Grade 300 Prestressing Strand and the Effect of Vertical Casting Position

James Christopher Carroll

Dissertation submitted to the faculty of the Virginia Polytechnic Institute and State University in partial fulfillment of the requirements for the degree of

Doctor of Philosophy
In
Civil Engineering

Tommy E. Cousins
Carin L. Roberts-Wollmann
Elisa D. Sotelino
Linbing Wang

August 20, 2009
Blacksburg, Virginia

Keywords: Transfer length, Development length, Prestressed concrete, Bond, Top-strand effect, Grade 300 strand, Flexural strength

Grade 300 Prestressing Strand and the Effect of Vertical Casting Position

James Christopher Carroll

ABSTRACT

The purpose of this study was to investigate the influence an increase in strand strength and the effect the as-cast vertical location had on transfer length, development length, and flexural strength and to resolve the discrepancies regarding the definition of the top-bar/strand effect. Two types of test specimens were fabricated and tested investigating each respective item. The increase in strand strength was found to influence transfer length, development length, and flexural strength, while the as-cast vertical location was only found to influence transfer length, and in turn development length. Contrary to the historical definition, the top-bar/strand effect was found to be more dependent on the amount of concrete cast above the strand than the amount below it, with transfer lengths showing a steady increase with a decrease in the amount of concrete cast above the strand. As a result of the findings of this study, a new transfer length equation was proposed and a previously proposed flexural bond length equation was recommended for use in lieu of the current code provisions. The current equations for flexural strength were found to give adequate estimates for flexural strength, although a decrease in ductility was noted.

DEDICATION

I would like to dedicate this dissertation to all those family members who have given their continual support and encouragement during my pursuit of my Ph.D. at Virginia Tech. I would also like to dedicate this to my Lord and Savior, Jesus Christ, for without his guidance I would not be where I am today.

ACKNOWLEDGEMENTS

First and foremost I would like to thank my Lord and Savior, Jesus Christ, for the opportunity and ability to pursue a Ph.D. To my committee, Dr. Cousins, Dr. Wollmann, Dr. Sotelino, and Dr. Wang, thank you for your continued guidance and support during my time at Virginia Tech. A special thanks to Dr. Cousins and Dr. Wollmann for their continued patience during my teaching endeavors and guidance in preparation for a career in academia. Thank you to Dr. Sotelino for providing me the opportunity to work with the History Channel.

I would like to thank the Department of Civil and Environmental Engineering and the College of Engineering for the opportunities that were provided for me to further prepare me for a career in academia. I would also like to thank the Virginia Transportation Research Council for funding this project.

On another note, I would like to thank Brett Farmer and Dennis Huffman for all their help during my time at the Structures Lab. I would also like to thank the numerous fellow students that helped in the ever daunting task of measuring DEMEC points. A special thanks to Hunter Hodges, Bryan Loflin, and Rob Cousins.

I would also like to thank my family for their continued support. I would specifically like to thank my mother for her always positive encouragement, my sister Felecia for her support, and my nephew Jacob for all the late nights he spent with me as I neared the completion of my dissertation.

No acknowledgements are necessary for photos, as all photos were taken by the author.

TABLE OF CONTENTS

LIST OF FIGURES

LIST OF TABLES

1.0 INTRODUCTION

1.1 Background

The nation's transportation infrastructure is a system comprised of roads and highways that interlock the eastern states to the western states, the northern states to the southern states, and those in between. The interstate system, initiated by former President Dwight D. Eisenhower in the mid 1950's and first created for military transport, has evolved into the primary arteries for the transportation of goods and people within the United States, proving to be a vital part of the country's continued success. Although the interstate highways provide the primary routes for transportation, a vast number of tributary routes consisting of state highways and local roads are also essential to the country. With an assortment of intricate routes weaving from one city to the next and an ever growing population and number of vehicles also comes the daunting task of maintenance and expansion, resulting in required revenues far surpassing anything one could have imagined 60 years ago.

The age of the overall system has far surpassed 50 years, with bridges beginning to deteriorate and the traffic volumes outgrowing the current routes. As a result, the nation's transportation infrastructure has turned into an ongoing process of demolition and reconstruction to ensure a continued efficient operation. No longer are two lanes in each direction adequate to support the volume of vehicles in specific areas of the country. Highways through major metropolitan areas require as many as 10 and 12 lanes in each direction, while highways through rural areas may even require three lanes in each direction. The expenses associated with such levels of maintenance and expansion have called for the use of more efficient materials in an effort to reduce costs. More durable asphalts and concretes have been created for road surfaces and more efficient designs have been implemented for bridges. Longer bridge spans have required engineers to be more innovative with their designs using steel plate girders, high-strength prestressed concrete girders, post-tensioned segmental sections, cable-stayed systems, and suspension bridges.

The use of prestressed concrete girders has become a common theme in bridge construction; however, span lengths have been limited by concrete compressive strengths and the maximum number of strands that can be placed in a section. In the past, high

concrete strengths have typically ranged between 6,000 psi and 8,000 psi, but recent advancements have resulted in concrete strengths well in excess of 10,000 psi. With higher concrete compressive strengths come increased allowable compressive and tensile stresses at transfer and service loads, as well as a small increase in flexural strength. Higher concrete compressive strengths also provide an opportunity for an increased resultant tensile force, however, the prestressing strands traditionally used are also limited by their cross-sectional areas and ultimate tensile strength. Historically, ½ in. diameter (0.153 $in.^2$) and ½ in. diameter super (0.167 $in.^2$) strands with an ultimate tensile strength of 270 ksi (Grade 270) have been used. In order to develop higher resultant tensile forces, a 0.6 in. diameter (0.217 $in.^2$) strand has been used in some cases, but has also been limited by the ultimate tensile strength of 270 ksi. As with concrete compressive strengths, recent developments have resulted in a higher strength strand with an ultimate tensile strength of 300 ksi (Grade 300 strand).

The Grade 300 prestressing strand was expected to provide an 11 percent increase in the available prestress force per strand, which in turn would provide two primary benefits. The first benefit of an increase in available prestress force would be a reduction in the number of strands needed in a member to provide the design prestress force of a beam originally containing Grade 270 strands. Such a reduction would result in a lower center of gravity of the strands, thus increasing the moment arm and flexural capacity of the member. The second benefit of an increase in available prestress force per strand would be an increased resultant tensile force using the same number of strands in a beam originally designed with Grade 270 strands, thus increasing the magnitude of the internal couple, and in turn increasing the flexural capacity. With an increase in flexural capacities also come economic benefits. An increased flexural capacity could allow for longer span lengths with the same number of girders in a bridge design compared to girders originally containing Grade 270 strands. On the other hand, an increased flexural capacity could also allow for a reduction in the number of girders transversely spaced in a bridge design originally designed for a specific span with girders containing Grade 270 strands. In either case, the use of girders containing Grade 300 strands could have a substantial economic impact on the bridge industry significantly reducing the costs associated with materials and the fabrication and construction processes.

1.2 Purpose Statement

The purpose of this investigation was to compare the effects an increase in strand strength had on transfer length, development length, and flexural strength in pretensioned, prestressed concrete girders to the traditional Grade 270 strand and current code equations. The current code provisions by the American Association of State Highway and Transportation Officials (AASHTO) and the American Concrete Institute (ACI) are based on years of experimental research on the traditional Grade 270 strand. The primary question that arose in this investigation was the possible effects an increase in strand strength might have on the existing provisions and if those provisions would still be adequate. In addition to the Grade 300 strand, the purpose of this investigation was also to consider the effect the as-cast vertical location of the strands (top-strand effect) had on transfer length, development length, and flexural strength and the importance of its recognition in the current codes for prestressed concrete.

1.3 Objectives

In an effort to fully determine the effects of the Grade 300 strand and the as-cast vertical location on transfer length, development length, and flexural strength, two types of test specimens were fabricated, each with varied objectives. The first type of test specimens were 24 ft long T-shaped, pretensioned, prestressed concrete girders and the second type of test specimens were groups of various sized 12 ft long, pretensioned, prestressed rectangular concrete blocks, referred to as the top-strand blocks. The T-beam test specimens had six objectives focused on their fabrication compared to the Grade 270 strand and current code provisions which were:

1. The effect the use of Grade 300 strand had on transfer length
2. The effect the use of Grade 300 strand had on development length
3. The effect the use of Grade 300 strand had on flexural strength
4. The effect a top-cast strand had on transfer length
5. The effect a top-cast strand had on development length
6. The effect a top-cast strand had on flexural strength

Contrary to the T-beam test specimens, the top-strand blocks had one primary objective. For over 50 years ACI and AASHTO have defined the top-bar effect in reinforced concrete to be dependent upon the amount of concrete cast beneath a bar

however, recent research has suggested otherwise. At the current time, neither ACI nor AASHTO include the top-bar effect in prestressed concrete, though it was assumed to have the same effect at the onset of this research. As a result of recent research, the primary objective of the top-strand blocks was to determine whether the top-strand effect was a factor of the amount of concrete cast below the strand or the amount of concrete cast above the strand.

The following sections of this report include background information for each of the aforementioned objectives, as well as a detailed description of research methodology. A discussion of the results is also provided followed by the conclusions and recommendations drawn from the study. Substantiation of current code provisions for use with the Grade 300 strand and effect of the as-cast vertical location of the strand are discussed as well as the recommended modifications as a result of the findings associated with this investigation.

2.0 BACKGROUND AND LITERATURE REVIEW

2.1 Introduction

Concrete is a material that has been used for countless construction projects throughout history. It is unique, in that concrete is placed in a plastic state, which allows it to be formed and molded into nearly any desirable shape. It was first invented by the Romans who mixed crushed stone with mortar to create small concrete panels. As this technology advanced, the Romans were able to use the material for the construction of larger, more ambitious projects such as the Pantheon. Concrete itself is a composite material, made up of various components, when mixed together cause a chemical reaction, resulting in a solidification of the mixture. With the application of load, concrete exhibits very different behavior with respect to the type of loading. Under a compressive load, concrete tends to have what is considered high strengths, typically ranging from 3,000 psi to 8,000 psi, while newer innovations have resulted in concrete compressive strengths in excess of 16,000 psi. On the other hand, when under tensile loads, concrete behaves very poorly, with tensile strengths generally in the range of 10 percent the respective compressive strength.

For members consistently loaded in compression, concrete can be a very efficient material due to its relatively high compressive strengths. However, when used in the construction of flexural members, members subject to bending stresses, the performance of concrete is limited by its low tensile strength. In order to compensate for the lack of tensile strength of the concrete, various types of steel reinforcing are placed in the areas expected to experience tensile stresses. This combination of concrete and steel is referred to as reinforced concrete, which takes advantage of both the high compressive strength of the concrete and the high tensile strength of the reinforcing steel creating an efficient composite material, dating back to the nineteenth century. Since its creation by Joseph Monier, reinforced concrete has seen much advancement in the use of reinforcement, from the simple iron cages used in Monier's early endeavors with flower pots, to the standard reinforcing bars (rebar) used today. Rebar has also evolved over time as continual research has led to the creation of more efficient deformation patterns as well as higher strengths, most commonly 60 ksi.

Reinforced concrete resists externally applied moments by an internal couple created from the resultant compressive force in the concrete and the resultant tensile force in the steel as shown in Figure 2.1. In order to develop tensile forces in the steel, the internal tensile stresses produced from bending must be transferred from the concrete to the steel, which occurs through the chemical and mechanical bond between the steel reinforcement and surrounding concrete. The chemical bond is the adhesion of the concrete to the steel, which contributes only a small portion of the overall bond, while the mechanical bond is the primary contributor, resulting from the shear interlock between the concrete and deformations along the reinforcing steel. Without the bond between the two materials, reinforced concrete would not be feasible.

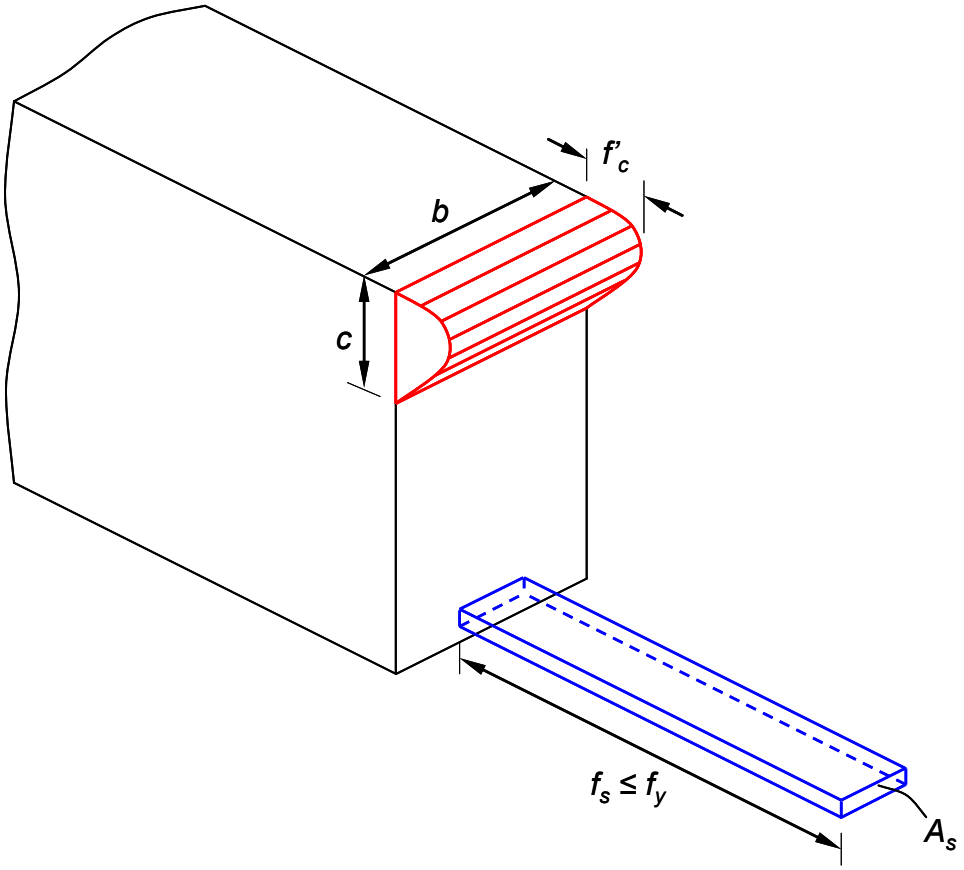

Figure 2.1. Internal Forces of a Reinforced Concrete Beam

The ability for reinforcing steel to adequately bond to the surrounding concrete is dependent upon a number of variables, the first of which being a sufficient embedment length. If the reinforcing steel is not embedded in the concrete for a long enough distance, under load, the bond stresses will exceed the bond strength of the concrete and

the reinforcing bar will simply pull through. ACI (2008) terms the minimum length required to fully develop a reinforcing bar as the development length and provides an empirical formula for its calculation shown as Equation (2-1).

$$L_d = \left(\frac{3}{40} \frac{f_y}{\lambda \sqrt{f_c'}} \frac{\psi_t \psi_e \psi_s}{\left(\frac{c_b + K_{tr}}{d_b} \right)} \right) d_b \qquad \text{Eq. (2-1)}$$

In Equation (2-1), factors take into consideration the yield strength of the bar (f_y), the as-cast vertical location (ψ_t), coating (ψ_e), bar size (ψ_s), bar diameter (d_b), the effect of using lightweight concrete (λ), the strength of the concrete (f'_c), and the amount of cover and confining reinforcement. The term $(c_b + K_{tr})/d_b$ accounts for the effects of cover and confinement, but the quantity is usually taken as 1.5 and in some cases 1.0 for conservatism. Since the adoption of the reinforcement location factor in the 1951 ACI Building Code, development lengths have been increased by a factor when bars are cast with more than 12 in. of fresh concrete beneath them, which was reduced from 1.4 to 1.3 in the 1989 Code (Wan et al. 2002a). In addition to location, development lengths are also increased by a factor to reflect the negative effect epoxy coating has on the bond between the reinforcement and surrounding concrete. Lightweight concrete also has a significant effect on development lengths, as well as the diameter of the bar. The use of lightweight concrete and larger diameter bars both result in longer development lengths. There is however, an additional factor (ψ_s), that accounts for the use of No. 6 bars and smaller, which have been shown to exhibit better bond characteristics, resulting in a decrease in development length (ACI 2008).

Reinforced concrete is an efficient use of the positive characteristics of both concrete and steel. There is, however, a more efficient use of both materials, which is becoming a more and more popular building material, prestressed concrete. With reinforced concrete, only a percentage of the material within the cross-section is utilized. Conventional analysis of reinforced concrete anticipates cracking of the cross-section. As a result of a cracked cross-section, increased deflections occur due to a decrease in stiffness. Prestressed concrete is similar to reinforced concrete, as it too relies on the tensile strength of the reinforcing steel to produce one component of the internal couple resisting externally applied loads; however, the concrete is precompressed prior to the

application of load thus reducing the amount of cracking under service loads. This precompression is made possible by use of high strength steel reinforcement, most notably, prestressing strands, which typically have ultimate tensile strengths of 270 ksi with recent developments resulting in strengths as high as 300 ksi.

Two types of prestressed concrete exist, pretensioned and post-tensioned. Pretensioned concrete, the focus of this research, relies on the bond of the prestressing strands to the surrounding concrete much like the bond between the rebar and surrounding concrete of reinforced concrete. Prior to casting structural members, prestressing strands are pulled in tension between two bulkheads until a target stress is reached in each strand, typically 75 percent of the strand's ultimate tensile strength. Following the stressing of the strands, the concrete is placed in the formwork around the strands and left to cure for a period of time allowing the concrete to reach an adequate strength for release. Upon sufficient strength gain, the prestressing strand is released and the force in the strands is transferred to the member through the bond between the prestressing strand and the surrounding concrete. In the case of flexural members, the prestressing strands are placed such that the induced force generally counteracts the expected moment, causing a precompression in the areas of the cross-section expected to experience tension, resulting in a very efficient use of the concrete.

Post-tensioned concrete is similar to pretensioned, as it too is precompressed, although the precompression of the concrete is induced after the structural member has already been cast. This precompression is applied by placing prestressing strands, also referred to as tendons, through ducts placed within the formwork prior to casting. Each strand is anchored at one end by an anchorage and pulled in tension to a specified stress on the opposite end. Subsequent to stressing the strands, the strands are anchored on the end at which stressing occurred, relying on the end anchorage to transfer the stress in the strand to the concrete.

As with reinforced concrete, pretensioned, prestressed concrete is also heavily dependent on the bond between the reinforcing steel and surrounding concrete in order to transfer the prestress forces and later the tensile stresses produced from external loadings. The chemical bond is again produced by the adhesion of the concrete to the steel, but is lost within the transfer zone during the transfer process, which is discussed with more

detail in Section 2.2 (Hanson and Kaar 1959). In addition to the mechanical bond, friction also plays a vital role in the development of tensile stresses in the prestressing strand due to external loadings.

Similar to reinforced concrete, the ability for prestressing steel to adequately bond to the surrounding concrete is dependent upon a number of variables, some of which are not taken into account by current building codes. Prestressing strand also must be embedded over an adequate length in order to develop its full tensile strength. If not, under load, the bond stresses will exceed the bond strength of the concrete and the prestressing strand will simply pull through. This type of failure is referred to as a bond failure, and is extremely undesirable in reinforced and prestressed concrete. The current ACI Building Code (2008) and AASHTO LRFD Specification (2006) provide an empirical formula for the calculation of the development length of prestressing strand shown as Equation (2-2) with units of psi.

$$L_d = \left(\frac{f_{se}}{3000}\right) d_b + \left(\frac{f_{ps} - f_{se}}{1000}\right) d_b \qquad \text{Eq. (2-2)}$$

Equation (2-2) takes into consideration the effective prestress (f_{se}), the stress in the strand at the nominal moment capacity (f_{ps}), and the diameter of the strand (d_b) and is broken up into two parts. The first term represents the transfer length and the second term represents the flexural bond length, each of which is defined and discussed with more detail in Sections 2.2 and 2.3, respectively. A number of researchers have shown the transfer and development lengths of prestressing strand to be dependent on a number of variables not included in Equation (2-2). Unlike the development length equation for standard reinforcing steel, Equation (2-2) neglects the effect of cover and confinement, the as-cast vertical location of the strand, the strength of the concrete, coating of the strand (i.e. rust or epoxy), and the effect of using lightweight concrete. In addition to the factors taken into consideration by Equation (2-1), the type of prestress release has also been shown to influence transfer and development lengths, as well as the fluidity of the concrete mixture, and possibly the water to cement ratio.

Equation (2-2) was adopted in the 1963 ACI Building Code and in the 1973 AASHTO Specification and is based on research conducted in the 1950's and 1960's by Hanson and Kaar and Kaar, Lafraugh, and Mass, and was later derived by Alan H.

Mattock (Tabatabai and Dickson 1993). The research by Hanson and Kaar was conducted on 250 ksi stress-relieved strand, with an initial prestress of 150 ksi, and a gradual method of release used in the transfer process. Over the past 50 years, the development length equation has remained for the most part constant, although numerous advancements have been made in the prestressed concrete industry. The type of prestressing strand has since evolved from the 250 ksi stress-relieved strand, to a more favorable 270 ksi low-relaxation strand, which has been the industry standard for more than 20 years and recent advancements have led to the development of a 300 ksi strand. In addition to the type of prestressing steel, concrete has also shown a steady progression to higher strengths and better quality. While materials have improved, a sudden release of prestress release has also become the standard method used by most prestressed concrete manufacturers. All of these changes over time contradict the parameters used in the derivation of the current code provisions.

In the following sections, detail is given to various topics associated with the research presented in this report. Sections 2.2 and 2.3 discuss the development and historical research contributions associated with transfer and development lengths, while Sections 2.4 and 2.5 discuss the bond characteristics of prestressed concrete and the factors affecting such. Section 2.6 focuses on the phenomenon known as the top-bar effect and its applicability to prestressed concrete. As previously discussed, adequate bond between the prestressing steel and the surrounding concrete is an essential part of prestressed concrete ensuring satisfactory performance, and is influenced by a number of factors not taken into consideration by current building codes. Attention is also given to the determination of the ultimate capacity of flexural members. As the primary objective of this report is the use of Grade 300 prestressing strand in flexural members, Section 2.7 reviews the previous use of the Grade 300 strand and its behavior, while Section 2.8 discusses the various methods used to calculate ultimate flexural capacities.

2.2 Transfer Length

2.2.1 Introduction

Pretensioned, prestressed concrete members rely on a precompression applied via internal bonded strands, which are tensioned prior to casting. Following the curing process, the force in the strand is released, typically accomplished by flame cutting the

strand and sometimes by gradual release using a hydraulic mechanism. The standard practice used by most prestressed manufacturers is the use of an acetylene torch to flame cut the strands. It should be noted that the strands are not actually cut, but heated to a point at which the strand yields in tension (Russell and Burns 1997). In either case, the force in the strand is transferred from the prestressing strand to the surrounding concrete via the chemical and mechanical bond between the two materials. Unlike nonprestressed reinforcement, the chemical bond has no effect within the transfer zone. The adhesion is lost with the violence associated with the transfer process, due to the tendency of the strand to slip into the member (Janney 1954). Leaving only the mechanical bond as the primary bond mechanism, the ability to transfer the prestress force from the prestressing strand to the surrounding concrete is achieved through the mechanical interlock of the strand within the concrete and the additional friction produced between the two materials from the expansion of the strand following the transfer process.

When a prestressing strand is tensioned, the strand elongates parallel to the direction of the applied load, causing a reduction in the cross-sectional area from the Poisson Effect. The concrete is then placed in the formwork with the strand fully tensioned, hardening around the strand with the reduced cross-sectional area. During the transfer process, when the strand is released, the strand tries to return to its original length and back to its original cross-sectional area. As the strand tries to pull through the concrete, the chemical bond, or adhesion, between the prestressing strand and surrounding concrete is broken. At the same time, the strand tries to expand, causing circumferential stresses along the length of the strand, commonly known as the Hoyer Effect (Janney 1954). Coupled with the mechanical interlock provided by the helical shape of the 7-wire strand, the friction forces produced from the Hoyer Effect add to the resistance of the strand to pull through the concrete, thus creating the bond between the strand and surrounding concrete. The distance required to obtain full bond of the prestressing strand to the surrounding concrete is the transfer length, formally defined by ACI as the distance over which the strand should be bonded to the concrete to develop the effective prestress in the prestressing steel, f_{se} (ACI 2008). The transfer length is assumed to vary linearly from zero bond at the end of the member to full bond, full transfer of the effective prestress, at the transfer length, where the strand ceases to slip

and the chemical component again contributes to the total bond between the two materials. However, the transfer length can be broken into a plastic and elastic zone, with a linear variation in strand stress and constant bond stress within the plastic zone and a parabolic variation in stress and descending bond stress within the elastic zone as shown in Figure 2.2.

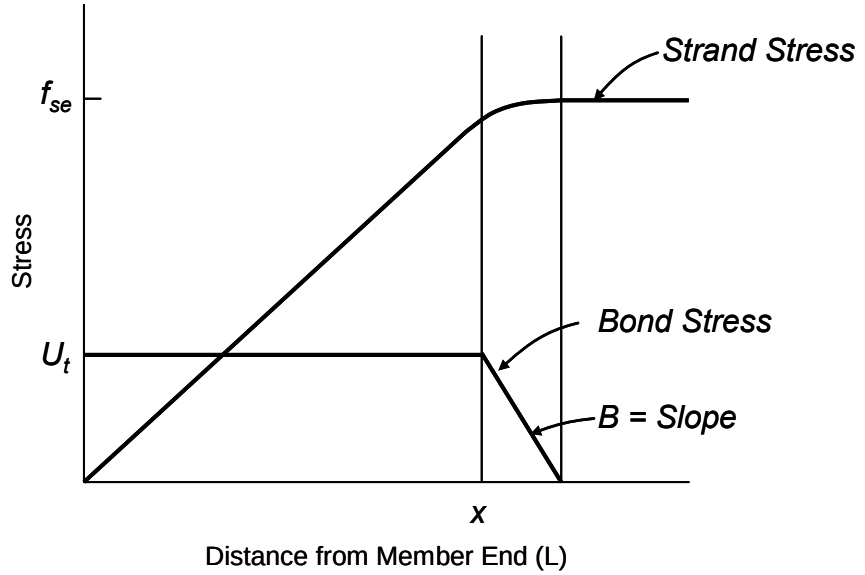

Figure 2.2. Stress behavior (Cousins et al. 1990b)

2.2.2 (Prior to 1990)

Criteria exist for transfer length calculations in both ACI and AASHTO with only slight variations between the two. As previously mentioned, the development length equation for prestressing strands is made up of two components, with the first term representing the transfer length and the second term representing the flexural bond length. The expression for transfer length in both ACI and AASHTO is shown as Equation (2-3) with f_{se} in units of ksi. Equation (2-3) is based on research performed in the late 1950's and early 1960's using 250 ksi stress-relieved strand coupled with a method of gradual release (Hanson and Kaar 1959).

$$L_t = \left(\frac{f_{se}}{3} \right) d_b \qquad \text{Eq. (2-3)}$$

Within the shear provisions of both codes, a value of 150 ksi is assumed for the effective prestress, f_{se}, after all losses, reducing Equation (2-3) to $50d_b$ (Equation 2-4). This assumption provides designers with a simplified method for obtaining the force in

the strand at any distance within the transfer zone and has generally been considered a conservative assumption. AASHTO increased this value by twenty percent to $60d_b$, accounting for higher jacking stresses typically used in industry as recommended by Buckner (1995).

Over the past 55 years, transfer length research has been an ongoing process with new equations proposed time and time again to no avail, with no significant changes being made to the code provisions. Some researchers claim transfer length to only be dependent on the effective stress in the strand and the diameter of the strand, while others say transfer lengths are dependent on a number of variables in addition to the two. Section 2.4 discusses, in detail, those variables shown to affect the bond between prestressing strand and surrounding concrete, while located at the end of Section 2.1, Table 2.1 and Table 2.2 list the proposed equations for transfer length and the contributing party associated with each from the past five decades.

Prior to 1960, the behavior of the bond between prestressing steel and concrete was not well understood. In an investigation published in 1954, Janney concluded that the stress along a concrete prism was directly proportional to the tensile stresses in the pretensioned wire, even though strain compatibility failed to exist in the end region (transfer zone) as a result of slip. Janney also concluded that the length of embedment necessary for the transfer of prestress increased with wire diameter (Janney 1954).

In response to questions associated with transfer and development length, significant studies were conducted in the late 1950's and early 1960's, leading to the development of the current ACI and AASHTO transfer and development length equations, the most significant by Hanson and Karr and Kaar et al. Hanson and Kaar investigated the bond characteristics in pretensioned, prestressed concrete beams containing 250 ksi stress-relieved strands, the industry standard at the time. The average bond stress for test specimens was found to be 400 psi, based on average transfer length measurements for ¼ in., ⅜ in., and ½ in. diameter strands pretensioned to 150 ksi. A gradual method of release was used in the transfer process and the test specimens contained concrete with a slump of 2 in. and a 1 ½ in. maximum size aggregate. Based on a 400 psi average bond stress, an equation could be derived calculating the transfer

length for 250 ksi stress relieved strand, shown as Equation (2-5) (Hanson and Kaar 1959).

$$L_t = \left(\frac{f_{se}}{2.94} \right) d_b \qquad \text{Eq. (2-5)}$$

In addition to the work on bond, Kaar et al. looked at the influence of concrete strength on transfer length. Again, 250 ksi stress-relieved strand was used for the investigation. The strands were flame cut; however, a period of preheating was conducted prior to transfer, gradually relieving a portion of the force in the strand. Variability did exist between cut and dead end transfer lengths, but the study showed no significant change in transfer lengths of strands up to ½ in. diameter for concrete strengths up to 5,000 psi (Kaar et al. 1963). Concurrent to the study by Kaar et al., a newer, high strength (270 ksi) strand was used in a transfer length study, which concluded, regardless of a 26 percent higher jacking stress, there was no significant increase in transfer length compared to conventional (250 ksi) strands (Janney 1963). Based on the studies of Hanson and Kaar and Kaar et al., the transfer length was shown to only be affected by the stress in the strand and the diameter of the strand, neglecting any effect concrete strength might have. As previously discussed, Alan Mattock of the Portland Cement Association (PCA) aided in the development and implementation of Equation (2-5) into the 1963 ACI Building Code, which was simplified into Equation (2-3) by what is now Committee 423 (Tabatabai and Dickson 1993).

Subsequent to the research basis for the ACI provisions, a number of factors were found to influence transfer lengths, and the original provisions were found to be unconservative with transfer lengths estimated to be 80 strand diameters ($80d_b$) (Equation 2-6) by Martin and Scott (1976). Zia and Mostafa further investigated transfer length also listing numerous factors influencing actual values, the majority of which are not included by the ACI provisions. With development length as the primary objective in the study, Zia and Mostafa focused on both components, deriving new expressions for the transfer and flexural bond lengths, with attention given to the type of release used for prestress transfer. Equations for transfer lengths were derived from linear regression for both release methods (sudden and gradual), selecting the equation for data having a sudden release as the final proposed equation, shown as Equation (2-7), which takes into

account the stress in the strand, strand diameter, and strength of the concrete at the time of release (Zia and Mostafa 1977). Selecting the equation for data having a sudden release ensured a conservative estimate for transfer lengths.

$$L_t = 1.5 \frac{f_{si}}{f_{ci}^{'}} d_b - 4.6 \qquad \text{Eq. (2-7)}$$

2.2.3 (1990 – 1999)

As prestressing strand advancements continued, concerns were raised about the amount of corrosion present in prestressed bridge girders, creating a high level of interest in epoxy-coated strand. Referring back to the development length equation for standard reinforcing bars, development lengths are known to increase for epoxy-coated rebar, thus questions arose regarding the effect epoxy coating may have on the bond of prestressing strand. In response to the concerns, a research project at North Carolina State University focused on the bond behavior of epoxy-coated prestressing strand, also using uncoated strands in control specimens.

Cousins et al. found transfer lengths for epoxy-coated strand to be less than transfer lengths for uncoated strand. Results showed transfer lengths for epoxy-coated strands, also heavily dependent on impregnated grit density, to be fairly well represented by the ACI/AASHTO equation (Equation 2-3) and Equation (2-7) proposed by Zia and Mostafa. On the other hand, the same equations were unconservative for uncoated strand. In response to the longer transfer lengths for uncoated strands, Cousins et al. proposed Equation (2-8), with recommended values of 6.7 and 300 psi/in. for U'_t and B, respectively for uncoated strands (Cousins et al. 1990b).

$$L_t = 0.5\left(\frac{U_t^{'}\sqrt{f_{ci}^{'}}}{B}\right) + \frac{f_{se}A_{ps}}{\pi d_b U_t^{'}\sqrt{f_{ci}^{'}}} \qquad \text{Eq. (2-8)}$$

The strands used by Cousins et al. were seven-wire, 270 ksi low-relaxation strands, stressed to approximately 80 percent of their ultimate tensile strength, about five percent higher than is typically used in industry today. The compressive strength of the concrete used was slightly higher than 4,000 psi for all test specimens. For the majority of the test specimens, a sudden release of prestress was used resulting in longer transfer lengths at the cut ends of test specimens (Cousins et al. 1990c). In all likelihood, the

combination of higher initial prestress values coupled with relatively low concrete strengths and a sudden release, would result in a worst case scenario with respect to those parameters.

In response to the work of Cousins et al., the Federal Highway Administration (FHWA) issued a memorandum in 1988 with various restrictions on the use of prestressing steel, one of which included the ban of 0.6 in. diameter strand for use in pretensioned, prestressed concrete girders, due to excessive transfer and development lengths (FHWA 1988). Additional restrictions were included in the memorandum, discussed further in Section 2.3 in relation to development length. Subsequent to the investigations performed in the late 1950's and early 1960's, few investigations were conducted related to transfer and development length between 1965 and 1985. In response to the 1988 FHWA Memorandum, the interest level of prestressed concrete related research shifted its focus to the bond characteristics between prestressing steel and concrete, resulting in a number of investigations looking at all aspects of transfer and development lengths.

In the early 1990's, a substantial amount of research was conducted on the transfer and development length of prestressing strand. Cousins continued work on the bond characteristics of prestressing strand, developing a simplified test representing the typical behavior between prestressing steel and concrete during the transfer process and the effect of varying strand spacing and cover. Cousins et al. looked at ½ in. diameter 270 ksi, low-relaxation prestressing strand, with varying surface conditions (clean, lightly rusted, and epoxy-coated) with results showing coated strand to have shorter transfer lengths and higher bond stresses, which sometimes have been shown to result in splitting of the concrete (Cousins et al. 1992). In the latter study, the influence of cover and spacing on transfer lengths of epoxy-coated, 270 ksi low-relaxation prestressing strand was also investigated. Transfer lengths of epoxy-coated strands were, again, found to be shorter than the ACI/AASHTO calculated values. This was attributed to the better bond with increased level of impregnated grit densities. Spacings less than those recommended by ACI/AASHTO resulted in significant cracking of the test specimens, resulting in considerably longer transfer lengths (Cousins et al. 1993). Additional

research was completed on the influence of reduced spacing of uncoated strands, but showed no significant impact on transfer length values (Cousins et al. 1994).

Concurrent to the work by Cousins et al., a number of studies were also in progress, including work by the Florida Department of Transportation (FDOT) and McGill University in Montreal, Quebec. The FDOT investigation focused on transfer lengths in full scale AASHTO girders, which is revisited by Deatherage et al. in a later study. FDOT researchers investigated the transfer lengths of AASHTO Type II girders containing ½ in. and 0.6 in. diameter strands with center-to-center spacings of 2 in. Some test specimens contained debonded strands, which is beyond the scope of this project. The authors found transfer lengths for both ½ in. and 0.6 in. diameter strands to exceed values specified by ACI and AASHTO, Equation (2-3). Strand spacing showed no significant effect on the results. However, based on the test results, it was recommended that the initial prestress, f_{si}, be substituted for the effective prestress, f_{se}, in Equation (2-3), which better estimated the experimental values (Shahawy et al. 1992). Similar results were found by Deatherage et al., with the same modifications presented for Equation (2-3), shown by Equation (2-9). Deatherage et al. did, however, find transfer lengths to be significantly shorter for the 0.6 in. diameter strands (Deatherage et al. 1994).

$$L_t = \left(\frac{f_{si}}{3} \right) d_b \qquad \text{Eq. (2-9)}$$

As previously discussed, the basis for Equation (2-3) was from tests completed on test specimens with a relatively low concrete strength in comparison with today's materials. Mitchell et al. investigated the influence of concrete strength on transfer and development length, looking at concrete strengths at the time of transfer from 3050 psi to 7250 psi and strand diameters of ⅜ in., ½ in., and 0.62 in. The ⅜ in. diameter strand was stress-relieved, while the ½ in. and 0.62 in. diameter strand was low-relaxation, and all strands were released using a gradual method of prestress release, which does fail to show the effects of sudden release. Based on the test results, Mitchell et al. concluded that transfer length did decrease with an increase in concrete strength regardless of strand diameter and proposed Equation (2-10) with f_{pi} being the stress in the strand immediately following transfer (Mitchell et al. 1993).

$$L_t = 0.33 f_{pi} d_b \sqrt{\frac{3}{f'_{ci}}} \qquad \text{Eq. (2-10)}$$

In response to the recommendations of research performed across the United States and Canada as a result of the 1988 FHWA Memorandum, the FHWA was forced to conduct an independent review of recent research efforts, clarifying discrepancies. Buckner noted the current ACI transfer length equation was derived based on a stress-relieved 250 ksi prestressing strand and a average bond stress of 400 psi and the actual area of a Grade 250 strand is $0.725*(\pi d_b/4)$, while the actual area of the newer 270 ksi low-relaxation prestressing strand is approximately 6 percent larger, $0.7685*(\pi d_b/4)$. Based on the equilibrium of forces over the transfer length of a 250 ksi strand, the following relationship is developed, where $4/3(\pi d_b)$ is the perimeter of a 7-wire strand with respect to the nominal diameter.

$$0.400\left(\frac{4\pi d_b}{3}\right) L_t = 0.725\left(\frac{\pi d_b^2}{4}\right) f_{se} \qquad \text{Eq. (2-11)}$$

Solving Equation (2-11) yields Equation (2-5) for transfer length. As previously stated, by assuming an effective prestress of 150 ksi, Equation (2-3) reduces to $50d_b$. However, substituting the area of a 270 ksi strand into Equation (2-11), and again solving for the transfer length, L_t, yields Equation (2-12). Assuming an effective prestress of 150 ksi would reduce Equation (2-12) to $54d_b$, which is slightly larger than the previous value of $50d_b$ for the 250 ksi strand.

$$L_t = \frac{f_{se} d_b}{2.78} \qquad \text{Eq. (2-12)}$$

Based on this comparison, Buckner stated that Equation (2-3) became invalid with the introduction of the 270 ksi low-relaxation strand, going on to recommend the use of Equation (2-9) for transfer length calculations, previously recommended by Shahawy et al. and Deatherage et al. Buckner also recommended that the assumed value for transfer length in shear design be increased by 20 percent to $60d_b$ (Equation 2-13), accounting for longer transfer lengths of Grade 270 strands.

For the most part, past research has been primarily focused on the use of ½ in. diameter prestressing strands. Prior studies by Cousins et al., Shahawy et al., Mitchell et

al., and Deatherage et al. have included the determination of transfer length for 0.6 in. diameter prestressing strands in their investigations, but not as the primary objective. The use of the larger 0.6 in diameter prestressing strand at the typical 2 in. spacing allows a 40 percent higher level of prestress than a typical ½ in. diameter strand and almost 30 percent higher level of prestress than a ½ in. diameter special strand. From an economic stand point, higher levels of prestress without an increase in the number of strands is extremely beneficial to the efficient use of higher strength concretes. With the moratorium placed on the use of 0.6 in. diameter prestressing strands, due to excessive transfer length measurements, a high level of attention was given to the ability of the 0.6 in. strand to sufficiently transfer its prestressing forces within a reasonable length (Russell and Burns 1997).

A study by Russell and Burns focused on the on the ability of the 0.6 in. strand to transfer its prestressing forces and the influence of flame cutting during the transfer process on transfer length measurements. Russell and Burns found 0.6 in. diameter strands to have a significantly longer transfer length and that transfer lengths at the ends adjacent to the cut end are generally much longer than those at the dead end. They note the ratio of average transfer lengths for 0.6 in. diameter strands to ½ in. diameter strands is approximately equal to the ratio of corresponding diameters. Russell and Burns found average transfer lengths to be $66.6d_b$ which, if compared to the recommendation of Buckner, correspond to transfer lengths calculated by Equation (2-9). Russell and Burns go on to recommend Equation (2-14) for the calculation of transfer lengths, noting modification could be made for the influence of concrete strength. Assuming an effective prestress of 160 ksi, Equation (2-14) reduces to $80d_b$ (Equation 2-6), which is approximately the average plus one standard deviation (Russell and Burns 1997). Subsequent to the work by Russell and Burns, Lane also proposed Equation (2-15) for the calculation of transfer lengths (Lane 1998).

$$L_t = \frac{f_{se} d_b}{2} \qquad \text{Eq. (2-14)}$$

$$L_t = \frac{4 f_{pt}}{f_c'} d_b - 5 \qquad \text{Eq. (2-15)}$$

2.2.4 (2000 – 2009)

Contradictory to the findings of Russell and Burns and those from previous studies, Barnes et al. found little difference in transfer length measurements from cut and dead ends, except for those containing rusted strands, which significantly increased at the cut end (Barnes et al. 2003). Also contrary to previous work, Kose and Burkett later found transfer lengths to decrease with an increase in strand diameter. In addition to strand diameter, Kose and Burkett also looked at the influence of concrete strength and effective prestress on transfer lengths, concluding an increase in concrete strength decreased the transfer length, while an increase in effective prestress increased the transfer length (Kose and Burkett 2005). With the three contributing factors taken into consideration, Barnes et al. proposed Equation (2-16) for the calculation of transfer lengths, while Kose and Burkett proposed Equation (2-17).

$$L_t = \alpha \frac{f_{pt}}{\sqrt{f_{ci}^{'}}} d_b \qquad \text{Eq. (2-16)}$$

$$L_t = 95 \frac{f_{pi}\left(1 - d_b\right)^2}{\sqrt{f_c^{'}}} \qquad \text{Eq. (2-17)}$$

As previously mentioned, numerous factors have been shown to influence transfer lengths, which are discussed in Section 2.4 with more detail. As research has progressed, transfer length equations have evolved from the ACI/AASHTO equation including only effective prestress and strand diameter to containing other factors, most notably concrete strength. In addition to the three primary contributing factors, one of the most influential may be the location of the strand within the cross-section. Petrou et al. (2000b) found top-strands to have significantly longer transfer lengths in prestressed concrete piles containing traditional concrete, while a recent study by Peterman has shown the vertical as-cast location to also strongly influence transfer lengths in Self Consolidating Concrete (SCC). As a result of the study by Peterman, Equation (2-18) was proposed for the calculation of transfer length, containing only strand diameter and as-cast vertical location where d_{cast} is the amount of concrete cast above the strand (Peterman 2007).

$$\begin{gathered} \text{For } d_{cast} < 8\text{”} \quad L_t = 90\left(90 - 5d_{cast}\right)d_b \\ \text{For } d_{cast} \geq 8\text{”} \quad L_t = 50 d_b \end{gathered} \qquad \text{Eq. (2-18)}$$

In a recent NCHRP report, researchers found concrete strength to strongly influence transfer length. As a result of the experimental testing in the NCHRP study, a simplified transfer length equation was proposed containing only strand diameter and concrete strength, shown as Equation (2-19). The recommended equation takes into account concrete strengths up to 6,000 psi. At a concrete strength of 4,000 psi the equation becomes equal to the current AASHTO recommended value of $60d_b$. As concrete strength increases, the calculated transfer lengths decrease, but are limited to a minimum value of $40d_b$, which corresponds to a concrete strength of 9,000 psi (NCHRP 2008).

$$L_t = \frac{120}{\sqrt{f'_{ci}}} d_b \geq 40d_b \qquad \text{Eq. (2-19)}$$

2.2.5 End-slip

For the most part, transfer length studies discussed herein have relied on the measurements of concrete surface strains, but transfer lengths can be determined by measuring the amount of slip occurring between the end of the strand and the end of the test specimen. End-slip measurements provide an easy way to obtain data for the calculation of transfer lengths, requiring less time and effort as opposed to concrete surface strain measurements. However, end-slip measurements sometimes are not always as reliable as measurements taken using surface mounted gauge points (Russell and Burns 1997).

At the onset of prestress release, the strand tries to slip through the concrete, but is resisted by the mechanical bond produced from the helical shape of the strand and the increased friction forces produced from the Hoyer Effect. The strand does, however, slip over the transfer length, until full bond is obtained. Figure 2.3 shows the relationship of concrete and steel strain with respect to the distance from the end of the member as discussed by Cousins et al (1990c). It is assumed that the strains have a linear variation from the end of the member to the end of the transfer length.

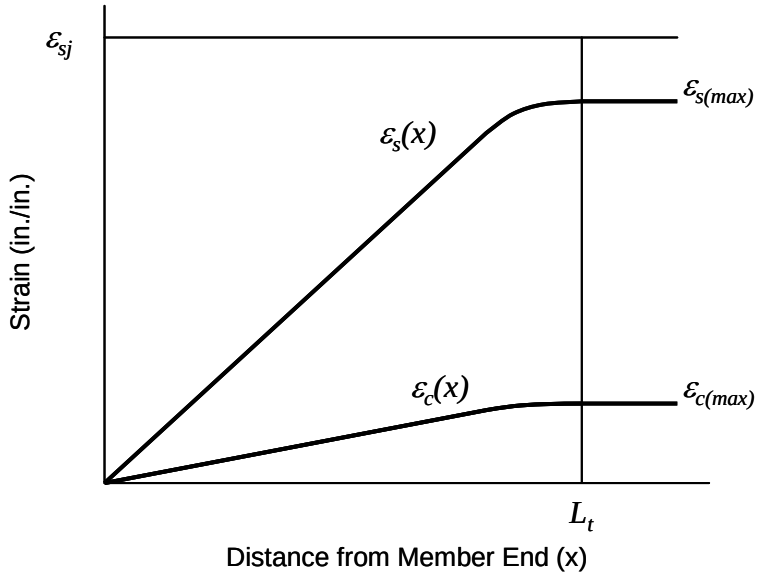

Figure 2.3. Concrete and Steel Strain versus Length (Cousins et al. 1990c)

Assuming a linear distribution of strains, the amount of elastic shortening occurring from the end of the specimen to the end of the transfer length in the specimen itself is equal to the area under the $\varepsilon_c(x)$ curve calculated by Equation (2-20), while the amount the strand shortens is equal to the area under the $\varepsilon_s(x)$ curve calculated by Equation (2-21). If perfect bond existed between the concrete and steel, the amount the concrete and the steel shorten would be equal, but because the strand slips along the transfer length, a discrepancy exists, referred to as end-slip, L_{es}, therefore the end slip is equal to the difference in δ_s and δ_c as shown in Equation (2-22).

$$\delta_c = \int_0^{L_t} \varepsilon_c(x)\,dx = \frac{\varepsilon_{c(\max)} L_t}{2} \qquad \text{Eq. (2-20)}$$

$$\delta_s = \int_0^{L_t} \varepsilon_s(x)\,dx = \frac{\varepsilon_{s(\max)} L_t}{2} \qquad \text{Eq. (2-21)}$$

$$L_{es} = \frac{\varepsilon_{s(\max)} L_t}{2} - \frac{\varepsilon_{c(\max)} L_t}{2} = \frac{L_t}{2}\left(\varepsilon_{s(\max)} - \varepsilon_{c(\max)}\right) \qquad \text{Eq. (2-22)}$$

By substituting the steel stress and the modulus of elasticity of the strand into Equation (2-22) in place of the steel strain, the transfer length can be solved for as shown in Equation (2-23) based on the assumption of linear variation for both concrete and steel strains.

$$L_t = \frac{2L_{es}E_{ps}}{f_{si} - E_{ps}\varepsilon_{ci}} \qquad \text{Eq. (2-23)}$$

In addition to the equation above, Equation (2-24) was derived by Guyon under the assumption of a constant bond stress (linear strain distribution) or a linear bond stress distribution (parabolic strain distribution) to calculate end-slip. The area labeled as L_{es} as shown in Figure 2.4 (a) and 2.4 (b), which varies with bond stress distribution, is equal to the end-slip. In Equation (2-24) α is modified depending on the bond stress distribution. With a constant bond stress distribution, $\alpha = 2$, while a linear bond stress distribution results in $\alpha = 3$ (Guyon 1948). Over time, researchers have proposed various α values based on experimental studies ranging in between the limits set forth by Guyon. Marti-Vargas (2007) found α to be 2.44 from a regression analysis of test results and Balazs (1993) found $\alpha = 2/(1 - b)$ where b is the power of the bond stress relationship. Balazs has also developed three nonlinear equations representing transfer length, Equations (2-25), (2-26), and (2-27).

$$L_t = \alpha \frac{L_{es}}{\varepsilon_{si}} \qquad \text{Eq. (2-24)}$$

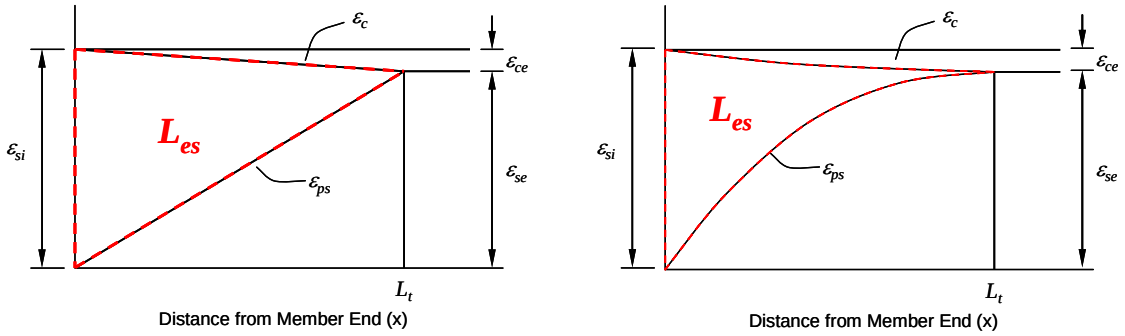

(a) Constant Bond Stress (b) Linear Bond Stress

Figure 2.4. Strain Distribution in the Transfer Zone (Balazs 1993)

$$L_t = 218\sqrt[4]{\frac{\sqrt{L_{es}^3}}{f_{ci}^{'}}}d_b \qquad \text{Eq. (2-25)}$$

$$L_t = 24.7\frac{L_{es}^{0.625}}{f_{ci}^{'0.15}\varepsilon_{si}^{0.4}} \qquad \text{Eq. (2-26)}$$

$$L_t = 0.158\frac{f_{si}}{\sqrt{f_{ci}^{'}\sqrt{L_{es}}}} \qquad \text{Eq. (2-27)}$$

Similar to the derivation of previous equations, Peterman derived Equation (2-28) by integrating under the strand stress versus transfer length curve and assuming a linear ascending branch of the curve. However, Peterman does not take into account the effect of the concrete strain, but the equation correlates very well with other expressions. If the stress and modulus of elasticity are changed to strain, Equation (2-28) is identical to Equation (2-24) by Guyon with $\alpha = 2$, which assumes a constant bond stress. In addition to the correlation to the equation by Guyon, assumed values of E_{ps} = 29,000 ksi and f_{si} = 197.4 ksi, Equation (2-28) is close to the expression by Russell and Burns (Equation 2-29) and Logan (Equation 2-30).

$$L_t = \frac{2L_{es}E_{ps}}{f_{si}} = 293.8L_{es} \qquad \text{Eq. (2-28)}$$

$$L_t = 294.9L_{es} \qquad \text{Eq. (2-29)}$$

$$L_t = 308L_{es} \qquad \text{Eq. (2-30)}$$

End-slip measurements are somewhat controversial, but can be very beneficial in the determination of transfer lengths if completed with a great deal of precision. Cousins et al. (1993) found transfer lengths calculated from end-slip measurements to have a good correlation to those calculated from concrete surface strains. Marti-Vargas et al. (2007), on the other hand, noted that a great variability existed with transfer lengths calculated from end-slip measurements and that, although transfer length calculations are relatively easy, it can lead to a false perception of variable transfer lengths.

2.2.6 Summary

Transfer length is an important aspect of pretensioned, prestressed concrete, especially with respect to shear design. Over the past five decades research has shown transfer lengths to be more complex than initially thought. The current ACI/AASHTO provisions calculate transfer lengths based on the effective prestress, after all losses, and the strand diameter, assuming a constant bond stress of 400 psi. Numerous researchers have shown transfer length results exceeding those calculated by current provisions and have made numerous recommendations from their conclusions. As previously stated, transfer length is a portion of the development length of prestressing strands. Looking back at Equation (2-1), numerous factors are included in the development length calculation for standard reinforcing bars, while the majority of these are neglected for prestressed concrete. It is evident from the literature that the current ACI/AASHTO provisions are insufficient for the calculations of transfer length, requiring additional research and revisions to the current code provisions.

Table 2.1. Historical Transfer Length Equations

Contributor	Year	Equation	Eq. No.
Hanson & Kaar	1959	$L_t = \frac{f_{se}}{2.94} d_b$	2-5
ACI	1963	$L_t = \frac{f_{se}}{3} d_b$	2-3
		$L_t = 50 d_b$	2-4
Martin & Scott	1976	$L_t = 80 d_b$	2-6
Zia & Mostafa	1977	$L_t = 1.5 \frac{f_{si}}{f_{ci}^{'}} d_b - 4.6$	2-7
Cousins et al.	1990	$L_t = 0.5 \left(\frac{U_t^{'} \sqrt{f_{ci}^{'}}}{B} \right) + \frac{f_{se} A_{ps}}{\pi d_b U_t^{'} \sqrt{f_{ci}^{'}}}$	2-8
Shahawy et al.	1992	$L_t = \frac{f_{si}}{3} d_b$	2-9
Mitchell et al.	1993	$L_t = 0.33 f_{pi} d_b \sqrt{\frac{3}{f_{ci}^{'}}}$	2-10
Deatherage et al.	1994	$L_t = \frac{f_{si}}{3} d_b$	2-9
Buckner	1995	$L_t = \frac{f_{si}}{3} d_b$	2-9
AASHTO	1995	$L_t = 60 d_b$	2-13
Russell & Burns	1997	$L_t = \frac{f_{se}}{2} d_b$	2-14
		$L_t = 80 d_b$	2-6
Lane	1998	$L_t = \frac{4 f_{pt}}{f_c^{'}} d_b - 5$	2-15
Barnes et al.	2003	$L_t = \alpha \frac{f_{pt}}{\sqrt{f_{ci}^{'}}} d_b$	2-16
Kose & Burkett	2005	$L_t = 95 \frac{f_{pi} \left(1 - d_b\right)^2}{\sqrt{f_c^{'}}}$	2-17
Peterman	2007	For $d_{cast} < 8$" $L_t = 90\left(90 - 5 d_{cast}\right) d_b$ For $d_{cast} \geq 8$" $L_t = 50 d_b$	2-18
NCHRP	2008	$L_t = \frac{120}{\sqrt{f_{ci}^{'}}} d_b \geq 40 d_b$	2-19

Table 2.2. Historical Transfer Length Equations (End-Slip)

Contributor	Year	Equation	Eq. No.
Guyon	1948	$L_t = \alpha \frac{L_{es}}{\varepsilon_{si}}$	2-24
Cousins et al.	1990	$L_t = \frac{2L_{es}E_{ps}}{f_{si} - E_{ps}\varepsilon_{ci}}$	2-23
Balasz	1992	$L_t = 218\sqrt[4]{\frac{\sqrt{L_{es}^3}}{f_{ci}^{'}}}d_b$	2-25
Balasz	1993	$L_t = 24.7\frac{L_{es}^{0.625}}{f_{ci}^{'0.15}\varepsilon_{si}^{0.4}}$	2-26
Balasz	1993	$L_t = 0.158\frac{f_{si}}{\sqrt{f_{ci}^{'}\sqrt{L_{es}}}}$	2-27
Russell & Burns	1996	$L_t = 294.9L_{es}$	2-29
Logan	1997	$L_t = 308L_{es}$	2-30
Peterman	2007	$L_t = \frac{2L_{es}E_{ps}}{f_{si}} = 293.8L_{es}$	2-28

2.3 Development Length

2.3.1 Introduction

Pretensioned, prestressed concrete members resist externally applied moments by an internal couple similar to the behavior of reinforced concrete, where the concrete ultimately takes the compressive force, while the prestressing strands take the tensile force. In order to develop that tensile force in the strands, the tensile stresses must be transferred from the concrete to the strand, which, again, occurs through the chemical and mechanical bond between the strand and the surrounding concrete. Beyond the transfer length, slip between the strand and surrounding concrete has not yet occured, therefore, the chemical bond is still present, but contributes very little to the overall bond.

As previously mentioned, the bond between the strand and the surrounding concrete is mainly dependent on an adequate embedment length in order to develop the full tensile strength of the strand. AASHTO defines the development length as the length required to anchor the strand to fully develop the stress in the strand at the nominal moment capacity of the member (AASHTO 2006). ACI and AASHTO provisions use Equation (2-2) for the calculation of the development length, with a 1.6 multiplier in AASHTO placed on development lengths for pretensioned members with a depth greater than or equal to 24 in.

$$L_d = \left(\frac{f_{se}}{3000}\right) d_b + \left(\frac{f_{ps} - f_{se}}{1000}\right) d_b \qquad \text{Eq. (2-2)}$$

Equation (2-2) is made of two components, the first term being the transfer length, discussed in Section 2.2, and the second term being the flexural bond length. The flexural bond length, L_{fb}, is the distance required to sufficiently increase the stress in the strand from the effective prestress to the stress in the strand at the nominal moment capacity, f_{ps}. Figure 2.5 shows an idealized relationship between the steel stress and distance from the free end of the beam at strength.

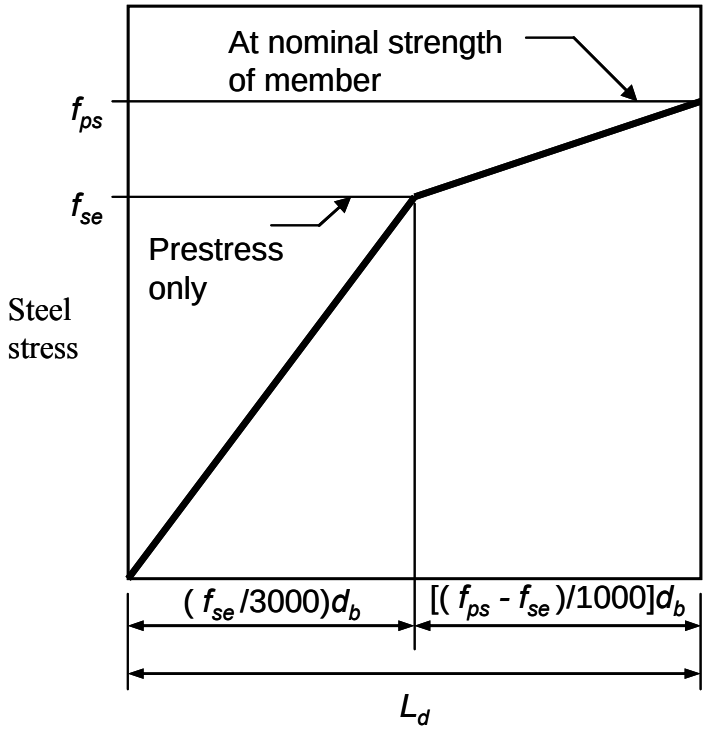

Figure 2.5. Idealized Bilinear Steel Stress Relationship at Strength (ACI 2008)

Subsequent to the transfer process, the tensile stress in the strand is converted to a compressive stress in the concrete via the bond between the strand and surrounding concrete as the strand becomes somewhat wedged in the concrete as a result of the Hoyer Effect. At this time, the entire cross-section may be subjected to an axial compression, depending on the cross-section, the amount of prestress, and eccentricity of the strands. As the member is subjected to externally applied moments, resulting in bending stresses (compression in the top and tension in the bottom), the compressive stress in the top portion of the cross-section will increase, while the compressive stress in the bottom portion of the cross-section will decrease. As the load is increased, the compressive stress in the bottom of the cross-section produced by the prestress force is overcome by the tensile stresses produced from bending, approaching the tensile strength of the concrete, resulting in flexural cracking. Upon overcoming the effective prestress in the cross-section, the prestressing strands are left to take all the tensile forces. When the tensile force is increased, the strain in the prestressing strand also increases, causing an elongation of the strand (Hanson and Kaar 1959). With an elongation of the strand also comes a slight reduction of the cross-sectional area due to the Poisson Effect. As the

cross-sectional area of the strand continues to reduce, the friction produced from the transfer process decreases, making the mechanical interlock of the strand within the concrete the primary contributor to bond (Janney 1954) (Cousins et al. 1990b). If the embedment length is shorter than the required development length, the bond stresses will exceed the bond strength of the surrounding concrete resulting in a bond failure in the end region of the beam and the strand being pulled through the concrete. If the embedment length is longer than the required development length, the strand will be capable of developing the stress required to reach the nominal moment capacity of the member.

2.3.2 (Prior to 1990)

ACI states in the commentary that provisions are based on tests of members with normal weight concrete and that tests may not be representative of low water-cementitious material ratios. ACI also states that the bond of the strand is a function of numerous factors, discussed with more detail in Section 2.4 and the test data was also based on tests performed in the late 1950's and early 1960's, primarily by Hanson and Kaar and Kaar et al. The research performed on transfer length over the past 55 years was generally part of research focused on development length beginning with Janney whose 1954 publication focused on the bond between pretensioned wire used in concrete members. Janney concluded that bond failures were a result of inadequate embedment lengths causing high bond stresses in excess of the resistance provided by the concrete. Janny also stated that rusted wire tended to perform better than clean wire as the clean wire slipped at lower bond stresses (Janney 1954). Hanson and Kaar also noted that slightly rusted strand did have better bond characteristics (Hanson and Kaar 1959).

Hanson and Kaar performed flexural bond tests of pretensioned, prestressed beams containing seven-wire strand, with a primary objective focused on the determination of the maximum diameter of seven-wire strand that could be safely used in a flexural member. They attribute bond failures of flexural members to a progressive wave propagating towards the ends of the beams. If the wave reaches the transfer zone, the reduction in cross-sectional area of the strand reduces the frictional resistance to an extent precipitating general bond slip. The helical shape of the strand does provide additional resistance following general bond slip, allowing for further application of load.

However, if the bond stresses exceed the strength of the surrounding concrete, a complete bond failure will occur, and the strand will pull through the concrete. Based on the results of Hanson and Kaar, Equation (2-2) was developed only after modifications of Mattock's original recommendation shown as Equation (2-31) with units of ksi (Tabatabai and Dickson 1993).

$$L_d = \left(1.11 f_{su} - 0.77 f_{se}\right) d_b \qquad \text{Eq. (2-31)}$$

Zia and Mostafa revisited development length following work by Martin and Scott and Anderson and Anderson. Martin and Scott, who first recommended transfer length to be increased to $80d_b$, also recommended flexural bond lengths of $160d_b$ (Equation 2-32a), $187d_b$ (Equation 2-32b),, and $200d_b$ (Equation 2-32c), for ¼ in., ⅜ in., and ½ in. diameter strand, respectively, far exceeding values from the ACI provisions (Martin and Scott 1976). However, Anderson and Anderson found no significant differences in experimental results when compared to the ACI provisions (Anderson and Anderson 1976). Zia and Mostafa noted that when looking at the equation for flexural bond length, $L_{fb} = (f_{ps} - f_{se})d_b$, an assumed bond stress of 250 psi was used, while the actual value computed from Hanson and Kaar test data was 233 psi, which indicates the flexural bond length portion of Equation (2-2) to be slightly unconservative. Zia and Mostafa recommended the average bond stress used for calculation purposes to be 200 psi (Zia and Mostafa 1977). As a result of their recommendation, the flexural bond length portion of Equation (2-2) was increased by 25 percent, when coupled with transfer length recommendations results in Equation (2-33).

$$L_d = 1.5\frac{f_{si}}{f_{ci}'} d_b - 4.6 + 1.25\left(f_{ps} - f_{se}\right) d_b \qquad \text{Eq. (2-33)}$$

2.3.3 (1990 – 1999)

Discussed in Section 2.2, corrosion in prestressed bridge girders became an area of concern resulting in the development of epoxy-coated prestressing strand. Development lengths of standard reinforcing bars with epoxy-coating are known to increase and this is taken into account in Equation (2-1). The anticipated use of epoxy-coated strand provided a level of uncertainty related to the bond integrity of the strand leading to a study conducted on the transfer and development length of epoxy-coated

strand at North Carolina State University. Hanson and Kaar described a bond failure as an increase in stress progressing as a wave. Cousins et al. also mentions this progression, noting that "as the moment increases, the stress in the strand increases and proceeds towards the end of the transfer length as a wave." If the stress wave reaches the transfer zone prior to the development of the ultimate moment capacity, a general bond failure will occur.

Cousins et al. breaks the flexural bond length into a plastic and elastic zone as was the model for transfer length, but assumes the plastic zone over the entire length of the flexural bond length. Based on this assumption, an equation was derived from equilibrium for the flexural bond length, resulting in Equation (2-34) for the calculation of development length, with recommended values of 6.7, 300 psi/in., and 1.32 for U'_t, B, and U'_d, respectively for uncoated strands (Cousins et al. 1990b). The constants were based on experimental results and derived from calculated transfer and flexural bond lengths. Flexural bond lengths were taken as the embedment length minus the corresponding calculated transfer length for each test, while the final development length was taken as the shortest embedment length resulting in a flexural failure. Test results showed experimental development lengths for uncoated strands to exceed the provisions provided by ACI and AASHTO, while development lengths for coated strands were below values calculated by ACI and AASHTO provisions (Cousins et al. 1990a).

$$L_d = 0.5\left(\frac{U'_t\sqrt{f'_{ci}}}{B}\right) + \frac{f_{se}A_{ps}}{\pi d_b U'_t\sqrt{f'_{ci}}} + \left(f_{ps} - f_{se}\right)\left(\frac{A_{ps}/\pi d_b}{U'_d\sqrt{f'_c}}\right) \qquad \text{Eq. (2-34)}$$

In response to the work of Cousins et al., the FHWA issued a memorandum in 1988 with various restrictions on the use of prestressing steel. Those restrictions included the ban of 0.6 in. diameter strand for use in pretensioned, prestressed concrete girders, a minimum strand spacing of $4d_b$, all calculated development lengths be multiplied by 1.6, and where a strand is debonded at the end of a member, the development should be two times the calculated value (FHWA 1988). As a result of the FHWA Memorandum, a number or research projects were taken underway focusing on the transfer and development length of prestressing strand.

With the 1.6 multiplier for development lengths imposed by AASHTO, some questions arose as to its applicability to piles. An FDOT study investigated the effect of pile embedment on the development length of prestressing strand. The construction of pile supported structures generally includes the use of pile caps, resulting in an embedment of the pile into the pile cap over a distance of 12 in. Shahawy and Issa state that shrinkage of the pile cap creates a confining force along the embedded portion of the pile, in turn reducing the development lengths. The tests performed by FDOT showed a decrease in development length due to the confining force (Shahawy and Issa 1992). However, in a later review of the development length of prestressing strands, Buckner disagreed with the initial assumption for the presence of confining forces as a result of shrinkage. FDOT later submitted a revised version of the current development length equation to AASHTO Committee T-10, to no avail. Equation (2-35) is the development equation proposed by FDOT, where k_b is a dimensionless constant for type of structural member and μ_{ave} is an assumed bond stress of 250 psi (Buckner 1995).

$$L_d = \frac{\left[\frac{f_{si}}{3} d_b + \left(f_{ps} - f_{se}\right) d_b\right]}{\left(k_b \mu_{ave}\right)} \qquad \text{Eq. (2-35)}$$

Concurrent to the study by FDOT, Mitchell et al. was investigating the influence of high strength concrete on transfer and development lengths at McGill University. The investigation by Mitchell et al. looked at concrete strengths at the time of transfer from 3050 psi to 7250 psi and 4500 psi to 12,900 psi at the time of testing and strand diameters of ⅜ in., ½ in., and 0.62 in. With an increase in concrete strength, transfer lengths decreased, the effective prestress increased, and the development lengths decreased (Mitchell et al. 1993). Although, it should be noted, a gradual method of release was used, however, Mitchell et al. proposed a modified version of the ACI equation for the condition of gradual release as shown in Equation (2-36) taking into account the influence of concrete strength on transfer and development length.

$$L_d = 0.33 f_{pi} d_b \sqrt{\frac{3}{f_{ci}'}} + \left(f_{ps} - f_{se}\right) d_b \sqrt{\frac{4.5}{f_c'}} \qquad \text{Eq. (2-36)}$$

In addition to the influence of concrete strength and confinement, the effect of strand spacing was the focus of research projects by Cousins et al. and Deatherage et al.

Cousins et al. looked at test specimens with strand spacings of 1.75 and 2 in. coupled with both a normal and high strength concrete mix. Tested embedment lengths for specimens with normal strength concrete resulted in a range of development lengths between 114 and 126 in. for strand spacings of 1.75 and 2 in, while development lengths for test specimens with high strength concrete were found to be less than 108 in. It was concluded that reducing the spacing of ½ in. diameter prestressing strands from 2 in. to 1.75 in. did not significantly affect the development length, though an increase in concrete strength did result in a decrease in development lengths. For the test specimens containing normal strength concrete, the test results did show the development lengths to be approximately 60 to 70 percent larger than those predicted by ACI (Cousins et al. 1994).

Deatherage et al. evaluated the transfer lengths of four different strand diameters as well as the effect of reducing strand spacing from $4d_b$ to $3.5d_b$ for ½ in. diameter strands. Results showed the flexural bond length of prestressing strand to be underestimated by the ACI and AASHTO equations by approximately 42 percent (Deatherage et al. 1994). It was recommended that the development length equation be modified as shown in Equation (2-37) including transfer length modifications as previously discussed and a 50 percent increase in the flexural bond length, later discounted by Buckner, due to erroneously large values of effective prestress. In agreement with the results of Cousins et al., a reduction in strand spacing did not significantly affect development lengths.

$$L_d = \left(\frac{f_{si}}{3} \right) d_b + 1.50 \left(f_{ps} - f_{se} \right) d_b \qquad \text{Eq. (2-37)}$$

As the main focus of a FHWA report, Buckner reviewed the research subsequent to the 1988 FHWA Memorandum pertaining to the development length of prestressing strand. In the review, an effort was made to resolve discrepancies among the recommendations from various studies. The report states that experimental results from most test programs showed lower bond strengths with an increase in strand strain. In test specimens with strand strains near the yield strain (0.010 in./in.), typical test results showed the ACI/AASHTO equation to adequately predict the development lengths, while test specimens having larger strand strains at failure (0.027 – 0.036 in./in.) experienced

strand slippage with embedment lengths as large as 1.7 times the ACI/AASHTO predicted values and in some cases failed to reach their expected moment capacities when tested at shorter embedment lengths. Thus, Buckner recommended that the development length be dependent on the level of strain in the strand at the time of failure. Coupled with the prior recommendations for transfer length, Buckner proposed a modification factor for the flexural bond length, taking the strain into consideration. Equation (2-38) shows the recommended equation for development length, where $\lambda = (0.6 + 40\varepsilon_{ps})$ (Buckner 1995). Lane also recommended Equation (2-39) from research completed at the FHWA (Lane 1998).

$$L_d = \left(\frac{f_{si}}{3}\right) d_b + \lambda\left(f_{ps} - f_{se}\right) d_b \qquad \text{Eq. (2-38)}$$

$$L_d = \frac{4 f_{pt}}{f_c'} d_b - 5 + \frac{6.4\left(f_{ps} - f_{se}\right) d_b}{f_c'} + 15 \qquad \text{Eq. (2-39)}$$

2.3.4 (2000 – 2009)

The studies following the 1988 FHWA Memorandum concentrated on the transfer and development length of prestressing strand, looking at various strand diameters, concrete strengths, and spacings. Results showed development lengths to increase with increasing strand diameter and to decrease with increasing concrete strength, while reduced spacings showed no significant effect on development lengths. Deatherage et al. (1994) did note that development lengths of 0.6 in. diameter strand failed to follow the trend of increasing development lengths with increasing strand diameters. Amongst the previous studies, the primary focus was never given to the 0.6 in. diameter strand, although the FHWA placed a moratorium on its use in the 1988 Memorandum.

Kose and Burkett later studied the behavior of 0.6 in. diameter strand, concluding that transfer and development lengths actually decreased with an increase in strand diameter. They also noted that transfer and development lengths decreased with increasing concrete strength. It should be noted that only ½ in. and 0.6 in. diameter strands were used in the study. Kose and Burkett showed no decrease in flexural bond lengths as concrete strengths increased; however, previous studies have shown flexural bond lengths to decrease. The development length was taken as the shortest embedment

length resulting in a flexural failure. Each flexural bond length was then determined by subtracting the average transfer length. In addition to the data obtained by test specimens of the study, additional test data were used from previous studies from the FHWA, Florida A&M/Florida State, Auburn University, University of Texas at Austin, and the University of Tennessee at Knoxville. As the primary objective, Equation (2-40) was derived from a linear regression model, for use with 270 ksi low-relaxation strand, with diameters ranging from ½ to 0.6 in. and concrete strengths ranging from 4000 to 14,000 psi. It was also assumed that initial prestress was taken as 75 percent of the ultimate tensile strength of the strand (Kose and Burkett 2005).

$$L_d = \left[95 \frac{f_{pi}\left(1 - d_b\right)^2}{\sqrt{f_c'}} \right] + \left[8 + 400 \frac{\left(f_{pu} - f_{pi}\right)\left(1 - d_b\right)^2}{\sqrt{f_c'}} \right] \qquad \text{Eq. (2-40)}$$

In a recent NCHRP study, as with transfer length, the results indicated concrete strength to be very influential on the determination of development length. As a result of the experimental testing, Equation (2-41) was proposed for the calculation of development length, accounting only for strand diameter and concrete strength. Based on the current AASHTO provisions, development length is approximately equal to $150d_b$. In the NCHRP study, the researchers assume transfer lengths equal to $60d_b$, which would correspond to a flexural bond length of $90d_b$. Assuming a concrete strength of 6,000 psi, the flexural bond length portion of Equation (2-41) reduces to $90d_b$. As with transfer length, an increase in concrete strength also results in a decrease in flexural bond length, however, a lower limit of $60d_b$ is placed on the flexural bond length, which corresponds to a concrete strength of 14,000 psi. As a result of the minimum allowable values for transfer and flexural bond lengths, the lower limit for development length is specified to be $100d_b$ (NCHRP 2008).

$$L_d = \left[\frac{120}{\sqrt{f_{ci}'}} + \frac{225}{\sqrt{f_c'}} \right] d_b \geq 100 d_b \qquad \text{Eq. (2-41)}$$

2.3.5 Summary

The development length of prestressing strand is a vital factor in the behavior of pretensioned, prestressed concrete. As with transfer length, research from the past five

decades has shown development lengths to be more complex than initially thought. The current ACI/AASHTO provisions only show development length to be dependent on strand stress at various times and the diameter of the strand. In some situations, the research discussed herein has shown development lengths to far exceed the predicted values. In response to inadequate predictions, multiple researchers have proposed new development length equations taking into account, concrete strength, strand diameter, stress level in the strand, strand strain at the time of failure, and type of structural member. Of the equations, summarized in Table 2.3, discrepancies exist among a number of them. Based on the evidence of conducted research, it is apparent the existing provisions for development length set forth by ACI and AASHTO are inadequate for a number of situations, requiring additional research and the development of more consistent equations.

Table 2.3. Historical Development Length Equations

Contributor	Year	Equation	Eq. No.
Hanson & Kaar	1959	$L_d = (1.11 f_{su} - 0.77 f_{se}) d_b$	2-31
ACI	1963	$L_d = \left(\frac{f_{se}}{3000}\right) d_b + \left(\frac{f_{ps} - f_{se}}{1000}\right) d_b$	2-2
Martin & Scott	1976	$L_t = 160 d_b$ for ¼ in. dia. strand $L_t = 187 d_b$ for ⅜ in. dia. strand $L_t = 200 d_b$ for ½ in. dia. strand	2-32a 2-32b 2-32c
Zia & Mostafa	1977	$L_d = 1.5 \frac{f_{si}}{f_{ci}^{'}} d_b - 4.6 + 1.25(f_{ps} - f_{se}) d_b$	2-33
Cousins et al.	1990	$L_d = 0.5\left(\frac{U_t^{'}\sqrt{f_{ci}^{'}}}{B}\right) + \frac{f_{se} A_{ps}}{\pi d_b U_t^{'}\sqrt{f_{ci}^{'}}} + (f_{ps} - f_{se})\left(\frac{A_{ps}/\pi d_b}{U_d^{'}\sqrt{f_c^{'}}}\right)$	2-34
Shahawy et al.	1992	$L_d = \frac{\left[\frac{f_{si}}{3} d_b + (f_{ps} - f_{se}) d_b\right]}{(k_b \mu_{ave})}$	2-35
Mitchell et al.	1993	$L_d = 0.33 f_{pi} d_b \sqrt{\frac{3}{f_{ci}^{'}}} + (f_{ps} - f_{se}) d_b \sqrt{\frac{4.5}{f_c^{'}}}$	2-36
Deatherage et al.	1994	$L_d = \left(\frac{f_{si}}{3}\right) d_b + 1.50(f_{ps} - f_{se}) d_b$	2-37
Buckner	1995	$L_d = \left(\frac{f_{si}}{3}\right) d_b + \lambda(f_{ps} - f_{se}) d_b$	2-38
Lane	1998	$L_d = \frac{4 f_{pt}}{f_c^{'}} d_b - 5 + \frac{6.4(f_{ps} - f_{se}) d_b}{f_c^{'}} + 15$	2-39
Kose & Burkett	2005	$L_d = \left[95 \frac{f_{pi}(1 - d_b)^2}{\sqrt{f_c^{'}}}\right] + \left[8 + 400 \frac{(f_{pu} - f_{pi})(1 - d_b)^2}{\sqrt{f_c^{'}}}\right]$	2-40
NCHRP	2008	$L_d = \left[\frac{120}{\sqrt{f_{ci}^{'}}} + \frac{225}{\sqrt{f_c^{'}}}\right] d_b \geq 100 d_b$	2-41

2.4 Bond Characteristics and Influential Factors

2.4.1 Introduction

The bond between prestressing steel and the surrounding concrete is the most significant component of pretensioned, prestressed concrete. Without the bond between the prestressing steel and surrounding concrete, pretensioned, prestressed concrete would not be feasible. In the calculation of the development length for standard reinforcing bars, the influence of cover and confining reinforcement, as-cast vertical location, coating, bar size, and effects of using lightweight concrete are taken into consideration. On the contrary, in the calculation of the development length (transfer and flexural bond lengths) for prestressing strand, only the stress in the strand and the strand diameter are taken into account, neglecting the effect of cover and confinement, as-cast vertical location, coating of the strand (i.e. rust or epoxy), effects of lightweight concrete, strength of the concrete, the type of prestress release, and the fluidity of the concrete mix. Over the past five decades, research has shown a number if not all of these factors to significantly effect the transfer and development length of prestressing strand.

The bond between the concrete and the prestressing strand is made up of three components, briefly discussed in previous sections. Janney first noted the factors contributing to bond to be the adhesion between the steel and concrete, friction between the steel and concrete, and the mechanical resistance of the deformations of the steel. With the transfer process, the adhesion is lost, which can only be present if no slip has occurred. If there was no slip between the concrete and steel, the reduction in steel strain would be equal to the increase in concrete strain within a member (Janney 1954). Hanson and Kaar later noted that seven-wire strand can further contribute to the mechanical bond allowing for additional strength of a flexural member after general bond slip has occurred (Hanson and Kaar 1959).

Section R12.9 of the ACI Commentary states the following:

> "The bond of strand is a function of a number of factors, including the configuration and surface condition of the steel, the stress in the steel, the depth of concrete beneath the strand, and the method used to transfer the force in the strand to the concrete. For bonded applications, quality assurance procedures should be used to confirm that the strand is capable of adequate bond. The precast concrete

manufacturer may rely on certification from the strand manufacturer that the strand has bond characteristics that comply with this section. Strand with a slightly rusted surface can have an appreciably shorter transfer length than clean strand. Gentle release of the strand will permit a shorter transfer length than abruptly cutting the strands (ACI 2008)."

2.4.2 Strand Stress

The transfer and development lengths have been shown to increase with an increase in strand stress. Janney first noted this increase in a study investigating a high strength strand (270 ksi) with respect to the conventional strand (250 ksi), stating that transfer length was greater by a small amount because of the high strength strand, but was thought to be an insignificant increase (Janney 1954). Cousins et al. later found an increase in strand stress to significantly increase transfer and development lengths well beyond the values predicted by the ACI/AASHTO provisions, with initial strand stresses up to 80 percent of the ultimate tensile strength of the strands (Cousins et al. 1990c). Studies by Shahawy et al. (1992) and Russell and Burns (1997) also indicated longer transfer lengths for larger values of strand stress, shown in the proposed equations, Equation (2-9) and Equation (2-14). More recent studies also recognize there to be a general agreement that strand stress does have a significant effect on transfer and development lengths, with proposed equation modifications consistently recommending the use of the initial prestress in lieu of the effective prestress used in the current ACI/AASHTO provisions.

2.4.3 Strand Diameter

The diameter of the strand has also been shown to be an influential factor on transfer and development lengths with a general consensus that transfer and development length increase with an increase in strand diameter. Early research by Hanson and Kaar (1959) showed increasing transfer lengths for increasing strand diameters up to ½ in. Zia and Mostafa (1977) showed development length to increase with increasing strand diameter, again for up to ½ in. diameter strands. Resulting from work by Cousins et al., 0.6 in. diameter strands were found to have excessive transfer and development lengths (Cousins et al. 1990b). In response to the findings, the FHWA placed a ban on the use of 0.6 in. diameter strands in the 1988 FHWA Memorandum. Further investigations later

coincided with the previous results, showing transfer and development length to increase with increasing strand diameter including 0.6 in. diameter strands. Contrary to the general agreement of increasing transfer and development lengths with increases in strand diameter, Deatherage et al. and Kose and Burkett found the transfer and development lengths to decrease for 0.6 in. diameter strands. Deatherage et al. found the historical trend to hold true up through strand diameters of $^{9}/_{16}$ in., but stated that the relationship did not hold true for 0.6 in. diameter strands (Deatherage et al. 1994). In the development of Equation (2-17), Kose and Burkett noticed a general trend showing transfer length to decrease as strand diameters ranged from ½ in. to 0.6 in. (Kose and Burkett 2005). Therefore, there is some disagreement as to the relationship between transfer and development lengths and strand diameters.

2.4.4 Spacing, Cover, and Confinement

The influence of spacing, cover, and confinement of prestressing strands has been the focus of numerous studies. During the transfer process and flexural testing, it is assumed there is a sufficient amount of concrete surrounding the strand to develop the bond between the strand and concrete. In situations where there is not adequate coverage, bond failures may occur as a result of splitting. Most precast manufacturers use a center-to-center spacing of 2 in., which is generally preferred. This spacing is based on the recommended values for strand spacing of $4d_b$ for ½ in. diameter strands. Research has proven a 1.75 in. and 2 in. spacing to be adequate for use with ½ in. and 0.6 in. diameter strands, respectively.

Cousins et al. looked at the influence of strand spacing and cover for epoxy-coated strand. Results of the study showed epoxy-coated strand to cause significant cracking at spacings and covers less than those recommended by ACI, while subsequent studies by Cousins et al. (1993) and Deatherage et al. (1994) found decreases in strand spacings to 1.75 in. had no significant effect on transfer and development length of ½ in. diameter, uncoated prestressing strand. One study, however, did show transfer lengths to increase with a reduction in bottom cover (Oh and Kim 2000). Zia and Mostafa noted that standard reinforcing bars were used to resist bursting in the end regions of test specimens, slightly reducing the transfer length, but not to a significant degree. Shahawy et al. (1992) looked at the influence of confinement on development lengths, showing a

significant decrease in development length with an applied confinement, later discounted by Buckner due to an unrealistic test situation. As research has shown, smaller spacings and small amounts of cover can result in bond issues, although the majority of these issues were at extreme limits or occurred with epoxy-coated strands due to excessive bond stresses. As the industry standard, a 2 in. spacing seems to be sufficient for all strand diameters up to 0.6 in. and does not appear to significantly influence transfer and development lengths of uncoated strands.

2.4.5 Top-bar Effect

Since the acknowledgement of the top-bar effect in the 1951 ACI Building Code, the development length of standard reinforcing bars have been multiplied by a factor when a horizontal bar is placed where there is more than 12 in. of concrete cast beneath it. Conversely, there currently are no provisions for prestressing strands with the same situation, although in the ACI commentary as previously stated, says that the bond of strand is a function of the depth of concrete beneath the strand. Traditionally, the top-bar effect has been accepted as the aforementioned definition, but recent research has resulted in questions surrounding the actual definition of the top-bar effect.

Research has shown top-cast bars to have less favorable bond characteristics than bottom-cast bars. A study by Jeanty et al. concluded that, in pairs of test specimens, one containing bottom-cast bars and the other containing top-cast bars, the development length of top-cast bars were approximately 20 percent larger than those of bottom-cast bars (Jeanty et al. 1988). In addition to research focused on standard reinforcement, the top-bar effect has also been seen in prestressed concrete applications, referred to as the top-strand effect, most notably in prestressed piles. As a result of excessive end-slip measurements found in prestressed concrete piles by the South Carolina Department of Transportation (SCDOT), a research project was launched to investigate the top-strand effect in prestressed concrete piles. Research by Petrou et al. (2000b) and Wan et al. (2002a) showed excessive strand end-slip measurements in both the top-cast and bottom-cast strands of prestressed concrete piles, with the top-cast strands exhibiting much higher end-slips than the bottom-cast strands. Although ACI and AASHTO define a top-cast bar as a horizontal bar with more than 12 in. of fresh concrete cast beneath it, Petrou et al. summarizes the top-strand definition defined by the EUROCODE, which refers to a

top-cast bar as one cast near the top as-cast surface of the member. Subsequent to the research by Petrou et al. and Wan et al., a study by Peterman (2007) revealed that the top-strand effect may in fact be dependent on the amount of concrete above the strand and not the amount of concrete beneath it. With this discovery comes a number of questions regarding the true definition of the top-strand effect, which is discussed in more detail in Section 2.6.

2.4.6 Surface Condition

The surface condition of the strand can highly influence the frictional component of the bond between the prestressing strand and surrounding concrete, increasing or decreasing the transfer and development length, depending on the level of friction between the strand and surrounding concrete. Strands are typically delivered in a "bright" condition, indicating the absence of rust, while an exposure to weather, may result in a slight rusting of the strand. As previously mentioned, corrosion became a concern in the bridge industry, resulting in the development of an epoxy-coated strand. Epoxy-coated rebar have been shown to have longer development lengths than uncoated rebar, resulting in the application of a modification factor. With the history of decreased bond in epoxy-coated rebar, an investigation was conducted with the surface condition of the strand as the primary variable.

Janney first noticed an improved bond behavior in rusted wire with respect to clean wire in a 1954 publication and later noted a significant decrease in transfer length of rusted strands (Janney 1954) (Janney 1963). Hanson and Kaar also noted improved bond characteristics resulting in an average increase in the moment at general bond slip of 30 percent (Hanson and Kaar 1959). Several other researchers recognized the increased bond characteristics from slightly rusted strand, although one study did show transfer lengths to greatly increase for strands with excessive rust located at the cut end of a test specimen. In an investigation of the bond characteristics of epoxy-coated strand, Cousins et al. found epoxy-coated strand without impregnated grit to have virtually no bond. However, as the density of impregnated grit increased, the transfer and development lengths decreased, having much more favorable bond characteristics than uncoated strand (Cousins et al. 1990b). In a later study, epoxy-coated strands were again observed to have smaller transfer lengths than uncoated strands (Cousins et al. 1993).

The bond between prestressing steel and surrounding concrete can be strongly influenced by the surface condition of the strand. The worst case can be assumed to be a clean, bright strand free of rust, excluding an epoxy-coated strand without impregnated grit. Rusted strand has been shown to have better bonding capabilities than clean, bright strand, but the level of rust would be difficult to measure and carelessly allowing strand to rust is strongly discouraged. Therefore, it is not recommended that the rusting of strands be taken into consideration for the calculation of transfer and development lengths. On the other hand, epoxy-coated strands with impregnated grit do have the potential for a reduction in transfer and development length, but should be investigated in more detail before any modification factors can be developed.

2.4.7 Concrete Strength

The compressive strength of the concrete is not included in the current ACI and AASHTO provisions for transfer and development length, while it may be one of the most influential factors. Research has shown a steady trend for transfer and development lengths to decrease with an increase in concrete strength. Kaar et al. (1963) claimed concrete strength to have little effect on transfer lengths for strand of up to ½ in. diameter, but it should be noted that concrete strengths were no higher than 5000 psi. Contrary to the results by Kaar et al., Zia and Mostafa proposed a transfer and development length equation incorporating concrete strength, reflecting a decrease in transfer length with increasing concrete strengths (Zia and Mostafa 1977). In later investigations, the influence of high strength concrete on transfer and development length of prestressing strand was studied. Concrete strengths ranged from 3050 to 7250 psi in one study resulting in a decrease in transfer length with increasing concrete strengths (Mitchell et al. 1993). In a second study, a 5300 psi mix and 8000 psi mix at transfer resulted in average transfer lengths of 56 and 37 in., respectively (Cousins et al. 1994). Additional studies by Oh and Kim (2000), Petrou et al. (2000b), and Wan et al. (2002b) also note concrete strength as a very influential factor, stating that excessive end-slip measurements of top-strands in piles could be a result of lower concrete strength in the top portion of the cross-section. In a more recent study, little correlation was found with relationships that omitted concrete strength in their development (Barnes et al. 2003).

Kose and Burkett also found transfer lengths to decrease with an increase in concrete strength (Kose and Burkett 2005).

Research has consistently shown concrete strength to significantly influence transfer and development lengths. Early work by Hanson and Kaar, from which the current ACI/AASHTO provisions are based, only considered concrete strengths up to 5000 psi, showing no significant impact (Hanson and Kaar 1959). The current ACI/AASHTO provisions fail to consider the concrete strength in calculations of transfer and development lengths, although numerous researchers have proposed equations doing so. Based on previous research, there is a clear indication that the influence of concrete strength should be taken into consideration with respect to bond.

2.4.8 Release Method

The force in the strands is transferred to the concrete using either a gradual or sudden release. ACI states that a gentle release will permit a shorter transfer length than abruptly cutting the strands. Although a gradual release does usually result in shorter transfer lengths, a sudden release has, for the most part, become the industry standard among precast manufacturers. Is it generally accepted that transfer lengths adjacent to the cut end are longer than transfer lengths adjacent to the dead end, and this conclusion is consistently supported by research.

Kaar et al. was the first to recognize an increase in transfer lengths adjacent to the cut end of test specimens, noting a 20 to 30 percent increase with respect to the dead end values (Kaar et al. 1963). Zia and Mostafa derived transfer length equations for both sudden and gradual prestress release, selecting only the equation for sudden release for a conservative estimate (Zia and Mostafa 1977). In subsequent studies, Cousins et al. (1994) found transfer lengths for ½ in. 270 ksi, low-relaxation strands to be 38 and 31 in. at the cut and dead ends, respectively, while Russell and Burns (1997) found similar results, 38.5 in. at the cut end and 28.7 in. at the dead end. Oh and Kim later found similar increases (Oh and Kim 2000).

Various researchers have proposed modified transfer length equations from tests having a gradual release as well as a sudden release, while proposed equations from tests using a gradual release may be unconservative for transfer lengths adjacent to cut ends. Two such equations are Equation (2-2), the current ACI transfer length equation, and

Equation (2-10) proposed by Mitchell et al. Taking into consideration the type of prestress release can be beneficial in the calculation of shear resistance in a flexural member, but for conservatism, as with the coating of the strand, it is recommended that all transfer length calculations assume a sudden release.

2.4.9 Additional Factors

In addition to the strand stress, diameter, spacing, cover and confinement, as-cast vertical location, coating, strength of concrete, and type of release, a number of other factors have been shown to influence transfer and development lengths. These additional factors include the effects of lightweight concrete, fluidity of the mix, admixtures, time effects, and cross-section size. The use of lightweight concrete has been shown to have a negative effect on bond as does an increased fluidity of the mix, typically in self consolidating concrete (SCC) (Peterman 2007). The influence of admixtures, such as retarder and superplasticizer, on transfer and development length are of interest, but are beyond the scope of this project. Transfer lengths have been shown by a number of researchers to increase with time, and Russell and Burns (1997) concluded transfer and development lengths are also dependent on the size of the cross-section.

2.4.10 Summary

Upon reviewing the literature to date with respect to bond, it is apparent there are multiple factors affecting bond in addition to the stress in the strand and strand diameter used in the ACI/AASHTO provisions. Typical spacing and cover requirements have been shown to be satisfactory to obtain adequate bond, while confinement has been shown to have little effect on transfer and development lengths. Unless coated with an epoxy containing impregnated grit, assuming the strand coating to benefit the bond of the strand may be unconservative. In addition, relying on a method of gradual release may also result in an unconservative estimate of transfer and development lengths. Therefore, the effects of spacing, cover, and confinement are assumed to be constant based on industry standards and any consideration of coating and gradual method of release will be neglected in the development of any equations for transfer and development length. The factors shown by previous research to most significantly influence the transfer and development lengths are the stress in the strand, the diameter of the strand, the strength of the concrete, and the as-cast vertical location of the strand.

2.5 Bond Quality

In order to ensure the bond characteristics of the prestressing strand, ACI requires quality assurance procedures to confirm the ability of the strand to obtain adequate bond. In the mid 1990's, a testing program by Rose and Russell evaluated simple bond tests finding little correlation with measured transfer lengths. During the same time period, three tests had originated: the PTI Bond Test, the Moustafa Test, and the North American Strand Producers (NASP) Bond test. It was found that the Moustafa and NASP test showed the best correlation as a measure of bond quality for prestressing strand related to measured transfer length (Ramirez and Russell 2007). Two of those tests for evaluating bond characteristics of prestressing strand are currently under consideration for adoption as standard test methods. These two tests are the Large Block Pullout Test (LBPT), formerly referred to as the Moustafa Pullout Test, and the NASP Test, each of which were used to verify the bond characteristics of each strand type used in the T-beam test specimens of this study (Ramirez and Russell 2007). The LBPT consists of 24 in. deep concrete blocks with a length and width dependent upon the number of strands in each block. Strands are placed in each block with a grid pattern of 12 in. by 8 in., with the 8 in. spacing throughout the longer dimension of the block as shown in Figure 2.6. Each strand used in the test extends 48 in. above the top surface of the block and 20 in. below the top surface of the block with the top 2 in. of embedded strand debonded, resulting in an embedment length of 18 in.

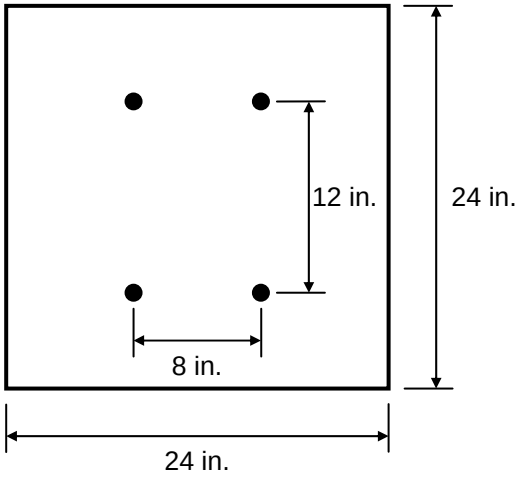

Figure 2.6. LBPT Strand Pattern (Loflin 2008)

Subsequent to adequate concrete strength development, typically ranging from 3500 to 5000 psi, each strand is loaded individually in tension using a hollow hydraulic ram at a load rate of 20 kips per minute until failure (Mote 2001). In addition to those used by Mote, similar test methods were used by Logan (1997) and Rose and Russell (1997). It is recommended that the minimum pullout force be 36 kips for a ½ in. diameter regular strand ensuring adequate bond characteristics for transfer and development lengths. Should the strand size increase, the minimum pullout force should also be increased by a factor equal to the ratio of the larger area to that of a ½ in. diameter regular strand, resulting in minimum pullout forces of 39 kips and 51 kips for a ½ in. diameter super strand and 0.6 in. diameter strand, respectively (Logan 1997).

The NASP Test consists of a 5 in. diameter steel pipe, 18 in. long with a ½ in. thick steel plate welded to one end used as a bearing surface. Each pipe contains a single concentrically placed prestressing strand placed throughout the entire length of the pipe, protruding approximately 20 in. through a ⅝ in. diameter hole located in the center of the bearing plate. As with the LBPT, the strand is debonded along the bottom 2 in. within the pipe (Loflin 2008). Figure 2.7 shows a typical NASP Test specimen.

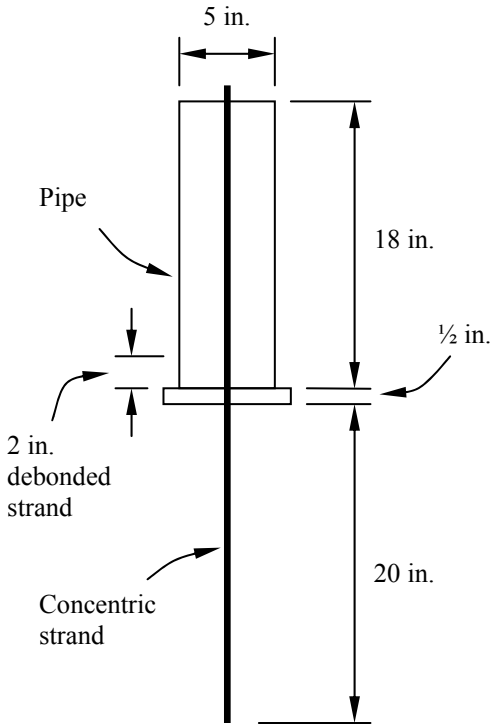

Figure 2.7. NASP Test Specimen (Loflin 2008)

The NASP Test uses a mortar consisting of Type III cement, sand, and water. At the time of casting, the mortar is required to have a flow between 100 and 125, while the strength is required to be between 4500 and 5000 psi at 24 hours (Ramirez and Russell 2007). The flow and strength limitations were selected to ensure consistent material properties in an attempt to provide uniformity across a spectrum of tests.

At approximately 24 hours each pipe was tested by loading the protruding strand in tension at a load rate of 7500 lbs per minute until failure. Failures being defined as the inability to carry any additional load or an end-slip value exceeding 1.5 in., with a minimum required average pullout force prior to 0.1 in. slip for a ½ in. diameter regular strand of 10.5 kips and a minimum pullout force of 9.0 kips for an individual test. As with the LBPT, these values were also increased by a factor equal to the ratio of the larger area to that of a ½ in. diameter regular strand for increased strand size. This increase resulted in an average minimum pullout force of 11.5 kips and 12.6 kips for a ½ in. diameter super and 0.6 in. strand, respectively, and a minimum pullout force for an individual test of 9.8 kips and 10.8 kips for a ½ in. diameter super and 0.6 in. diameter strand, respectively (Loflin 2008).

Both LBPT's and NASP tests were performed on each strand type used in the T-beam test specimens. The strand types investigated included Grade 270 and Grade 300 ½ in. diameter regular, Grade 270 and Grade 300 ½ in. diameter super, and Grade 270 0.6 in. diameter strands from Producer A, as well as Grade 270 ½ in. diameter super from Producer A2. LBPT specimens for each strand type were cast individually in groups of four strands in a single 24 in. cube as shown in Figure 2.8. All strands from Producer A performed with satisfactory results, each exceeding the minimum values as previously discussed, however, the ½ in. diameter super strand from Producer A2 fell slightly below the minimum required average pullout force of 39 kips. Table 2.4 lists a summary of the results for all strand types used in the LBPT's (Loflin 2008).

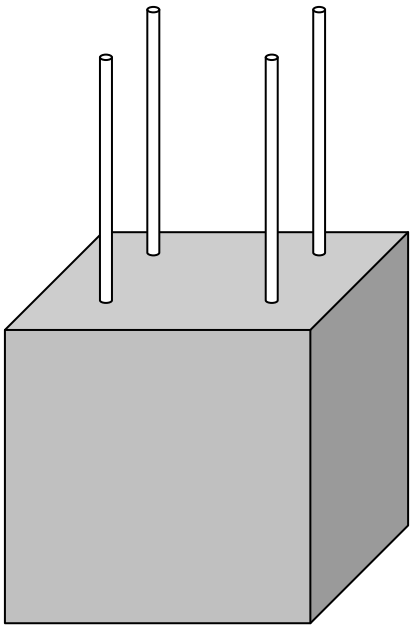

Figure 2.8. LBPT Specimen

Table 2.4 Summary of LBPT Results (Loflin 2008)

Strand Type	Average Maximum Load (kips)	Standard Deviation of Maximum Load (kips)	Concrete Strength (psi)	Minimum Required Load (kips)	Ratio of Average Maximum to Minimum Required Load
½ in. regular GR 270 A	42.1	0.58	8100	36	1.17
½ in. regular GR 300 A	43.5	2.66	6400	36	1.21
½ in. regular GR 300 A	46.2	3.46	8100	36	1.28
½ in. super GR 270 A	43.5	3.18	8100	39	1.11
½ in. super GR 270 A2	38.8	2.72	8100	39	0.99
½ in. super GR 300 A	49.4	1.63	8100	39	1.27
0.6 in. GR 270 A	55.4	2.81	6400	51	1.09

NASP test specimens were also cast for each strand type to investigate the bond characteristics of each. Six test specimens were cast for each strand type for a total of 36. As with the LBPT's, all strand types from Producer A satisfied the specified minimum required values for adequate bond, however, the average pullout force for the Grade 270 ½ in. diameter super strand from Producer A2 fell slightly below the minimum required value of 11.5 kips. Table 2.5 shows a summary of the NASP test results (Loflin 2008).

Table 2.5. Summary of NASP Test Results (Loflin 2008)

Strand	Average NASP Value (kips)	Grout Strength (psi)	Normalized NASP Value (kips)	Required NASP Value (kips)	Ratio of Normalized to Required Value
½ in. regular GR 270 A	14.6	4500	14.6	10.5	1.39
½ in. regular GR 300 A	12.5	4300	12.7	10.5	1.21
½ in. super GR 270 A	14.0	4400	14.2	11.5	1.23
½ in. super GR 270 A2	10.0	4000	10.6	11.5	0.92
½ in. super GR 300 A	14.6	4500	14.6	11.5	1.27
0.6 in. GR 270 A	16.6	4300	16.9	12.6	1.34

2.6 Top-strand Effect

As previously discussed, the as-cast vertical location of standard reinforcing bars has been shown by numerous researchers to influence development length. Known as the top-bar effect, it is generally understood that a larger amount of concrete cast below a horizontal bar will increase this effect. The top-bar effect is attributed to a decrease in concrete strength due to the upward migration of water toward the top of a specimen during the curing process and the effect of aggregate settlement underneath a horizontally cast bar, allowing lighter elements, such as cement, water, and entrapped air to rise to the top of the specimen. Settlement of the concrete is also thought to occur underneath the top-bars as a result of aggregate settlement. However, research has shown aggregate settlement to only occur under vibration, as the aggregate does not sink in typical concrete mixtures (Petrou et al. 2000a).

A top-bar is defined by ACI as a horizontal bar cast with more than 12 in. of fresh concrete beneath the bar (Jeanty et al. 1988). On the contrary, the EUROCODE (1992-1-1) defines a top-bar as a bar in the top half of a member with a thickness of more than 10 in. or within the top 12 in. of a member more than 24 in. in depth. The top-bar effect has been recognized since 1913 with modification factors first implemented in the 1951 ACI Building Code based on research by Clark (1946). For bond applications, the 1951 Code used allowable bond stresses, with a 0.7 modification factor applied to the allowable bond stress of top-cast bars. In the 1971 ACI Building Code, the allowable stress calculations were replaced by a development length equation. In addition to the development length equation, the top-bar modification factor was modified to be 1.4, resulting in a 40 percent increase in development length, analogous to the 30 percent reduction in bond strength from the 0.7 modification factor.

In the 1989 ACI Building Code , the modification factor was again revised, reducing from 1.4 to 1.3 based on research by Jirsa and Breen (1981) and Jeanty et al. (1988), while AASHTO retained the 1.4 modification factor for use in its designs. Jirsa and Breen recommended development length modification factors vary with concrete slump, while Jeanty et al. (1988) simply recommended a top-bar factor of 1.20 based on research performed on test specimens as shown in Figure 2.9. They also noted that the top-cast specimens displayed flexural cracking at lower loads than the counterpart bottom-cast specimens, indicating a reduction in concrete strength at the top of the casting.

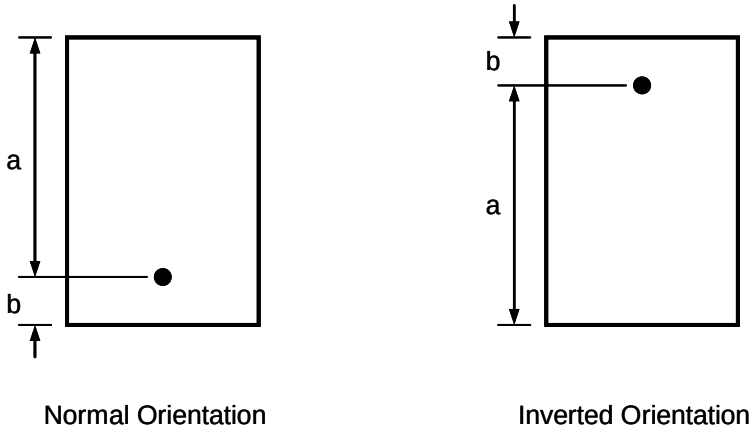

Figure 2.9. Jeanty et al. General Test Specimen Orientation

The current ACI provisions only consider the top-bar effect in the development length calculations for standard reinforcing steel, although the top-bar effect has been shown to exist in prestressed applications as well. In a review of development length research by the FHWA, Buckner noted that the top-bar effect, referred to as the top-strand effect in prestressed concrete, could influence the development length of prestressing strand. Buckner further recommends that development lengths of strands cast with more than 12 in. of concrete beneath them be increased by a factor of 1.3 similar to the current provisions for the development length of standard reinforcing bars (Buckner 1995).

In the late 1990's the South Carolina Department of Transportation (SCDOT) reported excessive strand end-slip values in prestressed concrete piles, with top-strands slipping as much as 1.5 in., significantly greater than estimated values of 0.1 in. In response to the SCDOT discovery, a research project on prestressed concrete piles was

undertaken, investigating the top-strand effect in prestressed concrete piles. The ratios of top-strand end-slip measurements to bottom-strand end-slip measurements in 24 in. prestressed concrete piles ranged between 1.15 and 5.15 with an average ratio of 2.12. The influence of concrete strength was one factor thought to contribute to the excessive end-slip measurements as concrete strength in the top portion of members is thought to be reduced as a result of aggregate settlement during vibration. It was recommended that the 1.3 modification factor used for the development length of standard reinforcing bars also be applied to prestressing strand considered as top-strands (Petrou et al. 2000b).

Subsequent research showed similar trends, resulting in an average top-strand end-slip of 0.140 in. and an average bottom-strand end-slip of 0.058 in., much less than previously reported values, but still in excess of typical accepted values. Ratios of end-slip measurements between top and bottom strands ranged from 1.17 to 3.36, verifying the presence of the top-strand effect (Wan et al. 2002a). In a later paper, the presence of retarder and confining reinforcement were mentioned as influential factors on top-strand effect. The use of spiral reinforcement may prevent adequate consolidation of the concrete around the top-strands (Wan et al. 2002b). In addition to the work on prestressed concrete piles, recent work by Larson et al. (2007) has shown transfer and development lengths in beams to increase for strands with more than 12 in. of fresh concrete cast beneath them.

For decades, the top-bar effect has been understood to be solely dependent on the amount of concrete cast beneath the bar. Research has shown the phenomenon to regularly occur in reinforced concrete (top-bar effect) and within the past ten years, has appeared to significantly impact the transfer and development length of prestressing strand (top-strand effect). A recent study has shown the top-strand effect to be more dependent on the amount of concrete cast above the strand rather than the amount of concrete cast below the strand, which has brought about concern regarding the historical definition of the top-bar/top-strand effect (Peterman 2007). Peterman investigated "The Effects of As-Cast Depth and Concrete Fluidity on Strand Bond" looking at the effects of vertical strand location and the use of high fluidity mixes, namely SCC, have on the transfer and development length of prestressing strand.

In order to investigate the effect of vertical casting position on transfer length, Peterman conducted a series of tests on rectangular blocks as shown in Figure 2.10. The test specimens allowed for a head-to-head comparison of the effect the amount of concrete cast above and below the strand had on transfer length. Both blocks were 12 ft in length and were 4 in. wide, containing no confining reinforcement. Block A was 28 in. tall, while Block B was only 16 in. tall. Using this type of test setup, the transfer lengths of the bottom three strands in Block A could be compared to the three strands in Block B, looking at the strands with the same amount of concrete cast below. In addition, the test setup also allowed for the comparison of the transfer lengths of the top three strands in Block A to the three strands in Block B, looking at strands with the same amount of concrete cast above. Results showed strands with the same amount of concrete cast above to have a better correlation than strands with the same amount of concrete cast below. In conclusion, Peterman recommended Equation (2-18) calculating the average transfer length, taking into consideration the distance from the as-cast top surface. Concurring with previous research, Peterman found transfer lengths in strands located in the top portion of test specimens to far exceed the provisions of ACI and AASHTO.

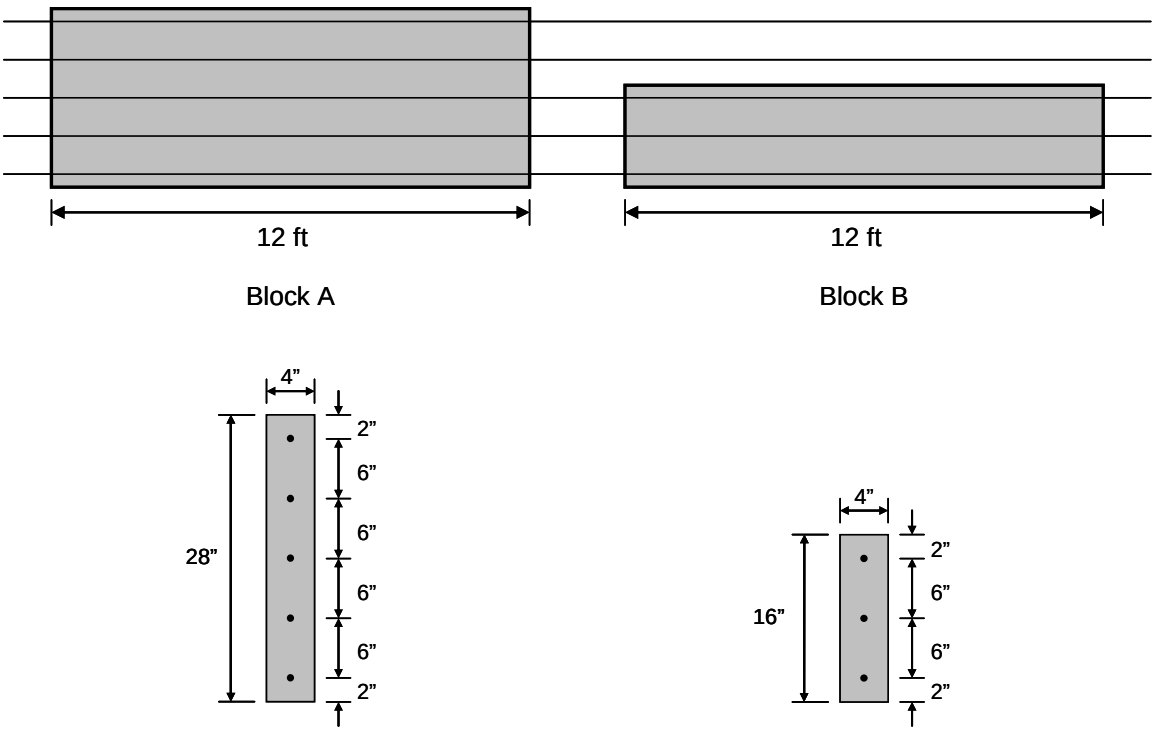

Figure 2.10. Peterman Test Setup (Peterman 2007)

$$\text{For } d_{cast} < 8\text{”} \quad L_t = 90\left(90 - 5d_{cast}\right)d_b$$
$$\text{For } d_{cast} \geq 8\text{”} \quad L_t = 50d_b \qquad \text{Eq. (2-18)}$$

The as-cast vertical locations of standard reinforcing steel and prestressing strand have been shown to significantly influence the bond between the steel and surrounding concrete resulting in longer development lengths. ACI and AASHTO currently have modification factors for the development length of standard reinforcing steel, but fail to recognize the influence of vertical casting position in the calculation of strand transfer and development lengths. A number of researchers have recommended modification factors similar to those used with standard reinforcing steel, and have yet to see any implementation. Recent research has challenged the historical definition of the top-bar/top-strand effect, concluding it is more dependent on the amount of concrete cast above the steel than below it. Regardless of the definition, the top-strand effect is of particular interest in the prestressed concrete industry, resulting in the need for additional research as well as more investigations focused on the determination of the actual top-bar/top-strand effect definition.

2.7 Grade 300 Strand

In the prestressed concrete industry, Grade 270 low-relaxation prestressing strand has been the industry standard for decades. ASTM A416 specifies that the ultimate stress for all tests completed on a Grade 270 strand must be no less than 270 ksi. It is also specified that the minimum yield stress be no less than 90 percent of the required ultimate stress at a strain of 0.01 in./in. and the ultimate elongation be at least 3.5 percent (A416-05/A416M-05 2005). There are currently no provisions for the Grade 300 strand; however, the ASTM limits were used as guidelines during material testing, thus the minimum required ultimate stress for a Grade 300 strand is 300 ksi, which corresponds to a minimum yield stress of 270 ksi at a strain of 0.01 in./in. The ultimate elongation limit of 3.5 percent was still used with the Grade 300 strand (Loflin 2008).

Material testing focused on a the development of the full stress/strain relationship for both the Grade 270 and Grade 300 strand used throughout this study. Table 2.6 shows a summary of the results for yield stress, ultimate stress, and ultimate elongation, which were used to create stress-strain curves for each strand type, and was used in the calculation of nominal moment capacities for beams tested in flexure.

Table 2.6. Summary of Material Testing Results (Loflin 2008)

Strand	Average Yield Stress (ksi)	Average Ultimate Stress (ksi)	Average Ultimate Elongation
½ in. regular GR 270 A	248	279	7.5%
½ in. regular GR 300 A	270	301	7.1%
½ in. regular GR 300 B	275	296	6.3%
½ in. super GR 270 A	239	268	7.2%
½ in. super GR 270 A2	236	273	7.4%
½ in. super GR 300 A	270	296	7.2%
0.6 in. GR 270 A	242	276	7.5%

Equation (2-42) was used to create an idealized stress-strain curve for Grade 270 low relaxation ½ in. diameter prestressing strand and was developed based on the results from 28 individual tensile tests. The coefficients, A, B, C, and D used in the equation were calculated to be 887, 27613, 112.4, and 7.360, respectively for those specific tests. It was noted that a large number of significant figures are necessary because the values of strand stress are sensitive to these constants (Devalapura and Tadros 1992). The coefficients used in the development of the stress-strain curves for strand used in this study were also calculated and are listed in Table 2.7.

$$f_{ps} = \varepsilon_{ps}\left[A + \frac{B}{\left(1+\left(C\varepsilon_{ps}\right)^{D}\right)^{1/D}}\right] \le f_{pu} \qquad \text{Eq. (2-42)}$$

Table 2.7. Constants for Stress-Strain Power Formulas (Loflin 2008)

Strand	A	B	C	D
½ in. regular GR 270 A	375.2	30162	118.2	5.306
½ in. regular GR 300 A	366.4	34132	122.5	5.466
½ in. regular GR 300 B	195.6	34224	120.2	5.148
½ in. super GR 270 A	410.6	35730	147.6	4.163
½ in. super GR 270 A2	448.9	25454	104.0	8.082
½ in. super GR 300 A	226.6	33078	117.8	5.427
0.6 in. GR 270 A	448.7	28845	116.6	6.905

2.8 Flexural Strength

The flexural strength of a member, also referred to as the nominal moment capacity, is a member's ability to resist externally applied moments with equal and opposite internal forces, again shown for a reinforced concrete member in Figure 2.11. The internal resultant compressive force is provided by the concrete and is calculated by integrating under the concrete stress distribution and multiplying by the appropriate width, essentially calculating a volume represented by the red shape. The internal resultant tensile force is provided by the steel and is calculated by multiplying the stress in the steel by the area of the steel, again essentially calculating a volume represented by the blue shape. The nominal moment capacity is equal to the internal couple produced by the two resultant forces. Various techniques can be used to calculate the flexural strength of the member and are based on some key assumptions (MacGregor and Wight 2005).

1. Plane sections before bending remain plane after bending.
2. The strain in the steel is equal to the strain in the concrete at the level of the steel (perfect bond).
3. The stresses in the concrete and steel can be computed from the strain using the stress-strain relationship for each material.
4. Concrete has no tensile strength.

With these assumptions made, the flexural strength of a member can be determined using various techniques. Both ACI and AASHTO have simplified calculation methods with AASHTO used in this study for comparative purposes. However, other techniques, such as strain compatibility can more accurately predict the behavior of a flexural member.

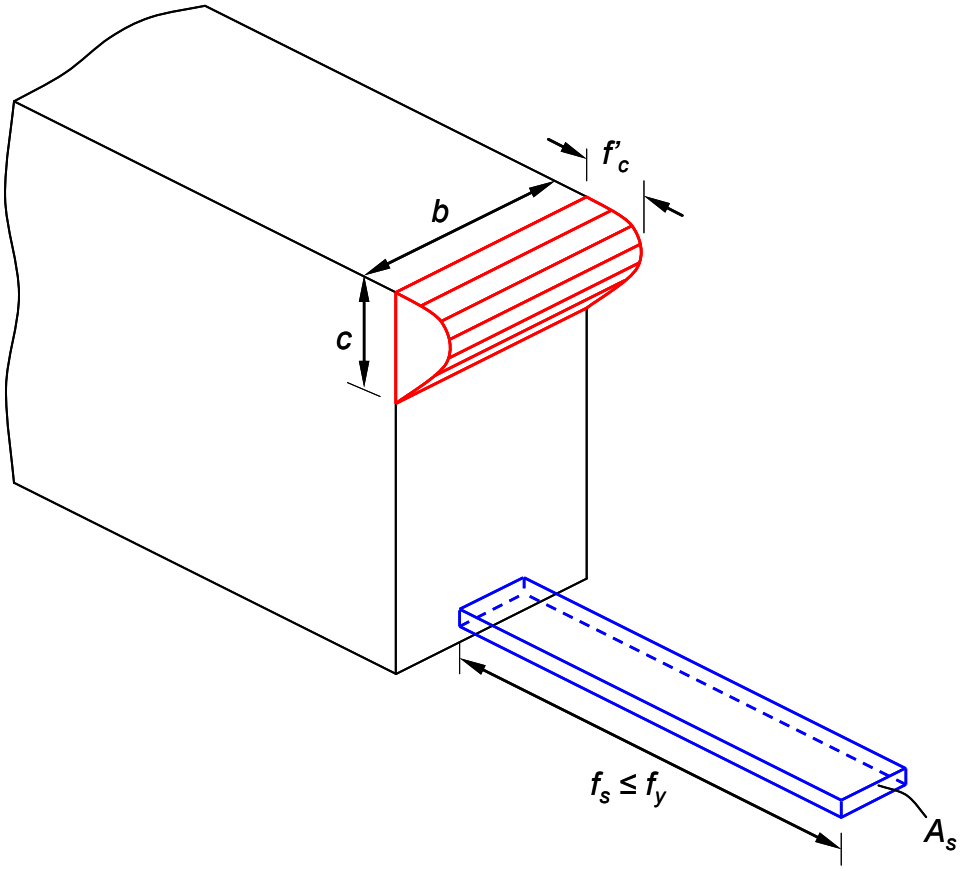

Figure 2.11. Internal Forces of a Reinforced Concrete Beam

The stress-strain relationship of concrete can be modeled in a variety of ways. Experimental tests have shown concrete to have a somewhat parabolic stress-strain behavior, which is idealized by two Hognestad models shown as Figure 2.12 (a) and 2.12 (b) (Park and Paulay 1975). In an effort to simply the calculation process, the stress-strain relationship for concrete is at times idealized with a bilinear relationship as shown in Figure 2.12 (c). In addition to those in Figure 2.12, an even more simplified approach is the equivalent rectangular stress block, used by ACI and AASHTO, where an average constant stress distribution is used over a specified depth, rather than the actual parabolic or idealized stress distribution.

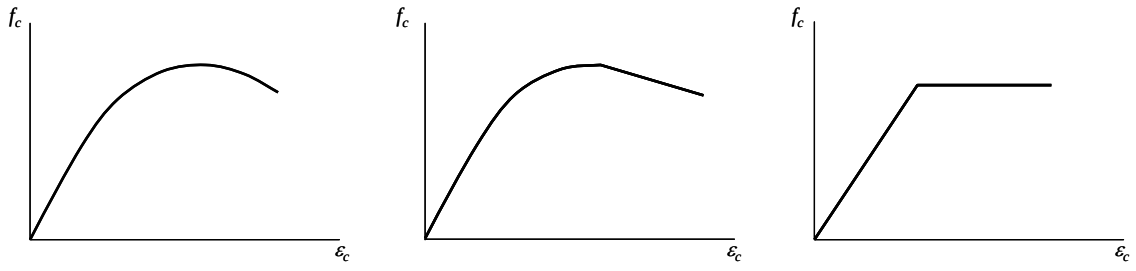

(a) (b) (c)

Figure 2.12. Concrete Stress-Strain Relationships

The stress-strain relationship of prestressing steel can also be modeled in a variety of ways. Experimental tests have shown both standard reinforcing steel and prestressing steel to have a linear relationship as the stress approaches yield. ACI limits the stress-strain relationship of standard reinforcing steel to be bilinear as shown in Figure 2.13 (a), neglecting any effect of strain hardening. Prestressing steel on the other hand can be modeled using either relationship shown in Figure 2.13 (b) and 2.13 (c). Figure 2.13 (b) shows a bilinear stress-strain relationship, while Figure 2.13 (c) shows the actual stress-strain relationship for prestressing steel. Both ACI and AASHTO have relationships for the calculation of the stress in the strand at the nominal moment capacity, shown as Equation (2-43) and Equation (2-44), respectively.

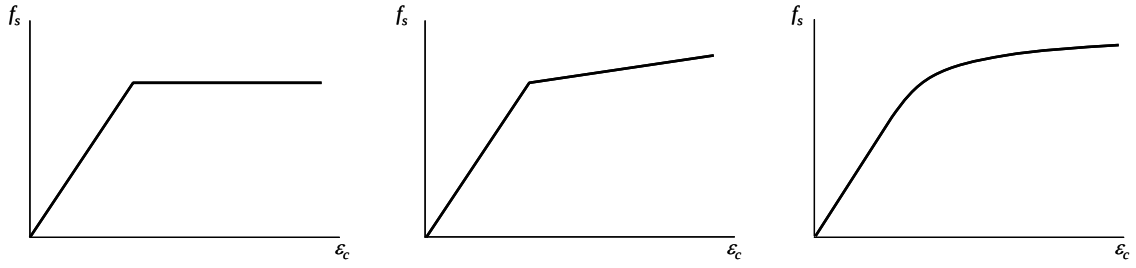

(a) (b) (c)

Figure 2.13. Steel Stress-Strain Relationships

$$f_{ps} = f_{pu}\left\{1-\frac{\gamma_p}{\beta_1}\left[\rho_p\frac{f_{pu}}{f_c^{'}}+\frac{d}{d_p}\left(\omega-\omega^{'}\right)\right]\right\} \qquad \text{Eq. (2-43)}$$

$$f_{ps} = f_{pu}\left(1-k\frac{c}{d_p}\right) \qquad \text{Eq. (2-44)}$$

Historically, nominal moment capacities have been calculated using the ACI and AASHTO provisions for comparative purposes in research. When predicting the actual flexural behavior, a more detailed approach is typically taken, using strain compatibility, taking into consideration the actual stress-strain behavior of the concrete and the steel. In addition to the stress-strain relationships discussed herein, an additional factor sometimes needing consideration in theoretical models is confinement of the concrete depending on the experimental testing method.

2.9 Summary

ACI and AASHTO currently have provisions for the calculation of transfer and development length. The current provisions have been in place for over five decades, while numerous advancements have been made in both prestressing steel and concrete. However, over the past few decades, a number of researchers have shown those equations to be unconservative. Research has shown multiple factors to affect transfer and development length that are not taken into consideration by the current code provisions, including the concrete strength and as-cast vertical location of the strand. Various equations have included either the concrete strength or as-cast vertical location, but an equation still fails to exist that incorporates all affecting factors at once.

In addition to the increase in knowledge regarding transfer and development length, materials have also advanced. With the development of the newer Grade 300 prestressing strand also come a number of questions surrounding its behavior in flexural members. Those questions include the effects of strand strength on transfer length, development length, and flexural capacity. To the knowledge of the author, research has not been completed on the Grade 300 strand prior to this study. There is a need for further verification of the behavior of the Grade 300 strand and the applicability of current code provisions for its implementation.

3.0 METHODOLOGY

3.1 Test Specimen Design

The scope of this project focused on the fabrication and testing of two specimen types in the investigation of the transfer length, development length, top-strand effect, and flexural strength for both Grade 270 and Grade 300 prestressing strands. The objective of the first portion of the investigation was to compare the behavior of test specimens containing the newer Grade 300 strand to those containing the traditional Grade 270 strand, which required the fabrication of twenty, 24 ft long T-beam test specimens. The objective of the second portion of the investigation was to study the top-strand effect which required the fabrication of four sets of top-strand blocks similar to those used in a previous investigation by Peterman (2007). Overall, 36 individual test specimens were constructed and tested in the Structures and Materials Laboratory at Virginia Tech from August 2005 to September 2008. Table 3.1 breaks down the test specimens into the groups in which they were constructed.

Table 3.1. Test Specimen Breakdown

Pour	No. of Specimens	Strand Type	Strand Grade	f_{si}	Description
1	2	0.5 in.	270 ksi 300 ksi	0.67*f_{pu}	T-beams
2	4	0.5 in.	270 ksi 300 ksi	0.67*f_{pu}	T-beams
3	4	0.5 in. super	270 ksi 300 ksi	0.67*f_{pu}	T-beams
4	2	0.5 in. super	270 ksi 300 ksi	0.67*f_{pu}	T-beams
5	4	0.5 in. super	270 ksi 300 ksi	0.75*f_{pu}	T-beams
6	2 2	0.5 in. super 0.6 in.	270 ksi	0.75*f_{pu}	T-beams
1	4	0.5 in.	270 ksi	0.75*f_{pu}	Top-strand blocks
2	4	0.5 in.	270 ksi	0.75*f_{pu}	Top-strand blocks
3	4	0.5 in. super	270 ksi	0.75*f_{pu}	Top-strand blocks
4	4	0.5 in. super	270 ksi	0.75*f_{pu}	Top-strand blocks

The T-beam specimens were 24 ft long, allowing for two flexural tests per specimen. The specimens included a transfer zone at each end of each specimen, which provided a total of 40 transfer zones. One of the transfer zones was lost due to a flash

setting of the concrete while casting the specimen. Of the twenty T-beam test specimens, the size of the cross-section varied with strand type: including low-relaxation ½ in. diameter regular, ½ in. diameter super, and 0.6 in. diameter strands each having a cross-sectional area of 0.153 in.^{2}, 0.167 in.^{2}, and 0.217 in.^{2}, respectively. With an increase in cross-sectional area, also comes an increase in the initial prestress force. Therefore, the prestress force in the beams containing 0.6 in. diameter strands was significantly higher than in those containing ½ in. diameter super strands and the prestress force in beams containing ½ in. diameter super strands was significantly higher than in those containing ½ in. diameter regular strands. For this reason, the size of the cross section varied with the strand type. In addition to the strand type, the size and shape of the cross-section was also influenced by the desired tensile strain in the strand at the ultimate flexural capacity of the member. Tests have shown development length to be dependent on the strain in the strand at the time of failure, thus as recommended by Buckner (1995), the cross section was designed such that the strain in the strand at the ultimate flexural capacity would be greater than the minimum required elongation of 3.5 percent. The relatively wide flanges of the T-beam specimens reduced the depth to the neutral axis, resulting in a high level of strain in the prestressing strands as recommended. The increase in tensile strain also provided a high level of ductility in the test specimens. The three cross sections used throughout the project are shown in Figure 3.1, while the section properties are shown in Table 3.2. The small, medium, and large beams each contained ½ in. diameter regular, ½ in. diameter super, and 0.6 in. diameter strands, respectively.

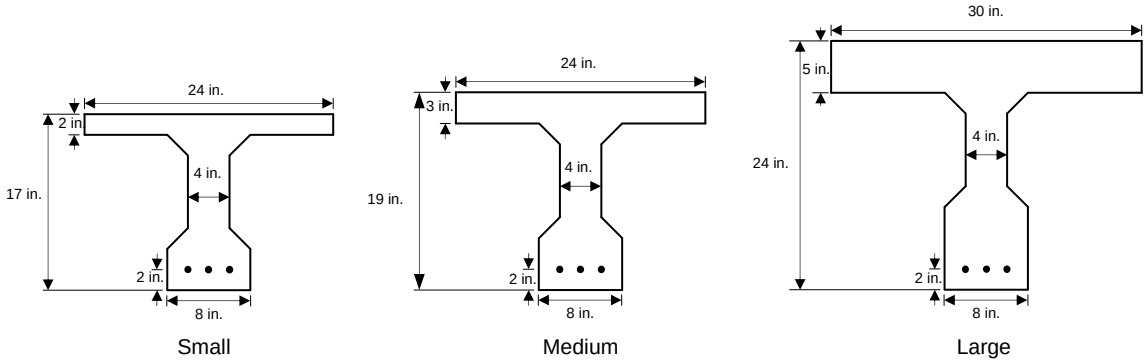

Figure 3.1. T-beam Cross-sections

Table 3.2. T-beam Section Properties

Section Property	Small	Medium	Large
A_g (in.^{2})	134	166	268.8
I_g (in.^{4})	4513	6684	15329
e_g (in.)	8.19	9.73	13.79
A_{gt} (in.^{2})	140.8	173.1	276.8
I_{gt} (in.^{4})	4858	7139	16344
e_{gt} (in.)	8.18	9.70	13.69

*Transformed properties based on f'c = 6000 psi

The three cross-sections were designed with the same dimensions in specific areas of the beams for simplicity throughout the fabrication process. Each cross-section had a web width of 4 in., an overall web height of 11 in., and a bottom flange width of 8 in. The use of the identical dimensions enabled the utilization of the same formwork with only slight modifications from pour to pour for different beam sizes. The top flange of the small size beams was 24 in. wide and 2 in. deep with the bottom flange depth adjusted such that the overall depth of the cross-section was 17 in. The top flange width of the medium size beams was also 24 in., but was 3 in. deep, while the overall depth was 19 in. Contrary to the small and medium size beams, the large size beams had a flange width and depth of 30 in. and 5 in., respectively, while the overall depth of the cross-section was 24 in. In each cross-section, three strands were placed 2 in. from the bottom of the formwork with a lateral center-to-center spacing of 2 in., which is typical in the prestressing industry.

In addition to prestressed reinforcement, longitudinal and transverse non-prestressed reinforcement was used in the top flange as well as shear reinforcement in the web and confining ties near the end of the transfer zone for each beam. Longitudinal reinforcement consisted of No. 4 bars equally spaced, located 1.125 in. from the face of the top flange. The small and medium size beams each contained three longitudinal bars in the top flange, while the large size beams contained five longitudinal bars in the top flange. Transverse reinforcement consisted of No. 3 bars spaced at 18 in. throughout the length of the beam, perpendicular to the longitudinal reinforcement, placed directly on

top of the longitudinal reinforcement. The shear reinforcement varied among the three cross-sections and was dependent upon the nominal moment capacity of each beam, with the maximum shear force calculated under the assumption each beam would reach its full nominal moment capacity during flexural testing. Applied loads were expected to be as close to the supports as 4 ft, which would result in significantly high shear forces in the end region of the beams. Modified compression field theory was used for the calculation of the concrete component of shear resistance (Collins et al. 1996). As for the steel component of shear resistance, No. 3 and No. 4 single leg stirrups were used with spacings adjusted accordingly. The small size beams contained No. 4 single leg stirrups placed every 4 in. over a distance of 8 ft from each end of each beam, while the middle 8 ft contained No. 3 single leg stirrups placed every 8 in. The medium size beams also contained No. 4 single leg stirrups placed every 4 in. in the end portions of the beams, however, No. 4 single leg stirrups were also used in the middle portion of the beam at a spacing of 8 in for added simplicity during the fabrication process. The large size beams were capable of supporting significantly higher loads, resulting in smaller stirrup spacings. The large beams contained No. 4 single leg stirrups placed every 3 in. over the end two-thirds of the beams, while the middle third contained No. 4 single leg stirrups placed every 6 in.

Single leg stirrups were selected because ACI spacing and cover requirements cannot be satisfied using double leg stirrups within a 4 in. web, considering a minimum inside bend diameter of $4d_b$. Use of double leg stirrups would have provided approximately ½ in. cover on each side, which is greater than the required cover of ⅜ in. specified by ACI, but that is assuming a perfectly bent stirrup, which was typically not the case. With such small tolerances, single leg stirrups were selected to ensure adequate cover of the shear reinforcing. It was desirable for the single leg stirrups to be located in the center of the web; however, this was not possible due to the location of the middle longitudinal bar forcing the leg of the stirrups to be slightly off-centered. For this reason, stirrups were alternately placed on each side of the middle longitudinal bar and slightly turned throughout the length of each beam, locating the leg of each stirrup as close to the web center as possible providing a symmetric layout of reinforcement as shown in Figure 3.2. In addition to longitudinal, transverse, and shear reinforcement, confining ties were

also placed at each end of each beam. Three triangular ties were placed within 1 ft of the end of each beam to prevent bursting during the transfer process. Figure 3.3 shows the typical reinforcement layout for the medium size beams.

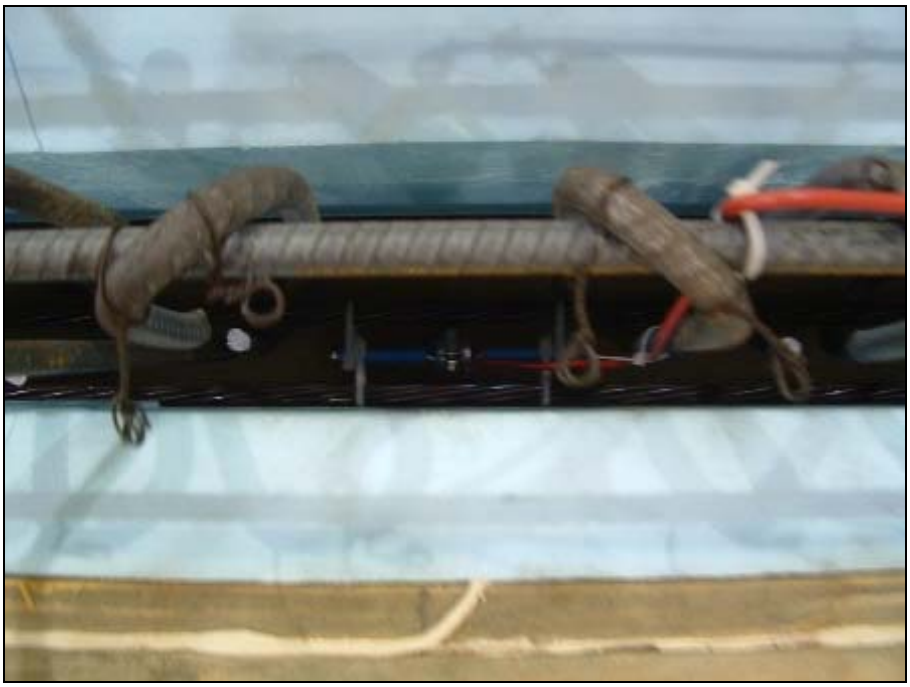

Figure 3.2. Stirrup Placement

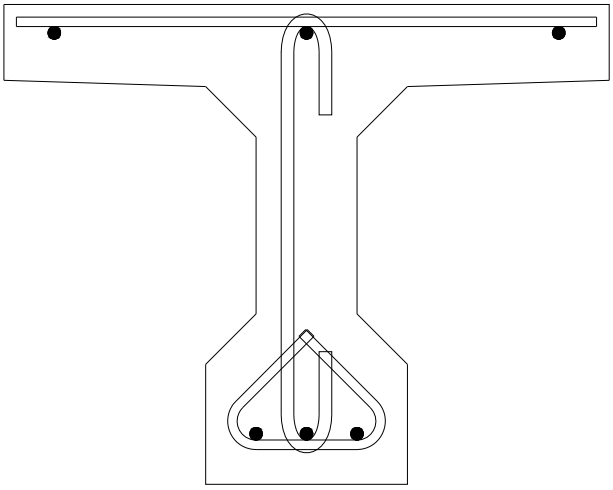

Figure 3.3. Typical Reinforcement Layout

The twenty T-beam test specimens were cast is six groups, each designated by pour, from Pour 1 to Pour 6. Each of the six groups included two types of strands, with

variations in cross-section and casting orientation from pour to pour. Cross-section variations were dependent on the strand type under investigation for a specific pour and the casting orientation was used to further investigate the influence of the top-strand effect on transfer and development length of flexural members. In an effort to investigate the top-strand effect, eight of the T-beam test specimens were cast up-side-down (inverted). Casting of the test specimens with an inverted orientation resulted in more than 12 in. of fresh concrete beneath the strand, which categorizes a strand as a "top-strand" based on the definition provided in the 2008 ACI Building Code for top reinforcing bars. Inverted orientations of small, medium, and large size beams resulted in respective depths of concrete cast beneath the strands of 15 in., 17 in., and 22 in., while maintaining a constant depth of 2 in. of concrete cast above the strand. In pours containing inverted beams, each inverted beam was cast on the same line of strands in succession with a counterpart beam having a normal orientation. This ensured a direct head-to-head comparison of beams cast with normal and inverted orientations. In addition to a head-to-head comparison, the variations in depths of concrete cast beneath the strands coupled with the constant depth of concrete cast above the strands also led to an analysis of the results with respect to reports claiming the top-strand effect to be dependent on the amount of concrete cast above the strand rather than the amount of concrete cast beneath the strand.

The small size beams were cast in Pours 1 and 2, containing ½ in. diameter regular strands stressed to an initial prestress of $0.67f_{pu}$. Pour 1 included two beams, one containing Grade 270 strands and one containing Grade 300 strands, both of which were cast with a normal orientation. Pour 2 included four beams, two containing Grade 270 strands and two containing Grade 300 strands. Of the four beams, one beam for each strand type was cast with an inverted orientation. The medium size beams were cast in Pours 3, 4, and 5 containing ½ in. diameter super strands. Strands from Pours 3 and 4 were stressed to an initial prestress of $0.67f_{pu}$, while strands from Pour 5 were stressed to an initial prestress of $0.75f_{pu}$. Pours 3 and 5 contained four beams, two in each containing Grade 270 strands and two in each containing Grade 300 strands, while Pour 4 contained only two beams, one cast with Grade 270 strands and one cast with Grade 300 strands. Both beams cast in Pour 4 were cast with a normal orientation, while one containing each

strand type was cast with an inverted orientation in Pours 3 and 5. Pour 6 differed slightly as it contained two different sizes of strand (½ in. diameter super and 0.6 in. diameter) having the same strength, Grade 270, due to the inability of obtaining 0.6 in. diameter Grade 300 strand from the strand manufacturer. As with previous pours, each type of strand was used in two beams, one of each cast with an inverted orientation, all of which were cast with an initial prestress of $0.75f_{pu}$. In order to distinguish each individual transfer length measurement location, a unique identification scheme was created, with an example shown in Figure 3.4. The identification scheme designates pour, strand grade, strand size, casting orientation, beam end, and beam side. It should be noted that the beam side is dependent on the beam end. The right and left sides of each beam are denoted by looking from the live, or cut end, towards the dead end.

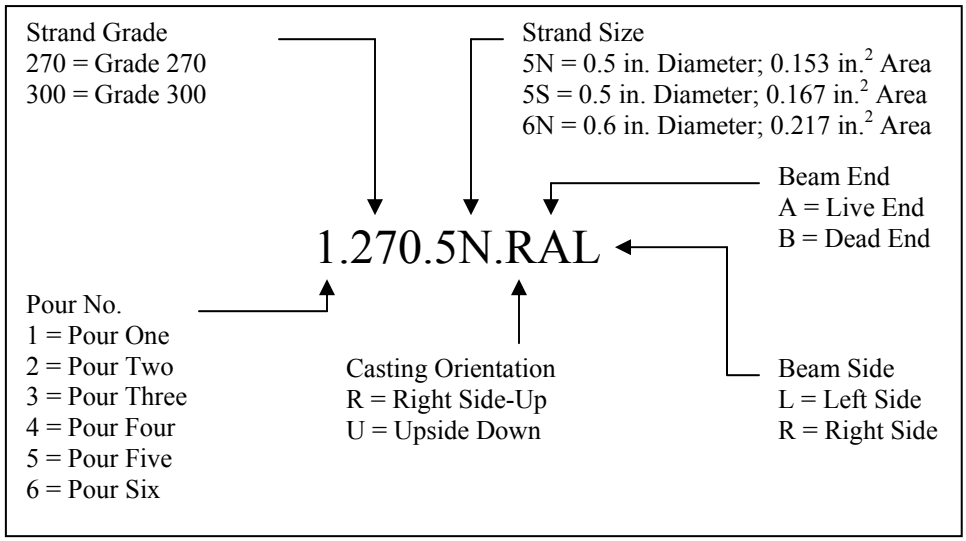

Figure 3.4. Identification Scheme

The top-strand block test specimens, similar to those used by Peterman (2007), were cast in groups of four blocks, each containing one large block, one small block, and two control blocks. The large block was 12 ft long, 24 in. tall and 4 in. wide. The small block was 12 ft long, 14 in. tall and 4 in. wide, and the two control blocks were 12 ft long and had a 4 in. by 4 in. cross-section. The 24 in. tall block was referred to as Block A and the 14 in. tall block was referred to as Block B, while the two 4 in. by 4 in. blocks were referred to as the control blocks. The design of the test specimens allowed for a dual comparison of transfer length for strands having the same amount of concrete cast above or below each. In the blocks used by Peterman, a vertical spacing of 6 in. was

used in between strands, while the blocks used in this investigation had a vertical spacing of 5 in. due to limitations of the existing stressing abutments. Block A contained five strands, Block B contained three strands, and each control block contained a single concentric strand. Figure 3.5 shows the strand layout for Blocks A and B. The strands located within Block A were labeled A – E from top to bottom and the strands in Block B were labeled F – H from top to bottom, while the strand in the two control specimens was labeled I and J (same strand in two control blocks placed in succession). Table 3.3 lists each strand and the amount of concrete cast above and below the strand.

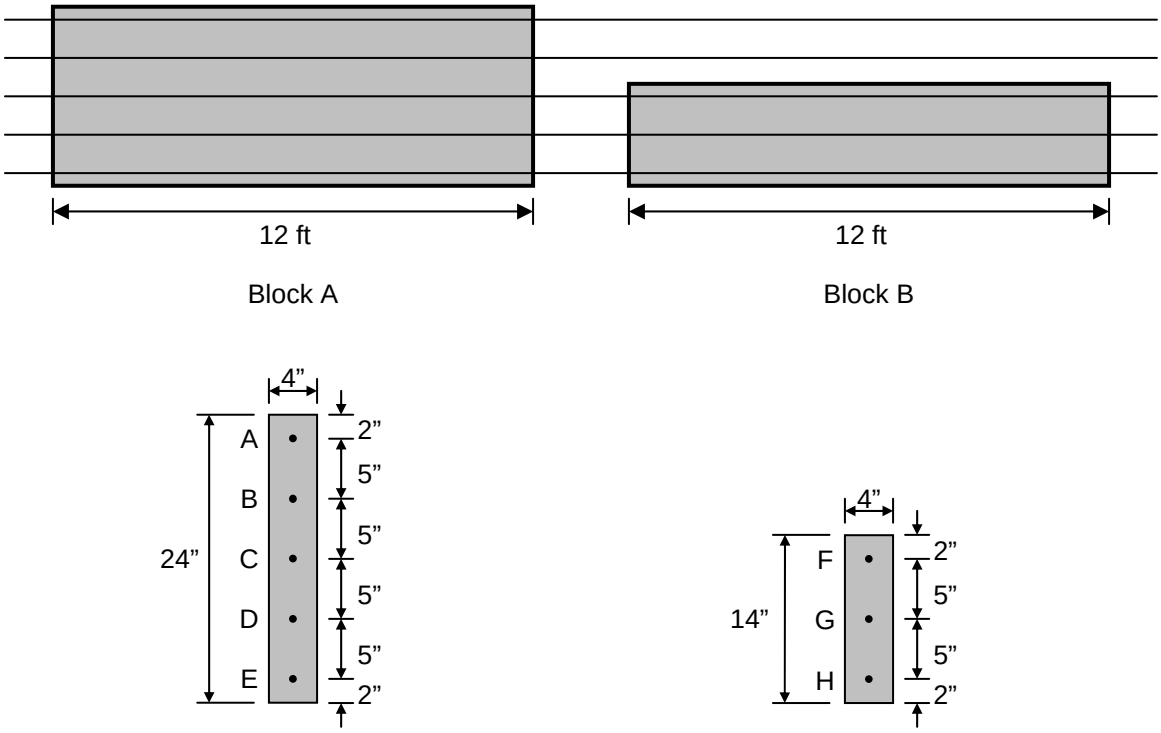

Figure 3.5. Top-strand Blocks

Table 3.3. Amount of Concrete Cast Above and Below Strands

Block	Strand	Distance from Top of Specimen (in.)	Distance from Bottom of Specimen (in.)
A	A	2	22
	B	7	17
	C	12	12
	D	17	7
	E	22	2
B	F	2	12
	G	7	7
	H	12	2
C*	I	2	2
C*	J	2	2

*C denotes Control Block

Of the four sets of top-strand blocks two variables were selected in addition to strand location for the investigation, the water to cement ratio and the size of strand (½ in. diameter regular and ½ in. diameter super). Pours 1 and 2 contained ½ in. diameter regular strands, while Pours 3 and 4 contained ½ in. diameter super strands. Although the concrete compressive strength was chosen to remain constant for all top-strand block specimens with a target release strength of 4500 psi and a target 28 day strength of 6000 psi, the water to cement ratios were varied to investigate the effect, if any, the amount of water in each mix had on transfer length. Pours 1 and 3 each had a design water to cement ratio of 0.40, while Pours 2 and 4 each had a design water to cement ratio of 0.45. The mix designs are discussed in more detail in Section 3.5.

3.2 Fabrication of Test Specimens

The fabrication of all test specimens was completed in the Structures and Materials Laboratory at Virginia Tech. In order to fabricate the pretensioned, prestressed concrete beams, two prestressing beds were created on a portion of the reaction floor inside the laboratory. The reaction floor consists of 60 ft long, 36 in. deep wide flange steel girders fully embedded in concrete, two of which were used for the creation of the prestressing beds. At each end of the two floor beams, one of four steel abutments was bolted to the floor beam as shown in Figure. 3.6.

Figure 3.6. Stressing Abutment

Since the test specimens were cast in a laboratory setting rather than by a precast manufacturer, an effort was made to replicate as closely as possible the casting process typically used in industry. The industry casting procedure usually entails stressing of the strands during the first part of the day, followed by the addition of mild reinforcement, and finally formwork prior to casting on the same day. In the laboratory setting, this process is not feasible because of time constraints and lack of manpower; therefore, slight modifications were made to the casting process. In addition to time constraints and lack of manpower, the fabrication of the inverted beams also added to the complexity of the overall process. For the purposes of direct comparisons of normal and inverted beams, it was desirable for each beam cast with a normal orientation to have a nearly identical counterpart beam cast with an inverted orientation. As previously mentioned, two types of strand were used with each set of beams, each on a corresponding floor beam, typically with one beam having a normal orientation and one beam having an inverted orientation. In order to fabricate beams with normal and inverted orientations along the same line of strands, the beams with a normal orientation were elevated. Figure 3.7 shows the plan view of a typical pour along with sections of both beam orientations.

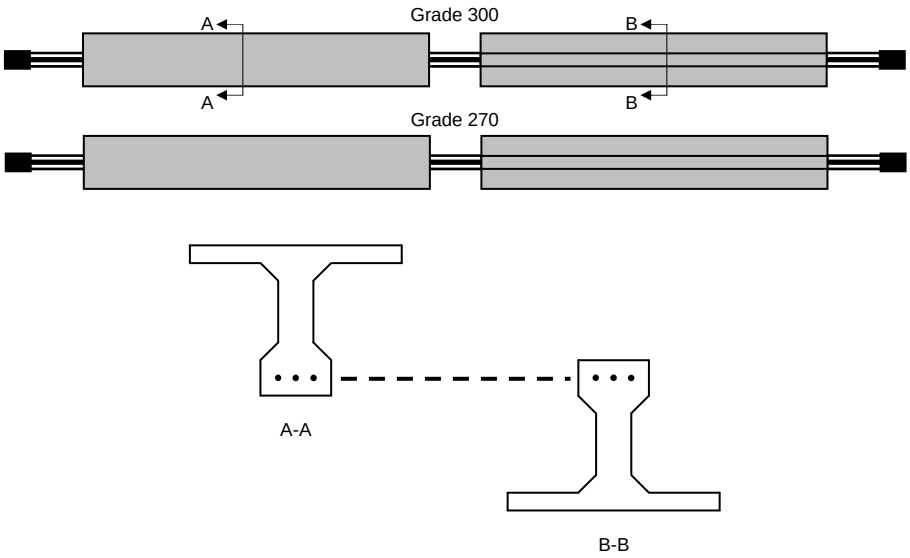

Figure 3.7. Plan View of Typical Pour Layout

The fabrication process for the T-beams generally took about four weeks from initial setup to prestress transfer with the assembly of formwork being the first step. The formwork for the T-beam specimens included four parts, base boards, L-shaped side forms, flange forms, and Styrofoam. Each L-shaped side form was 8 ft long and was constructed of 2x4 studs, ¾ in. plyform, and sheetrock screws. Three of the L-shaped side forms were joined together for each side prior to casting and remained together throughout the duration of the fabrication process. A number of problems arose with the L-shaped side forms, which are discussed with more detail in Section 3.3. The base boards were also 8 ft long, three of which were spliced together for a total length of 24 ft at the beginning of the formwork assembly. For the beams cast with a normal orientation, the L-shaped side forms were then joined to the base boards, held in place by sheetrock screws. Steel angles were then attached to the top of the L-shaped side forms and ¼ in. diameter threaded rods were placed through the angles later aiding in the placement of reinforcement also providing added lateral strength during casting. The prestressing strands were then placed through the formwork, unstressed, followed by longitudinal reinforcing bars, placed by hanging the bars from the threaded rods, with the lateral reinforcement later placed on top of the longitudinal bars. Stirrups were then placed, hanging from the middle longitudinal bar, hooked underneath the middle prestressing strand. Following the addition of the non-prestressed reinforcement,

trapezoidal shaped pieces of Styrofoam were glued to the inside of the side forms, used as a web block-out.

The inverted beams were assembled in a similar manner, with the 8 ft long base boards spliced together by overlapping flange forms. One-quarter inch diameter slick rods were used with the wooden flange forms in lieu of threaded rods. The slick rods were only laid in place and were not attached, as lateral support was not needed at the bottom of the formwork. Longitudinal bars were placed on top of the ¼ in. diameter slick rods and tied in place with lateral reinforcement later tied underneath the longitudinal bars, followed by stirrups hooked underneath the middle longitudinal bar. At that point, the L-shaped side forms were attached to the flange forms and screwed in place. Prestressing strands were then pulled through the formwork with the stirrups hooked over the middle strand. Following the addition of the prestressing strands, the Styrofoam was glued in place for the inverted beams. Figure 3.8 shows an exploded view of the formwork for the medium size beams with both a normal and inverted orientation, while Figure 3.9 shows the assembled view of the formwork for the medium size beams with both orientations. It should be noted, as was previously discussed, the beams cast with a normal orientation were elevated during the casting process, so the same line of strands were used simultaneously for a beam with a normal orientation and a beam with an inverted orientation. Figure 3.10 and Figure 3.11 show the assembled formwork and the general layout of one set of T-beam specimens prior to casting.

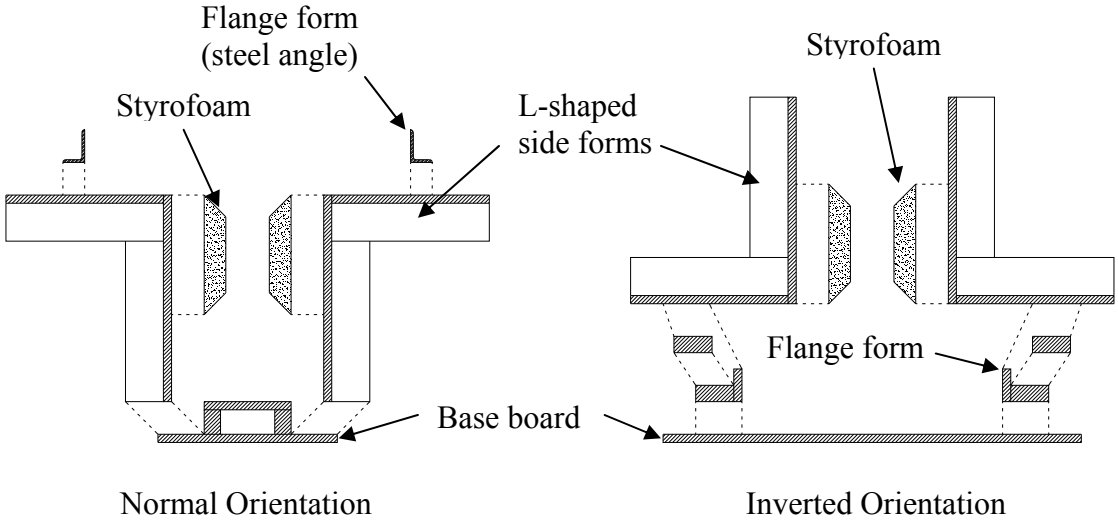

Figure 3.8. Formwork Assembly (Exploded)

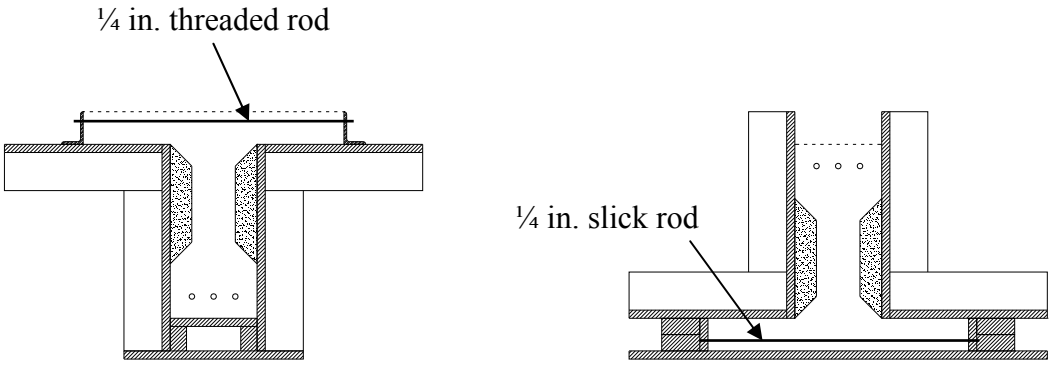

Figure 3.9. Formwork Assembly (Assembled)

Figure 3.10. Formwork Prior to Casting

Figure 3.11. General Pour Layout

Following the assembly of the formwork, the prestressing strands were stressed to an initial prestress as previously discussed. Each strand was stressed individually beginning with the middle strand, followed by each subsequent strand using a hollow cylinder hydraulic actuator as shown in Figure 3.12. The hydraulic actuator was controlled with an electric pump. At one end (dead end) of each floor beam, the strands were anchored by a prestressing chuck with a load cell located on each strand in between the chuck and bearing plate as shown in Figure 3.13 (a) for load monitoring. At the opposite end (live end), after the strands had been tensioned, another chuck was slid in place against the bearing plate as shown in Figure. 3.13 (b). Although seating losses were minimized by tapping the chuck teeth in place on the live end with a welding hammer, the strands were stressed slightly above the desired initial prestress to maximize the stress in the strand after transfer. At that point, the end boards were attached and final modifications were made to the formwork as needed. Strands were typically stressed one day prior to casting, resulting in a small amount of prestress loss from strand relaxation. On the morning of casting, the strands were re-stressed to the specified initial prestress and small spacers were inserted in between the chuck and bearing plate.

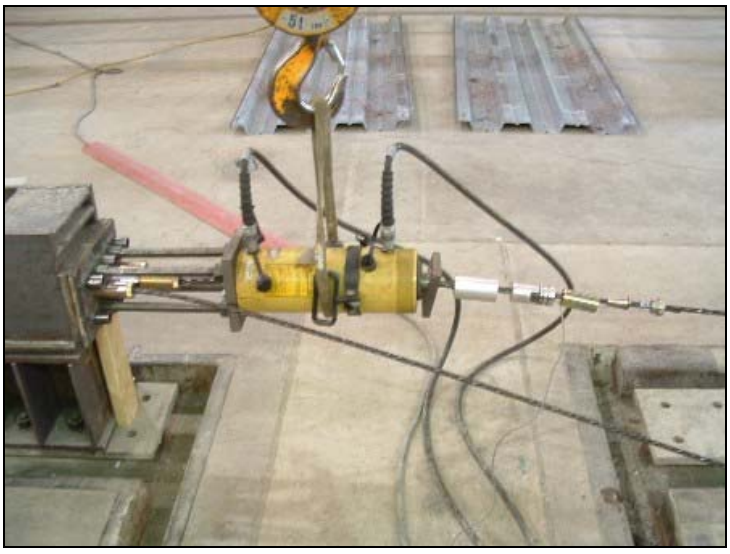

Figure 3.12. Stressing Apparatus

(a) (b)

Figure 3.13. Stressing Abutments

Subsequent to the assembly of the formwork and stressing of the strands, the test specimens were cast beginning with the inverted beams. It was found to simplify the casting process by casting the inverted beams first, as the workability of the concrete decreased with time. The concrete used in the T-beam test specimens was provided by a local ready mix batch plant and was internally vibrated during the casting process. The top surface of each beam was leveled using a vibrating screed and later floated to obtain the desired finish. Following casting, wet burlap was placed on each beam, covered with plastic up to the point of transfer. During this time, the formwork was removed and preparations made for transfer length measurements, which are discussed in Section 3.6.

The casting process for the top-strand blocks was very similar to that of the T-beam specimens. The fabrication process generally took approximately two weeks from initial setup to the transfer of prestress and formwork was again constructed in sections prior to casting, consisting of three parts, the side forms, base boards, and end boards. Each section of formwork was 12 ft long and was constructed of 2x4 studs, ¾ in. plyform, and sheetrock screws, having various heights dependent upon block type. With no additional reinforcement, the formwork assembly of the top-strand blocks was relatively easy, usually taking two days. The side forms were attached to the base boards with three or four sheetrock screws per side. The end boards were then screwed to the end of the side forms and were used to square-up the formwork. Subsequent to the addition of the end boards, additional screws were added to the connection of the side forms and the base boards. As with the T-beam test specimens, ¼ in. diameter threaded rods were used as cross-ties adding lateral restraint to the formwork during casting.

Following the formwork assembly, prestressing strands were pulled through the formwork and prestressing abutments. Figure 3.14 shows an exploded view of the formwork for the small and large blocks, while Figure. 3.15 shows the assembled view of the formwork for both blocks. Figure 3.16 shows the general layout of the top-strand blocks.

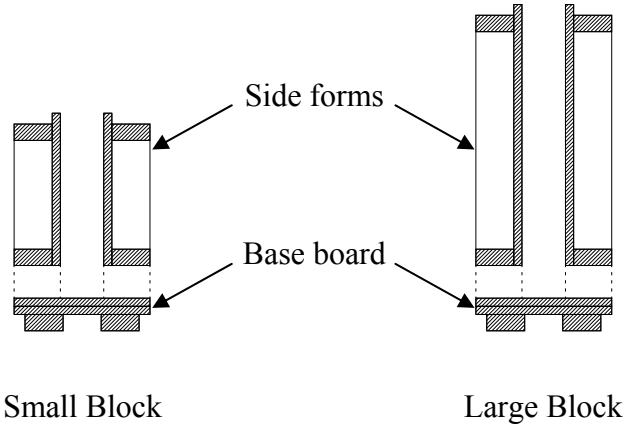

Figure 3.14. Top-strand Block Formwork Assembly (Exploded)

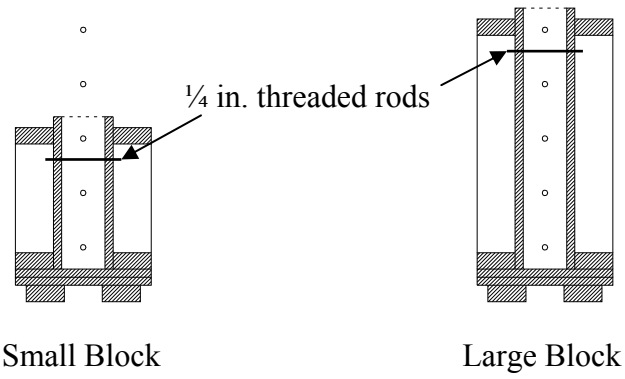

Figure 3.15. Top-strand Block Formwork Assembly (Assembled)

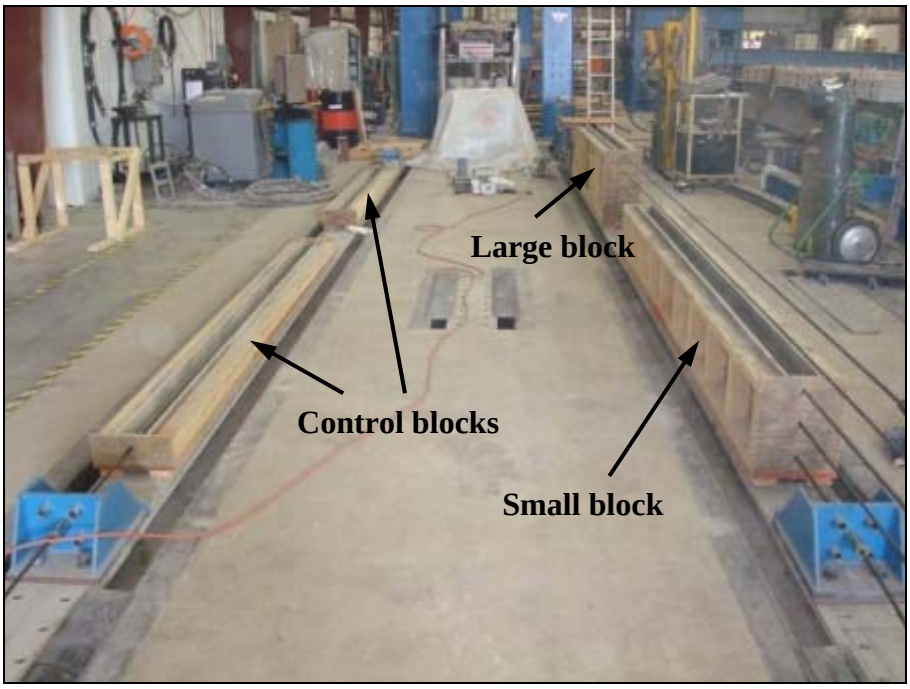

Figure 3.16 Top-strand Blocks General Layout

Following the assembly of the formwork, the prestressing strands were stressed to the specified initial prestress, with a slightly different process. The single strand of the control blocks was stressed first followed by each of the five strands used in the small and large blocks. With a vertical spacing, the top-strand block strands were stressed proceeding upward beginning with the bottom strand. As with the T-beam specimens, at one end (dead end) of each floor beam, the strands were anchored by a prestressing chuck with a load cell located on each strand in between the chuck and bearing plate as shown in Figure 3.17 (a), (b), and (c), for the bottom, 2nd and 3rd, and 4th and 5th strands, respectively. The stressing abutments used in the fabrication of the top-strand blocks were those used in the fabrication of the T-beam test specimens and from a study focused on support conditions used in single-span flexural testing. Note that the abutment heights were adjusted by using 1 in. thick steel plates as spacers.

(a) (b) (c)

Figure 3.17. Top-strand Blocks Stressing Abutments

Because of existing abutment limitations, the abutments were used in sequence along one floor beam. Figure 3.18 (a) shows the three abutments located at the dead end (anchored end) of the test specimens, spaced approximately 12 to 18 in. apart. At the live end (stressing end), shown in Figure 3.18 (b), the abutments were placed in the same order, but with approximately six feet in between each abutment. A larger spacing was used allowing adequate space for the stressing apparatus, previously shown in Figure 3.12, to fit in between abutments during the stressing of the bottom, and the 2nd and 3rd strands from the bottom.

(a) (b)

Figure 3.18. Layout of Stressing Abutments for Top-strand Blocks

Contrary to the T-beam test specimens, the concrete used in the fabrication of the top-strand blocks was mixed in the laboratory to ensure a higher level of quality control

of the mix proportions. The total volume used in the fabrication of each set of top-strand blocks was approximately 18 ft^3. However, the mixer used in the batching process had a capacity of only 7 ft^3; therefore, three batches of 6.25 ft^3 were mixed continuously during the casting process with special care given to the material proportions used in each batch. Prior to the batching process, the material proportions were weighed out to speed up mixing and to provide a somewhat continuous supply of fresh concrete. In each batch, the coarse and fine aggregates were first mixed with a small amount of water, while the additional water and cement were simultaneously added in small amounts. Although the super plasticizer was added last, the air entrainment was combined with the water prior to mixing, and was thus added throughout the mixing process. As each batch finished mixing, the concrete was emptied from the mixer into a concrete bucket attached to the overhead crane, then transported and placed in the formwork. Internal vibration was again used ensuring adequate consolidation of the concrete around each strand. Following casting, wet burlap was placed on each block and covered with plastic for seven days up to the point of transfer. During this time, as with the T-beam test specimens, the formwork was removed and preparations were made for transfer length measurements.

3.3 Formwork Design

The formwork used in the fabrication of the T-beam test specimens was designed using traditional 2x4 studs and plyform. Throughout the fabrication of the T-beam test specimens, the formwork was extremely difficult to remove. Initially, the formwork was designed to have a ¼ in. drop from the bottom edge of the flange to the face of the web. This was accomplished by slightly rotating upward the horizontal 2x4 of the inverted L-shaped stud shown in Figure 3.19 (a). With the horizontal 2x4 rotated, four sheetrock screws were placed in the joint of horizontal and vertical 2x4's. These L-shaped studs were then attached, at a spacing of 16 in. on center, to 8 ft long, longitudinal 2x4's, later covered with plyform sheets. Figure 3.20 shows a small section of the assembled frame. The use of that design resulted in two significant problems in the removal of the formwork following casting. The first problem arose from the lack of rigidity in the L-shaped stud joint. Even with the use of four screws and a ¼ in. drop, the formwork was still unable to adequately support the weight of the overhanging flange. As a result, the

formwork became wedged underneath the flange of the beams and was extremely difficult to remove. The second problem was the way the plyform was attached to the frame. The vertical piece of plyform overlapped the edge of the horizontal piece and in some cases, the top surface of the vertical piece extended above the top surface of the horizontal piece causing the concrete to entrap the top edge of the vertical piece.

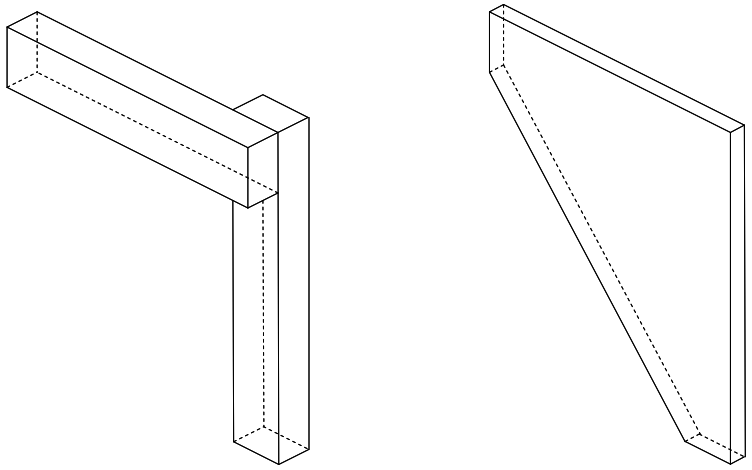

(a) (b)

Figure 3.19. Formwork Studs

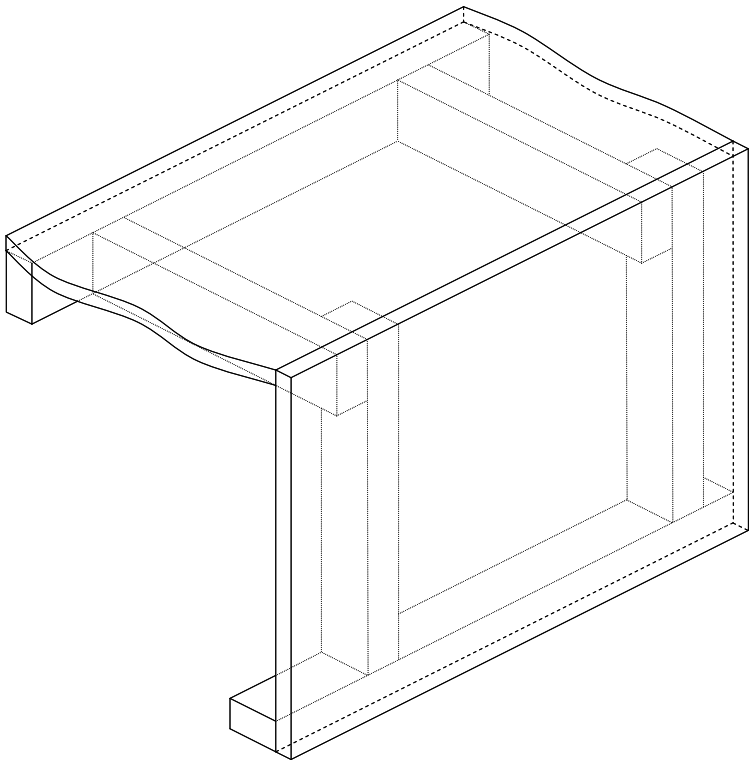

Figure 3.20. Original Formwork Assembly

In an effort to reduce the difficulty associated with formwork removal, the formwork was redesigned for a succeeding project using the same cross-sections. Rather than using 2x4 studs, single triangular shaped studs were cut from ¾ in. plywood with a ½ in. drop from the bottom edge of the flange to the face of the web, shown in Figure 3.19 (b). The plywood studs were joined together with longitudinal 2x4 pieces in pairs as shown in Figure 3.21, with a center-to-center spacing of 12 in. These were then attached to 12 ft long, longitudinal 2x4's, later covered with sheets of plyform as shown in Figure 3.22. It should also be noted that in Figure 3.22, the horizontal piece of formwork overlaps the edge of the vertical piece. The use of plywood studs resulted in a significantly more rigid section and the change in overlaps of the plyform sheets eliminated the possibility of entrapment of the cross-section, resulting in a much easier removal of formwork.

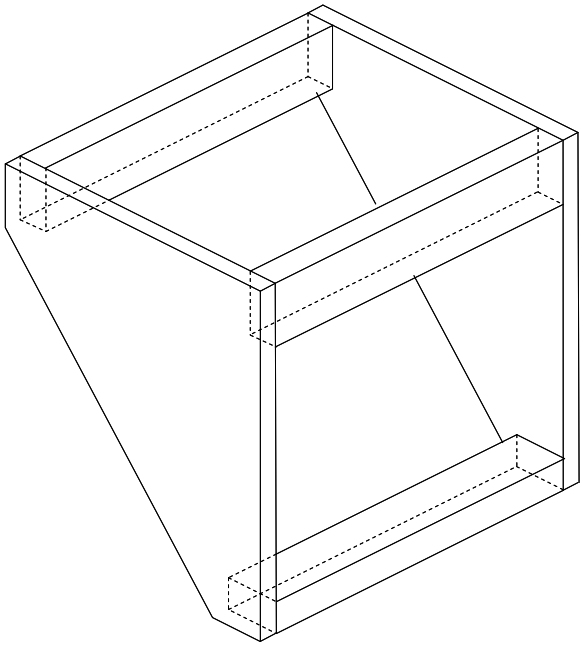

Figure 3.21. Plywood Stud Assembly

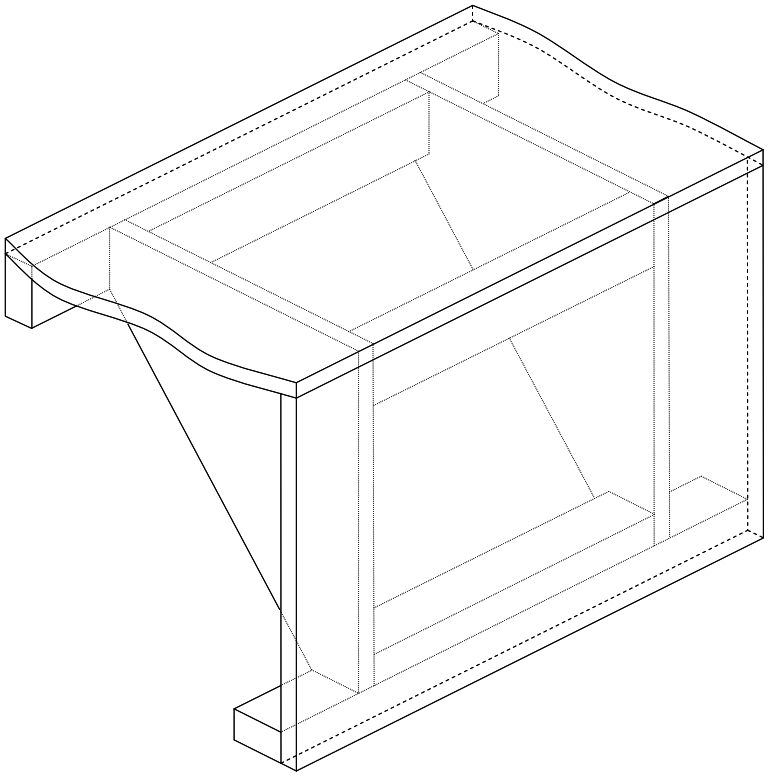

Figure 3.22. Revised Formwork Assembly

3.4 Initial Prestress

Initial prestress has been shown to affect both transfer and development lengths of prestressing strand. A number of studies have used initial prestress values anywhere from $0.60f_{pu}$ to $0.80f_{pu}$, resulting in an increase in transfer length with an increase in initial prestress. While the industry standard is to use an initial prestress equal to $0.75f_{pu}$, two levels of initial prestress were selected for this study, $0.67f_{pu}$ and $0.75f_{pu}$. The T-beam test specimens in Pours 1, 2, 3, and 4 were fabricated with an initial prestress of $0.67f_{pu}$, while those in Pours 5 and 6 were fabricated with an initial prestress of $0.75f_{pu}$. Two levels of initial prestress resulted in an additional variable in the investigation of transfer and development length. The researchers were able to compare the effect strand stress coupled with casting position had on the transfer and development lengths of Grade 270 and 300 strands. With only four sets of top-strand blocks, it was decided to limit the number of variables in addition to casting position to as few as possible. The water to cement ratio and strand size were chosen to be those additional variables, therefore, the initial prestress selected for the top-strand blocks was a constant $0.75f_{pu}$ throughout testing.

3.5 Material Properties

The concrete mixture used in the T-beam test specimens was designed to be a normal weight concrete with a target compressive strength of 4500 psi at transfer and a 28 day compressive strength of 6000 psi. The mix consisted of a ⅜ in. maximum aggregate, natural sand, Portland cement, fly ash, water, and various admixtures. The initial mix design, as shown in Table 3.4 had a water to cement ratio of 0.38 and called for the use of a super plasticizer. Following a flash set during the first pour, the initial mix design was slightly modified, also shown in Table 3.4, increasing the water to cement ratio to 0.40 and adding a retarding admixture.

Table 3.4. Concrete Mix Proportions

Component	Quantity (per yd^3)	
	Initial	Revised
No. 78 Stone	1443 lb	1443 lb
Natural Sand	1083 lb	1083 lb
Portland Cement	600 lb	600 lb
Fly Ash	150 lb	150 lb
Water	34 gal	36 gal
Air Entrainment	3-5%	3-5%
Super Plasticizer	19 oz.*	19 oz.*
Retartder	None	19 oz.#
W:C	0.38	0.40

*Not used in Pours 2-5
#Used in Pours 2-6

The concrete supplier provided batch information with each delivery, allowing for on-site manipulation of the mix to more accurately control the water to cement ratio. Throughout the duration of the project, there was little correlation between slump measurements and the amount of super plasticizer used. The provided batch information was based on moisture contents for coarse and fine aggregates calculated by the concrete supplier. It was thought that these moisture contents lacked a high level of accuracy and overestimated the amount of water in each mix. When manipulating each batch of concrete, water to cement ratios were adjusted to match those shown in Table 3.4, providing a constant water to cement ratio throughout the project with the exception of Pour 1 where a water to cement ratio of 0.38 was intended. Again, adjustments were made based on provided batch information and the accuracy of the calculated moisture contents. Table 3.5 lists the "actual" amounts of water and water to cement ratios for

each pour. The final slump values along with the compressive strength of the concrete at transfer and the average compressive strength at the time of flexural testing for each pour are shown in Table 3.6, while Figure 3.23 shows the concrete strength gain plots for each pour.

Table 3.5. Actual Concrete Mix Proportions

Component	Pour 1	Pour 2	Pour 3	Pour 4	Pour 5	Pour 6
Concrete Volume (yd^3)	4.5	4.5	5.5	3.5	7.5	8.5
Target Water (gal)	153	162	198	126	270	306
Actual Water (gal)	139	139	173	117	255	273
Actual W:C	0.34	0.34	0.35	0.37	0.38	0.36

Table 3.6. T-beam Concrete Properties

Pour	Final Slump (in.)	HRWR Used (oz)	f'_{ci} (psi)	f'_c (psi)	f_r (psi)	E_c (ksi)
1	2.75	76	4900	6500	600	4600
2	7.5	NA	5300	6400	600	4500
3	6.5	NA	6000	8200	700	5100
4	7.5	NA	4900	6300	700	4600
5	6.25	NA	5000	6500	600	4600
6	11.5	128*	6400	8300	700	5200

*Mid-way through casting an additional 28 oz was added

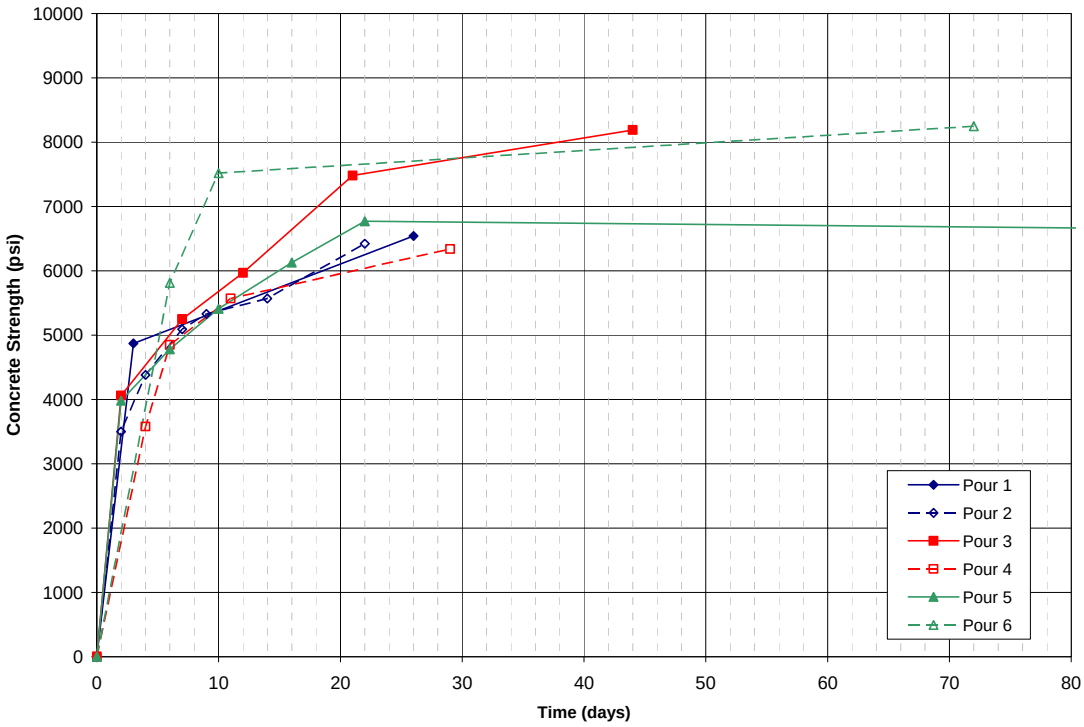

Figure 3.23. T-beam Test Specimens Concrete Strength Gain

The concrete mixture used for the top-strand block test specimens was similar to that used for the T-beam test specimens, with target values of 4500 to 5000 psi at transfer and 6000 psi at 28 days. As previously discussed, the variables used in the fabrication of the top-strand blocks were limited to strand type and water to cement ratio in addition to the as-cast vertical location of the strands, while all other possible variables remained as constant as possible. Two water to cement ratios were used to examine the effect, if any, the amount of water in a mix had on transfer lengths. Given that the compressive strength of concrete is generally dependent on the water to cement ratio, other modifications to the material proportions were necessary to obtain a relatively constant compressive strength for each mix. These modifications were made using an air entraining admixture, when added to a mix has been shown to decrease the compressive strength of the concrete. Table 3.7 and Table 3.8 show the specified and actual batch proportions for mixes with a 0.40 and 0.45 water to cement ratio.

Table 3.7. Specified Concrete Mix Proportions

Component	Quantity (per yd^3)	
	0.40 W:C	0.45 W:C
No. 78 Stone	1677 lb	1677 lb
Natural Sand	1112 lb	1112 lb
Portland Cement	926 lb	926 lb
Water	44.4 gal	49.9 gal
Air Entrainment	5.5 oz.	3.7 oz.
Super Plasticizer	22.8 oz.	22.8 oz.

Table 3.8. Actual Concrete Mix Proportions

Component	Quantity (per yd^3)			
	Pour 1	Pour 2	Pour 3	Pour 4
No. 78 Stone	1677 lb	1677 lb	1677 lb	1677 lb
Natural Sand	1112 lb	1112 lb	1112 lb	1112 lb
Portland Cement	926 lb	926 lb	926 lb	926 lb
Water	44.4 gal	49.9 gal	44.4 gal	49.9 gal
Air Entrainment	5.5 oz.	3.7 oz.	5.5 oz.	3.7 oz.
Super Plasticizer	22.8 oz.	22.8 oz.	32.9 oz.	22.8 oz.
W:C	0.40	0.45	0.40	0.45

Mixing the concrete used for the top-strand blocks in the laboratory allowed for a high level of quality control as was shown with the actual mix proportions in Table 3.8. Other than the super plasticizer used in Pour 3, all components remained constant throughout casting. Concrete strength was monitored up to and following the transfer process, testing cylinders at 1, 4, 7, 14, 21, and 28 days for each pour. The concrete strengths were fairly consistent throughout testing with the strength gain plots for each pour shown in Figure 3.24. In addition to the strength gain plot, Table 3.9 lists the measured slump and air content for each pour with amount of super plasticizer used as well as concrete strengths at transfer and 28 days.

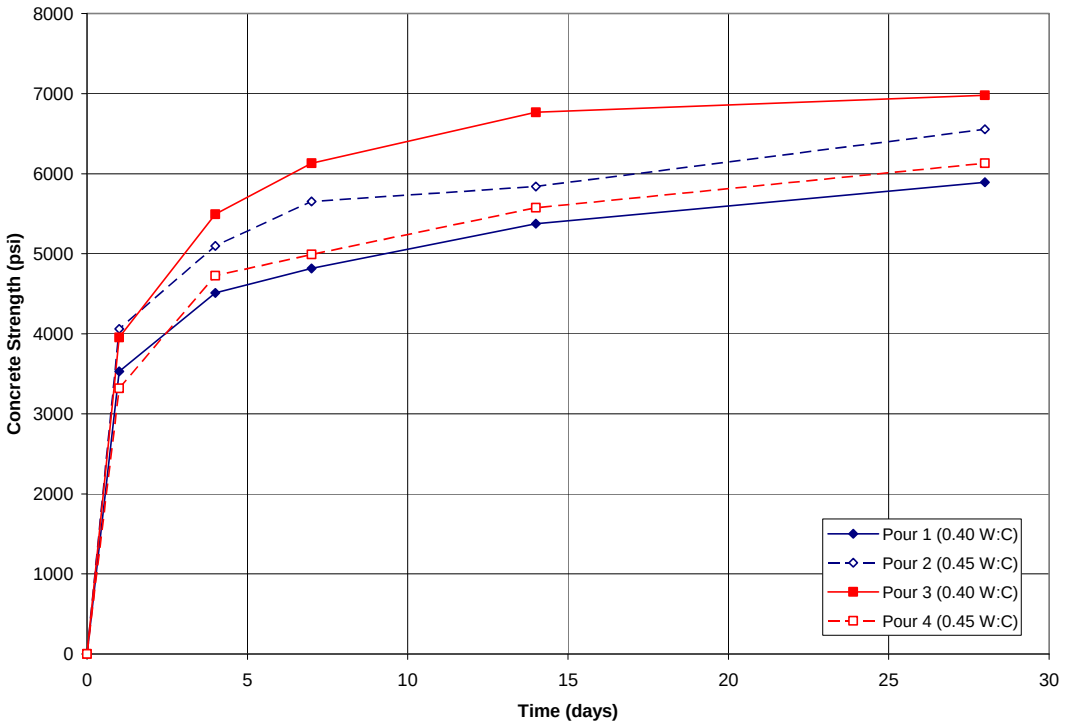

Figure 3.24. Top-strand Block Concrete Strength Gain

Table 3.9. Top-strand Block Concrete Properties

Pour	Average Slump (in.)	MRWR Used (oz/yd^3)	Average Air %	f'_{ci} (psi)	f'_c (psi)
1	6.25	22.8	8.3	4800	5900
2	3.75	22.8*	5.2**	5700	6600
3	5.75	32.9	7.7	6100	7000
4	8.75	22.8	6.3	5000	6100

*an additional 1.7 oz. was added to the third batch

**only two air contents were taken of the three batches

3.6 Transfer Length Measurements

Transfer length measurements were taken at each end of each T-beam and each end of each top-strand block for each strand, corresponding to the live and dead end of each test specimen. The live end of the specimen was the end at which the strand was torch cut (in between two test specimens cast on the same line of strands), while the dead end of the specimen was the end at which the strand was anchored to the supporting abutments. Transfer length measurements were taken using two techniques. The primary method used was to measure the concrete surface strain at the level of the strand in each

specimen, while the secondary method used was to measure end-slip of the strand. A total of 39 transfer zones were studied for the T-beams, while a total of 80 transfer zones were studied for the top-strand blocks.

Concrete surface strains were measured using a DEmountable MEChanical (DEMEC) strain gauge and surface mounted gauge points. The DEMEC gauge had a gauge length of 7.874 in. (200 mm) and the gauge points were approximately ¼ in. in diameter with a small, fine point indention located at the approximate center. These points were placed on the test specimens at the level of the strands at a spacing of 1.969 in. (50 mm) and 3.937 in. (100 mm). A spacing of 1.969 in. was used in areas expected to be within the anticipated transfer zone, ensuring a defined ascending branch of the strain plot. The remaining points located beyond the anticipated transfer zone, corresponding to the strain plateau were spaced at 3.937 in. Each individual strain reading was based on the total gauge length of 7.874 in., so adjacent strain readings would overlap aiding in the development of a smooth strain plot. Figure 3.25 and Figure 3.26 show the typical layout of DEMEC points used on a T-beam specimen and a top-strand block specimen.

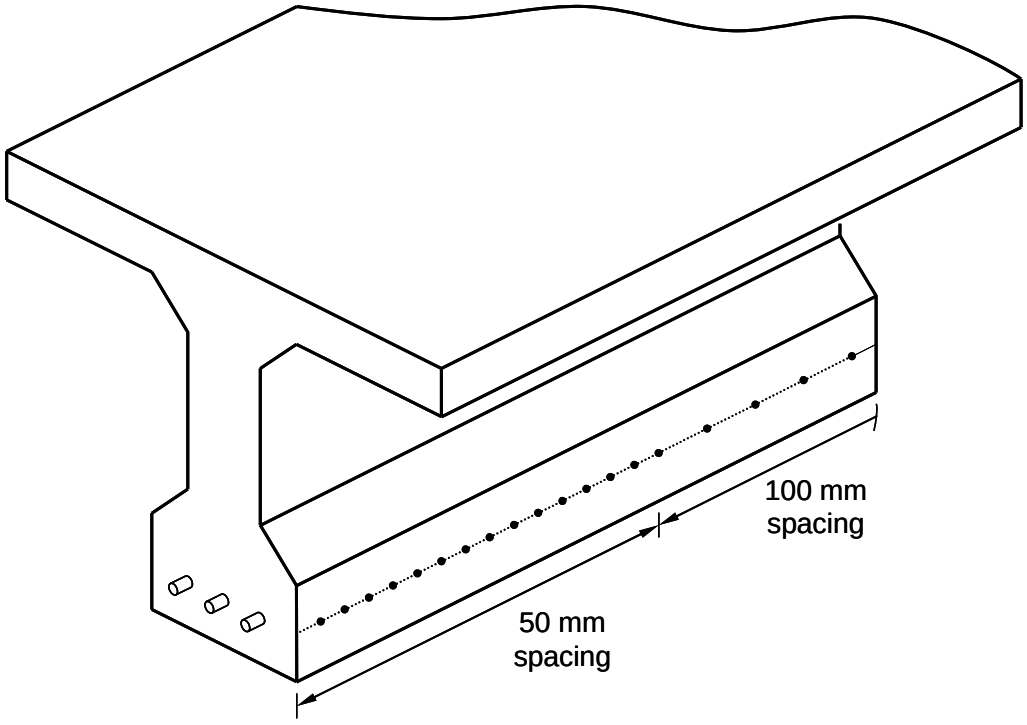

Figure 3.25. T-beam DEMEC Point Layout

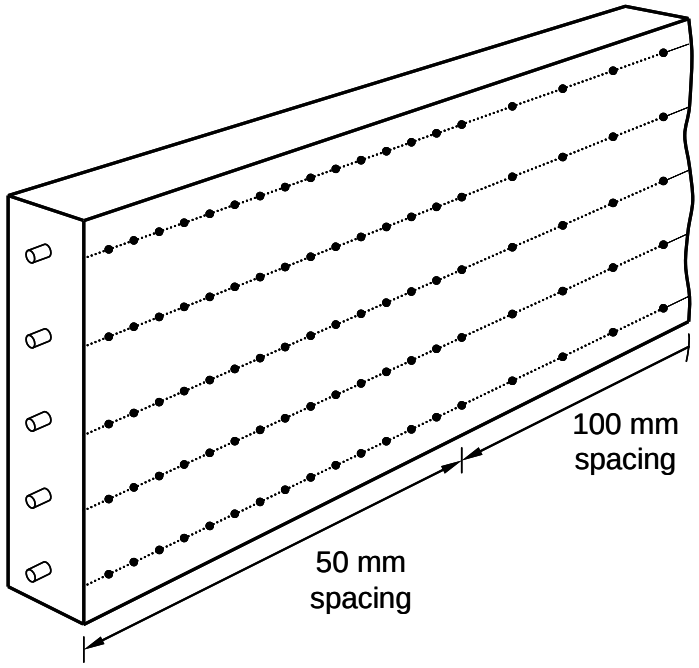

Figure 3.26. Top-strand Block DEMEC Point Layout

DEMEC points were attached in the days leading up to transfer. On average, approximately 25 points were placed on each side of each T-beam end, for a total of 100 per beam, while the top-strand blocks used approximately 800 DEMEC points per pour. Demec points were attached by hand using a five minute epoxy and then labeled. Prior to the transfer process, it is extremely important to define the initial distances between each set of points therefore the initial distance between each set of points was measured three times and then averaged to ensure an accurate starting point for all future measurements. During the initial measurements, a tolerance of 0.005 mm was used with each set of measurements allowing for the elimination of any outlying measurements. When a spurious measurement was recorded, a fourth measurement was taken to provide a more accurate starting point.

Subsequent to the initial readings, the strands were flame cut using an acetylene torch. It should be noted, as previously mentioned, the strands are not physically cut, but are gradually heated until the strands yield in tension. For the T-beam test specimens, the middle strand was cut first followed by each of the two outer strands. This pattern of cutting was used to first apply a uniform compressive stress along the middle of the cross-section to resist any possible weak axis bending resulting from the lateral eccentricity of the outside strands. For the top-strand block test specimens, previously

shown in Figure 3.5, the strand located within the control blocks (I and J) was first cut followed by strands D/G, B, C/F, E/H, and A of the large and small blocks. Strand D/G was cut first applying a uniform compressive stress to the small block, and coupled with the release of strand B created a uniform compressive stress on the large block. Subsequent strands, C/F, E/H, and A were then cut. Following the transfer of prestress, T-beams or top-strand blocks, the DEMEC points were again measured and recorded. The difference between the two readings (before and after transfer) at any one location provided the change in length from the point at which zero prestress force was applied to the point at which the entire prestress force was applied. The change in length was then divided by the gauge length, resulting in the average strain across the gauge length for that location. A number of researchers have shown transfer lengths to increase over time by approximately ten percent, therefore, additional measurements are usually taken. For the T-beam specimens, the second set of readings were taken one to two weeks after transfer, while the second set of readings were taken seven days after transfer for the top-strand blocks.

Based on each set of concrete surface strains recorded using the DEMEC gauge, a strain profile similar to Figure 3.27 was created for each transfer zone and the 95 percent Average Maximum Strain (AMS) method was used with slight modifications to estimate initial and the second set of transfer lengths (Russell and Burns 1993). The point at which the strain plateau began (apex) was visually identified and the AMS was determined based on those points beyond the apex of the ascending branch. The AMS was then reduced by five percent and a horizontal line plotted. Using the apex point, a linear trend line was fit to the data located between the end of the beam and that apex. Using the equation produced by the trend line, the intersection of the 95 percent AMS line and the best fit ascending line was determined, which corresponds to the transfer length. Equation (3-1) shows this equation.

$$m \cdot L_t + y_{\text{int}} = 95\% AMS \qquad \text{Eq. (3-1)}$$

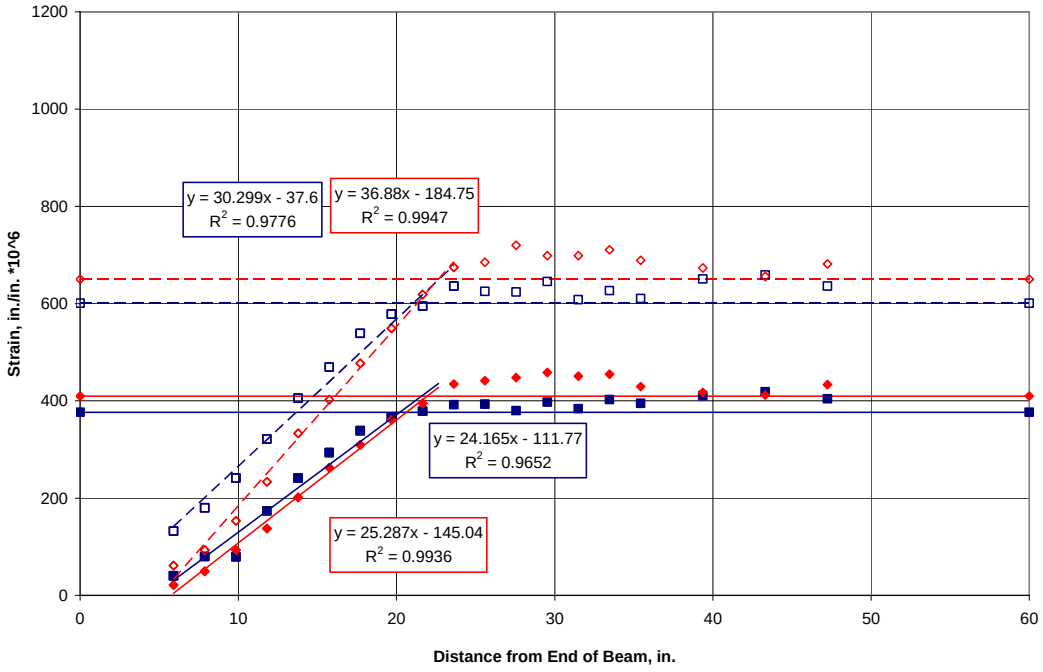

Figure 3.27. Transfer Length Strain Profile

The slope of the ascending branch of the strain plot was used rather than the intersection of the strain profile to the 95% AMS because there exists the possibility of spurious strain values. Shown in Figure 3.28 is a detailed view of the intersection of both the best fit line and the line of connected data points to the 95% AMS for a specific transfer zone. A discrepancy can be noted between the two methods for the red line. If the line of connected data points was used, a longer transfer length would be calculated. In the case of overestimation of transfer lengths, added conservatism is not of concern, but in the case of underestimation of transfer lengths, a lack of conservatism would be of concern. Therefore, the use of a best fit line to the ascending branch of each strain profile was used and was expected to give the most accurate and consistent results.

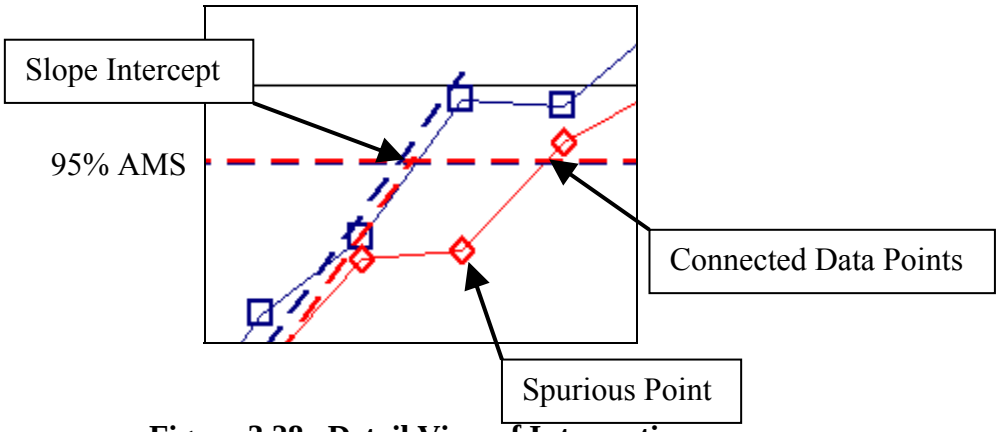

Figure 3.28. Detail View of Intersection

In addition to measuring changes in concrete surface strains, end-slip was also measured on the dead end of each specimen. As previously discussed, transfer length can be related to the amount of slip occurring between the strand and the end of the beam and various researchers have developed equations for the calculation of transfer length, some more complex than others. Over the course of transfer length research a number of methods have been used when taking end-slip measurements including, a piece of tape on the strand, brackets mounted to the strand, or a small notch cut in the strand. Placing a piece of tape on the strand is the easiest method, but the least accurate. Mounting brackets is probably the most difficult method, but produces fairly consistent results. Notching a strand may be the most accurate of the three methods, but is also the most dangerous and is not recommended. End-slip measurements reported herein were taken using a depth micrometer and, in order to obtain accurate results, it is imperative that solid reference points be established before measurements are taken.

A small U-bracket was placed approximately one inch from the face of the test specimen on each strand with a hose clamp providing a stationary reference point for measurements before and after transfer. A small aluminum flat bar was also embedded in the concrete during casting to provide a smooth flat surface for measuring. Figure 3.29 (a) shows the setup used for end-slip measurements. As with DEMEC points, three initial measurements were taken prior to transfer and averaged to ensure an accurate reference point. Following transfer, measurements were again taken with the end-slip equal to the difference between the initial and final measurements minus the elastic shortening of the protruding strand. It should be noted that it was only possible to obtain end-slip measurements at the dead end of the test specimens. When using a flame-cut

release, the strand tends to fray, as shown in Figure 3.29 (b), at the live end causing the U-brackets to bend or the hose clamps to break. Therefore, measurements at the live end were not possible. Following end-slip measurements, transfer lengths were calculated using various equations as discussed in Section 2.2 and compared to transfer lengths calculated from concrete surface strain profiles.

(a) (b)

Figure 3.29. End-slip Measurements Setup

3.7 Development Length Measurements

The development length tests were designed to establish the minimum development length for each of the five strand types used throughout the duration of the project. A single point bending test was performed on each end of the 24 ft long T-beam test specimens with a test span of 16 ft, allowing for two tests per beam. Figure 3.30 shows the test setup for one of the single point bending tests. The initial location of the point load (P), and the embedment length (L_e) from the end of the beam was based upon the calculated development length. A schematic diagram of the test setup is shown in Figure 3.31.

Figure 3.30. Single Point Bending Test Setup

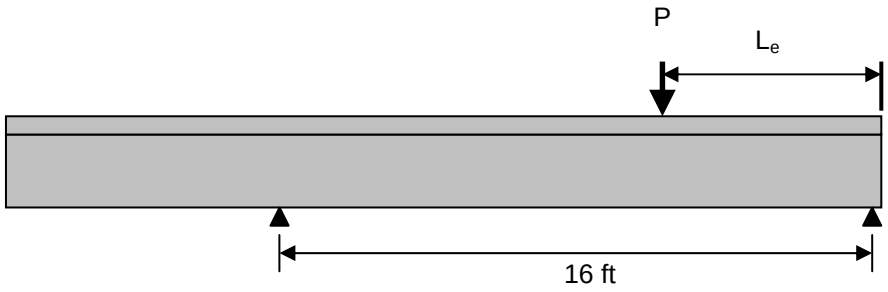

Figure 3.31. Single Point Bending Test Schematic

With each test arose the possibility of three failure types, flexural, bond, or in some cases a combination thereof. A flexural failure is defined by either crushing the concrete in the compression zone or by rupturing the strands in very ductile test specimens, both of which are easily discernable and shown in Figure 3.32. Leading up to each type of failure, a test specimen will typically see very little increase in applied load with substantial increases in deflection. At this point, some tests were considered flexural failures, while in other cases, load application was continued until complete failure of the specimen. It should be noted that with a single point load, the concrete was confined by the load itself, resulting in an increase in compressive strength of the concrete. The impacts of confined concrete on the compressive strength are discussed in more detail in Section 3.8. A bond failure was defined by the amount of average slip occurring between the end of the strand and the end of the test specimen, with a limit of 0.01 in., also usually resulting in the formation of shear cracks. End-slip measurements during flexural testing were measured with linear variable differential transducers (LVDT's), with an accuracy of 0.001 in. Three LVDT's were attached to the end of the

test specimen corresponding to the embedment length in question, mounted with a small frame constructed of small aluminum channel as shown in Figure 3.33. In most cases, a full bond failure would allow the strand to pull into the end of the test specimen, pulling away from the tip of the LVDT's. Figure 3.34 shows a typical bond failure where the strands are no longer in contact with the LVDT's.

Concrete Crushing

Strands Fractured

Figure 3.32. Flexural Failures

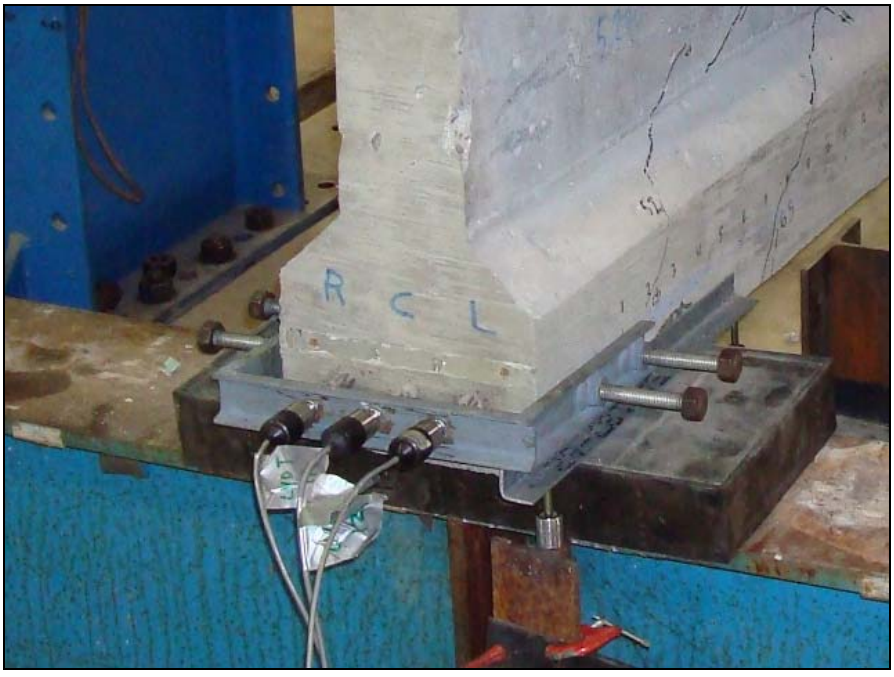

Figure 3.33. End-slip Measurement Setup

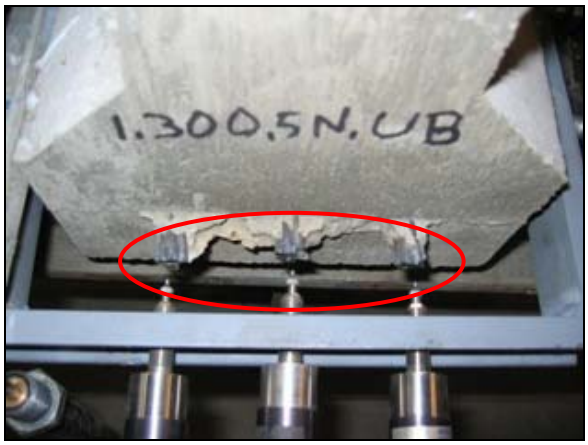

Figure 3.34. Typical Bond Failure

The application of load during the single point bending tests were conducted in 2 kip increments until cracking, then 5 kip increments thereafter. During the single point bending tests, a flexural failure would indicate that the selected embedment length was longer than the actual development length, in which case the succeeding test of a new specimen would incorporate a shorter embedment length. A test resulting in a bond failure, an average slip of 0.01 in. or greater, would indicate that the selected embedment length was shorter than the actual development length, in which case the succeeding test of a new specimen would incorporate a larger embedment length. This process was repeated for each strand type with the intention of determining the minimum flexural bond length to result in a flexural failure. Upon the completion of each test, the flexural bond length was taken as the tested embedment length minus the corresponding transfer length.

3.8 Flexural Strength

The flexural strength, also referred to as the nominal moment capacity and ultimate flexural capacity, was determined experimentally by single point bending tests used in the determination of the development length as well as theoretically based on the provisions of ACI and AASHTO, and strain compatibility. The flexural strength was determined experimentally for each test specimen assuming the strand was fully developed. When calculating the nominal flexural capacity of a section using the ACI or AASHTO provisions, the assumption of perfect bond between the strand and surrounding concrete is made, although that may not be true in every situation. Therefore, the value obtained by ACI or AASHTO provisions for each test specimen is the maximum nominal

moment capacity. Strain compatibility also makes the assumption of perfect bond and will also result in a maximum nominal moment capacity, slightly higher than that calculated by ACI or AASHTO. As mentioned in Section 3.7, the application of load used in the single point bending tests added a confinement in the compression zone of the test specimen, resulting in an increase in compressive strength of the concrete. Taking this confinement into consideration, the calculated nominal moment capacities based on strain compatibility used a concrete stress-strain relationship as shown in Figure 3.35.

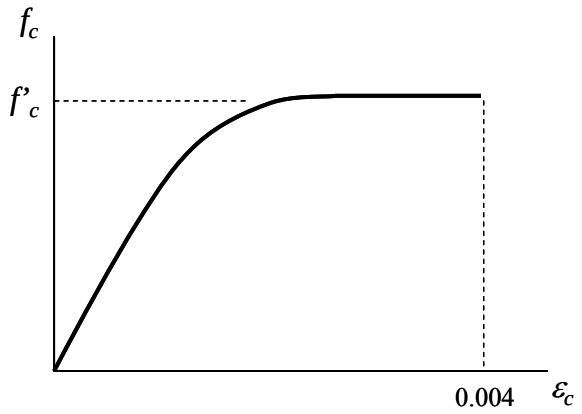

Figure 3.35. Modified Confined Concrete Stress vs. Strain Diagram

In addition to the monitoring of end-slip during flexural testing, the applied load and deflection directly under the load point were measured. The applied load was measured using a strain gauge type load cell having a precision of approximately 100 lb, while the deflection was determined using a single wire pot, with a precision of approximately 0.001 in. The support conditions were assumed to be simply supported using neoprene bearing pads at each end of the beam, typically used in industry, which incur a small amount of displacement under the applied load as well as some rotation as a result of vertical deflection in the beam during loading. In order to take into consideration the vertical displacement and displacement from rotation in the pad, large scale LVDT's were used to monitor the support displacements as shown in Figure 3.36. Some concern was raised about the possibility of the neoprene bearing pads supplying horizontal restraint to the beam creating an arching action rather than a truly simply supported condition. Therefore, an independent study was conducted on the support conditions of simply supported flexural tests, which showed no significant differences in the flexural capacity of rectangular beams supported with neoprene bearing pads versus a

traditional pin and roller support system. Based on the test results, the applied moment versus deflection was plotted for each test specimen with the displacements of the neoprene bearing pads taken into account and the end-slip relationship with moment is also shown in Figure 3.37

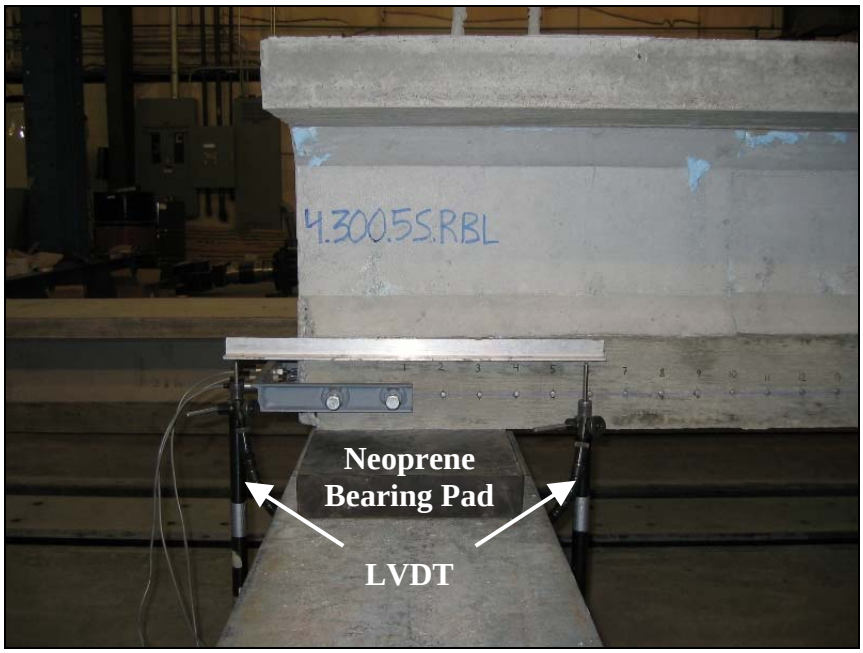

Figure 3.36. Support Displacement Monitoring

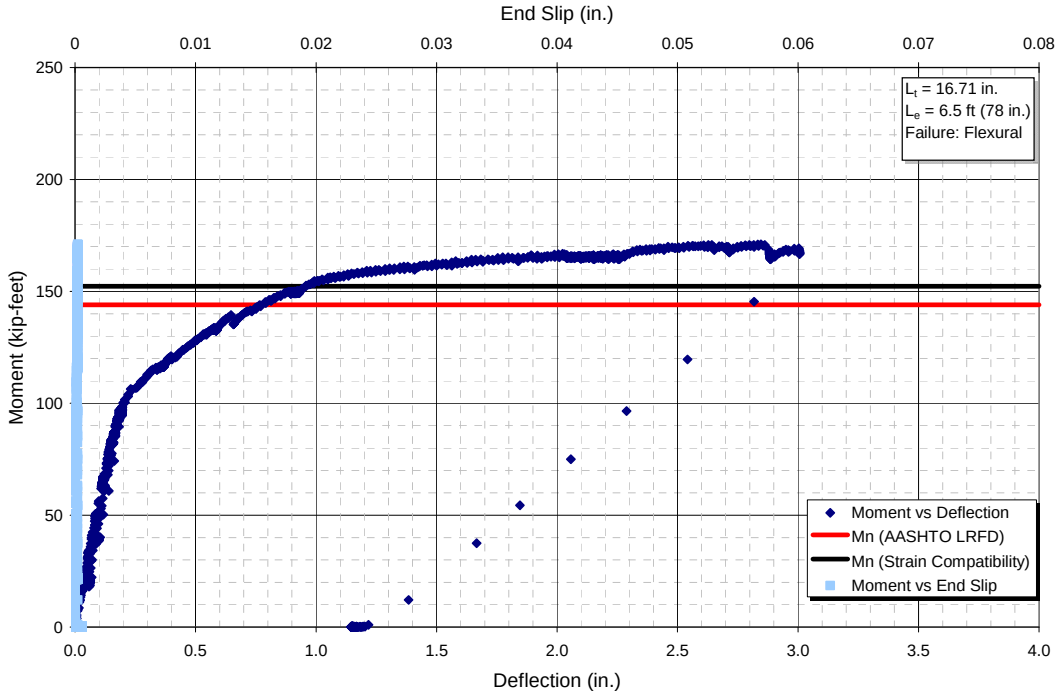

Figure 3.37. Typical Moment versus Deflection Relationship

3.9 Practical Modeling Technique for Transfer Length

A practical modeling technique for transfer length was developed for use in finite element analyses of pretensioned, prestressed concrete members. The modeling technique included the use of nonlinear springs in an effort to model the force versus slip relationship between prestressing strand and the surrounding concrete. As previously discussed, the strand tends to slip along the transfer length until full bond of the strand and concrete is present. However, the force versus slip behavior of the prestressing strand and surrounding concrete was unknown and found to be dependent on the size of the strand and the jacking stress. Two and three-dimensional models were constructed in the analysis and later compared to verify the use of two-dimensional elements with a plane-stress condition. In addition to the type of element used, the size of the elements was varied to verify the mesh size. Although the models were small, only half of each test specimen was modeled since each was symmetrical about its center-line. Figure 3.38 shows a two-dimensional model of one end of the 4 in. by 4 in. control blocks of the top-strand block test specimens, while Figure 3.39 shows a three-dimensional model of the same test specimen. In order to verify the use of two-dimensional elements and the size

of the mesh, a number of two and three-dimensional models with various element sizes were constructed and the results compared. The results showed models with two-dimensional elements to have nearly identical results compared to the three-dimensional models. The results also showed meshes with 2 in., 1 in. and ½ in. elements to have nearly identical results, indicating either of the three mesh sizes to be adequate in the analyses.

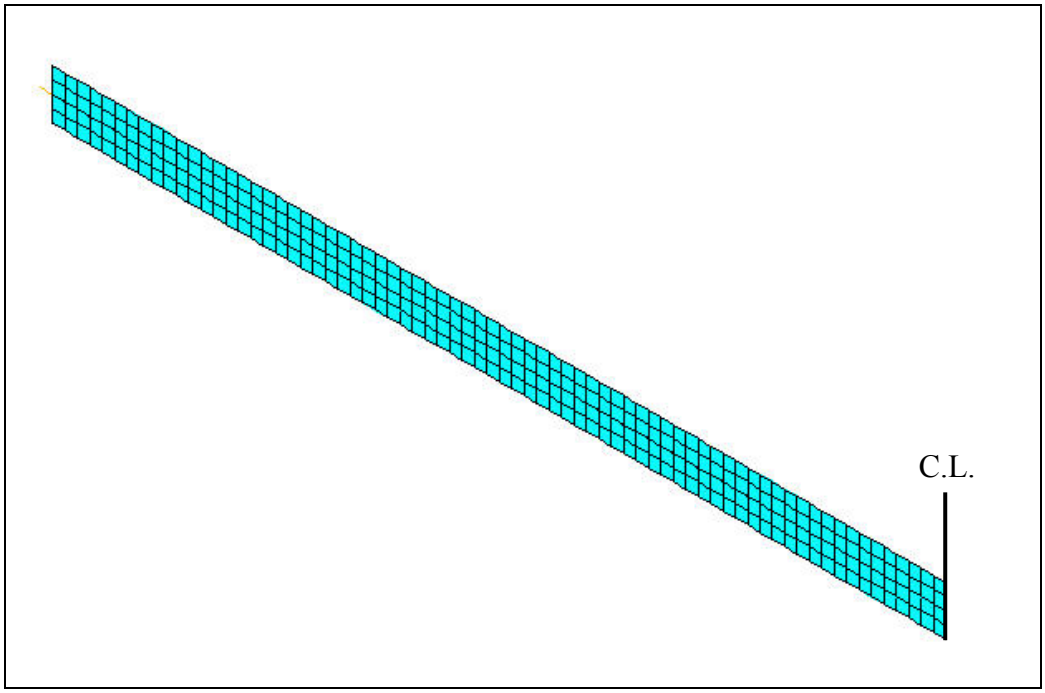

Figure 3.38. Two-dimensional Finite Element Model

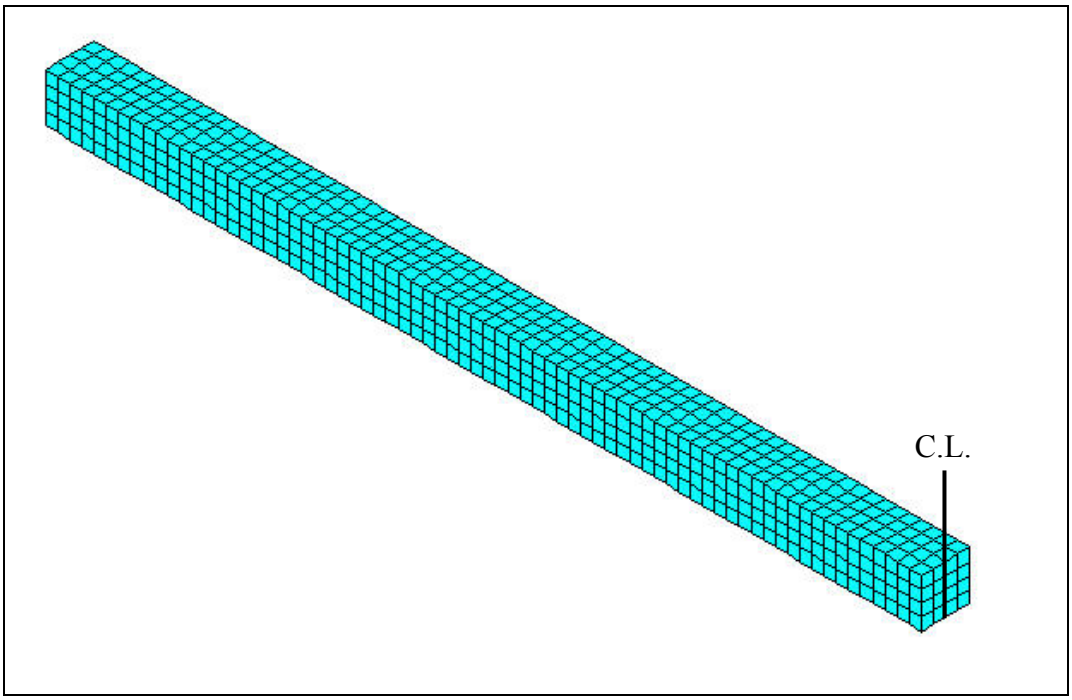

Figure 3.39. Three-dimensional Finite Element Model

As previously mentioned, the force versus slip relationship between the prestressing strand and surrounding concrete was modeled using nonlinear springs. In order to adequately model this behavior, the prestressing strand (represented by truss members) could not be directly attached to nodes connected to the finite elements. This was accomplished by generating a line of duplicate nodes along the line of the prestressing strand. The duplicate nodes were then joined to their counterparts with a longitudinal nonlinear spring. To prevent instabilities, each duplicate node was tied to its counterpart in the vertical direction with master and slave commands. Each model was supported in the longitudinal direction at all nodes located along the center-line of the test specimen. However, only the bottom node was supported in the vertical direction. These boundary conditions allowed for the lateral expansion associated with the Poisson Effect resulting from an axially applied load. Figure 3.40 shows the boundary conditions and the layout of duplicate nodes and corresponding truss members for a generic model. The large arrows represent supports, while the small arrows represent joint ties.

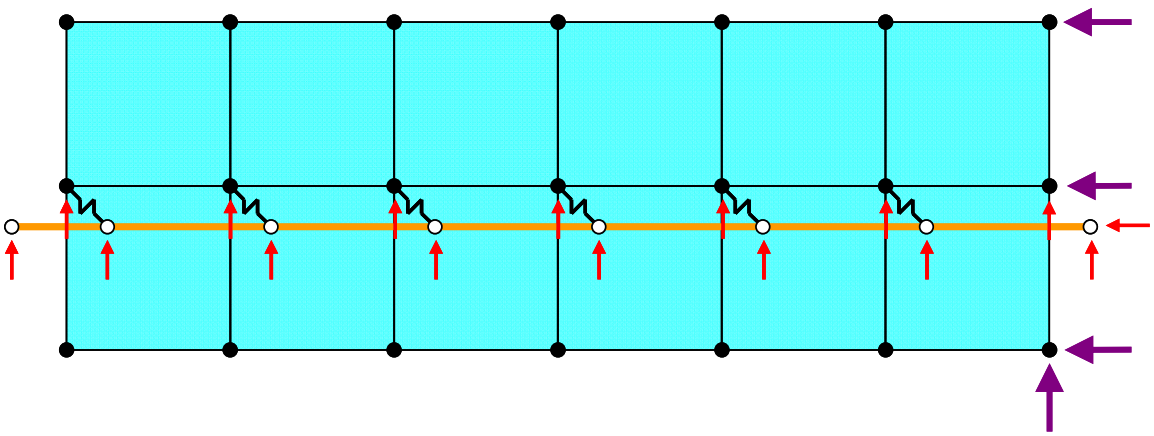

Figure 3.40. Generic Model

The prestressed force was applied to the model using a temperature load added to each of the truss members representing the prestressing strand. When a prestressing strand is pulled in tension, it develops a level of axial tensile strain that is constant throughout its length. Subsequent to the transfer process, the strand tries to contract, but is restrained by the surrounding concrete. If slip between the strand and surrounding concrete did not occur and elastic shortening of the concrete did not take place, the tensile strain in the strand would remain constant. Likewise, a truss member fixed at both ends subjected to a change in temperature also develops a level of constant strain. In the presence of a temperature reduction, the truss member tries to contract, but develops tensile strains because of the restraints at each end. Figure 3.41 shows an example of a temperature load on a truss member with two fixed supports.

$$P = \sigma A = \varepsilon EA$$

$$\varepsilon = \Delta T \alpha$$

$$P = \Delta T \alpha EA$$

$$P = (-1100)\left(6.5x10^{-5}\right)(28500)(0.153) \approx 31.2^{kips}$$

Figure 3.41. Temperature Load on Truss Member

Assuming a fixed-fixed condition at the ends of the truss member, a temperature change of approximately -1100 ºF would produce a strain in the member equivalent to the strain produced from an axial tensile force of 31.2 kips. If perfect bond was present, each truss member representing the prestressing strand would have a force equal to the initial

prestress force minus the loss of force from the elastic shortening of the elements representing the concrete. However, prestressing strand does not have full bond throughout its entire length due to the slip associated with the transfer process. For that reason, the truss member is allowed to shorten and displace relative to the concrete elements, which is represented by the nonlinear springs. At the end of the member, a large amount of slip between the strand and the surrounding concrete would result in a significant loss of prestress force in the strand, but would result in a significant force increase in the nonlinear spring. Moving along the transfer length, the amount of slip between the strand and surrounding concrete reduces, resulting in an increase of force in the stand and a force decrease in the nonlinear spring.

The nonlinear springs used in the finite element models have the capability for nonlinear force versus displacement relationships, however, linear force versus slip relationships were used throughout this study. In order to determine the spring stiffness corresponding to a specific transfer length, a relationship for transfer length and spring stiffness was established. This was accomplished by using a range of spring stiffnesses for each model. Figure 3.42 shows a sample of the linear spring stiffnesses used in this development. It was found that a reduction in spring stiffness resulted in an increase in distance required for the force in the strand to reach its maximum as shown in Figure 3.43. ACI states the transfer length to be the distance required to fully transfer the force in the strand to the member. However, to obtain reasonable results, the transfer length for the models herein was taken as the distance required for the truss member to obtain 99 percent of the maximum force in any one truss member. Figure 3.44 shows a typical plot for the force in the strand against the distance from the end of the member. The horizontal dashed line shows 99 percent of the maximum force in the strand, while the vertical dashed line shows the point at which the force versus location curve intersects the 99 percent plateau, or the transfer length.

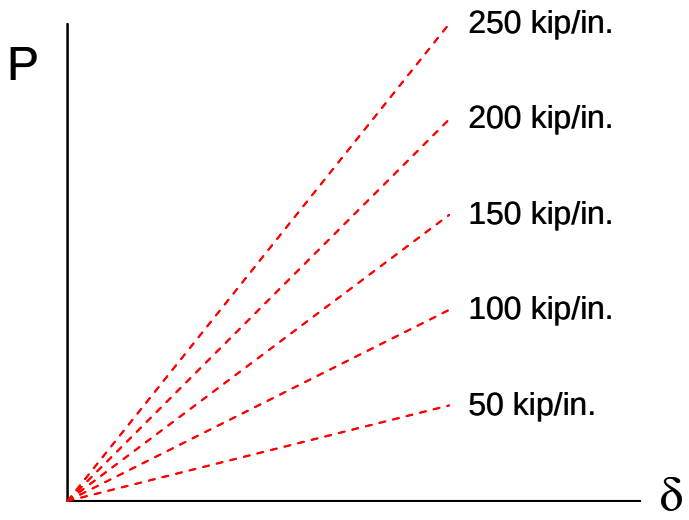

Figure 3.42. Sample Spring Stiffnesses

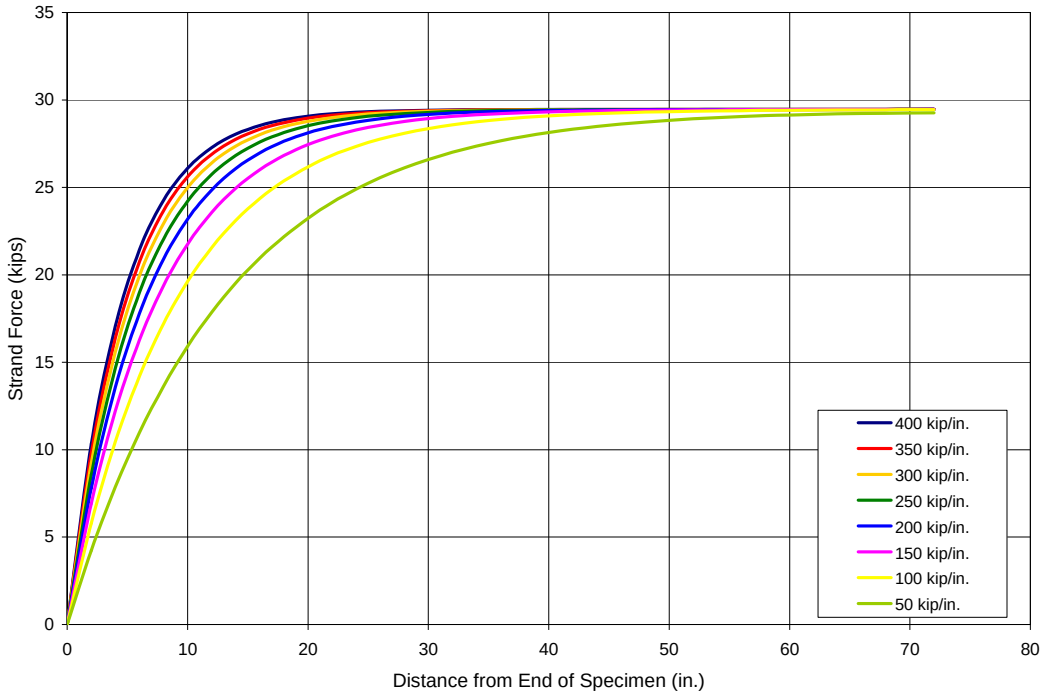

Figure 3.43. Transfer Length versus Spring Stiffness

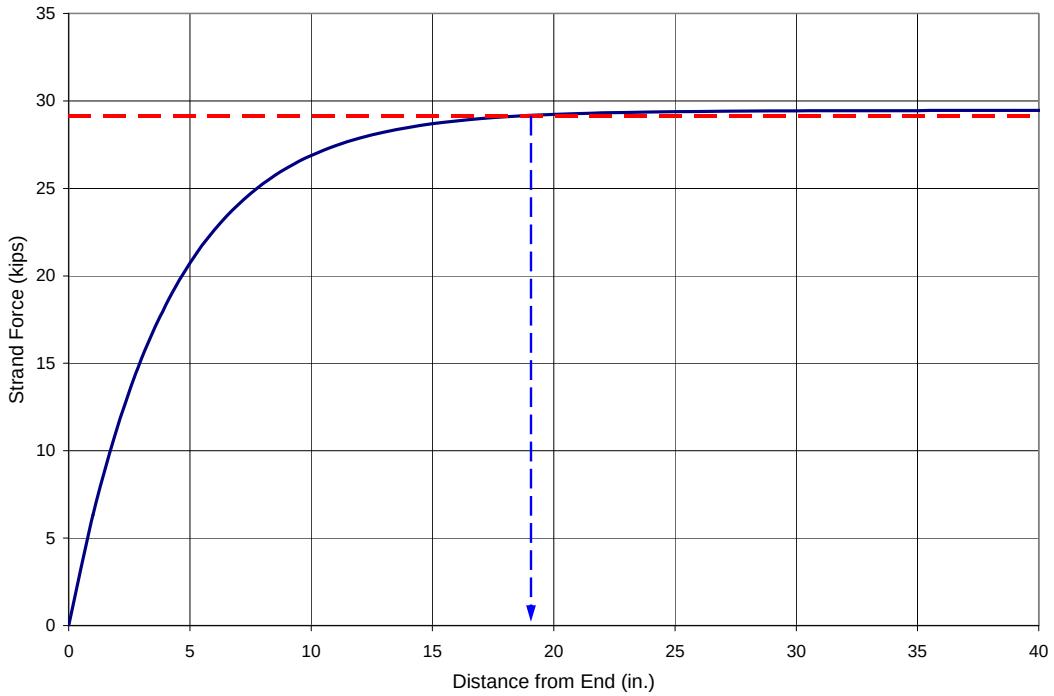

Figure 3.44. Strand Force vs. Distance from End of Member

Subsequent to the determination of each transfer length, the transfer lengths were plotted against each respective spring stiffness as shown in Figure 3.45. This relationship was developed for each test specimen investigated and a best fit line added to each plot. At that point, an engineer could select a spring stiffness for the finite element model based on either experimentally determined or calculated transfer lengths.

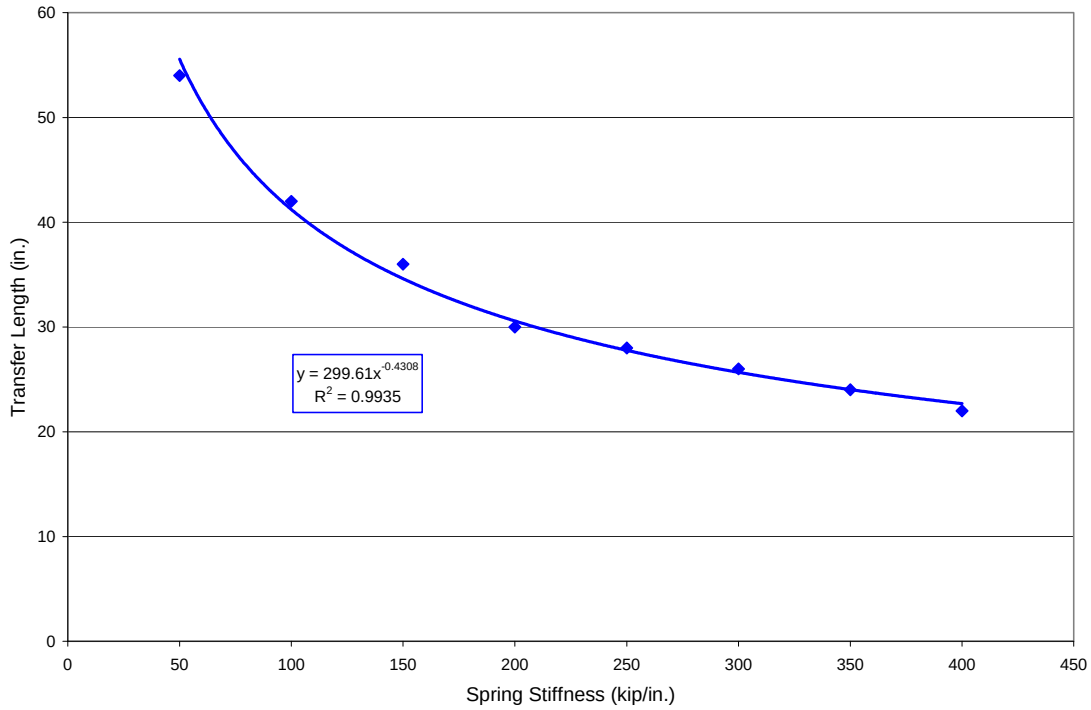

Figure 3.45. Transfer Length versus Spring Stiffness

The nonlinear analysis used in this study was based on the Newton Raphson-Method of convergence. A tolerance of 0.001 and a maximum number of iterations set at 10 were specified. To verify the tolerance used throughout this study, a few models were ran with a tolerance of 0.0001 and were found to have the same results. As previously mentioned, a linear force versus displacement relationship was used for the nonlinear springs, therefore, each analysis was essentially linear, converging in two or three iterations.

4.0 RESULTS AND DISCUSSION

4.1 Transfer Length

4.1.1 Introduction

Transfer lengths were determined for 119 transfer zones from both the T-beam test specimens and the top-strand block test specimens using measurements of concrete surface strains at the time of transfer and one to two weeks thereafter. For consistency, transfer lengths taken at the time of transfer were used in comparisons unless otherwise noted, since the time of the second measurements varied with each set of test specimens. Of the 119 transfer zones, the T-beam test specimens account for 39 transfer zones (20 Dead End, 19 Live End), while the top-strand blocks accounted for the remaining 80 transfer zones (40 Dead End, 40 Live End). In addition to concrete surface strains, end-slip measurements were taken for 57 of the transfer zones at the time of transfer, from which transfer lengths were again determined and later compared to those obtained from surface strain measurements. As previously discussed, end-slip measurements were only taken at the dead end of the specimens due to the strands' tendency to fray at the live end upon transfer.

Historically, transfer length has been shown to be affected by a number of contributing factors such as method of release, strand diameter, effective prestress, concrete strength, strand surface conditions, time, and as-cast vertical location, all of which were discussed in detail in Section 2.4. As were relevant to the determination of and comparison of transfer lengths in this project, the influence of a number of these factors were evaluated. The influence of release method was first looked at, comparing the measured transfer lengths of ends adjacent to flame cutting (Live End) to those adjacent to support abutments (Dead End). The effect of strand strength was compared in a similar manner as was casting orientation for the transfer lengths associated with the T-beam test specimens and the effect of time as initial and second sets of measurements were compared for all transfer zones. Proving to have a significant effect on transfer length measurements, the as-cast vertical location of the strand, also referred to as the top strand effect, was given a large amount of attention in the determination of its influence.

In addition to the factors affecting transfer length, transfer length measurements were compared to the current code provisions from ACI and AASHTO as well as a

number of previously recommended transfer length equations, each of which was discussed in Section 2.2. The values of effective and initial prestress used in the comparisons were determined by subtracting the amount of prestress losses calculated by current AASHTO provisions. Historically, ACI and AASHTO have only included effective prestress and the strand diameter in the calculation of transfer lengths. However, over the past 35 years, a number of researchers have recommended various equations also taking into account concrete strength and recently Peterman (2007) has recommended an equation incorporating the as-cast vertical location and strand diameter, but neglects stress in the strand and concrete strength. With the absence of an equation incorporating the four main contributing factors, an equation was also developed taking into account effective prestress, concrete strength, strand diameter, and the as-cast vertical location.

4.1.2 Influence of Release Method

A number of researchers have shown transfer lengths of strands released by and adjacent to a flame cutting process to be longer with respect to those located away from the flame cutting process or adjacent to support abutments. This increase is important in the development of transfer length equations. In the past, some equations have been derived based on a gradual release method, while the standard method of release used in the prestressing industry is typically the flame cutting process. Thus, the influence of release method is vital in the derivation of a conservative transfer length equation, which is shown in Table 4.1 for the T-beam test specimens with both casting orientations.

The average increase of transfer lengths at the live ends versus transfer lengths at the dead ends for the T-beam test specimens cast with a normal orientation was 45 percent, while those cast with an inverted orientation increased by 49 percent. Note that transfer lengths for members 2.300.5N.U and 2.300.5S.U, both containing Grade 300 prestressing strands and cast with an inverted orientation, increased by 84 and 95 percent, respectively. There is a possibility these excessively long values were influenced by the high levels of bleed water, as transfer lengths have been shown to increase with highly fluid mixes. This only occurred with the beams containing Grade 300 strands and may be a result of the larger prestress force coupled with a mix of high fluidity. Because of the excessive transfer lengths, there was speculation of inadequate consolidation of the

concrete around the strand. For verification purposes, autopsies were performed on beams from Pour 1 and Pour 2 to compare the interface between the prestressing steel and surrounding concrete. No differences were observed between the concrete around the strands following the autopsies. Therefore, it was concluded that the concrete surrounding the strands had adequate consolidation.

Table 4.1. Influence of Release Method (T-beam Test Specimens)

		f_{sj}	f_{si}	f_{se}	f'_{ci}	f'_c	Transfer Length (in.)		
	Beam	ksi	ksi	ksi	psi	psi	Live	Dead	Live/Dead
Normal	1.270.5N.R	180.9	168.4	157.0	4900	6500	16.7	12.3	1.36
	2.270.5N.R	180.9	168.4	162.3	5300	6400	18.1	12.5	1.46
	3.270.5S.R	180.9	169.1	158.6	6000	8200	21.1	13.6	1.55
	4.270.5S.R	180.9	168.3	157.8	4900	6300	17.5	15.5	1.13
	5.270.5S.R	202.5	187.5	162.5	5000	6500	20.2	12.8	1.58
	6.270.5S.R	202.5	188.8	174.3	6400	8300	20.7	16.7	1.24
	1.300.5N.R	201.0	186.9	175.8	4900	6500	NA	14.6	NA
	2.300.5N.R	201.0	187.0	180.0	5300	6400	21.2	14.2	1.50
	3.300.5S.R	201.0	187.7	176.2	6000	8200	20.8	13.5	1.53
	4.300.5S.R	201.0	186.9	175.5	4900	6300	18.4	14.1	1.30
	5.300.5S.R	225.0	208.1	181.2	5000	6500	20.6	13.9	1.47
	6.270.6N.R	202.5	188.4	173.0	6400	8300	19.3	10.7	1.80
	Average Increase								**1.45**
Inverted	2.270.5N.U	180.9	168.4	161.7	5300	6400	30.2	24.5	1.23
	3.270.5S.U	180.9	169.1	157.5	6000	8200	25.6	19.8	1.29
	5.270.5S.U	202.5	187.5	162.4	5000	6500	26.3	19.9	1.32
	6.270.5S.U	202.5	188.8	173.6	6400	8300	21.3	17.8	1.20
	2.300.5N.U	201.0	187.0	179.3	5300	6400	43.3	23.6	1.84
	3.300.5S.U	201.0	187.7	175.1	6000	8200	41.1	21.1	1.95
	5.300.5S.U	225.0	208.1	180.9	5000	6500	24.3	19.2	1.27
	6.270.6N.U	202.5	188.4	172.4	6400	8300	23.1	12.9	1.79
	Average Increase								**1.49**

In addition to the tabulated values, Figure 4.1 also shows the relationship of transfer lengths at the live end of a test specimen compared to the transfer lengths at the dead end of a test specimen with transfer lengths measured in strand diameters. Again, a general increase is shown for all T-beam test specimens with the largest differences in live and dead end measurements shown in the inverted beams. All live and dead end transfer lengths for beams cast with a normal orientation fall below current code provisions of ACI and AASHTO, $50d_b$, $f_{se}/3$, and $60d_b$, and although all of the dead end transfer lengths of the inverted beams fall below code values, five live end transfer lengths exceed the $50d_b$ value from ACI, three of which exceeded the $60d_b$ value from AASHTO. These excessive transfer lengths could prove problematic in the design for shear in prestressed concrete members.

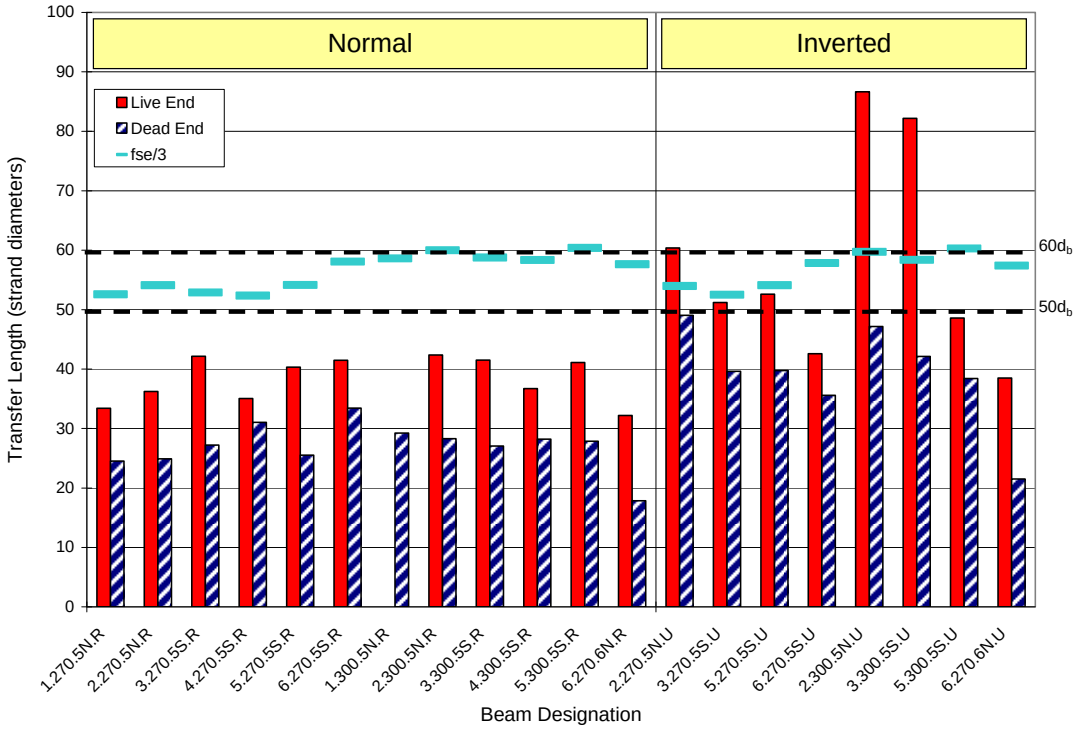

Figure 4.1. Influence of Release Method on Transfer Length (T-beams)

In addition to the T-beam test specimens, the transfer lengths at the live and dead ends of the top-strand blocks were also compared and plotted versus current code provisions. Table 4.2 lists the transfer lengths for both the live and dead ends of each set of top-strand blocks as well as the corresponding steel stresses and concrete strengths. The average increase in transfer length was one percent for Pour 1, 19 percent for Pour 2, 9 percent for Pour 3, and 13 percent for Pour 4. The largest increase among all top-strand transfer zones was Strand H in Pour 2. This strand was located 2 in. from the bottom of the specimen, while the two strands in the T-beam test specimens exhibiting excessive increases in transfer length were located 2 in. from the top of the as-cast specimen. It is unknown as to the cause of the increase, as the top-strand blocks were typically cast with a much stiffer concrete.

Complimenting Table 4.2, Figures 4.2 though 4.5 give a graphical presentation of the data compared with current code provisions. As with the T-beam test specimens, a general increase was seen for live end transfer lengths compared to dead end transfer lengths, with only a few exceptions. Contrary to the T-beam test specimens, the majority of the transfer lengths fell at or below current code provisions. However, values do not

remain constant and show an additional trend of decreasing transfer length from left to right on the plots. This is discussed with greater detail in Section 4.1.8.

Overall, the comparison of transfer lengths for live and dead ends was in agreement with previous research. An average overall increase in transfer length of 22 percent was seen between live and dead ends, showing the necessity of measurements taken adjacent to the ends of test specimens having a sudden release to be incorporated in the development of transfer length equations.

Table 4.2. Influence of Release Method (Top-strand Block Test Specimens)

		f_{sj}	f_{si}	f_{se}	f'_{ci}	f'_c	Transfer Length (in.)		
	Strand	ksi	ksi	ksi	psi	psi	Live	Dead	Live/Dead
Pour 1	A	202.5	188.7	178.0	4800	5900	21.2	17.8	1.19
	B	202.5	188.7	178.0	4800	5900	19.6	16.3	1.20
	C	202.5	188.7	178.0	4800	5900	18.3	17.7	1.04
	D	202.5	188.7	178.0	4800	5900	19.0	16.4	1.16
	E	202.5	188.7	178.0	4800	5900	18.8	15.8	1.18
	F	202.5	188.4	177.5	4800	5900	28.9	46.8	0.62
	G	202.5	188.4	177.5	4800	5900	25.7	30.2	0.85
	H	202.5	188.4	177.5	4800	5900	25.4	24.7	1.03
	I	202.5	186.7	174.6	4800	5900	23.7	30.8	0.77
	J	202.5	186.7	174.6	4800	5900	25.4	24.2	1.05
	Average Increase								**1.01**
Pour 2	A	202.5	189.6	179.9	5700	6600	19.4	15.9	1.22
	B	202.5	189.6	179.9	5700	6600	19.6	15.5	1.26
	C	202.5	189.6	179.9	5700	6600	18.3	16.1	1.13
	D	202.5	189.6	179.9	5700	6600	15.0	14.5	1.04
	E	202.5	189.6	179.9	5700	6600	16.1	14.5	1.11
	F	202.5	189.3	179.4	5700	6600	23.4	20.4	1.15
	G	202.5	189.3	179.4	5700	6600	21.7	18.9	1.15
	H	202.5	189.3	179.4	5700	6600	22.4	14.3	1.57
	I	202.5	187.7	176.8	5700	6600	21.5	19.6	1.09
	J	202.5	187.7	176.8	5700	6600	19.2	16.3	1.18
	Average Increase								**1.19**
Pour 3	A	202.5	189.0	179.4	6100	7000	22.6	21.1	1.07
	B	202.5	189.0	179.4	6100	7000	23.5	17.3	1.36
	C	202.5	189.0	179.4	6100	7000	19.0	16.7	1.14
	D	202.5	189.0	179.4	6100	7000	18.5	16.4	1.13
	E	202.5	189.0	179.4	6100	7000	17.6	16.2	1.08
	F	202.5	188.8	179.0	6100	7000	21.3	34.2	0.62
	G	202.5	188.8	179.0	6100	7000	24.0	24.0	1.00
	H	202.5	188.8	179.0	6100	7000	22.6	17.4	1.30
	I	202.5	187.0	176.2	6100	7000	25.2	21.8	1.15
	J	202.5	187.0	176.2	6100	7000	25.4	24.4	1.04
	Average Increase								**1.09**
Pour 4	A	202.5	188.0	177.2	5000	6100	29.3	30.9	0.95
	B	202.5	188.0	177.2	5000	6100	23.2	21.4	1.08
	C	202.5	188.0	177.2	5000	6100	20.7	19.0	1.09
	D	202.5	188.0	177.2	5000	6100	20.0	17.3	1.16
	E	202.5	188.0	177.2	5000	6100	18.8	16.5	1.14
	F	202.5	187.7	176.7	5000	6100	25.0	25.7	0.97
	G	202.5	187.7	176.7	5000	6100	25.5	21.3	1.20
	H	202.5	187.7	176.7	5000	6100	30.5	19.1	1.60
	I	202.5	185.8	173.7	5000	6100	28.7	30.8	0.93
	J	202.5	185.8	173.7	5000	6100	29.7	25.5	1.17
	Average Increase								**1.13**

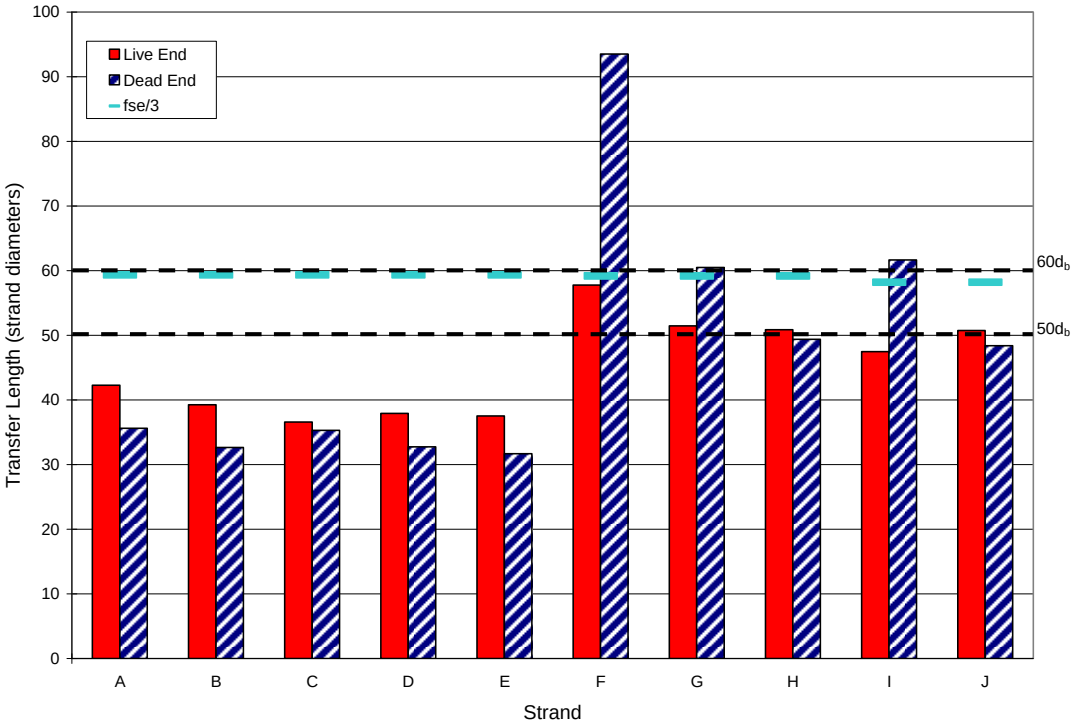

Figure 4.2. Influence of Release Method on Transfer Length (TSB-Pour 1)

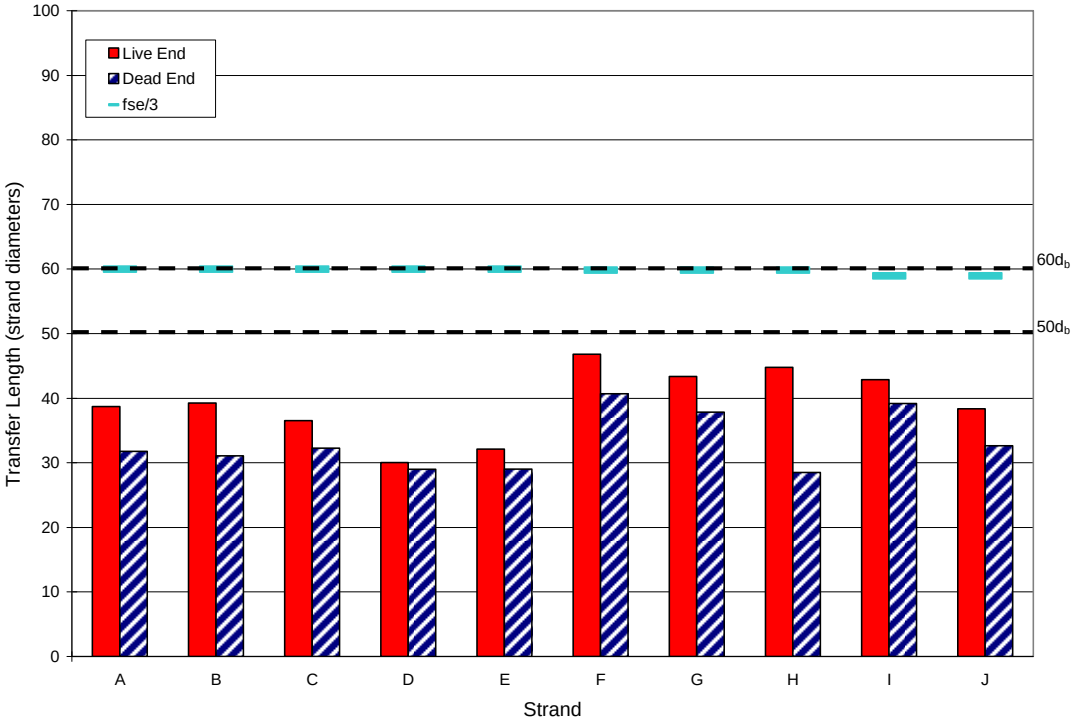

Figure 4.3. Influence of Release Method on Transfer Length (TSB-Pour 2)

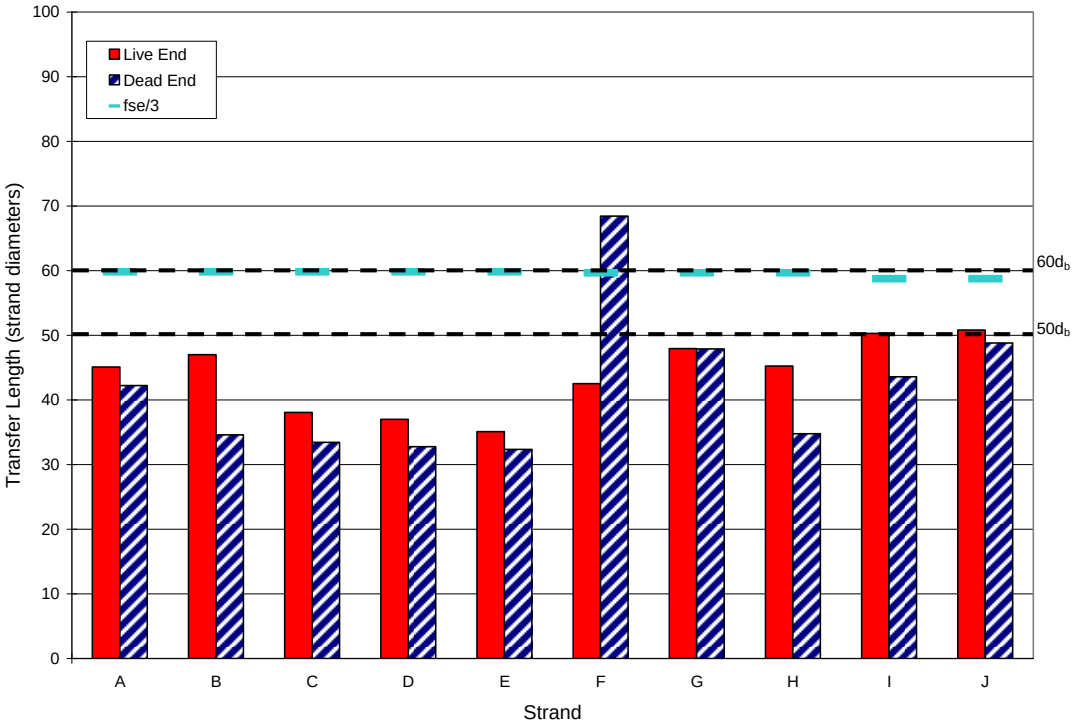

Figure 4.4. Influence of Release Method on Transfer Length (TSB-Pour 3)

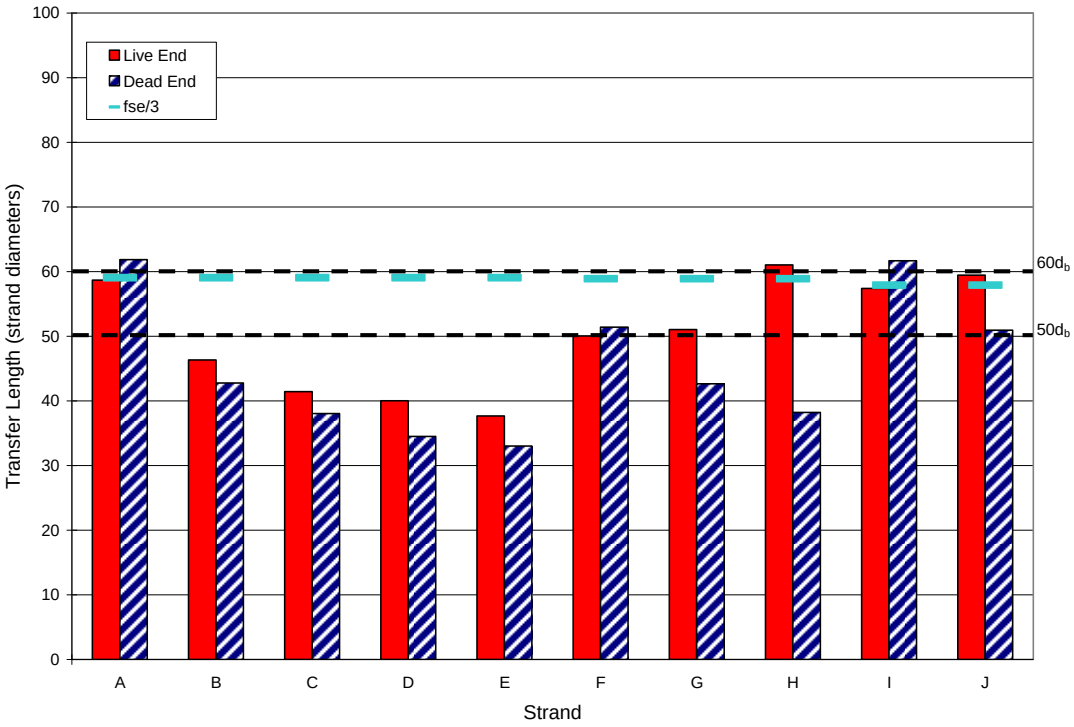

Figure 4.5. Influence of Release Method on Transfer Length (TSB-Pour 4)

4.1.3 Influence of Strand Strength

As the primary objective, the anticipated industry use of the Grade 300 strand relied on a number of items in question, one of which was the transfer length of Grade 300 prestressing strands compared to the traditionally used Grade 270 strand and more importantly, the current code provisions. As with the influence of release method on transfer length, it was believed that an increase in strand strength, which resulted in larger effective prestress values, would also result in an increase in transfer lengths. Grade 300 strand allows for an 11 percent increase in initial prestress as compared to the traditional Grade 270 strand, which was expected to increase transfer lengths. Table 4.3 lists the transfer lengths of both the Grade 300 and Grade 270 strands also giving ratios of the results for each. It should be noted that Pour 6 did not include Grade 300 strands, but used Grade 270, 0.6 in. diameter strands instead and was not included in average calculations. The average increase of transfer lengths for Grade 300 strands versus Grade 270 strands of the T-beam test specimens cast with a normal orientation was 6 percent for both the live and dead ends, respectively. The average increase of transfer lengths for Grade 300 strands verses Grade 270 strand of the T-beams cast with an inverted orientation was 32 percent at the live ends, but failed to show an increase at the dead ends. Note that increases of 43 percent and 61 percent were seen in Pour 2 and Pour 3 for the inverted beams. As was discussed in the previous section, it is unknown as to the cause of this behavior, but is believed to be a combination of an increase in strand strength coupled with the fluidity of the concrete mix.

Table 4.3. Influence of Strand Strength

				Transfer Length (in.)				Ratios	
		f'_{ci}	f'_c	Live		Dead		Live	Dead
	Pour	psi	psi	300	270	300	270	300/270	300/270
Normal	1	4900	6500	NA	16.7	14.6	12.3	NA	1.19
	2	5300	6400	21.2	18.1	14.2	12.5	1.17	1.14
	3	6000	8200	20.8	21.1	13.5	13.6	0.98	0.99
	4	4900	6300	18.4	17.5	14.1	15.5	1.05	0.91
	5	5000	6500	20.6	20.2	13.9	12.8	1.02	1.09
	6	6400	8300	19.3	20.7	10.7	16.7	0.93	0.64
	Average Increase							**1.05**	**1.06**
Inverted	2	5300	6400	43.3	30.2	23.6	24.5	1.43	0.96
	3	6000	8200	41.1	25.6	21.1	19.8	1.61	1.06
	5	5000	6500	24.3	26.3	19.2	19.9	0.92	0.97
	6	6400	8300	23.1	21.3	12.9	17.8	1.08	0.73
	Average Increase							**1.32**	**1.00**

In conjunction with Table 4.3, Figures 4.6 and 4.7 show the comparison of transfer lengths, in strand diameters, for the T-beam test specimens cast with a normal and inverted orientation, respectively. The transfer lengths shown in Figure 4.6 all fall below both ACI and AASHTO values, with transfer lengths of Grade 300 strands having slightly larger values. Contrary to the transfer length of the T-beam test specimens cast with a normal orientation, five of the transfer lengths for the T-beam test specimens cast with an inverted orientation exceeded the ACI provision of $50d_b$, three of which exceeded the AASHTO provision of $60d_b$. As previously mentioned, the live end transfer lengths of the Grade 300 strand in Pour 2 and Pour 3 far exceed other measurements as well as code provisions. As shown on Figures 4.6 and 4.7, Pours 1 through 4 used a jacking stress of $0.67f_{pu}$, while Pours 5 and 6 used a jacking stress of $0.75f_{pu}$. It is reasonable to recommend that if the Grade 300 strands used in Pour 2 and Pour 3 were initially stressed to $0.75f_{pu}$, the transfer lengths could have very well been $97d_b$ and $92d_b$, respectively, by multiplying the original values by the ratio of initial prestresses.

Overall, an average increase of 10 percent was shown for all transfer lengths of Grade 300 strand compared to transfer lengths of the Grade 270 strand as expected. For T-beam test specimens cast with a normal orientation, all measured values fell below current code provisions however for T-beam test specimens cast with an inverted orientation, some of the measured transfer lengths exceeded the current code provisions, in the predicted cases of Pours 2 and 3, by almost 95 percent. Thus, results have shown strands cast near the as-cast top of the test specimen to exhibit longer transfer lengths regardless of strand grade or beam end.

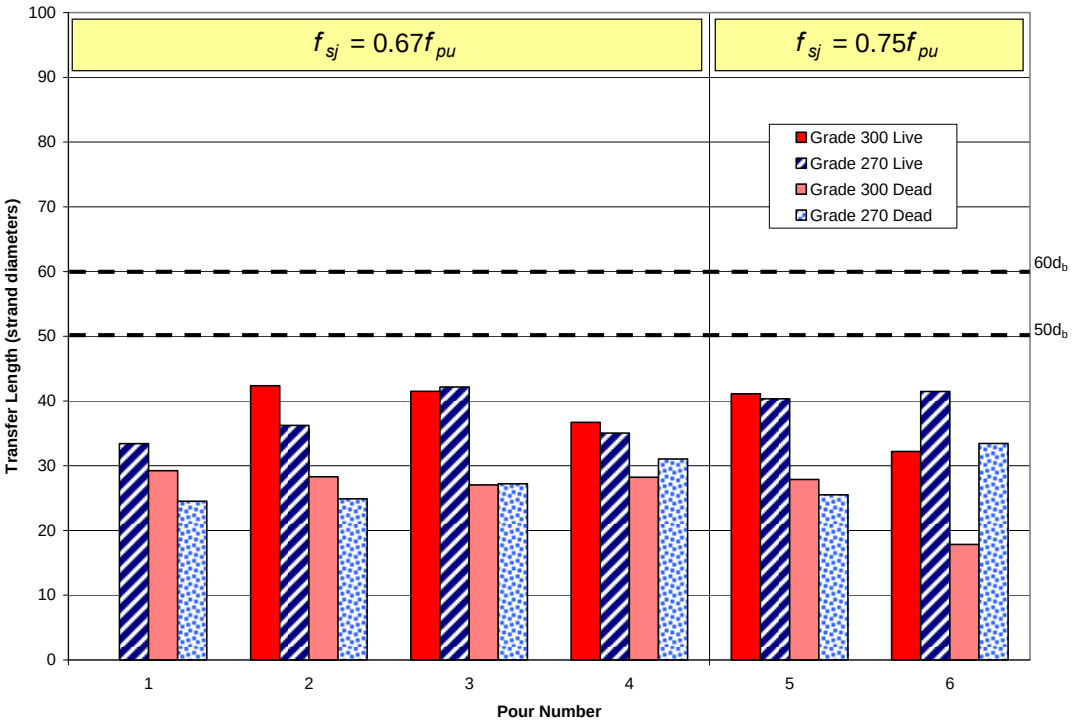

Figure 4.6. Influence of Strand Grade (T-beams – Normal Orientation)

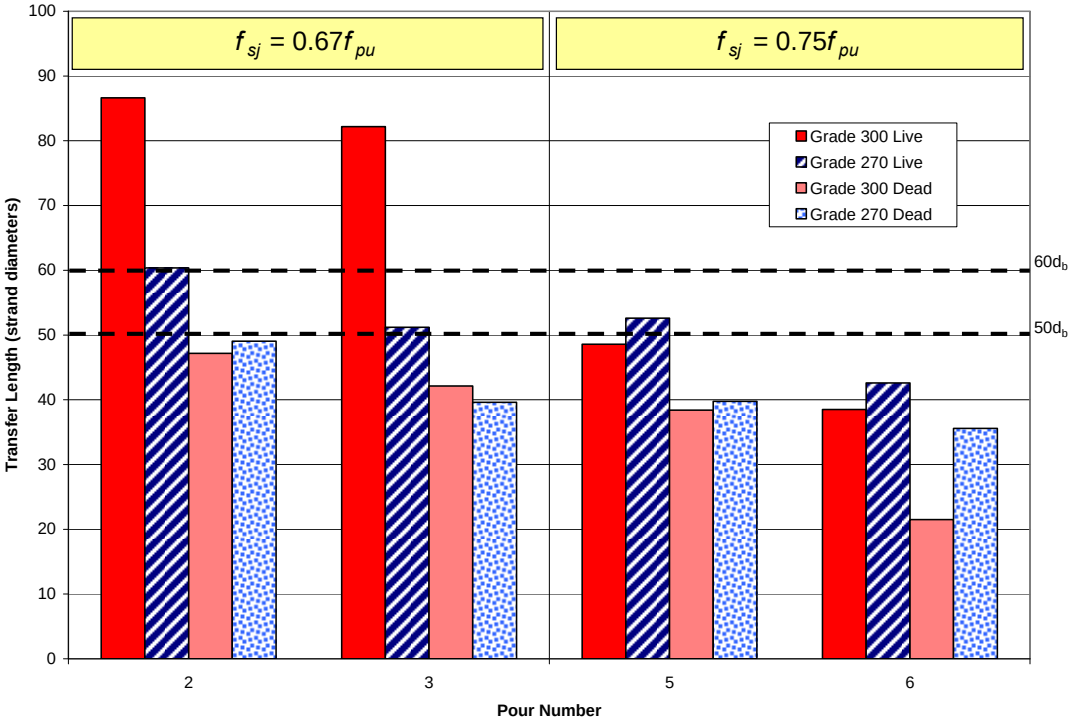

Figure 4.7. Influence of Strand Grade (T-beams – Inverted Orientation)

4.1.4 Influence of Strand Diameter/Area

Strand diameter has been shown to influence transfer length by a number of researchers. Most have found transfer length to increase with strand diameter, while some have shown transfer lengths to decrease when using 0.6 in. diameter prestressing strands. Three strand types were used throughout this study, including ½ in. regular, ½ in. super, and 0.6 in. diameter strands. The majority of the test specimens were constructed with ½ in. regular or ½ in. super strands, with only two T-beam test specimens containing 0.6 in. diameter strands, so no definitive conclusions with respect to 0.6 in. diameter strands and their influence on transfer length could be made, although transfer lengths did appear to decrease.

Table 4.4 lists the average transfer length measurements with respect to strand area and diameter, along with standard deviation as a measure of variability for the data. Maximum and minimum values for measurements taken at the live end, dead end, and both ends combined were also included. Figure 4.8 shows each transfer length measurement plotted with respect to strand diameter as well as averages plus and minus two standard deviations denoted by the red bars. Assuming a normal distribution, the range produced by the average plus and minus two standard deviations would include approximately 95 percent of the data. The total average transfer length for the ½ in. diameter strands was 21.3 in. with a standard deviation of 6.0 in. The total average transfer length for the 0.6 in. diameter strands was 16.5 in. with a standard deviation of 5.0 in. While strand diameter may be a contributing factor in the determination of transfer lengths, based on the scatter amongst transfer length measurements shown in Figure 4.8, it is unreasonable to say transfer length is solely or primarily dependent on strand diameter.

In addition to strand diameter, each transfer length measurement was also plotted against the corresponding strand area as shown in Figure 4.9. Again average transfer lengths plus and minus two standard deviations are also shown along with the experimental data by the red bars. The total average transfer length for the ½ in. diameter regular strands was 20.8 in. with a standard deviation of 6.7 in. The total average transfer length for the ½ in. diameter super strands was 21.6 in. with a standard deviation of 5.3 in. and the total average transfer lengths for the 0.6 in. diameter strands was 16.5 in. with

a standard deviation of 5.0 in. As with strand diameter, there is no significant trend indicating transfer length to be solely or primarily dependent on the area of the strand. As previously discussed with other contributing factors, the effect of casting position could be influential in the amount of scatter associated with the transfer length data plotted against strand diameter and strand area. With respect to historical research that has shown transfer length to be dependent upon strand diameter, the diameter of the strand was still considered in the derivation of the proposed transfer length equation in Section 4.1.10.

Table 4.4. Influence of Strand Diameter and Strand Area

		Transfer Lengths (in.)				
		Strand Area ($in.^2$)			Diameter (in.)	
		0.153	0.167	0.217	0.5	0.6
Live	AVE	22.1	23.4	21.2	22.9	21.2
	STD	5.7	4.7	1.9	5.2	1.9
	MAX	43.3	41.1	23.1	43.3	23.1
	MIN	15.0	17.5	19.3	15.0	19.3
Dead	AVE	19.6	19.8	11.8	19.7	11.8
	STD	7.3	5.2	1.1	6.2	1.1
	MAX	46.8	34.2	12.9	46.8	12.9
	MIN	12.3	12.8	10.7	12.3	10.7
Total	AVE	20.8	21.6	16.5	21.3	16.5
	STD	6.7	5.3	4.9	6.0	4.9
	MAX	46.8	41.1	23.1	46.8	23.1
	MIN	12.3	12.8	10.7	12.3	10.7

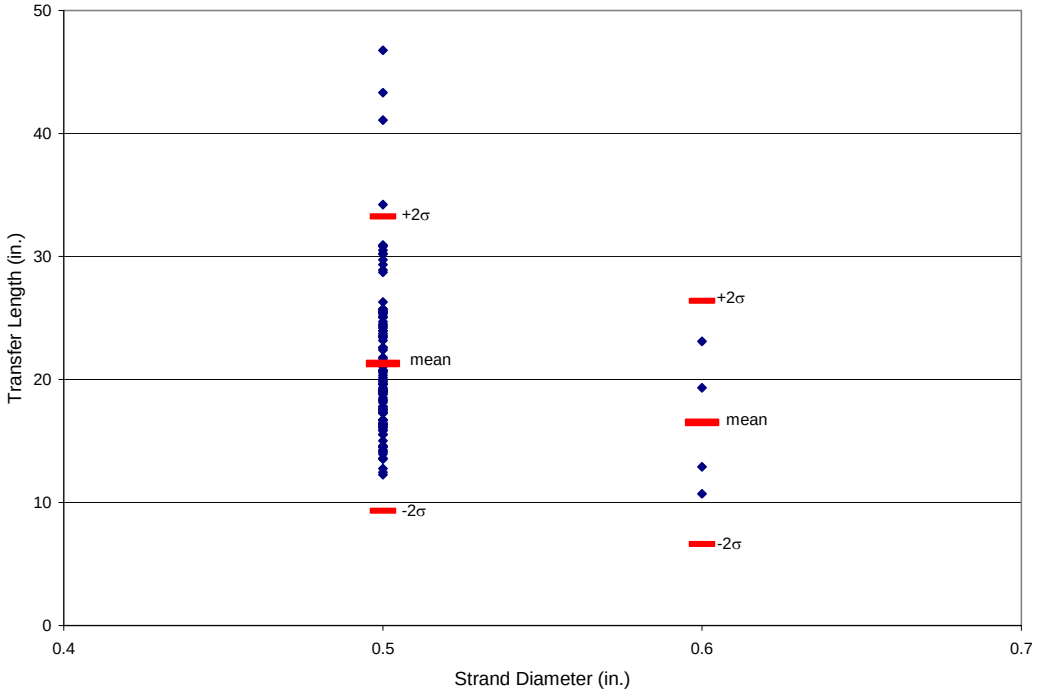

Figure 4.8. Influence of Strand Diameter

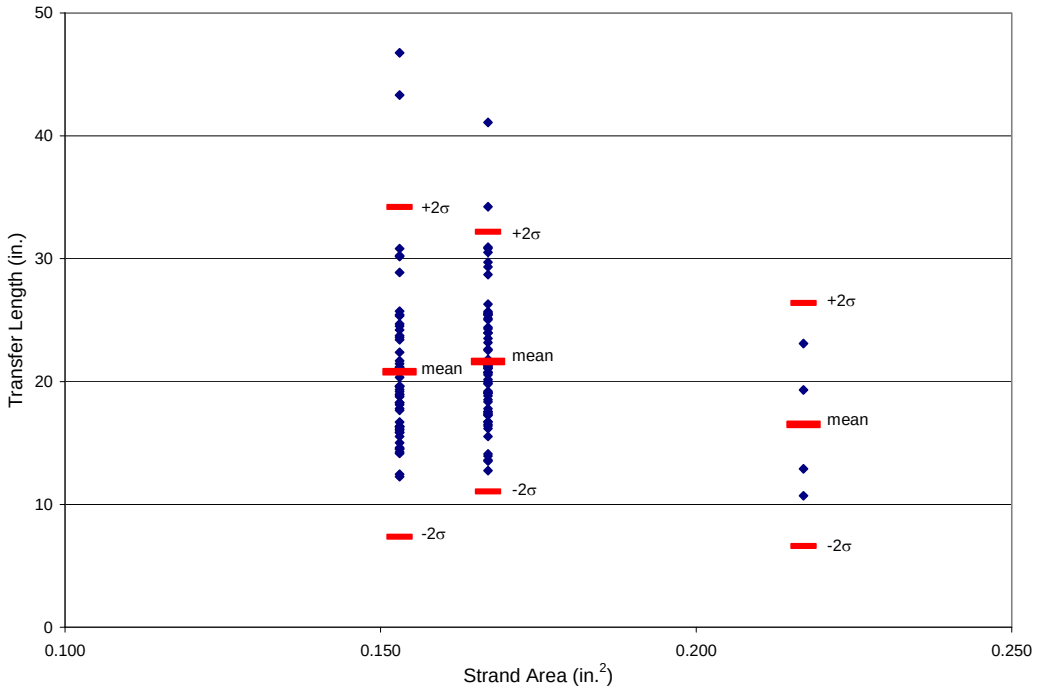

Figure 4.9. Influence of Strand Area

4.1.5 Influence of Effective Prestress

The effective prestress f_{se} (stress in the strand after all losses) has been used in the calculation of transfer length since the implementation of Equation (2-2) in the ACI Building Code, however, research over the past few decades has shown transfer lengths to be more dependent on the initial prestress f_{si} (stress in the strand just after transfer) rather than the effective prestress. In retrospect, using the initial prestress in place of the effective prestress seems more logical, since the initial prestress is the stress in the strand transferred to the surrounding concrete. In either case, a number of researchers have shown transfer length to increase with effective and initial prestress. For that reason, two levels of prestress were used throughout this study, $0.67f_{pu}$ and $0.75f_{pu}$, for some level of variability in the stress at transfer between test specimens. Figure 4.10 shows the relationship between the effective prestress and transfer length while Figure 4.11 shows the relationship between the initial prestress and transfer length. In either case, a significant amount of scatter exists, failing to produce any definitive trends relating transfer length to effective or initial prestress. As with strand diameter, transfer lengths have shown a significant tendency to increase with increased levels of prestress. Although no definitive trends exist from this study relating strand stress and transfer length, the initial prestress remained a factor in the derivation of the proposed transfer length equation in Section 4.1.10.

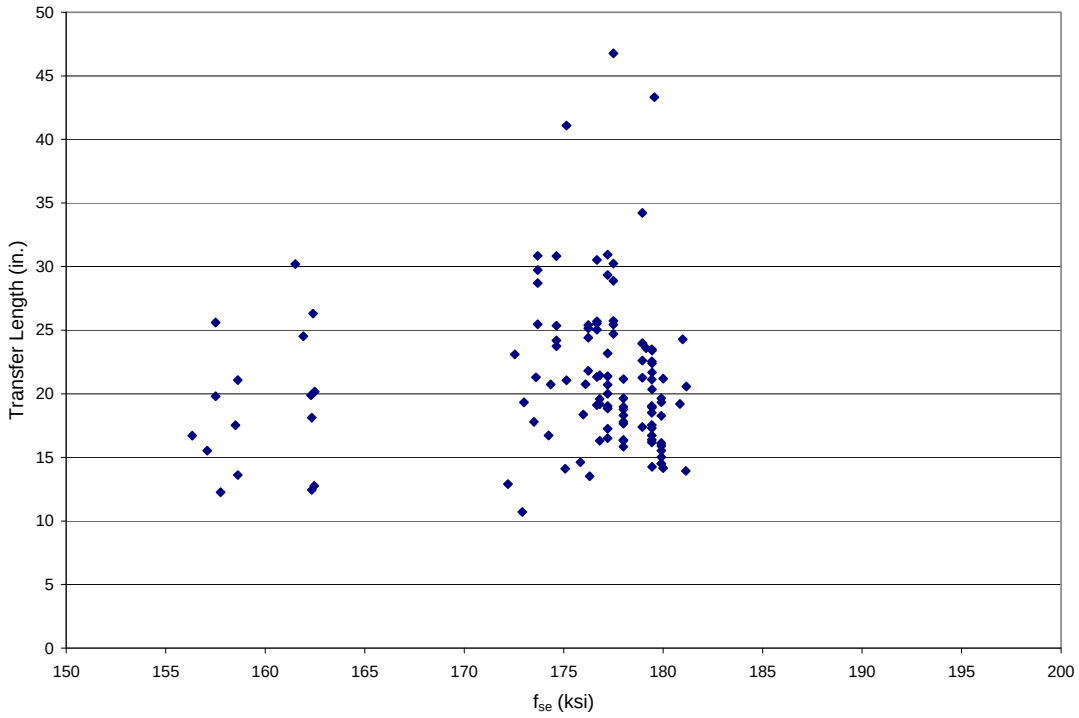

Figure 4.10. Influence of Effective Prestress

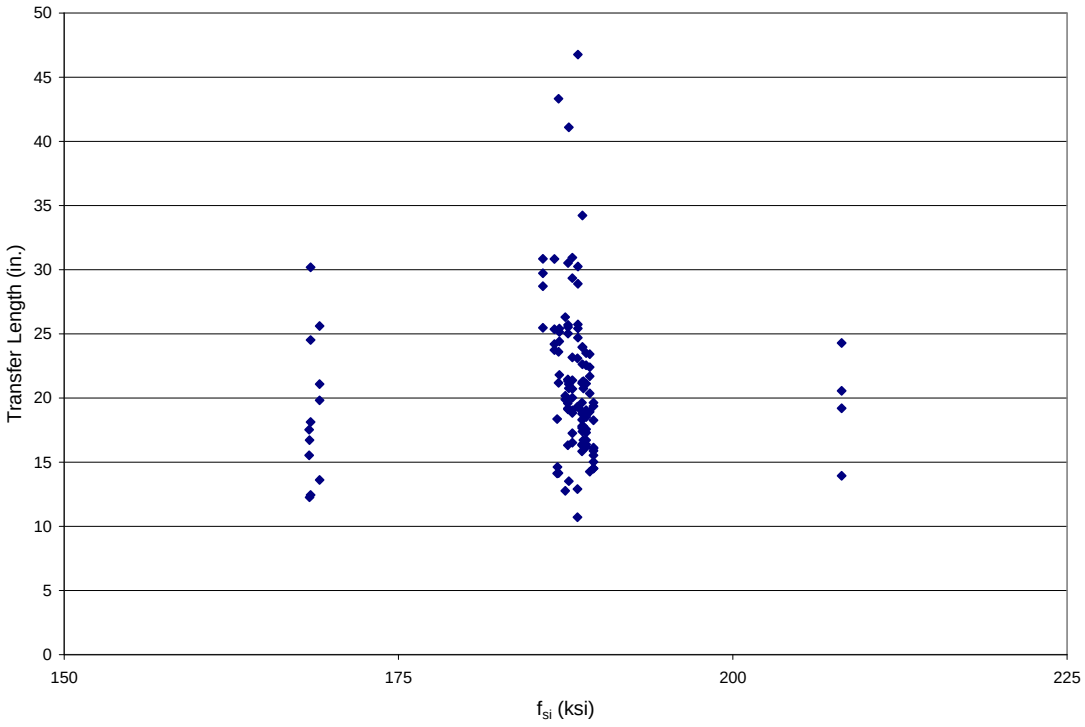

Figure 4.11. Influence of Initial Prestress

4.1.6 Influence of Concrete Strength

Although the current code provisions do not account for the strength of concrete, research has shown an increase in concrete strength reduces transfer length, especially those in excess of 10,000 psi. Of the equations proposed by various researchers over the past few decades, the majority incorporate the concrete strength at transfer or the square root of the concrete strength at transfer in the denominator of each equation. Among the 10 sets of test specimens cast in this study, eight different concrete strengths existed at the time of transfer as shown in Table 4.5. The concrete strengths ranged from 4800 psi to 6400 psi. In comparison to the achievable concrete strengths, this range is somewhat small, but was still considered in the evaluation of factors influencing transfer lengths

Average transfer lengths ranged from 14.1 in. to 28.2 in. with standard deviations as high as 9.8 in. Table 4.5 lists the average transfer length for each concrete strength at the live end, the dead end, and both ends combined. The standard deviations as well as the maximum and minimum values are also listed showing the level of variability in the measurements. In conjunction with Table 4.5, Figure 4.12 plots each transfer length measurement against the square root of each corresponding concrete strength. The data shows a significant amount of scatter, but does show a slight trend of decreasing transfer length with an increase in concrete strength at transfer. As previously noted, the range of concrete strengths was very small, but considered typical with respect to those used in the bridge industry therefore the effect of high strength concretes was not investigated in this study. Based on prior research, as with the stress in the strand and strand diameter, the concrete strength was included in the derivation of the proposed transfer length equation in Section 4.1.10.

Table 4.5. Influence of Concrete Strength

		Transfer Lengths (in.)							
		Concrete Strength (psi)							
		4800	4900	5000	5300	5700	6000	6100	6400
Live	AVE	22.6	17.5	24.5	28.2	19.6	27.1	22.0	21.1
	STDEV	3.5	0.7	3.9	9.8	2.6	8.3	2.6	1.4
	MAX	28.9	18.4	30.5	43.3	23.4	41.1	25.4	23.1
	MIN	18.3	16.7	18.8	18.1	15.0	20.8	17.6	19.3
Dead	AVE	24.1	14.1	21.0	18.7	16.6	17.0	20.9	14.5
	STDEV	9.3	1.2	5.4	5.4	2.1	3.5	5.3	2.9
	MAX	46.8	15.5	30.9	24.5	20.4	21.1	34.2	17.8
	MIN	15.8	12.3	12.8	12.5	14.3	13.5	16.2	10.7
Total	AVE	23.3	15.6	22.7	23.4	18.1	22.1	21.5	17.8
	STDEV	7.1	2.0	5.0	9.2	2.8	8.1	4.2	4.0
	MAX	46.8	18.4	30.9	43.3	23.4	41.1	34.2	23.1
	MIN	15.8	12.3	12.8	12.5	14.3	13.5	16.2	10.7

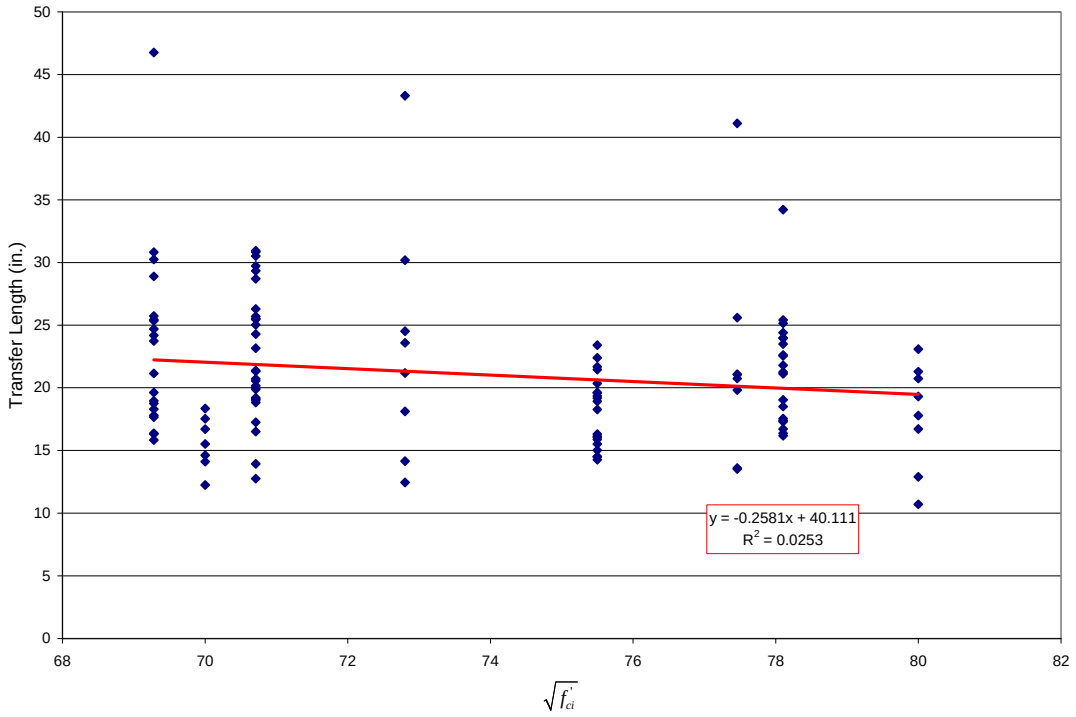

Figure 4.12. Influence of Concrete Strength

4.1.7 Influence of Time

As with strand diameter, effective prestress, and method of release, transfer lengths have also been shown to increase with time, usually occurring within the first few weeks following transfer. Transfer length measurements in this study were taken at the time of transfer and one to two weeks thereafter. Table 4.6 lists the initial and

succeeding, or last, transfer length measurements for the T-beam test specimens along with ratios of the last to initial measurements. Transfer lengths at the live ends of the T-beam test specimens with both normal and inverted casting orientations showed an average increase of 4 percent, while the transfer lengths at the dead ends of the T-beam test specimens with normal and inverted casting orientations showed an average increase of 13 and 11 percent, respectively, while the overall average increase of initial to last transfer length measurements was 8 percent. Figure 4.13 shows a graphical representation of the data plotting the ratio of the last to initial measurements. As Figure 4.13 shows, transfer lengths at the dead ends of T-beam test specimens show a tendency for a larger increase with time.

Table 4.6. Influence of Time (T-beams)

		Beam	fsj ksi	fsi ksi	fse ksi	f'ci psi	f'c psi	Transfer Length (in.) Initial	Last	L/l
Normal	Live	1.270.5N.RA	180.9	168.4	156.3	4900	6500	16.7	17.4	1.04
		2.270.5N.RA	180.9	168.4	162.3	5300	6400	18.1	19.3	1.06
		3.270.5S.RA	180.9	169.1	158.6	6000	8200	21.1	21.9	1.04
		4.270.5S.RA	180.9	168.3	158.5	4900	6300	17.5	18.3	1.04
		5.270.5S.RA	202.5	187.5	162.5	5000	6500	20.2	21.3	1.06
		6.270.5S.RA	202.5	188.8	174.4	6400	8300	20.7	21.2	1.02
		1.300.5N.RA	NA	NA	NA	NA	NA	NA	NA	NA
		2.300.5N.RA	201.0	187.0	180.0	5300	6400	21.2	21.5	1.02
		3.300.5S.RA	201.0	187.7	176.1	6000	8200	20.8	21.2	1.02
		4.300.5S.RA	201.0	186.9	176.0	4900	6300	18.4	19.9	1.08
		5.300.5S.RA	225.0	208.1	181.2	5000	6500	20.6	21.9	1.07
		6.270.6N.RA	202.5	188.4	173.0	6400	8300	19.3	19.3	1.00
		Average Increase								**1.04**
	Dead	1.270.5N.RB	180.9	168.4	157.8	4900	6500	12.3	13.3	1.08
		2.270.5N.RB	180.9	168.4	162.3	5300	6400	12.5	12.7	1.02
		3.270.5S.RB	180.9	169.1	158.6	6000	8200	13.6	14.5	1.06
		4.270.5S.RB	180.9	168.3	157.1	4900	6300	15.5	18.3	1.18
		5.270.5S.RB	202.5	187.5	162.5	5000	6500	12.8	15.2	1.19
		6.270.5S.RB	202.5	188.8	174.2	6400	8300	16.7	18.2	1.09
		1.300.5N.RB	201.0	186.9	175.8	4900	6500	14.6	15.9	1.09
		2.300.5N.RB	201.0	187.0	180.0	5300	6400	14.2	15.4	1.09
		3.300.5S.RB	201.0	187.7	176.3	6000	8200	13.5	14.6	1.08
		4.300.5S.RB	201.0	186.9	175.1	4900	6300	14.1	16.3	1.15
		5.300.5S.RB	225.0	208.1	181.1	5000	6500	13.9	17.1	1.23
		6.270.6N.RB	202.5	188.4	172.9	6400	8300	10.7	14.4	1.35
		Average Increase								**1.13**
Inverted	Live	2.270.5N.UA	180.9	168.4	161.5	5300	6400	30.2	30.1	1.00
		3.270.5S.UA	180.9	169.1	157.5	6000	8200	25.6	28.2	1.10
		5.270.5S.UA	202.5	187.5	162.4	5000	6500	26.3	28.0	1.06
		6.270.5S.UA	202.5	188.8	173.6	6400	8300	21.3	21.5	1.01
		2.300.5N.UA	201.0	187.0	179.6	5300	6400	43.3	44.1	1.02
		3.300.5S.UA	201.0	187.7	175.1	6000	8200	41.1	43.0	1.05
		5.300.5S.UA	225.0	208.1	181.0	5000	6500	24.3	25.4	1.05
		6.270.6N.UA	202.5	188.4	172.5	6400	8300	23.1	24.0	1.04
		Average Increase								**1.04**
	Dead	2.270.5N.UB	180.9	168.4	161.9	5300	6400	24.5	26.1	1.07
		3.270.5S.UB	180.9	169.1	157.5	6000	8200	19.8	23.0	1.16
		5.270.5S.UB	202.5	187.5	162.3	5000	6500	19.9	21.3	1.07
		6.270.5S.UB	202.5	188.8	173.5	6400	8300	17.8	17.8	1.00
		2.300.5N.UB	201.0	187.0	179.1	5300	6400	23.6	24.8	1.05
		3.300.5S.UB	201.0	187.7	175.1	6000	8200	21.1	25.5	1.21
		5.300.5S.UB	225.0	208.1	180.8	5000	6500	19.2	20.8	1.08
		6.270.6N.UB	202.5	188.4	172.2	6400	8300	12.9	15.7	1.21
		Average Increase								**1.11**

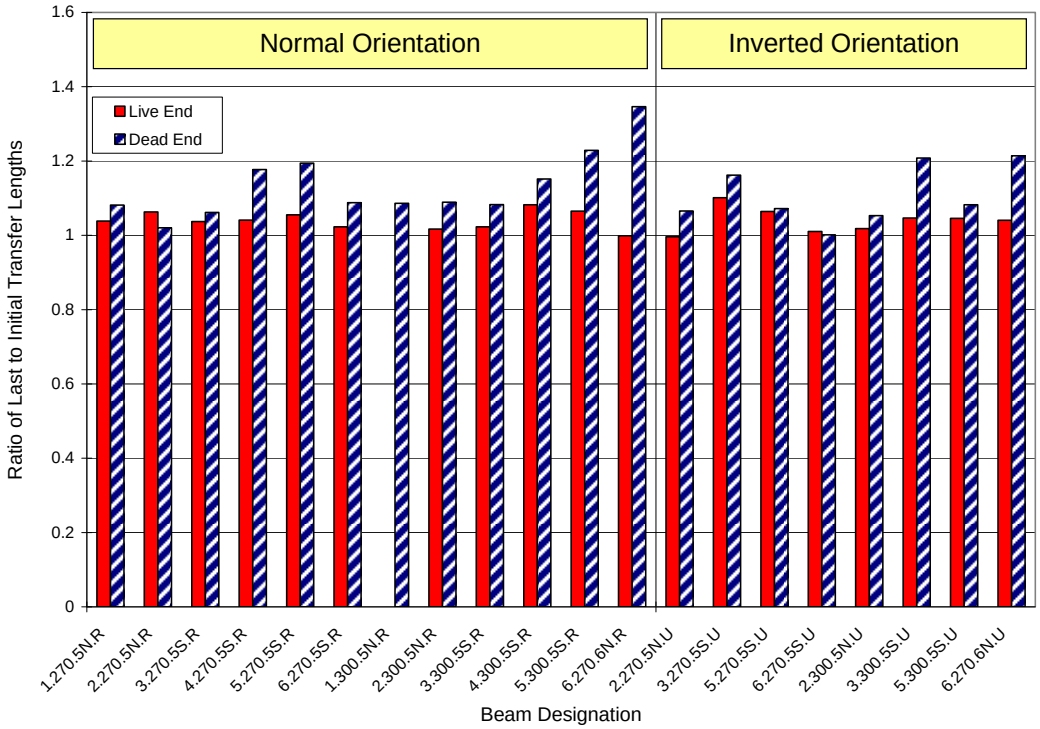

Figure 4.13. Influence of Time (T-beams)

In addition to the comparisons drawn with the T-beam test specimens, the initial and last set of transfer lengths were also compared for each set of transfer length measurements associated with the top-strand blocks. Table 4.7 compares initial and last transfer length measurements for the top-strand block test specimens, while Figure 4.14 shows the average ratios between initial and last transfer length measurements for each set of test specimens. Additional tables with individual results can be seen in Appendix D, while additional figures with individual comparisons can be seen in Appendix E. The transfer lengths at both ends of all top-strand block test specimens showed an average increase of 8 percent, consistent with the average increase in transfer length for the T-beam test specimens.

Table 4.7. Influence of Time (Top-strand Blocks)

	Pour	fsj	fsi	fse	f'ci	f'c	Average Transfer Length (in.)		
		ksi	ksi	ksi	psi	psi	Initial	Last	L/I
Live	1	202.5	Varied	Varied	4800	5900	22.6	24.4	1.08
	2	202.5	Varied	Varied	5700	6600	19.6	21.3	1.08
	3	202.5	Varied	Varied	6100	7000	22.0	23.3	1.06
	4	202.5	Varied	Varied	5000	6100	25.2	27.8	1.10
	Average Increase								**1.08**
Dead	1	202.5	Varied	Varied	4800	5900	24.1	25.4	1.06
	2	202.5	Varied	Varied	5700	6600	16.6	18.1	1.09
	3	202.5	Varied	Varied	6100	7000	20.9	22.8	1.09
	4	202.5	Varied	Varied	5000	6100	22.8	25.2	1.11
	Average Increase								**1.08**

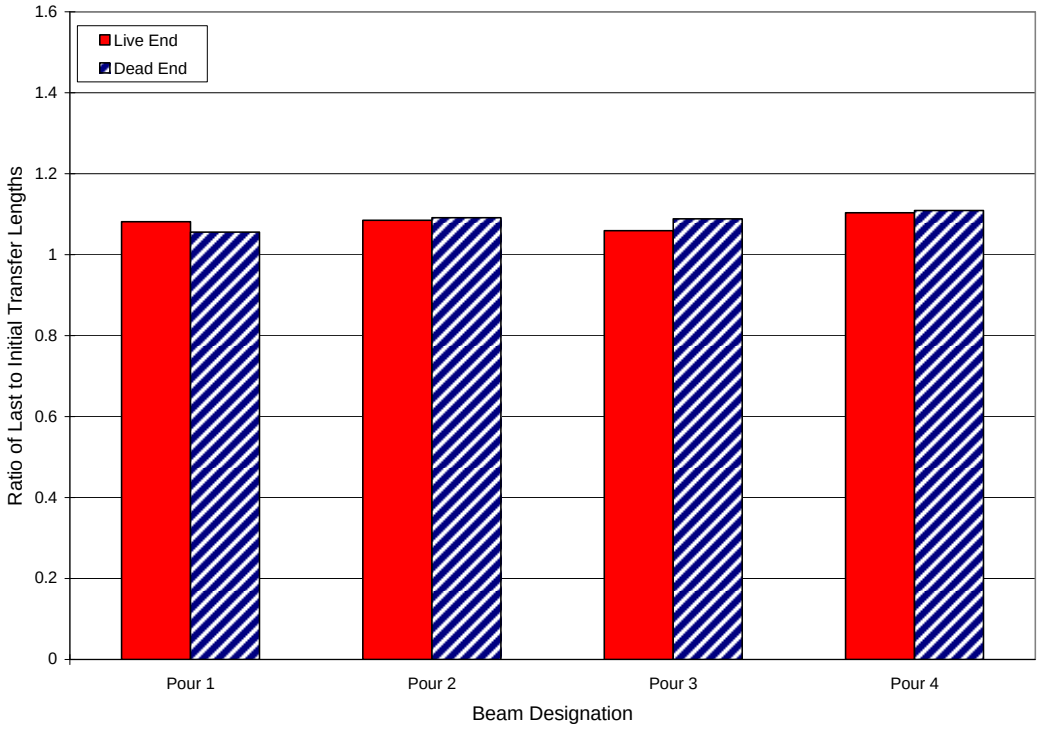

Figure 4.14. Influence of Time (Top Strand Blocks)

4.1.8 Influence of Casting Orientation

The influence of the top-bar effect has been seldom investigated in prestressed concrete, but has been an area of concern in reinforced concrete. As defined in the current ACI and AASHTO codes, the top-bar effect has been thought to be dependent on the amount of concrete cast beneath the bar. In the case of prestressed concrete, it was also expected to be dependent on the amount of concrete cast beneath the strand. Initially a secondary objective of the project, the top-strand effect was investigated by casting eight of the twenty T-beam test specimens with an inverted orientation. Table 4.8 lists

the transfer lengths of each beam cast with a normal orientation and adjacent inverted beam as well as comparative ratios. In addition to Table 4.8, Figure 4.15 gives a graphical representation of the data in strand diameters coupled with current code provisions.

The average increase in transfer length at the live end of beams cast with an inverted orientation and an initial prestress of $0.67f_{pu}$ was 73 percent, while the average increase in transfer length at the dead end was 67 percent. For beams cast with an initial prestress of $0.75f_{pu}$, the average increase in transfer length at the live and dead ends was 18 and 30 percent, respectively. It should be noted that the significant increase in transfer length for the beams cast with an initial prestress of $0.67f_{pu}$ may attributed to the high fluidity of the mixes used in Pour 2 and Pour 3. However, regardless of consistency, it is evident that the casting orientation of the T-beam test specimens was highly influential on transfer length measurements.

Table 4.8. Influence of Casting Orientation

				Transfer Length (in.)				Ratios	
		f'_{ci}	f'_c	Live		Dead		Live	Dead
	Beam	psi	psi	Normal	Inverted	Normal	Inverted	Inv/Nor	Inv/Nor
$0.67f_{pu}$	2.270.5N	5300	6400	18.12	30.19	12.45	24.52	1.67	1.97
	2.300.5N	5300	6400	21.18	43.32	14.15	23.59	2.05	1.67
	3.270.5S	6000	8200	21.08	25.60	13.61	19.81	1.21	1.46
	3.300.5S	6000	8200	20.75	41.09	13.52	21.07	1.98	1.56
	Average Increase							**1.73**	**1.66**
$0.75f_{pu}$	5.270.5S	5000	6500	20.17	26.30	12.76	19.88	1.30	1.56
	5.300.5S	5000	6500	20.56	24.29	13.94	19.20	1.18	1.38
	6.270.5S	6400	6400	20.74	21.30	16.72	17.79	1.03	1.06
	6.270.6N	6400	6400	19.32	23.09	10.71	12.90	1.20	1.20
	Average Increase							**1.18**	**1.30**

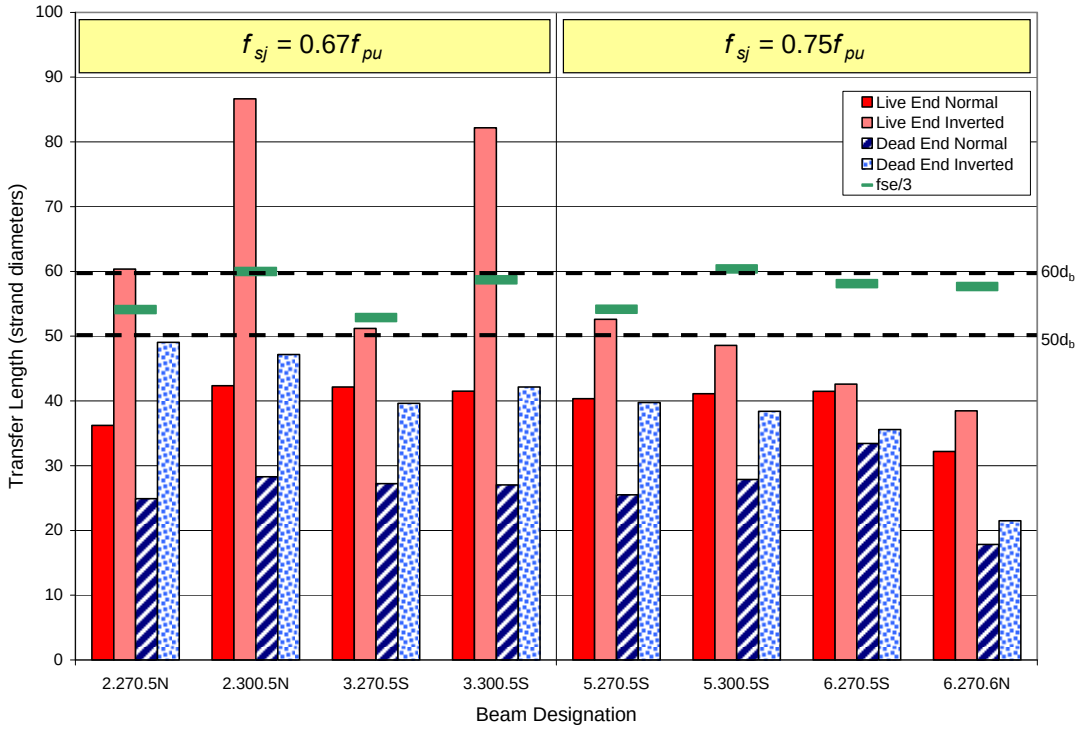

Figure 4.15. Influence of Casting Orientation

Concurrent to this investigation, another study revealed that the top-strand effect may be more dependent on the amount of concrete cast above the strand rather than the amount of concrete cast beneath the strand, thus raising a number of questions associated with the true definition of the top-strand effect (Peterman 2007). In an effort to determine the correlation of transfer lengths and the amount of concrete cast above and beneath the strand, the transfer length for each of the T-beam test specimens was first plotted against the amount of concrete cast below the strand and again plotted against the amount of concrete cast above the strand.

Figure 4.16 shows each transfer length plotted against the amount of concrete cast beneath the strand (b_{cast}), showing a slight correlation between transfer length and depth of concrete. Looking at Figure 4.16 alone, a conclusion could be drawn supporting the traditional definition of the top-strand effect claiming transfer lengths to increase with an increase in the depth of concrete cast beneath the strand. However, in the inverted T-beam test specimens, as the amount of concrete beneath the strand increased, the amount of concrete above the strand remained constant at 2 in. Contrary to Figure 4.16 and the traditional definition of the top-strand effect, Figure 4.17 shows each transfer length

plotted against the amount of concrete cast above the strand (d_{cast}) with a better correlation existing than was shown in Figure 4.16. In addition to the representation of the data in Figure 4.16 and 4.17, the data was separated with respect to strand type, but no conclusions were drawn. Although, there seemed to be a better correlation between measured transfer lengths and d_{cast} than measured transfer lengths and b_{cast}, an overall definitive conclusion could not be drawn from the T-beam test specimens alone. Therefore, a series of top-strand blocks were cast to further investigate the top-strand effect in prestressed concrete.

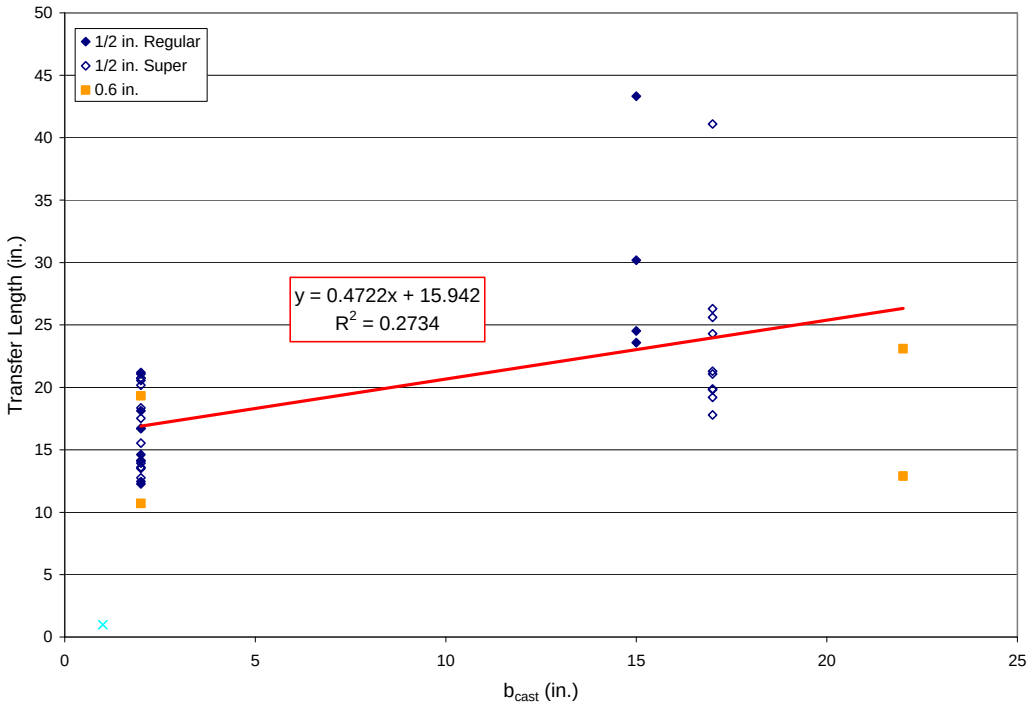

Figure 4.16. Transfer Length vs. b_{cast} (T-beams)

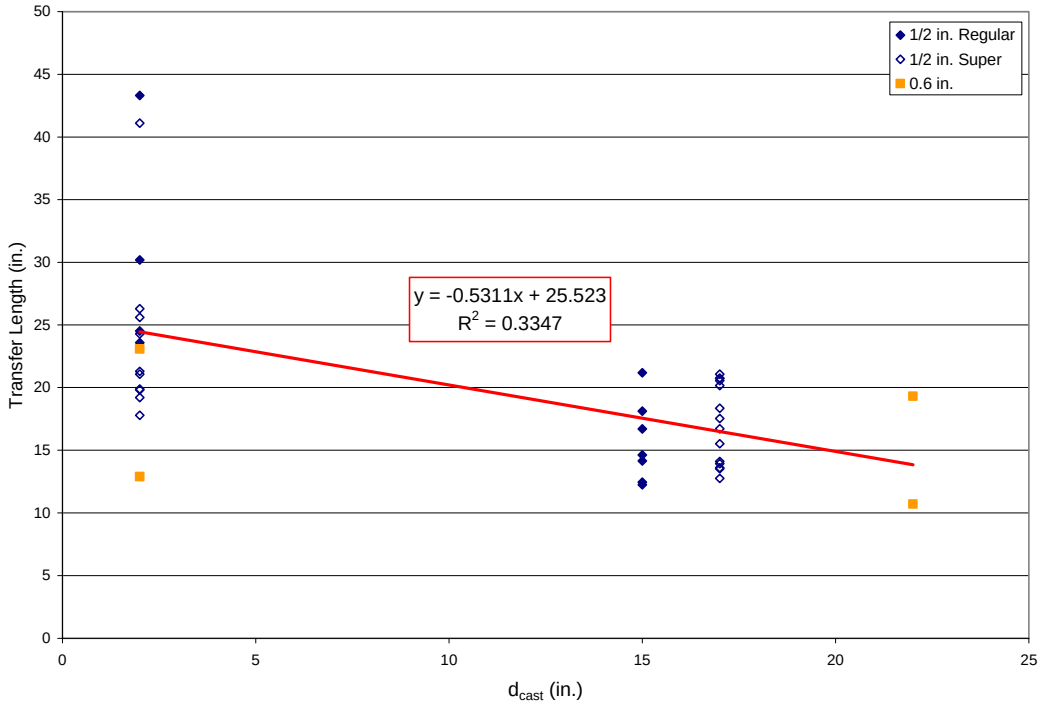

Figure 4.17. Transfer Length vs. d_{cast} (T-beams)

Four sets of top-strand block test specimens were cast, which allowed for two comparisons. The first compared the transfer lengths in two separate specimens with the same amount of concrete cast beneath the strand, while having different amounts of concrete cast above the strand. The second compared the transfer lengths in two separate specimens with the same amount of concrete cast above the strand, while having different amounts of concrete cast below the strand. Figure 4.18 compares the transfer lengths of strands having the same amount of concrete cast beneath them. Transfer lengths at both the live and dead ends for strands F, G, and H were compared to the transfer lengths for strands C, D, and E, respectively, corresponding to concrete depths of 12 in., 7 in., and 2 in. below the strands. On the contrary, Figure 4.19 compares the transfer lengths of strands having the same amount of concrete cast above them. Transfer lengths at both the live and dead ends for strands F, G, and H were compared to the transfer lengths for strands A, B, and C, respectively, corresponding to concrete depths of 2 in, 7 in., and 12 in. above the strands. Figure 4.18 and Figure 4.19 did seem to have more scatter than previous studies and is attributed to possible material variations in fabrication. Although a high level of quality control was used in the fabrication of the test specimens, some

variation did exist in concrete properties from batch to batch and strand stress after transfer. Additionally, the cutting sequence was not evaluated, but could have influenced transfer length measurements as well.

Coefficients of correlation (R^2) were calculated for both comparisons with respect to a line of perfect correlation. However, due to the amount of scatter away from the line of perfect correlation, the R^2 values were unreasonable. Although R^2 values were unreasonable, a best fit trend line was fit to each set of data passing through zero. By visual inspection, the best fit line in Figure 4.19 (same amount of concrete cast above the strand) showed a better relationship to the line of perfect correlation than did the best fit line in Figure 4.18. In an effort to verify that observation, the difference in values of strands in the small block to values of corresponding strands in the large block were evaluated with respect to the line of perfect correlation. The transfer lengths corresponding to strands with the same amount of concrete cast beneath the strand had an average ratio of 1.37 with a standard deviation of 0.24 with respect to the line of perfect correlation, while transfer lengths corresponding to strands with the same amount of concrete cast above the strand had an average ratio of 1.20 with a standard deviation of 0.25. Therefore, it was concluded that strands cast with the same amount of concrete above the strand had a better correlation than did those with the same amount of concrete cast beneath the strand.

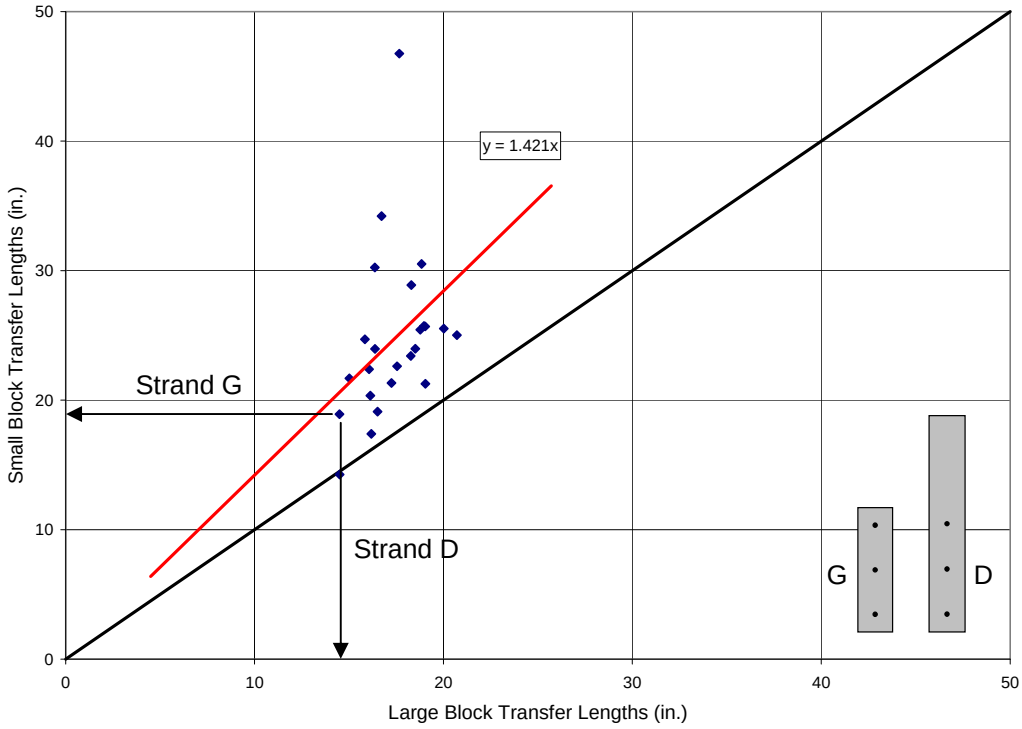

Figure 4.18. Transfer Length Correlation with same b_{cast}

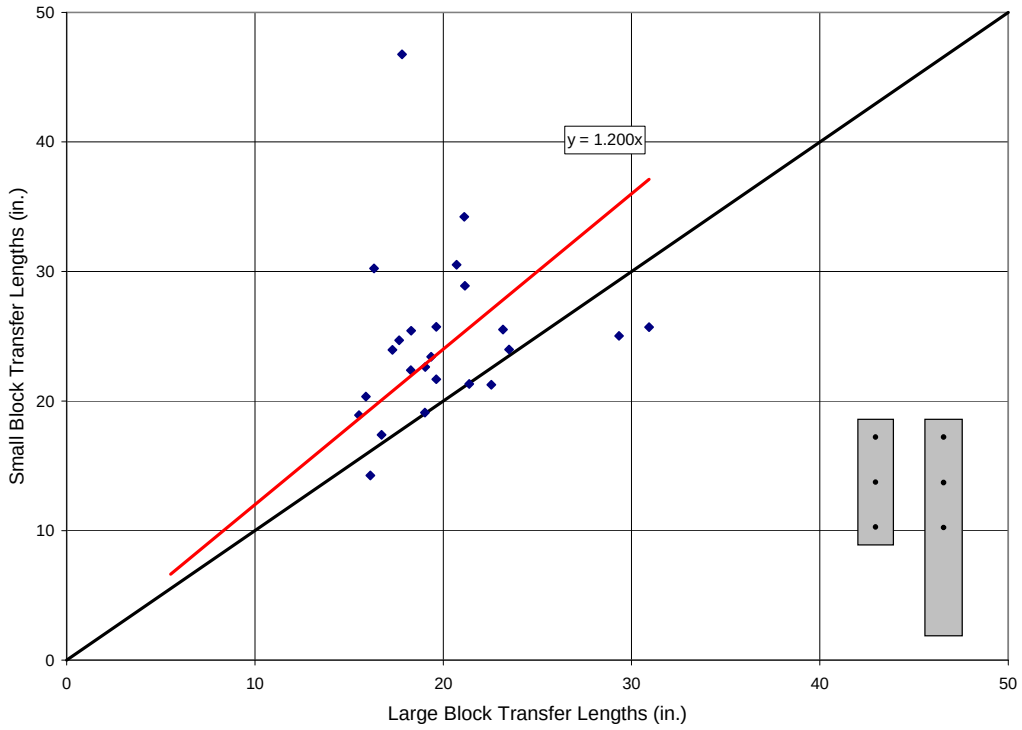

Figure 4.19. Transfer Length Correlation with same d_{cast}

In an effort to further verify the relationship between transfer length and the as-cast vertical location, each of the 119 transfer length measurements were plotted against the amount of concrete cast beneath the strand and the amount of concrete cast above the strand. Figure 4.20 shows the relationship between transfer length measurements and the amount of concrete cast beneath the strand, while Figure 4.21 shows the relationship between transfer length measurements and the amount of concrete cast above the strand. The data plotted in Figure 4.21 showed a much better correlation than did the data in Figure 4.20 with a significantly better value for the coefficient of correlation. Table 4.9 further summarizes and verifies these relationships with average transfer lengths for each amount of concrete cast below and above the strands as well as standard deviations for each amount of concrete. The average standard deviation for transfer lengths compared to the amount of concrete cast below the strand was 5.58 in. The average standard deviation for transfer lengths compared to the amount of concrete cast above the strand was 3.58 in. A smaller standard deviation indicates there was a better correlation for transfer lengths of strands compared to the amount of concrete cast above the strand than those compared to the amount of concrete cast below the strand.

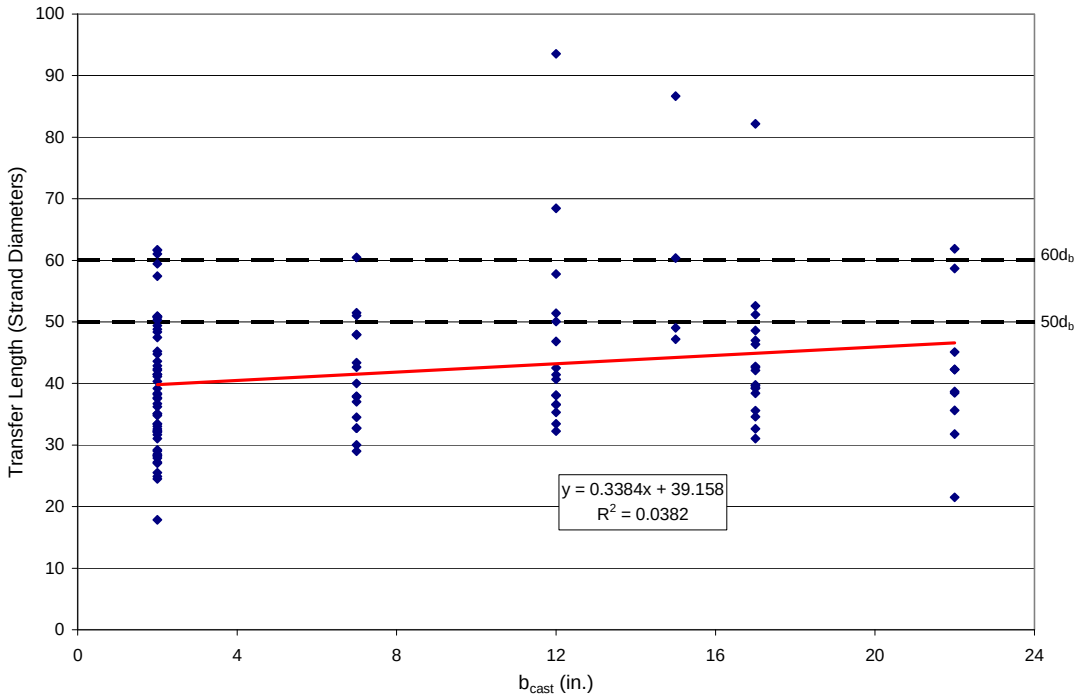

Figure 4.20. Transfer Length vs. b_{cast} (All Test Specimens)

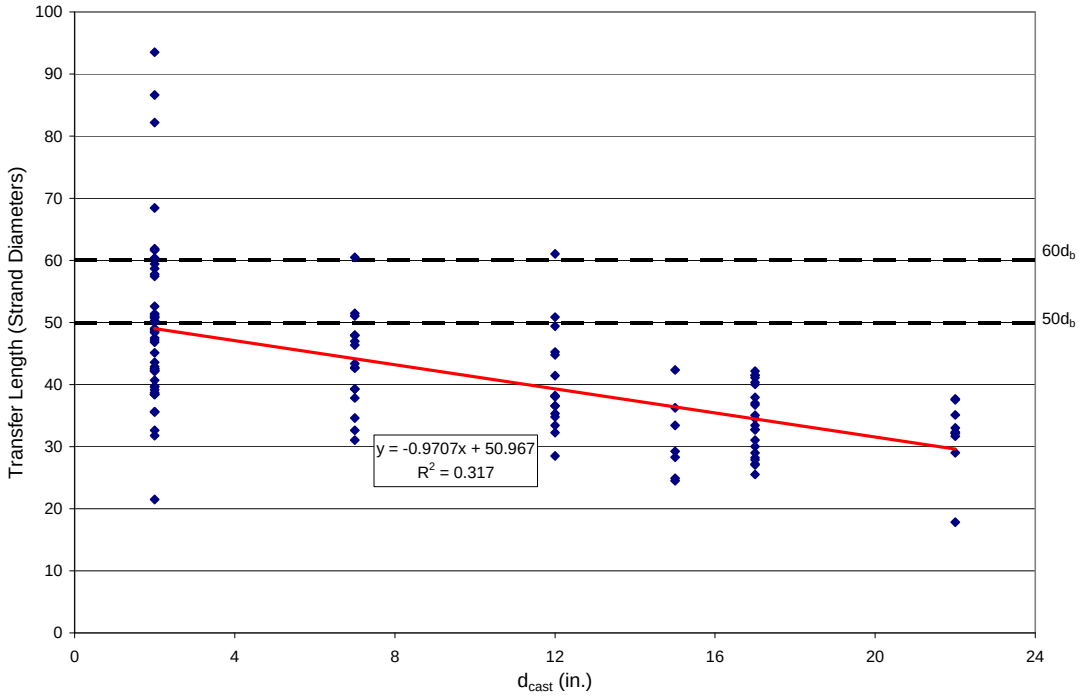

Figure 4.21. Transfer Length vs. d_{cast} (All Test Specimens)

Table 4.9. As-cast Vertical Location Correlations

			Transfer Lengths (in.)					
			Depth of Concrete (in.)					
			2	7	12	15	17	22
Concrete Below	Live	AVE	21.7	21.2	21.9	36.8	24.9	23.1
		STDEV	3.8	3.5	3.5	6.6	6.1	3.4
		MAX	30.5	25.7	28.9	43.3	41.1	29.3
		MIN	16.1	15.0	18.3	30.2	19.6	19.4
	Dead	AVE	17.7	19.9	24.6	24.1	18.7	19.7
		STDEV	5.4	4.8	10.1	0.5	1.9	6.2
		MAX	30.8	30.2	46.8	24.5	21.4	30.9
		MIN	10.7	14.5	16.1	23.6	15.5	12.9
	Total	AVE	19.7	20.5	23.2	30.4	21.8	21.4
		STDEV	5.1	4.3	7.7	7.9	5.5	5.3
		MAX	30.8	30.2	46.8	43.3	41.1	30.9
		MIN	10.7	14.5	16.1	23.6	15.5	12.9
Concrete Above	Live	AVE	26.0	22.9	22.2	18.7	19.2	18.1
		STDEV	5.8	2.2	3.9	1.9	1.7	1.2
		MAX	43.3	25.7	30.5	21.2	21.1	19.3
		MIN	19.2	19.6	18.3	16.7	15.0	16.1
	Dead	AVE	23.5	20.6	18.1	13.4	15.0	14.8
		STDEV	7.1	4.5	2.9	1.0	1.5	2.1
		MAX	46.8	30.2	24.7	14.6	17.3	16.5
		MIN	12.9	15.5	14.3	12.3	12.8	10.7
	Total	AVE	24.8	21.7	20.1	15.6	17.1	16.4
		STDEV	6.6	3.7	4.0	3.0	2.7	2.4
		MAX	46.8	30.2	30.5	21.2	21.1	19.3
		MIN	12.9	15.5	14.3	12.3	12.8	10.7

4.1.9 Current and Recommended Equations

Since the 1963 ACI Building Code was published, transfer length has been calculated by Equation (2-3). Equation (2-3) takes into consideration the strand diameter and the effective prestress in the strand after all losses. However, Equation (2-3) fails to account for the strength of the concrete and the vertical casting location.

$$L_t = \left(\frac{f_{se}}{3} \right) d_b \qquad \text{Eq. (2-3)}$$

Over the past 35 years, a number of researchers have proposed various equations incorporating concrete strength and have recommended using the prestress just after transfer in place of the effective prestress. Some equations have proved to be adequate in the estimation of transfer length, while others have failed to reproduce conservative values. Taking into consideration the recommendations of past researchers, the transfer lengths calculated in this study were compared to 14 different transfer length equations,

shown again in Table 4.10. Figure 4.22 through Figure 4.35 show this comparison to each of those equations with a line of perfect correlation. Actual values were plotted on the ordinate axis while the predicted values from each equation were plotted on the abscissa axis with a line of perfect correlation aiding in interpretation of the data. If the predicted value for a specimen is larger than the measured value, a conservative estimate, the point would fall below the line of perfect correlation. However, if the predicted value for a specimen is smaller than the measured value, an unconservative estimate, the point would fall above the line of perfect correlation.

The first equation evaluated, shown in Figure 4.22, was the traditional equation from ACI (Equation 2-3). Figure 4.22 indicated Equation (2-3) gives a relatively constant transfer length, which in some cases exhibited unconservative estimations. In a similar manner, Equation (2-4), shown in Figure 4.23, provided even more constant values for transfer length, proving to be even more unconservative with respect to the data from this study. On the contrary, Equation (2-6) by Martin and Scott (Figure 4.24) produced extremely conservative results even though the predicted values again remained relatively constant.

Equation (2-7), shown in Figure 4.25, proposed by Zia and Mostafa, was one of the first equations to account for concrete strength, producing very good average results. Average results are satisfactory if all data points fall on or close to the line of perfect correlation, but in this case, a number of data points were above the line of perfect correlation, indicating a lack of conservatism. On the other hand, Equation (2-8), shown in Figure 4.26, produced a conservative estimation of transfer lengths, also showing a good range in the estimations. Equation (2-9) goes back to only including the stress in the stand and diameter of the strand, but replaces the effective prestress with the initial prestress. However, as shown in Figure 4.27, the results again produce a relatively constant value for transfer length, which may be too conservative in favorable situations, but also may be unconservative in highly fluid mixes or members subject to the top-strand effect.

Of the additional equations shown in Figure 4.28 through Figure 4.35, Equation (2-10) and Equation (2-16) prove to be unconservative in their estimation of transfer lengths as compared to those measured in this study. Equations (2-13), (2-14), (2-18),

and (2-19) provide conservative estimates, but also produce relatively constant values with a very small range in predicted values. Equations (2-15) and (2-17) produced acceptable estimations for this data, with Equation (2-17) by Kose and Burkett estimating the transfer lengths of the 0.6 in. diameter strands much better than previous equations.

Through this comparison, it is evident that transfer length is dependent upon more than just effective prestress and strand diameter. Of the 14 equations examined, six used the initial prestress instead of the effective prestress, seven included the strength of the concrete, and one included the influence of casting position. Of the 14 equations and the various factors considered, none of the 14 takes into account the initial prestress, the concrete strength, the strand diameter, and the casting position simultaneously. Based on the previous comparisons of the factors affecting transfer length and the evaluation of the current code provisions and recommended transfer length equations, an equation incorporating each of these four factors is proposed.

Table 4.10. Historical Transfer Length Equations

Contributor	Year	Equation	Eq. No.
Hanson & Kaar	1959	$L_t = \frac{f_{se}}{2.94} d_b$	2-5
ACI	1963	$L_t = \frac{f_{se}}{3} d_b$	2-3
		$L_t = 50 d_b$	2-4
Martin & Scott	1976	$L_t = 80 d_b$	2-6
Zia & Mostafa	1977	$L_t = 1.5 \frac{f_{si}}{f_{ci}^{'}} d_b - 4.6$	2-7
Cousins et al.	1990	$L_t = 0.5 \left(\frac{U_t^{'} \sqrt{f_{ci}^{'}}}{B} \right) + \frac{f_{se} A_{ps}}{\pi d_b U_t^{'} \sqrt{f_{ci}^{'}}}$	2-8
Shahawy et al.	1992	$L_t = \frac{f_{si}}{3} d_b$	2-9
Mitchell et al.	1993	$L_t = 0.33 f_{pi} d_b \sqrt{\frac{3}{f_{ci}^{'}}}$	2-10
Deatherage et al.	1994	$L_t = \frac{f_{si}}{3} d_b$	2-9
Buckner	1995	$L_t = \frac{f_{si}}{3} d_b$	2-9
AASHTO	19??	$L_t = 60 d_b$	2-13
Russell & Burns	1997	$L_t = \frac{f_{se}}{2} d_b$	2-14
		$L_t = 80 d_b$	2-6
Lane	1998	$L_t = \frac{4 f_{pt}}{f_c^{'}} d_b - 5$	2-15
Barnes et al.	2003	$L_t = \alpha \frac{f_{pt}}{\sqrt{f_{ci}^{'}}} d_b$	2-16
Kose & Burkett	2005	$L_t = 95 \frac{f_{pi} \left(1 - d_b\right)^2}{\sqrt{f_c^{'}}}$	2-17
Peterman	2007	For $d_{cast} < 8$" $L_t = 90\left(90 - 5 d_{cast}\right) d_b$ For $d_{cast} \geq 8$" $L_t = 50 d_b$	2-18
NCHRP	2008	$L_t = \frac{120}{\sqrt{f_{ci}^{'}}} d_b \geq 40 d_b$	2-19

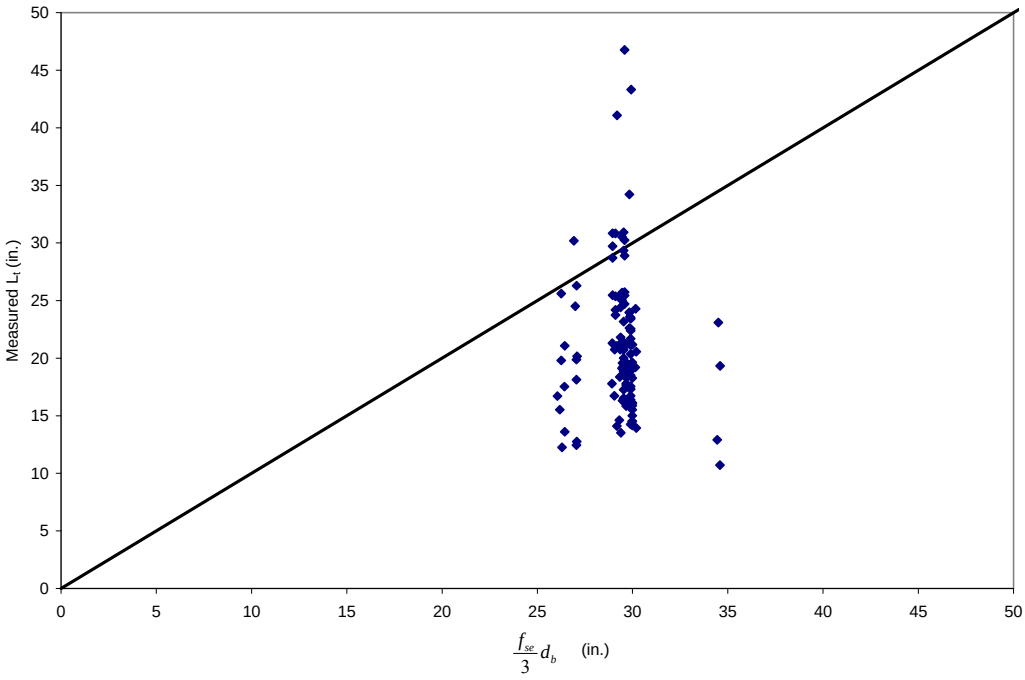

Figure 4.22. Measured Transfer Lengths vs. ACI (Eq. 2-3)

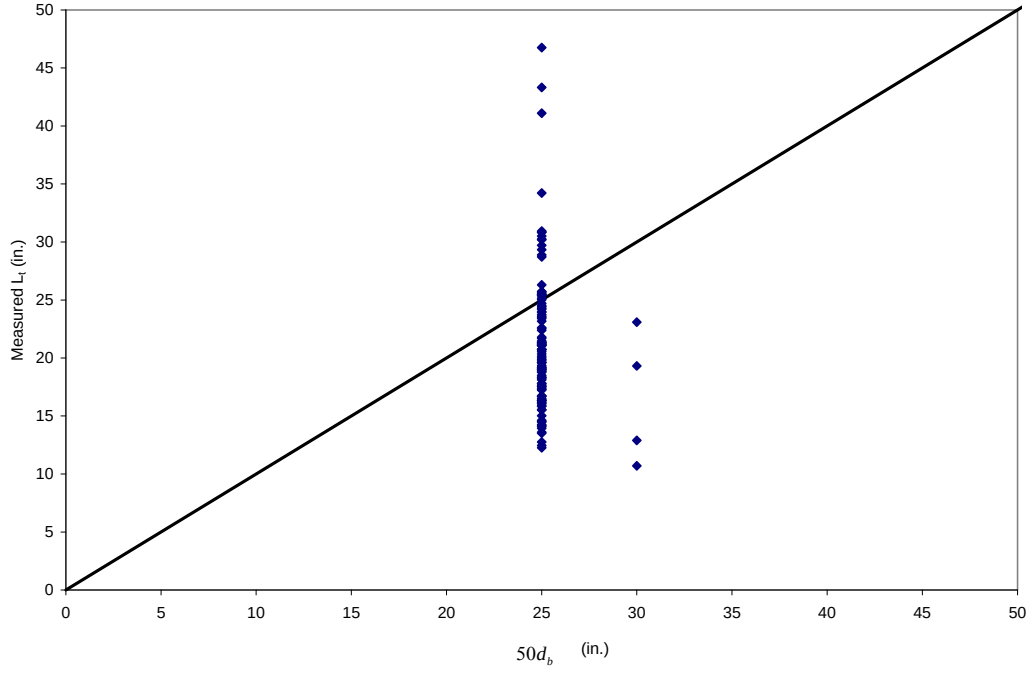

Figure 4.23. Measured Transfer Lengths vs. Alt. ACI (Eq. 2-4)

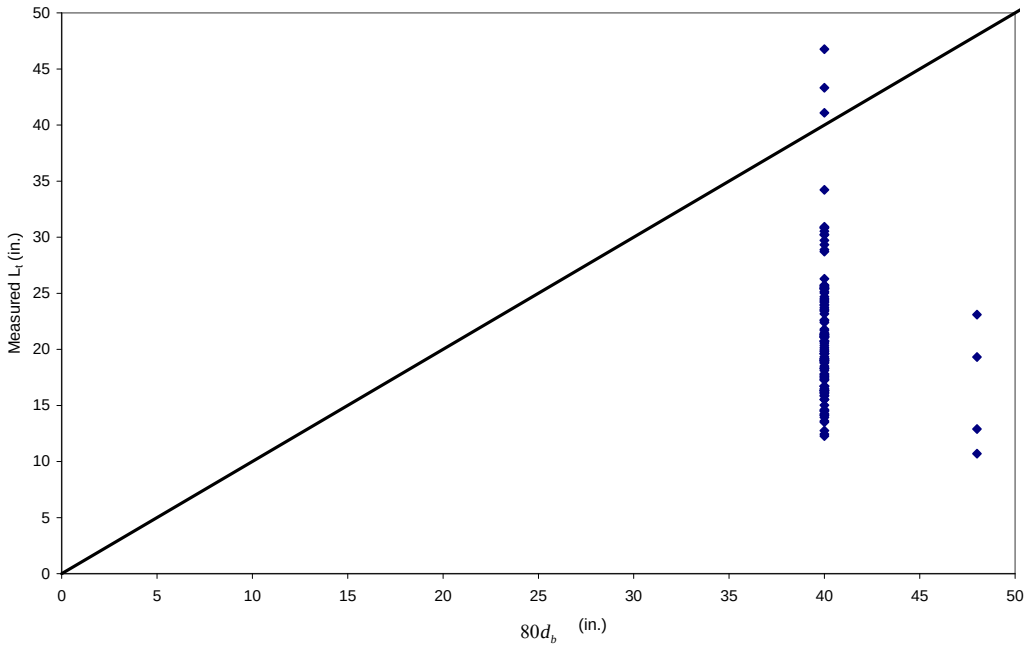

Figure 4.24. Measured Transfer Lengths vs. Martin and Scott (Eq. 2-6)

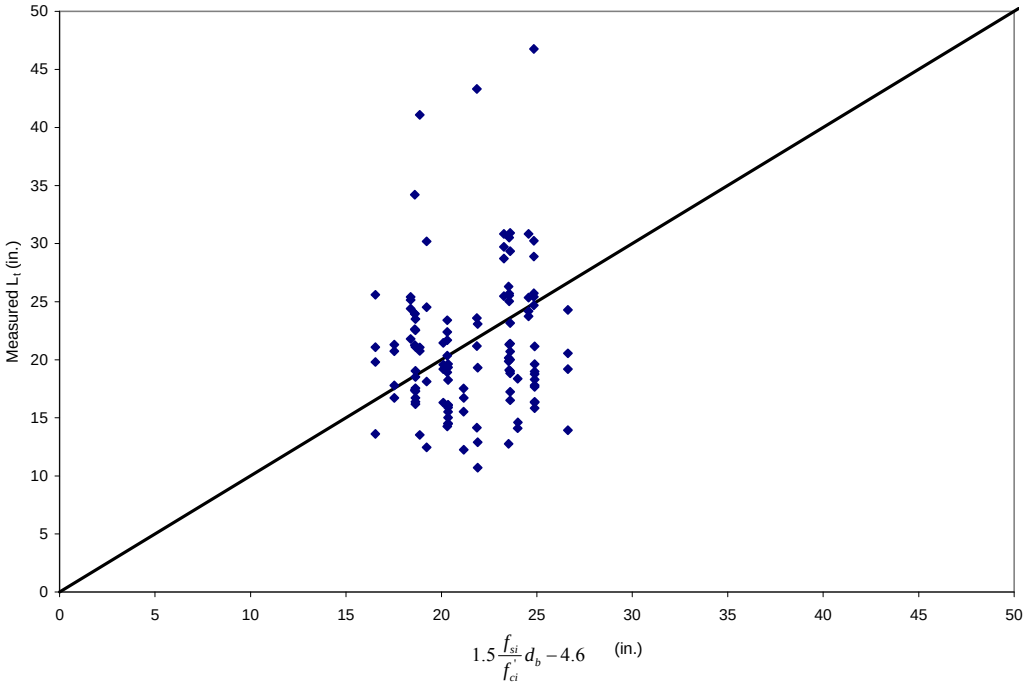

Figure 4.25. Measured Transfer Lengths vs. Zia and Mostafa (Eq. 2-7)

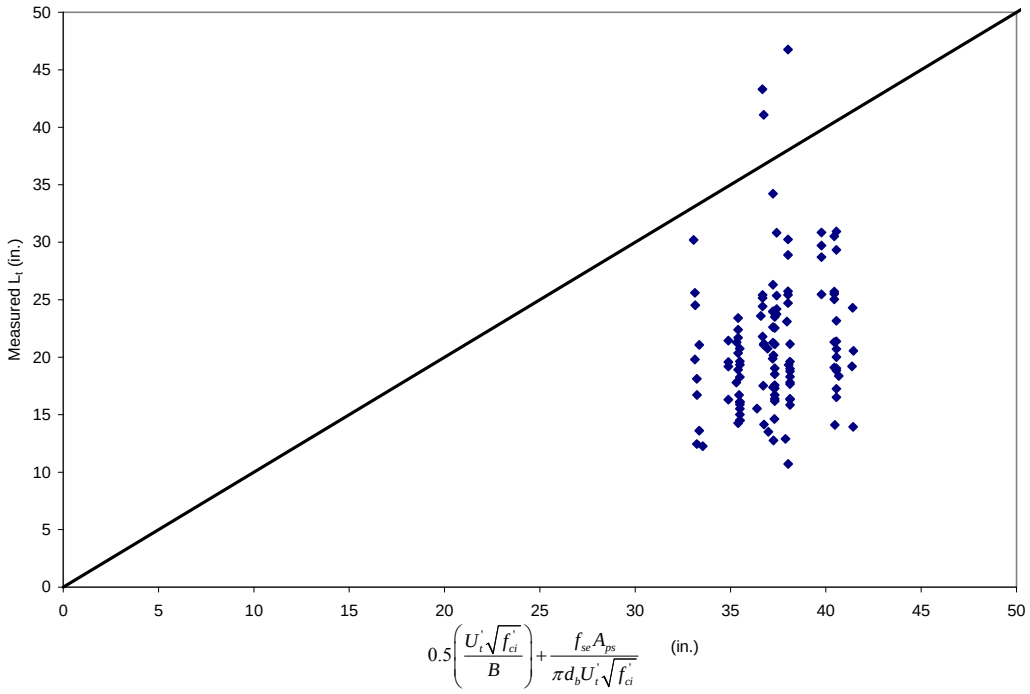

Figure 4.26. Measured Transfer Lengths vs. Cousins et al. (Eq. 2-8)

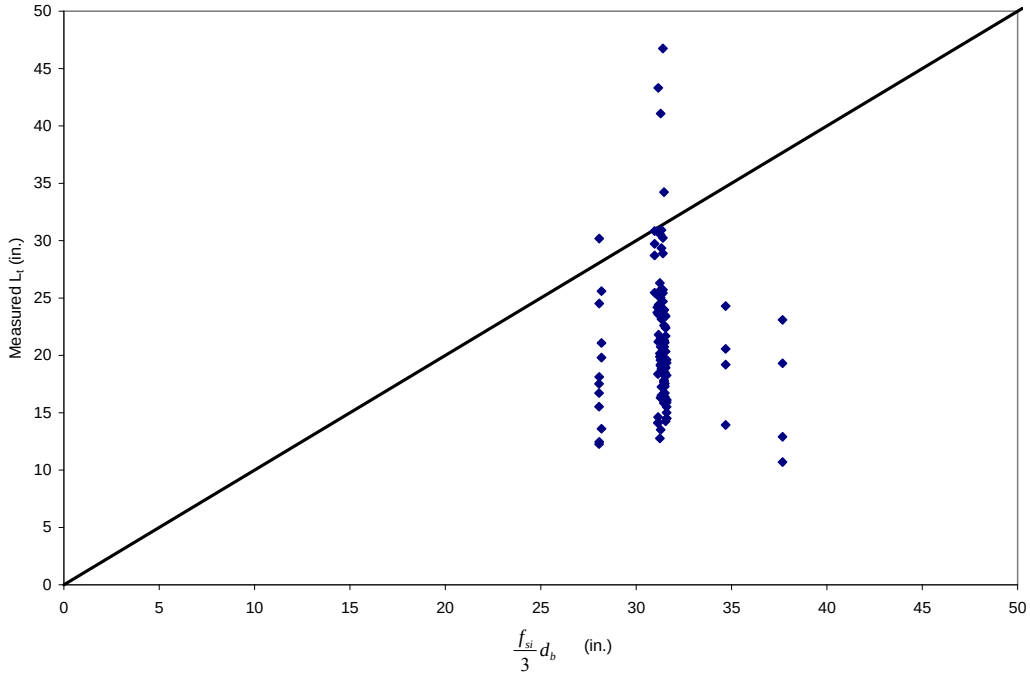

Figure 4.27. Measured Transfer Lengths vs. Shahawy et al. (Eq. 2-9)

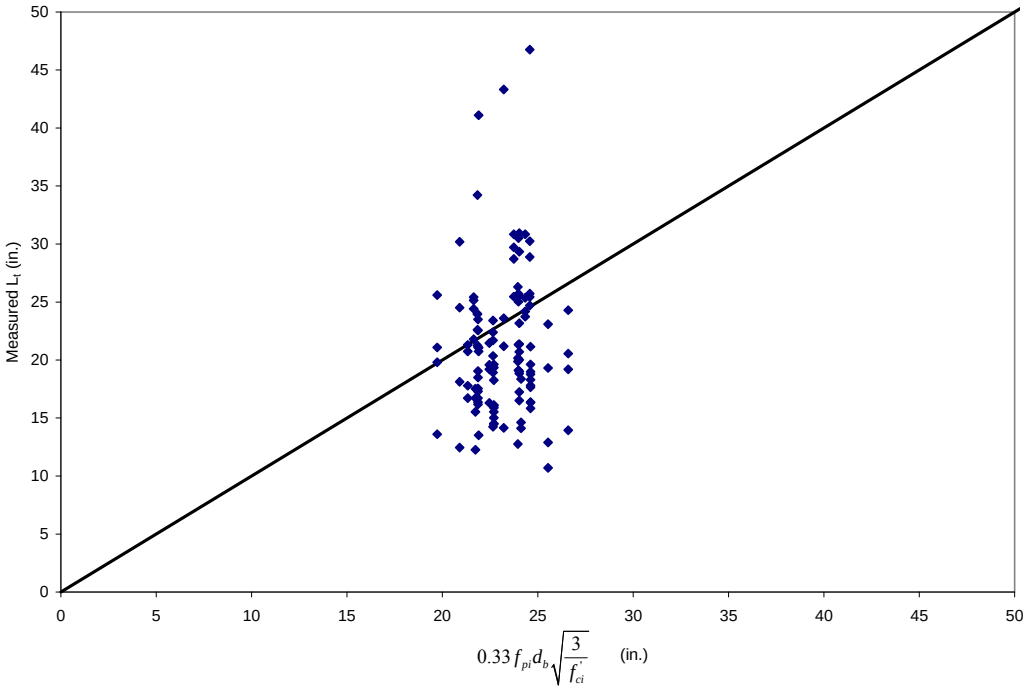

Figure 4.28. Measured Transfer Lengths vs. Mitchell et al. (Eq. 2-10)

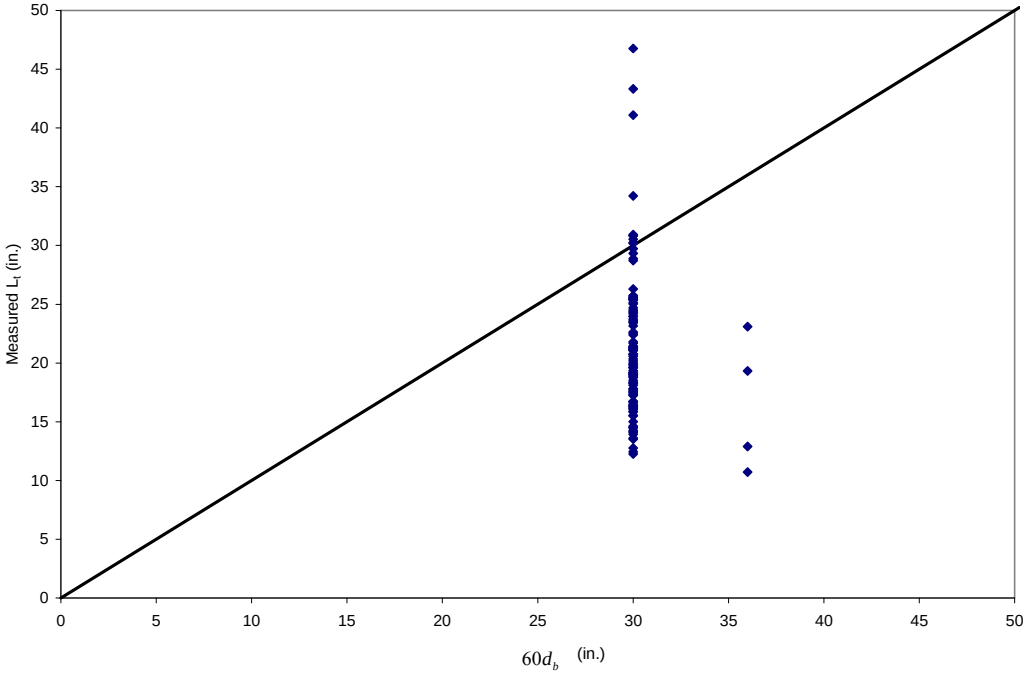

Figure 4.29. Measured Transfer Lengths vs. AASHTO (Eq. 2-13)

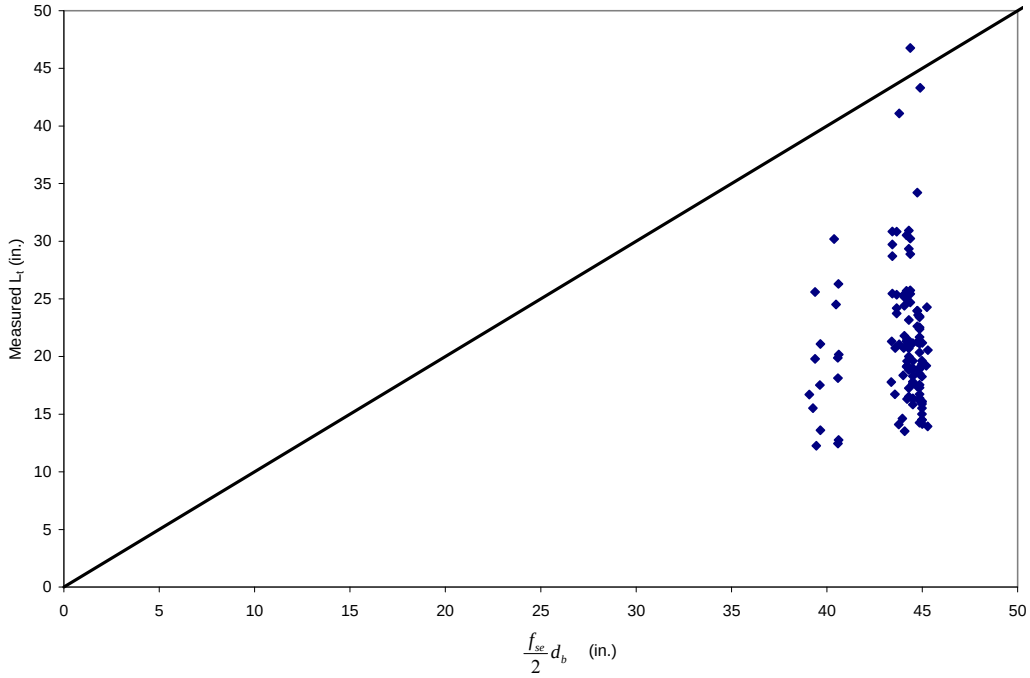

Figure 4.30. Measured Transfer Lengths vs. Russell and Burns (Eq. 2-14)

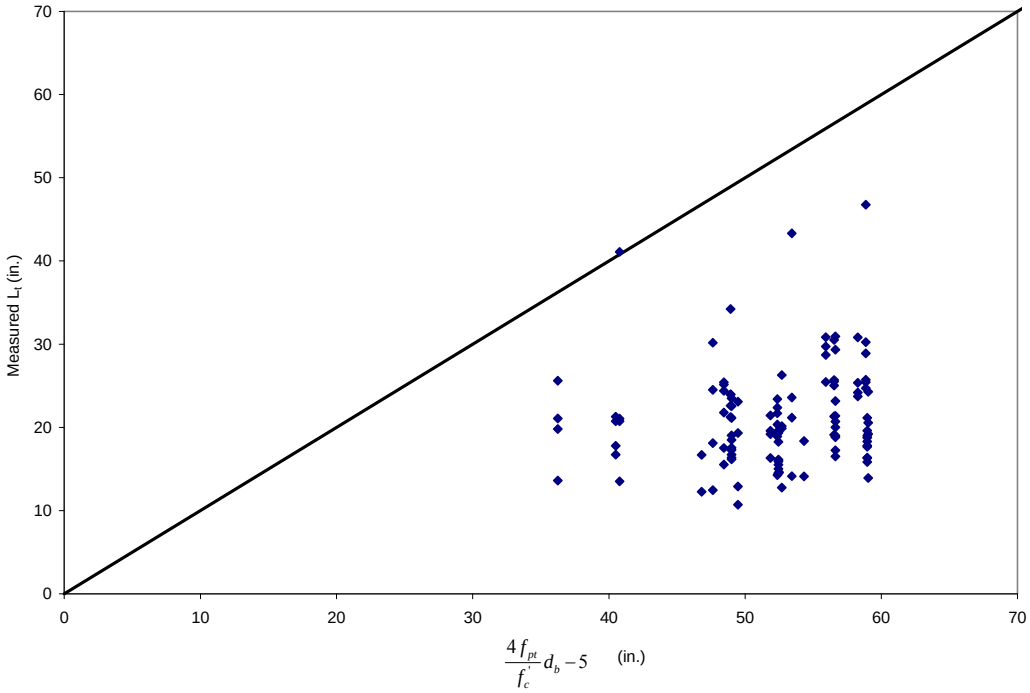

Figure 4.31. Measured Transfer Length vs. Lane (Eq. 2-15)

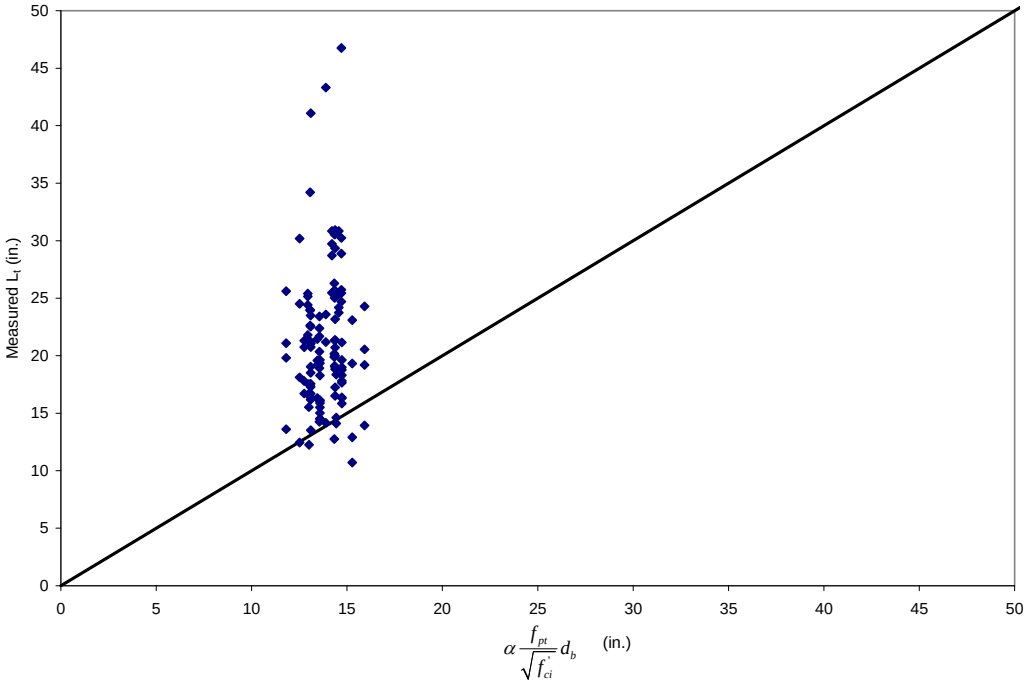

Figure 4.32. Measured Transfer Lengths vs. Barnes et al. (Eq. 2-16)

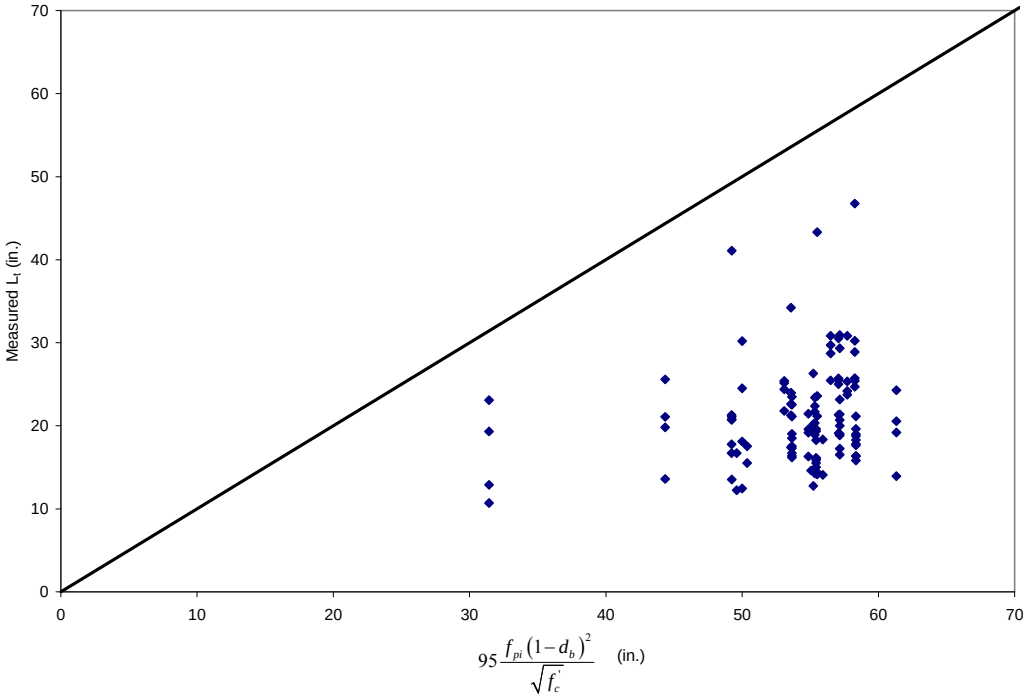

Figure 4.33. Measured Transfer Lengths vs. Kose and Burkett (Eq. 2-17)

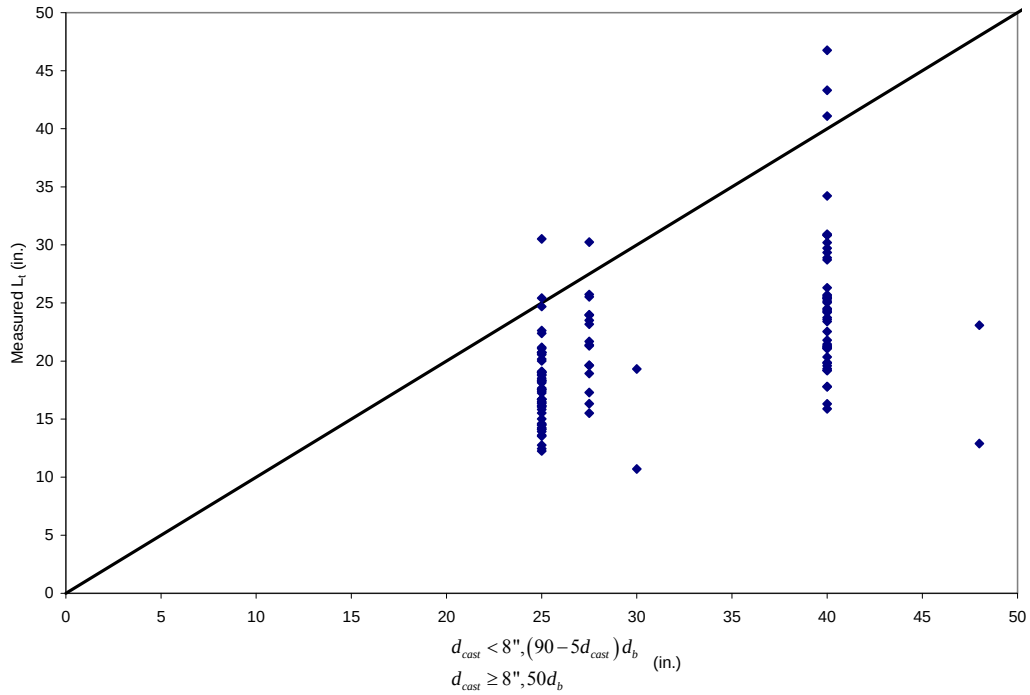

Figure 4.34. Measured Transfer Lengths vs. Peterman (Eq. 2-18)

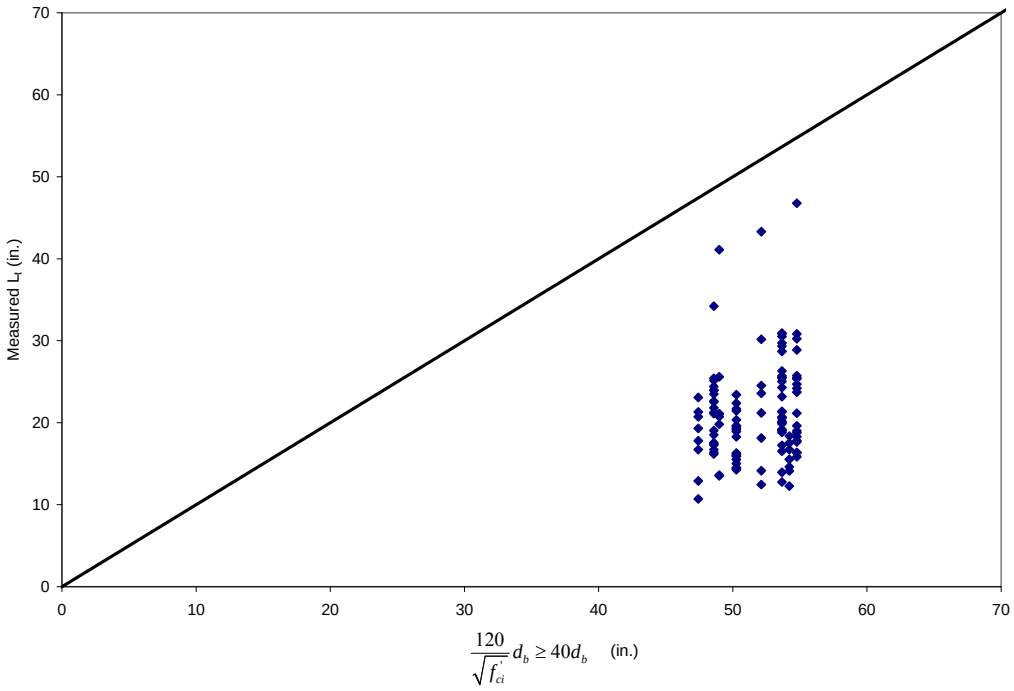

Figure 4.35. Measured Transfer Lengths vs. NCHRP (Eq. 2-19)

4.1.10 Proposed Transfer Length Equation

The derivation of the proposed transfer length equation, shown as Equation (4-1), was a step-by-step process involving a number of iterations and statistical analyses for the final determination of coefficients X, Y, and Z and the later addition of ζ.

$$\text{For } d_{cast} < 24 \text{ in. } L_t = X \frac{f_{si}}{\sqrt{f'_{ci}}} d_b + \zeta \frac{(24 - d_{cast})^Y}{Z}$$
$$\text{For } d_{cast} \geq 24 \text{ in. } L_t = X \frac{f_{si}}{\sqrt{f'_{ci}}} d_b \qquad \text{Eq. (4-1)}$$

Figure 4.21 showed the relationship of the measured transfer lengths and the amount of concrete cast above the strand. Transfer lengths were found to be heavily dependent on the amount of concrete cast above the strand. In Figure 4.21, a linear best fit line was used in lieu of a polynomial equation to maintain simplicity. Using a polynomial equation did result in an insignificant increase in the coefficient of correlation. Had a polynomial equation been used as shown by the dashed line in Figure 4.36, it could be noted that the average transfer lengths tended to level off when d_{cast} reached approximately 24 in. It was assumed that a strand cast with more than 24 in. of concrete above it would not experience any top-strand effect. The proposed equation is broken up into two terms because the effect of vertical casting position appeared to be independent of the initial prestress, strand diameter, and concrete strength after evaluation of those factors. The first term in the proposed equation is the basic transfer length equation for the calculation for bottom-cast strands (d_{cast} > 24 in.). The second term is the top-strand factor that accounts for the increases in transfer length associated with a decrease in d_{cast}. The relationship of the two equations can be seen in Figure 4.36, where the horizontal line is from the first term where there was more than 24 in. of concrete cast above the strand and the sloped line is from the second term where transfer length tends to increase with less than 24 in. of concrete cast above the strand.

The first step in the derivation was to determine the coefficient X or where the two lines intersect. In other words, by plotting the transfer length minus the basic transfer length equation of strands with less than 24 in. of concrete cast above the strand against (24 – d_{cast}), the best fit line would intersect at point B in Figure 4.36. Focusing on

the sloped portion of the solid line in Figure 4.36, Figure 4.37 plots all of the data from this study, which had less than 24 in. of concrete cast above the strand. This was accomplished by subtracting the first term in Equation (4-1) from the existing transfer length measurements by iterating X until the y-intercept was equal to zero, resulting in X = 10.89. It can also be observed in Figure 4.37 that average transfer length measurements tend to increase approximately ½ in. with a 1 in. decrease of d_{cast}. Therefore, for the data reported herein, the average transfer lengths could be approximated by Equation (4-2) with X rounded to 11 and the slope of the best fit line in Figure 4.37 rounded to ½ or Z = 2 and Y = 1 as shown in Equation (4-1).

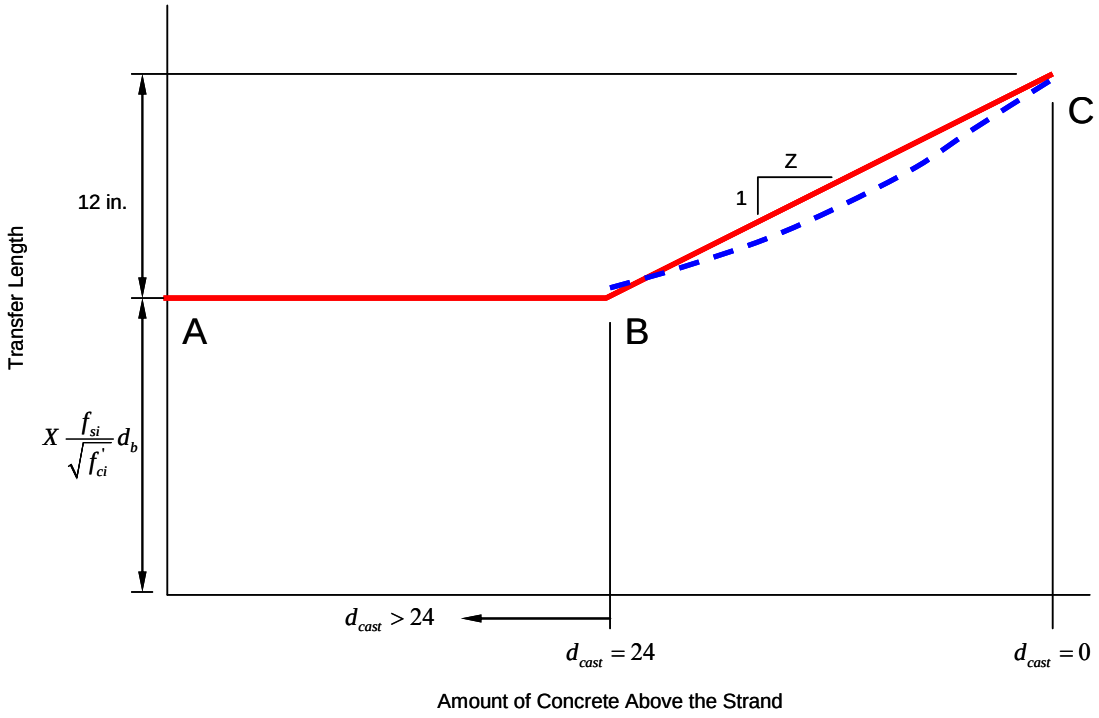

Figure 4.36. Average Predicted Transfer Length vs. d_{cast}

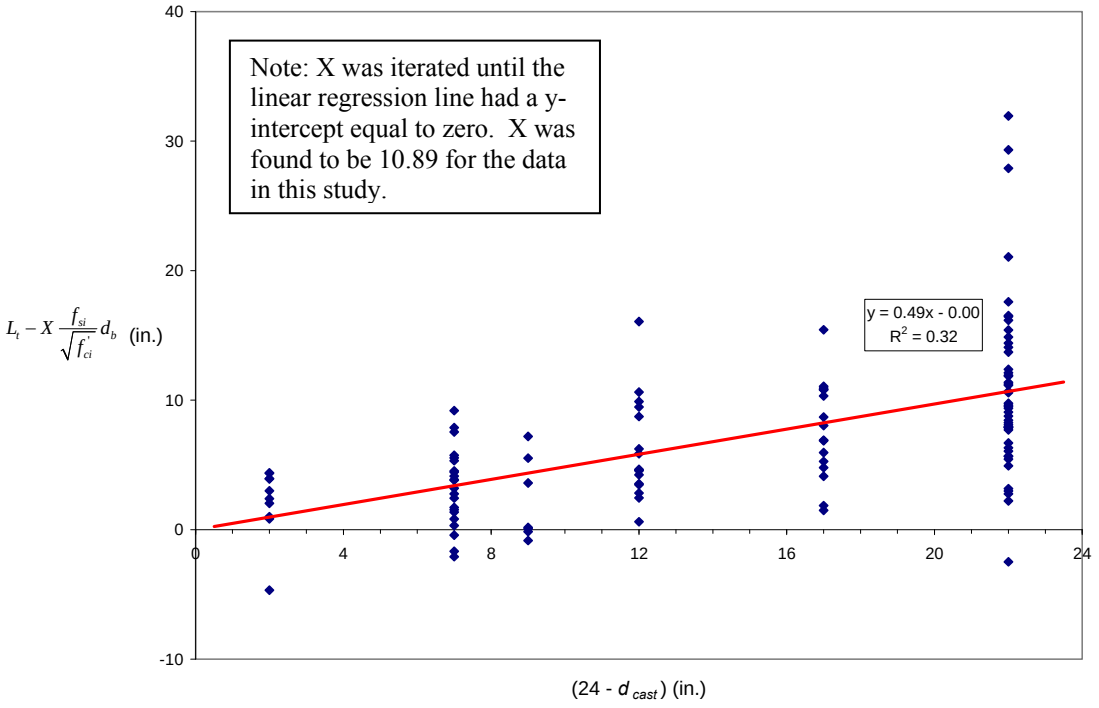

Figure 4.37. Transfer Length – $X(f_{si}/f'^{1/2}_{ci})d_b$ vs. $(24 - d_{cast})$

$$\text{For } d_{cast} < 24 \text{ in. } L_t = 11\frac{f_{si}}{\sqrt{f'_{ci}}}d_b + \frac{(24 - d_{cast})}{2}$$

$$\text{For } d_{cast} \geq 24 \text{ in. } L_t = 11\frac{f_{si}}{\sqrt{f'_{ci}}}d_b \qquad \text{Eq. (4-2)}$$

The transfer lengths from this study were plotted against Equation (4-2) as shown in Figure 4.38. The bold line in Figure 4.38 is the best fit linear regression line, which is nearly aligned with the line of perfect correlation, showing a very good representation of an average estimate for transfer length. As shown in Figure 4.38, about half the data is above the line of perfect correlation showing unconservative estimations by Equation (4-2). It is unreasonable to expect an equation to result in 100 percent conservative estimates. Therefore, a 95 percent limit was selected for estimated values to be considered conservative, similar to the derivation of other equations in the past that have used the 95 percent confidence interval. Equation (4-2) was modified to Equation (4-3) by trial and error. Note that the $(24 - d_{cast})$ term was squared in the transition, which tended to show a slightly better correlation for the data, especially for situations where

d_{cast} was extremely small. Figure 4.39 shows the measured transfer lengths plotted against predicted values using Equation (4-3), which resulted in a conservative estimation for 96.6 percent of the data.

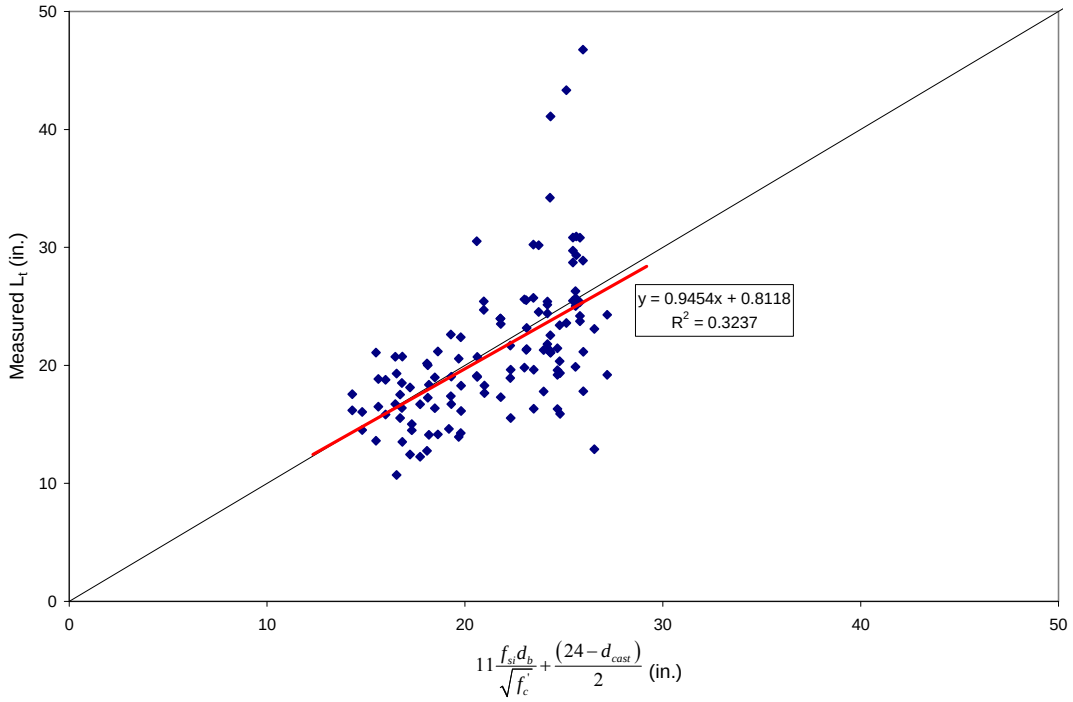

Figure 4.38. Measured Transfer Length vs. Equation (4-2)

$$\text{For } d_{cast} < 24 \text{ in. } \quad L_t = 20\frac{f_{si}}{\sqrt{f_{ci}'}}d_b + \frac{(24-d_{cast})^2}{40}$$

$$\text{For } d_{cast} \geq 24 \text{ in. } \quad L_t = 20\frac{f_{si}}{\sqrt{f_{ci}'}}d_b \qquad \text{Eq. (4-3)}$$

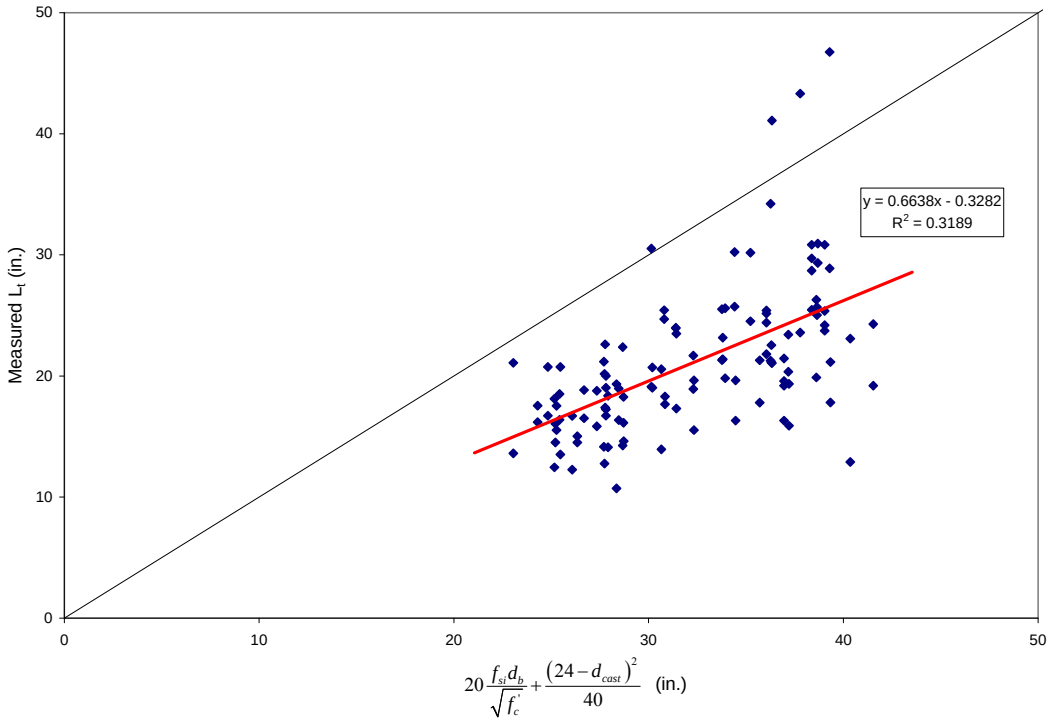

Figure 4.39. Measured Transfer Length vs. Equation (4-3)

Subsequent to the derivation of Equation (4-3), transfer length measurements from seven previous studies were also compared to the estimates from the modified equation. Figure 4.40 shows the measured transfer lengths from all seven studies plotted against Equation (4-3) with a best fit linear regression line shown by the red line. The relationship showed a small range along the abscissa, giving unconservative estimates for 25.3 percent of the data, while having a coefficient of correlation of only 0.179, indicating a poor fit of the data with the current form of the equation. In order to better estimate transfer lengths, it was imperative for the proposed equation to incorporate a larger data set from various researchers. Therefore, the coefficients were again modified until a reasonable amount of the data fell below the line of perfect correlation. The X coefficient was changed from 20 to 35 accounting for a number of longer reported transfer lengths for strands with more than 24 in. of concrete cast above the strand, while the Y and Z coefficients remained the same. The further modified equation is listed as Equation (4-4).

$$\text{For } d_{cast} < 24 \text{ in. } \; L_t = 35\frac{f_{si}}{\sqrt{f_{ci}^{'}}}d_b + \frac{(24 - d_{cast})^2}{40}$$

$$\text{For } d_{cast} \geq 24 \text{ in. } \; L_t = 35\frac{f_{si}}{\sqrt{f_{ci}^{'}}}d_b \qquad \text{Eq. (4-4)}$$

Figure 4.41 shows the measured transfer lengths from the seven previous studies plotted against Equation (4-4). Each data set is plotted separately to distinguish differences among sets. All of the data except the measurements taken by Peterman were for mixes using conventional concrete, while Peterman used mixes with high fluidity. Overall, 6 percent of the data fell above the line of perfect correlation, indicating a somewhat unconservative relationship. In addition to the amount of data in excess of the predicted values, the coefficient of correlation was 0.176. As shown by Peterman, the transfer lengths for the mixes with high levels of fluidity had transfer lengths far surpassing those reported herein with respect to casting position. For that reason, the factor ζ was added to Equation (4-4) resulting in Equation (4-5).

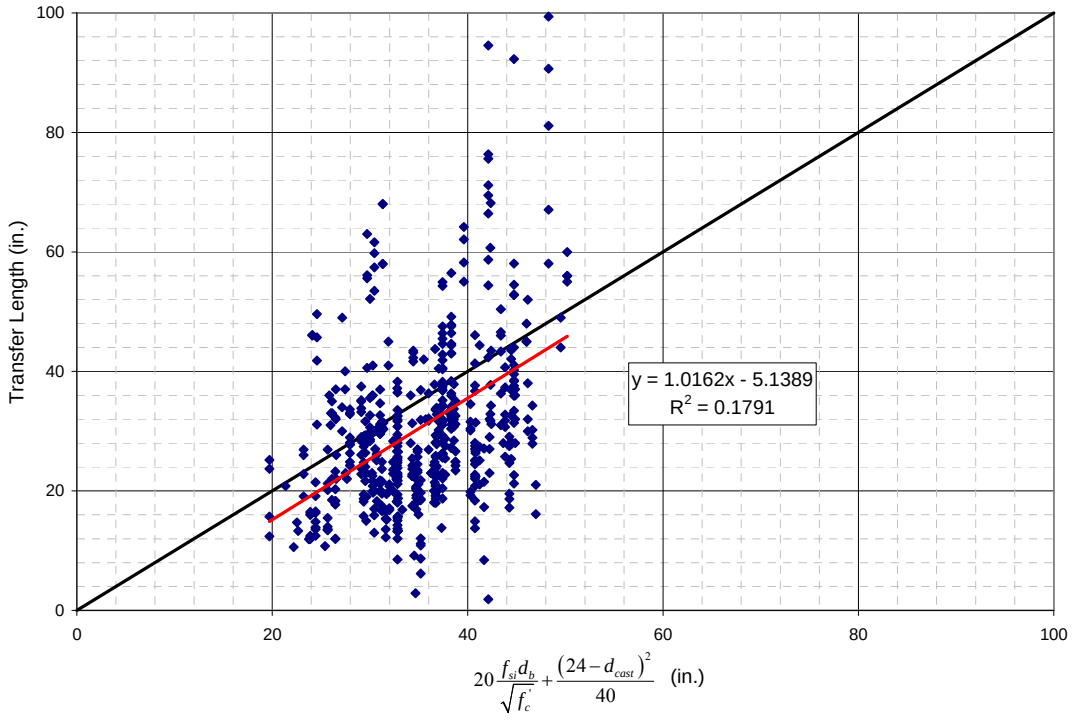

Figure 4.40. Measured Transfer Length from Prior Studies vs. Equation (4-3)

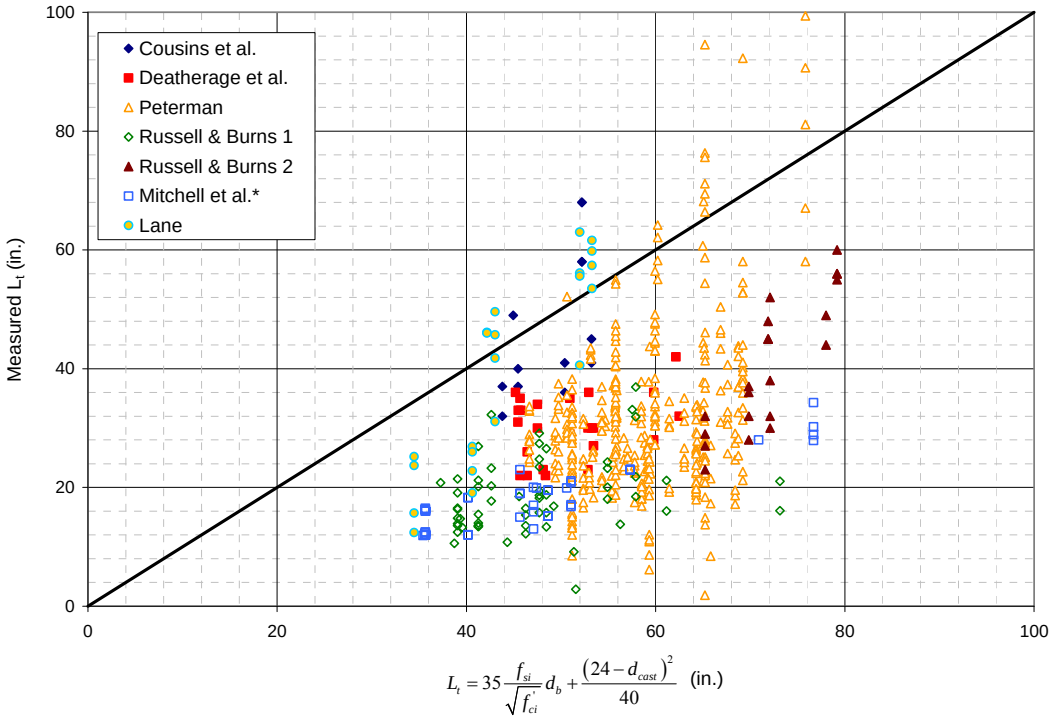

Figure 4.41. Measured Transfer Length from Prior Studies vs. Equation (4-4)

$$\text{For } d_{cast} < 24 \text{ in. } \quad L_t = 35\frac{f_{si}}{\sqrt{f'_{ci}}}d_b + \zeta\frac{(24-d_{cast})^2}{40}$$

$$\text{For } d_{cast} \geq 24 \text{ in. } \quad L_t = 35\frac{f_{si}}{\sqrt{f'_{ci}}}d_b \qquad \text{Eq. (4-5)}$$

Of the 6 percent of the data falling above the line of perfect correlation, almost half of those data points were from the Peterman data for mixes of high fluidity. It should also be noted that the Peterman data was obtained using end-slip measurements. The incorporation of the ζ factor allows for the increased influence of the top-strand effect in members containing mixes of high fluidity. For the data used in this report, mixes of high fluidity are limited to those used by Peterman where self consolidating concrete was used. The data in Figure 4.41 was plotted again in Figure 4.42 using Equation (4-5) and corresponding ζ values. A value of ζ = 1 was used for the data using a conventional concrete mix and a value of ζ = 2 was applied to the Peterman data associated with the high fluidity mixes. At the current time, high fluidity mixes are defined as the SCC mixes used by Peterman. As a result of the modification, only 4.2

percent of the data fell above the line of perfect correlation, ensuring that at least 95% of the predicted values were equal to or greater than the measured values. After a number of iterations $\zeta = 2.1$ was found to have the best correlation, but was rounded down to 2 for simplicity. A discrepancy does exist between $\zeta = 1$ and $\zeta = 2$, a gap that is thought to be dependent upon fluidity which was not investigated in this study.

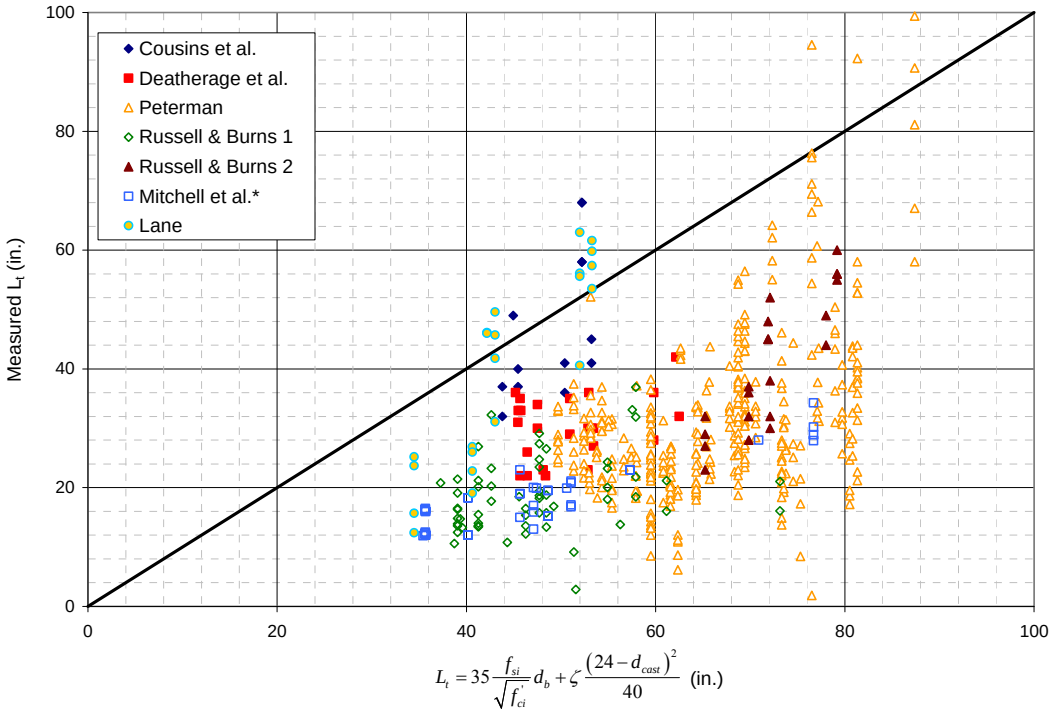

Figure 4.42. Measured Transfer Length from Prior Studies vs. Equation (4-5)

Based on the evaluation of the data from this study and the seven previous studies, Equation (4-5) was derived for the calculation of transfer length.

$$\text{For } d_{cast} < 24 \text{ in. } \quad L_t = 35\frac{f_{si}}{\sqrt{f'_{ci}}}d_b + \zeta\frac{(24-d_{cast})^2}{40}$$

$$\text{For } d_{cast} \geq 24 \text{ in. } \quad L_t = 35\frac{f_{si}}{\sqrt{f'_{ci}}}d_b \qquad \text{Eq. (4-5)}$$

4.2 End-slip

4.2.1 End-slip Measurements for Calculating Transfer Lengths

In addition to the use of concrete surface strains in the determination of transfer lengths, end-slip measurements were also taken for 57 transfer zones and used in various equations to calculate transfer lengths. The transfer length equations for use with end-slip are shown again in Table 4.11. As previously noted, end-slip measurements were only taken at the dead end of each test specimen as a result of fraying of the strand at the live end upon transfer. The transfer lengths calculated from concrete surface strains are listed in Table 4.12 along side the measured end-slips (L_{es}) for the T-beam test specimens. Also included are the calculated transfer lengths based on eight different equations relating end-slip to transfer length. Table 4.13 through Table 4.16 list the transfer lengths calculated from concrete surface strains, corresponding end-slip values, and the eight different end-slip based transfer length calculations for each of the four sets of top-strand block test specimens.

Transfer lengths were plotted against end-slip values as shown in Figure 4.43, which shows an approximately linear relationship. In addition to the tabulated values, the transfer lengths calculated from concrete surface strains are plotted against each of the eight equations using end-slip measurements for the calculation of transfer lengths along with best fit lines, shown in Figures 4.44 through 4.51. In the past, transfer lengths calculated form concrete surface strains have shown better consistency (Russell and Burns 1993) (Marti-Vargas et al. 2007). Of the eight equations, all but one showed a good correlation between surface strain based transfer lengths and end-slip based transfer lengths. The average ratio of calculated to measured transfer lengths was computed for each equation, shown in Table 4.11. Equation (2-29), used by Russell and Barnes had the lowest ratio, 1.01, Equations by Peterman and Logan had ratios of 1.04 and 1.06, respectively, while the equation by Cousins et al. had a ratio of 1.11. Guyon's equation had a ratio of 1.21, while the three equations by Balasz failed to show a favorable correlation having much higher ratios. Low average ratios of calculated to measured transfer lengths indicated end-slip measurements to be a reliable method for the determination of transfer lengths with the use of the correct equation. It should be noted, however, that some equations fail to include the compressive strain in the concrete.

Neglecting the strain in the concrete could lead to false estimations of transfer lengths. Thus, it is recommended that equations including the strain in the concrete be used for the calculation of transfer lengths based on end-slips measurements.

Table 4.11. Historical Transfer Length Equations (End-Slip)

Contributor	Year	Equation	Eq. No.	$\frac{L_{t(Calc)}}{L_{t(Meas)}}$
Guyon	1948	$L_t = \alpha \frac{L_{es}}{\varepsilon_{si}}$	2-24	1.21
Cousins et al.	1990	$L_t = \frac{2L_{es}E_{ps}}{f_{si} - E_{ps}\varepsilon_{ci}}$	2-23	1.11
Balasz	1992	$L_t = 218\sqrt[4]{\frac{\sqrt{L_{es}^3}}{f_{ci}^{'}}}d_b$	2-25	1.38
Balasz	1993	$L_t = 24.7\frac{L_{es}^{0.625}}{f_{ci}^{'0.15}\varepsilon_{si}^{0.4}}$	2-26	1.37
Balasz	1993	$L_t = 0.158\frac{f_{si}}{\sqrt{f_{ci}^{'}\sqrt{L_{es}}}}$	2-27	1.40
Russell & Burns	1996	$L_t = 294.9L_{es}$	2-29	1.01
Logan	1997	$L_t = 308L_{es}$	2-30	1.06
Peterman	2007	$L_t = \frac{2L_{es}E_{ps}}{f_{si}} = 293.8L_{es}$	2-28	1.04

Table 4.12. Transfer Lengths from End-slip Measurements (T-beams)

	Measured		Calculated							
	L_t	Ave. L_{es}								
Beam	(in.)	(in.)	Eq. 2-23	Eq. 2-24	Eq. 2-25	Eq. 2-26	Eq. 2-27	Eq. 2-28	Eq. 2-29	Eq. 2-30
2.270.5N.RB	12.5	0.0341	12.4	14.6	20.2	18.1	26.9	10.1	10.5	11.6
3.270.5S.RB	13.6	0.0401	14.5	16.5	20.8	19.7	24.4	11.8	12.4	13.5
4.270.5S.RB	15.5	0.0491	18.2	19.6	23.7	23.1	25.5	14.5	15.1	16.6
5.270.5S.RB	12.8	0.0451	14.8	16.7	22.8	20.9	28.7	13.3	13.9	13.7
6.270.5S.RB	16.7	0.0511	16.6	18.4	22.5	21.7	24.8	15.1	15.7	15.4
3.300.5S.RB	13.5	0.0461	15.1	17.0	22.0	20.6	26.1	13.6	14.2	14.0
4.300.5S.RB	14.1	0.0552	18.4	19.8	24.7	23.8	27.5	16.3	17.0	16.8
5.300.5S.RB	13.9	0.0490	14.5	16.4	23.5	21.1	31.3	14.5	15.1	13.4
6.270.6N.RB	10.7	0.0501	16.4	18.2	26.8	21.4	24.9	14.8	15.4	15.2
2.270.5N.UB	24.5	0.0581	21.3	22.7	24.7	25.3	23.5	17.1	17.9	19.7
3.270.5S.UB	19.8	0.0581	21.2	22.6	24.0	24.8	22.2	17.1	17.9	19.6
5.270.5S.UB	19.9	0.0631	20.8	22.2	25.9	25.7	26.4	18.6	19.4	19.2
6.270.5S.UB	17.8	0.0611	19.7	21.4	24.0	24.2	23.7	18.0	18.8	18.4
2.300.5N.UB	23.6	0.0892	29.5	30.2	29.0	31.7	23.5	26.3	27.5	27.2
3.300.5S.UB	21.1	0.0781	25.4	26.7	26.8	28.6	22.9	23.0	24.1	23.7
5.300.5S.UB	19.2	0.0670	20.0	21.4	26.5	25.6	28.9	19.8	20.6	18.4
6.270.6N.UB	12.9	0.0571	18.8	20.3	28.1	23.3	24.1	16.8	17.6	17.3

Table 4.13. Transfer Lengths from End-slip Measurements (TSB-Pour 1)

	Measured		Calculated							
	L_t	Ave. L_{es}								
Strand	(in.)	(in.)	Eq. 2-23	Eq. 2-24	Eq. 2-25	Eq. 2-26	Eq. 2-27	Eq. 2-28	Eq. 2-29	Eq. 2-30
A	17.8	0.0641	20.3	22.4	26.3	26.1	27.1	18.9	19.7	19.4
B	16.3	0.0494	15.6	17.9	23.8	22.2	28.9	14.6	15.2	14.9
C	17.7	0.0714	22.6	24.6	27.4	27.9	26.3	21.1	22.0	21.6
D	16.4	0.0657	20.8	22.9	26.5	26.5	26.9	19.4	20.2	19.9
E	15.8	0.0617	19.5	21.6	25.9	25.5	27.3	18.2	19.0	18.6
F	46.8	0.1497	48.1	48.3	36.1	44.4	21.8	44.2	46.1	45.3
G	30.2	0.1044	33.3	34.6	31.6	35.4	23.9	30.8	32.2	31.6
H	24.7	0.0717	23.1	24.7	27.4	28.0	26.3	21.2	22.1	21.7
I	30.8	0.1122	36.4	37.3	32.4	37.2	23.3	33.1	34.6	34.3
J	24.2	0.0705	22.8	24.5	27.2	27.8	26.1	20.8	21.7	21.5

Table 4.14. Transfer Lengths from End-slip Measurements (TSB-Pour 2)

	Measured		Calculated							
	L_t	Ave. L_{es}								
Strand	(in.)	(in.)	Eq. 2-23	Eq. 2-24	Eq. 2-25	Eq. 2-26	Eq. 2-27	Eq. 2-28	Eq. 2-29	Eq. 2-30
A	15.9	0.0310	9.8	12.3	19.2	16.1	29.9	9.1	9.6	9.3
B	15.5	0.0297	9.3	11.9	18.9	15.7	30.2	8.8	9.1	8.9
C	16.1	0.0447	14.1	16.4	22.0	20.3	27.3	13.2	13.8	13.4
D	14.5	0.0504	15.8	18.1	23.0	21.8	26.5	14.8	15.5	15.1
E	14.5	0.0607	19.1	21.2	24.7	24.5	25.3	17.9	18.7	18.2
F	20.4	0.0584	18.3	20.6	24.3	23.9	25.5	17.2	18.0	17.6
G	18.9	0.0487	15.3	17.7	22.7	21.4	26.7	14.4	15.0	14.7
H	14.3	0.0477	15.0	17.4	22.5	21.1	26.8	14.1	14.7	14.4
I	19.6	0.0685	21.9	23.8	25.8	26.5	24.3	20.2	21.1	20.8
J	16.3	0.0588	18.9	20.9	24.4	24.1	25.2	17.3	18.1	17.9

Table 4.15. Transfer Lengths from End-slip Measurement (TSB-Pour 3)

	Measured		Calculated							
	L_t	Ave. L_{es}								
Strand	(in.)	(in.)	Eq. 2-23	Eq. 2-24	Eq. 2-25	Eq. 2-26	Eq. 2-27	Eq. 2-28	Eq. 2-29	Eq. 2-30
A	21.1	0.0807	25.7	27.3	27.0	29.0	22.7	23.8	24.9	24.3
B	17.3	0.0651	20.7	22.6	24.9	25.4	23.9	19.2	20.0	19.6
C	16.7	0.0581	18.5	20.5	23.9	23.6	24.6	17.1	17.9	17.5
D	16.4	0.0591	18.8	20.8	24.0	23.9	24.5	17.4	18.2	17.8
E	16.2	0.0651	20.7	22.6	24.9	25.4	23.9	19.2	20.0	19.6
F	34.2	0.1234	39.4	40.3	31.6	37.9	20.4	36.4	38.0	37.3
G	24.0	0.0741	23.7	25.4	26.1	27.5	23.1	21.8	22.8	22.4
H	17.4	0.0741	23.7	25.4	26.1	27.5	23.1	21.8	22.8	22.4
I	21.8	0.0688	22.4	24.0	25.4	26.4	23.4	20.3	21.2	21.0
J	24.4	0.0645	21.0	22.7	24.8	25.4	23.7	19.0	19.9	19.7

Table 4.16. Transfer Lengths from End-slip Measurement (TSB-Pour 4)

	Measured		Calculated							
	L_t	Ave. L_{es}								
Strand	(in.)	(in.)	Eq. 2-23	Eq. 2-24	Eq. 2-25	Eq. 2-26	Eq. 2-27	Eq. 2-28	Eq. 2-29	Eq. 2-30
A	30.9	0.1101	35.5	36.4	31.9	36.4	23.1	32.5	33.9	33.4
B	21.4	0.0658	21.2	22.9	26.3	26.4	26.2	19.4	20.3	19.9
C	19.0	0.0731	23.5	25.2	27.3	28.2	25.5	21.6	22.5	22.2
D	17.3	0.0628	20.2	22.0	25.8	25.6	26.5	18.5	19.3	19.0
E	16.5	0.0684	22.0	23.8	26.7	27.1	26.0	20.2	21.1	20.8
F	25.7	0.0898	29.2	30.3	29.5	32.1	24.2	26.5	27.7	27.3
G	21.3	0.0768	24.9	26.3	27.8	29.1	25.2	22.6	23.7	23.3
H	19.1	0.0851	27.5	28.9	28.9	31.0	24.6	25.1	26.2	25.9
I	30.8	0.1206	39.9	40.0	33.0	38.7	22.3	35.6	37.1	37.0
J	25.5	0.0759	25.1	26.3	27.7	29.0	25.0	22.4	23.4	23.3

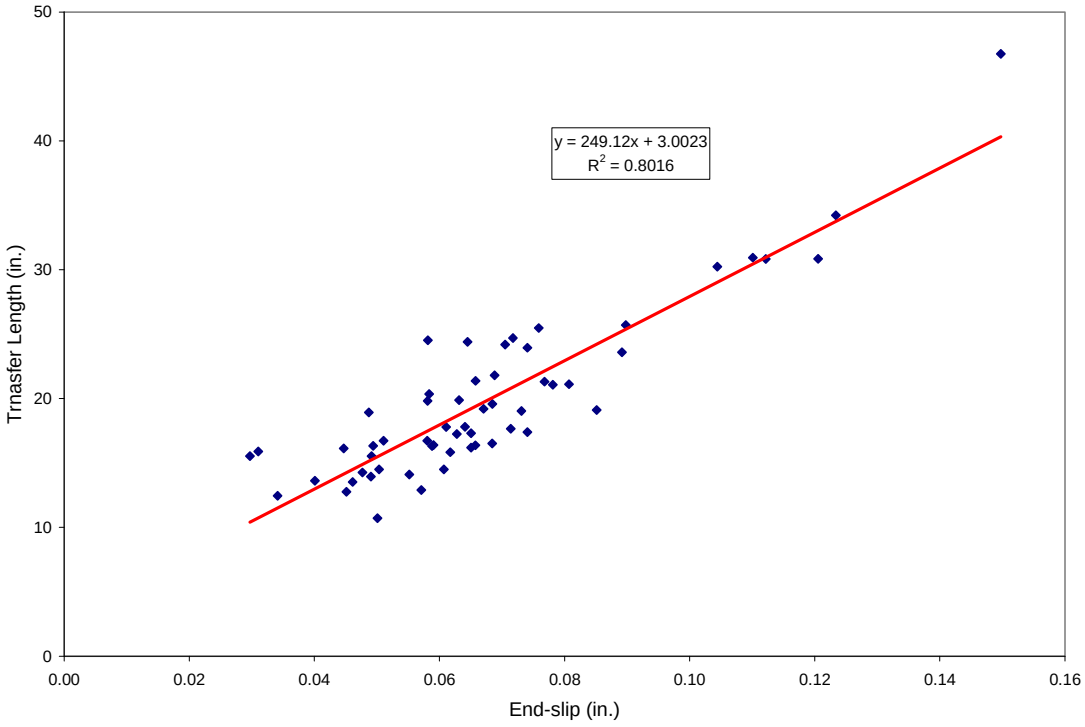

Figure 4.43. Measured Transfer Length vs. End-slip Measurements

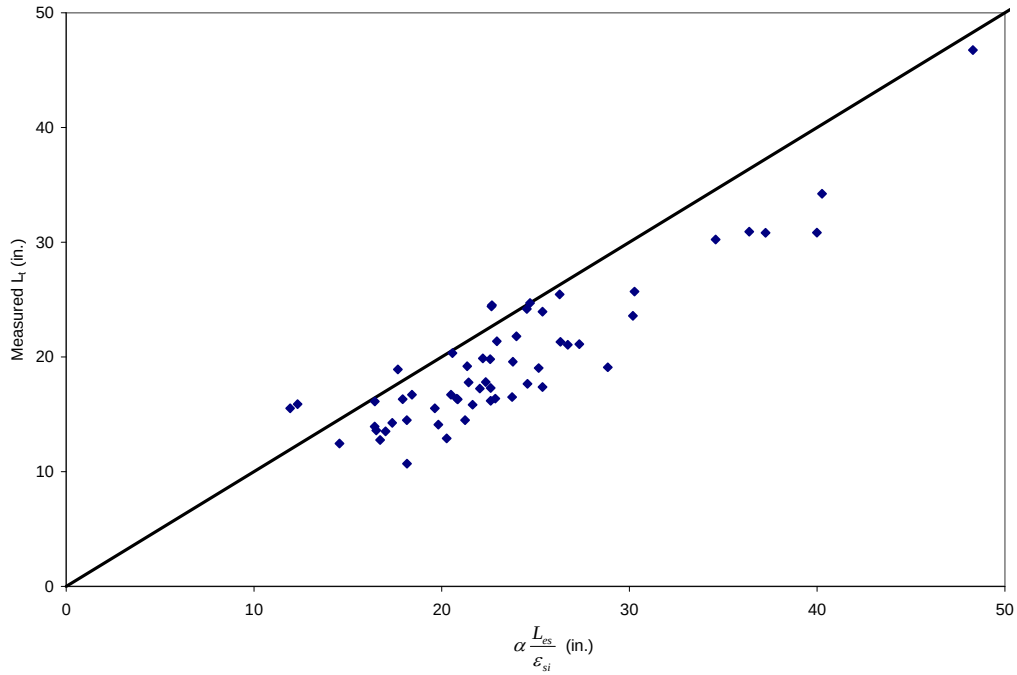

Figure 4.44. Measured Transfer Lengths vs. Guyon (Eq. 2-24)

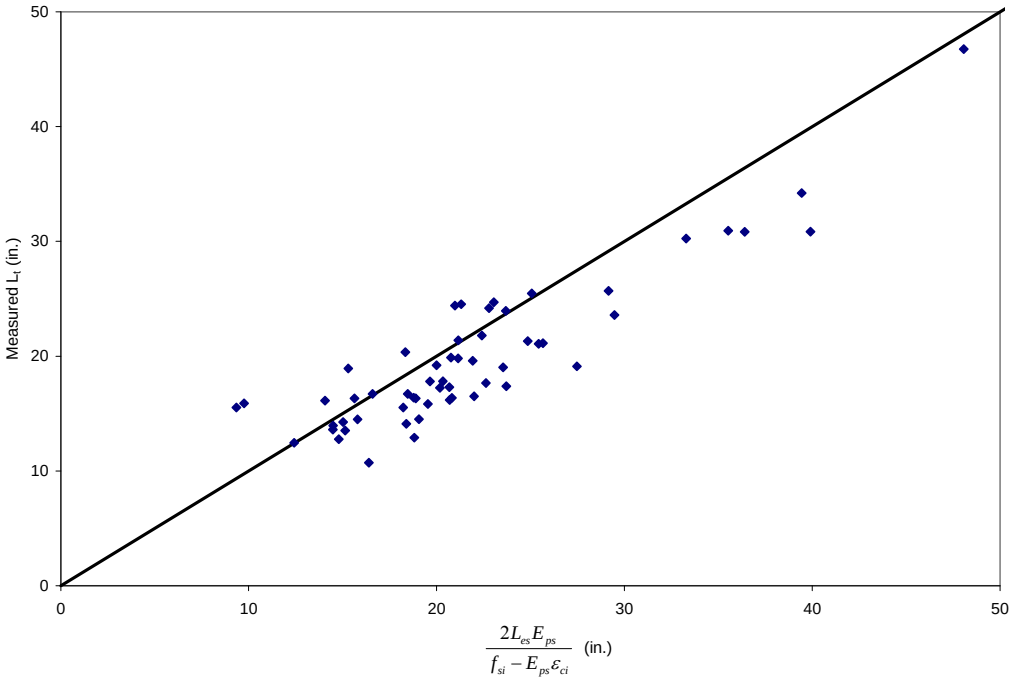

Figure 4.45. Measured Transfer Lengths vs. Cousins et al. (Eq. 2-23)

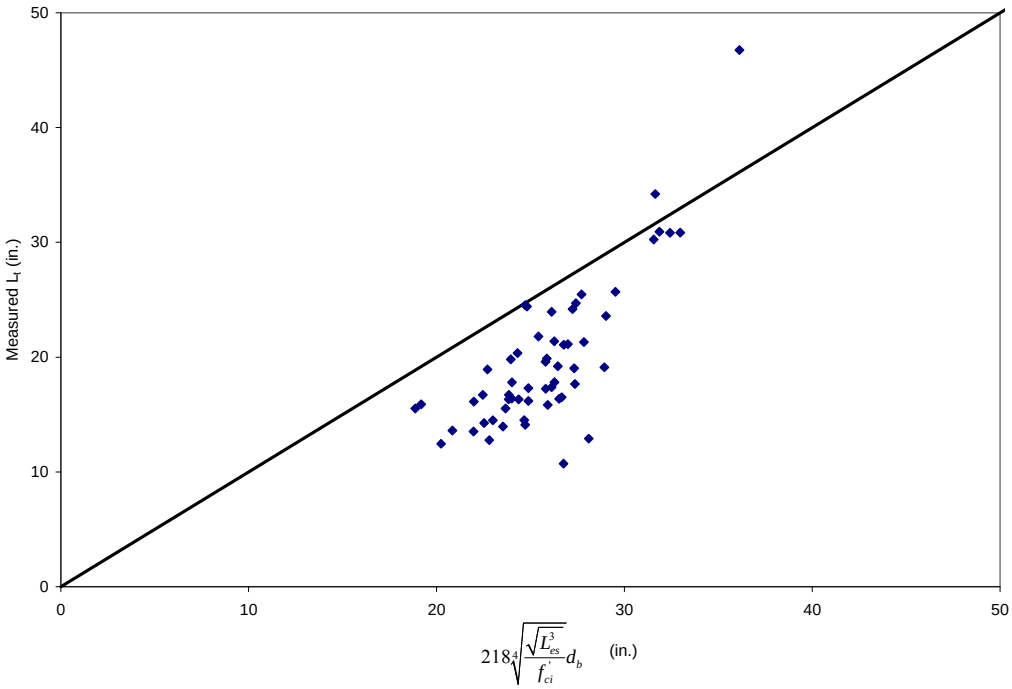

Figure 4.46. Measured Transfer Lengths vs. Balasz (Eq. 2-25)

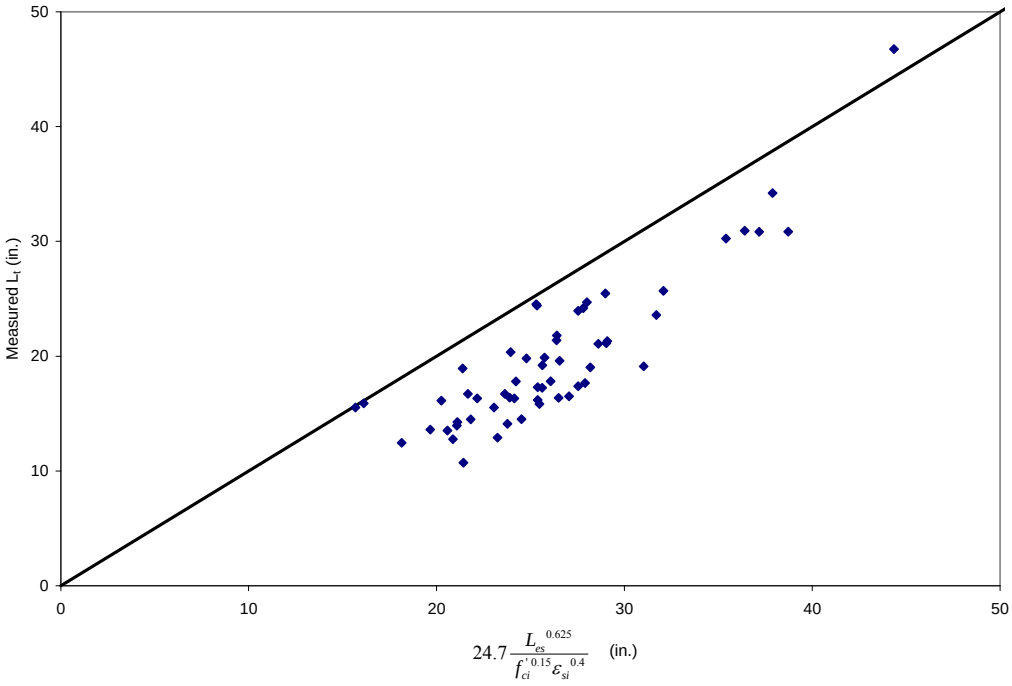

Figure 4.47. Measured Transfer Lengths vs. Balasz (Eq. 2-26)

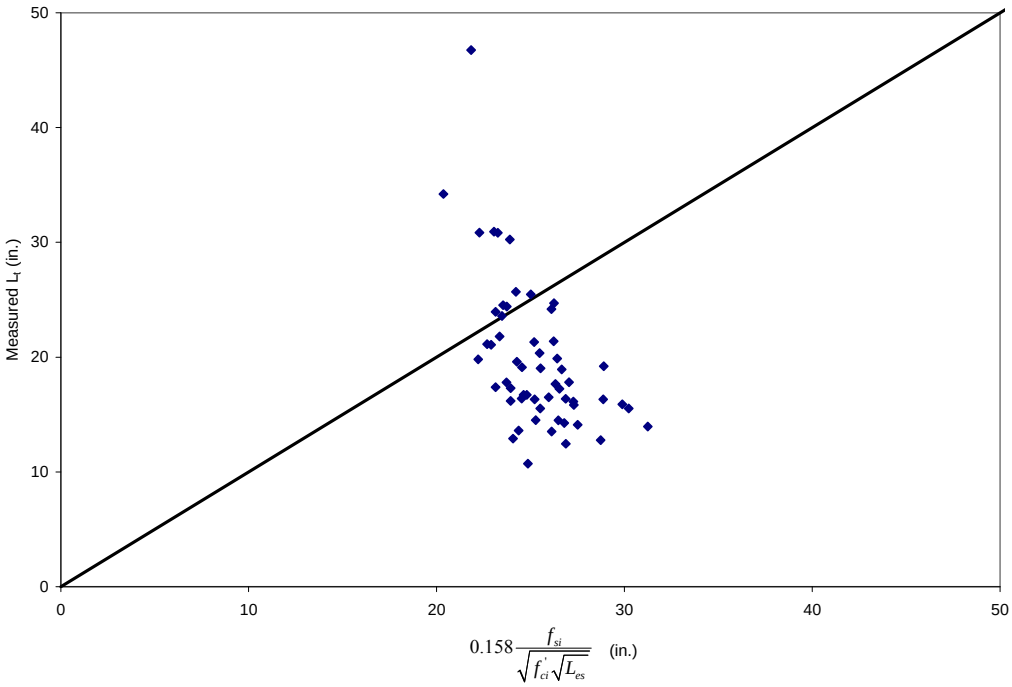

Figure 4.48. Measured Transfer Lengths vs. Balasz (Eq. 2-27)

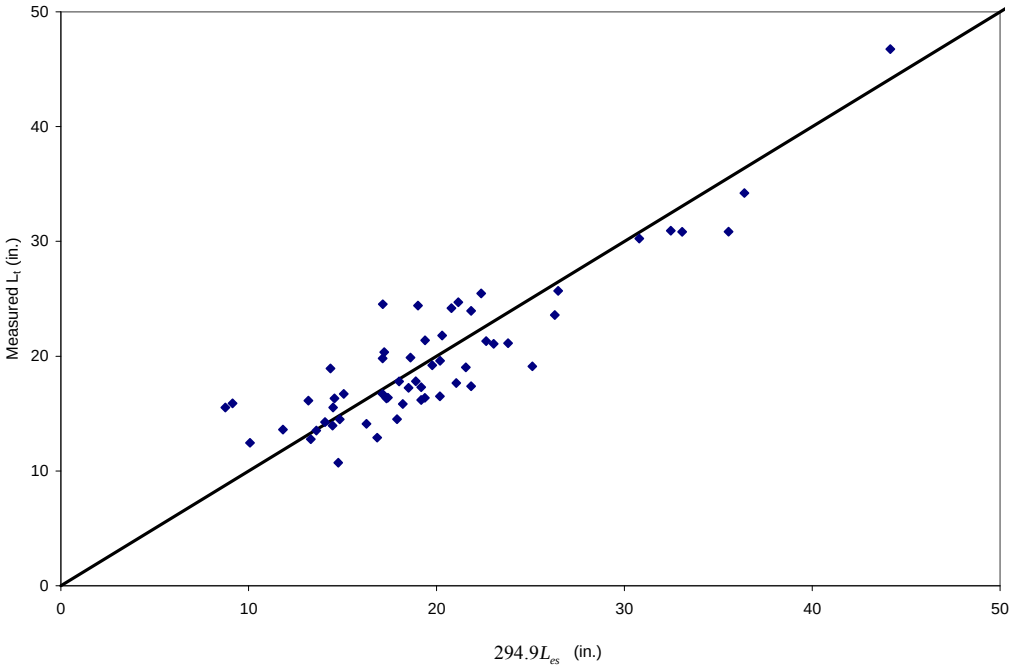

Figure 4.49. Measured Transfer Lengths vs. Russell and Barnes (Eq. 2-29)

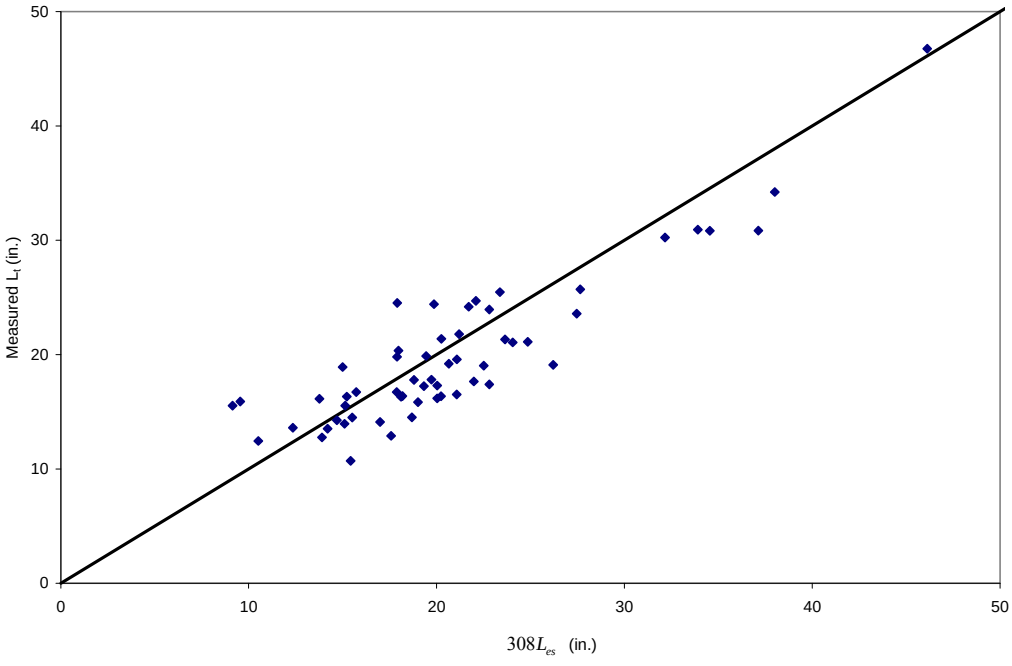

Figure 4.50. Measured Transfer Lengths vs. Logan (Eq. 2-30)

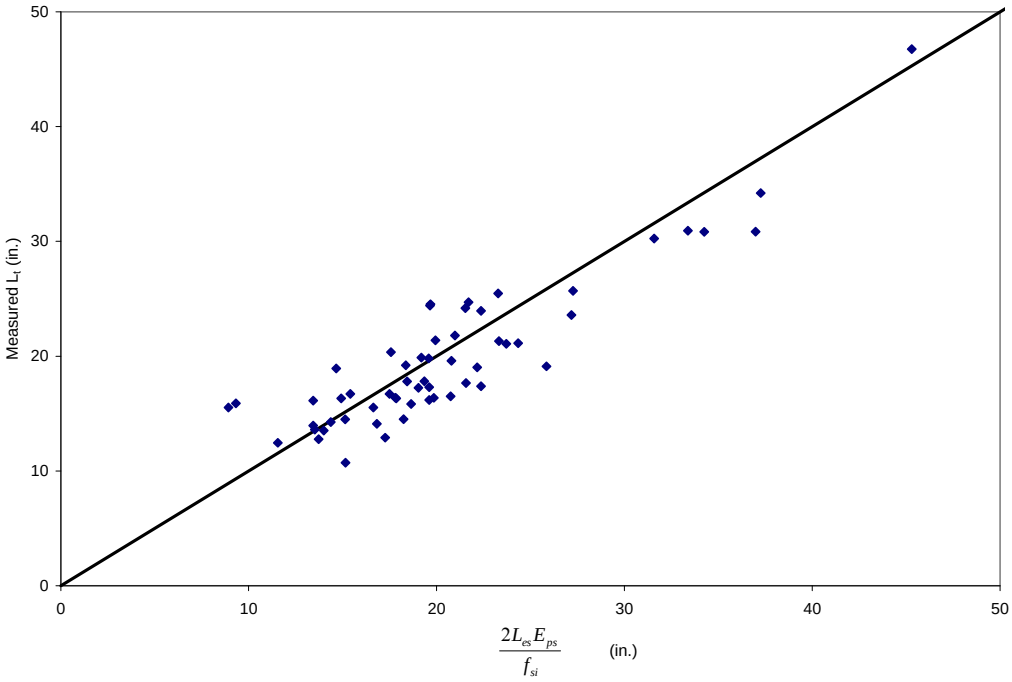

Figure 4.51. Measured Transfer Lengths vs. Peterman (Eq. 2-28)

4.2.2 Transfer Length and Bond Stress

During the transfer process, as the strand tries to slip within the concrete, causing end-slip, bond stresses develop between each individual strand and the surrounding concrete creating a resistance to the strands tendency to slip. As the distance from the end of the specimen increases, the amount of slip between the strand and concrete decreases until the slip reaches zero at the end of the transfer zone and the stress in the strand is fully transferred to the surrounding concrete. In the current provisions for the calculation of transfer length, ACI assumes a constant bond stress of 400 psi. The ACI value is assumed to be conservative and a number of researchers have reported bond stresses far surpassing the assumed value of 400 psi.

Bond stresses were calculated for each transfer zone using the relationship from Equation (2-11), which assumes a linear relationship in steel stress from the end of the member to the end of the transfer length and the perimeter of a strand equal to $4/3\pi d_b$ (Buckner 1995). A summary of calculated bond stresses are listed in Table 4.17. When previously comparing transfer length to casting position, transfer length was shown to be highly dependent on the amount of concrete cast above the strand. Plotting bond stresses

against the amount of concrete above the strand as shown in Figure 4.52 also showed the same trend, indicating that as d_{cast} is increased, bond stresses increase, thus reducing transfer lengths. In addition to bond stresses, the bond quality of each strand type used in the T-beam test specimens was also compared to transfer length measurements and is shown in Figures 4.53 and 4.54 for the LBPT and NASP test, respectively (Loflin 2008). All of the strands considered to be bottom-cast strands had satisfactory transfer length results, but when plotted against LBPT and NASP test values, as previous studies have done (Ramirez and Russell 2007), no correlation existed between transfer lengths and LBPT and NASP test values. Taking into consideration the relationships previously discussed with respect to the amount of concrete cast above the strand, the transfer lengths were again plotted against LBPT and NASP test values normalized with d_{cast} and the concrete strength. Figures 4.55 and 4.56 show the transfer lengths potted against LBPT and NASP values, respectively, with casting position and concrete strength taken into consideration. The data in Figure 4.55 and 4.56 both show a linear trend indicating transfer lengths to be directly proportional to LBPT and NASP test values. Of the strand tested, one strand did not meet the minimum values for each test, however, the strand did have satisfactory transfer lengths. LBPT results were also plotted against NASP test results which did show a good correlation as shown in Figure 4.57.

Table 4.17. Experimentally Determined Bond Stresses

		Bond Stress (ksi)							
		Concrete Strength (psi)							
		4800	4900	5000	5300	5700	6000	6100	6400
Live	AVE	0.623	0.771	0.637	0.512	0.716	0.563	0.696	0.745
	STDEV	0.096	0.031	0.109	0.154	0.102	0.134	0.090	0.057
	MAX	0.753	0.812	0.807	0.679	0.922	0.721	0.859	0.842
	MIN	0.476	0.736	0.490	0.315	0.591	0.364	0.587	0.704
Dead	AVE	0.642	0.964	0.776	0.759	0.845	0.872	0.757	1.132
	STDEV	0.195	0.072	0.211	0.220	0.102	0.182	0.158	0.275
	MAX	0.870	1.056	1.191	0.988	0.970	1.107	0.932	1.519
	MIN	0.294	0.864	0.480	0.502	0.680	0.681	0.440	0.846
Total	AVE	0.633	0.881	0.706	0.635	0.781	0.718	0.726	0.938
	STDEV	0.154	0.112	0.182	0.227	0.121	0.222	0.132	0.277
	MAX	0.870	1.056	1.191	0.988	0.970	1.107	0.932	1.519
	MIN	0.294	0.736	0.480	0.315	0.591	0.364	0.440	0.704

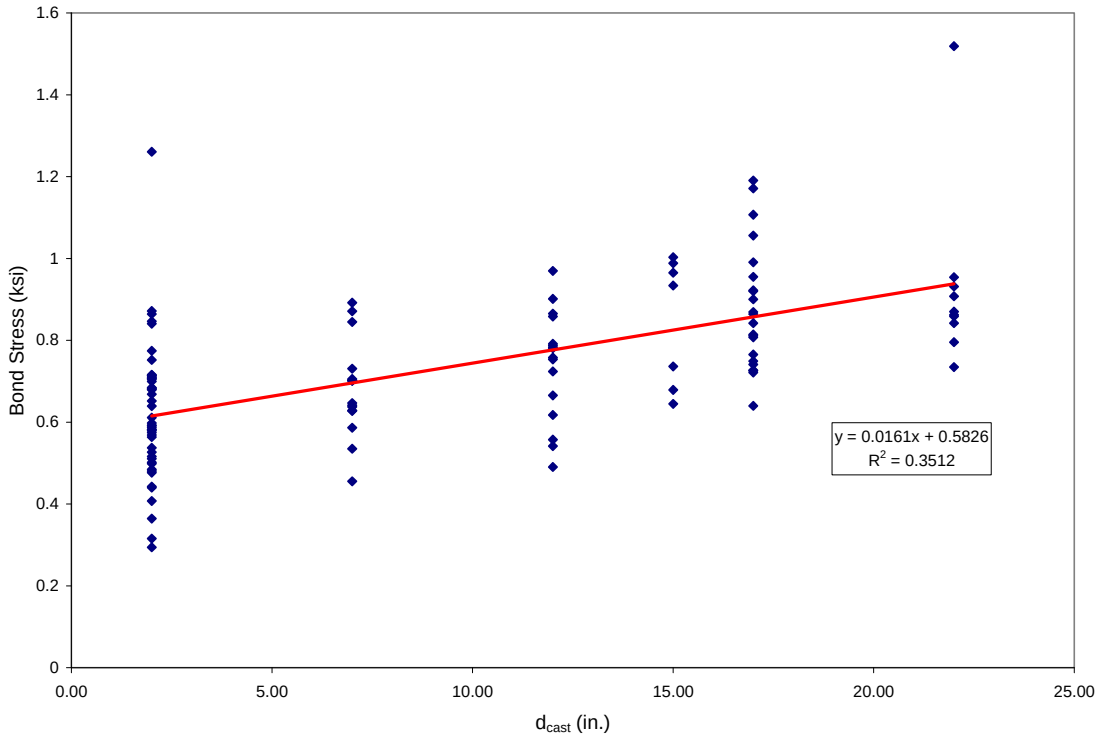

Figure 4.52. Bond Stress vs. d_{cast}

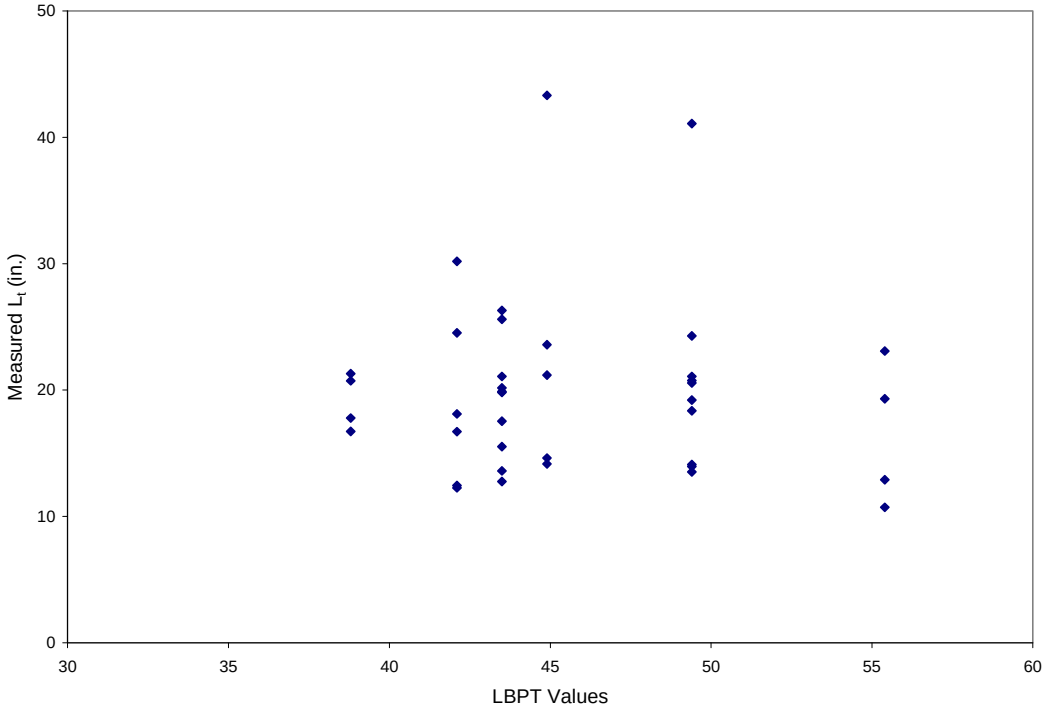

Figure 4.53. Measured Transfer Lengths vs. LBPT Values

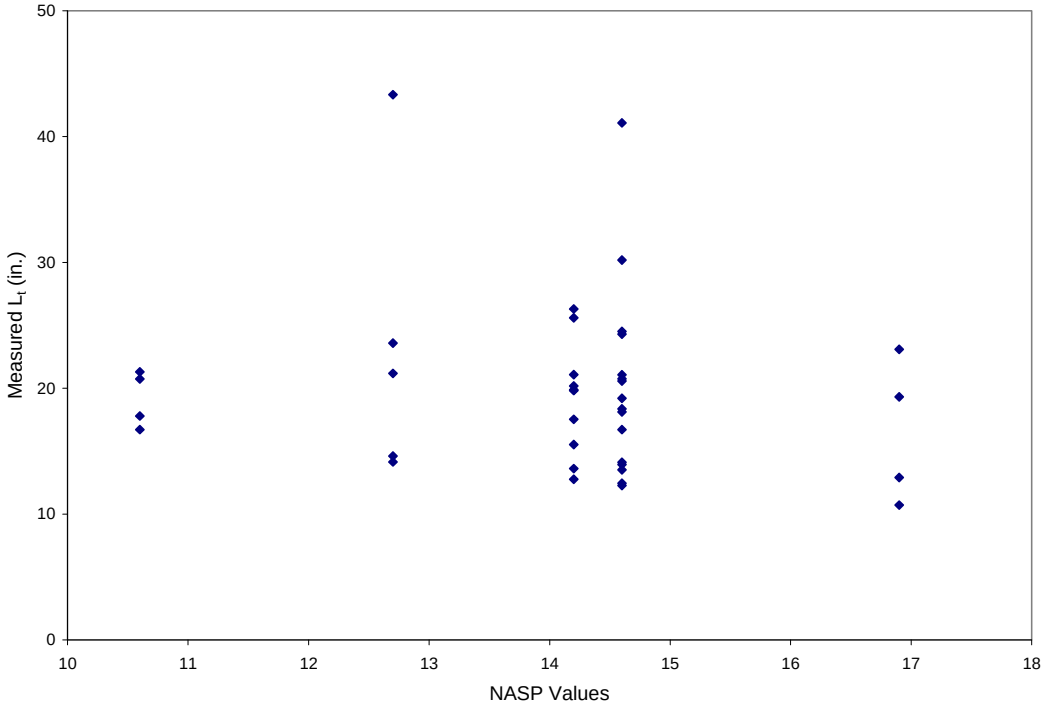

Figure 4.54. Measured Transfer Lengths vs. NASP Test Values

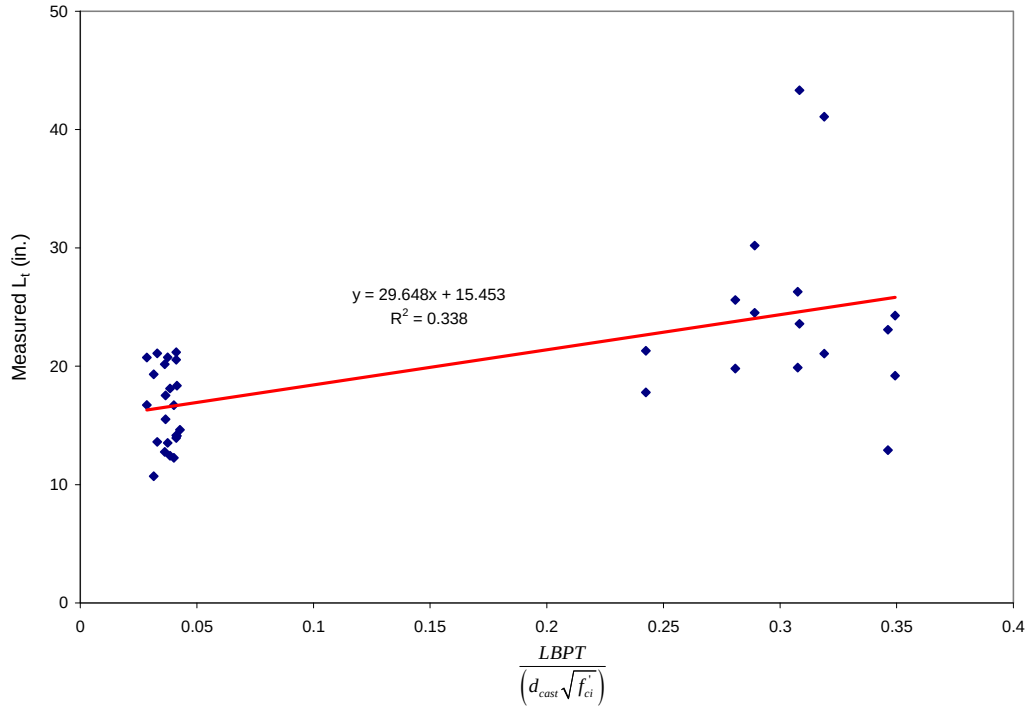

Figure 4.55. Measured Transfer Lengths vs. LBPT/(d_{cast}*f'$_c$^0.5)

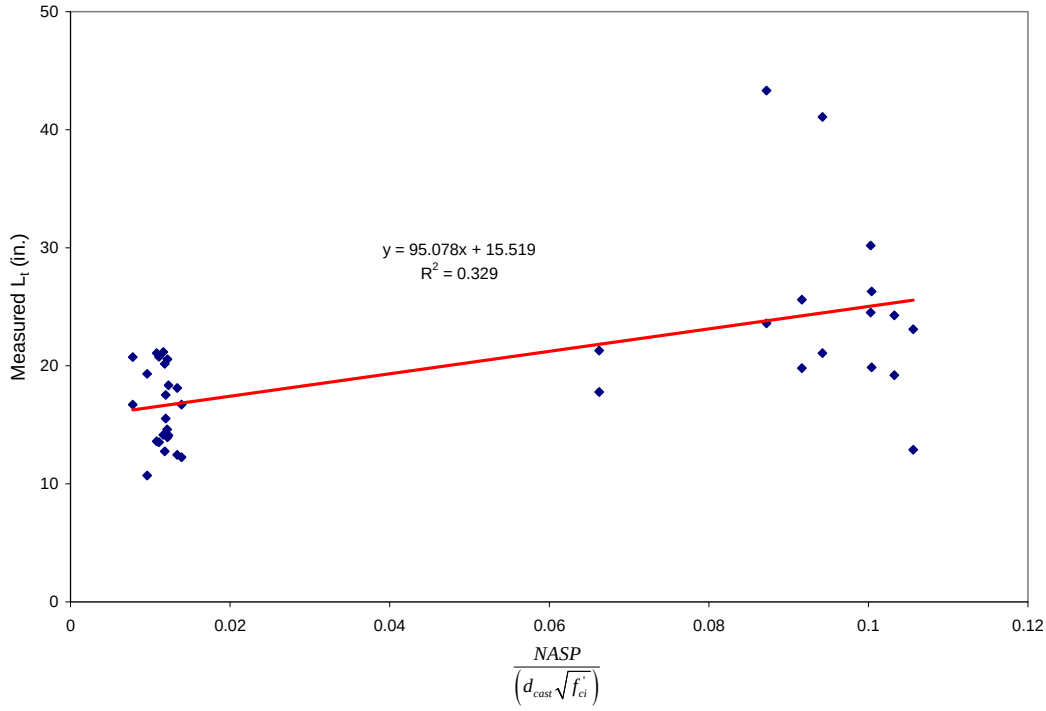

Figure 4.56. Measured Transfer Lengths vs. NASP/(d_{cast}*f'$_c$^0.5)

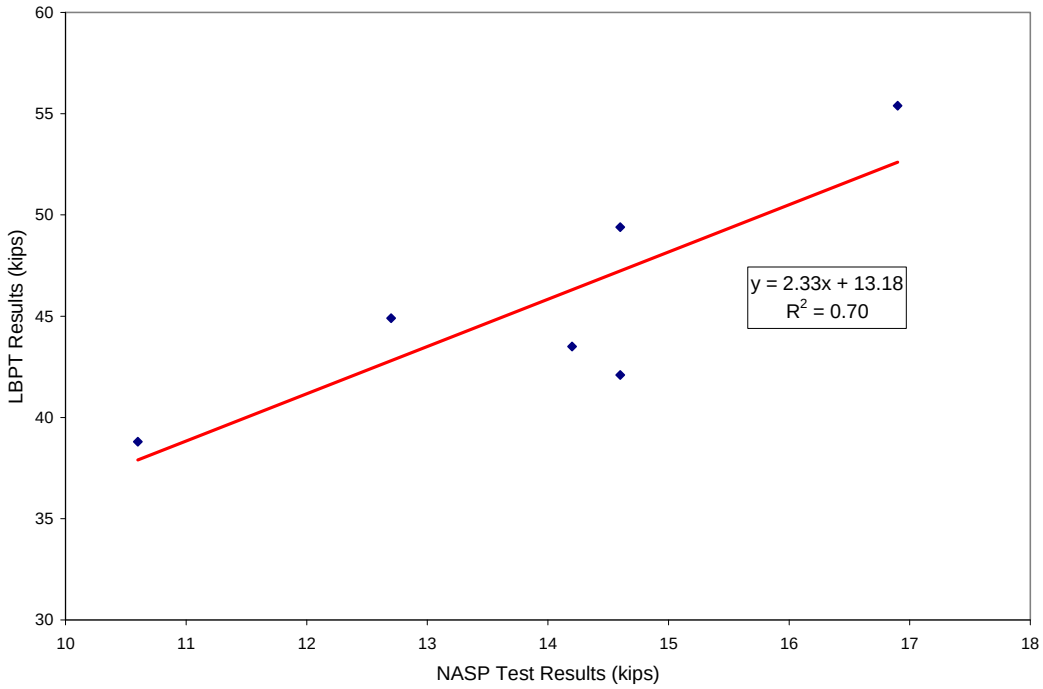

Figure 4.57. LBPT Results vs. NASP Test Results

4.3 Practical Modeling Technique for Transfer Length

As previously discussed, transfer length increased with a decrease in the amount of concrete cast above the strand. With an increase in transfer lengths also came a decrease in bond stress and an increase in end-slip between the concrete and strand. Therefore, it can be concluded that transfer length is directly proportional to end-slip and the force versus displacement relationship between the strand and the surrounding concrete. In common practice, the stresses from the prestress force within a member are of concern at transfer and various other times throughout the life of the member. Stresses are calculated at the time of transfer to ensure no cracking of the concrete will occur and the transfer length is later used in the determination of the shear resistance of the member. The transfer length is calculated using either Equation (2-3), (2-4), or (2-13), depending on the code used and is typically estimated by Equation (2-4) or (2-13) in the calculation of shear strength.

In most cases, conventional methods could be used for the calculations of stresses and shear strength with code assumed transfer length values. In other cases, such as deep beams or members containing various voids, traditional methods may not be sufficient

and may require the use of measured transfer length values and a more detailed analysis method, such as strut and tie models or finite element analysis. In the case of finite element models, to accurately predict the behavior within the end-zone of the member, the slip between the strand and the surrounding concrete must be modeled. This behavior was successfully determined with the details of its development described herein.

The development of the strand-slip behavior was determined based on the experimental results from this study for strands with a jacking stress of $0.75f_{pu}$, but can be modified for any strand size, jacking stress, and concrete strength with sufficient model verification. To effectively use the modeling technique, the transfer length must be known prior to the model development. Ideally, the transfer length would be from experimentally determined values, via concrete surface strains or strand end-slips, but in some cases transfer lengths may be needed for design prior to member fabrication. When the transfer length is unknown or needed prior to member fabrication, it should be calculated using Equation (4-5) taking into consideration, the initial prestress, concrete strength, strand size, and the amount of concrete cast above the strand. As mentioned in other sections, there is a force versus displacement relationship between the strand and the surrounding concrete, which is unknown and the first item in need of determination.

Finite element models were constructed for the 12 ft long, 4 in. by 4 in. concrete prisms from the top-strand blocks in Pours 1 through 4. Using the actual material properties of the concrete and prestressing steel, four individual models were constructed and transfer length versus spring stiffness curves developed for each. The first two models contained ½ in. diameter 270 ksi prestressing strands with concrete compressive strengths of 4800 psi and 5700 psi, respectively. The third and fourth models contained ½ in. diameter super 270 ksi prestressing strands with concrete compressive strengths of 6100 psi and 5000 psi, respectively. Shown in Figure 4.58 and Figure 4.59 are the relationships for transfer length versus spring stiffness for the ½ in. diameter and ½ in. diameter super strands, respectively. It was determined that the small range of concrete strengths in this study had little to no effect on the transfer length versus spring stiffness behavior as the two curves on each plot nearly overlapped. However, there was a slight difference as a result of strand size. In other cases, a wider range of concrete strengths may affect the relationship shown in Figure 4.58 and Figure 4.59, but this would be

determined when developing that relationship for a specific model, since concrete strength is a required property of the finite element model. With concrete strength having little effect on these models, an average best fit curve was fit to the data resulting in Equation (4-6) for calculating transfer length as a function of spring stiffness for the ½ in. diameter regular strand, while Equation (4-7) was fit to the data for the ½ in. diameter super strand.

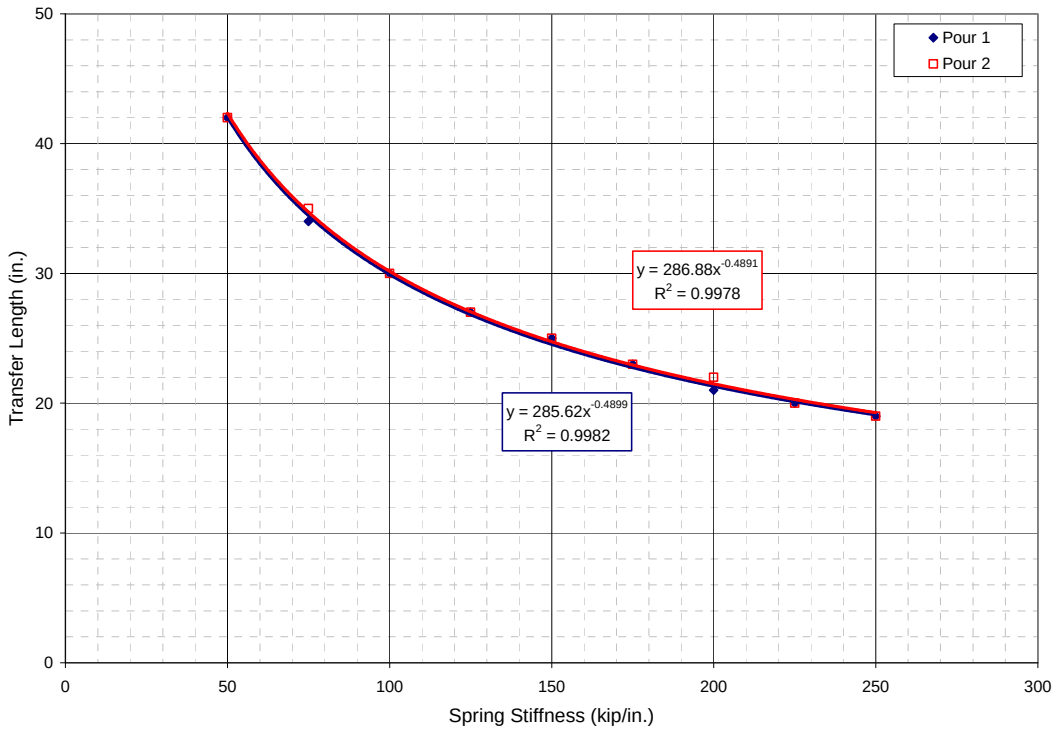

Figure 4.58. Transfer Length vs. Spring Stiffness (½ in. diameter regular)

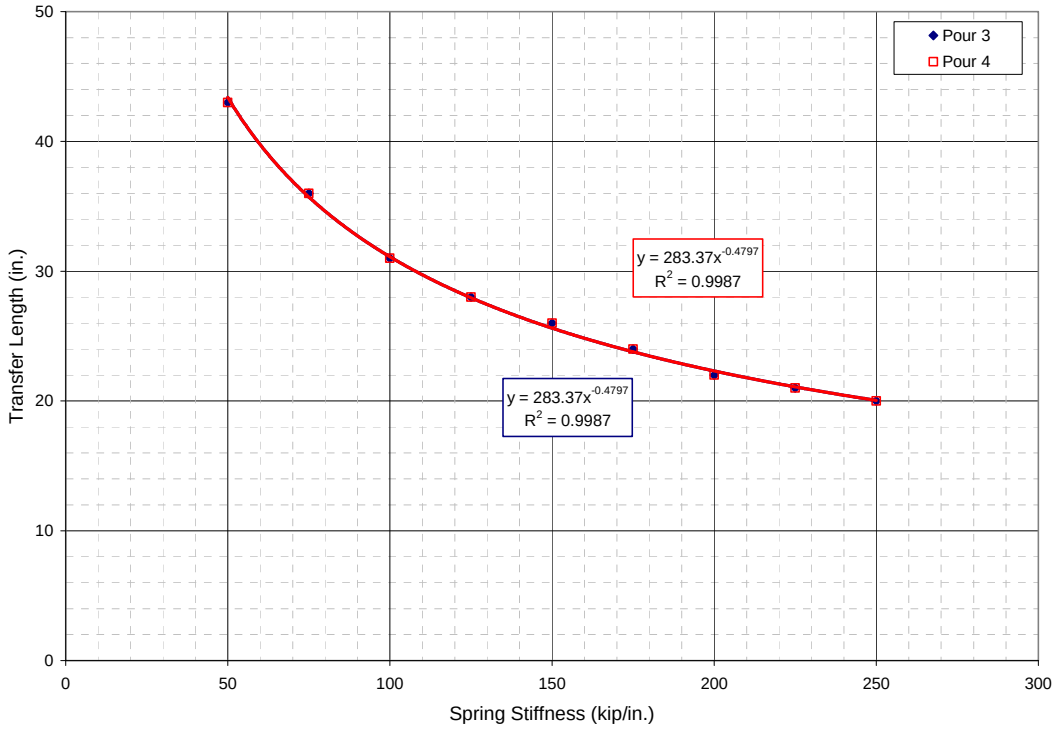

Figure 4.59. Transfer Length vs. Spring Stiffness (½ in. diameter super)

$$L_t = 286k^{-0.490} \qquad \text{Eq. (4-6)}$$

$$L_t = 283k^{-0.480} \qquad \text{Eq. (4-7)}$$

In addition to the 4 in. by 4 in. concrete prisms, the relationship of transfer length and spring stiffness was also evaluated for the large blocks (24 in. tall by 4 in. wide) of the top-strand block test specimens to study the effect one strand may have on an adjacent strand and the effect of a larger cross-section. Again, four models were developed including specific strand sizes and concrete strengths, all of which used 1 in. by 1 in. elements. The first two models contained ½ in. diameter, 270 ksi strands with concrete strengths of 4800 psi and 5700 psi, respectively. The third and fourth models contained ½ in. diameter super, 270 ksi strands and had respective concrete strengths of 6100 psi and 5000 psi. Figures 4.60 through 4.63 show the relationships for transfer length versus spring stiffness for large block of the top-strand blocks of Pours 1, 2, 3, and 4, respectively. Note that only strands A, B, and C were included in each plot. The relationship of transfer length to spring stiffness for strand D was found to be identical to strand B and strand E was found to be identical to strand A because of their respective

locations within the model. As with the 4 in. by 4 in. prisms, the ½ in. diameter regular strands and the ½ in. diameter super strands had a different relationship between transfer length and spring stiffness and the small range of concrete strengths were again found to have little effect. Average best fit curves were fit to the data for each strand size resulting in Equations (4-8) and (4-9) for calculating transfer length as a function of spring stiffness for the ½ in. diameter regular strand and ½ in. diameter super strand, respectively.

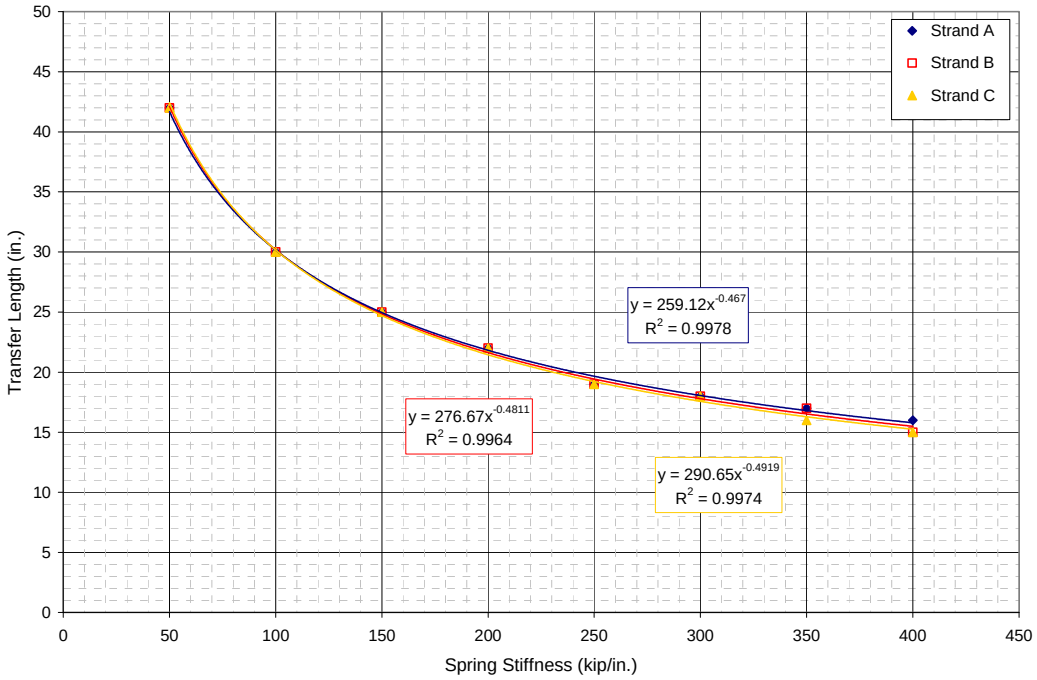

Figure 4.60. Transfer Length vs. Spring Stiffness (TSB-Pour 1)

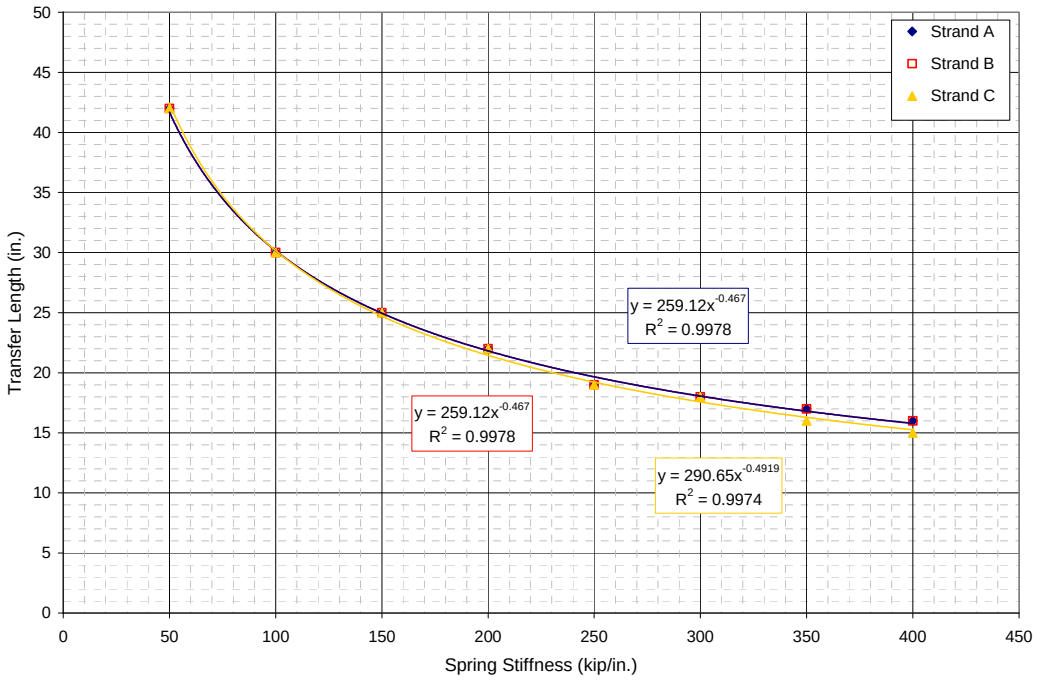

Figure 4.61. Transfer Length vs. Spring Stiffness (TSB-Pour 2)

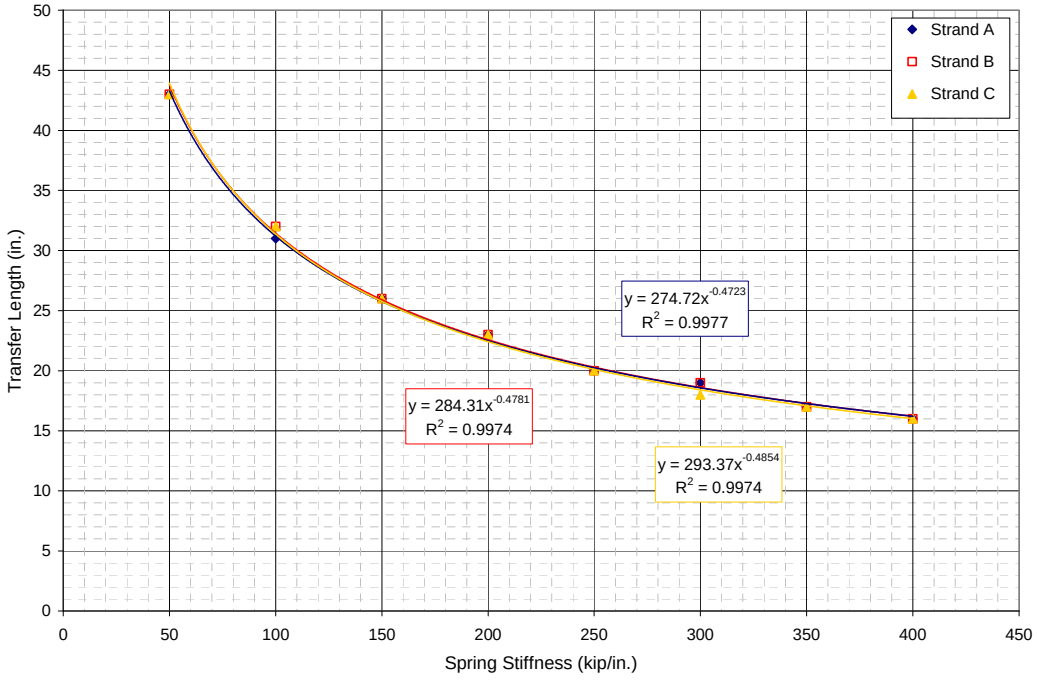

Figure 4.62. Transfer Length vs. Spring Stiffness (TSB-Pour 3)

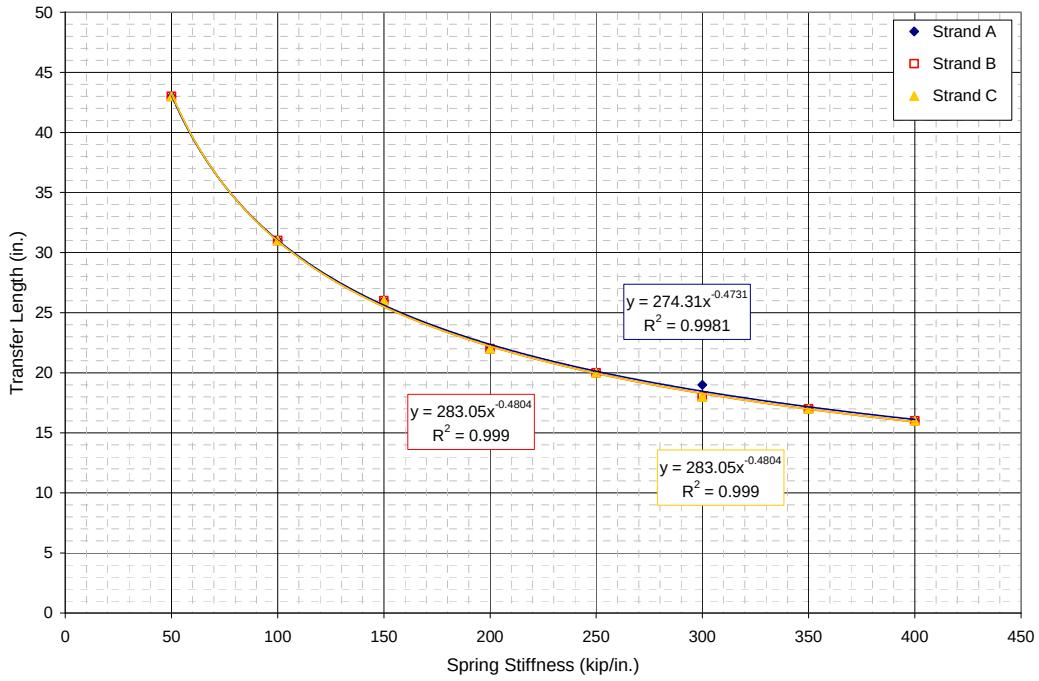

Figure 4.63. Transfer Length vs. Spring Stiffness (TSB-Pour 4)

$$L_t = 272k^{-0.478} \qquad \text{Eq. (4-7)}$$

$$L_t = 282k^{-0.478} \qquad \text{Eq. (4-8)}$$

With the transfer length versus spring stiffness relationships known for each strand type, the correct stiffness for the nonlinear springs was then chosen corresponding to the measured transfer lengths as shown in Figure 4.64 for the dead end of the large block of the top-strand blocks in Pour 4. Each respective stiffness was then applied to each strand in the model and an additional nonlinear analysis performed as with previous models. Individual transfer lengths were recalculated for each strand to verify the same conditions in the analytical model as the experimental test specimen. Subsequent to verification of the finite element based transfer lengths, the model was in a completed stage and could be used for the analysis of stresses and strains. Figure 4.65 shows the stress contours in the X-direction as a result of the various prestressing strands in the model. As previously noted, if the transfer lengths were unknown, the transfer lengths should be determined using Equation (4-5).

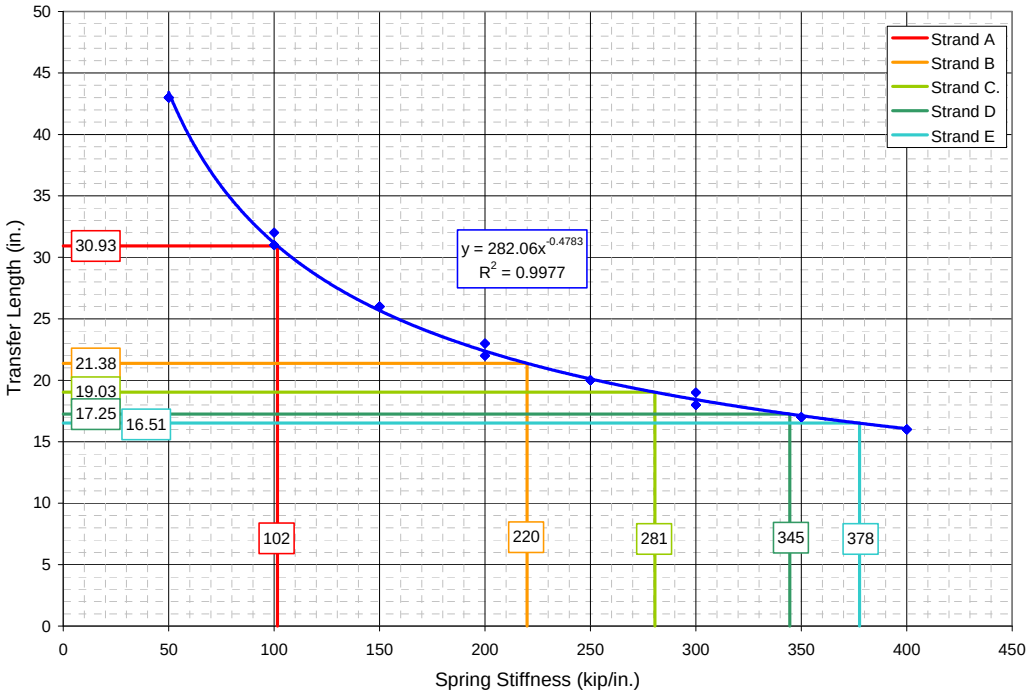

Figure 4.64. Selection of Spring Stiffnesses

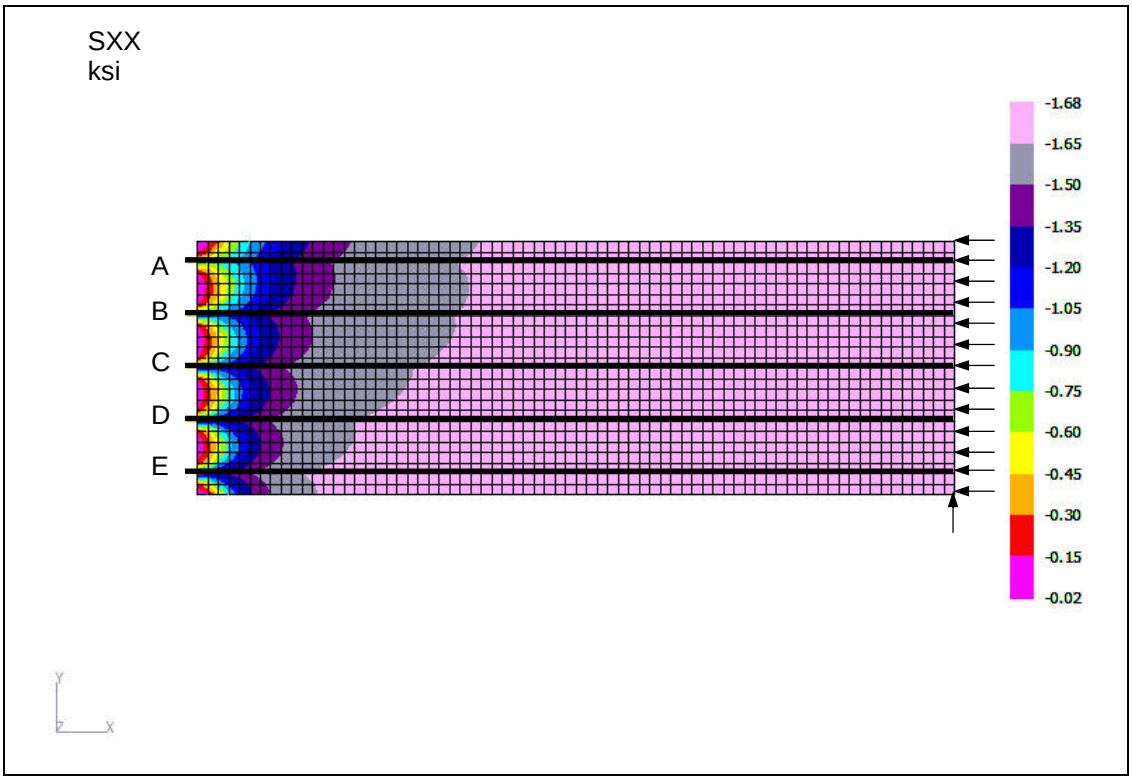

Figure 4.65. Normal Horizontal Stress Contours for TSB-4 Large Block

This modeling technique could be used to model the transfer length in a variety of pretensioned, prestressed concrete members. The relationships developed herein are specific to a jacking stress of $0.75f_{pu}$, ½ in. diameter regular or super prestressing strands, and the specified cross-sections used in this development. This technique can be extremely useful in the calculation of stresses at transfer and shear strength of cross-sections where conventional methods may not be appropriate. As previously mentioned, the transfer length must be known either by experimental methods or analytical calculations to select an appropriate spring stiffness. After the construction of a finite element model, the transfer length versus spring stiffness relationship must be developed for the given cross-section, strand type, and jacking stress. Following the development of that relationship, spring stiffnesses corresponding to measured or predicted transfer lengths would be chosen and applied to the model. Subsequent to verification of transfer lengths, the model would be complete and could be used for the purpose of analysis.

The models used in the development of this method only encountered axial deformation. In this situation, a linear quadrilateral element can be used. In the case of a member subjected to bending, linear quadrilateral elements may not produce sufficient results and a quadratic quadrilateral element should be used. Sample input files for the finite element models used in this development are located in Appendix F as well as an additional model of a T-beam from the experimental portion of this study using quadratic quadrilateral elements.

4.4 Development Length

4.4.1 Introduction

The development length of standard reinforcing bars is simply the embedment length in concrete required to fully develop the yield stress of the steel, while the development length of prestressing strand consists of two components, transfer length and flexural bond length. As previously discussed, transfer length is the distance required to transfer the effective prestress from the prestressing strand to the concrete. The flexural bond length is the additional distance required to effectively increase the stress in the strand from the effective stress to the stress at the nominal moment capacity. Analogous to transfer length, research has shown flexural bond length to also be affected by various contributing factors, such as the required increase in the strand stress, the

strand diameter, the concrete strength, and as-cast vertical location. As were relevant to the determination of and comparison of flexural bond lengths, the influence of these factors were evaluated.

In order to determine the minimum embedment length required to fully develop each strand type, single-point bending tests were performed on 39 T-beam test specimens, each test resulting in one of three types of failure: flexural, hybrid, or bond. A flexural failure was defined as a beam exceeding the nominal moment capacity calculated by AASHTO provisions with less than 0.01 in. of average end-slip. A hybrid failure was defined as a beam with more than 0.01 in. of average end-slip occurring after the nominal moment capacity was reached and a bond failure was defined as a beam having more than 0.01 in. average end-slip prior to reaching the calculated nominal moment capacity. The moment versus deflection and end-slip was plotted for each test. Each plot also included the nominal moment capacity calculated by the current AASHTO LRFD provisions and by strain compatibility. Figure 4.66 shows the aforementioned relationships for a typical flexural failure. Figure 4.67 shows the same relationships for a typical hybrid failure and Figure 4.68 shows the same relationships for a typical bond failure. Plots for each of the 39 tests are located in Appendix C. In addition to individual plots, a table of overall results is located in Appendix D listing the results for all test specimens.

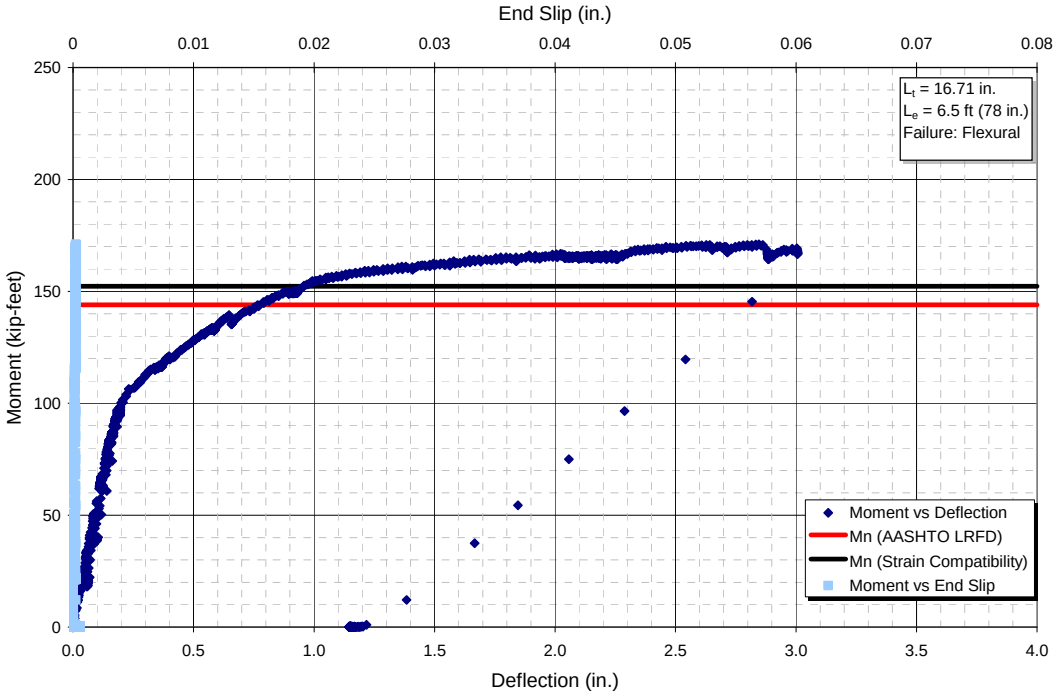

Figure 4.66. Moment versus Deflection and End-slip (Flexural Failure)

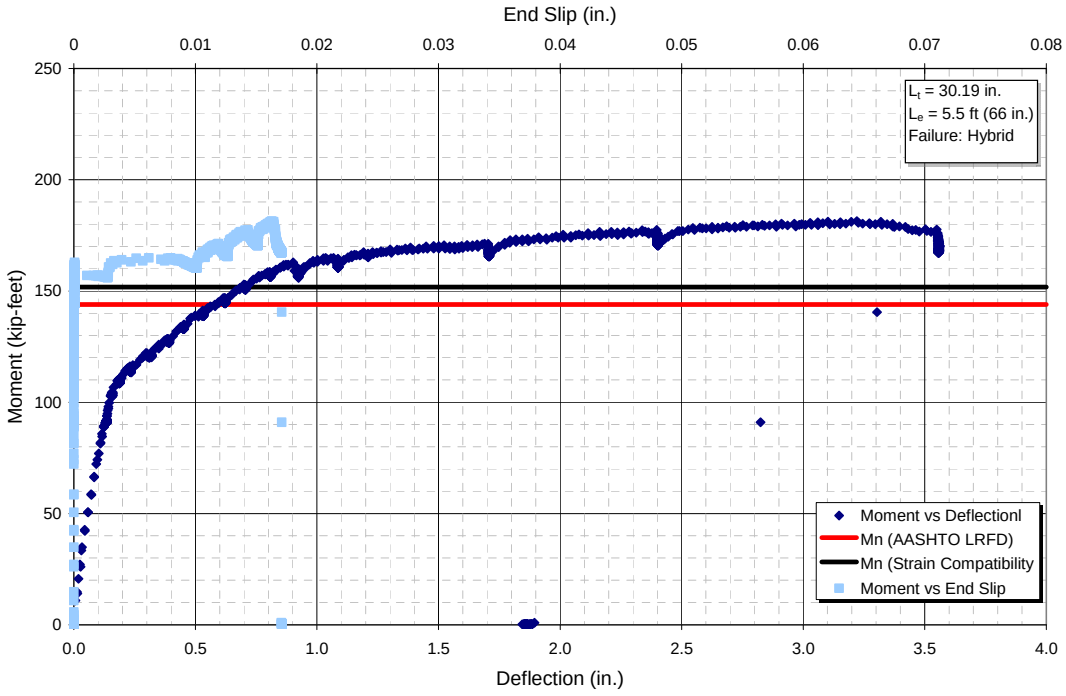

Figure 4.67. Moment versus Deflection and End-slip (Hybrid Failure)

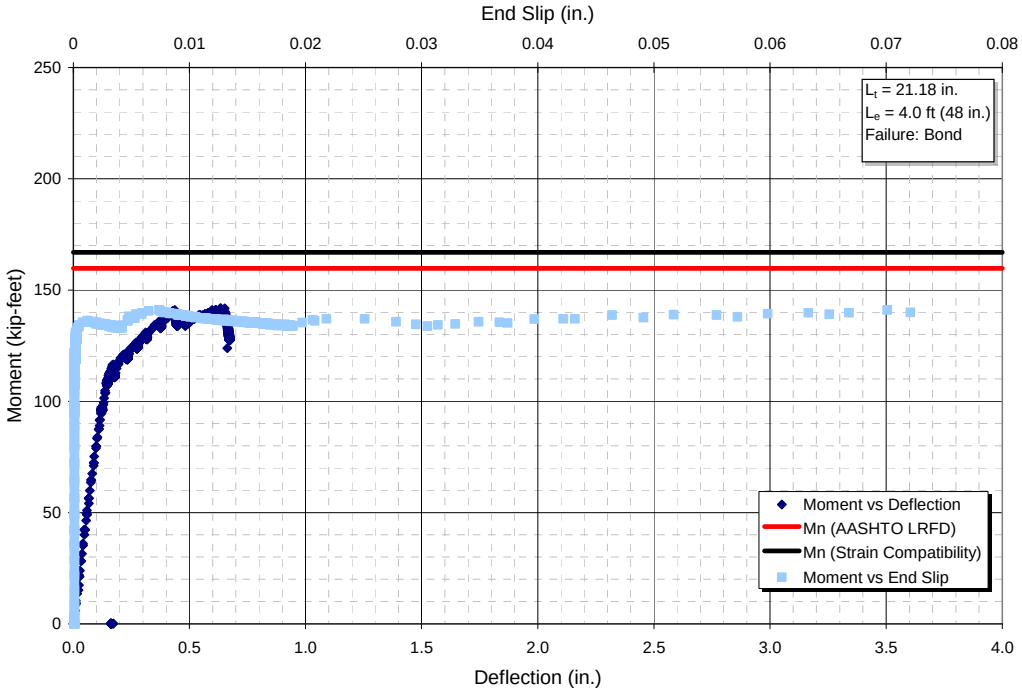

Figure 4.68. Moment versus Deflection and End-slip (Bond Failure)

4.4.2 Influence of Strand Strength

As with transfer length, the primary objective was the development of the Grade 300 strand relying on a number of items in question, the second of which was the development length. With the Grade 300 strand, there was a slight increase in the difference between the effective prestress and the stress in the strand at the nominal moment capacity, which was expected to increase the flexural bond length. Historically, development length equations separate transfer length and flexural bond length. Therefore, for each test specimen, the transfer length was subtracted from the tested embedment length ($L_e - L_t$) to focus on the determination of the flexural bond length. When ($L_e - L_t$) was equal to or greater than the minimum required flexural bond length, a flexural failure occurred. On the contrary, when ($L_e - L_t$) was less than the minimum flexural bond length, a bond or hybrid failure would occur. Of the test specimens containing ½ in. diameter regular Grade 300 strands, the minimum flexural bond length resulting in a flexural failure was 45.9 in., while the minimum flexural bond length resulting in a flexural failure for the test specimens containing ½ in. diameter regular Grade 270 strands was 47.6 in., showing relatively no difference in flexural bond length.

The test specimen containing the Grade 300 strand did have 0.003 in. of slip, while the test specimen containing the Grade 270 strand had no slip. This possibly indicated that the required flexural bond length for the test specimen containing Grade 300 strand may have been somewhat longer than the flexural bond length for the test specimen containing Grade 270 strand. For the test specimens containing ½ in. diameter super Grade 300 strands, the minimum flexural bond length resulting in a flexural failure was 45.4 in., while the minimum flexural bond length resulting in a flexural failure for the test specimens containing ½ in. diameter super Grade 270 strands was 46.1 in. Both test specimens had less than 0.001 in. of slip, but the beam containing the Grade 270 strands was an inverted beam, which may have increased the flexural bond length. Comparisons for beams containing Grade 300 0.6 in. diameter strands were not possible because the Grade 300, 0.6 in. diameter strands was not being manufactured at the time. Overall, the Grade 300 strand performed very similarly to the Grade 270 strand. A summary of the results for strand type are shown in Table 4.18. Although the Grade 300 strand may have a slightly higher flexural bond length, it was not possible to determine this with anymore precision as the interval of embedment lengths tested was 6 in. It should be noted that one test specimen containing Grade 300 ½ in. diameter super strands with a $(L_e - L_t)$ value of 47.6 in. did encounter a hybrid/shear failure.

Table 4.18. Summary of Results for Strand Grade and Size

	Minimum Determined Flexural Bond Length (in.)		
Strand Strength	½ in. diameter	½ in. diameter super	0.6 in. diameter
Grade 270	47.6	46.1	46.7
Grade 300	45.9	45.4	NA

4.4.3 Influence of Strand Diameter/Area

Strand diameter has been shown by a number of researchers to affect the flexural bond length of prestressing strand. As with transfer length, most have found flexural bond length to increase with strand diameter, while some have shown flexural bond length to decrease when using 0.6 in. diameter prestressing strand. As previously mentioned, three types of strand were used throughout the study, including ½ in. regular, ½ in. super, and 0.6 in. diameter strands. All but two beams contained ½ in. diameter strands, with the majority being ½ in. diameter super strands, so, as with transfer length,

no conclusions were made with respect to 0.6 in. diameter strand and their influence on flexural bond length.

The minimum flexural bond length resulting in a flexural failure for the ½ in. diameter strands, including both Grade 270 and Grade 300 strand, was 45.4 in., while the minimum flexural bond length resulting in a flexural failure for the 0.6 in. diameter Grade 270 strand was 46.7 in. As with the influence of strand strength, the strand diameter showed only a small increase in flexural bond length for an increase in strand diameter, but only four tests were performed with 0.6 in. diameter strands. In addition to strand diameter, flexural bond lengths were also evaluated for each corresponding strand area. The minimum flexural bond length resulting in a flexural failure for the ½ in. diameter regular strand was 45.9 in., while the minimum flexural bond length resulting in a flexural failure for the ½ in. diameter super strand was 45.4 in. The minimum flexural bond length resulting in a flexural failure for the 0.6 in. diameter strand was 46.7 in. as previously stated. Again, no definitive trend was shown between strand type or strand grade in this study, which can be seen in multiple comparisons of the data in Table 4.18.

4.4.4 Influence of Effective Prestress

Transfer length has been shown to increase with an increase in effective prestress. Since two levels of initial prestress and two strengths of strand were used resulting in various levels of effective prestress, $(L_e - L_t)$ for each test was plotted against each corresponding effective prestress, as shown in Figure 4.69. As was shown in Table 4.18, it can be observed in Figure 4.69 that the minimum flexural bond lengths required for flexural failures are in the range of 45 to 50 in. regardless of strand size or grade. A significant amount of scatter existed in the plot among those test specimens failing in flexure indicating there to be no definitive trend.

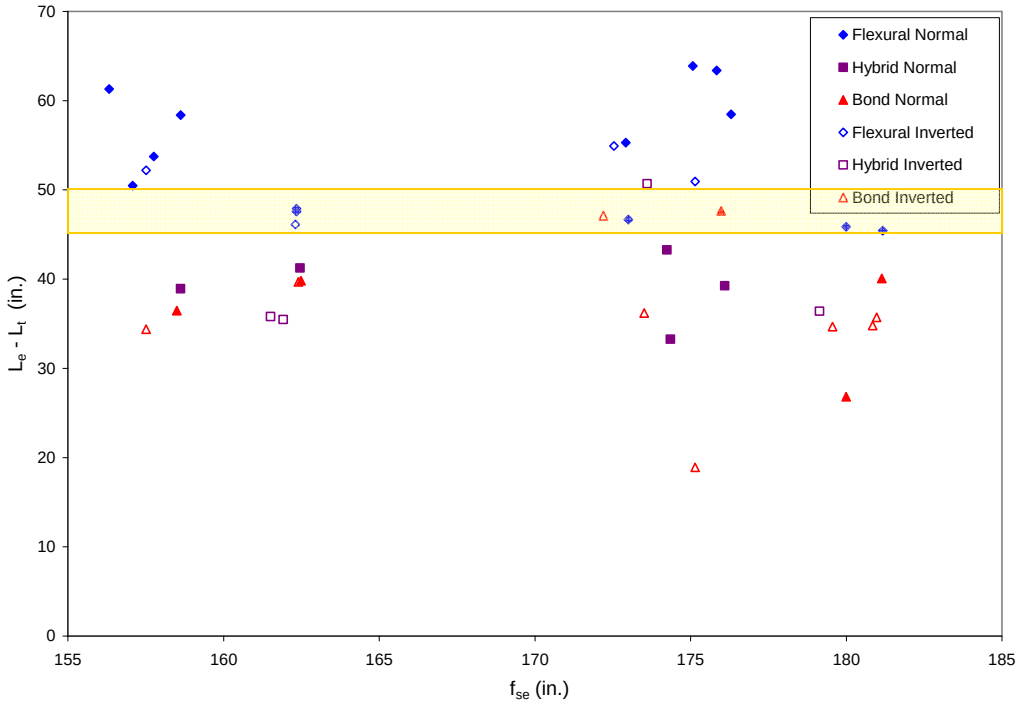

Figure 4.69. (L_e - L_t) versus Effective Prestress

4.4.5 Influence of ($f_{ps} - f_{se}$)

The difference in the stress in the strand at the nominal moment capacity f_{ps} and the effective prestress f_{se} has been used in the calculation of the flexural bond length since the implementation of Equation (2-2) in the ACI Building Code and has been incorporated into numerous proposed equations for the calculation of the flexural bond length. Figure 4.70 shows the relationship of ($L_e - L_t$) for various failure types and ($f_{ps} - f_{se}$). As with strand diameter, although ($f_{ps} - f_{se}$) has been shown to influence the flexural bond length, neither an increase nor decrease was observed for values of ($L_e - L_t$) resulting in a flexural failure when compared to variations in ($f_{ps} - f_{se}$). It appeared the flexural bond length for all strand types was in the range of 45 to 50 in.

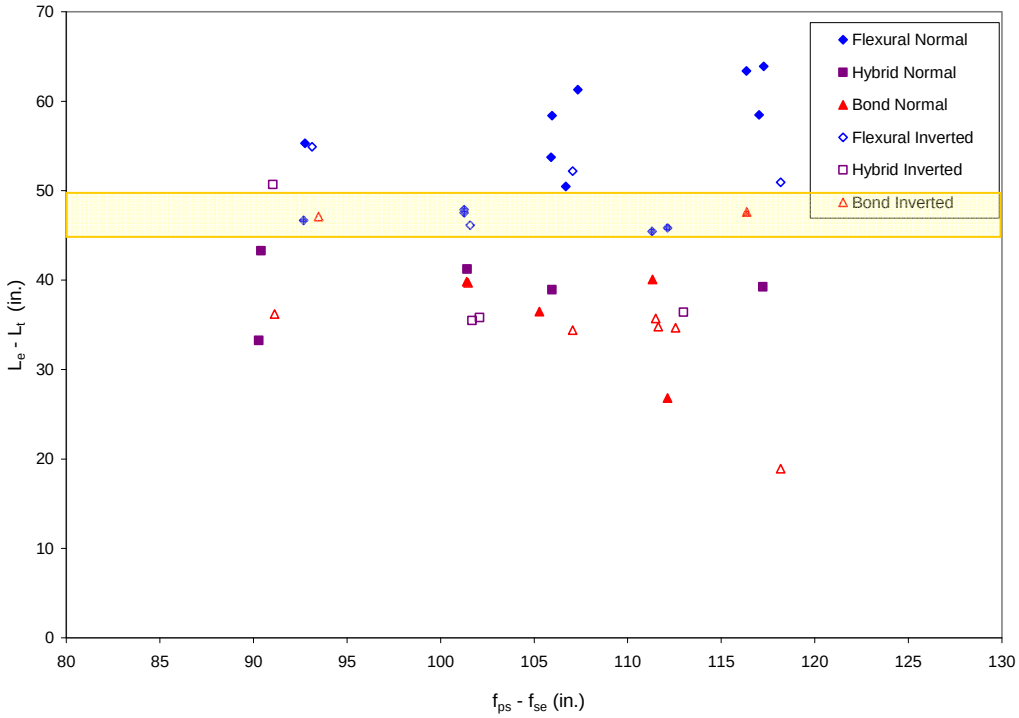

Figure 4.70. ($L_e - L_t$) versus ($f_{ps} - f_{se}$)

4.4.6 Influence of Concrete Strength

As with transfer length, the current code provisions do not account for the strength of the concrete in the calculation of flexural bond length. Although the strength of concrete is not accounted for, some researchers have shown flexural bond length to decrease with an increase in concrete strength, while others have shown very little correlation. Among the six sets of test specimens cast in this study for the development length tests, five different concrete strengths existed at the time of testing, ranging from 6300 to 8300 psi, which was representative of concrete strengths typically used in the bridge industry. Figure 4.71 plots ($L_e - L_t$) values against the square root of each corresponding concrete strength. Again the flexural bond lengths appear to be between 45 and 50 in. for all test specimens. There does however, appear to be a trend of increasing flexural bond length with an increase in concrete strength. This goes against other studies and is attributed to the small amount of data points for higher concrete strengths in this study.

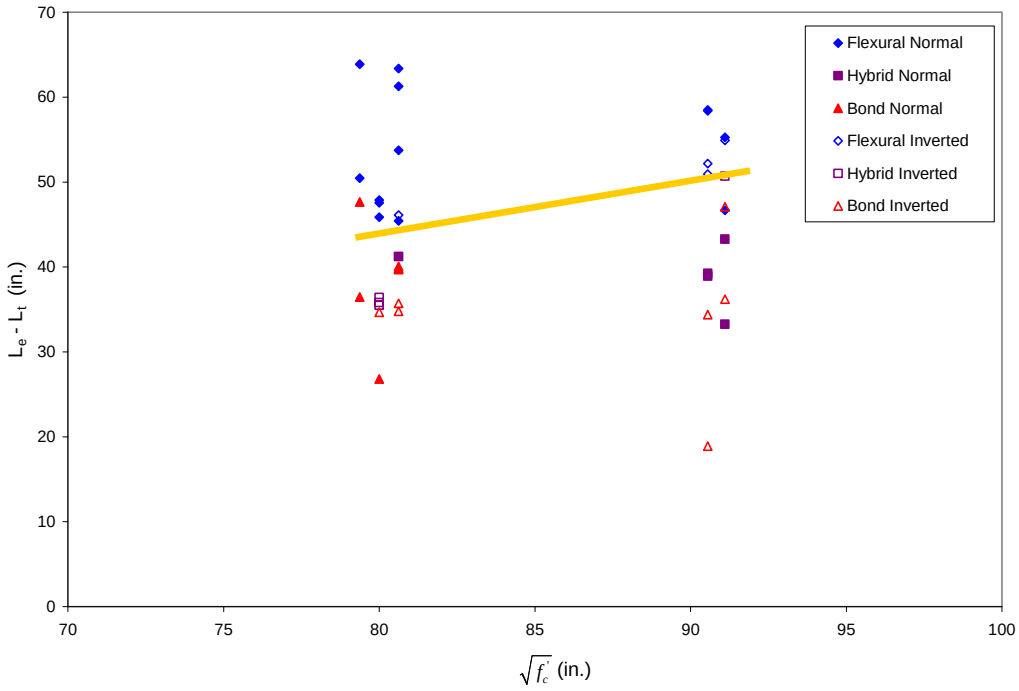

Figure 4.71. ($L_e - L_t$) versus Concrete Strength

4.4.7 Influence of Casting Orientation

The top-strand effect proved to be very influential on transfer length measurements and with respect to standard reinforcing bars, is very influential in the calculation of development lengths. Looking at the development lengths alone for prestressing strand, the top-strand effect appeared to have a significant influence. Figure 4.72 shows the relationship of embedment length and the amount of concrete cast below the strand. A number of the points with different failure types overlap as they had the same embedment length, but had different transfer lengths. The plot failed to show any solid relationship between any of the failure types and the amount of concrete cast below the strand because of the overlap. However, by subtracting out the measured transfer lengths, the transfer length and ($L_e - L_t$) were uncoupled, showing the top-strand effect to have very little effect on the flexural bond length. By subtracting out the transfer length, only looking at ($L_e - L_t$) values, the overlap was removed. Figure 4.73 shows the relationship of ($L_e - L_t$) values and the amount of concrete cast below the strand. Once again the minimum values of ($L_e - L_t$) resulting in a flexural failure appear to be between 45 and 50 in, showing no correlation to the amount of concrete cast beneath the strand.

As previously discussed, transfer lengths were found to be more dependent on the amount of concrete cast above the strand than the amount of concrete cast below the strand. Therefore, the embedment length and ($L_e - L_t$) values from each test were plotted against the amount of concrete cast above the strand. Figure 4.74 shows the relationship of the embedment length and the amount of concrete cast above the strand. A number of the points, again, overlapped from having the same embedment lengths, showing no correlation between any of the failure types and the amount of concrete cast above the strand. Again, the transfer lengths were subtracted out of each corresponding embedment length, resulting in ($L_e - L_t$) values. Figure 4.75 shows the relationship of the ($L_e - L_t$) values and the amount of concrete cast above the strand. The overlap was removed, but there was no correlation between ($L_e - L_t$) values resulting in flexural failures and the amount of concrete cast above the strand. Again, the range of minimum flexural bond lengths appears to be between 45 and 50 in.

By evaluation of the development length only, the top-strand effect appeared evident, however, by also evaluating the flexural bond lengths for each test, unlike transfer lengths, it was determined that the top-strand effect failed to have a significant influence on the flexural bond length. However, the development length equation consists of both the transfer and flexural bond lengths therefore the top-strand effect does influence the development length through the transfer length.

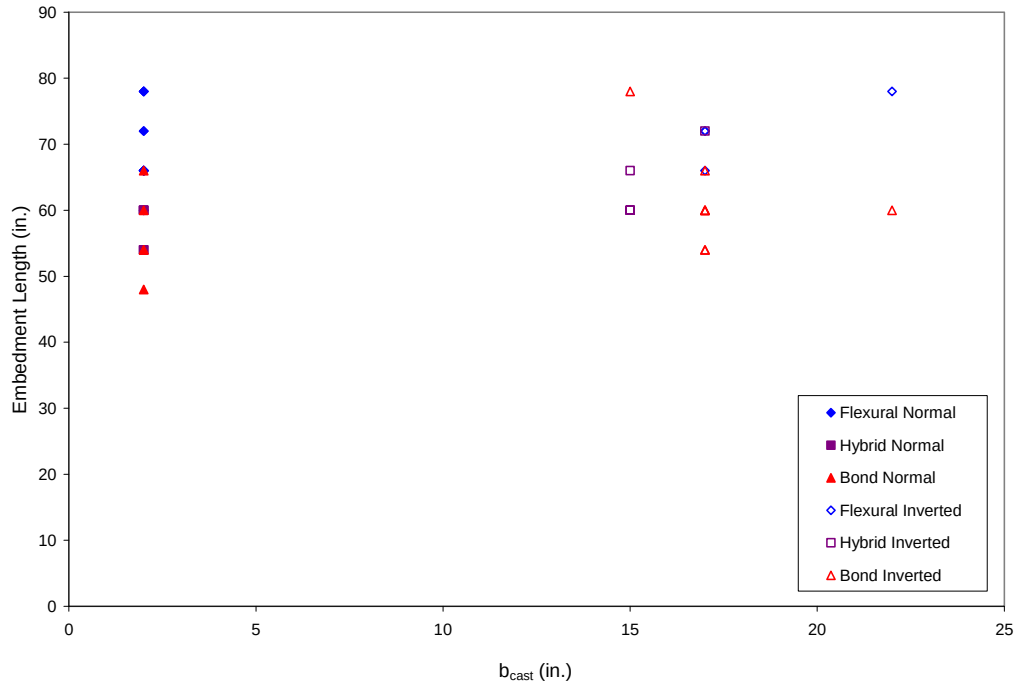

Figure 4.72. Embedment Length versus b_{cast}

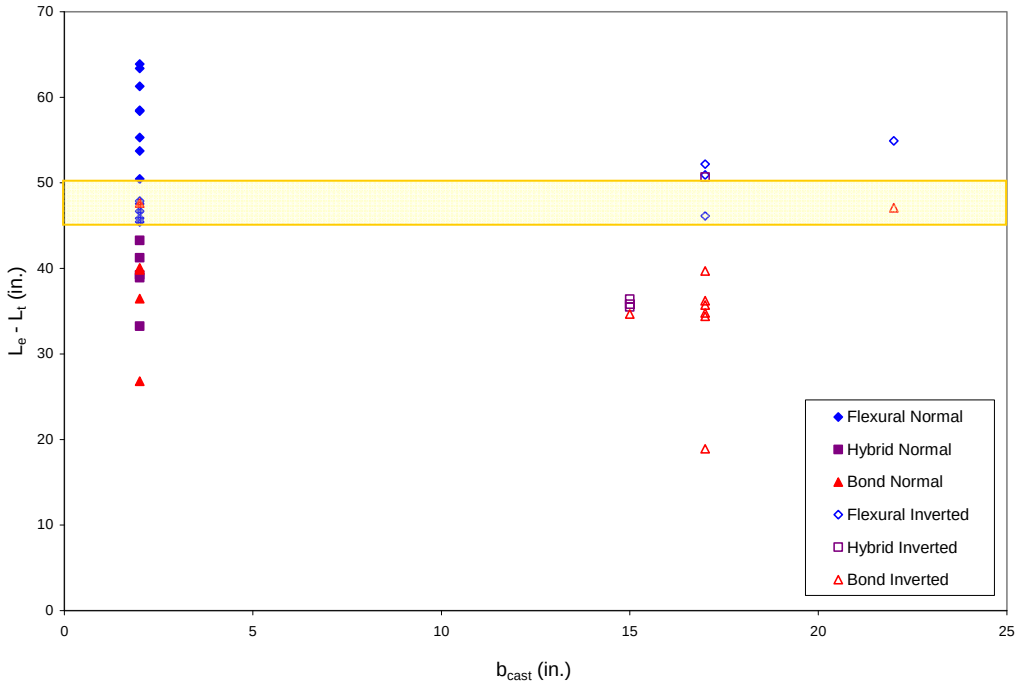

Figure 4.73. (L_e - L_t) versus b_{cast}

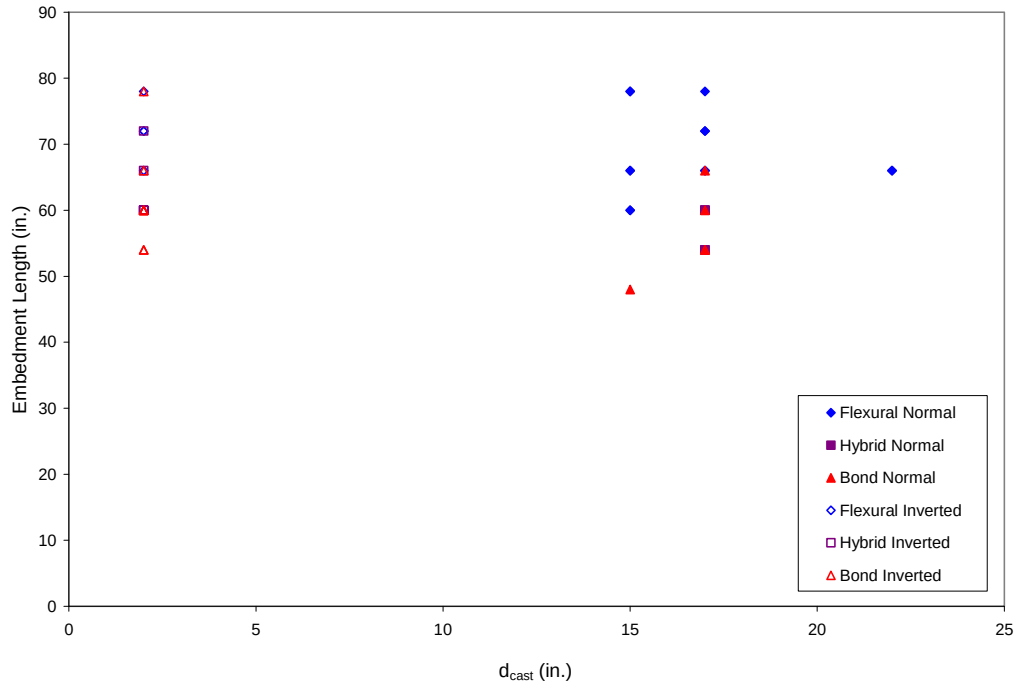

Figure 4.74. Embedment Length versus d_{cast}

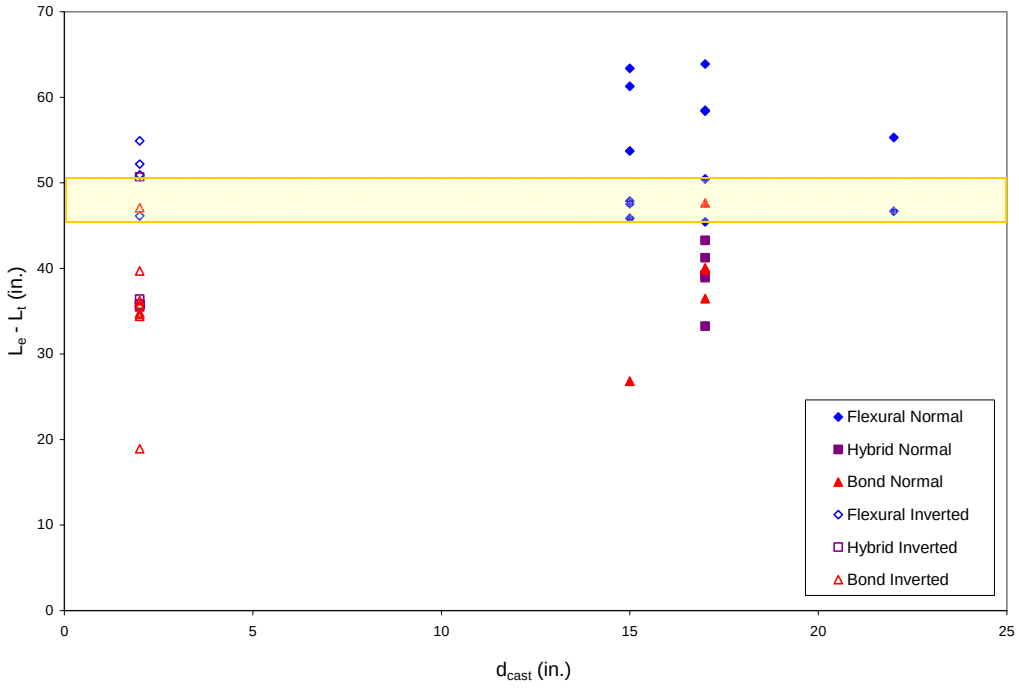

Figure 4.75. (L_e - L_t) versus d_{cast}

4.4.8 Current and Additional Recommended Equations

Since the 1963 ACI Building Code, development length has been calculated by Equation (2-2) taking into consideration the effective prestress in the strand after all losses, stress in the strand at the nominal moment capacity, and the diameter of the strand. Over the past 35 years, as with transfer length, the proposed equations have evolved to include the strength of the concrete. Again, as with transfer lengths, some equations have proved to be adequate estimators of development length, while others have not. Similar to Kose and Burkett (2005) the embedment lengths and ($L_e - L_t$) values were compared to nine different development length/flexural bond length equations for comparative purposes. Figure 4.76 through Figure 4.84 show the comparison to each of those equations with a line of perfect correlation. Actual values were plotted on the ordinate axis while the predicted values were plotted on the abscissa axis with a line of perfect correlation aiding in visual observation of the data. Contrary to the transfer length comparisons, all of the data points for the embedment length and ($L_e - L_t$) values did not have to fall below the line of perfect correlation for conservatism. Ideally, the points for a flexural failure would fall just above the line of perfect correlation, while the bond failure would fall below the line and the hybrid failures would fall nearly on the line. However, that was not the case with most comparisons and would show no conservatism. The equations are listed again in Table 4.19.

The first equation evaluated, shown in Figure 4.76, was the traditional equation from ACI (Equation 2-2). Figure 4.76a showed that all values were conservative however there is very little range in the data. Figure 4.76b showed very good correlation and had an increased range of data. Equation (2-33), shown in Figure 4.77 also showed very clustered predictions for development length, but showed very favorable predictions for the flexural bond length. Comparably, Equation (2-34) and Equation (2-37) also showed very conservative predictions for the development length and showed conservative predictions for the flexural bond length also with good correlation as shown in Figure 4.78 and Figure 4.80, respectively.

Contrary to the four equations already mentioned, Equation (2-36) proposed by Mitchell et al. and Equation (2-41) of a recent NCHRP report showed unconservative predictions for both development length and flexural bond length as shown in Figure 4.79

and Figure 4.84, respectively. The remaining equations, by Buckner and Lane had good correlations, while the proposed equation by Kose and Burkett seemed to excessively overestimate both the development length and flexural bond length.

Although, most of the equations did not produce predicted development length values with good correlations, overall, all but three equations predicted reasonable flexural bond lengths with adequate levels of conservatism. Even though, a number of researchers have found flexural bond length to be influenced by concrete strength, the results in this study failed to support that trend. Of the proposed equations, Equation (2-38) by Buckner seemed to be the most logical for the data presented herein. The λ factor included in Equation (2-38) takes into account the strain in the strand at the nominal moment capacity of the member. With transfer length, the Hoyer Effect causes the strand to expand increasing the bond. Development length has a behavior quite the opposite with the strand contracting as the stress is increased and if the embedment length was smaller than the required development length, the bond between the prestressing steel and surrounding concrete would fail resulting in a bond failure. Buckner's equation proved to have the most relevance to the data presented herein, thus there was no derivation of an equation for the flexural bond length. The second portion of Equation (2-38), shown as Equation (4-6) is recommended for the calculation of flexural bond length, where λ is taken as ($0.6 + 40\varepsilon_{ps}$) with lower and upper bounds of 1.0 and 2.0, respectively.

$$L_{fb} = \lambda\left(f_{ps} - f_{se}\right)d_b \qquad \text{Eq. (4-6)}$$

Table 4.19. Historical Development Length Equations

Contributor	Year	Equation	Eq. No.
Hanson & Kaar	1959	$L_d = (1.11 f_{su} - 0.77 f_{se}) d_b$	2-31
ACI	1963	$L_d = \left(\frac{f_{se}}{3000}\right) d_b + \left(\frac{f_{ps} - f_{se}}{1000}\right) d_b$	2-2
Martin & Scott	1976	$L_t = 160 d_b$ for 1/4 in. dia. strand $L_t = 187 d_b$ for 3/8 in. dia. strand $L_t = 200 d_b$ for 1/2 in. dia. strand	2-32a 2-32b 2-32c
Zia & Mostafa	1977	$L_d = 1.5 \frac{f_{si}}{f_{ci}'} d_b - 4.6 + 1.25(f_{ps} - f_{se}) d_b$	2-33
Cousins et al.	1990	$L_d = 0.5\left(\frac{U_t' \sqrt{f_{ci}'}}{B}\right) + \frac{f_{se} A_{ps}}{\pi d_b U_t' \sqrt{f_{ci}'}} + (f_{ps} - f_{se})\left(\frac{A_{ps}/\pi d_b}{U_d' \sqrt{f_c'}}\right)$	2-34
Shahawy et al.	1992	$L_d = \frac{\left[\frac{f_{si}}{3} d_b + (f_{ps} - f_{se}) d_b\right]}{(k_b \mu_{ave})}$	2-35
Mitchell et al.	1993	$L_d = 0.33 f_{pi} d_b \sqrt{\frac{3}{f_{ci}'}} + (f_{ps} - f_{se}) d_b \sqrt{\frac{4.5}{f_c'}}$	2-36
Deatherage et al.	1994	$L_d = \left(\frac{f_{si}}{3}\right) d_b + 1.50(f_{ps} - f_{se}) d_b$	2-37
Buckner	1995	$L_d = \left(\frac{f_{si}}{3}\right) d_b + \lambda (f_{ps} - f_{se}) d_b$	2-38
Lane	1998	$L_d = \frac{4 f_{pt}}{f_c'} d_b - 5 + \frac{6.4(f_{ps} - f_{se}) d_b}{f_c'} + 15$	2-39
Kose & Burkett	2005	$L_d = \left[95 \frac{f_{pi}(1 - d_b)^2}{\sqrt{f_c'}}\right] + \left[8 + 400 \frac{(f_{pu} - f_{pi})(1 - d_b)^2}{\sqrt{f_c'}}\right]$	2-40
NCHRP	2008	$L_d = \left[\frac{120}{\sqrt{f_{ci}'}} + \frac{225}{\sqrt{f_c'}}\right] d_b \geq 100 d_b$	2-41

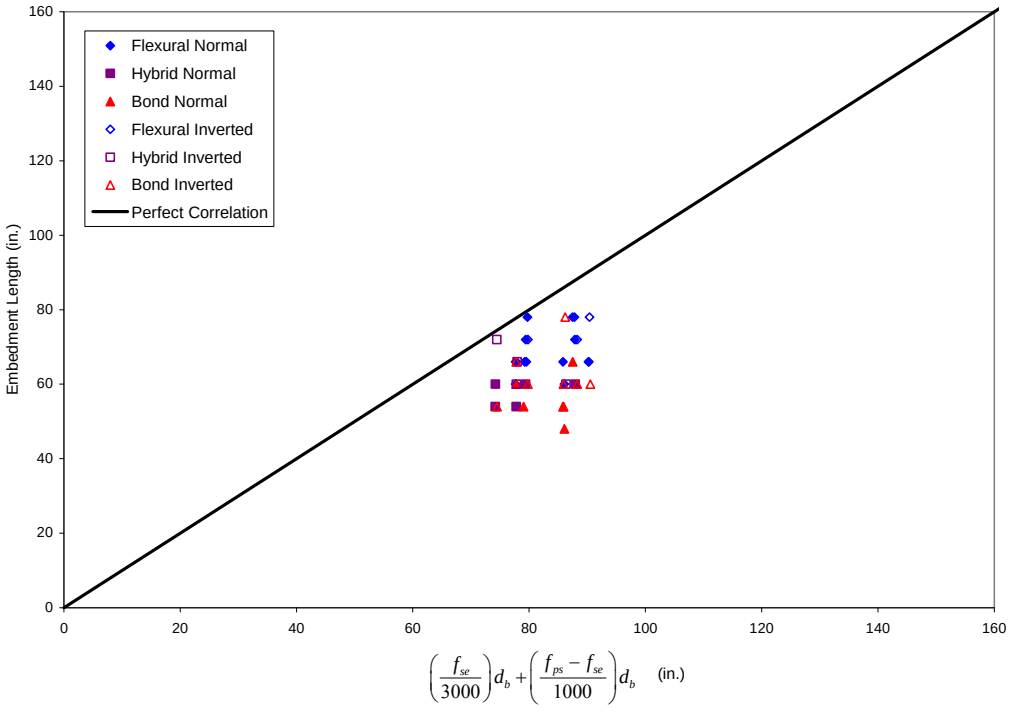

Figure 4.76a. Embedment Length vs. ACI (Eq. 2-2)

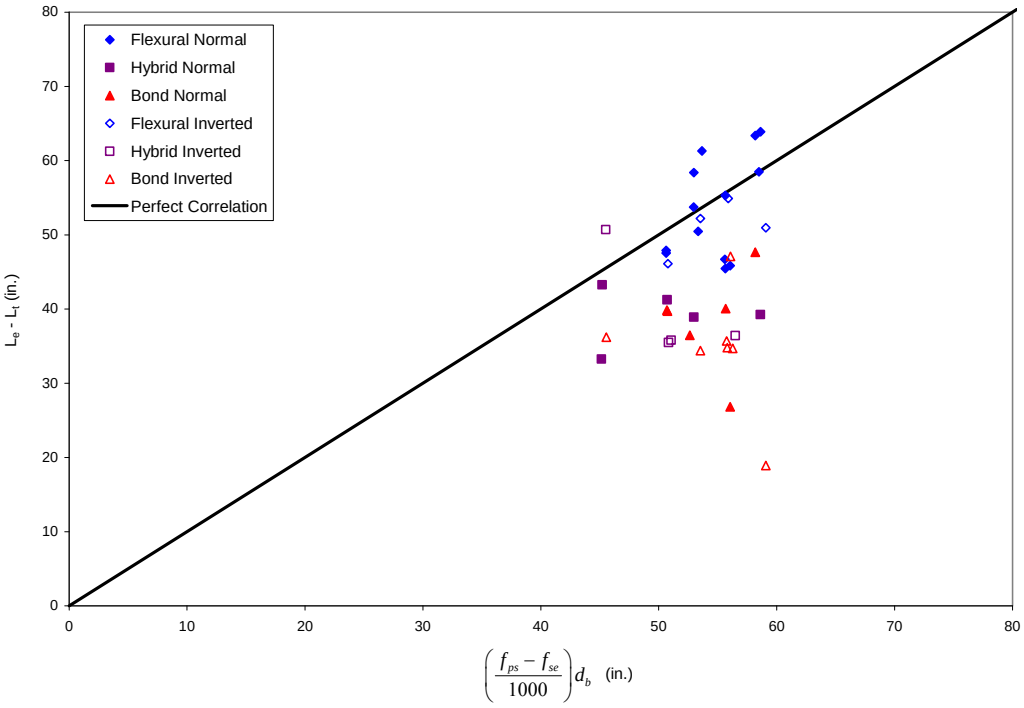

Figure 4.76b. (L_e - L_t) vs. ACI (Eq. 2-2)

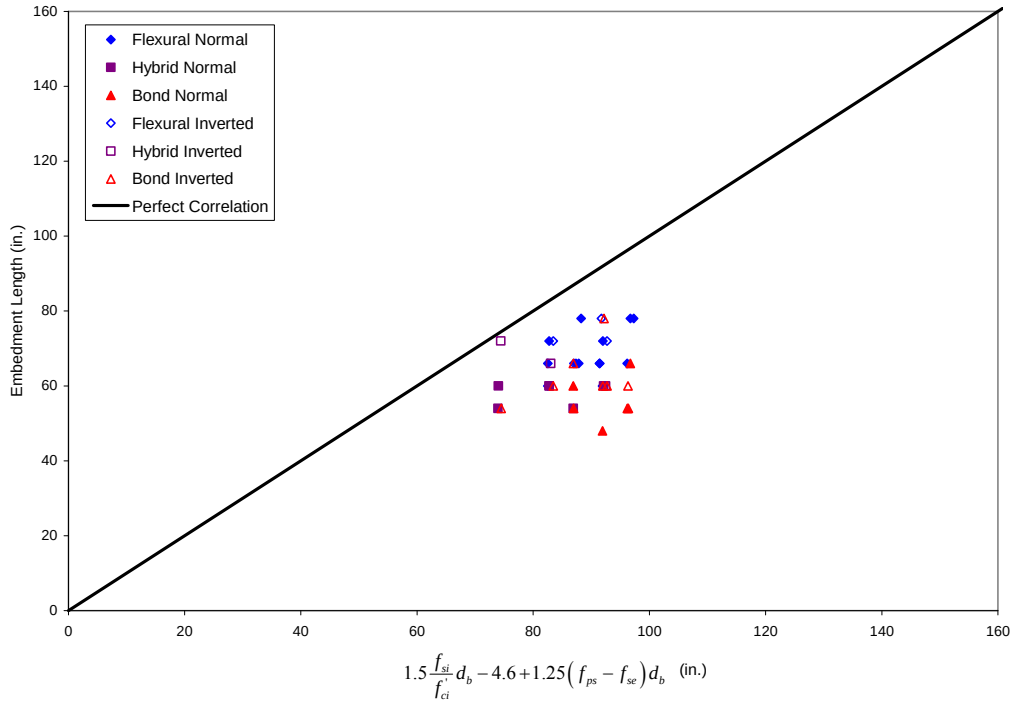

Figure 4.77a. Embedment Length vs. Zia and Mostafa (Eq. 2-33)

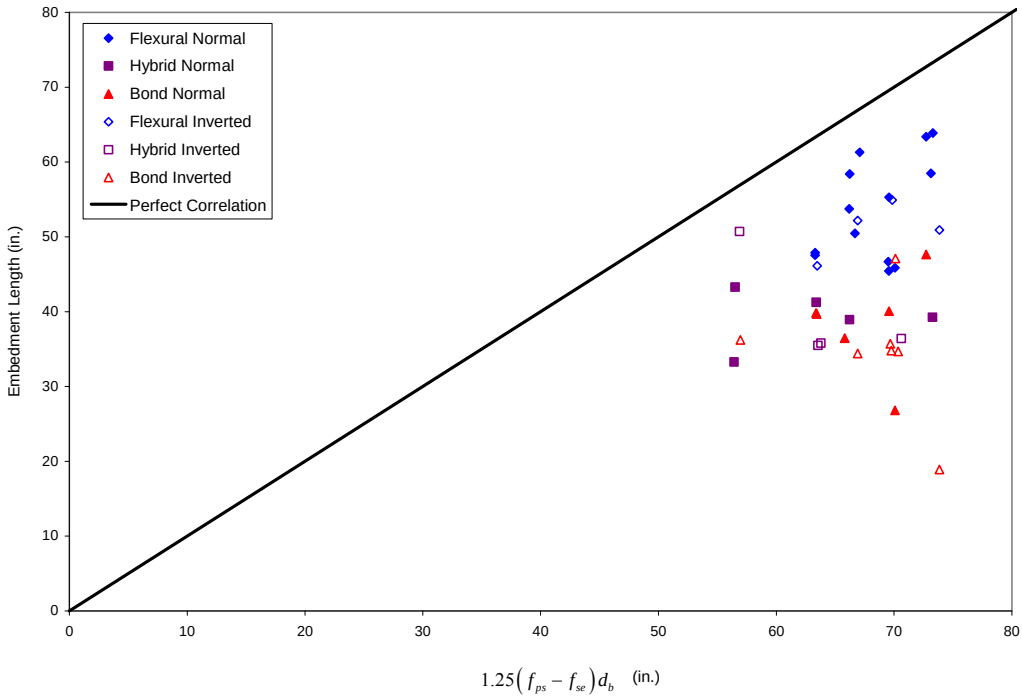

Figure 4.77b. (L_e - L_t) vs. Zia and Mostafa (Eq. 2-33)

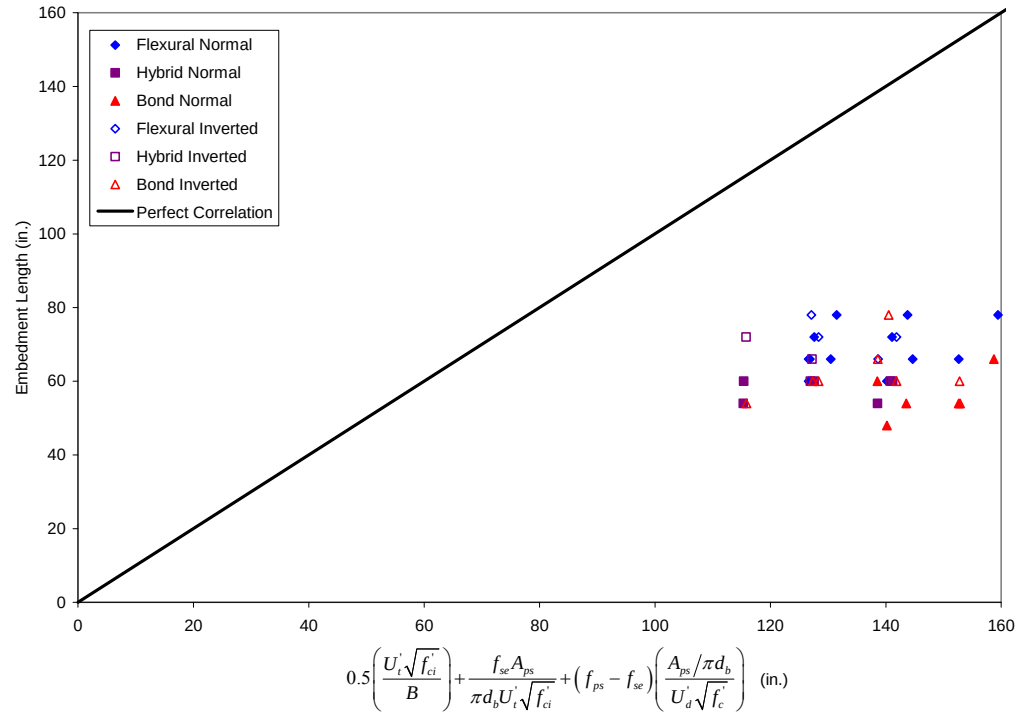

Figure 4.78a. Embedment Length vs. Cousins et al. (Eq. 2-34)

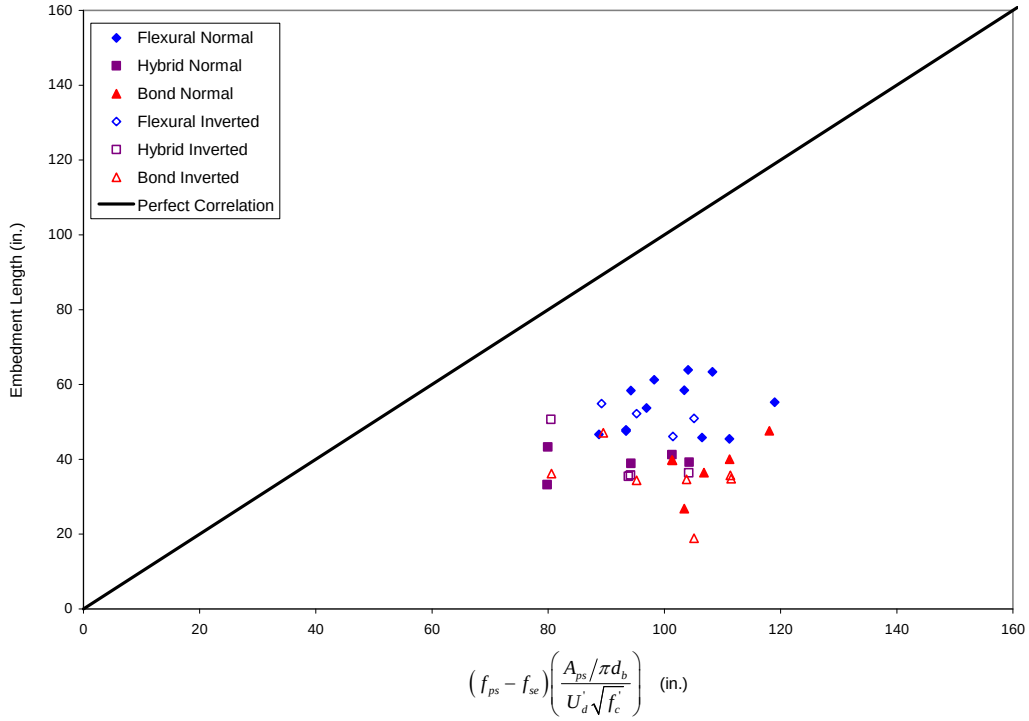

Figure 4.78b. (L_e - L_t) vs. Cousins et al. (Eq. 2-34)

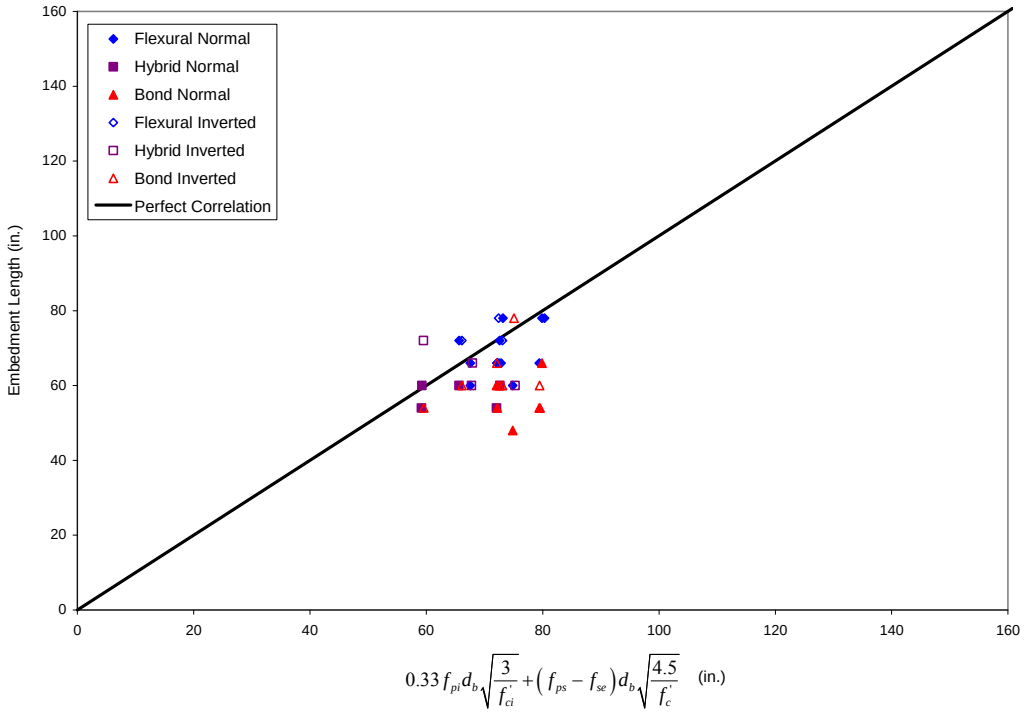

Figure 4.79a. Embedment Length vs. Mitchell et al. (Eq. 2-36)

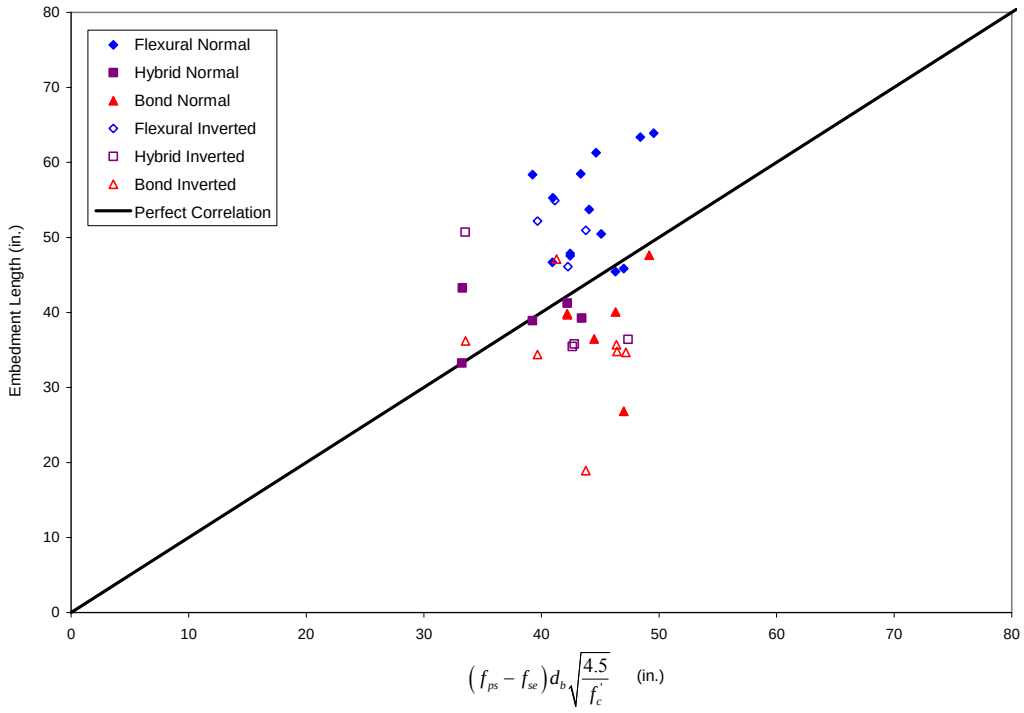

Figure 4.79b. (L_e - L_t) vs. Mitchell et al. (Eq. 2-36)

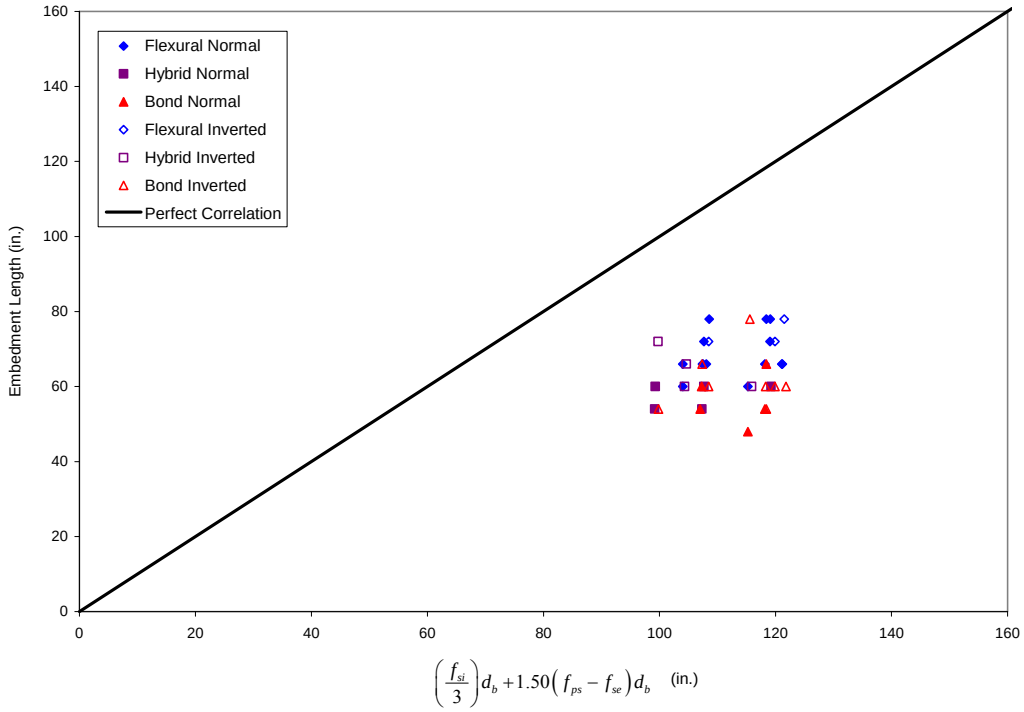

Figure 4.80a. Embedment Length vs. Deatherage et al. (Eq. 2-37)

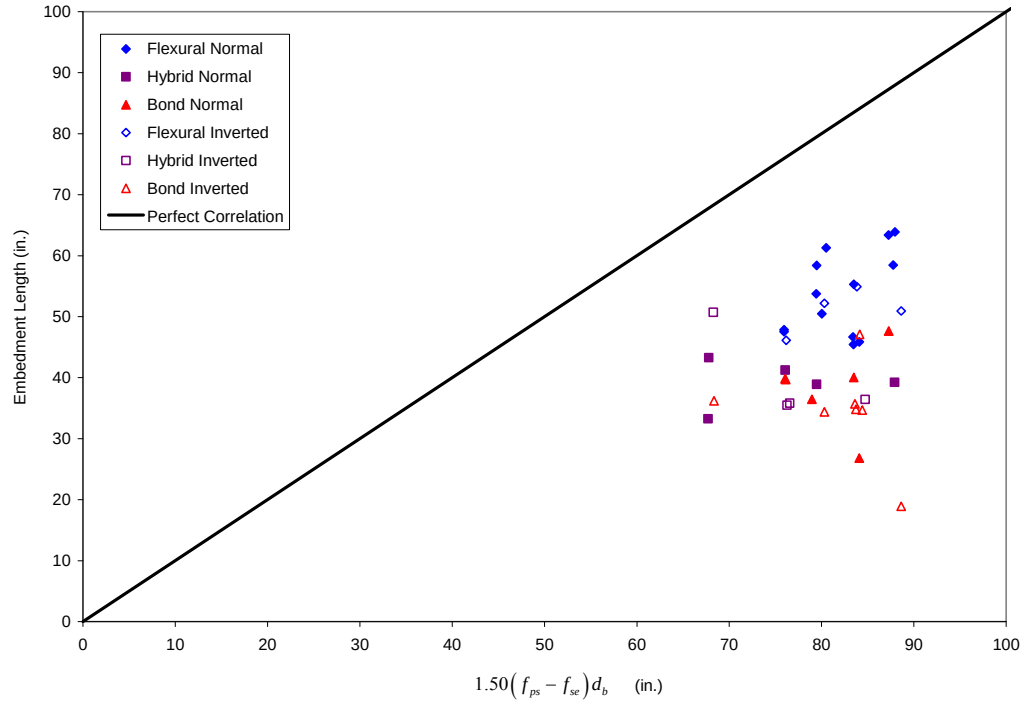

Figure 4.80b. (L_e - L_t) vs. Deatherage et al. (Eq. 2-37)

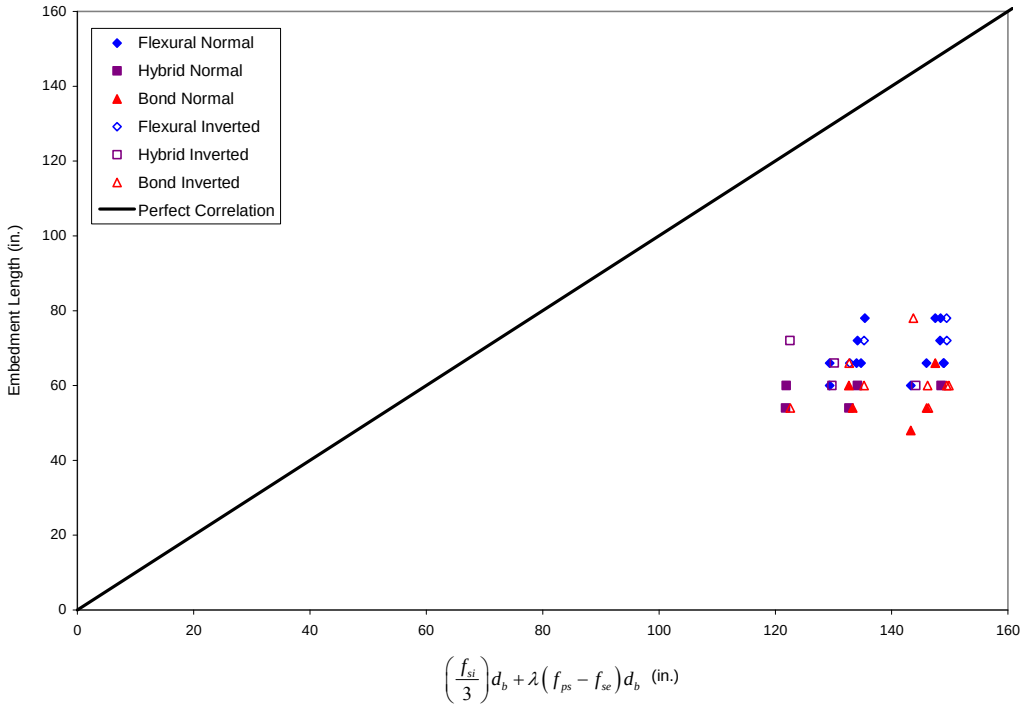

Figure 4.81a. Embedment Length vs. Buckner (Eq. 2-38)

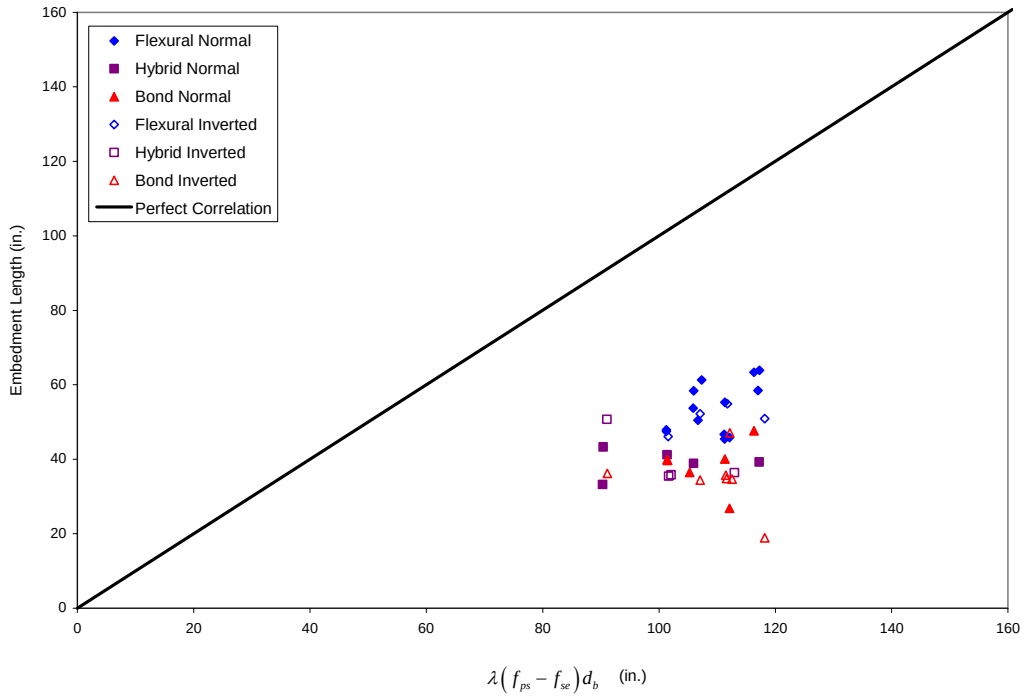

Figure 4.81b. (L_e - L_t) vs. Buckner (Eq. 2-38)

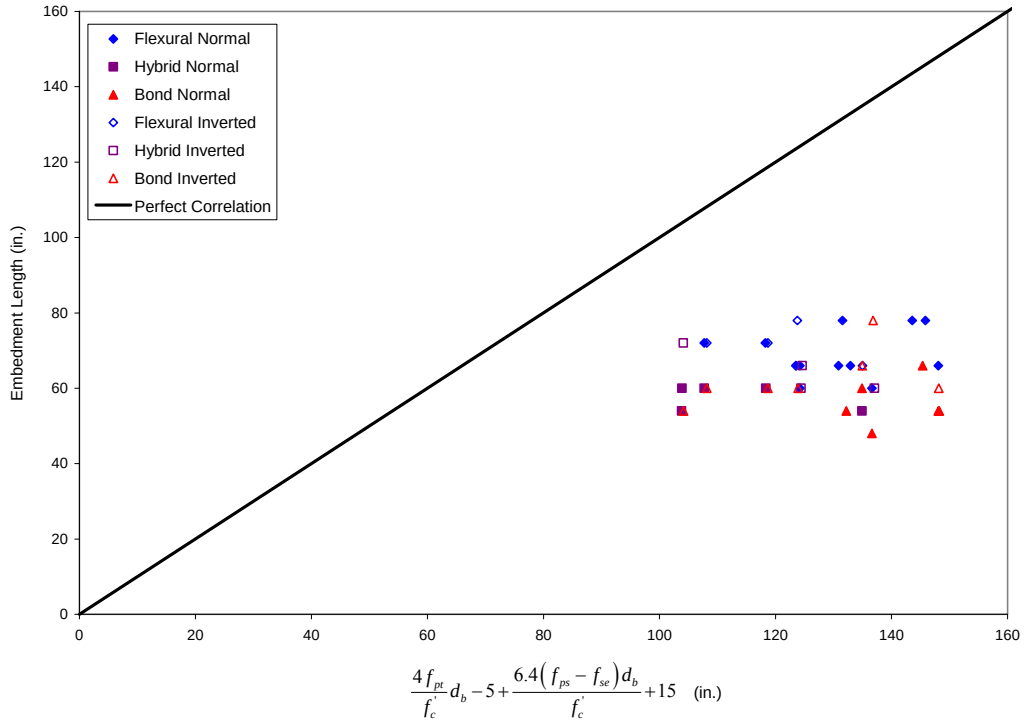

Figure 4.82a. Embedment Length vs. Lane (Eq. 2-39)

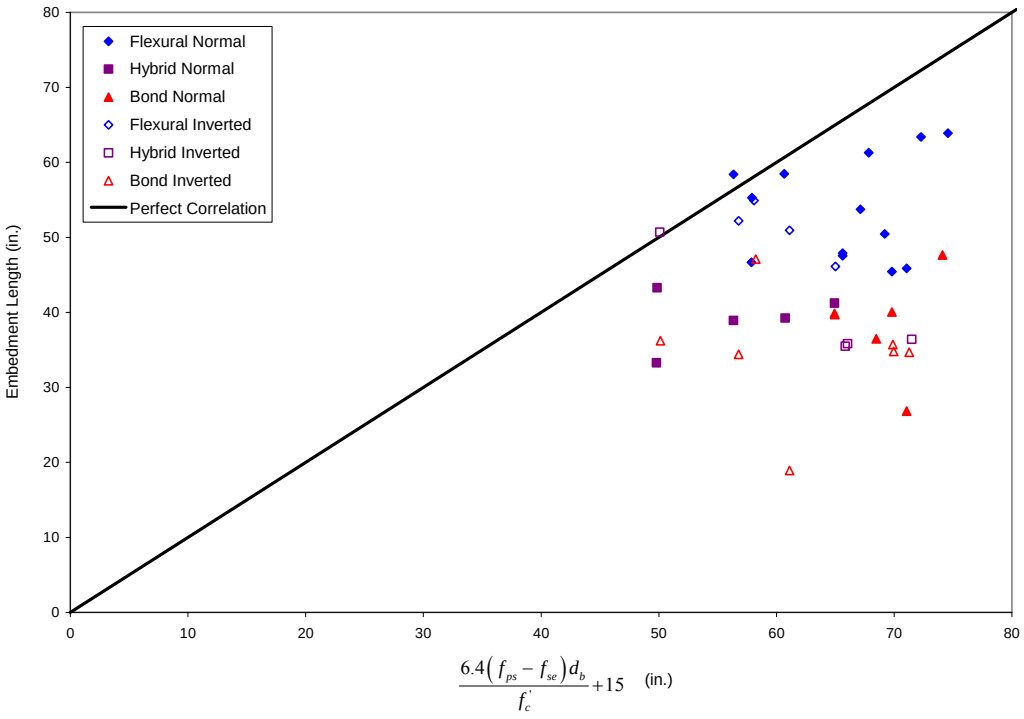

Figure 4.82b. (L_e - L_t) vs. Lane (Eq. 2-39)

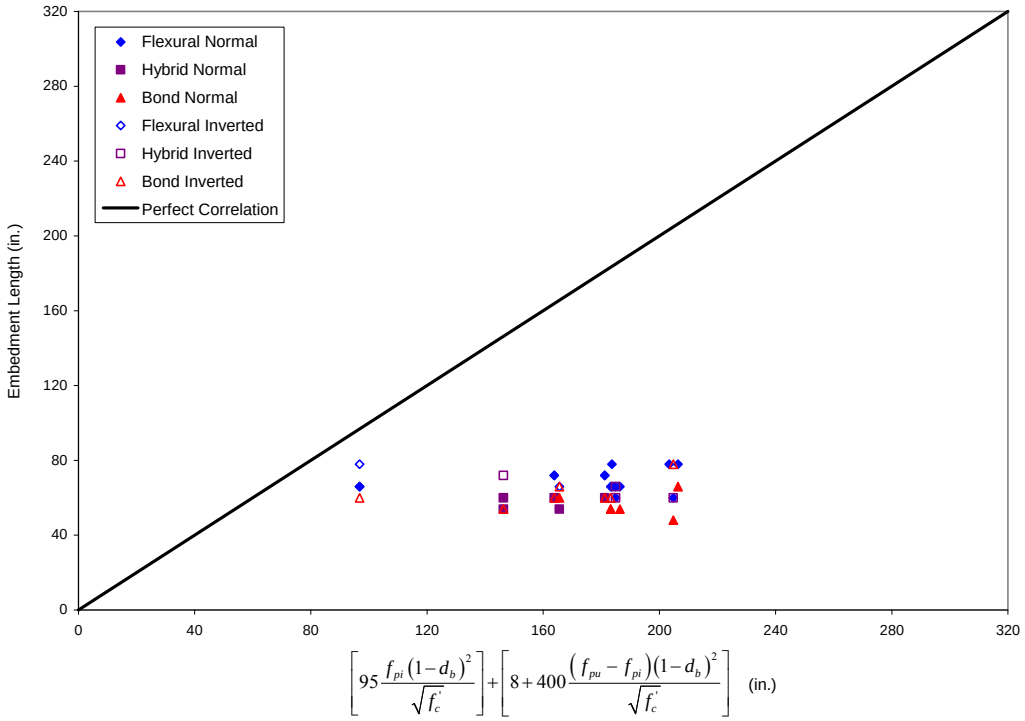

Figure 4.83a. Embedment Length vs. Kose and Burkett (Eq. 2-40)

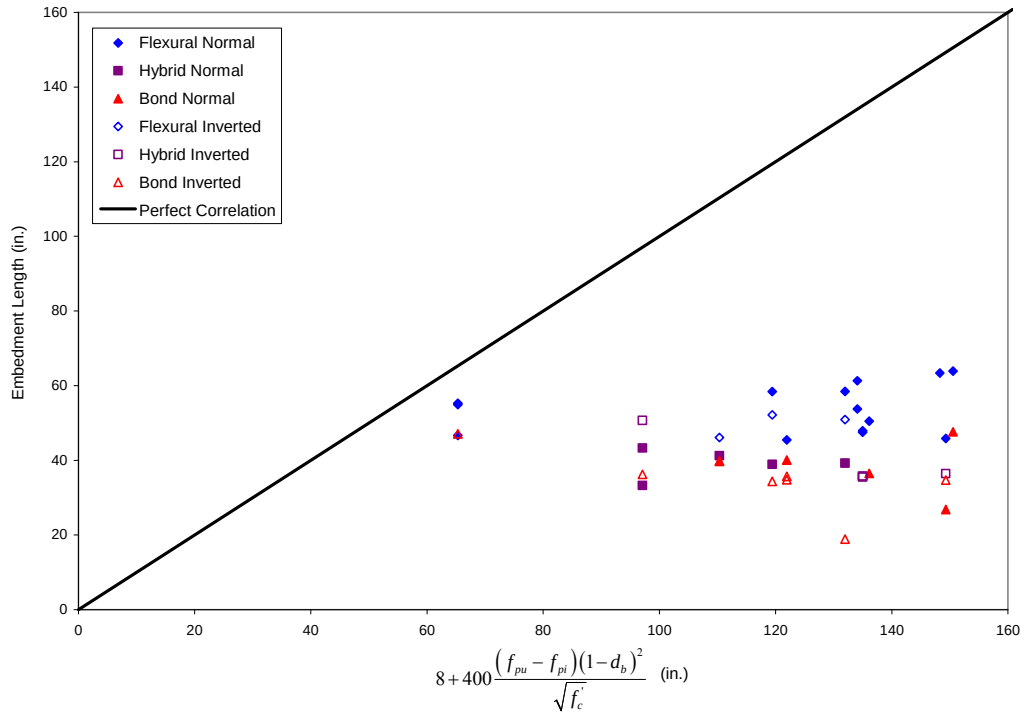

Figure 4.83b. (L_e - L_t) vs. Kose and Burkett (Eq. 2-40)

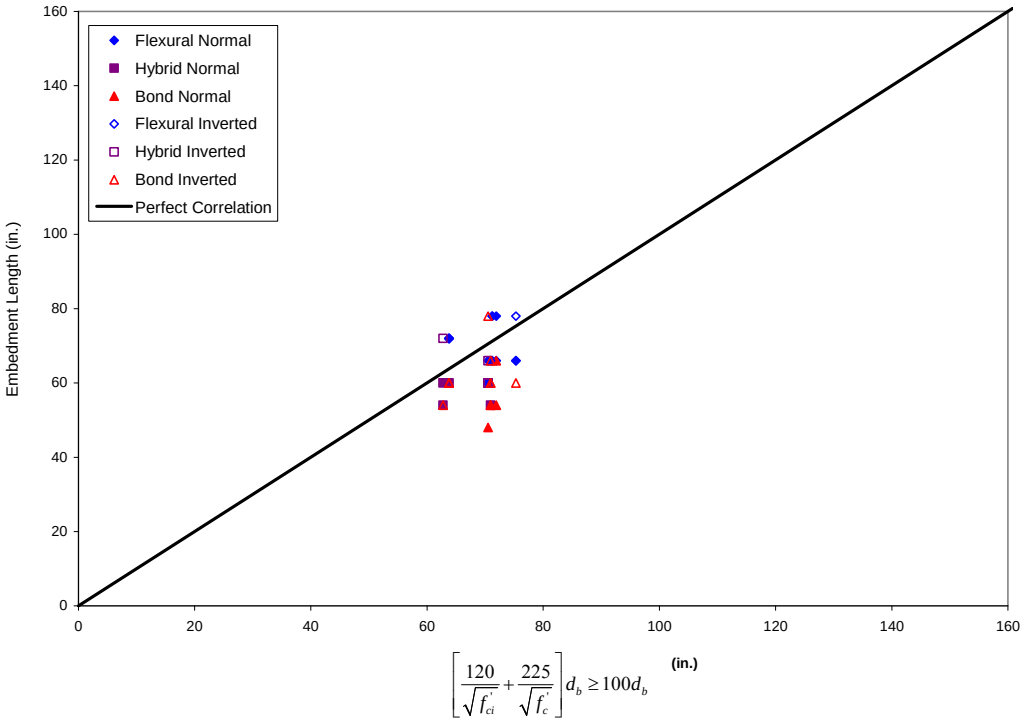

Figure 4.84a. Embedment Length vs. NCHRP (Eq. 2-41)

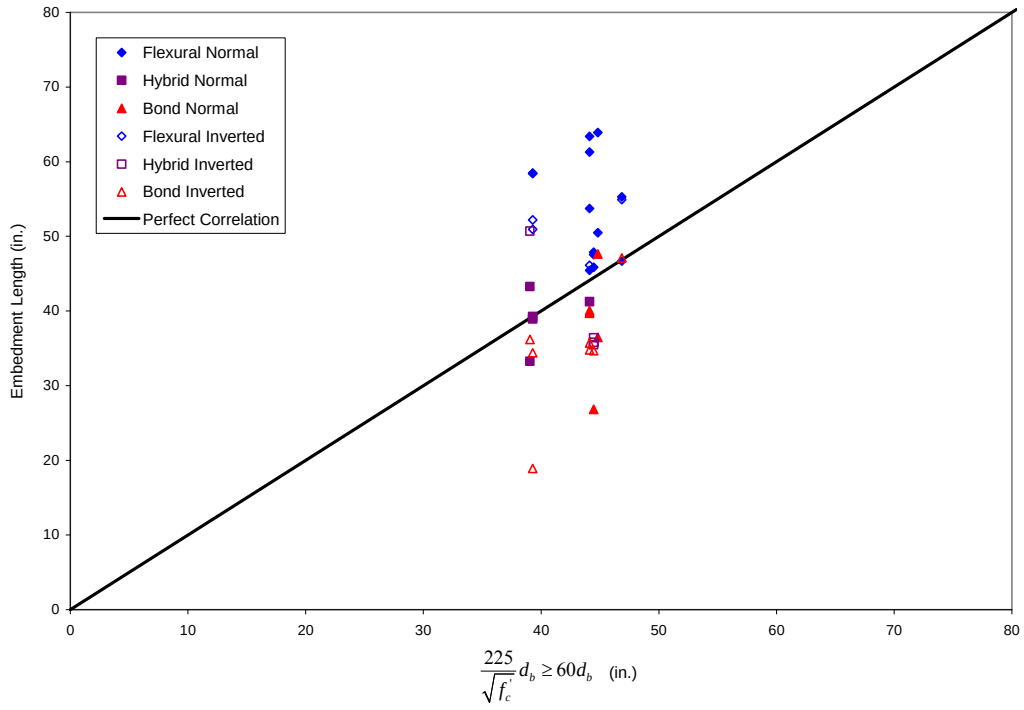

Figure 4.84b. (L_e - L_t) vs. NCHRP (Eq. 2-41)

4.5 Flexural Strength

4.5.1 Introduction

The single-point bending development length tests served two purposes, not only evaluating development lengths, but also the flexural strength of each member for cases where the prestressing strand was fully developed. The primary objective in the evaluation of flexural strength was to determine the applicability of the current code provisions for use with the newer, higher strength Grade 300 strand. The flexural strength was also compared for beams containing Grade 300 strands and beams containing Grade 270 strands, as well as the flexural strength of beams cast with a normal orientation and beams cast with an inverted orientation. In addition to flexural strength evaluation, analytical curvature values were also determined and compared based on an assumed ultimate compressive strain in the concrete of 0.004.

4.5.2 Comparison of Flexural Strength

Each of the experimentally determined values for flexural capacity was compared to the code calculated value. Table 4.20 lists a general summary of the flexural tests, including the ratio of M_{ACTUAL}/M_{AASHTO} for each type of strand. In addition to Table 4.20, plots similar to Figures 4.66 through 4.68 are located in Appendix C for each T-beam test specimen. Of the beams having less than 0.01 in. of slip prior to reaching the nominal moment capacity based on current AASHTO provisions (flexural or hybrid failure), the average overstrength of the T-beam test specimens was 15 percent and the maximum overstrength was 26 percent. For beams containing Grade 300 strands, the average overstrength was 16 percent while those containing Grade 270 strands had an overstrength of 14 percent. The maximum overstrength for beams containing Grade 300 strands was 21 percent, while the beams containing Grade 270 strands had a maximum overstrength of 26 percent. As for the beams cast with a normal orientation, the average overstrength was 14 percent and the average overstrength was 16 percent for the beams cast with an inverted orientation, while both beams cast with a normal and inverted orientation had a maximum overstrength of 26 percent.

Table 4.20. Summary of Flexural Tests Compared to AASHTO

Strand Strength	Average Ratio of M_{ACTUAL}/M_{AASHTO}		
	½ in. diameter	½ in. diameter super	0.6 in. diameter
Grade 270	1.14	1.15	1.13
Grade 300	1.16	1.15	NA

As the primary objective of the study, the calculated flexural capacities for each strand grade were compared. As expected, the Grade 300 strand produced an average increase in nominal flexural capacity of 11 percent. On the contrary, members containing Grade 300 strands showed about a 6 percent decrease in curvature, or ductility at the nominal moment capacity. Experimental comparisons were not made because identical members having different strand strengths were not always tested at the same embedment lengths and did not provide identical flexural failures for comparisons. Calculated ductilities were also the only values compared as ductility was also not measured experimentally. Tables 4.21 and 4.22 show the tabulated values discussed herein for the flexural tests. Overall the T-beam test specimens performed very well in comparison to the current AASHTO provisions. The beams containing Grade 300 strands showed no significant differences with respect to the beams containing Grade 270 strands and the beams cast with an inverted orientation also showed similar behavior to those cast with a normal orientation.

Table 4.21 Summary of Calculated Flexural Strength for Casting Orientation

Average Ratio of M_{300L}/M_{270}		
½ in. diameter	½ in. diameter super	0.6 in. diameter
1.11	1.11	NA

Table 4.22. Summary of Calculated Curvature Comparison

Ratio of Calculated Curvatures			
Pour	Strand Size	Concrete Strength	ϕ_{300}/ϕ_{270}
1	½ in. regular	6500	0.941
2	½ in. regular	6400	0.941
3	½ in. super	8200	0.946
4	½ in. super	6300	0.938
5	½ in. super	6500	0.934
6	½ in. super/0.6 in.	8300	NA

5.0 CONCLUSIONS AND RECOMMENDATIONS

5.1 Summary

Twenty pretensioned, prestressed concrete T-beam test specimens and four sets of top-strand block test specimens were fabricated and tested over the course of three years. Transfer lengths were determined for 119 individual transfer zones, including three strand sizes, two strand strengths, two levels of initial prestress, and various amounts of concrete cast above and below each strand. Thirty-nine flexural tests were performed for the purpose of development length and flexural strength determination. Minimum embedment lengths and flexural bond lengths were determined for each strand size and grade, while the effect of vertical casting position was also evaluated. Of the parameters taken into consideration, the amount of concrete cast above the strand was found to have the most influence on transfer length, but showed no significant effect on flexural bond lengths or flexural strength. Test specimens containing the Grade 300 strands proved to have considerably longer transfer lengths and development lengths, as well as an increase in flexural strength compared to test specimens containing the traditional Grade 270 strands.

5.2 Conclusions

5.2.1 Initial Objectives

The purpose of this study was to investigate the effects an increase in strand strength and the as-cast vertical location of the strand had on transfer length, development length, and flexural strength in pretensioned, prestressed concrete girders and to resolve the discrepancies regarding the definition of the top-strand effect.

5.2.2 Grade 300 Strand

Transfer lengths of the Grade 300 strand had an average increase of 10 percent compared to the transfer lengths of the Grade 270 strand. Development lengths for the Grade 300 strand were also shown to increase compared to the Grade 270 strand. However, flexural bond lengths were found to be relatively the same for both strand strengths, indicating the increase to be primarily dependent on the increase in transfer length. Minimum flexural bond lengths that resulted in flexural failures were found to be in the range of 45 to 50 in. for both strand strengths. The influence of strand strength on flexural strength was also evaluated. As expected, members cast with ½ in. diameter,

Grade 300 strands had about 11 percent higher nominal moment capacities than did those cast with ½ in. diameter, Grade 270 strands. Although increases were seen in nominal moment capacities, reductions in calculated ductilities were also noted in beams cast with Grade 300 strands, on average about 6 percent lower than beams cast with Grade 270 strands.

5.2.3 Effect of Vertical Casting Position

The effect of vertical casting position proved to be the primary conclusion drawn from this study. The results from this study showed the top-strand effect to be more dependent on the amount of concrete cast above the strand than the amount of concrete cast beneath the strand. The amount of concrete cast above the strand had the maximum impact on transfer length, resulting in an average increase of ½ in. for every 1 in. reduction in the amount of concrete cast above a strand. As a result of the findings associated with this study, the current code provisions for the calculation of transfer lengths were found to be unconservative mainly due to the effect of the as-cast vertical location, which was found to be significantly more dependent upon the amount of concrete cast above the strand rather than the amount of concrete cast below the strand. Following a comparison of the results from this study and a number of previous studies, Equation (4-5) was derived for the calculation of transfer length, taking into account the initial prestress, the concrete strength at the time of transfer, the strand diameter, and the amount of concrete cast above the strand.

$$\text{For } d_{cast} < 24 \text{ in. } L_t = 35\frac{f_{si}}{\sqrt{f_{ci}'}}d_b + \zeta\frac{\left(24 - d_{cast}\right)^2}{40}$$
$$\text{For } d_{cast} \geq 24 \text{ in. } L_t = 35\frac{f_{si}}{\sqrt{f_{ci}'}}d_b \qquad \text{Eq. (4-5)}$$

As with transfer length, the development length was also found to be highly influenced by a number of the same factors. However, the flexural bond length was not shown to be affected by those same factors, indicating any influence on development length to be primarily from the initial impact of those factors on transfer lengths. As with strand strength, the minimum flexural bond lengths resulting in flexural failures were in the range of 45 to 50 in. When comparing beams cast with normal orientations to

those cast with inverted orientations, no definitive conclusions were made, but based on the ratios of actual to calculated flexural strengths, beams cast with an inverted orientation had very similar results as those cast with a normal orientation.

5.2.4 Practical Modeling Technique for Transfer Length

In addition to the proposed transfer length equation, a method for modeling transfer length within a finite element model was also developed. The modeling technique was established using nonlinear springs. Relationships between transfer length and spring stiffness were developed for two strand types and cross sections in this study. The technique was developed for use with any member type. However, measured or calculated transfer length values are required and it should be noted that the technique does use an idealized linear force versus slip relationship between the prestressing strand and the surrounding concrete.

5.2.5 Other Conclusions

In addition to the primary objectives associated with this study, a number of items were evaluated and notable conclusions established. In addition to strand strength and the as-cast vertical location, transfer length was found to increase with a sudden release, a decrease in concrete strength, and time, while previously defined influencing factors, strand diameter and effective/initial prestress, showed no significant impact on transfer length. Transfer lengths showed an average increase of 22 percent for strands having a sudden release compared to those with a gradual release. A decrease in concrete strength resulted in a slight increase in transfer length, while the influence of time proved to extend transfer lengths by an average of about 8 percent. End-slip measurements were also used for the calculation of transfer lengths and were compared to transfer lengths calculated from concrete surface strains, showing a very good correlation. When calculated from end-slip measurements, equations by Cousins et al., Russell and Barnes, Logan, and Peterman all showed high levels of accuracy in the calculation of transfer lengths, confirming the reliability of end-slip measurements.

As with transfer length, a number of equations were evaluated for development length including the current code provisions and those recommended by various researchers. The current code expressions used by ACI and AASHTO had a lack of conservatism looking at the flexural bond length portion of the equation, however

equations by Zia and Mostafa, Cousins et al., Deatherage et al., and Buckner all showed a reasonable level of conservatism while still having an appropriate trend. Of the four, equations proposed by Zia and Mostafa, Deatherage et al., and Buckner used factors applied to ($f_{ps} - f_{se}$) of 1.25, 1.50, and λ, respectively, which proved adequate in the estimation of flexural bond lengths. Of the three, the equation by Buckner is the only equation that takes into account the effect of an increased level of tensile strain in the strand at the ultimate flexural capacity of the member.

5.3 Recommendations

As a result of this investigation, the following recommendations were made:

1. The current ACI and AASHTO provisions for the calculation of nominal moment capacity be used for flexural members containing Grade 300 prestressing strands.
2. The proposed Equation (4-5), which takes into account the initial prestress, concrete strength, strand diameter, and as-cast vertical location, be implemented into the provisions of ACI and AASHTO for the calculation of transfer length as current equations were shown to be unconservative.
3. The modeling technique developed herein be used in finite element analyses of pretensioned, prestressed concrete members. If experimentally determined transfer length measurements are unavailable, Equation (4-5) should be used for the calculation of transfer lengths.
4. The proposed Equation (2-38), by Buckner, which takes into account the level of strain in the strand at the nominal moment capacity, be used for the calculation of the flexural bond length portion of the development length.

5.4 Future Research

Although the Grade 300 strand showed favorable results, the ductility of members containing the newer high strength strand was not investigated with great depth in this study. With standard reinforcing, an increase in strength tends to result in a decrease in ductility. Therefore, to ensure an adequate level of ductility for members containing Grade 300 prestressing strands, additional research is recommended on the flexural strength of members containing Grade 300 prestressing strands with an additional focus on the ductility associated with an increase in strand strength.

Equation (4-5) takes into account the level of prestress in the strand just after transfer, the concrete strength, the strand diameter, and the amount of concrete cast above the strand. The first term of the equation correlated very well with transfer length measurements of members with at least 24 in. of concrete cast above the strand. For members with less than 24 in. of concrete cast above the strand, the second term engages, increasing transfer lengths with a reduction in d_{cast}. The term ζ takes into consideration the fluidity of the concrete and ranges from 1 to 2, increasing with fluidity. At the current time, it is recommended that a value of 2 be used for highly fluid mixes, although, the relationship between values of 1 and 2 is not yet known. It is reasonable to assume ζ may be a factor of slump, thus it is recommended that further research by conducted on the relationship between the top-strand effect and the slump of the concrete.

The modeling technique presented herein is a practical method for modeling transfer length in a finite element analysis of pretensioned, prestressed concrete members and allows engineers the ability to accurately account for the effect of transfer length in those models. As previously noted, this technique is simplified for practical use by assuming the force versus slip relationship of the strand and surrounding concrete to be linear. In a continued effort to more accurately predict the effects of transfer length on the end-zones of pretensioned, prestressed concrete members, it is recommended that further attention be given to the force versus slip relationship between the prestressing strand and surrounding concrete.

LIST OF REFERENCES

A416-05/A416M-05, A. (2005). *Standard Specification for Steel Strand, Uncoated Seven-wire for Prestressed Concrete*, American Society for Testing and Materials, West Conshohocken, PA.

AASHTO. (2006). *AASHTO LRFD Bridge Design Specification*, Washington, D.C.

ACI, A. C. I. (2008). *Building Code Requirements for Structural Concrete and Commentary*, Farmington Hills, Michigan.

Anderson, A. R., and Anderson, R. G. (1976). "An Assurance Criterion for Flexural Bond in Pretensioned Hollow Core Units." *ACI Journal*, 73(8), 457-464.

Balazs, G. L. (1993). "Transfer Length of Prestressing Strand as a Function of Draw-In and Initial Prestress." *PCI Journal*, 38(2), 86-93.

Barnes, R. W., Grove, J. W., and Burns, N. H. (2003). "Experimental Assessment of Factors Affecting Transfer Length." *ACI Structural Journal*, 100(6), 740-748.

Buckner, C. D. (1995). "A Review of Strand Development Length for Pretensioned Concrete Members." *PCI Journal*, 40(2), 84-105.

Clark, A. P. (1946). "Comparative Bond Efficiency of Deformed Concrete Reinforcing Bars." *ACI Journal*, 43(4), 381-400.

Collins, M. P., Mitchell, D., Adebar, P., and Vecchio, F. J. (1996). "A General Shear Design Method." *PCI Journal*, 93(1), 36-45.

Cousins, T. E., Badeaux, M. H., and Moustafa, S. (1992). "Proposed Test for Determining Bond Characteristics of Prestressing Strand." *PCI Journal*, 37(1), 66-73.

Cousins, T. E., Francis, L. H., Stallings, J. M., and Gopu, V. (1993). "Spacing and Concrete Cover Requirements for Epoxy-Coated Prestressing Strand in Unconfined Sections." *PCI Journal*, 38(5), 76-84.

Cousins, T. E., Johnston, D. W., and Zia, P. (1990a). "Development Length of Epoxy-Coated Prestressing Strand." *ACI Materials Journal*, 87(4), 309-318.

Cousins, T. E., Johnston, D. W., and Zia, P. (1990b). "Transfer and Development Length of Epoxy Coated and Uncoated Prestressing Strand." *PCI Journal*, 35(4), 92-103.

Cousins, T. E., Johnston, D. W., and Zia, P. (1990c). "Transfer Length of Epoxy-Coated Prestressing Strand." *ACI Materials Journal*, 87(3), 193-203.

Cousins, T. E., Stallings, J. M., and Simmons, M. B. (1994). "Reduced Strand Spacing in Pretensioned, Prestressed Members." *ACI Structural Journal*, 91(3), 277-286.

Deatherage, J. H., Burdette, E. G., and Chew, C. K. (1994). "Development Length and Lateral Spacing Requirements of Prestressing Strand for Prestressed Concrete Bridge Girders." *PCI Journal*, 39(1), 70-83.

Devalapura, R. K., and Tadros, M. K. (1992). "Stress-Strain Modeling of 270 ksi Low-Relaxation Prestressing Strands." *PCI Journal*, 37(2), 100-105*.

ENV. (1992-1-1). *Eurocode 2: Design of Concrete Structures*.

FHWA. (1988). *Prestressing Strand for Pretension Applications - Development Length Revisited*, Chief, Bridge Division, Federal Highway Administration, McLean, VA.

Guyon, Y. (1948). *Beton Precontraint*, Gand, France.

Hanson, N. W., and Kaar, P. H. (1959). "Flexural Bond Tests of Pretensioned Prestressed Beams." *ACI Journal*, 56(1), 783-802.

Janney, J. R. (1954). "Nature of Bond in Pre-Tensioned Prestressed Concrete." *ACI Journal*, 50(9), 717-736.

Janney, J. R. (1963). "Report of Stress Transfer Length Studies on 270 k Prestressing Strand." *PCI Journal*, 8(1), 41-45.

Jeanty, P. R., Mitchell, D., and Mirza, M. S. (1988). "Investigation of "Top Bar" Effects in Beams." *ACI Structural Journal*, 85(3), 251-257.

Jirsa, J. O., and Breen, J. E. (1981). "Influence of Casting Position and Shear on Development and Splice Length - Design Recommendation." Center for Transportation Research, University of Texas at Austin.

Kaar, P. H., LaFraugh, R. W., and Mass, M. A. (1963). "Influence of Concrete Strength on Strand Tranfer Length." *PCI Journal*, 8(5), 47-67.

Kose, M. M., and Burkett, W. R. (2005). "Formulation of New Development Length Equation for 0.6 in. Prestressing Strand." *PCI Journal*, 50(5), 96-105.

Lane, S. H. (1998). *A New Development Length Equation for Pretensioned Strands in Bridge Beams and Piles*, Structures Division, Federal Highway Administration, McLean, VA.

Larson, K. H., Peterman, R. J., and Esmaeily, A. (2007). "Bond Characteristics of Self-consolidating Concrete for Prestressed Bridge Girders." *PCI Journal*, 52(4).

Loflin, B. J. (2008). *Bond and Material Properties of Grade 270 and Grade 300 Prestressing Strands*, Virgina Tech, Blacksburg, VA.

Logan, D. R. (1997). "Acceptance Criteria for Bond Quality of Strand for Pretensioned Prestressed Concrete Applications." *PCI Journal*, 42(2), 52-90.

MacGregor, J. C., and Wight, J. K. (2005). *Reinforced Concrete, Mechanics and Design*, Pearson Prentice Hall, Upper Saddle River, NJ.

Marti-Vargas, J. R., Arbelaez, C. A., Serna-Ros, P., and Castro-Bugallo, C. (2007). "Reliability of Transfer Length Estimation from Strand End Slip." *ACI Structural Journal*, 104(4), 487-494.

Martin, A. R., and Scott, N. L. (1976). "Development of Prestressing Strand in Pretensioned Member." *ACI Journal*, 73(8), 453-456.

Mitchell, D., Cook, W. D., Khan, A. A., and Tham, T. (1993). "Influence of High Strength Concrete on Transfer and Development Length of Pretensioning Strand." *PCI Journal*, 38(3), 52-66.

Mote, J. (2001). *Bond Mechanics of Steel Prestressing Strand*, University of Oklahoma, Norman Oklahoma.

NCHRP. (2008). "WAI 146 - Transfer and Development of PS Strand."

Oh, B. H., and Kim, E. S. (2000). "Realistic Evaluation of Transfer Lengths in Pretensioned, Prestressed Concrete Members." *ACI Structural Journal*, 97(6), 821-830.

Park, R., and Paulay, T. (1975). *Reinforced Concrete Structures*, John Wiley & Sons, Inc., New York.

Peterman, R. J. (2007). "The Effects of As-Cast Depth and Concrete Fluidity on Strand Bond." *PCI Journal*, 52(3), 72-101.

Petrou, M. F., Wan, B., Gadala-Maria, F., Kolli, V. G., and Harries, K. A. (2000a). "Influence of Mortar Rheology on Aggregate Settlement." *ACI Materials Journal*, 97(3), 479-485.

Petrou, M. F., Wan, B., Joiner, W. S., Trezos, C. G., and Harries, K. A. (2000b). "Excessive Strand End Slip in Prestressed Piles." *ACI Structural Journal*, 97(5), 774-782.

Ramirez, J. A., and Russell, B. W. (2007). "Draft Final Report NCHRP 12-60 - Transfer, Development, and Splice Length for Strad/Reinforcement in High-Strength Concrete." Purdue University, School of Civil Engineering, West Lafayette, IN.

Rose, D. R., and Russell, B. W. (1997). "Investigation of Standardized Tests to Measure the Bond Perfomance of Prestressing Strand." *PCI Journal*, 42(4), 56-80.

Russell, B. W., and Burns, N. H. (1993). "Design Guidelines for Transfer, Development and Debonding of Large Diameter Seven Wire Strands in Pretensioned Concrete Girders.", University of Texas at Austin, Austin, TX.

Russell, B. W., and Burns, N. H. (1997). "Measurement of Transfer Lengths on Pretensioned Concrete Elements." *Journal of Structural Engineering*(May), 541-549.

Shahawy, M. A., and Issa, M. (1992). "Effect on Pile Embedment on the Development Length of Prestressing Strands." *PCI Journal*, 37(6), 44-59.

Shahawy, M. A., Issa, M., and Batchelor, B. d. (1992). "Strand Transfer Lengths in Full Scale AASHTO Prestressed Concrete Girders." *PCI Journal*, 37(3), 84-96.

Tabatabai, H., and Dickson, T. J. (1993). "The History of the Prestressing Strand Development Length Equation." *PCI Journal*, 38(6), 64-75.

Wan, B., Harries, K. A., and Petrou, M. F. (2002a). "Transfer Length of Strands in Prestressed Concrete Piles." *ACI Structural Journal*, 99(5), 577-585.

Wan, B., Petrou, M. F., Harries, K. A., and Hussein, A. A. (2002b). "Top Bar Effects in Prestressed Concrete Piles." *ACI Structural Journal*, 99(2), 208-214.

Zia, P., and Mostafa, T. (1977). "Development Length of Prestressing Strands." *PCI Journal*, 22(5), 54-63.

APPENDIX A

Nomenclature

a = depth of equivalent rectangular stress block (in.)
A = coefficient used in stress-strain development for prestressing strand
A_g = gross area of concrete section (in.^{2})
A_{gt} = gross transformed area of concrete section (in.^{2})
A_{ps} = area of prestressing strand (in.^{2})
A'_s = are of compression reinforcement (in.^{2})
b = width of compression face of member (in.)
b_{cast} = depth of concrete cast beneath the strand (in.)
B = slope of the bond stress in the plastic zone (Cousins et al.)
B = coefficient used in stress-strain development for prestressing strand
c = distance from extreme compressive fiber to neutral axis (in.)
c_b = smaller of: (a) the distance from center of bar or wire to nearest concrete surface, and (b) one-half the center-to-center spacing of bars or wires being developed
C = coefficient used in stress-strain development for prestressing strand
d = distance from extreme compressive fiber to centroid of tensile steel (in.)
d' = distance from extreme compression fiber to centroid of compression steel (in.)
d_b = diameter of standard reinforcing bar or prestressing strand (in.)
d_{cast} = depth of concrete cast above the strand (in.)
d_p = distance from extreme compression fiber to centroid of prestressing steel (in.)
D = coefficient used in stress-strain development for prestressing strand
e_g = eccentricity of prestressing strands in the gross section (in.)
e_{gt} = eccentricity of prestressing strands in the gross transformed section (in.)
E_c = modulus of elasticity of concrete (ksi)
E_{ci} = modulus of elasticity of concrete at the time of transfer (ksi)
E_{ps} = modulus of elasticity of prestressing strand (ksi)
E_s = modulus of elasticity of standard reinforcing steel (ksi)
f'_c = 28 day concrete compressive strength (psi)
f'_{ci} = concrete compressive strength at transfer (psi)
f_{pi} = stress in the prestressing strand just after transfer (ksi)
f_{ps} = stress in the prestressing strand at nominal moment capacity (ksi)
f_{pu} = ultimate tensile strength of prestressing strand (ksi)
f_{pt} = stress in the prestressing strand just after transfer (ksi)
f_r = modulus of rupture of concrete (psi)
f_{se} = stress in the prestressing strand after all losses at the time of testing
f_{si} = stress in the prestressing strand just after transfer (ksi)
f_{sj} = jacking stress of the prestressing strand (ksi)
f_{su} = ultimate tensile strength of prestressing strand (ksi)
f_y = yield strength of standard reinforcing steel (ksi)
h = overall height of member (in.)
I_g = gross moment of inertia (in.^{4})
I_{gt} = gross transformed moment of inertia (in.^{4})
k = nonlinear spring stiffness (kips/in.)
k = strand type factor
k_b = factor for member type (Shahawy and Issa)
K_{tr} = transverse reinforcement index

L_d = development length (in.)
L_e = embedment length (in.)
L_{es} = end-slip (in.)
L_{fb} = flexural bond length (in.)
L_t = transfer length (in.)
m = slope of ascending branch of strain profile (in./in.)
M_n = nominal moment capacity (kip-feet)
U'_d = development length constant (Cousins et al.)
U'_t = transfer length constant (Cousins et al.)
X = basic transfer length equation constant
y_{int} = y-intercept of ascending branch of strain profile (in.)
Y = top-strand factor exponent
Z = top-strand factor constant

α = transfer length constant (Barnes et al.)
α = modifier for shape of bond stress distribution (Guyon)
β_1 = factor relating depth of equivalent rectangular stress block to neutral axis depth
γ_p = factor for type of prestressing steel
δ_c = deflection of concrete due to prestressing force (in.)
δ_s = deflection of steel due to prestressing force (in.)
ΔT = change in temperature (ºF)
ε_c = strain in the concrete (in./in)
ε_{ci} = initial strain in the concrete (in./in.)
ε_{cu} = ultimate compressive strain in the concrete (in./in.)
ε_{pu} = ultimate tensile strain in the prestressing steel (in./in.)
ε_{ps} = strain in the prestressing steel at nominal moment capacity (in./in.)
ε_s = stain in the prestressing steel (in./in.)
ε_{si} = initial strain in the prestressing steel (in./in.)
λ = modification factor reflecting the reduced mechanical properties of lightweight concrete all relative to normalweight concrete of the same compressive strength
λ = modification factor for flexural bond length dependent upon the strain in the strand at the nominal moment capacity (Buckner)
ρ_p = ratio of A_{ps} to bd_p
μ_{ave} = average bond stress (psi)
ψ_e = factor used to modify development length based on reinforcement coating
ψ_s = factor used to modify development length based on reinforcement size
ψ_t = factor used to modify development length based on reinforcement location
ω = tension reinforcement index
ω' = compression reinforcement index
ζ = fluidity multiplier for top-strand factor

APPENDIX B

Surface Strain Plots

The following strain profiles were generated from transfer length measurements taken throughout the duration of the project. In an effort to increase the clarity of each plot, the legend was removed. The legend is consistent for all plots and is shown below.

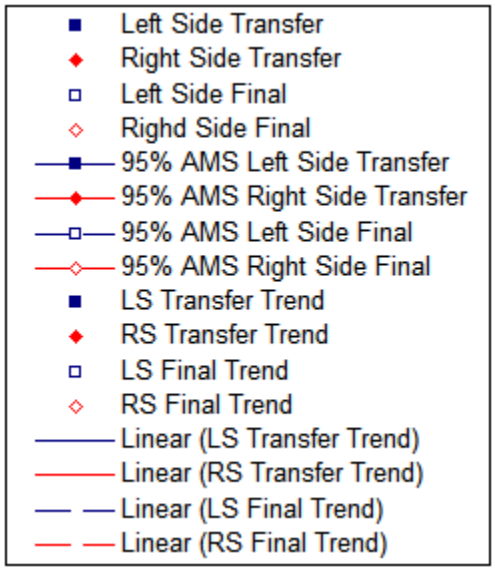

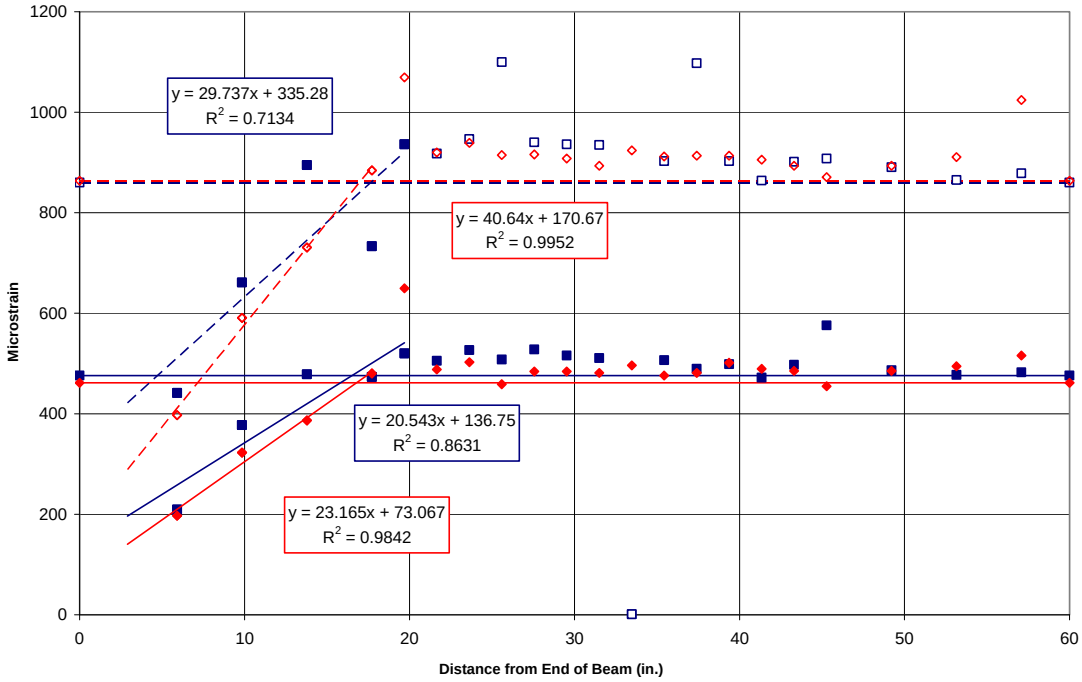

Figure B.1 – 1.270.5N.RA

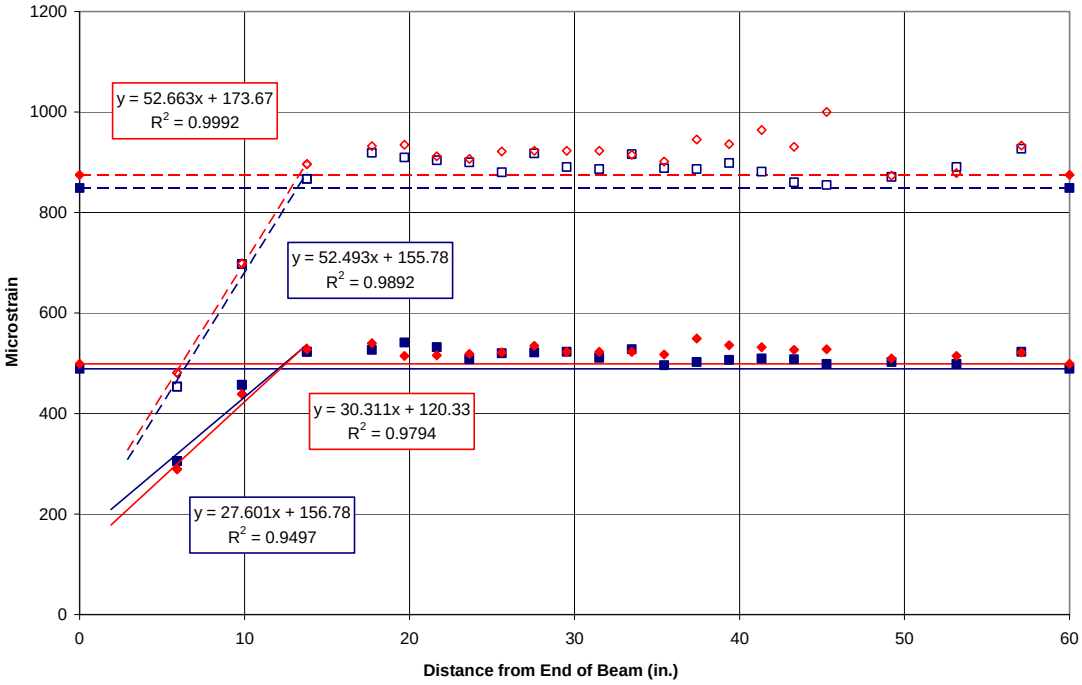

Figure B.2 – 1.270.5N.RB

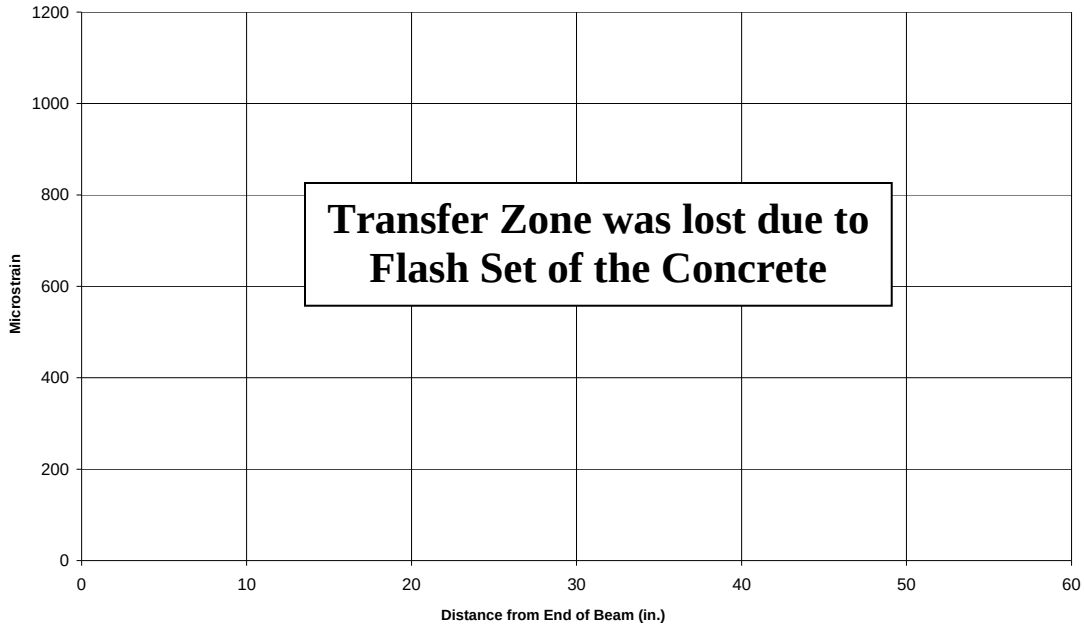

Figure B.3 – 1.300.5N.RA

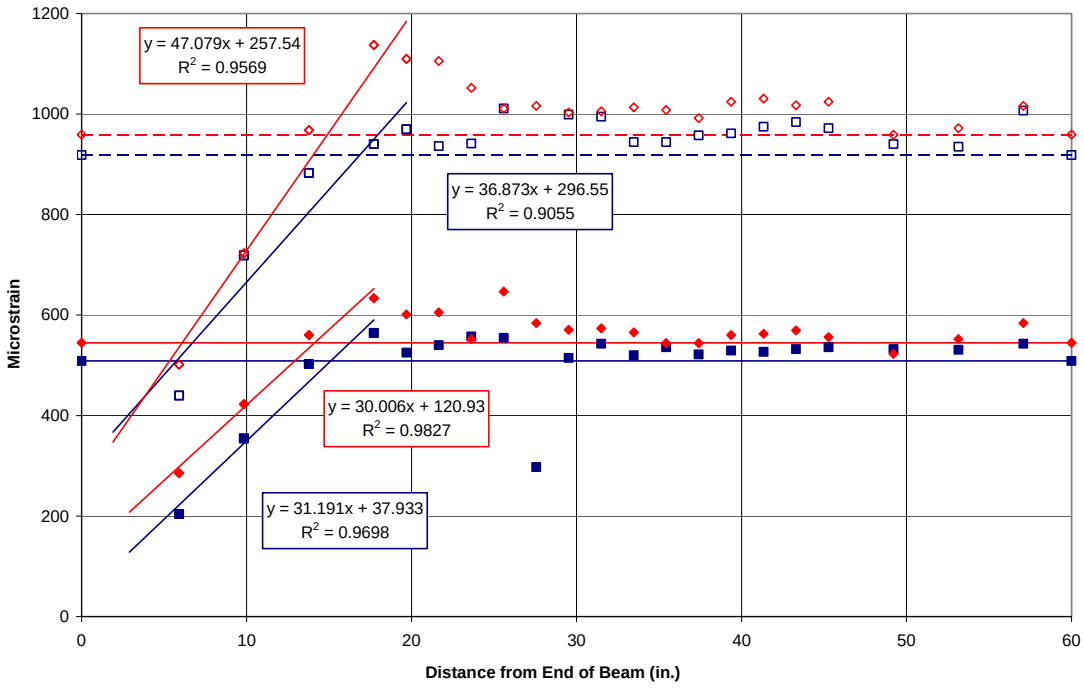

Figure B.4 – 1.300.5N.RB

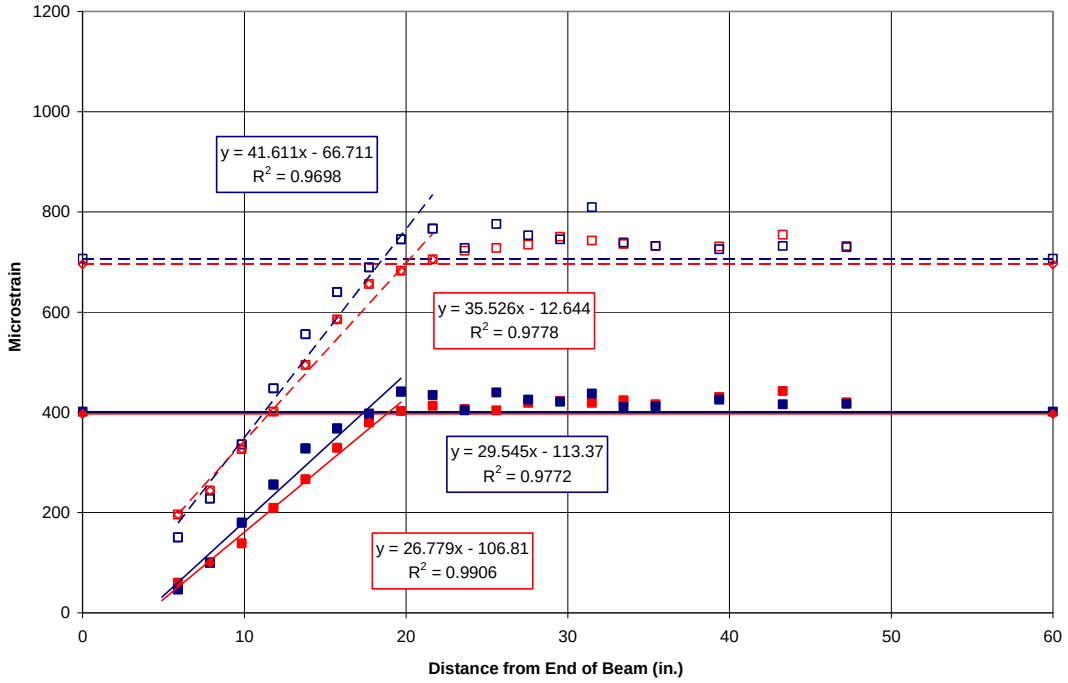

Figure B.5 – 2.270.5N.RA

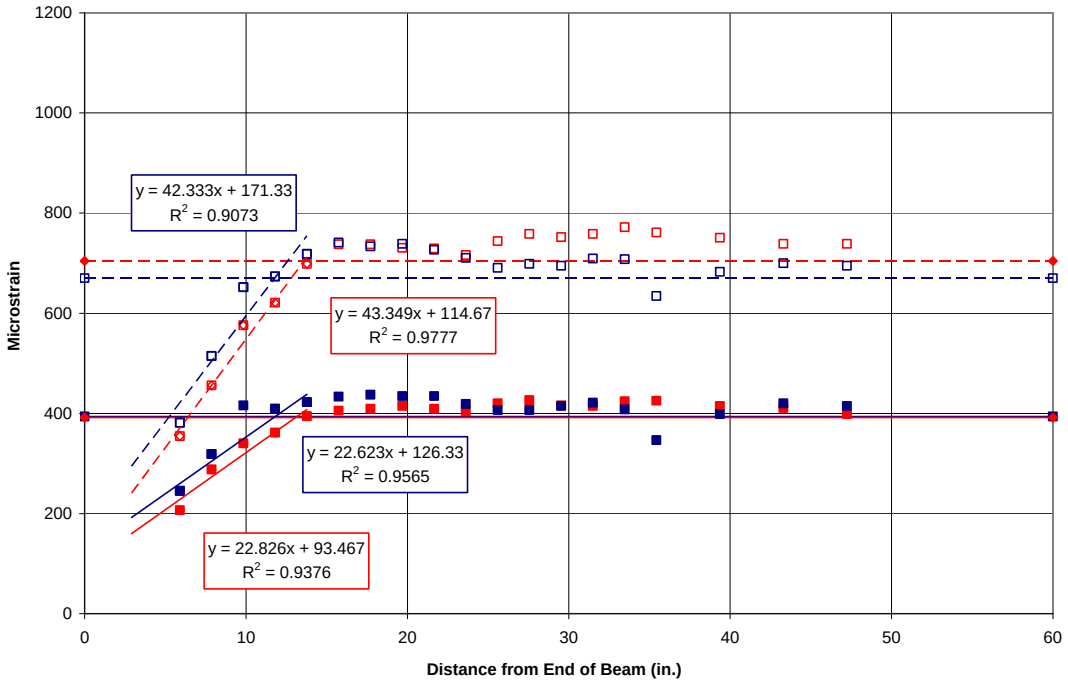

Figure B.6 – 2.270.5N.RB

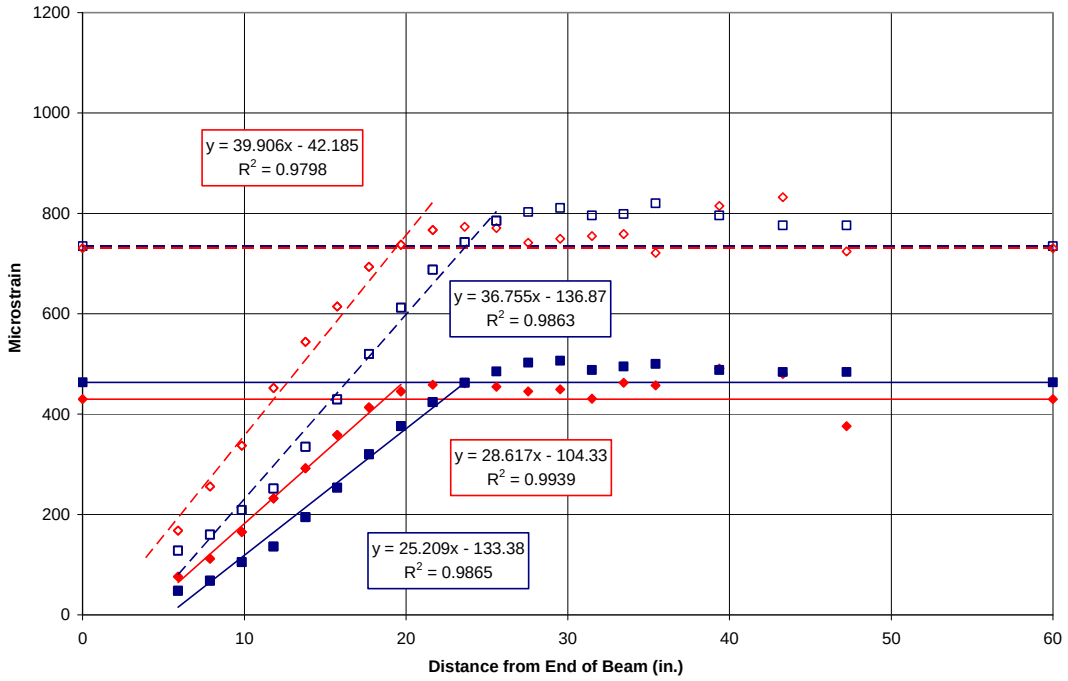

Figure B.7 – 2.300.5N.RA

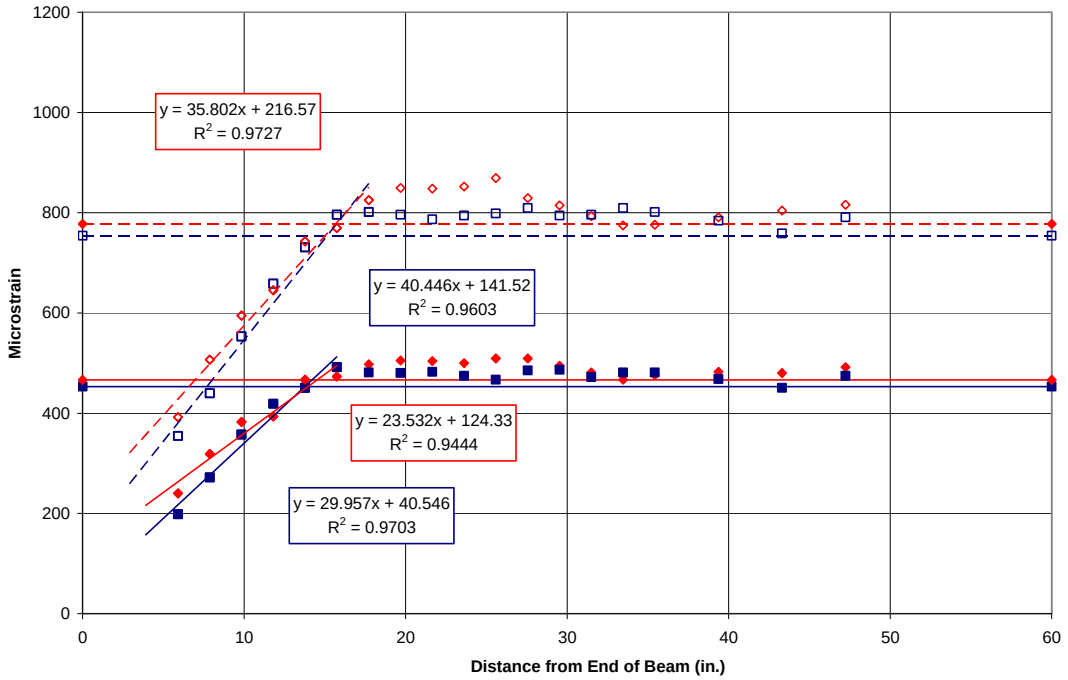

Figure B.8 – 2.300.5N.RB

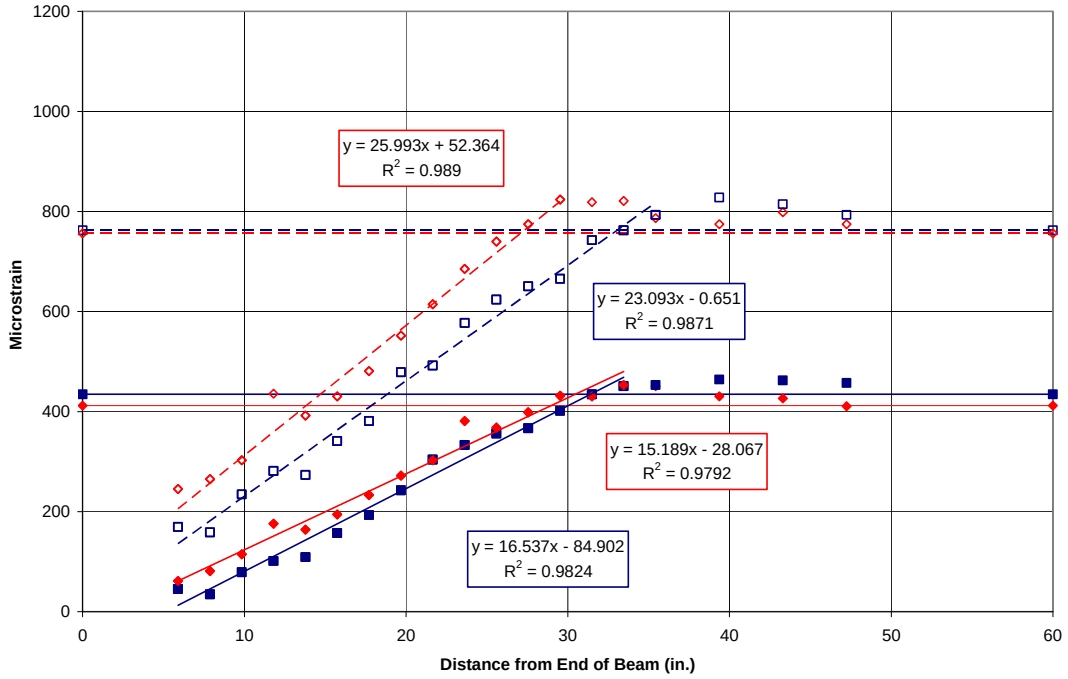

Figure B.9 – 2.270.5N.UA

1.270.5N.UB

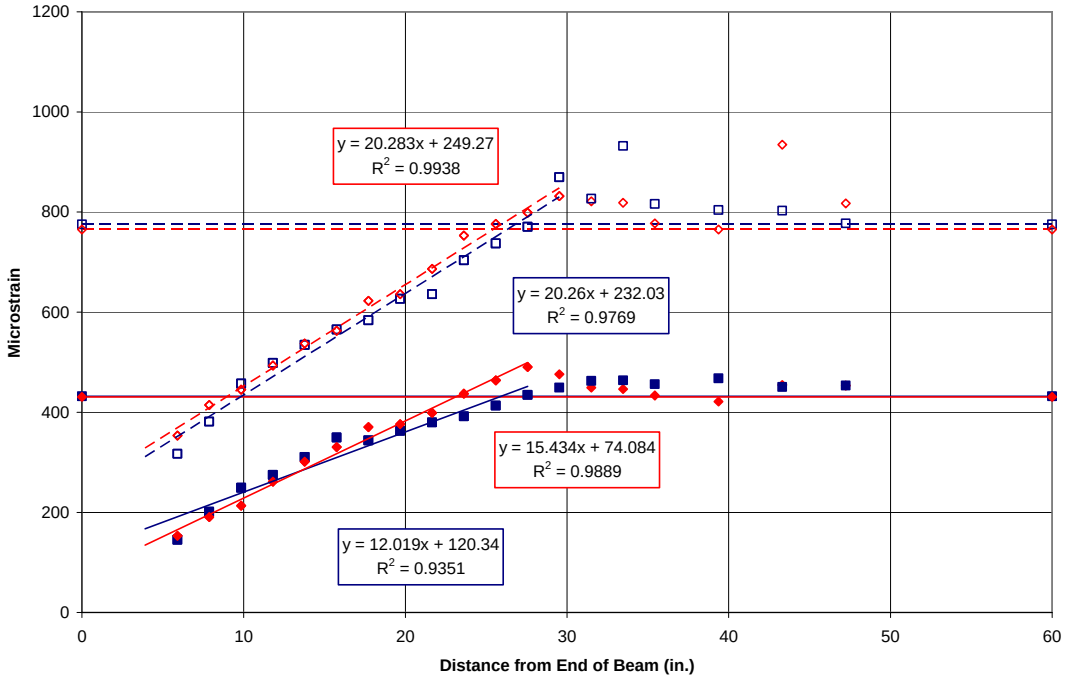

Figure B.10 – 2.270.5N.UB

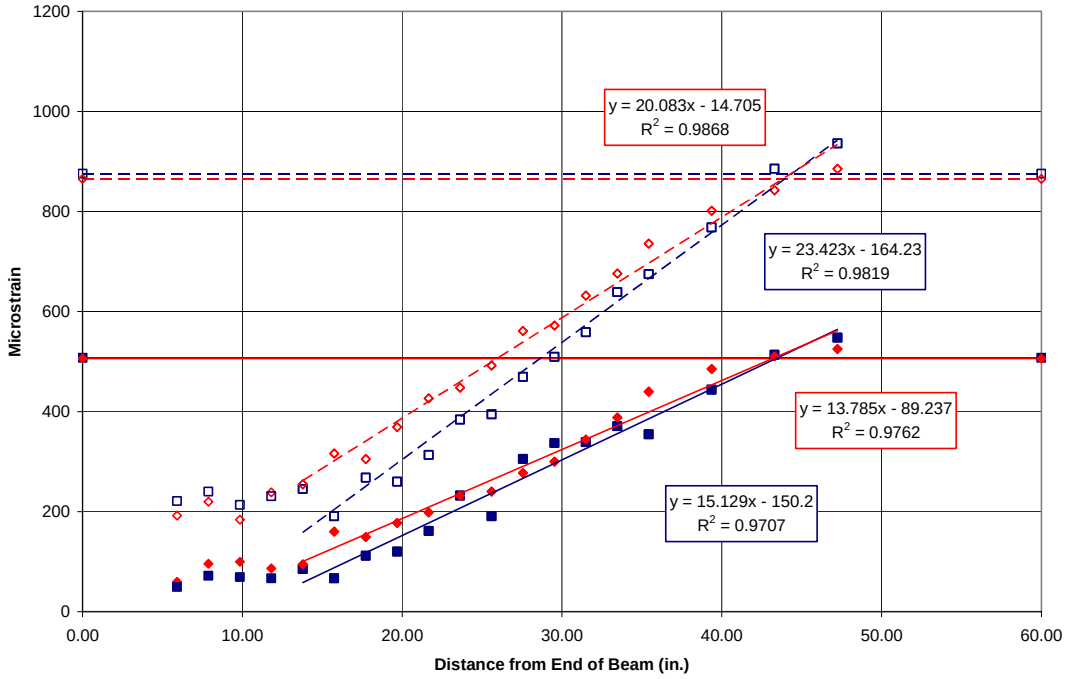

Figure B.11 – 2.300.5N.UA

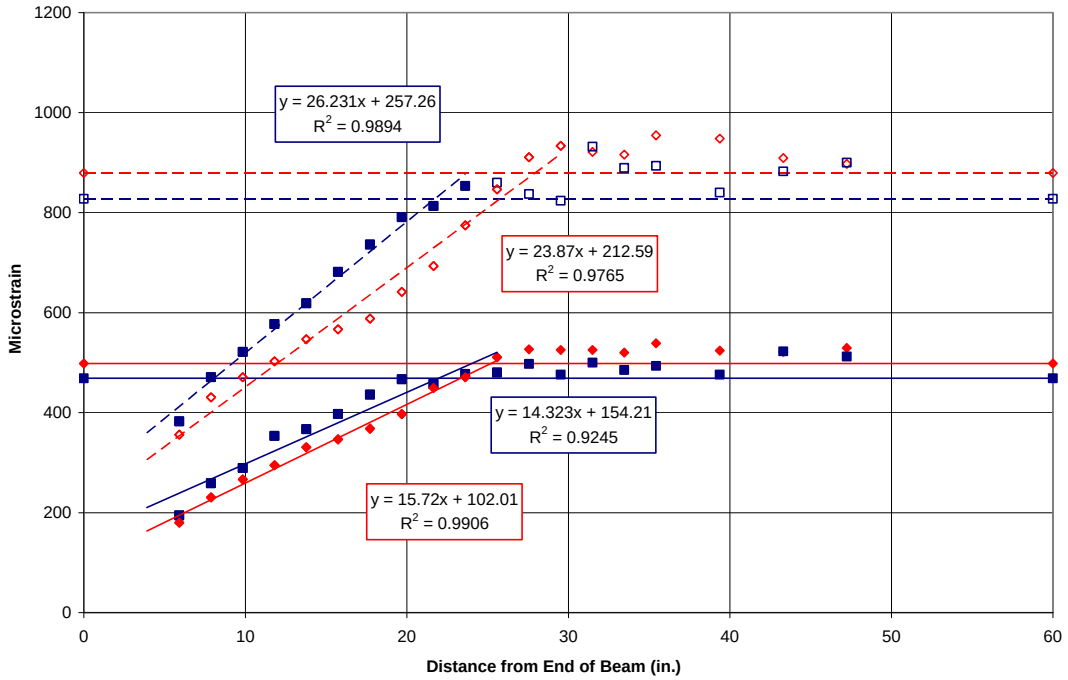

Figure B.12 – 2.300.5N.UB

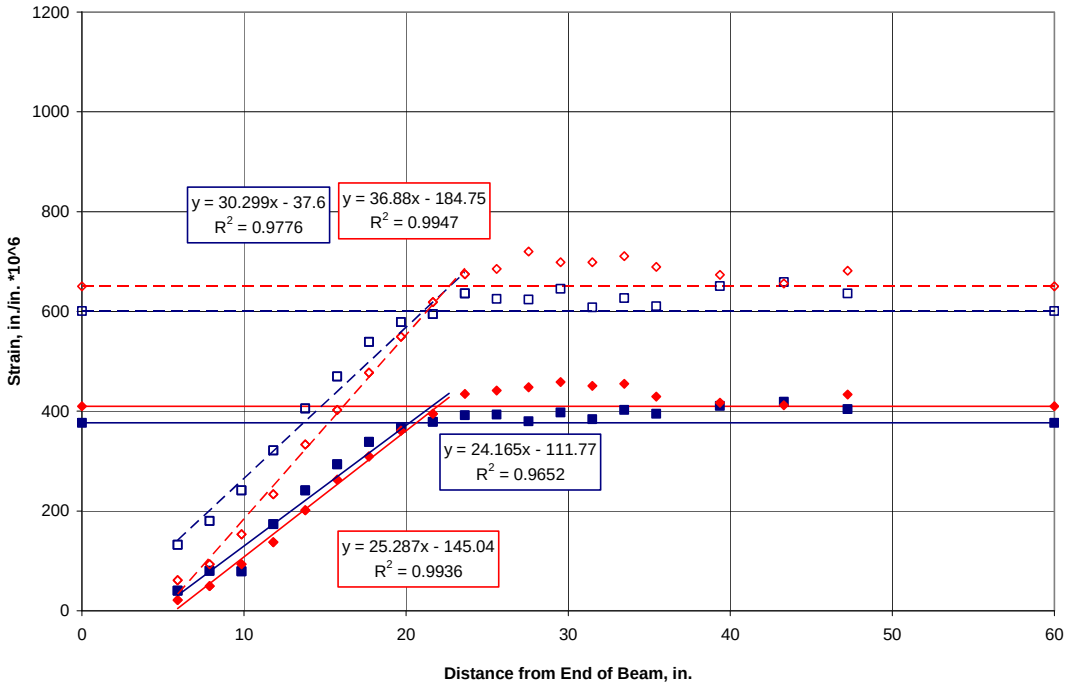

Figure B.13 – 3.270.5S.RA

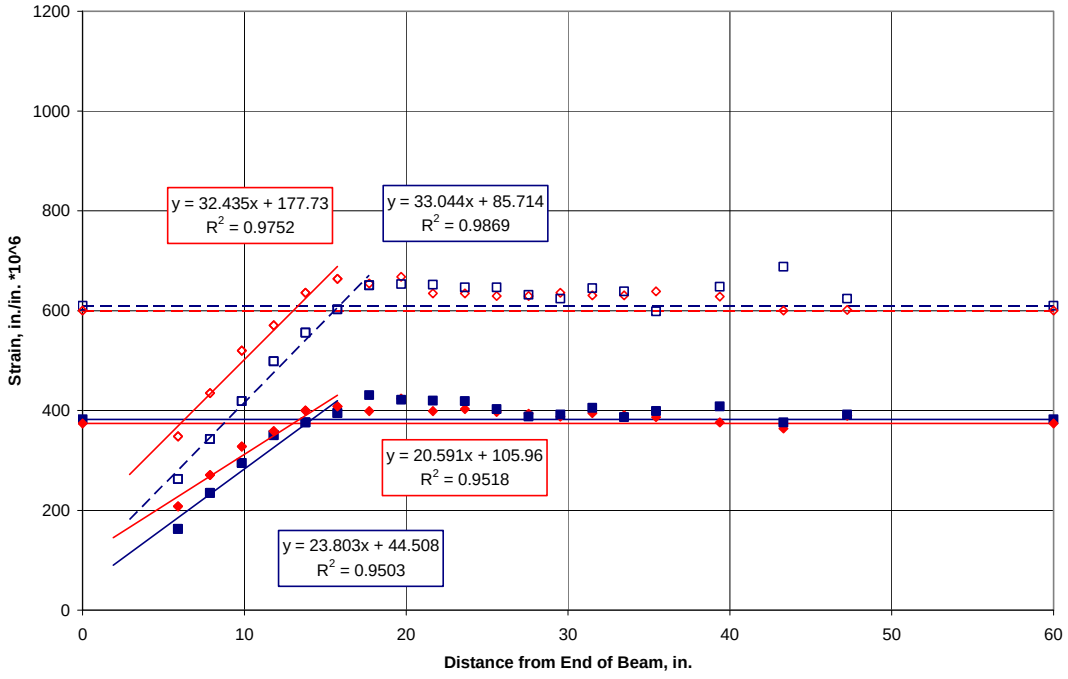

Figure B.14 – 3.270.5S.RB

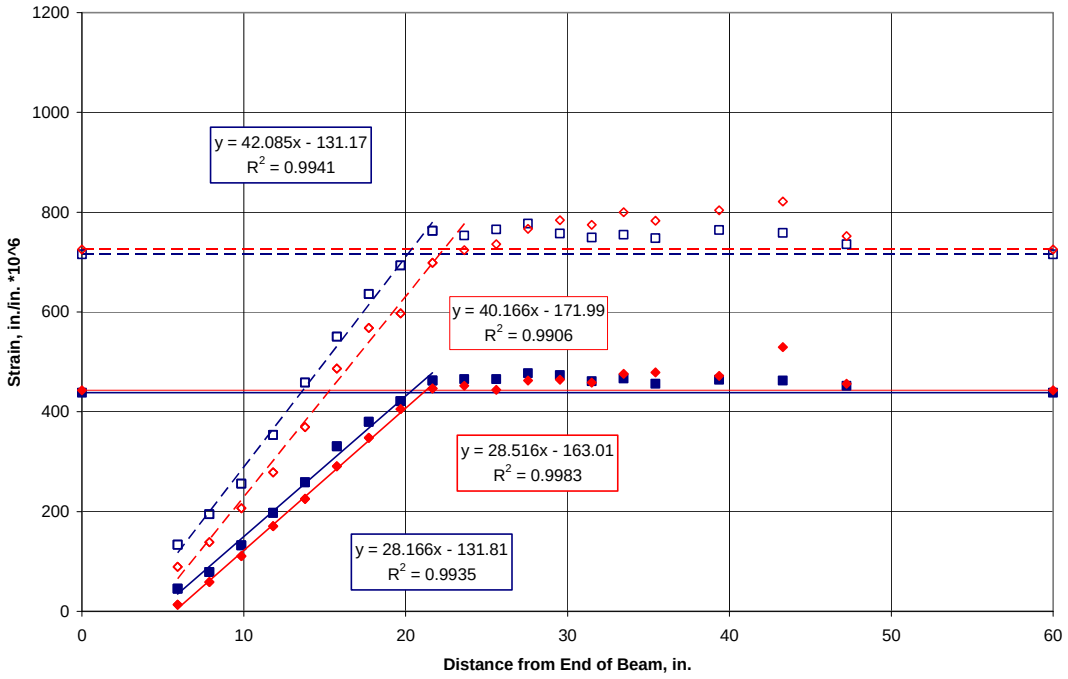

Figure B.15 – 3.300.5S.RA

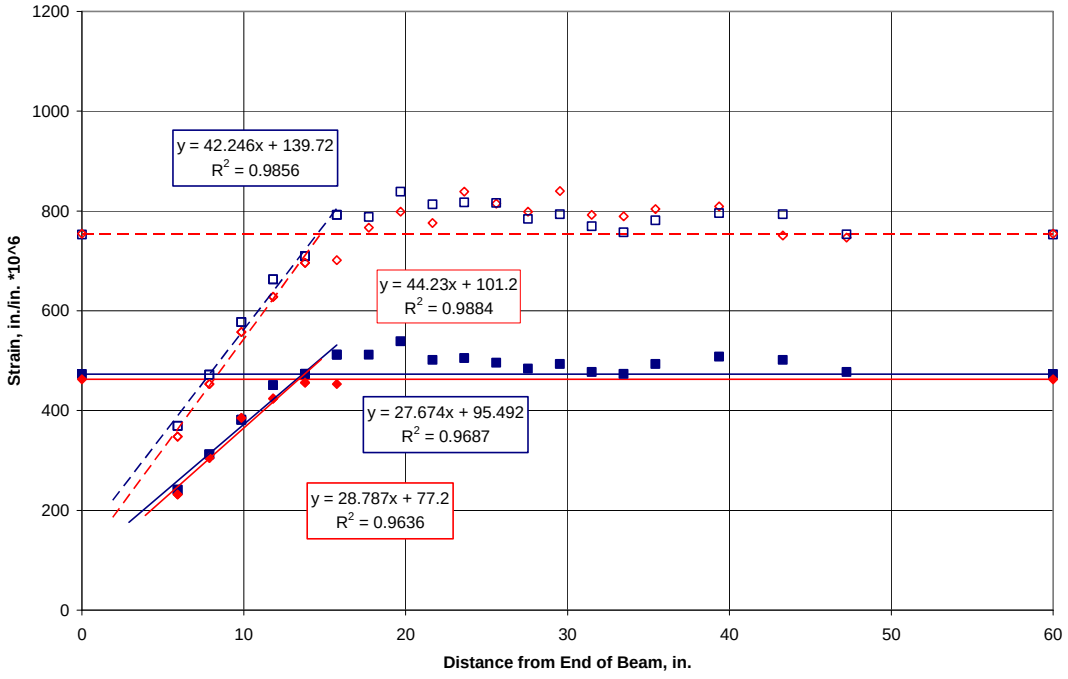

Figure B.16 – 3.300.5S.RB

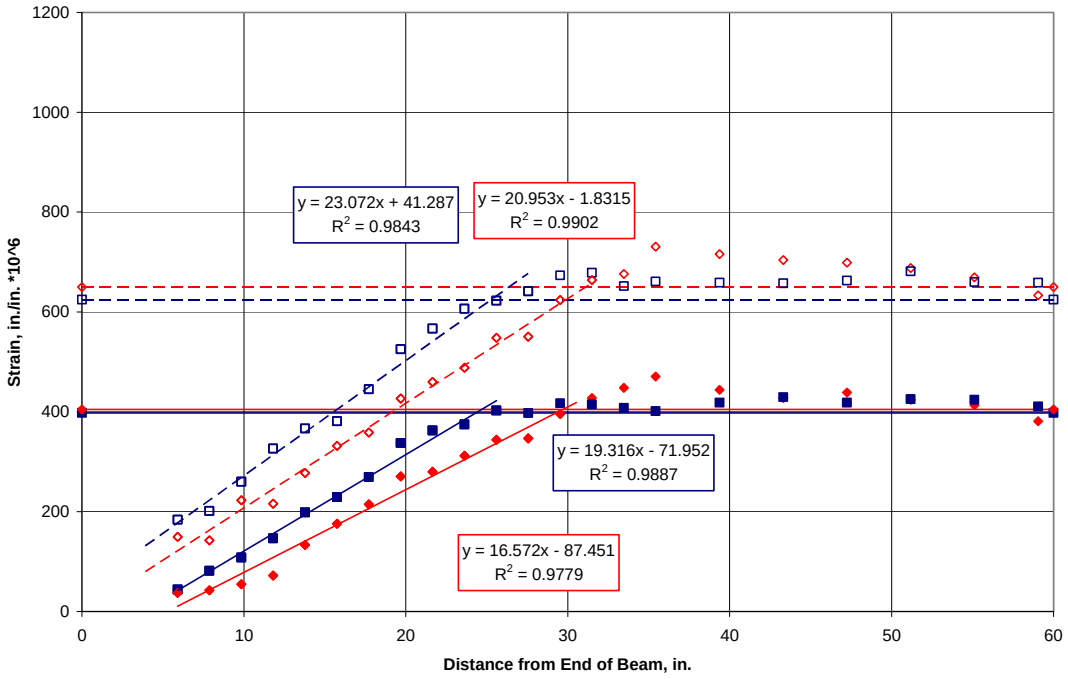

Figure B.17 – 3.270.5S.UA

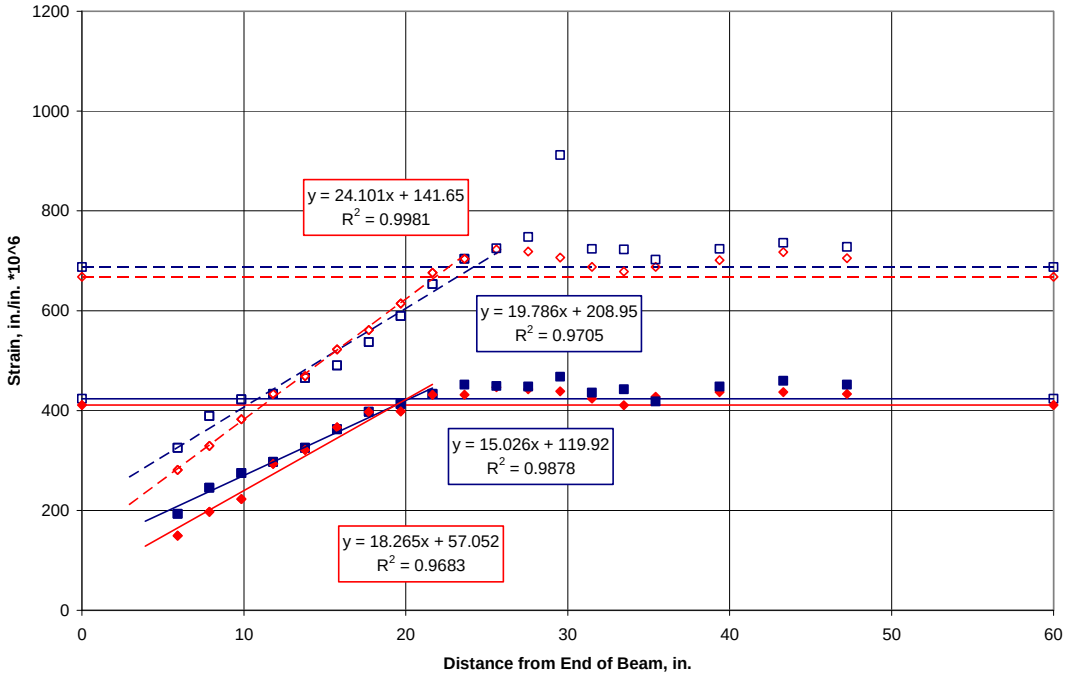

Figure B.18 – 3.270.5S.UB

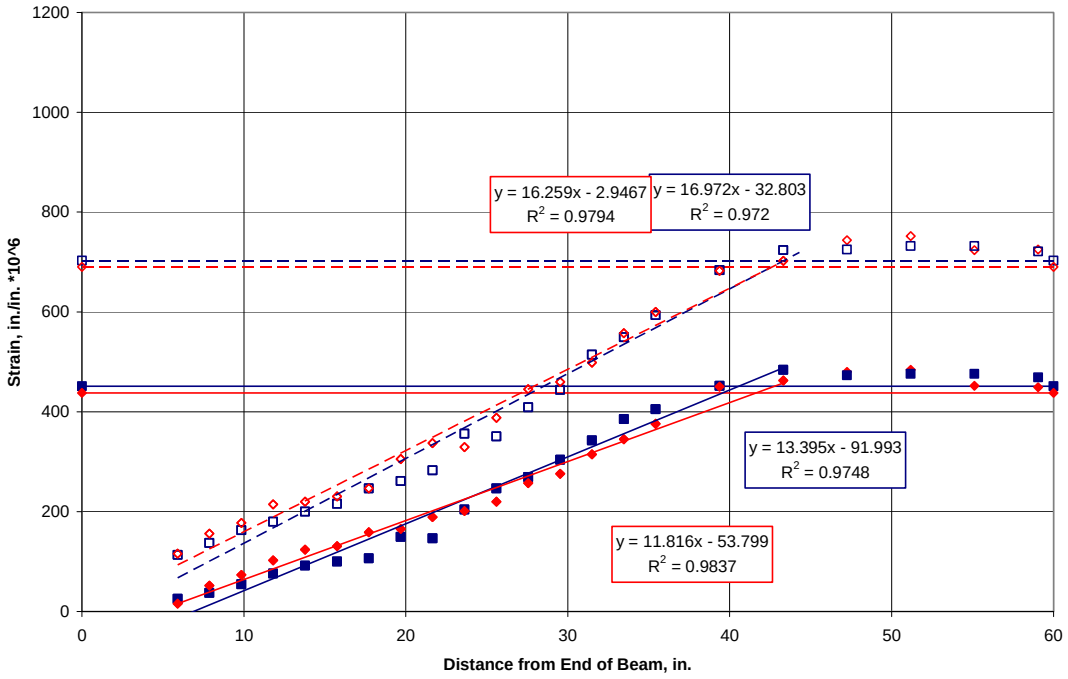

Figure B.19 – 3.300.5S.UA

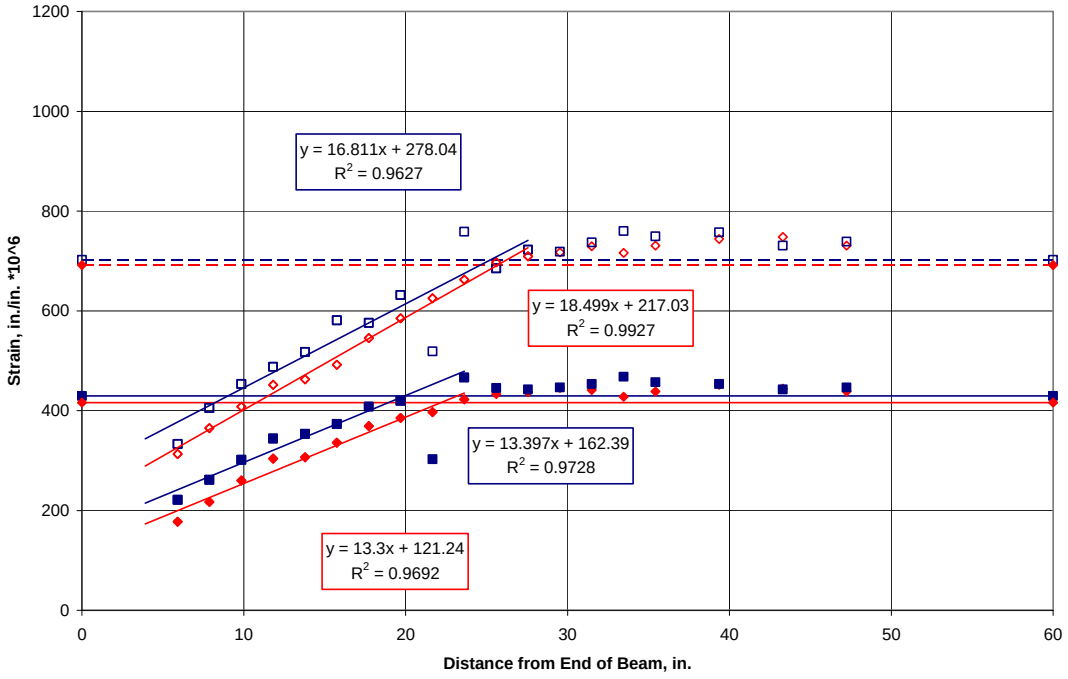

Figure B.20 – 3.300.5S.UB

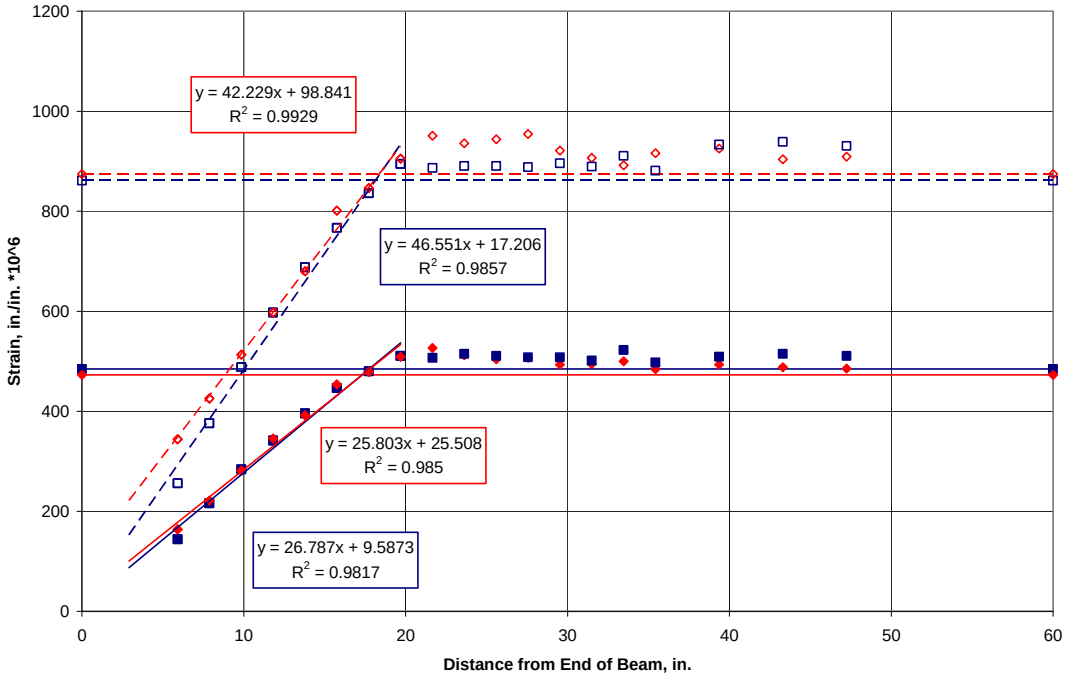

Figure B.21 – 4.270.5S.RA

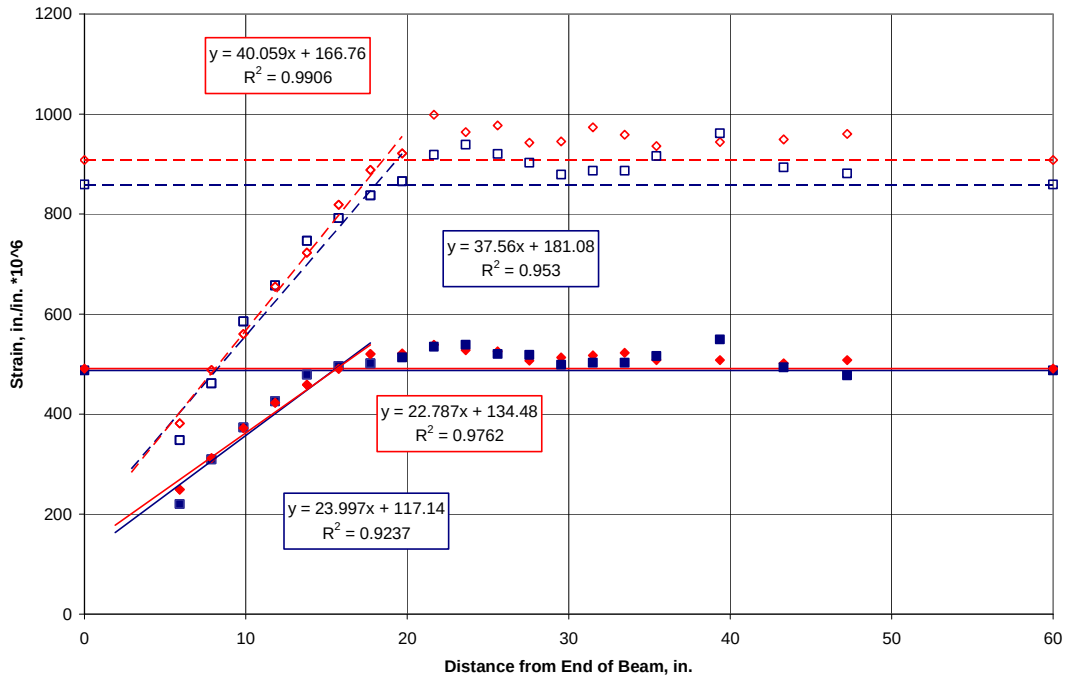

Figure B.22 – 4.270.5S.RB

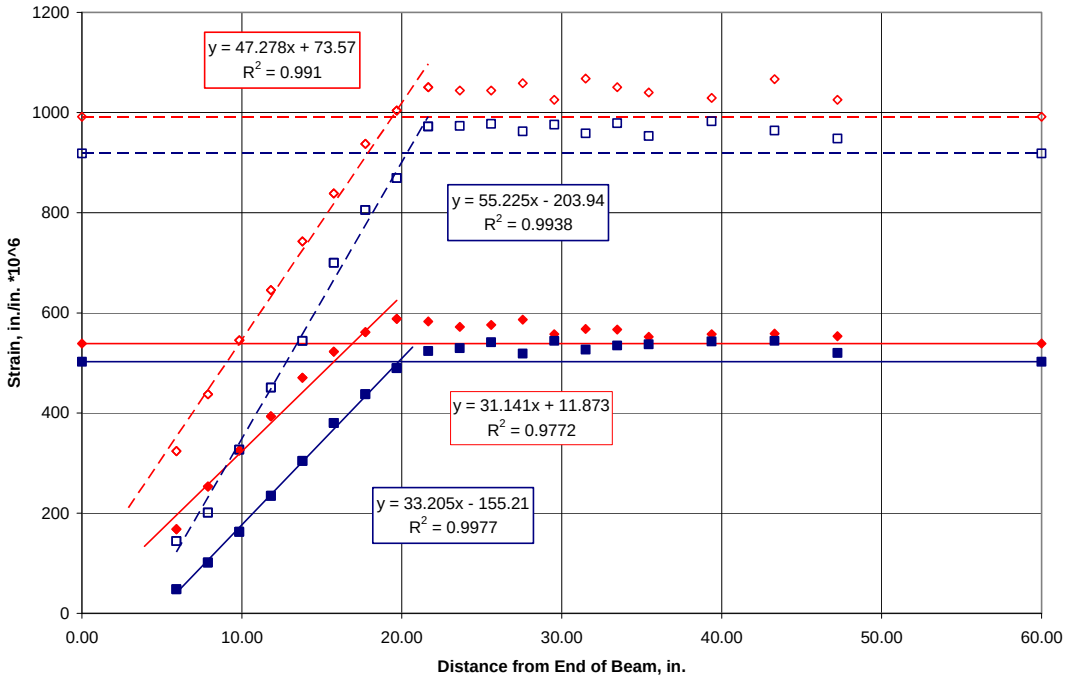

Figure B.23 – 4.300.5S.RA

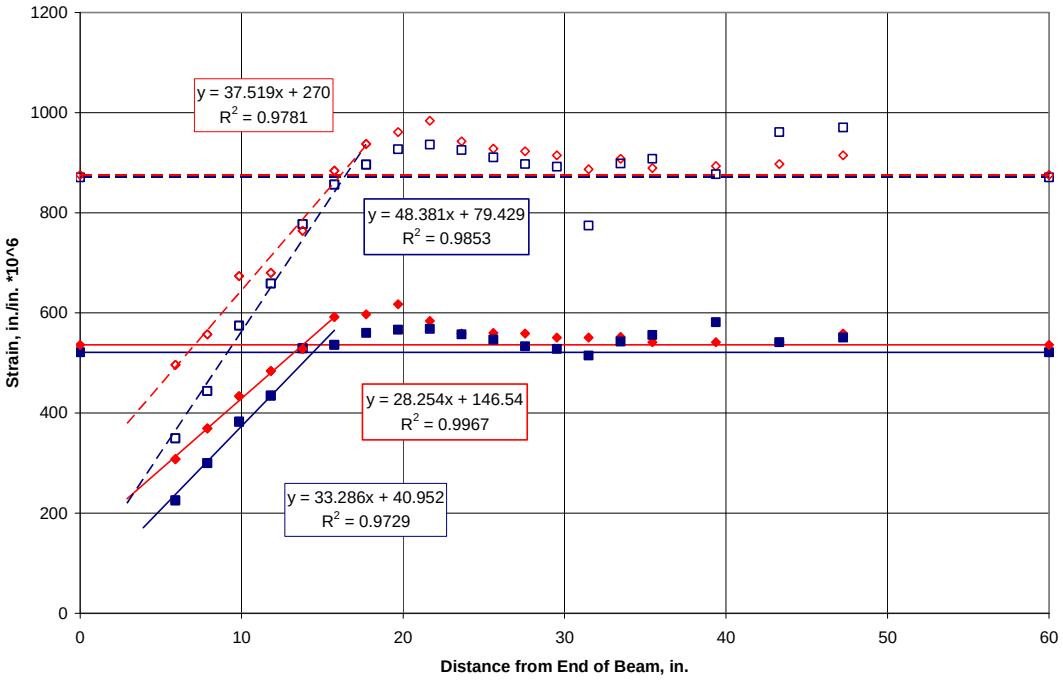

Figure B.24 – 4.300.5S.RB

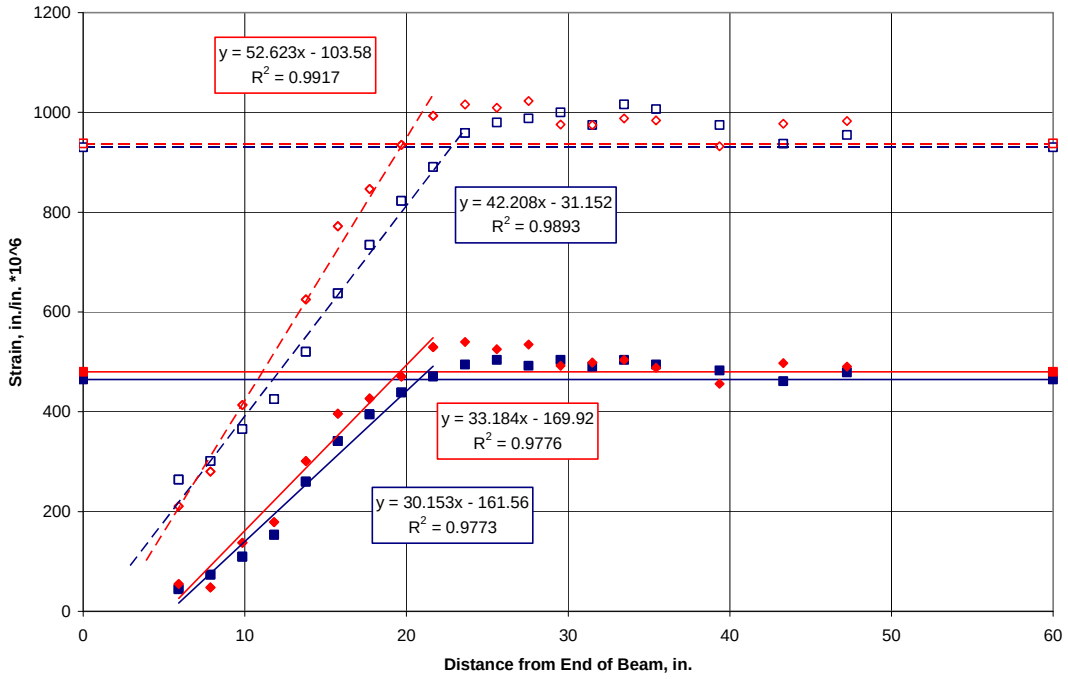

Figure B.25 – 5.270.5S.RA

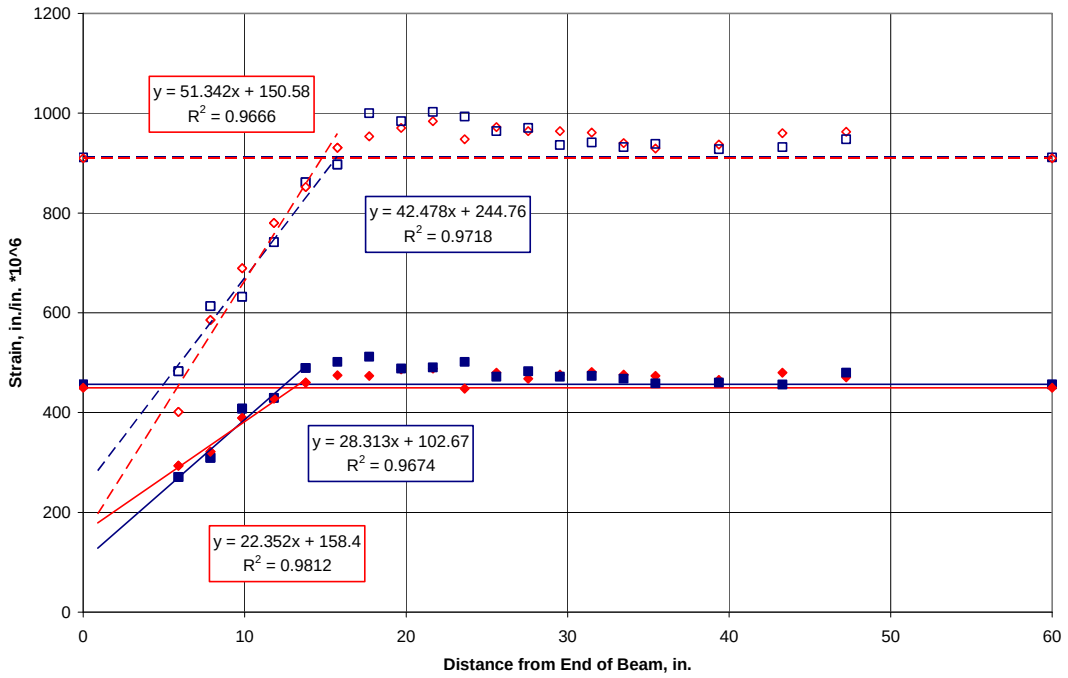

Figure B.26 – 5.270.5S.RB

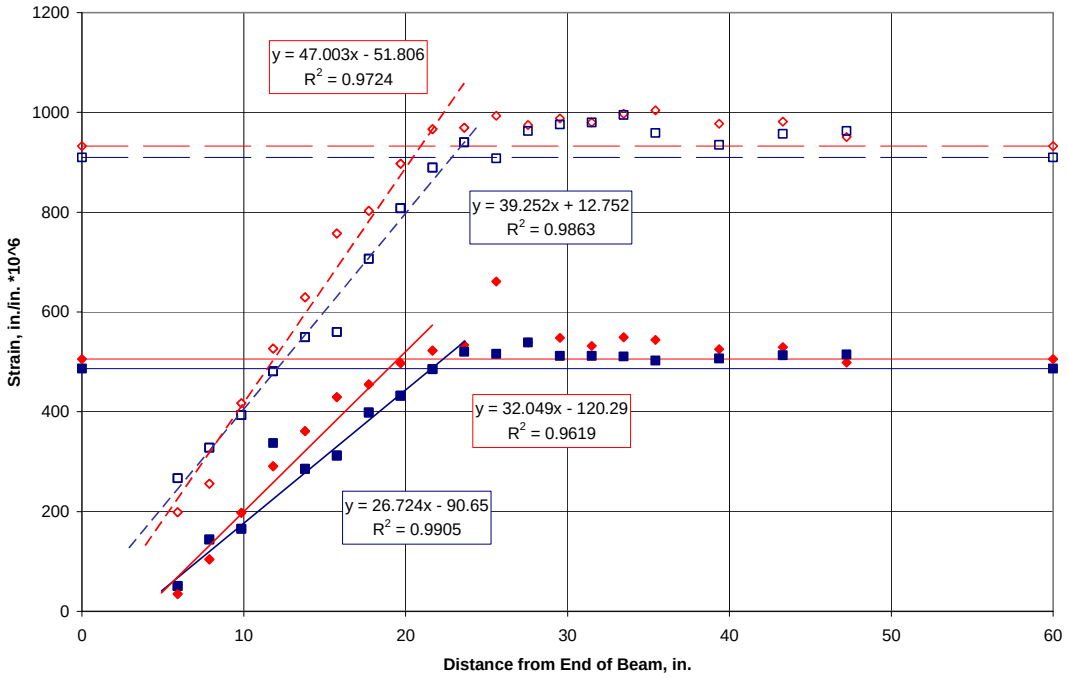

Figure B.27 – 5.300.5S.RA

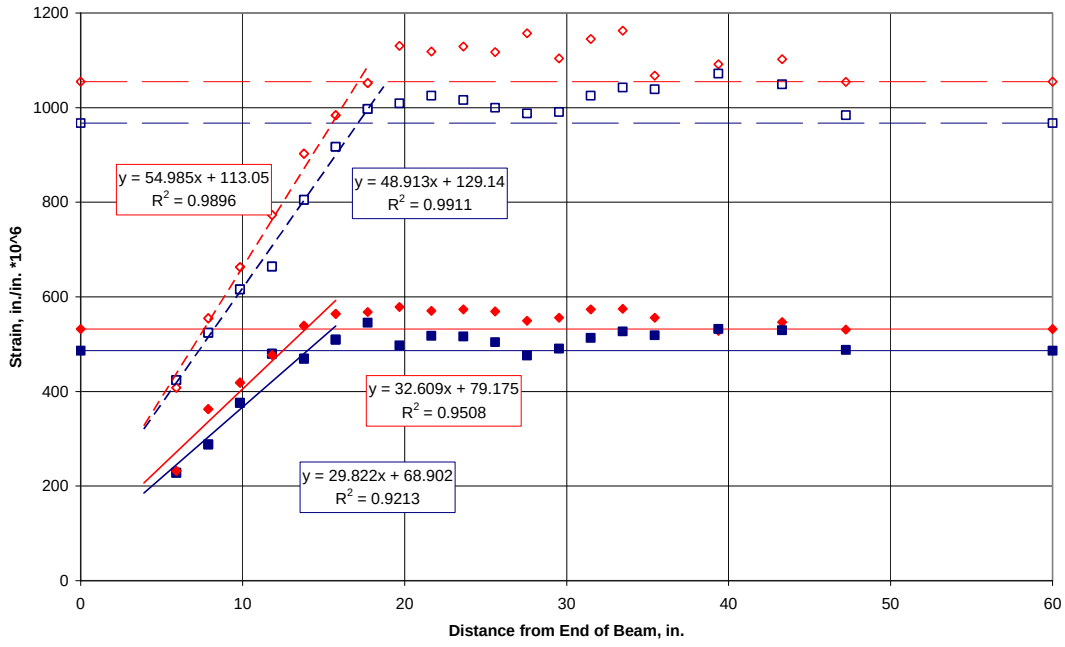

Figure B.28 – 5.300.5S.RB

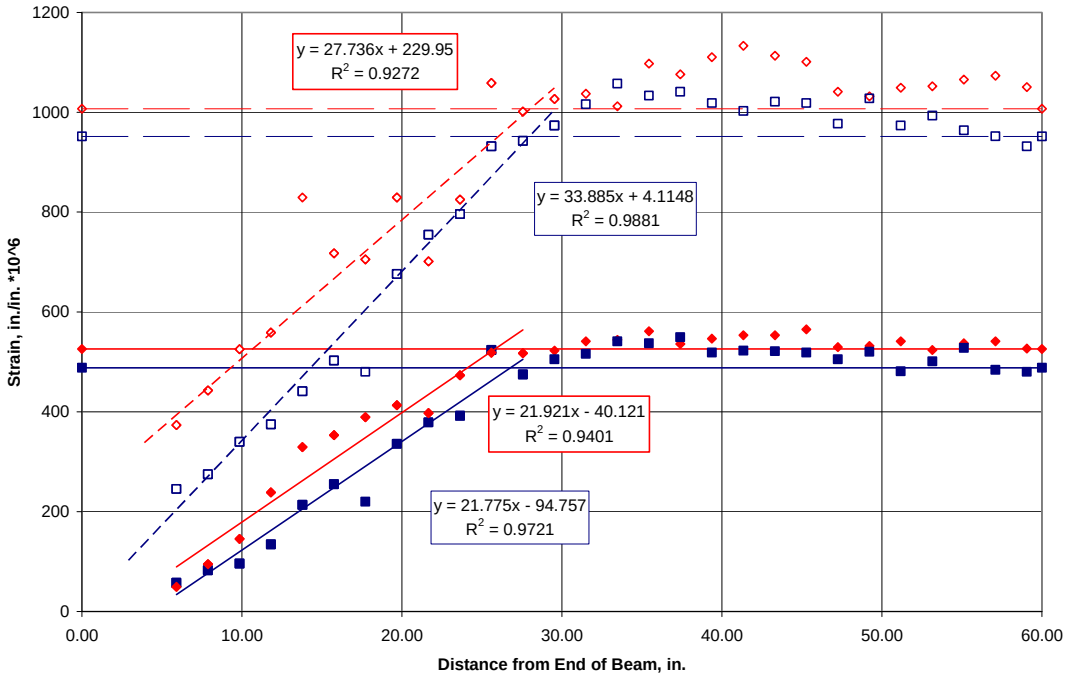

Figure B.29 – 5.270.5S.UA

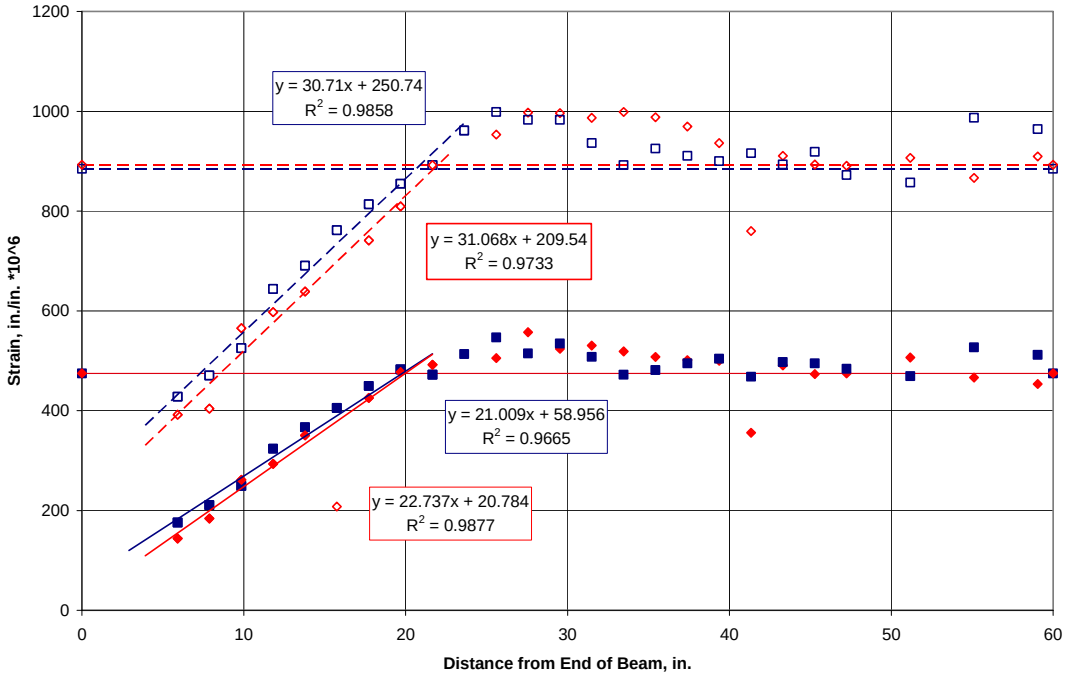

Figure B.30 – 5.270.5S.UB

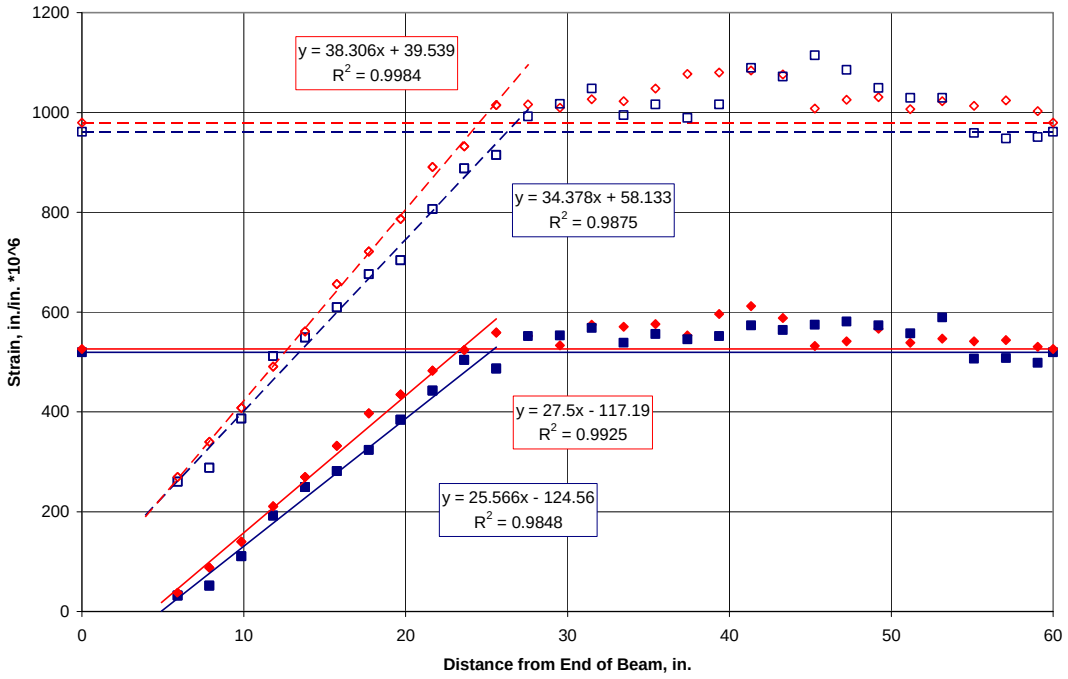

Figure B.31 – 5.300.5S.UA

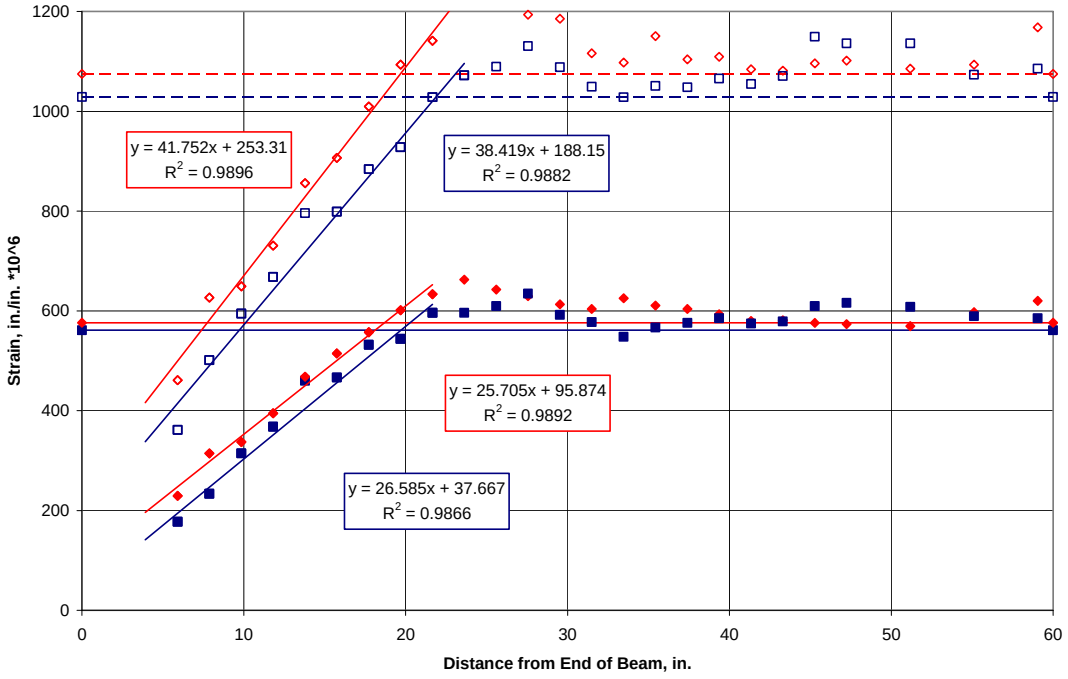

Figure B.32 – 5.300.5S.UB

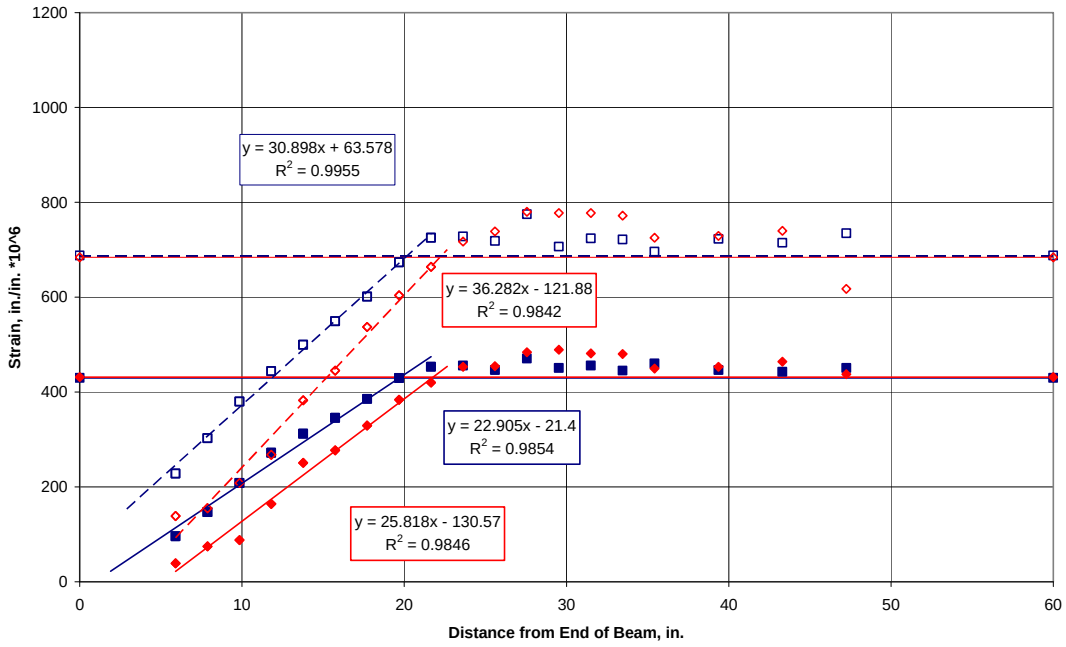

Figure B.33 – 6.270.5S.RA

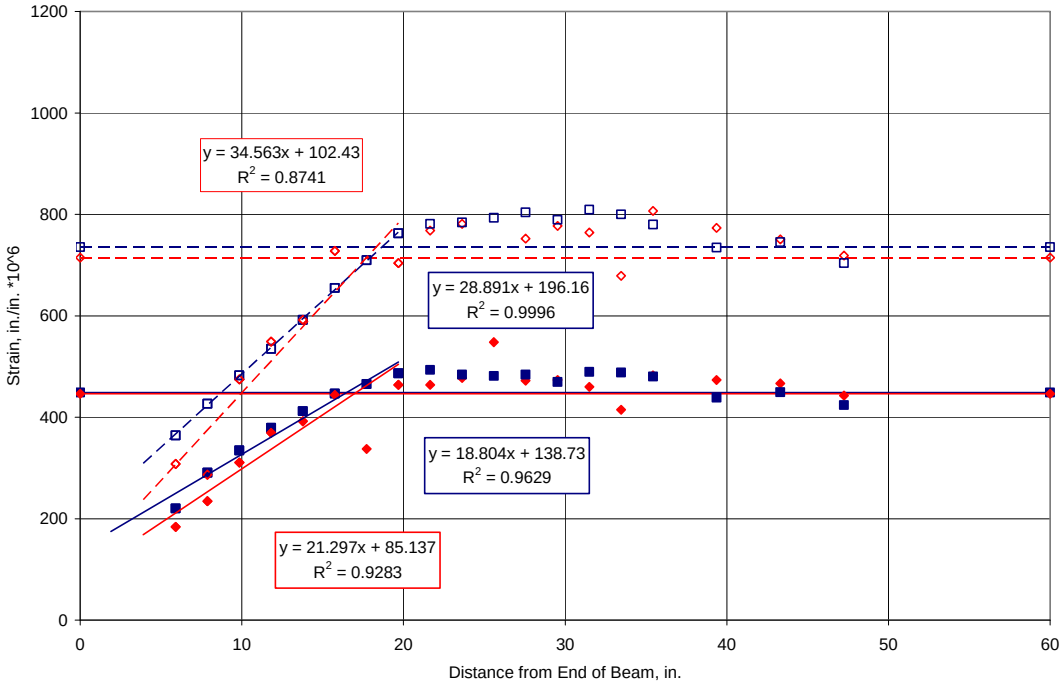

Figure B.34 – 6.270.5S.RB

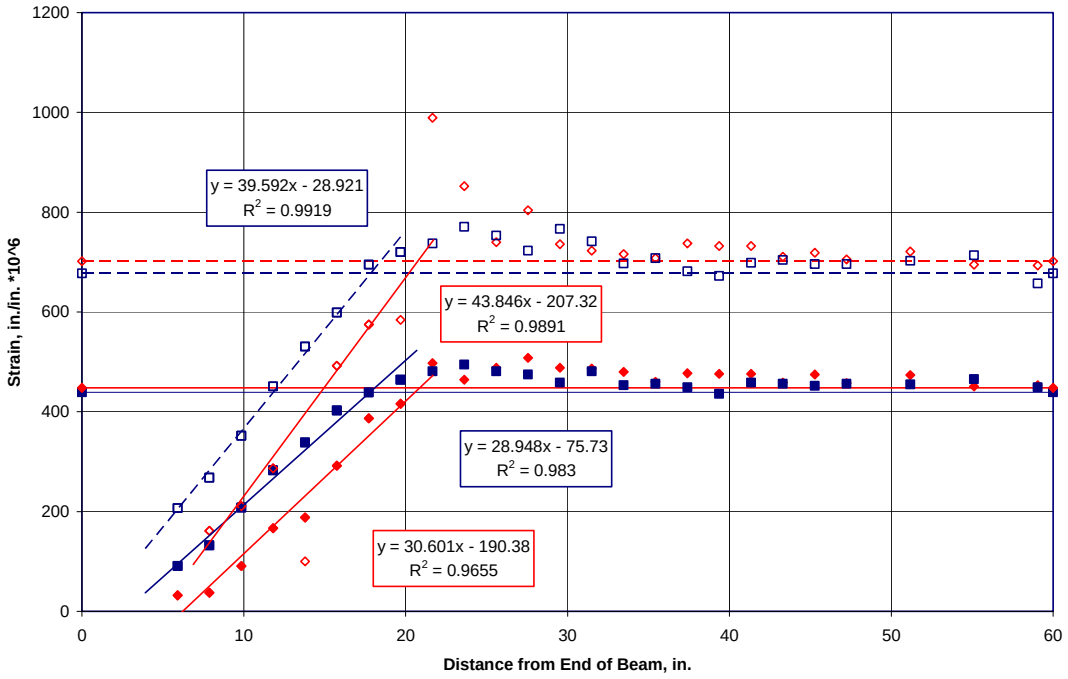

Figure B.35 – 6.270.6N.RA

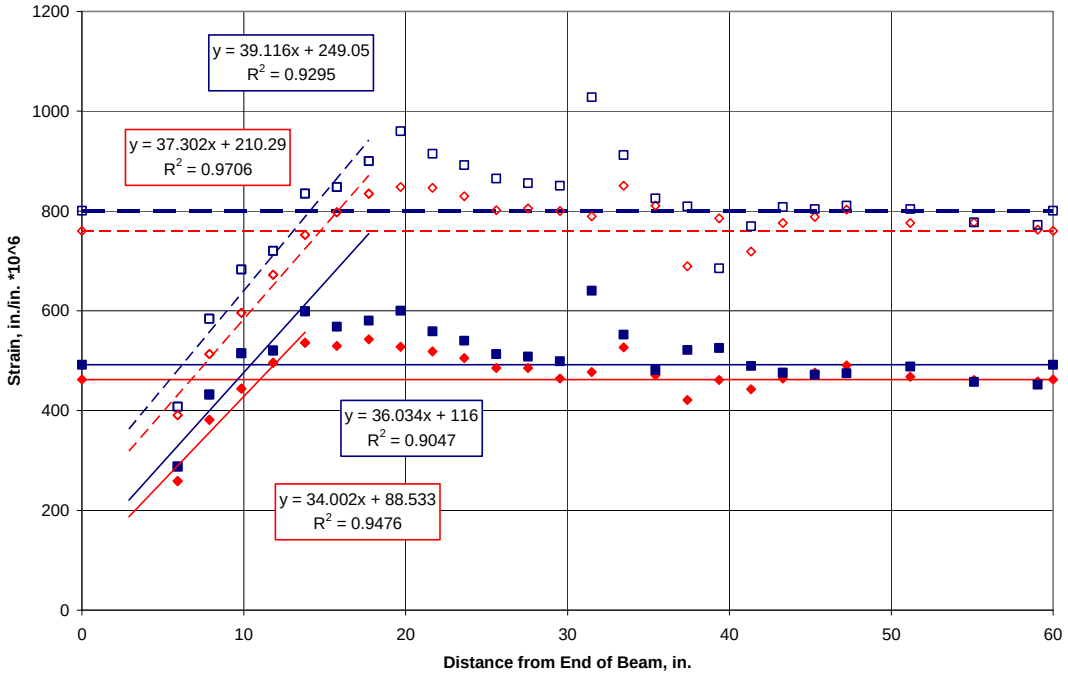

Figure B.36 – 6.270.6N.RA

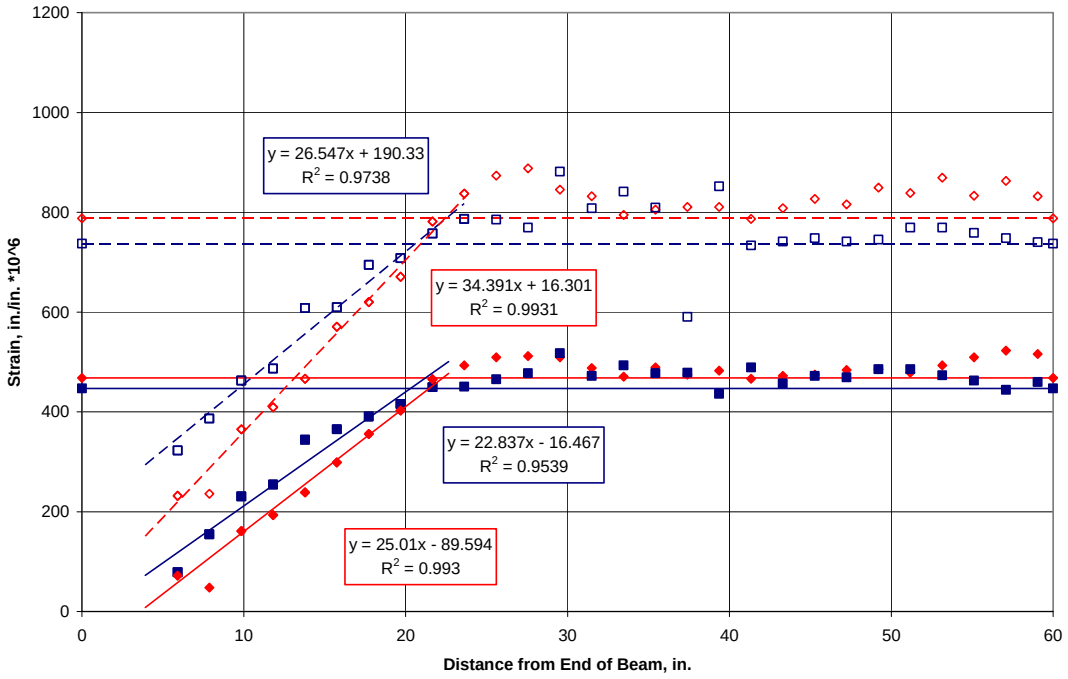

Figure B.37 – 6.270.5S.UA

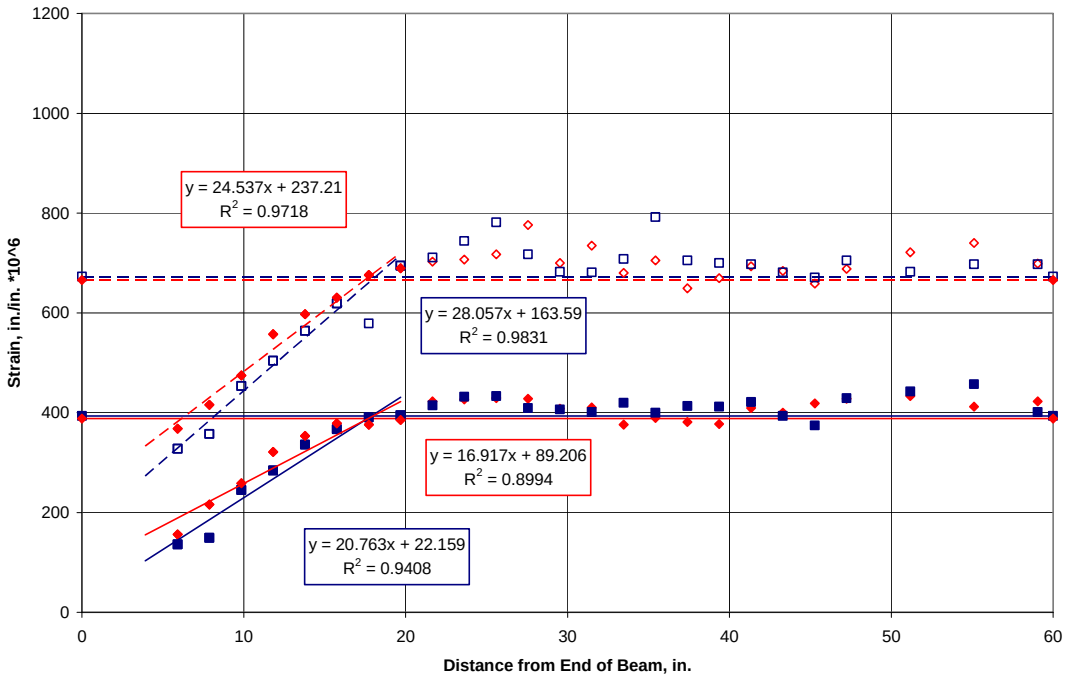

Figure B.38 – 6.270.5S.UB

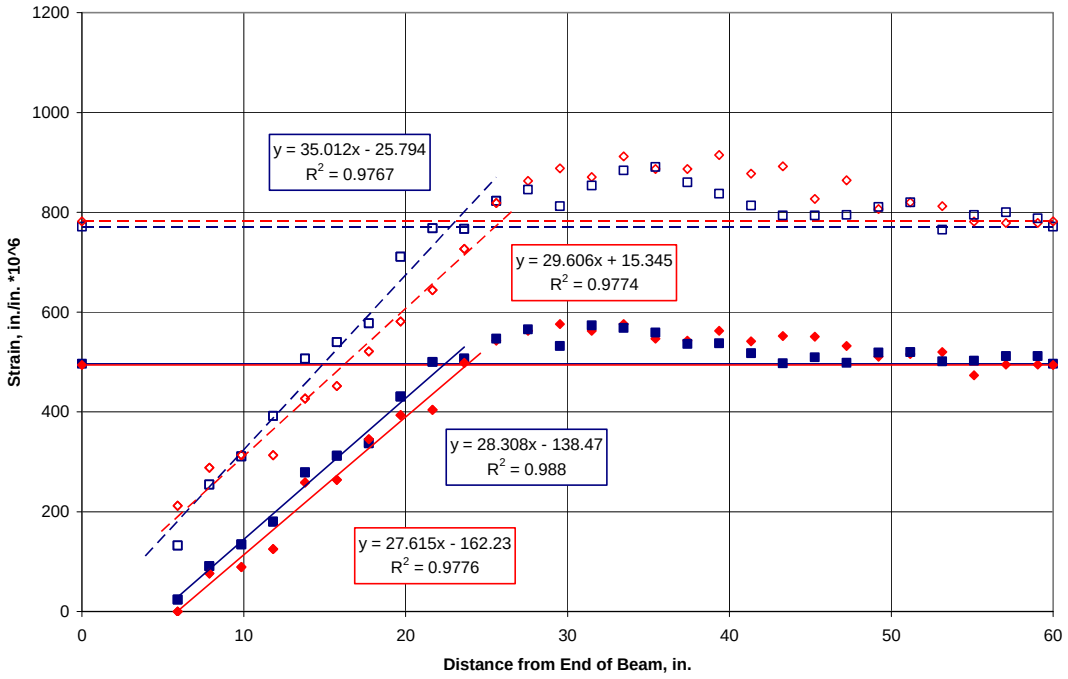

Figure B.39 – 6.270.6N.UA

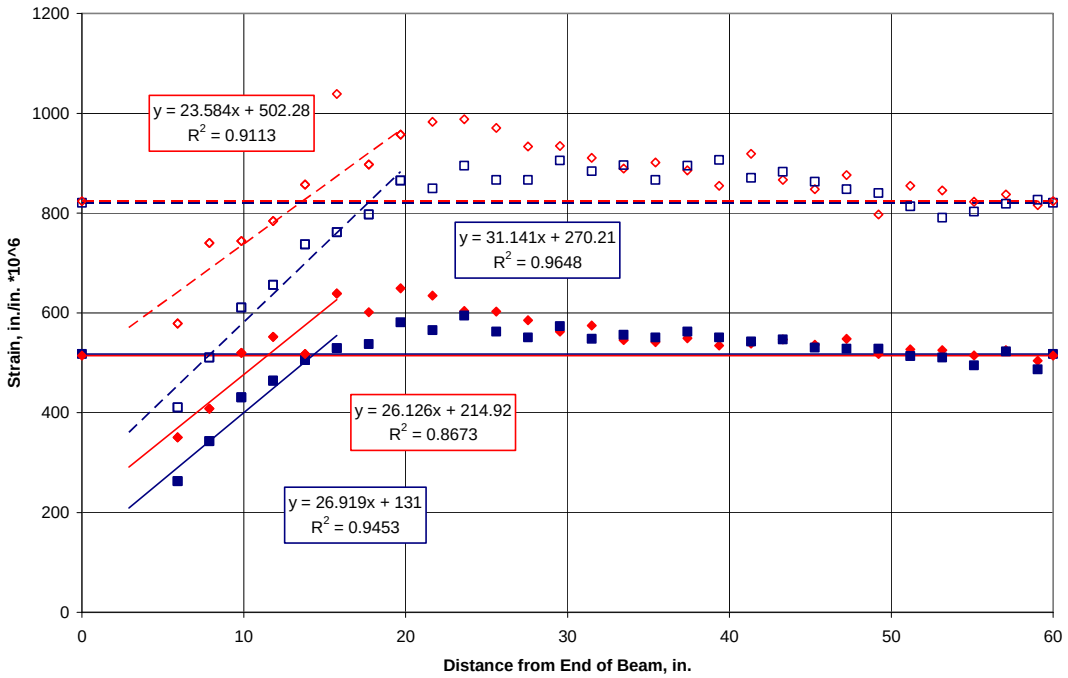

Figure B.40 – 6.270.6N.UB

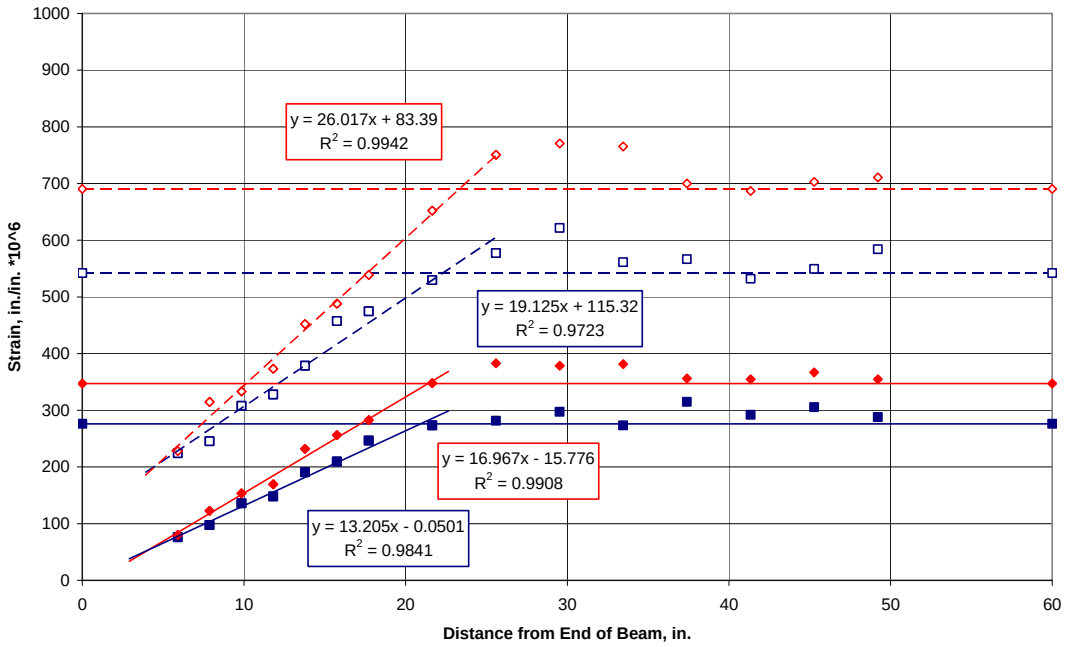

Figure B.41. Pour 1 Strand A Live End Surface Strains

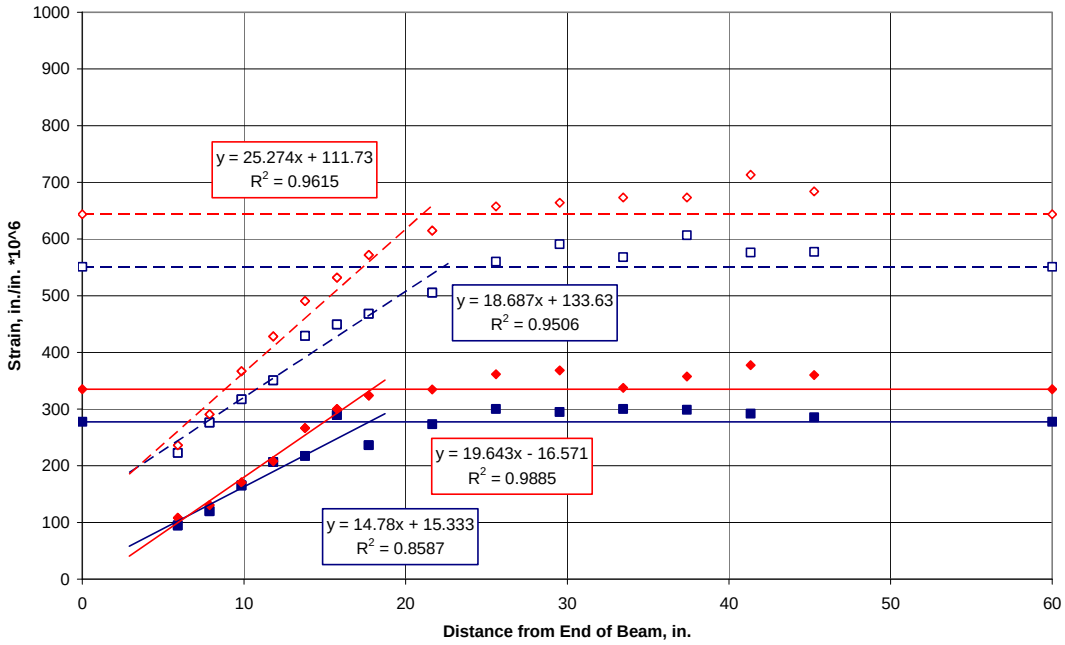

Figure B.42. Pour 1 Strand A Dead End Surface Strains

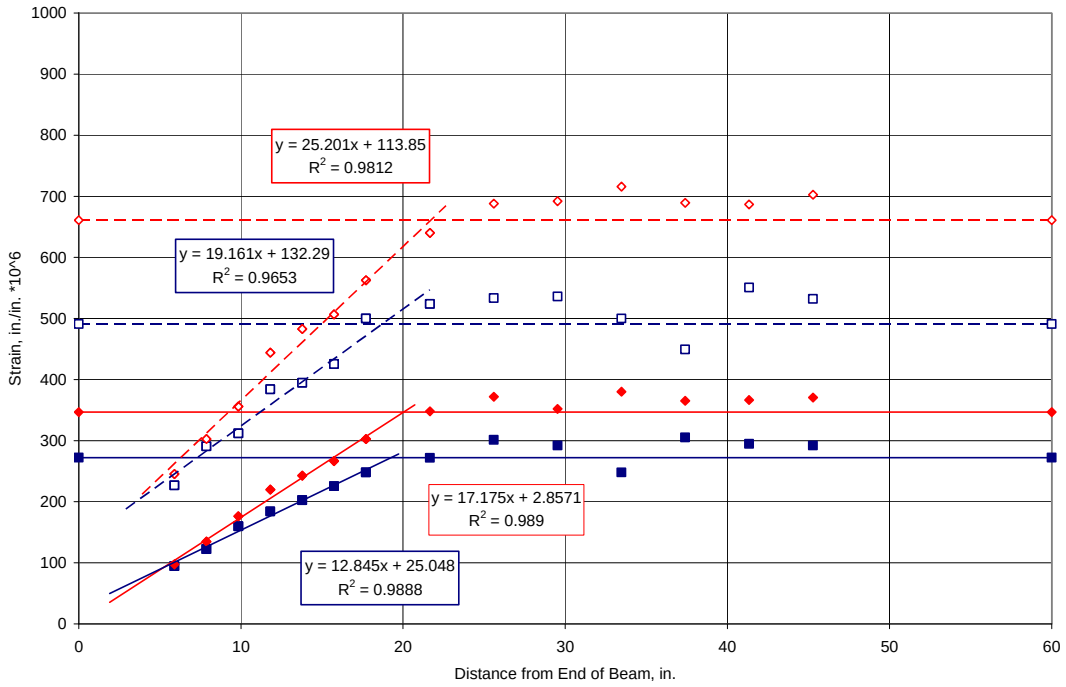

Figure B.43. Pour 1 Strand B Live End Surface Strains

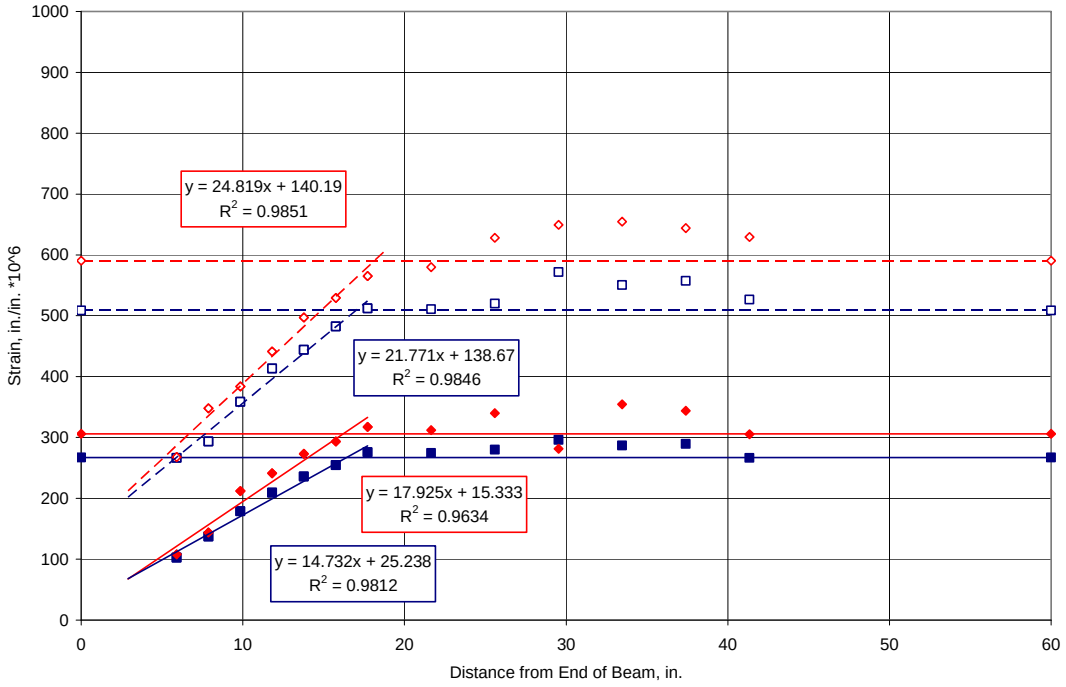

Figure B.44. Pour 1 Strand B Dead End Surface Strains

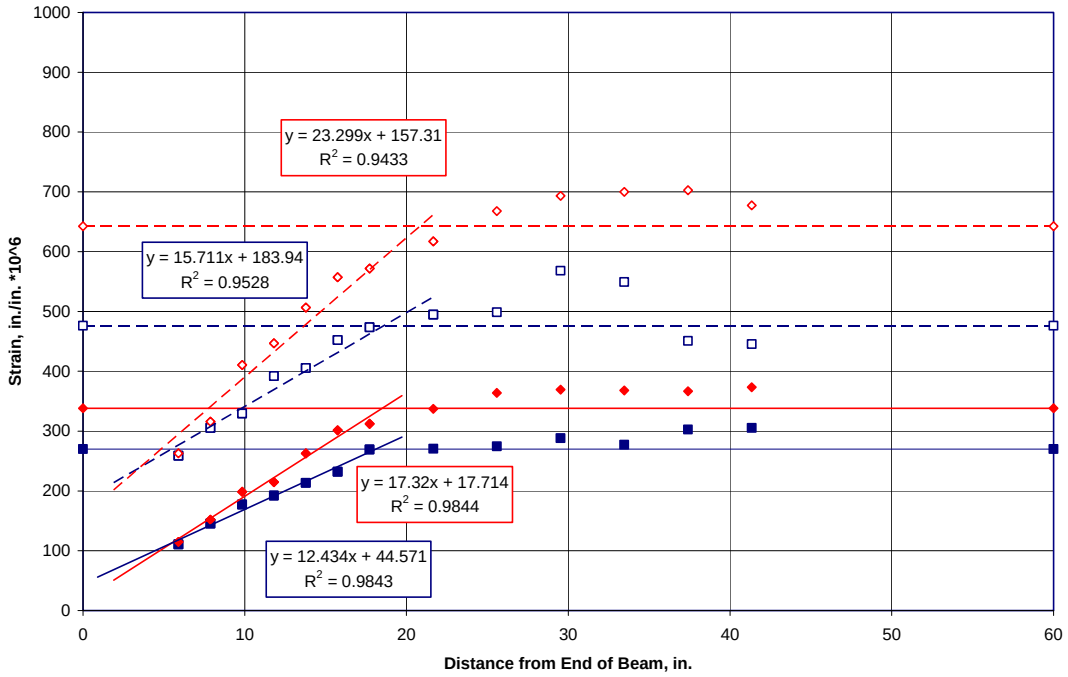

Figure B.45. Pour 1 Strand C Live End Surface Strains

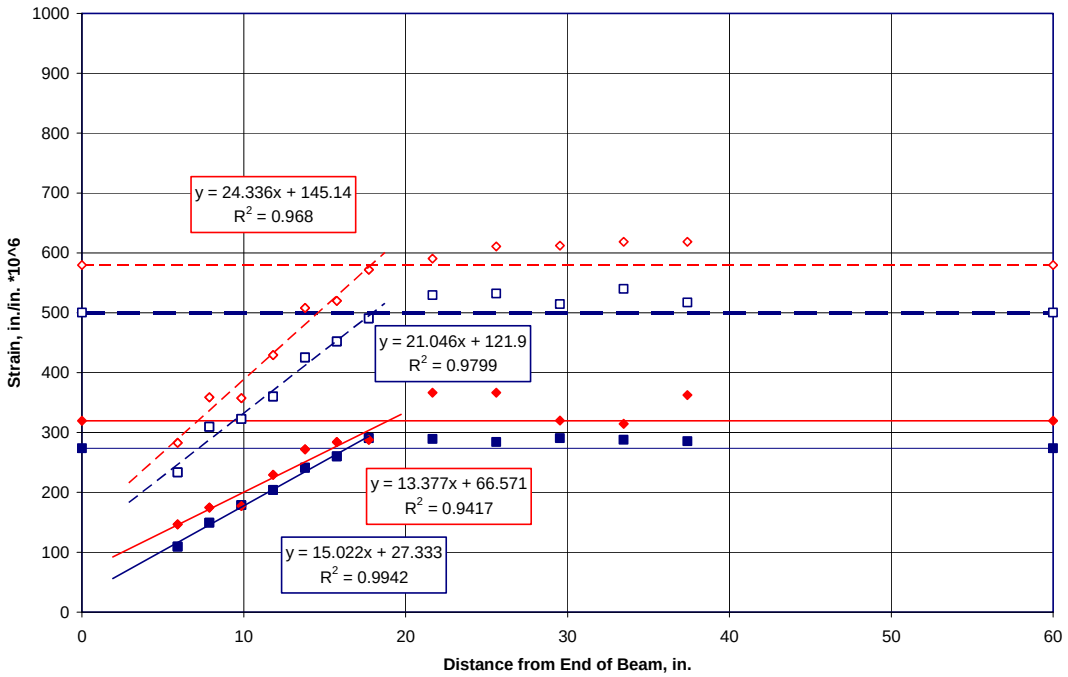

Figure B.46. Pour 1 Strand C Dead End Surface Strains

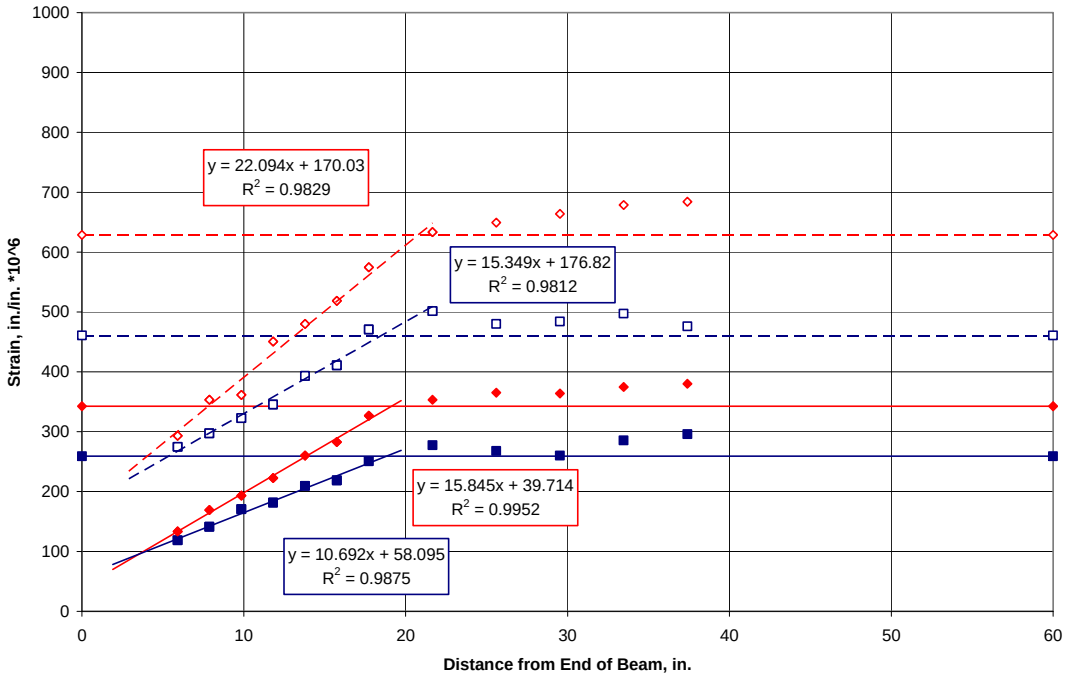

Figure B.47. Pour 1 Strand D Live End Surface Strains

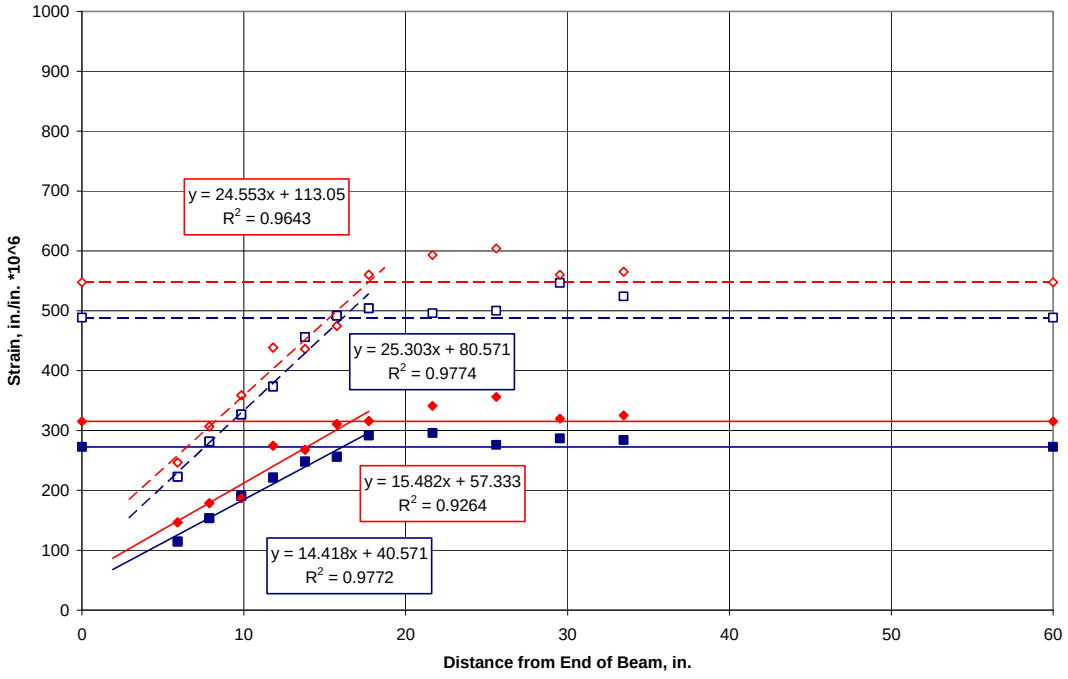

Figure B.48. Pour 1 Strand D Dead End Surface Strains

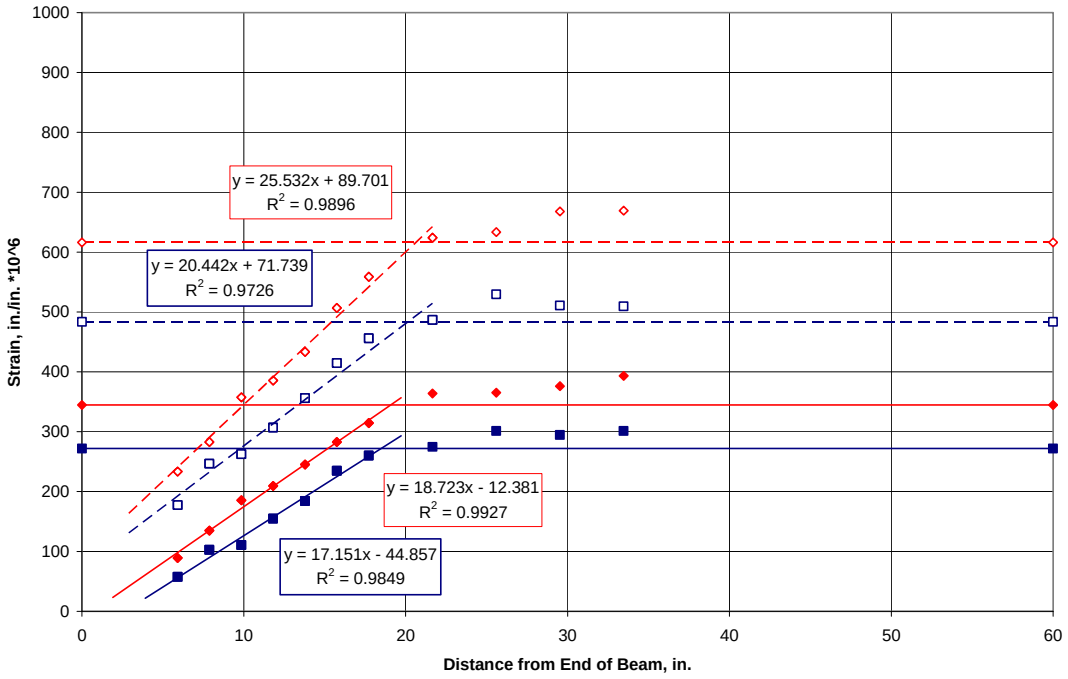

Figure B.49. Pour 1 Strand E Live End Surface Strains

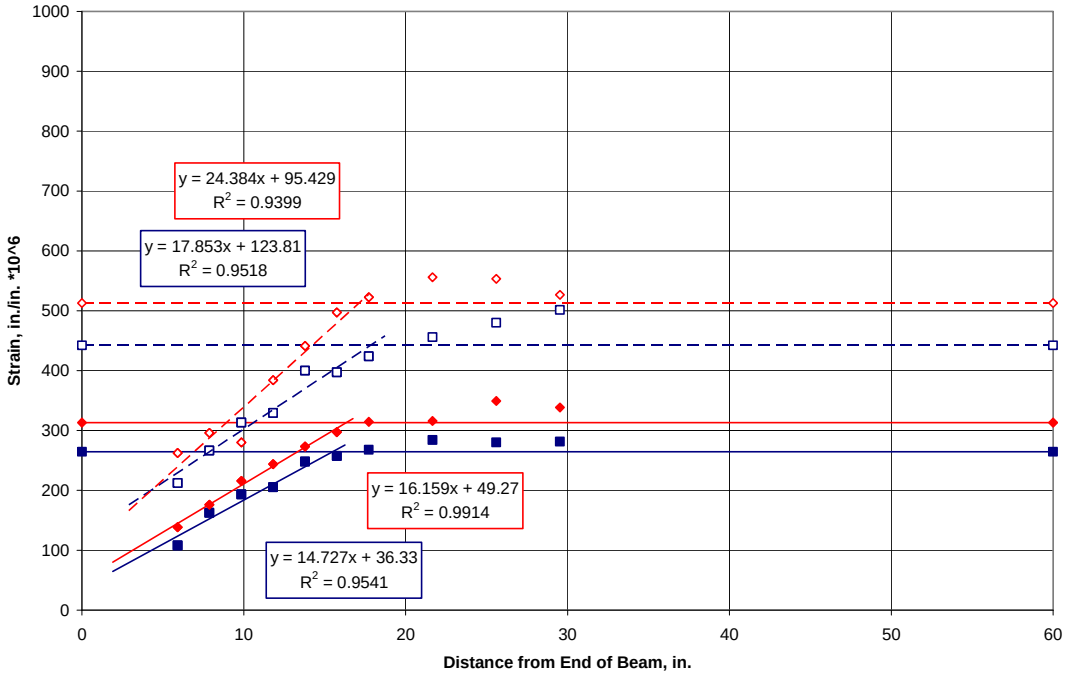

Figure B.50. Pour 1 Strand E Dead End Surface Strains

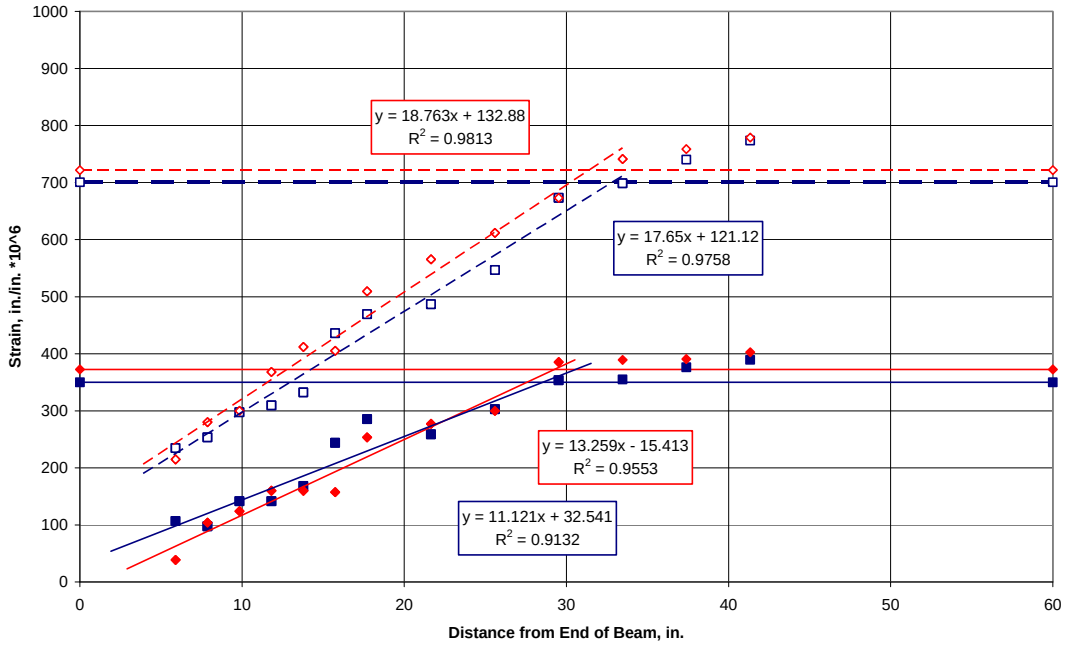

Figure B.51. Pour 1 Strand F Live End Surface Strains

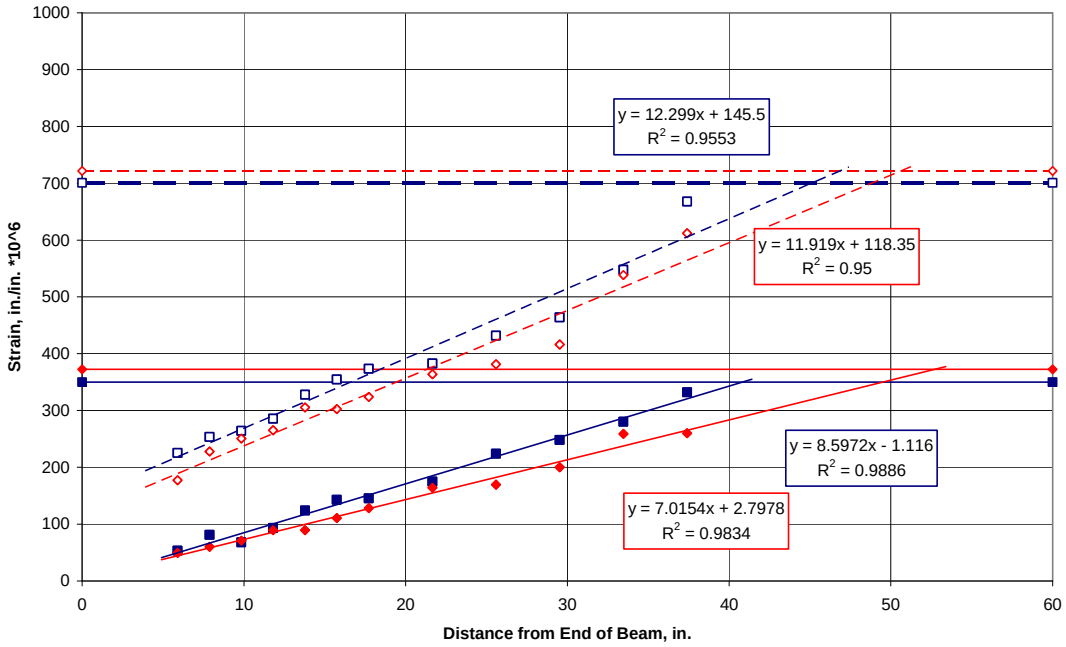

Figure B.52. Pour 1 Strand F Dead End Surface Strains

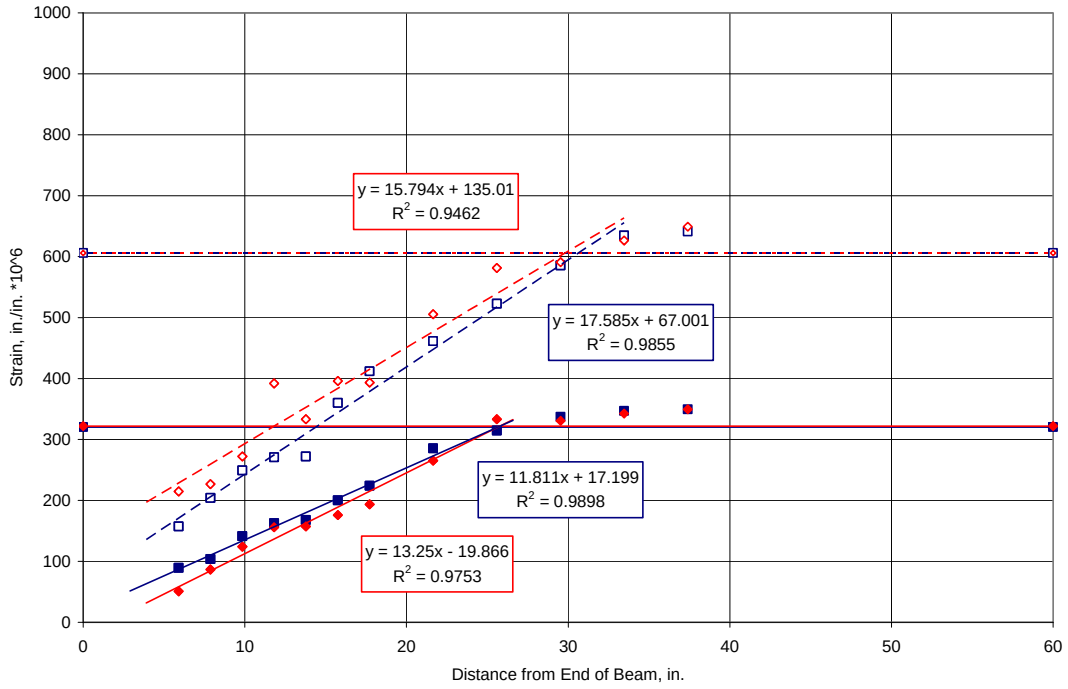

Figure B.53. Pour 1 Strand G Live End Surface Strains

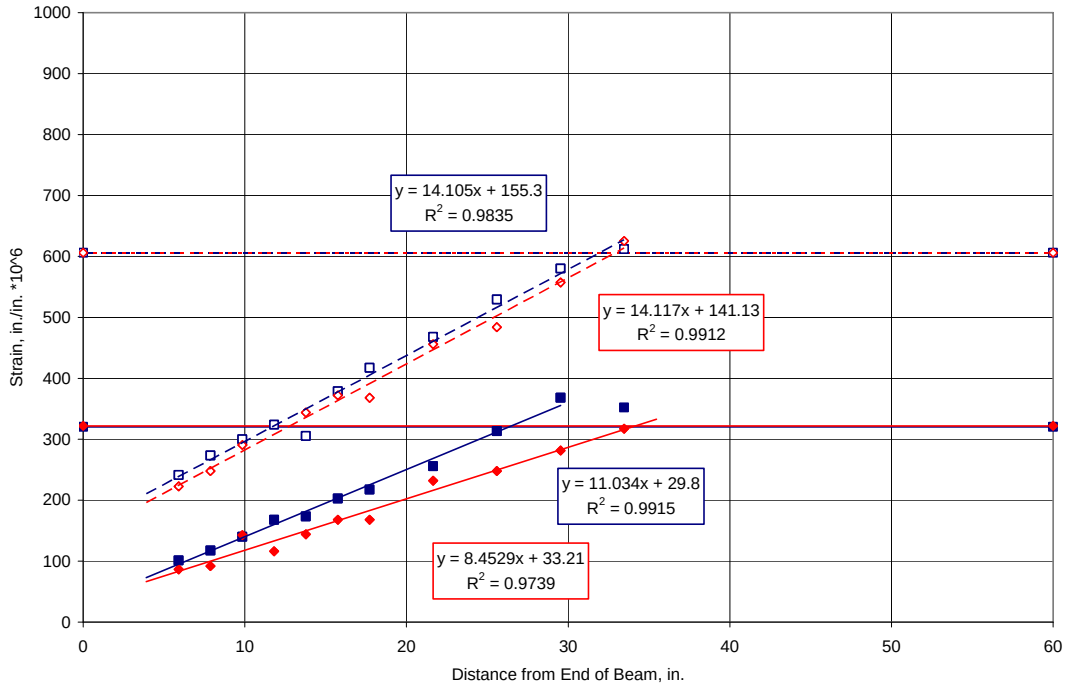

Figure B.54. Pour 1 Strand G Dead End Surface Strains

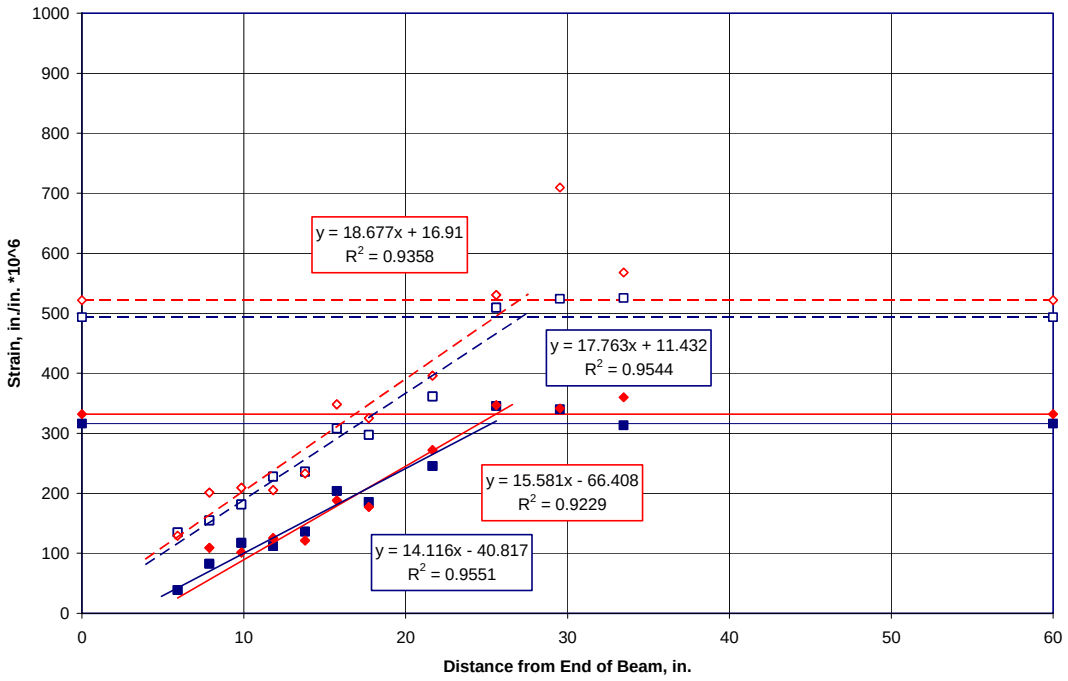

Figure B.55. Pour 1 Strand H Live End Surface Strains

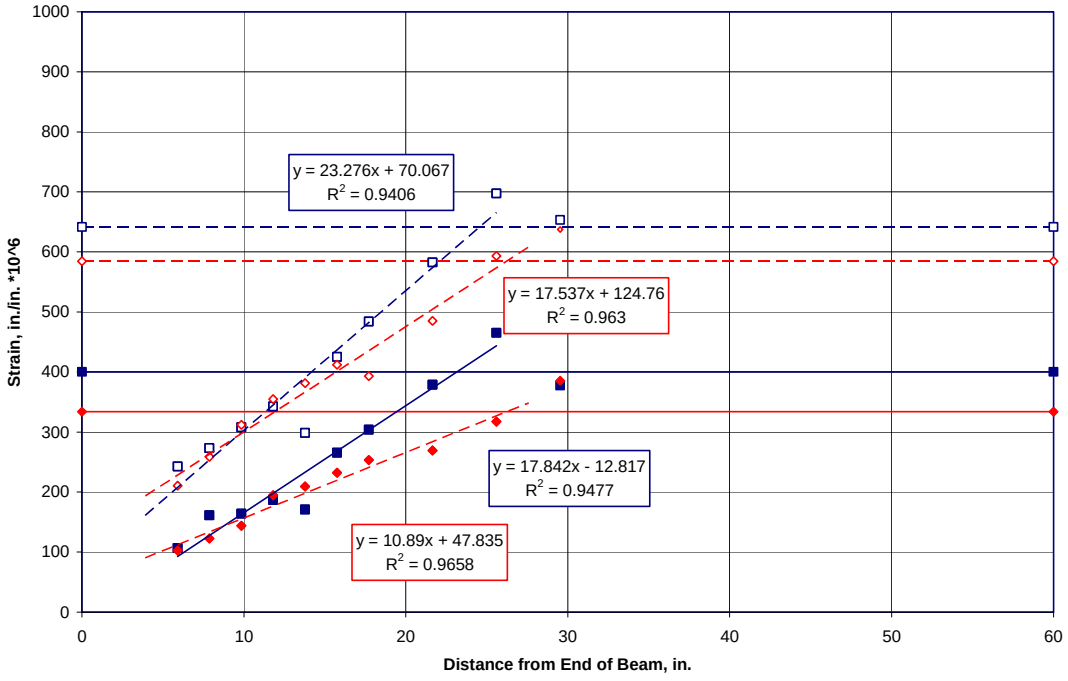

Figure B.56. Pour 1 Strand H Dead End Surface Strains

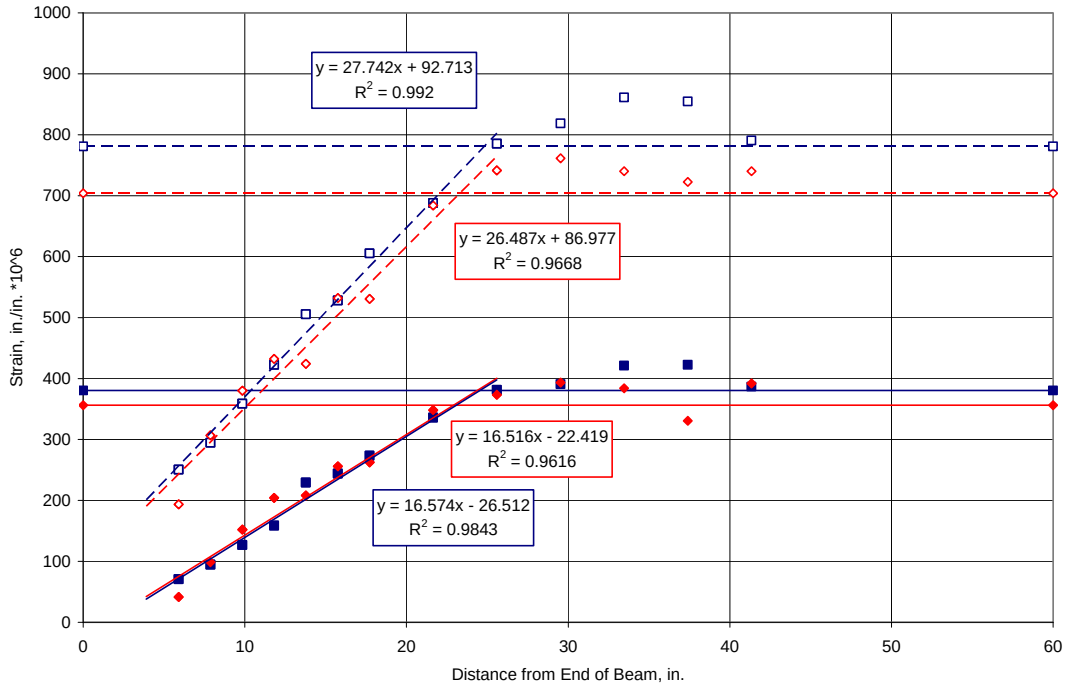

Figure B.57. Pour 1 Strand I Live End Surface Strains

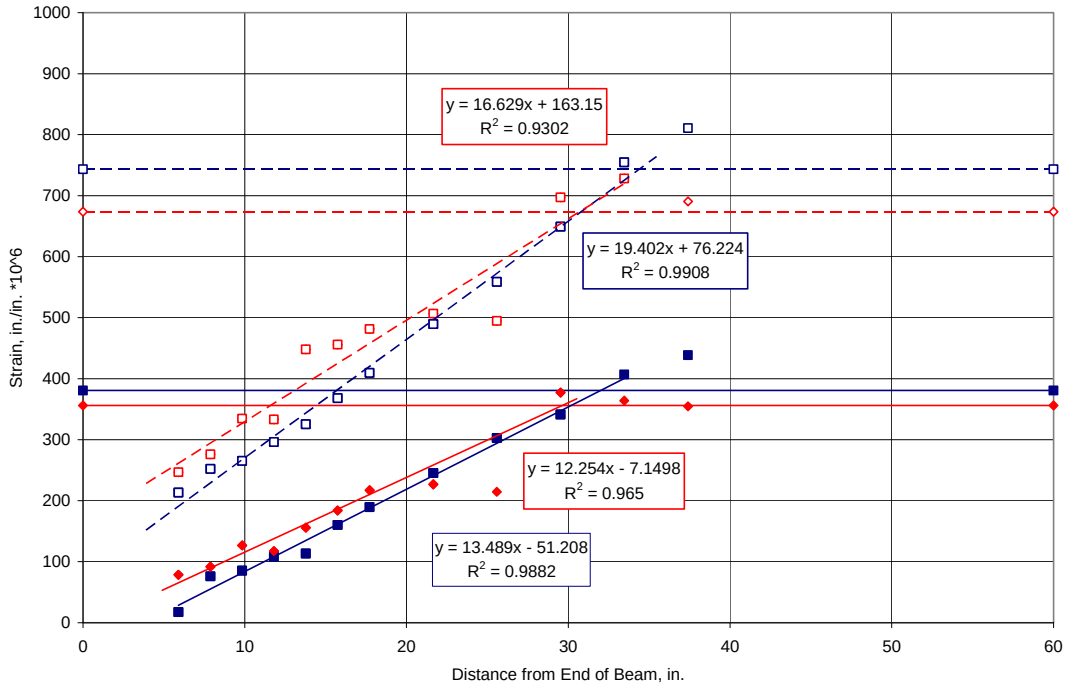

Figure B.58. Pour 1 Strand I Dead End Surface Strains

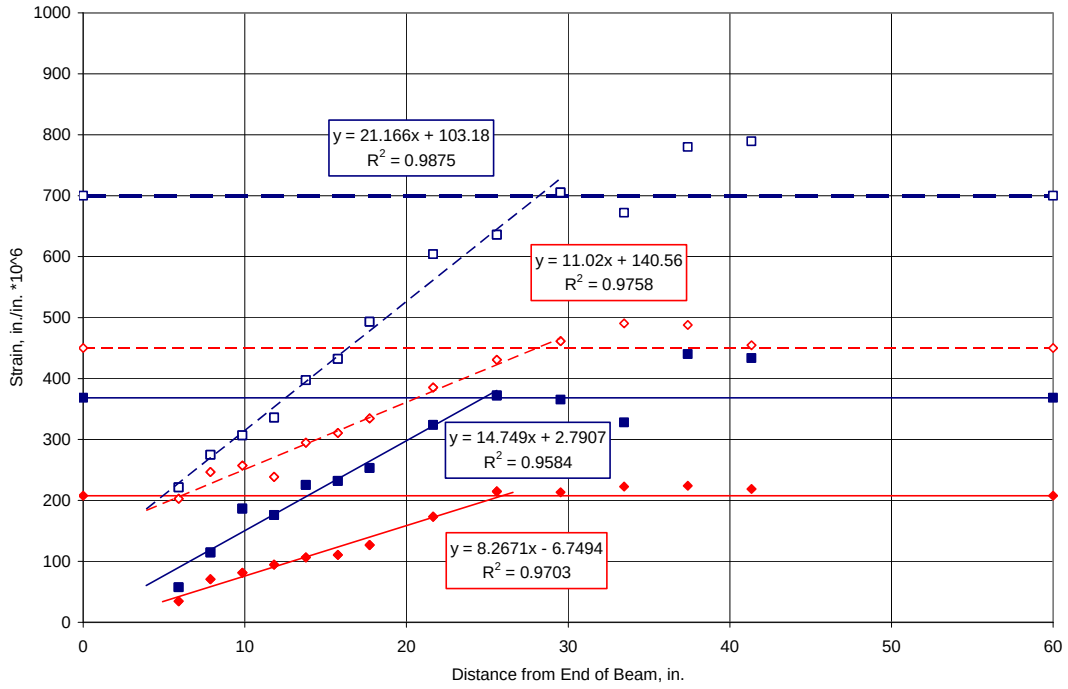

Figure B.59. Pour 1 Strand J Live End Surface Strains

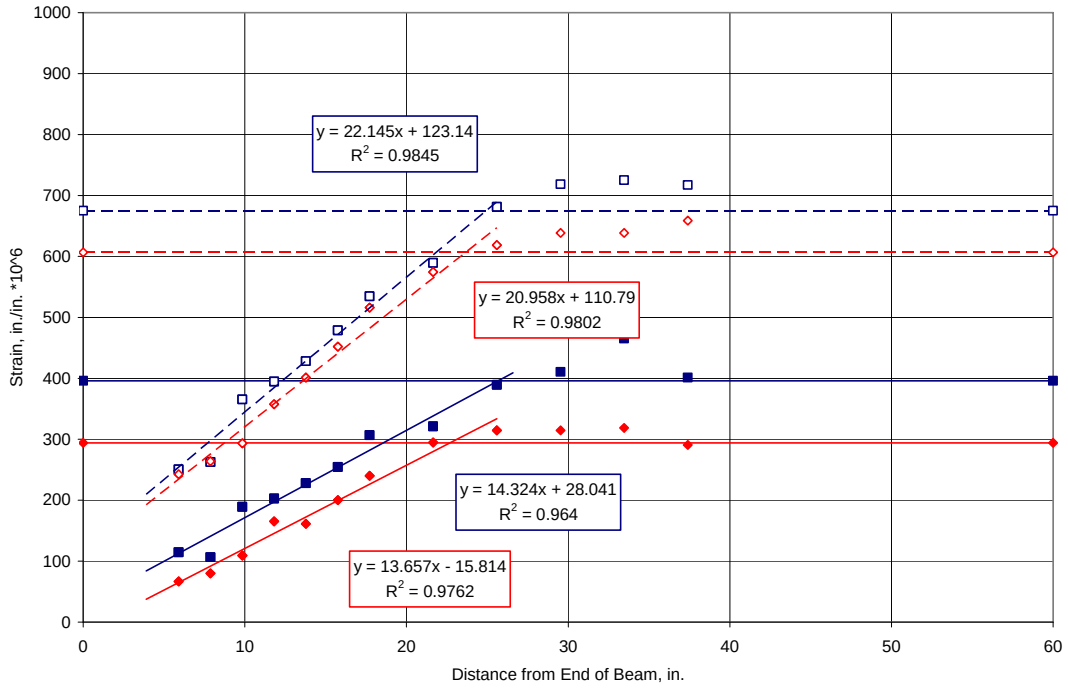

Figure B.60. Pour 1 Strand J Dead End Surface Strains

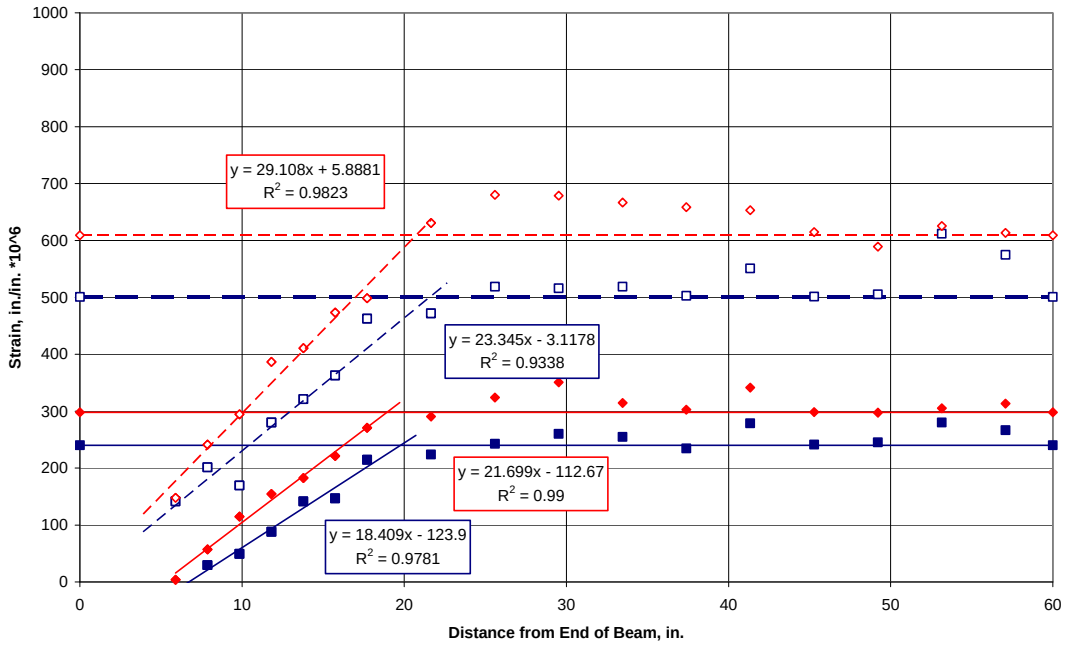

Figure B.61. Pour 2 Strand A Live End Surface Strains

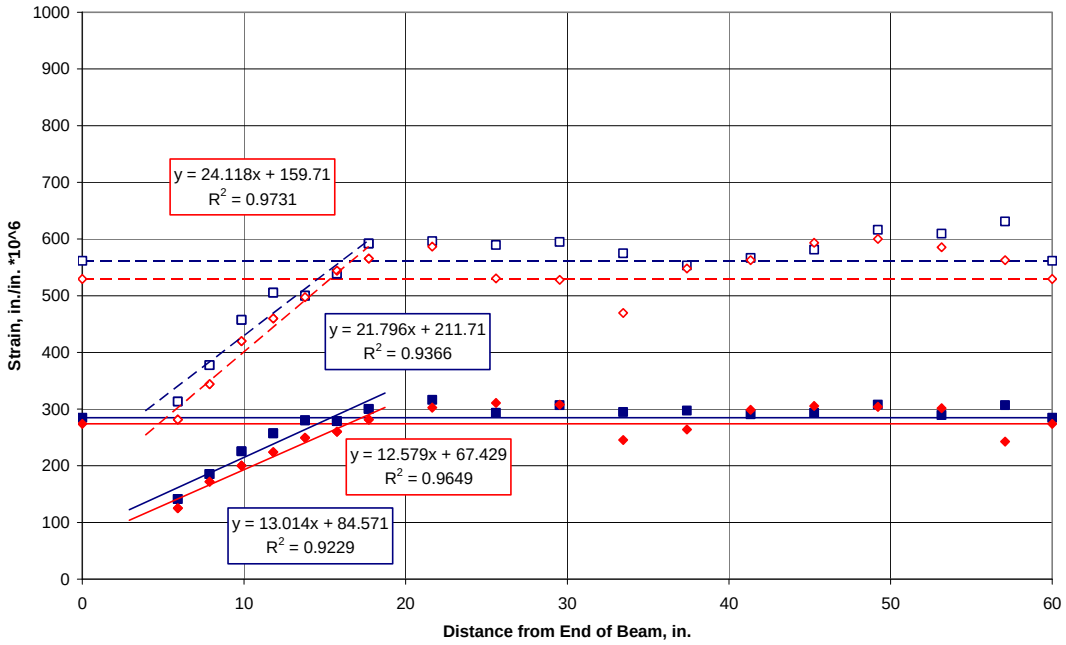

Figure B.62. Pour 2 Strand A Dead End Surface Strains

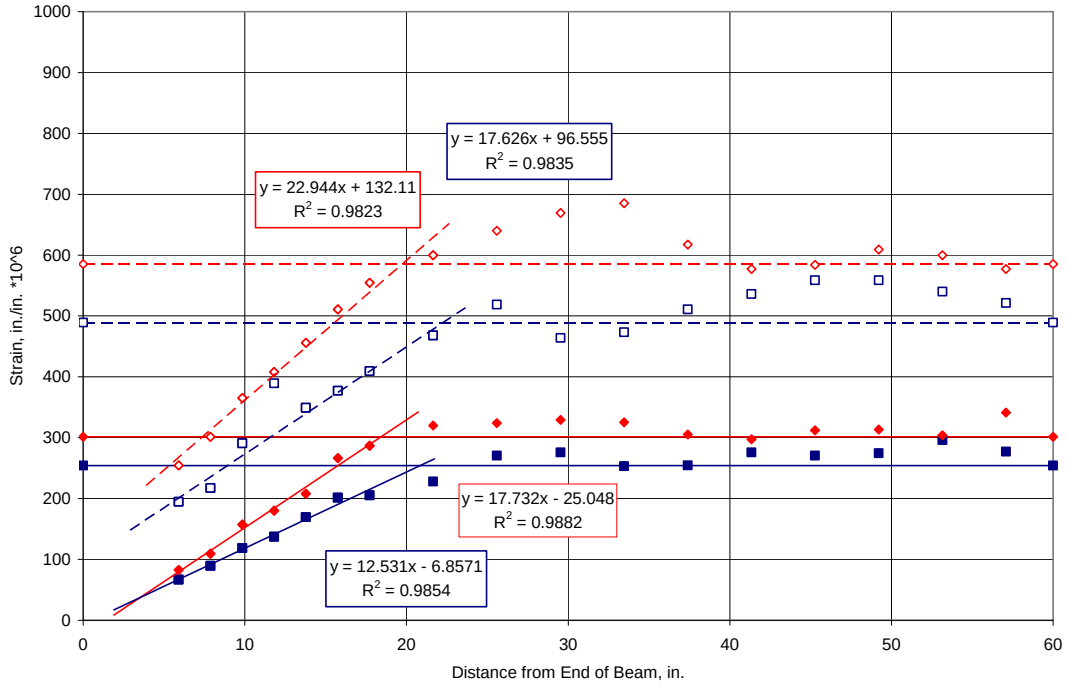

Figure B.63. Pour 2 Strand B Live End Surface Strains

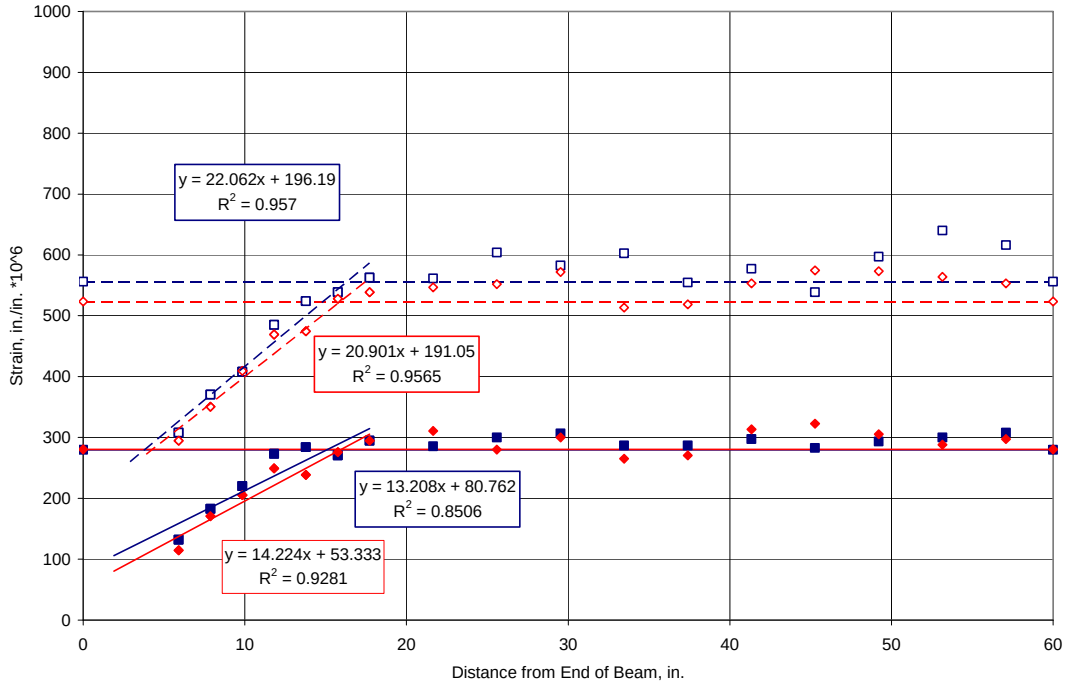

Figure B.64. Pour 2 Strand B Dead End Surface Strains

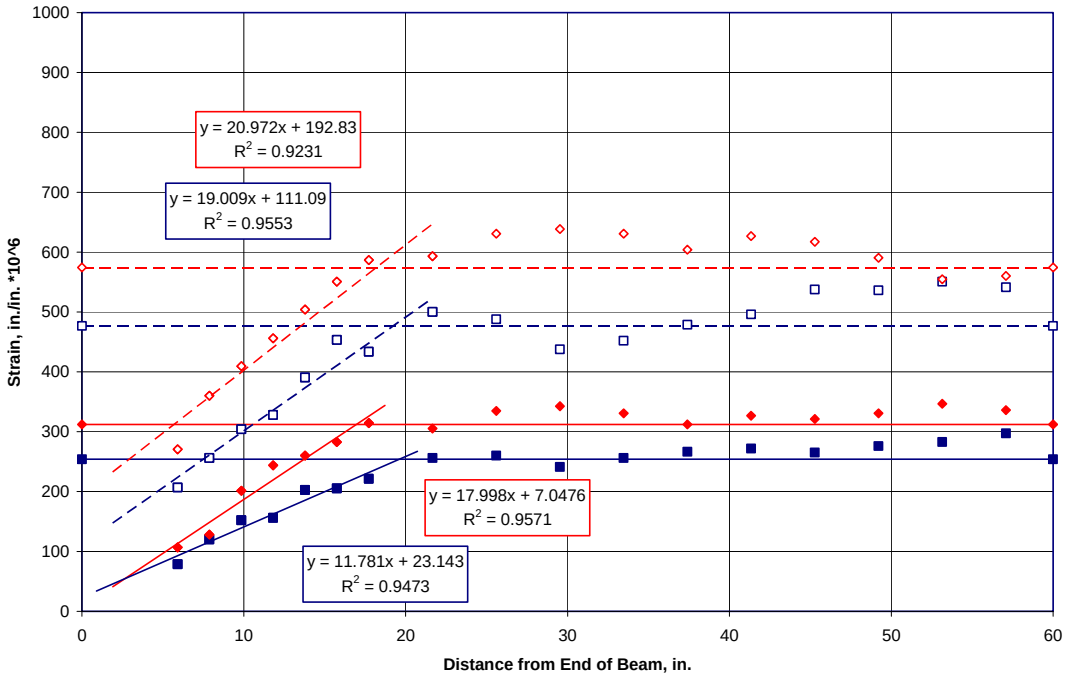

Figure B.65. Pour 2 Strand C Live End Surface Strains

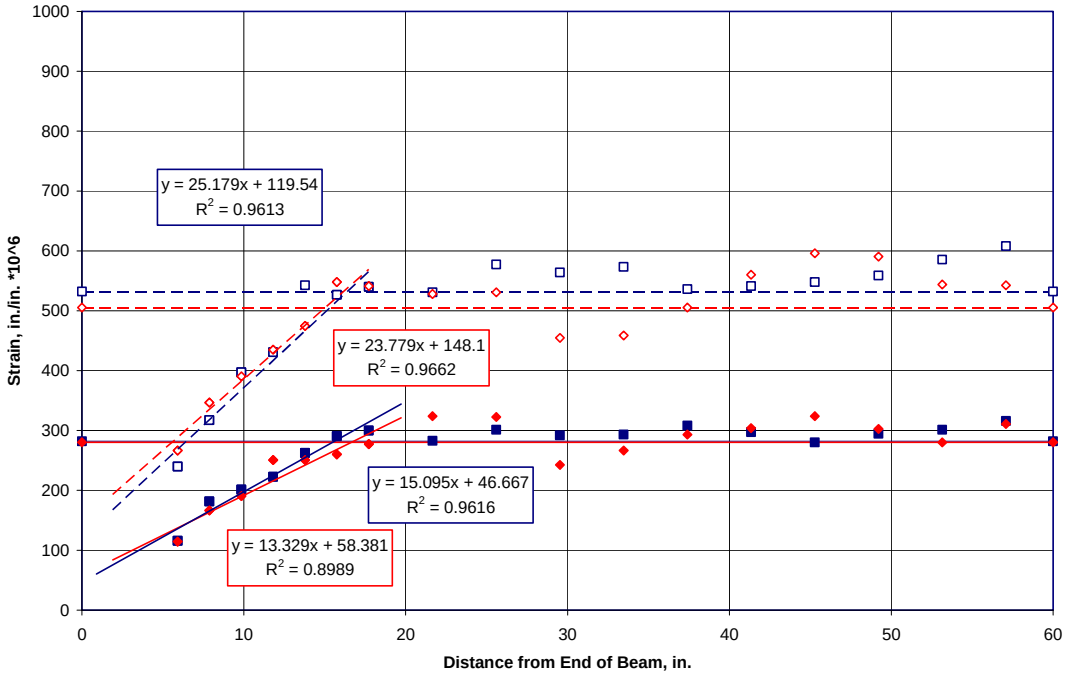

Figure B.66. Pour 2 Strand C Dead End Surface Strains

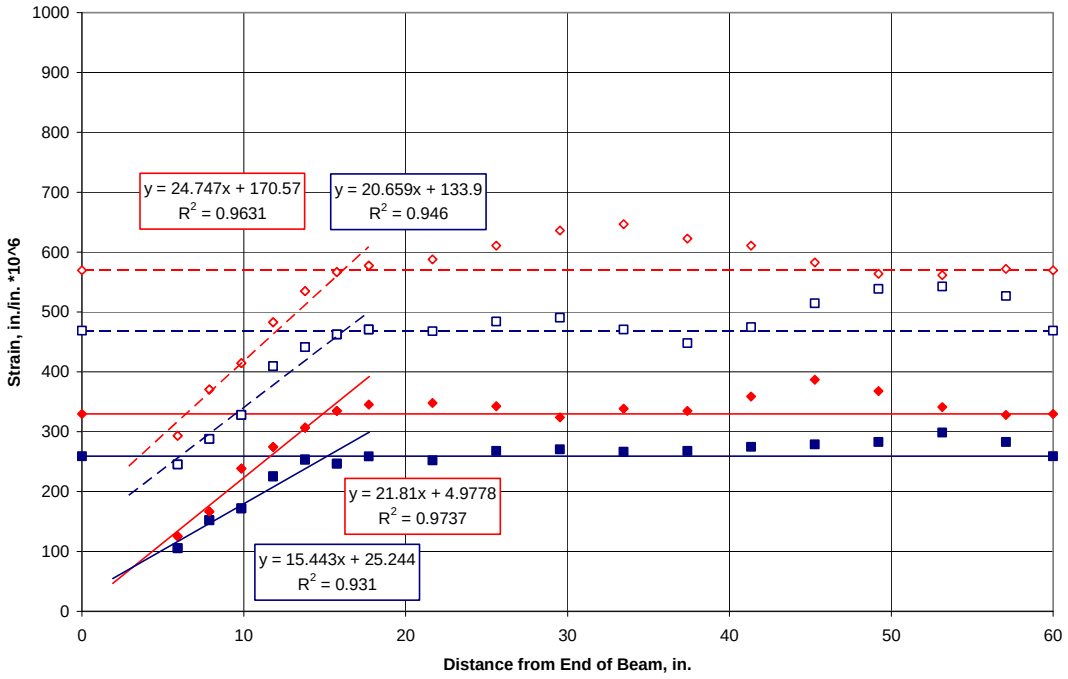

Figure B.67. Pour 2 Strand D Live End Surface Strains

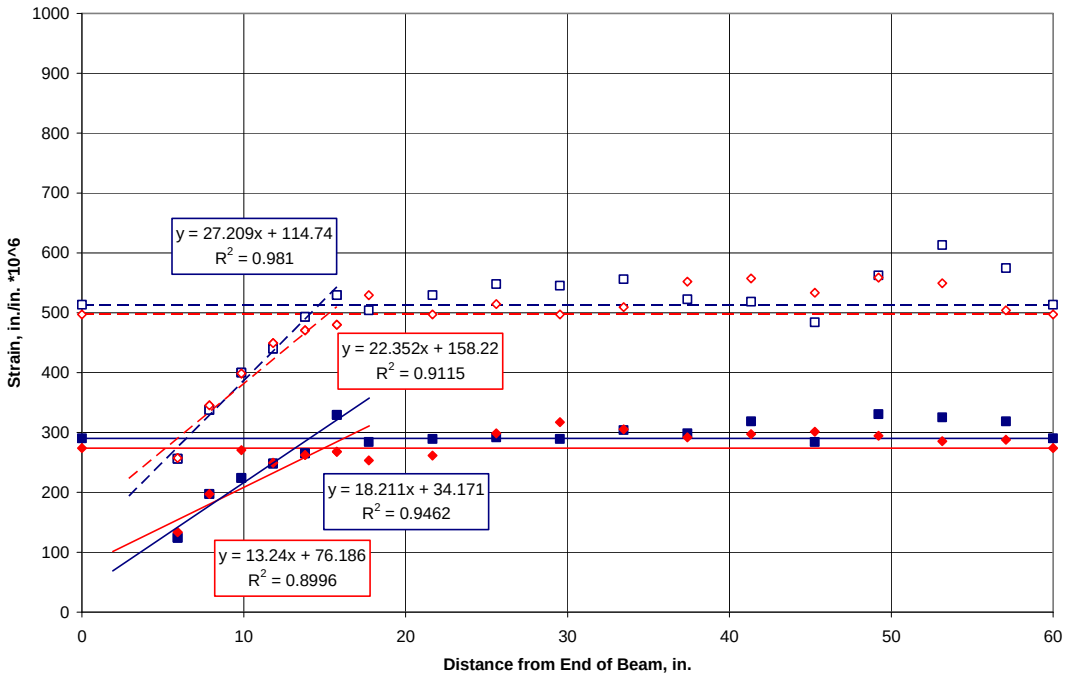

Figure B.68. Pour 2 Strand D Dead End Surface Strains

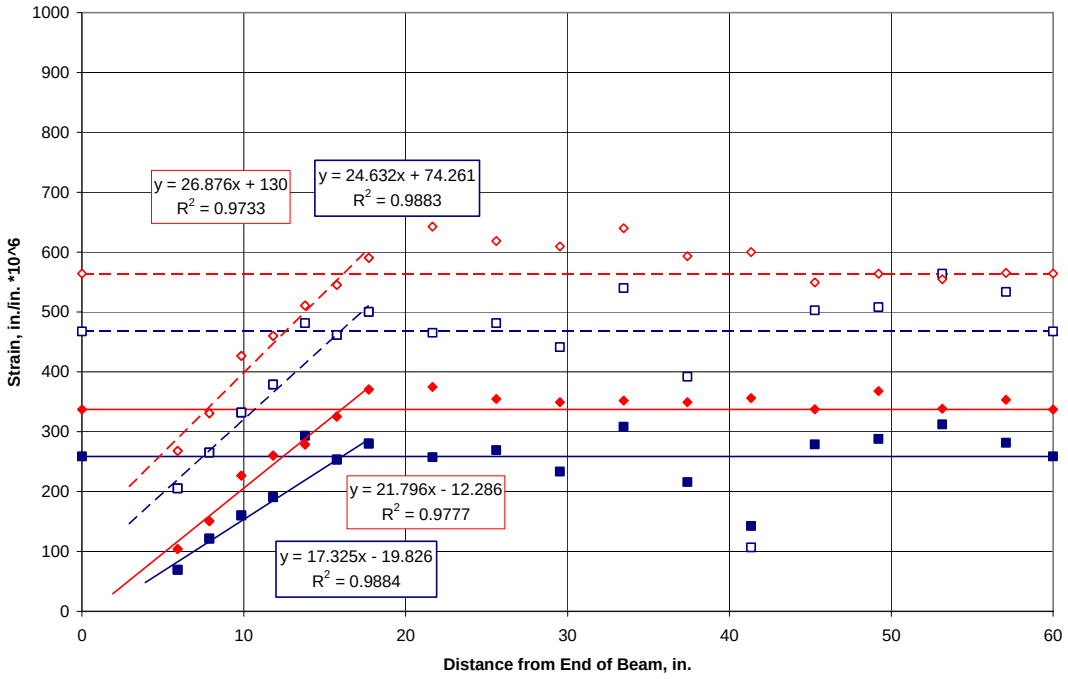

Figure B.69. Pour 2 Strand E Live End Surface Strains

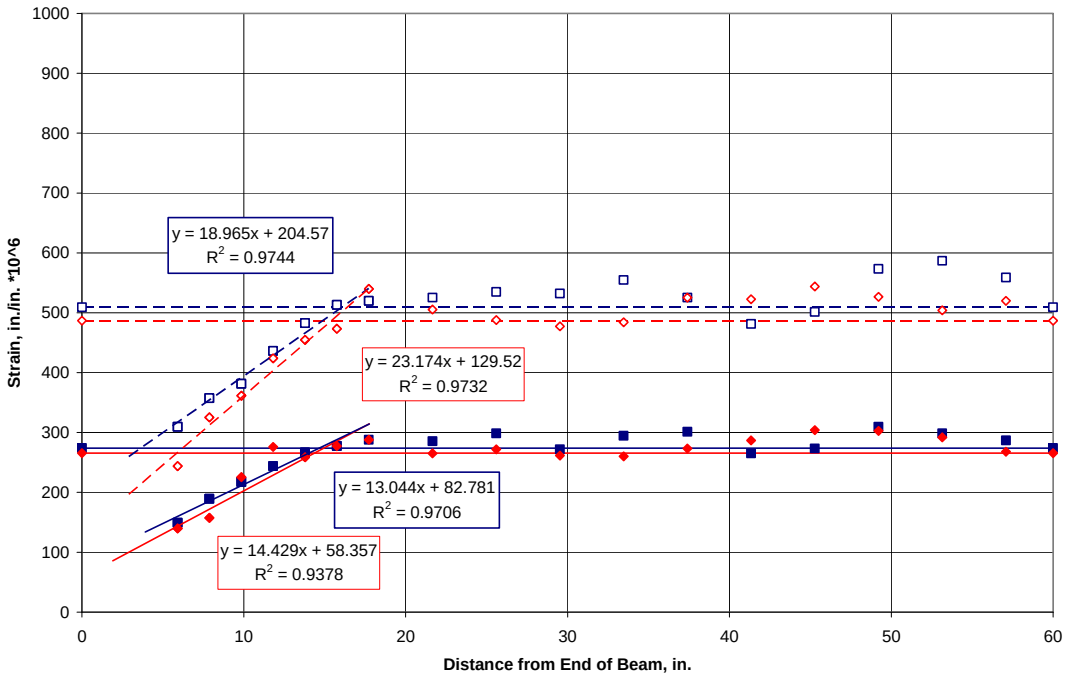

Figure B.70. Pour 2 Strand E Dead End Surface Strains

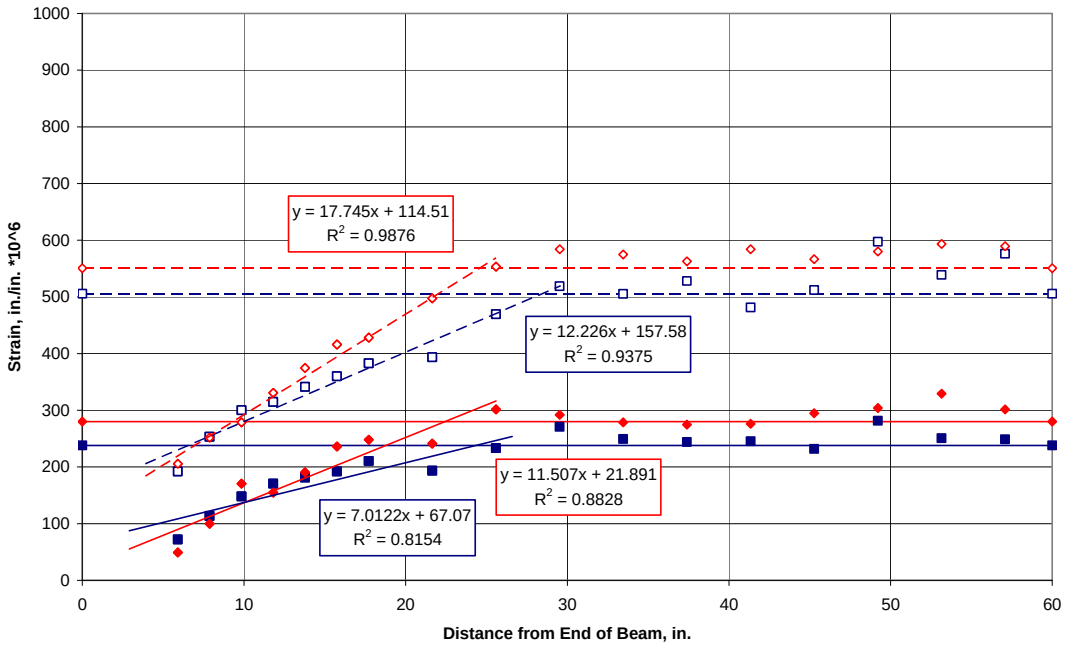

Figure B.71. Pour 2 Strand F Live End Surface Strains

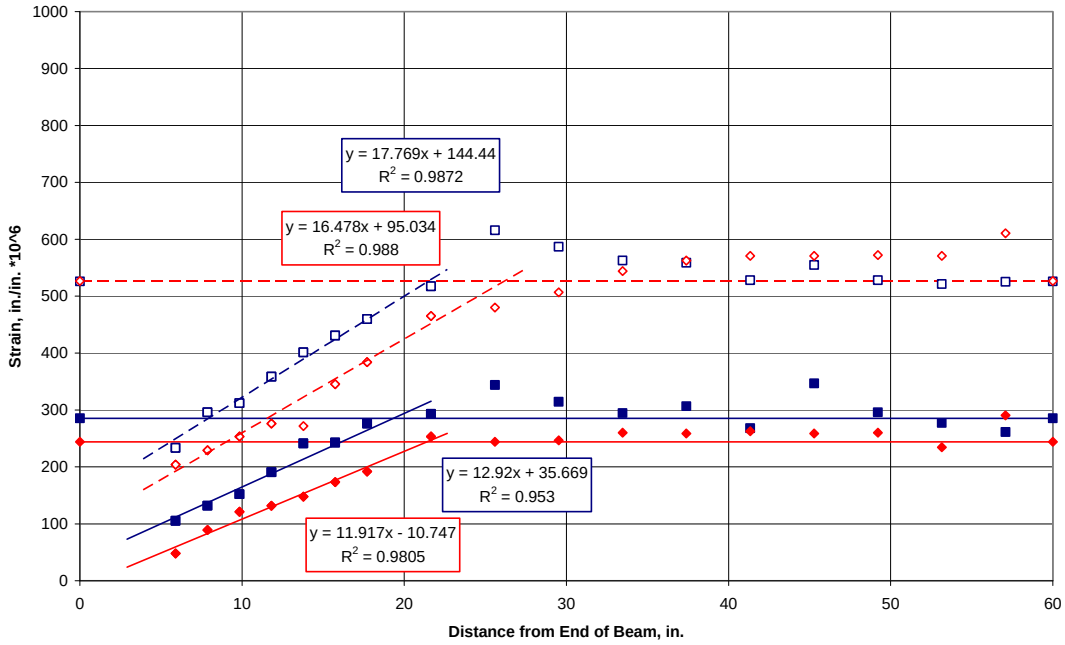

Figure B.72. Pour 2 Strand F Dead End Surface Strains

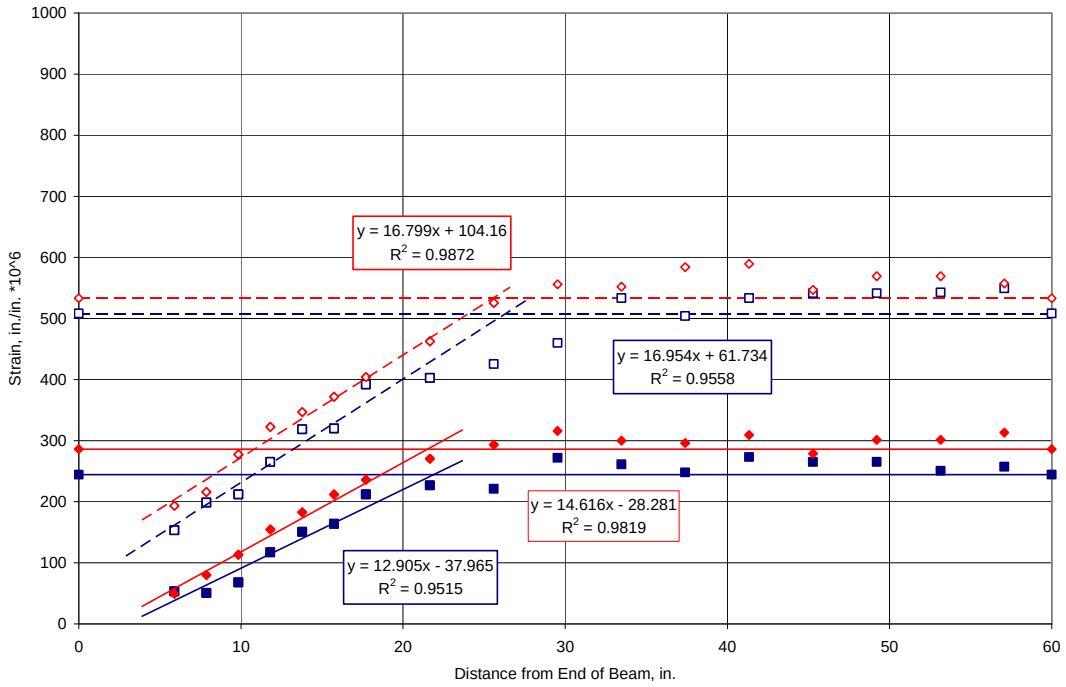

Figure B.73. Pour 2 Strand G Live End Surface Strains

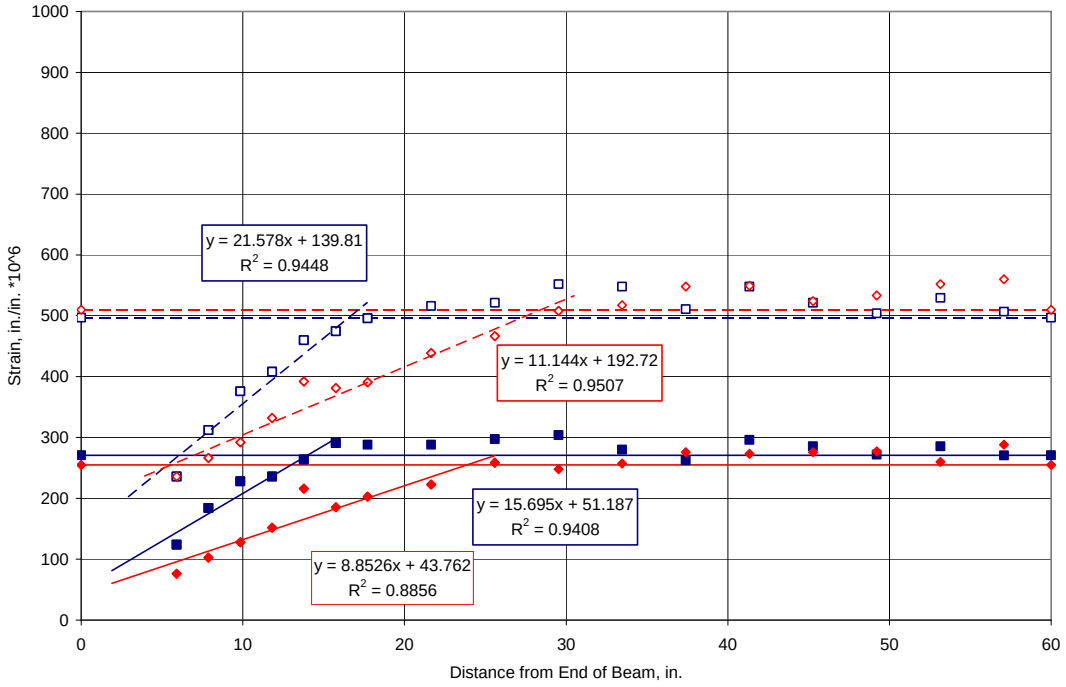

Figure B.74. Pour 2 Strand G Dead End Surface Strains

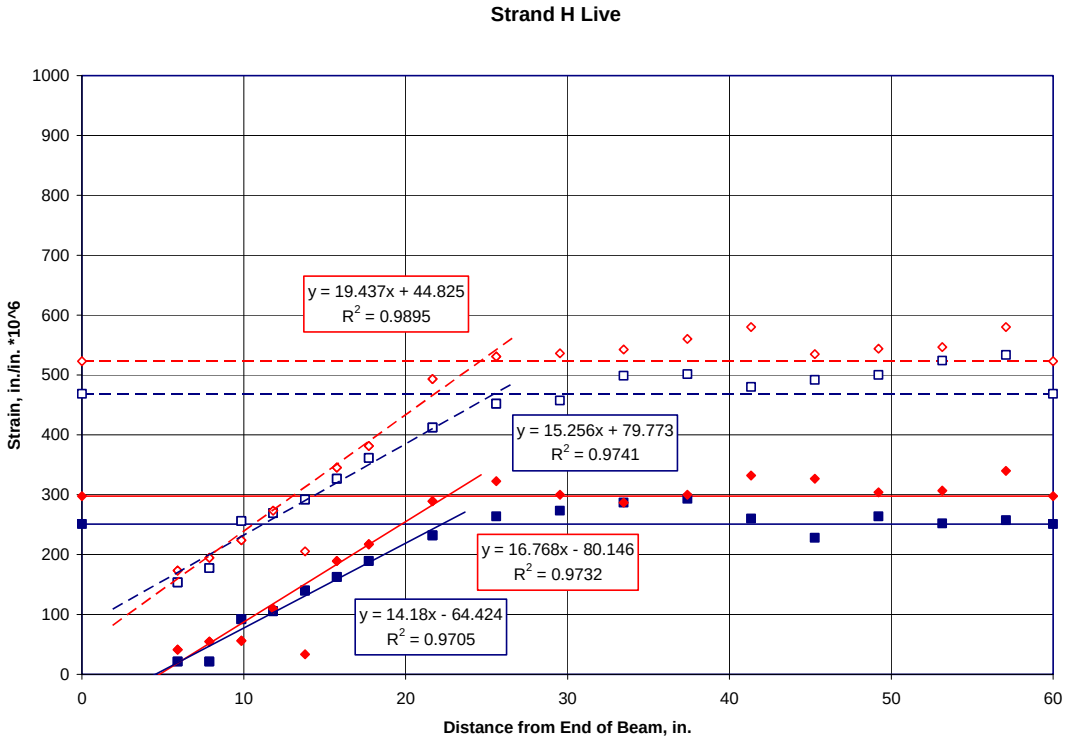

Figure B.75. Pour 2 Strand H Live End Surface Strains

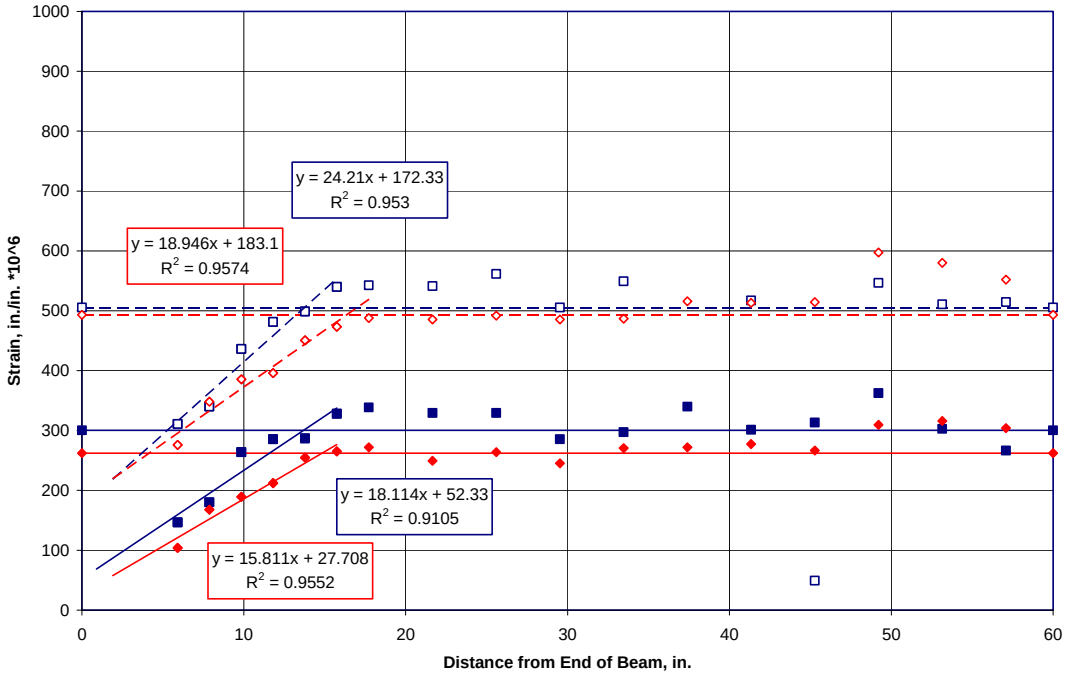

Figure B.76. Pour 2 Strand H Dead End Surface Strains

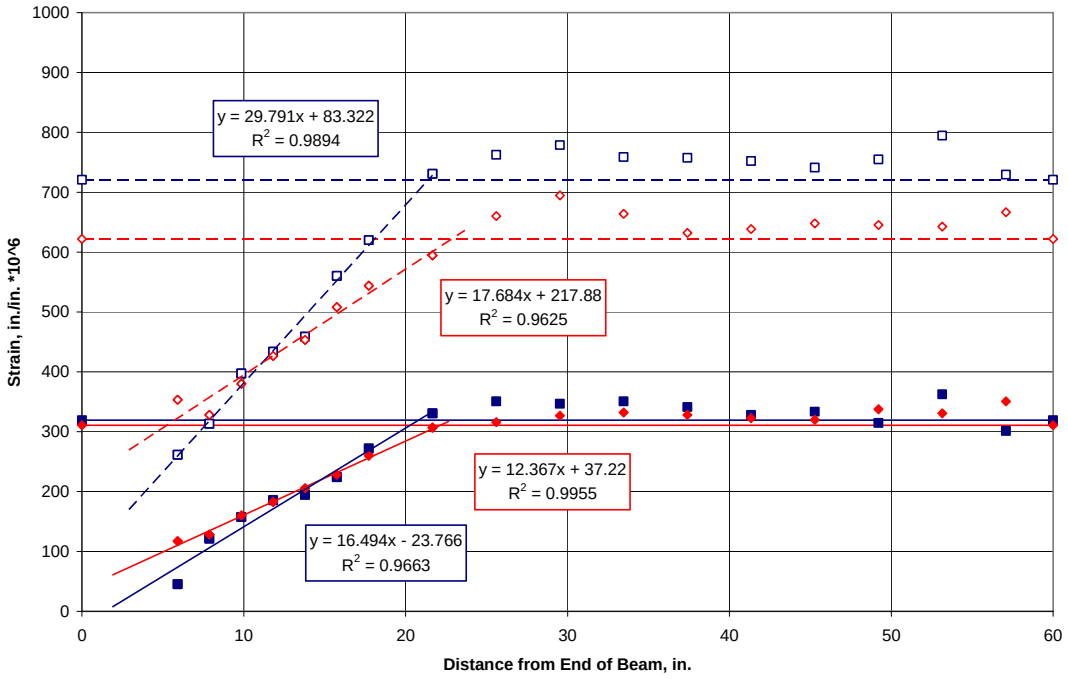

Figure B.77. Pour 2 Strand I Live End Surface Strains

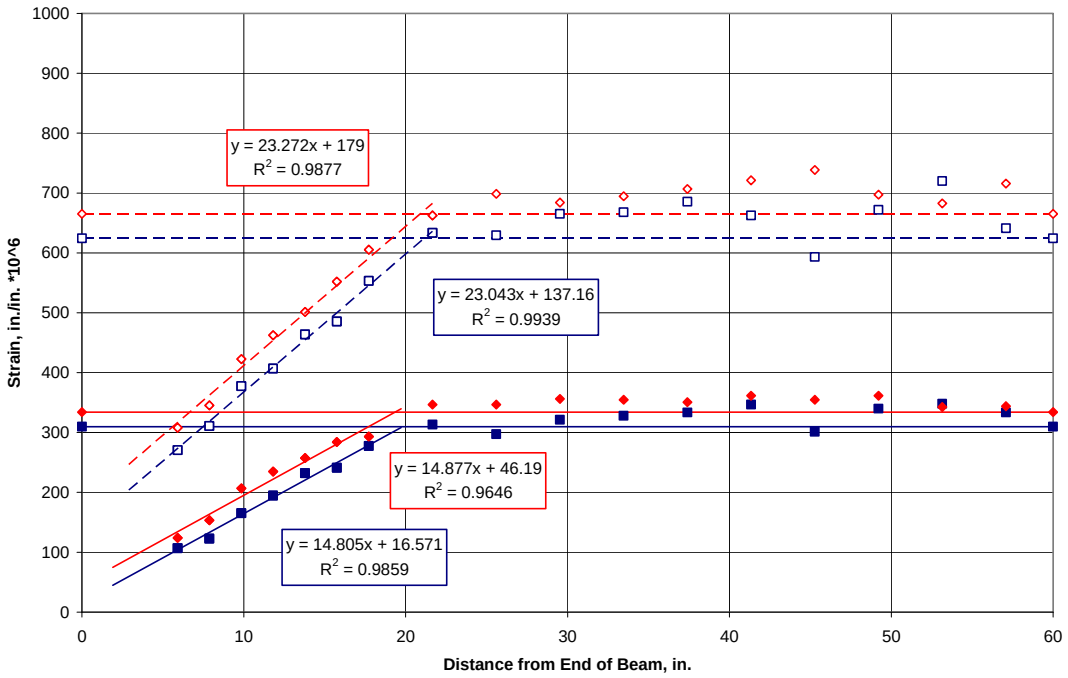

Figure B.78. Pour 2 Strand I Dead End Surface Strains

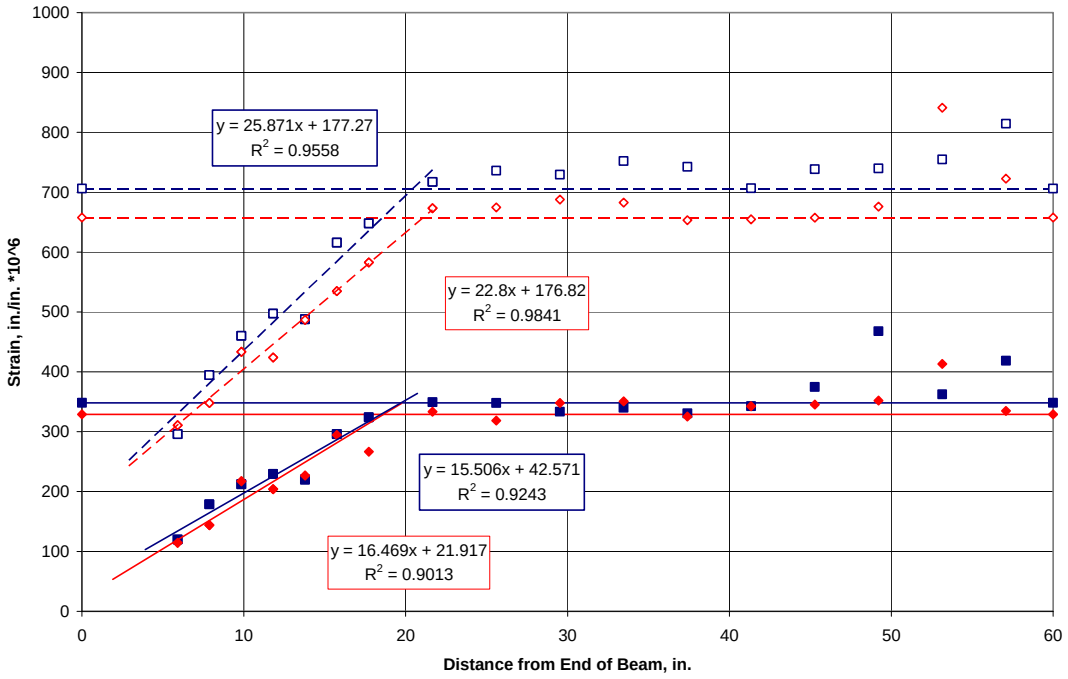

Figure B.79. Pour 2 Strand J Live End Surface Strains

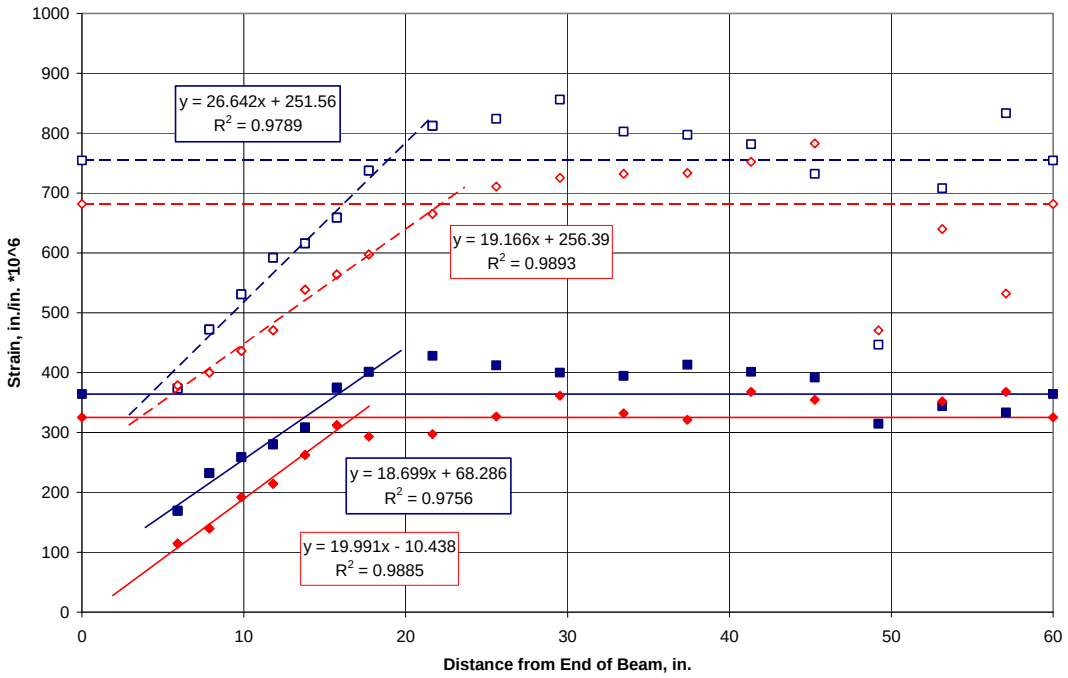

Figure B.80. Pour 2 Strand J Dead End Surface Strains

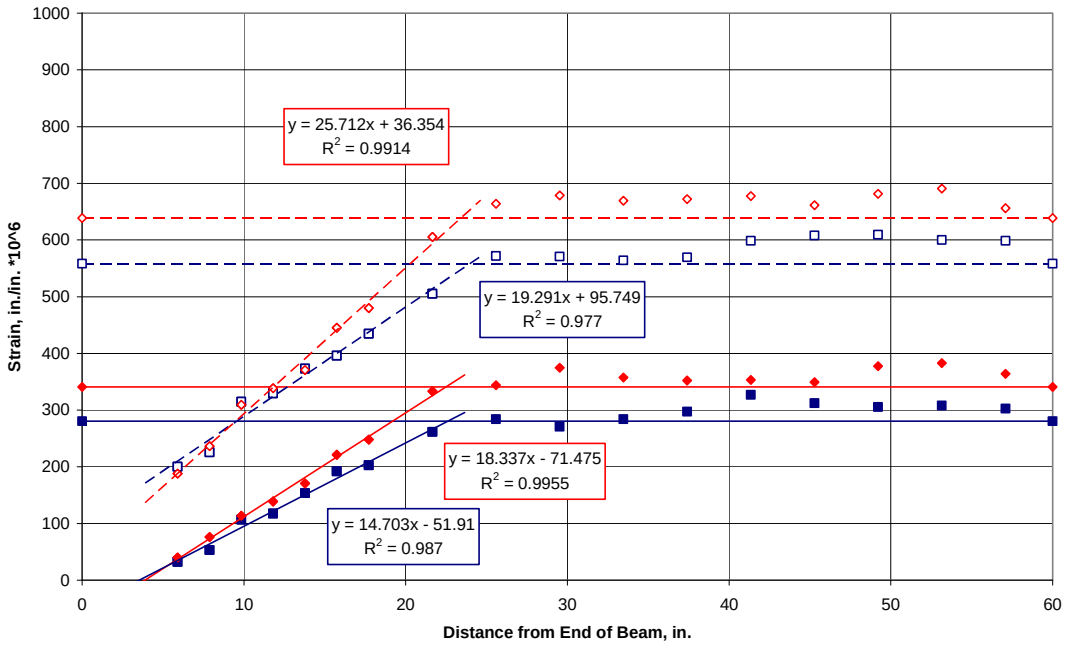

Figure B.81. Pour 3 Strand A Live End Surface Strains

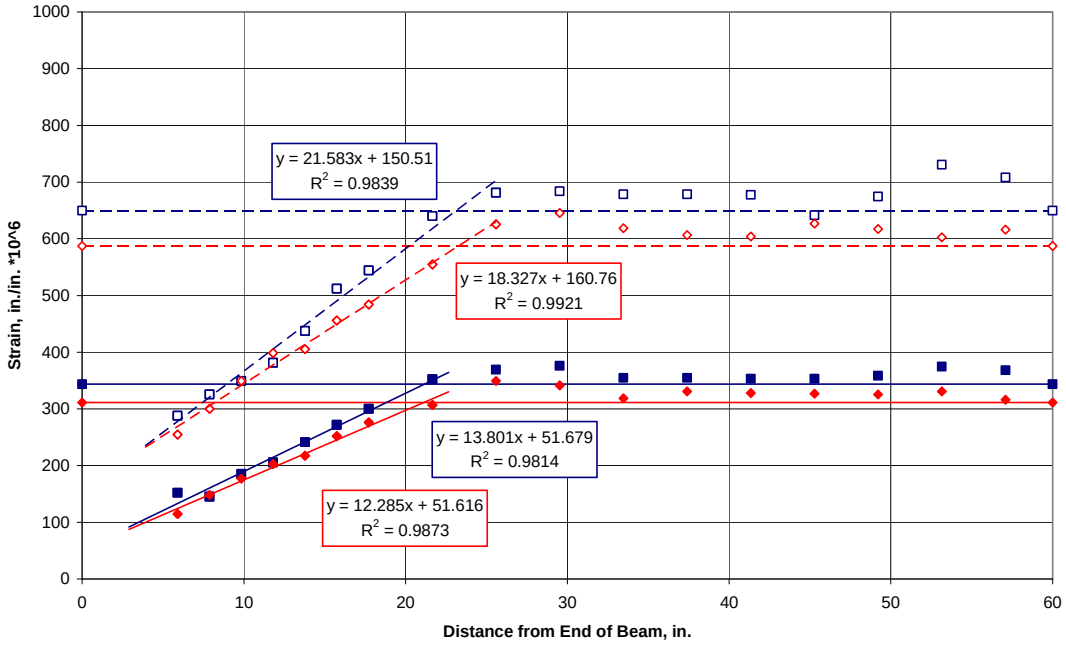

Figure B.82. Pour 3 Strand A Dead End Surface Strains

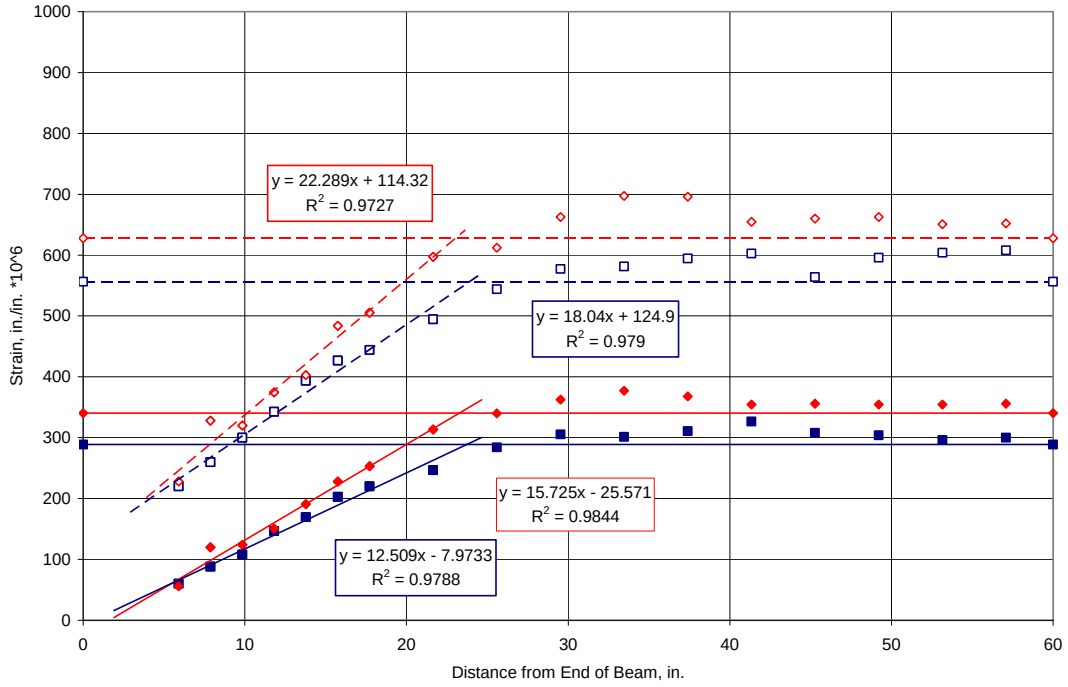

Figure B.83. Pour 3 Strand B Live End Surface Strains

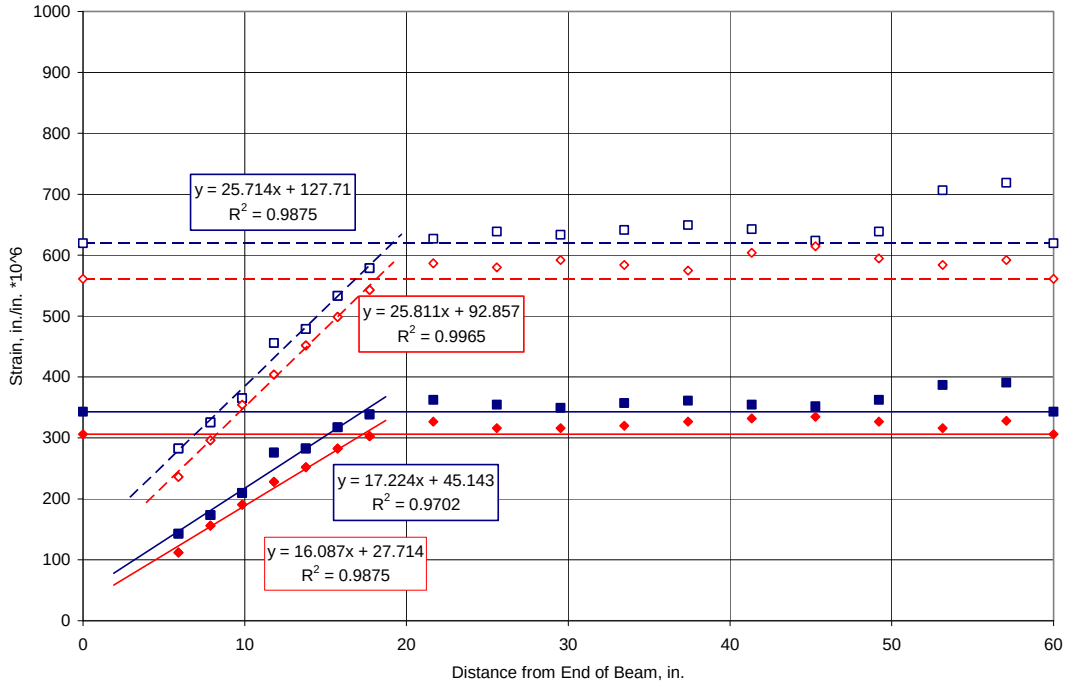

Figure B.84. Pour 3 Strand B Dead End Surface Strains

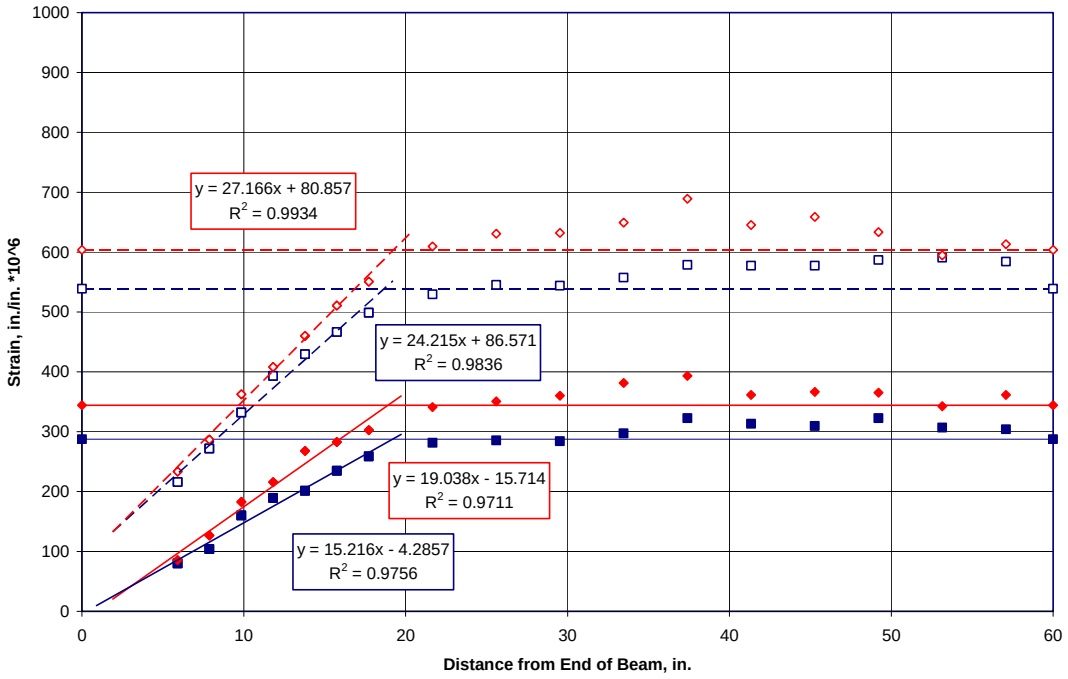

Figure B.85. Pour 3 Strand C Live End Surface Strains

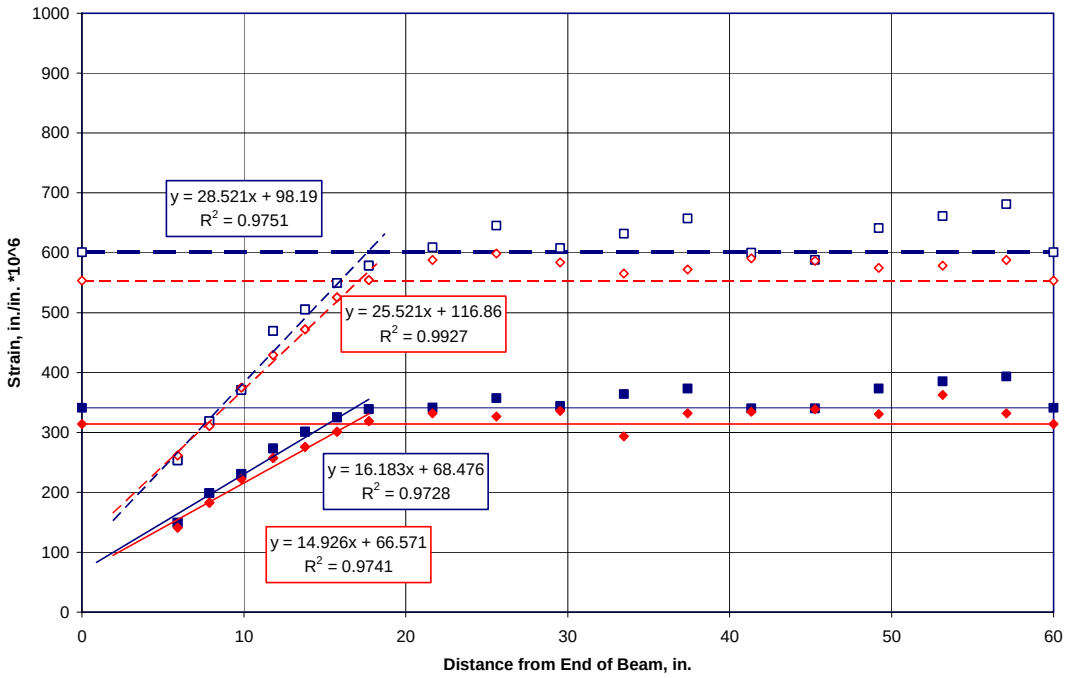

Figure B.86. Pour 3 Strand C Dead End Surface Strains

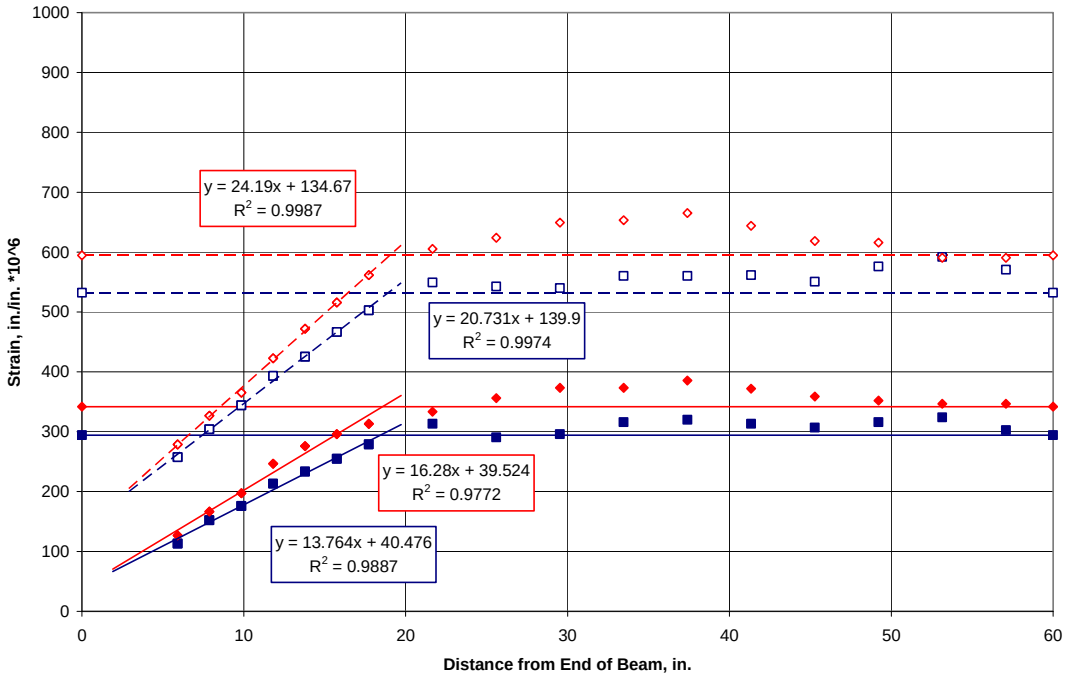

Figure B.87. Pour 3 Strand D Live End Surface Strains

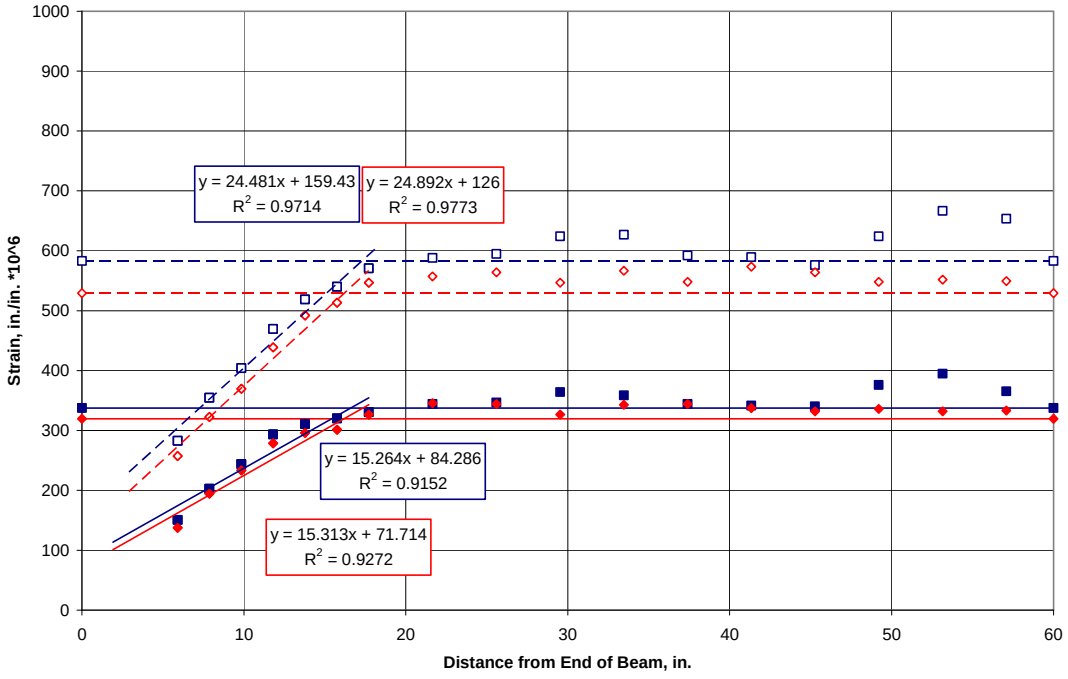

Figure B.88. Pour 3 Strand D Dead End Surface Strains

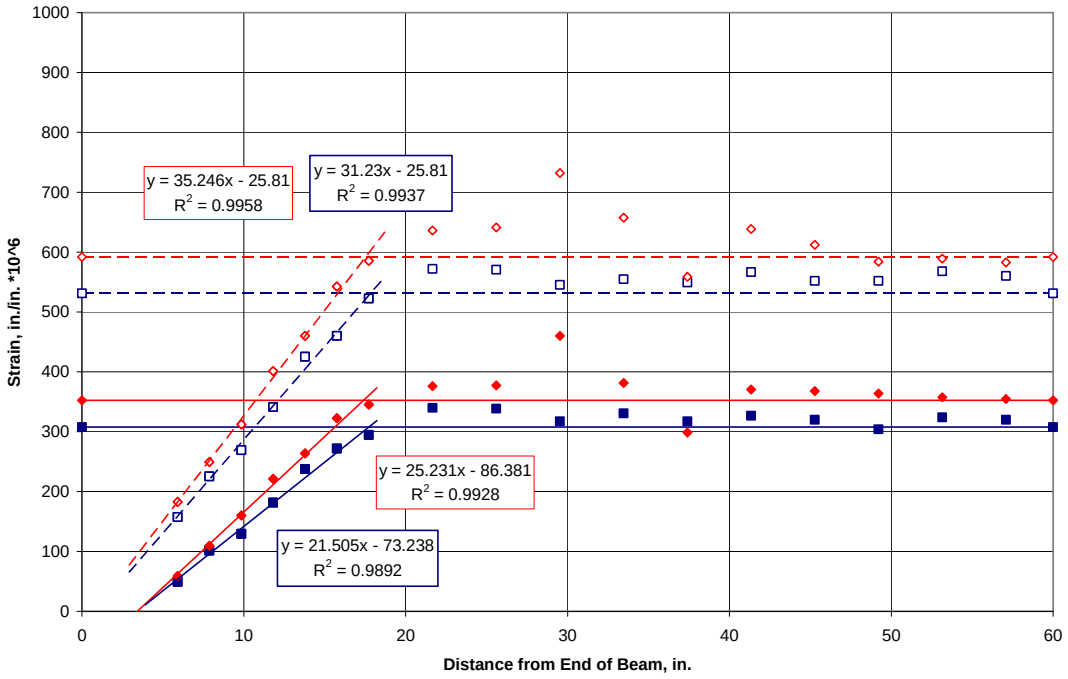

Figure B.89. Pour 3 Strand E Live End Surface Strains

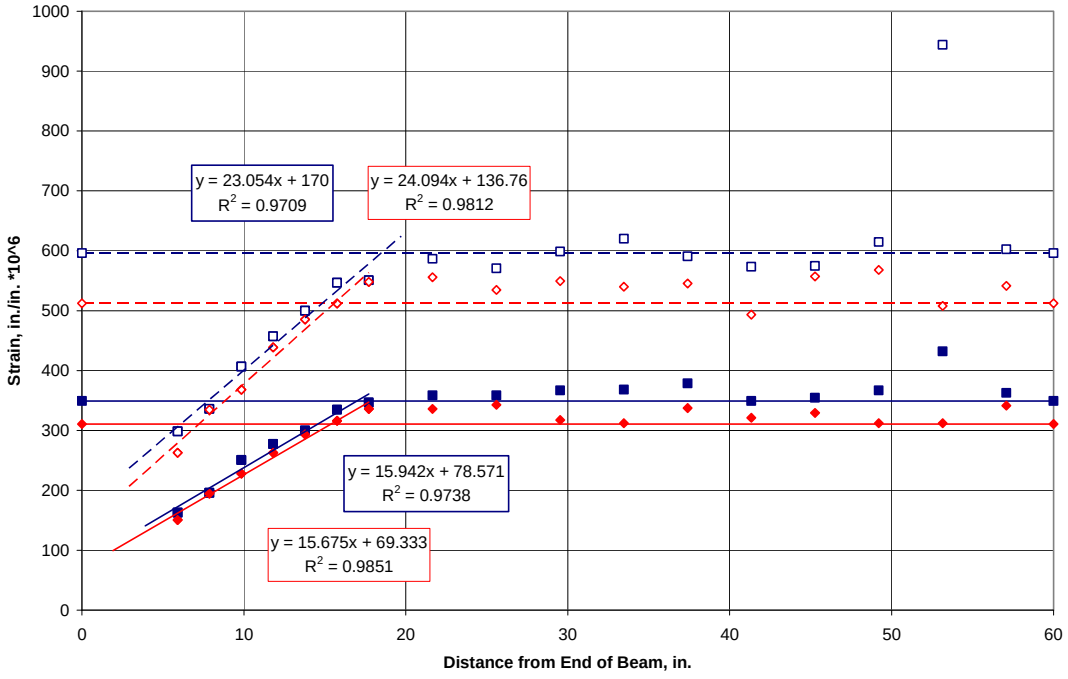

Figure B.90. Pour 3 Strand E Dead End Surface Strains

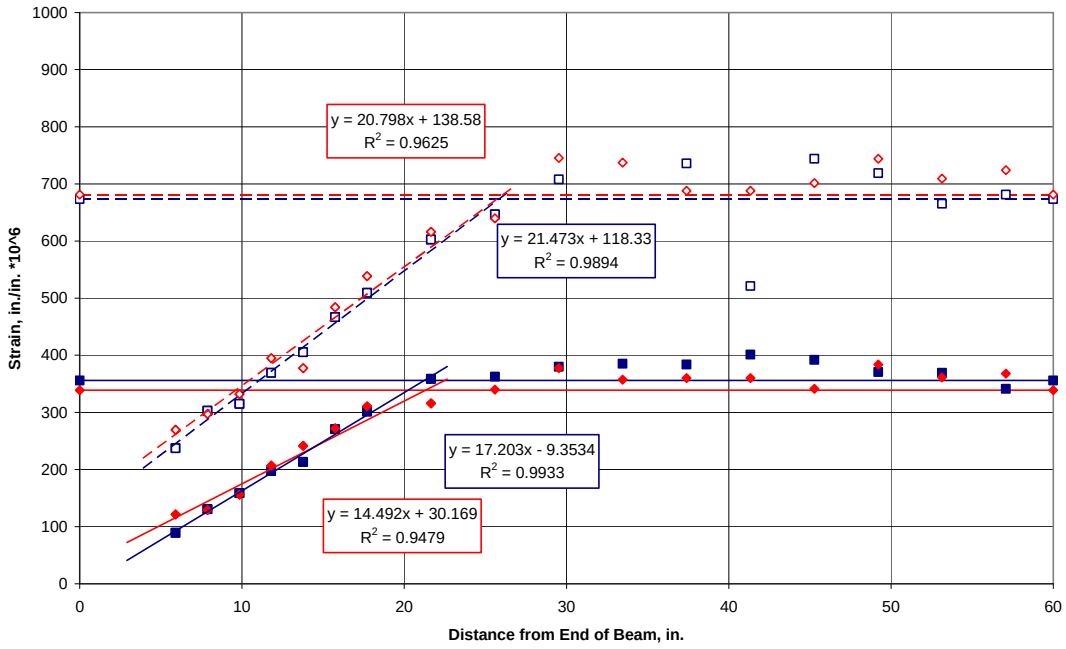

Figure B.91. Pour 3 Strand F Live End Surface Strains

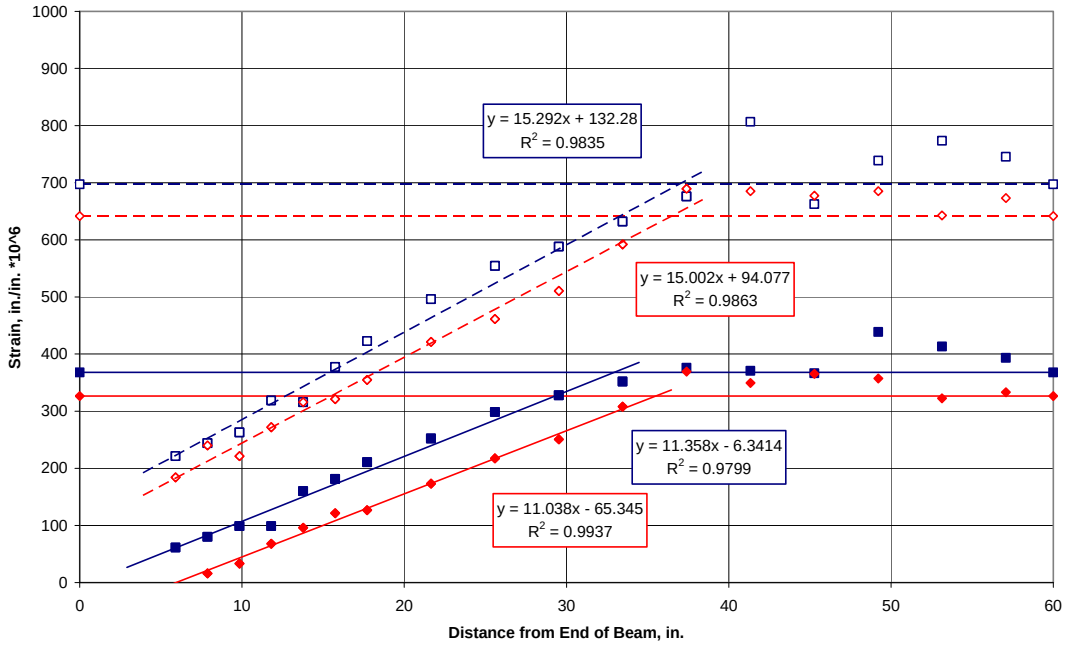

Figure B.92. Pour 3 Strand F Dead End Surface Strains

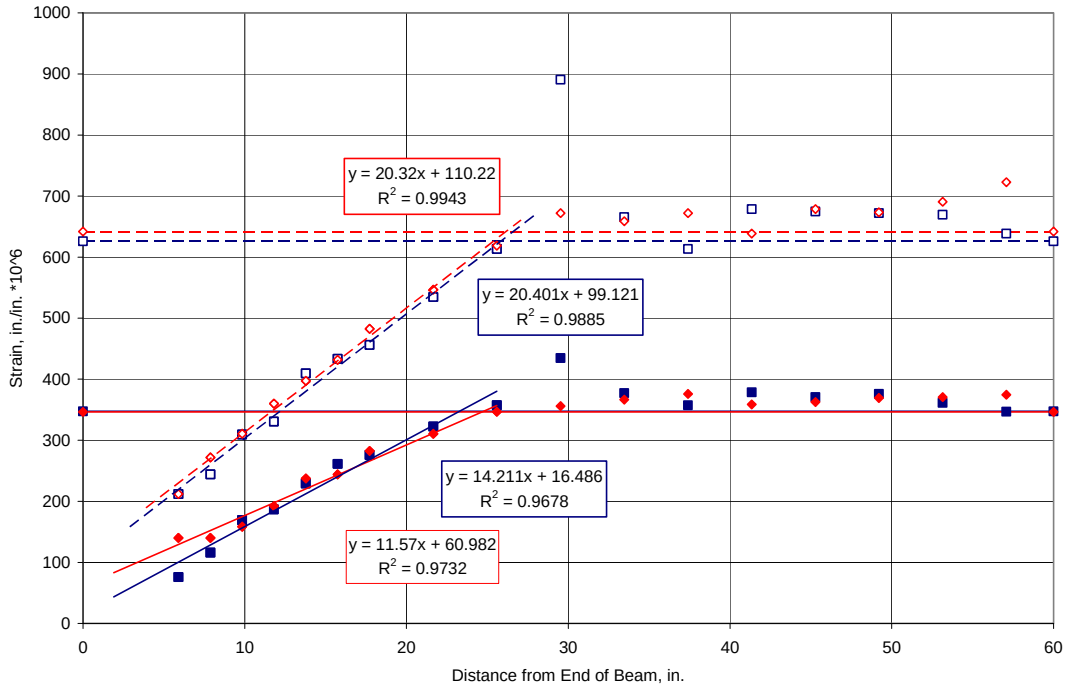

Figure B.93. Pour 3 Strand G Live End Surface Strains

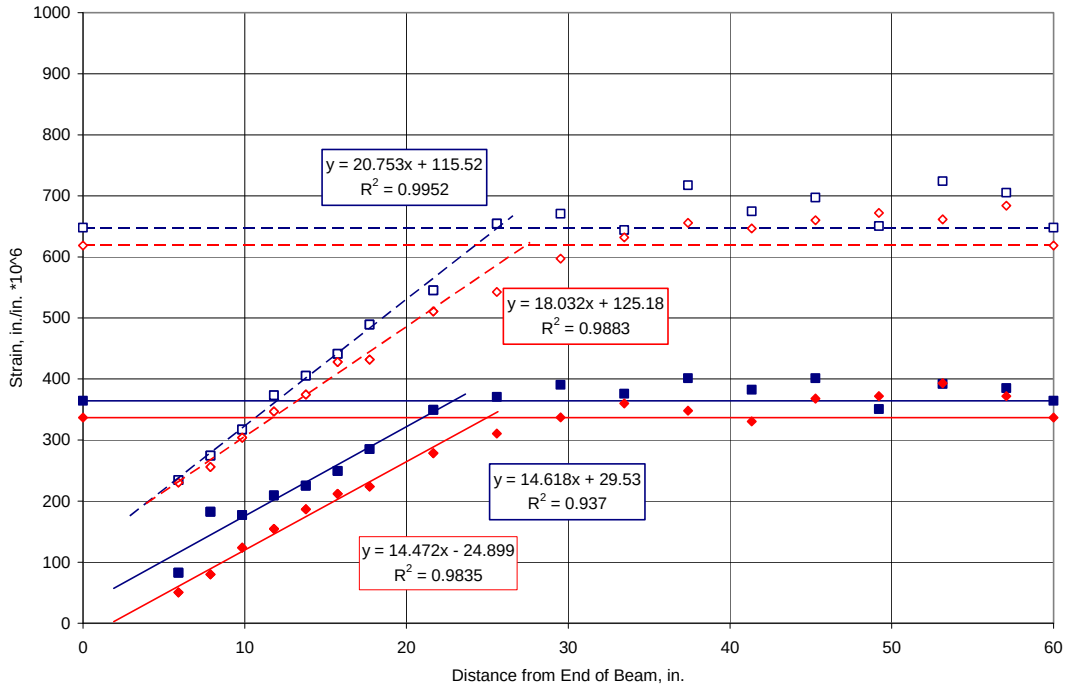

Figure B.94. Pour 3 Strand G Dead End Surface Strains

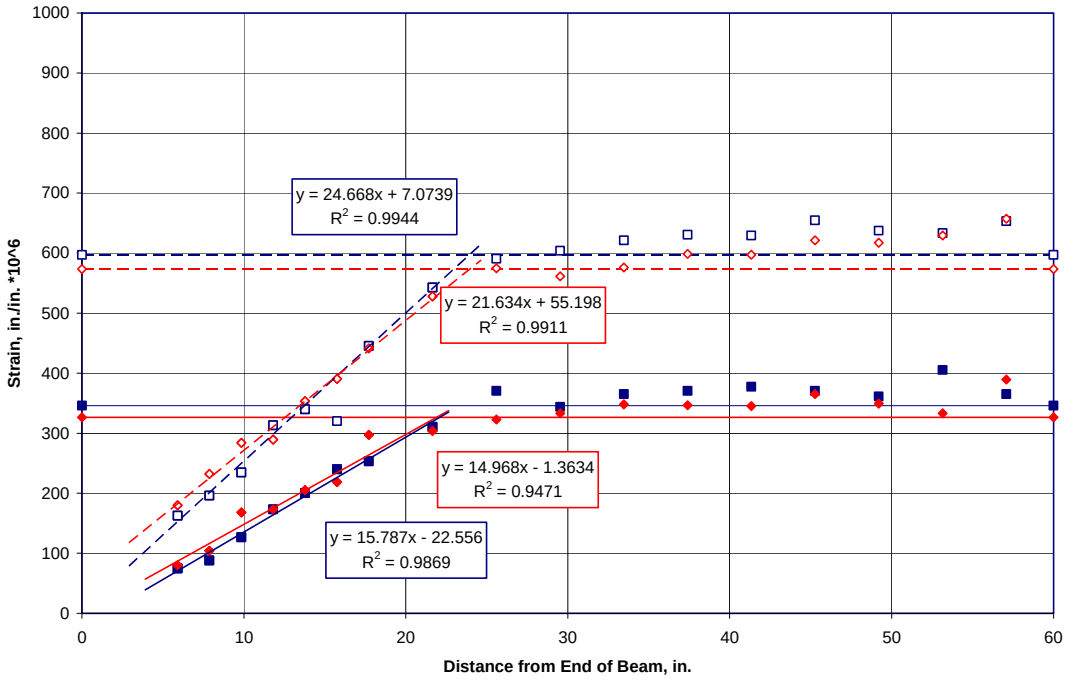

Figure B.95. Pour 3 Strand H Live End Surface Strains

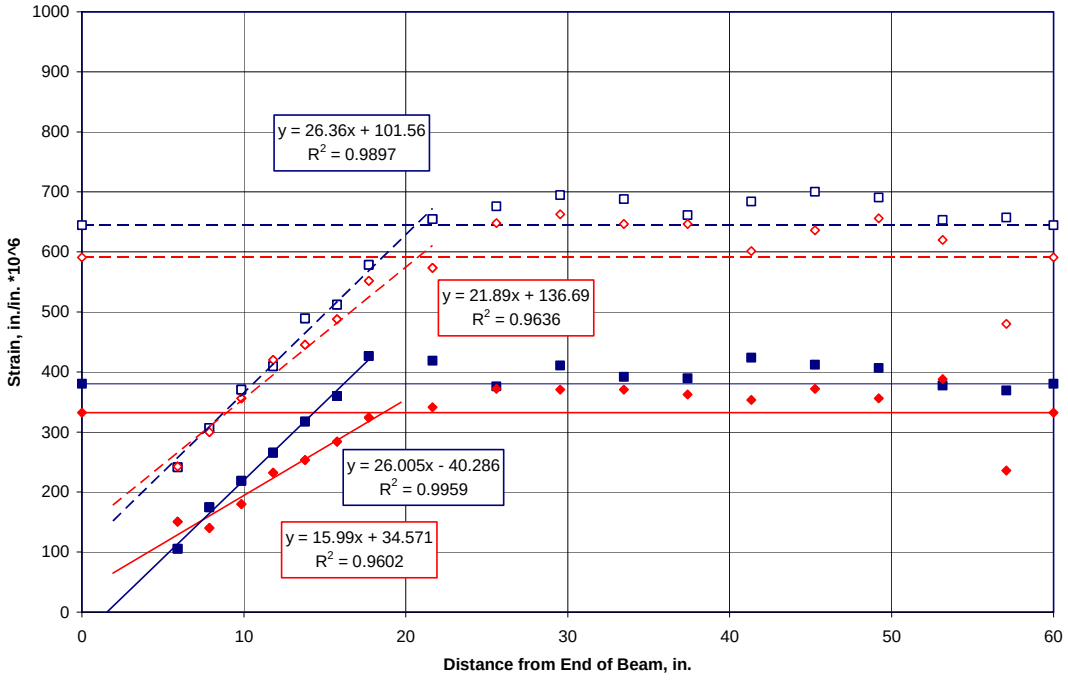

Figure B.96. Pour 3 Strand H Dead End Surface Strains

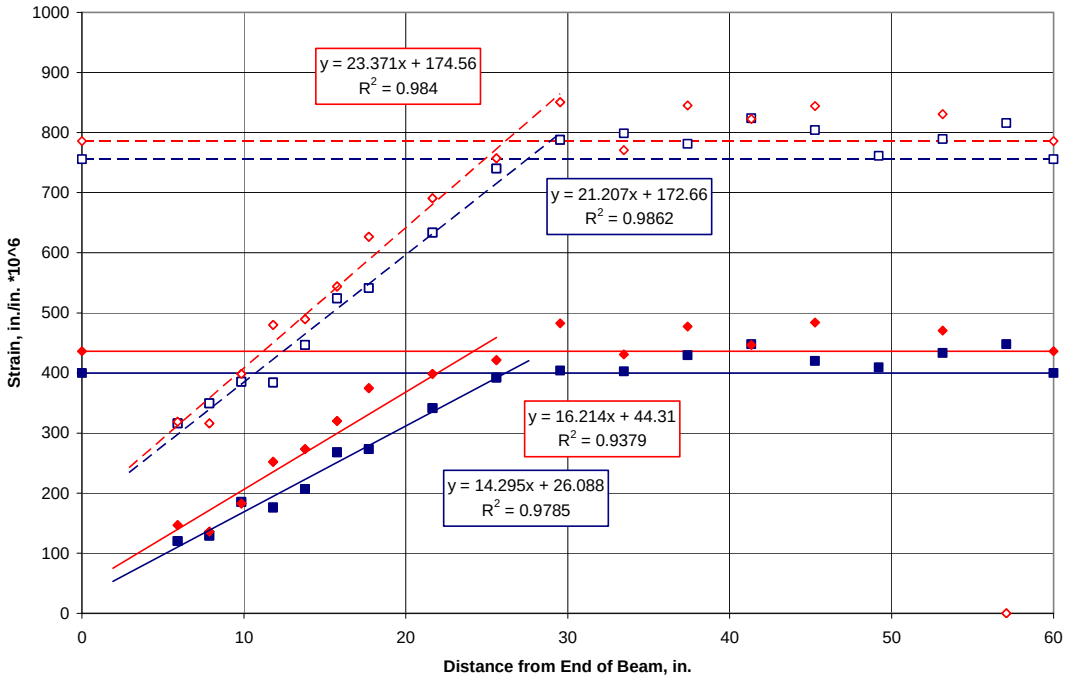

Figure B.97. Pour 3 Strand I Live End Surface Strains

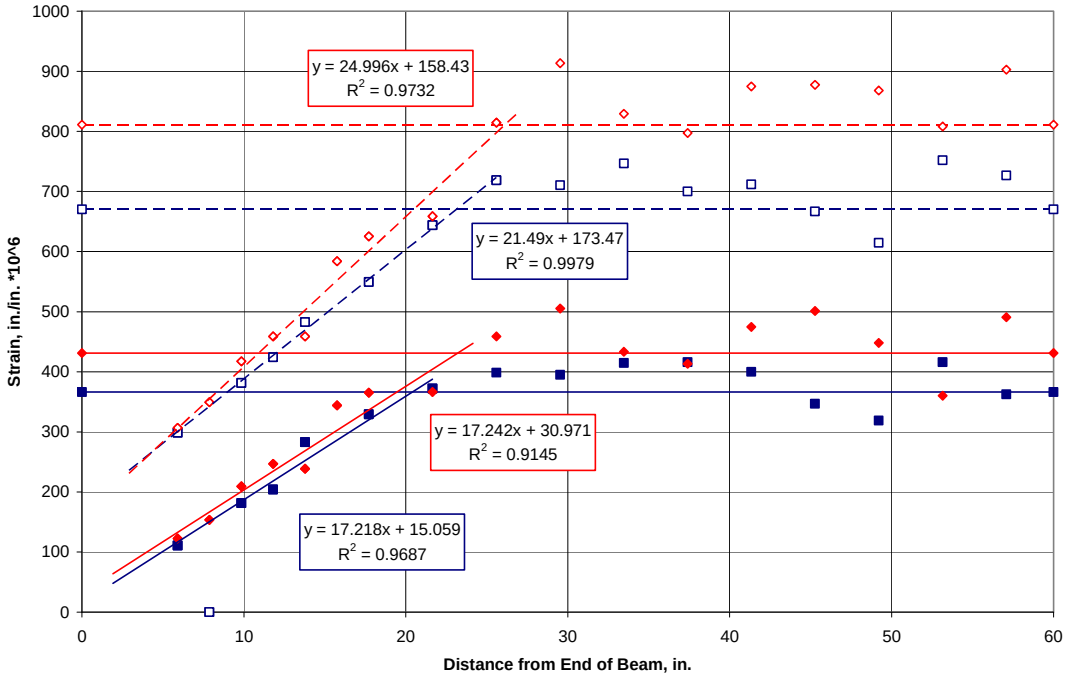

Figure B.98. Pour 3 Strand I Dead End Surface Strains

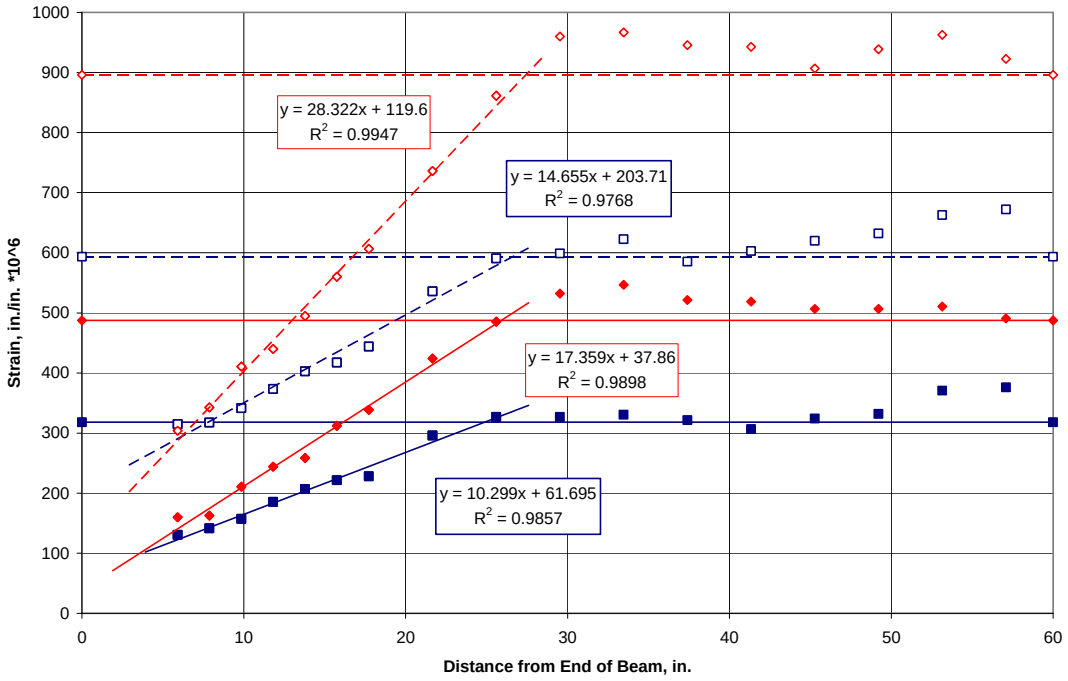

Figure B.99. Pour 3 Strand J Live End Surface Strains

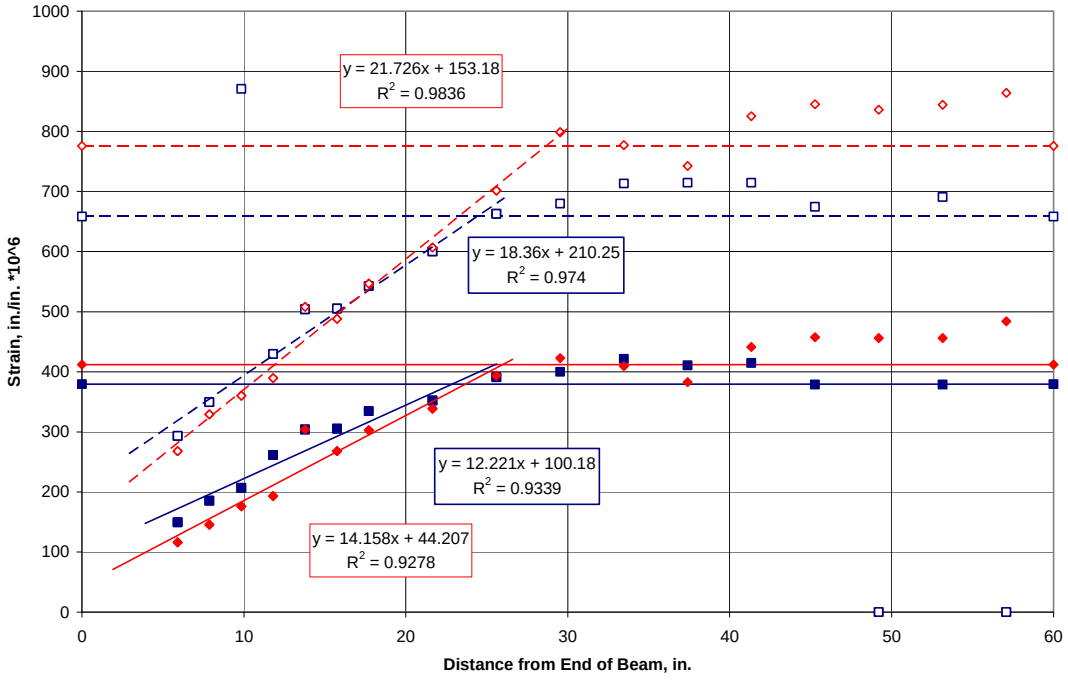

Figure B.100. Pour 3 Strand J Dead End Surface Strains

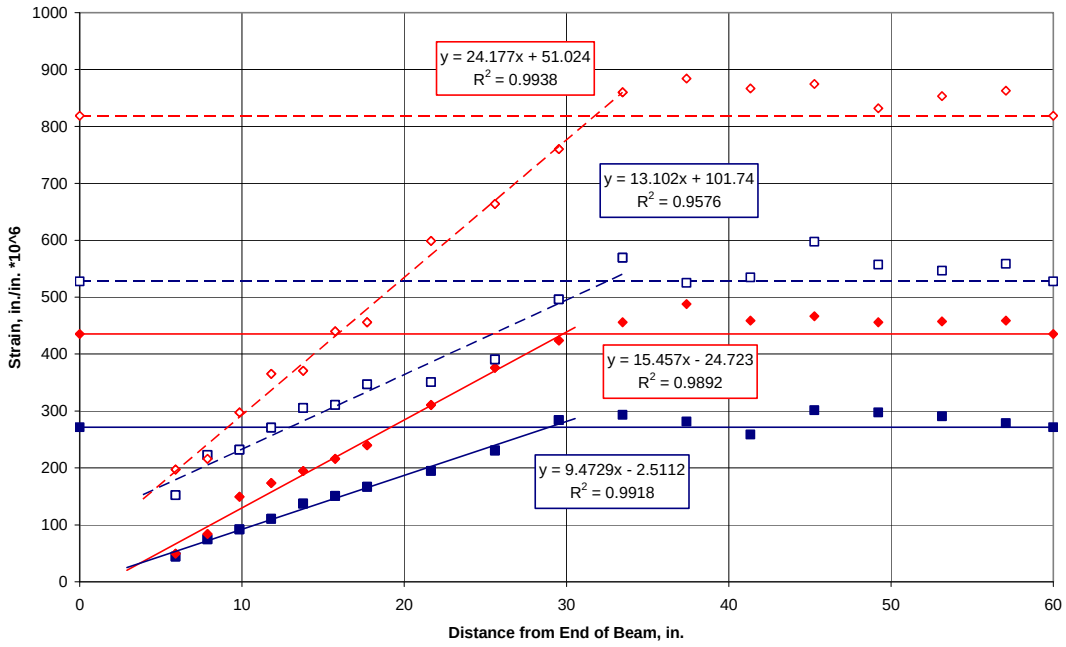

Figure B.101. Pour 4 Strand A Live End Surface Strains

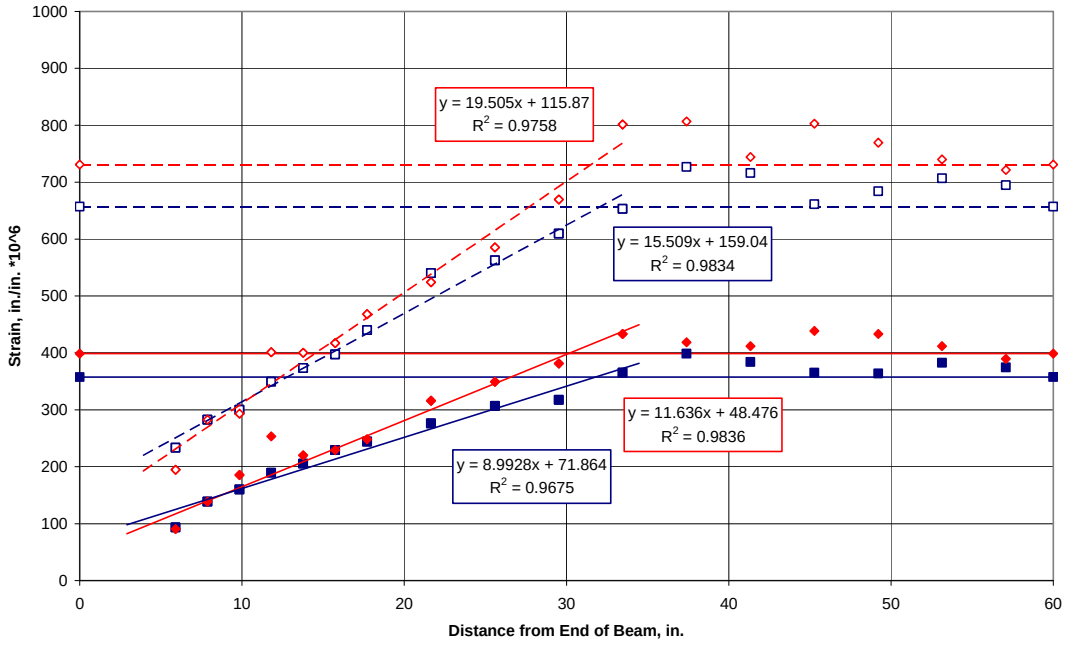

Figure B.102. Pour 4 Strand A Dead End Surface Strains

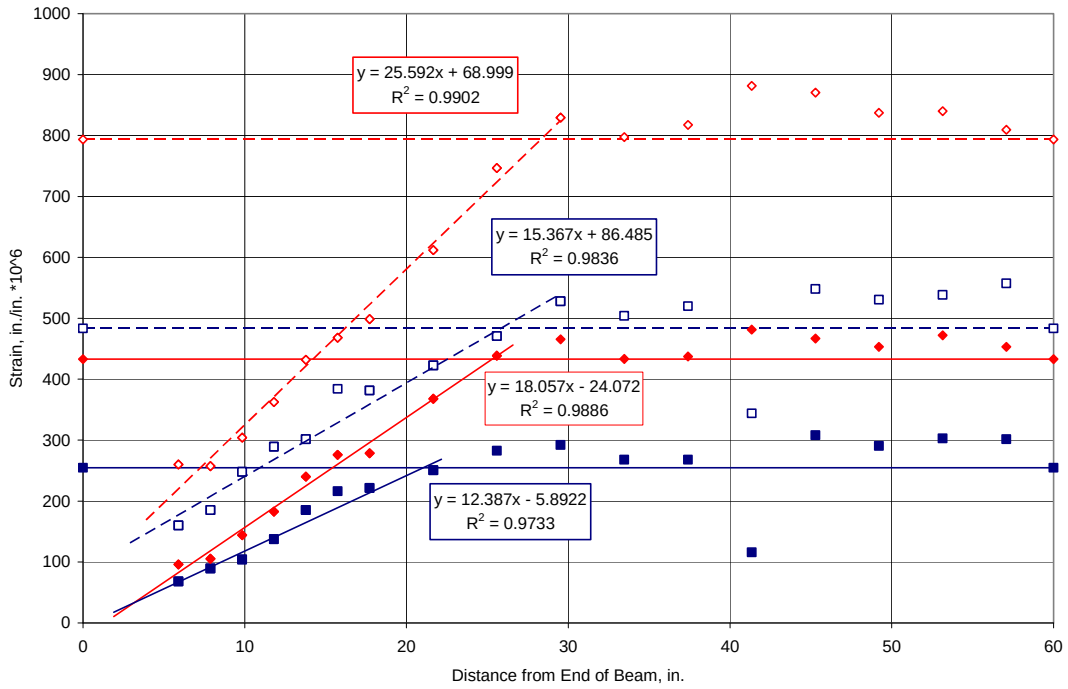

Figure B.103. Pour 4 Strand B Live End Surface Strains

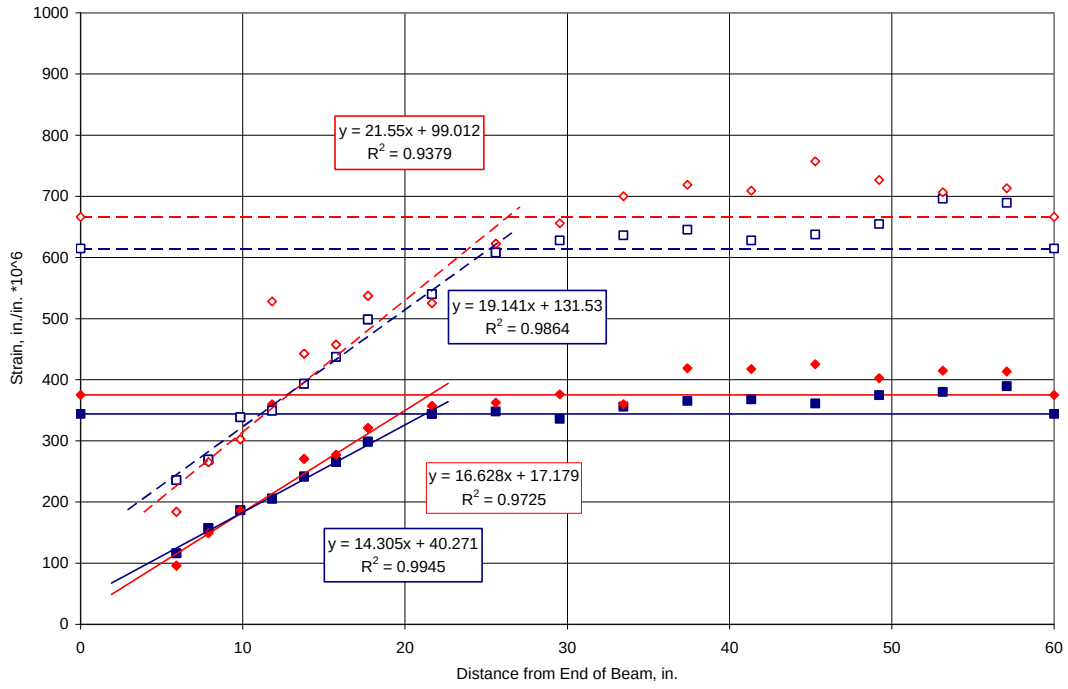

Figure B.104. Pour 4 Strand B Dead End Surface Strains

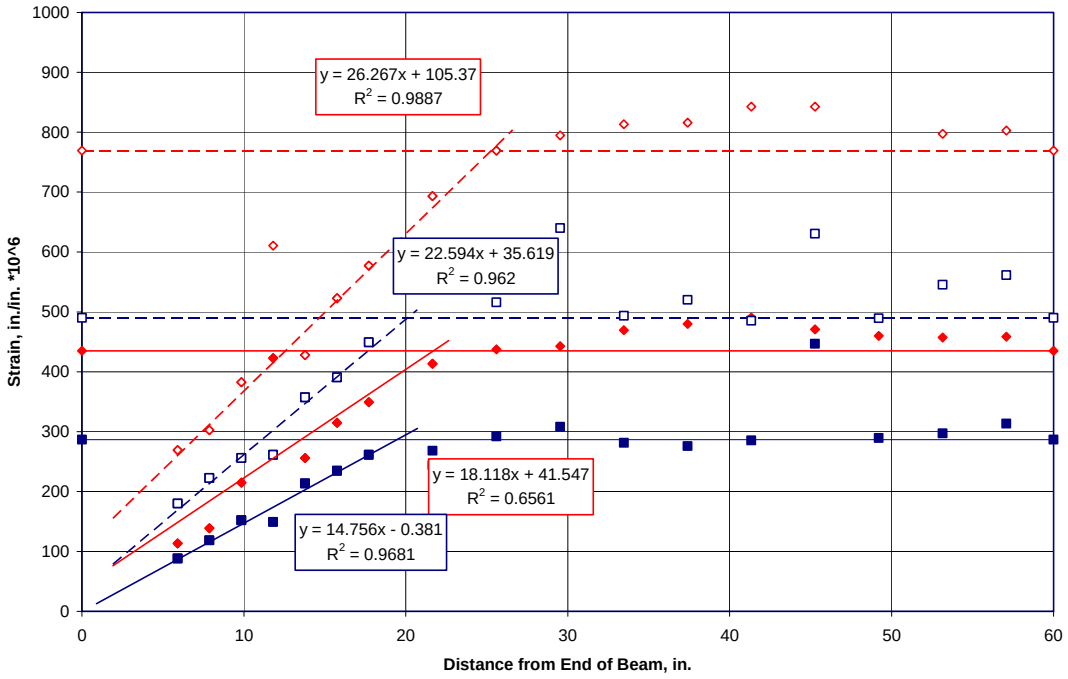

Figure B.105. Pour 4 Strand C Live End Surface Strains

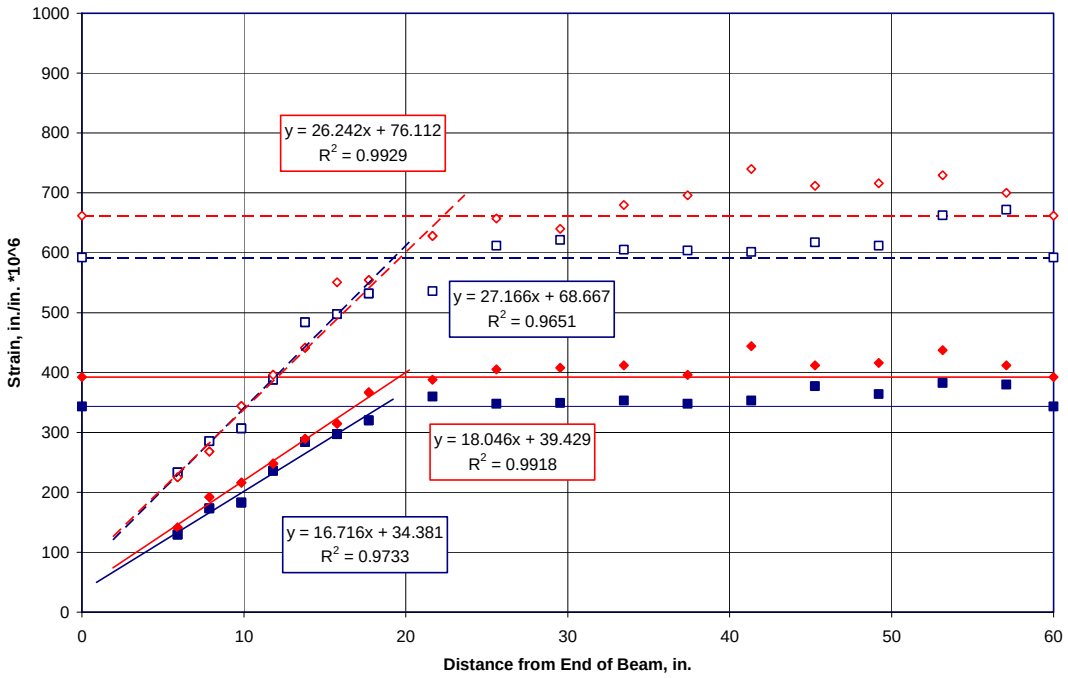

Figure B.106. Pour 4 Strand C Dead End Surface Strains

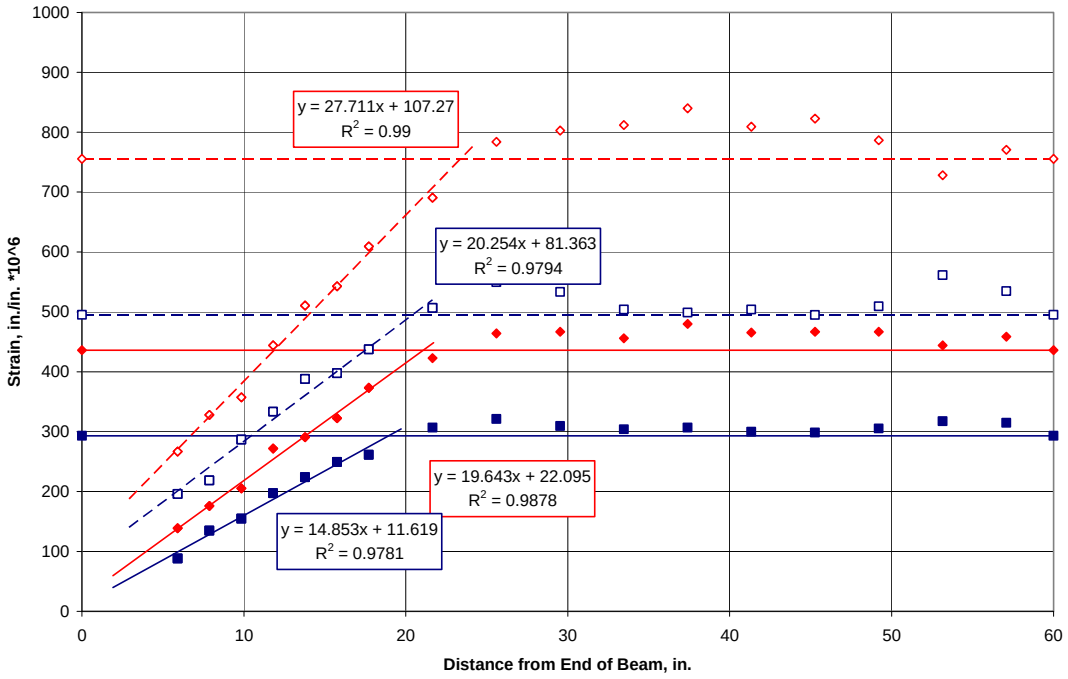

Figure B.107. Pour 4 Strand D Live End Surface Strains

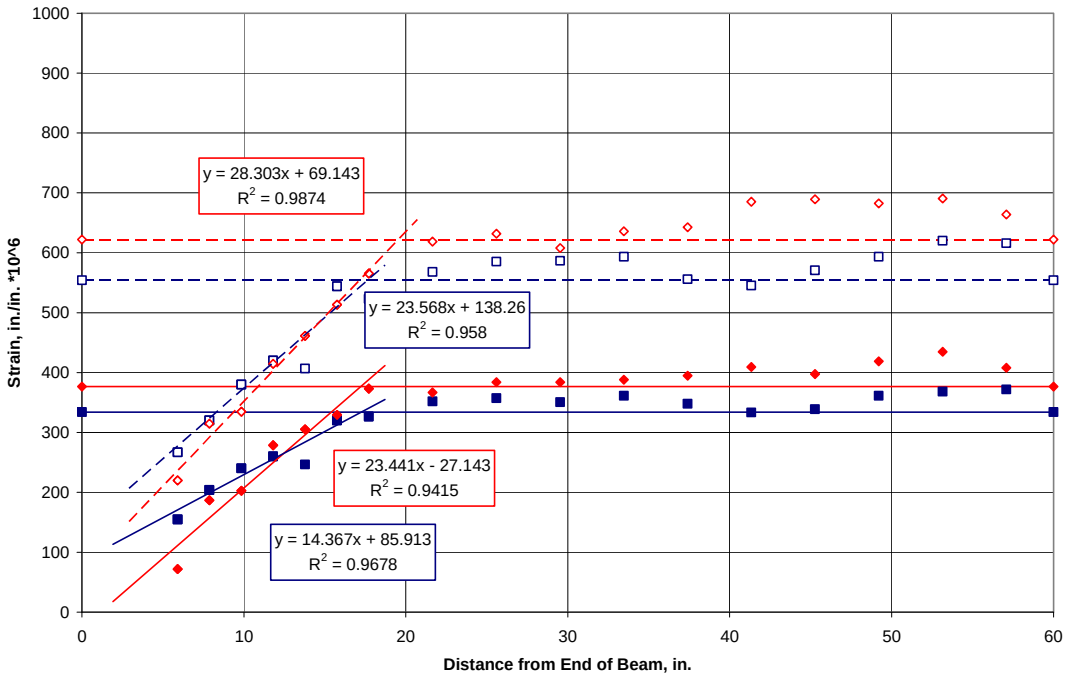

Figure B.108. Pour 4 Strand D Dead End Surface Strains

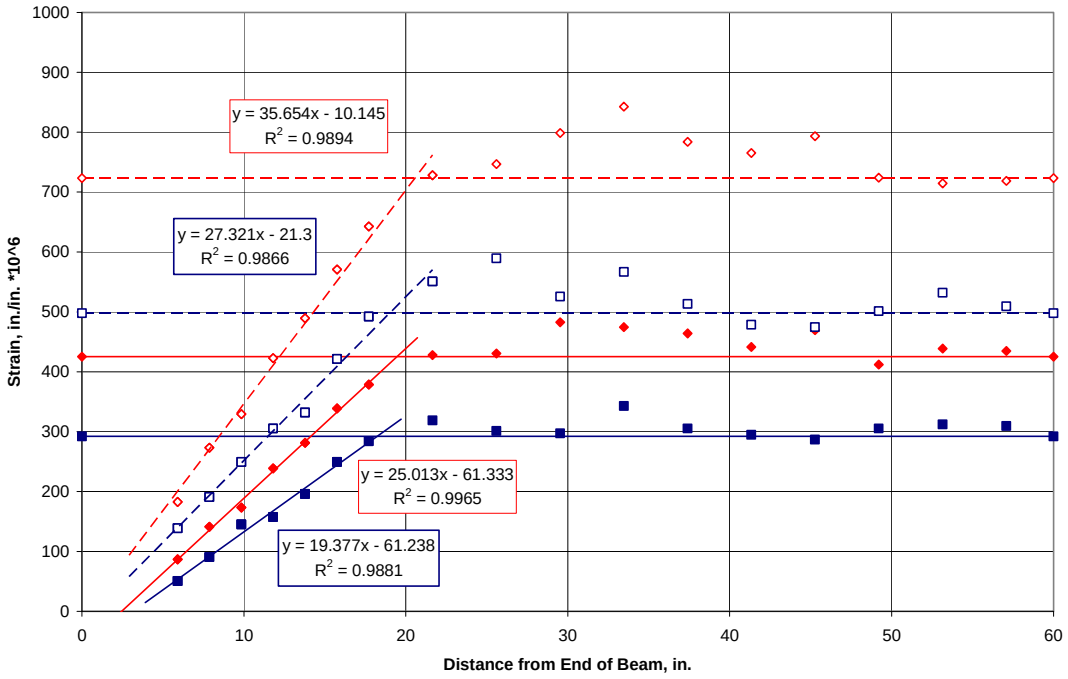

Figure B.109. Pour 4 Strand E Live End Surface Strains

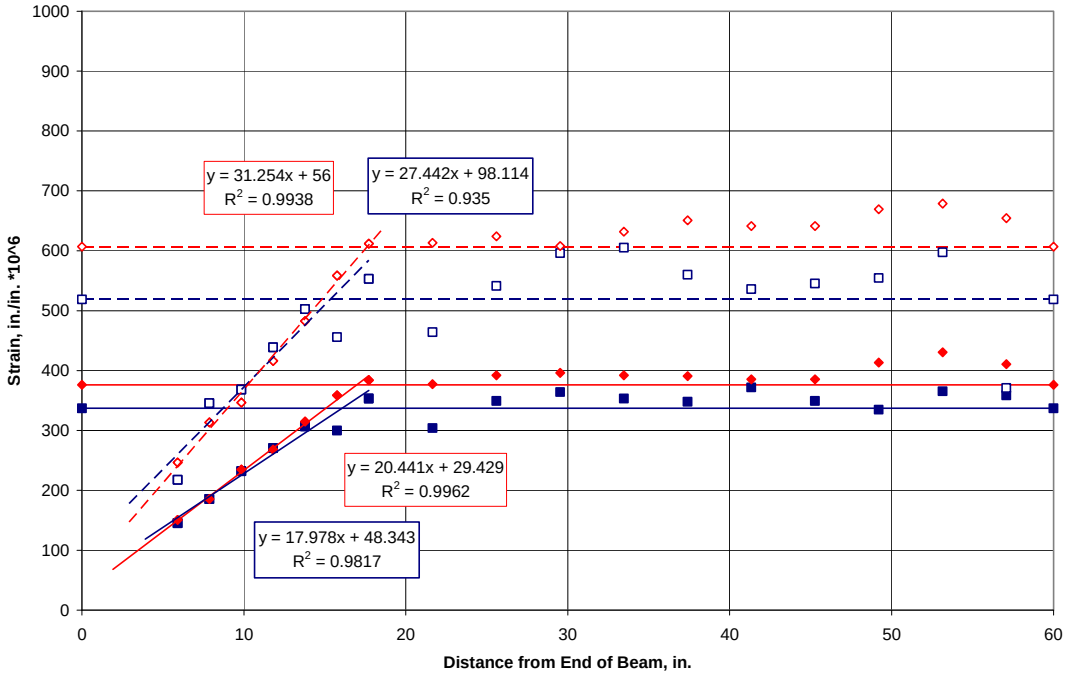

Figure B.110. Pour 4 Strand E Dead End Surface Strains

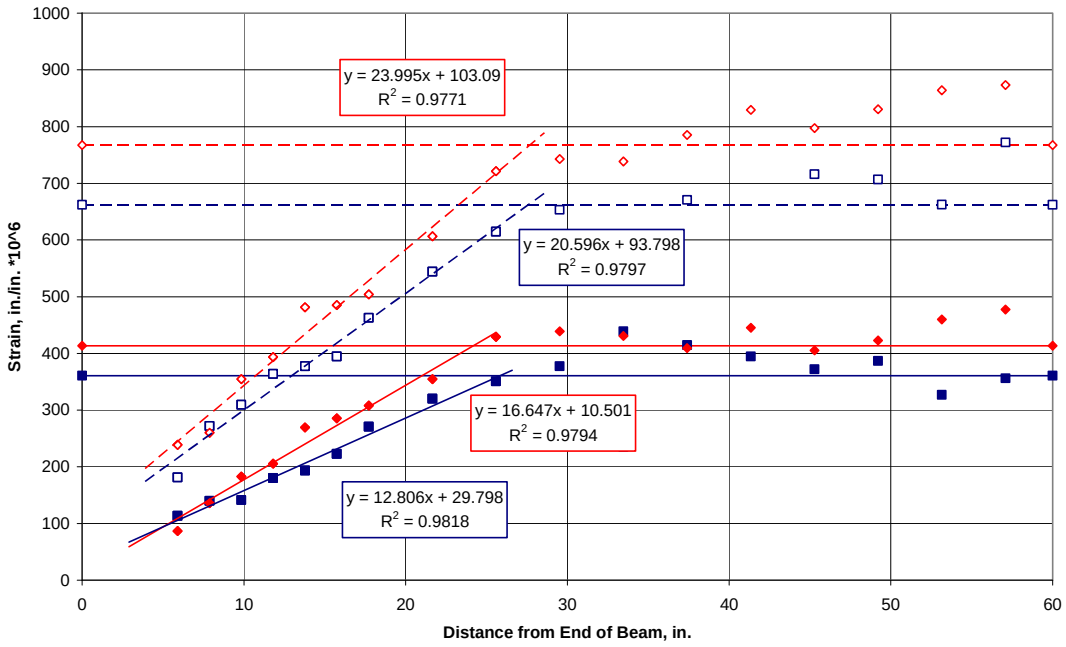

Figure B.111. Pour 4 Strand F Live End Surface Strains

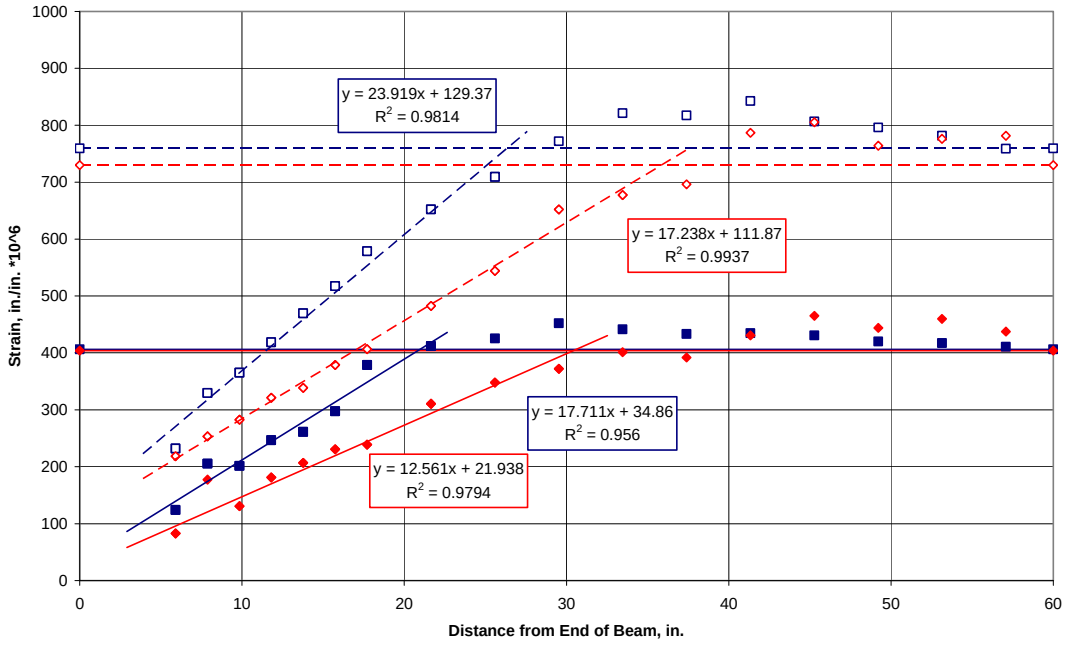

Figure B.112. Pour 4 Strand F Dead End Surface Strains

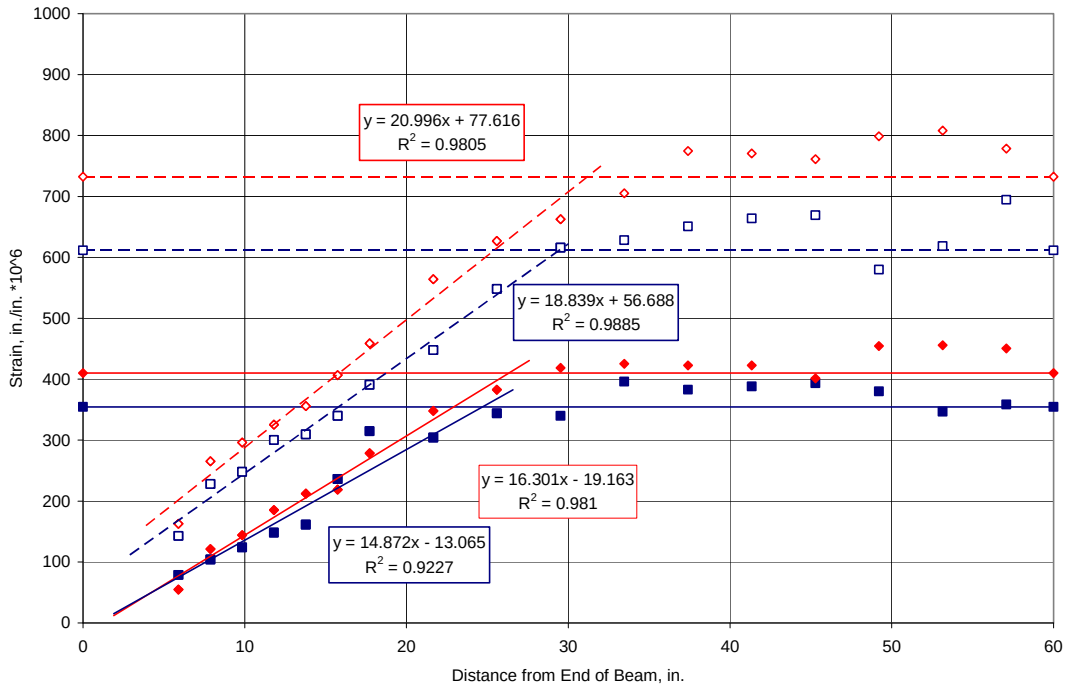

Figure B.113. Pour 4 Strand G Live End Surface Strains

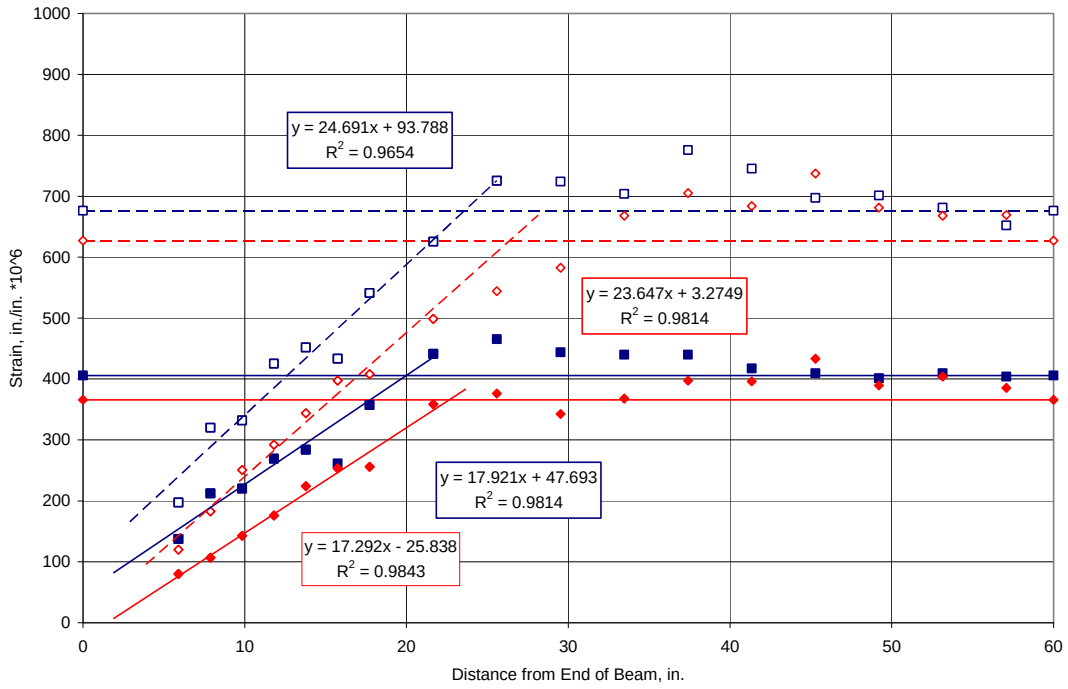

Figure B.114. Pour 4 Strand G Dead End Surface Strains

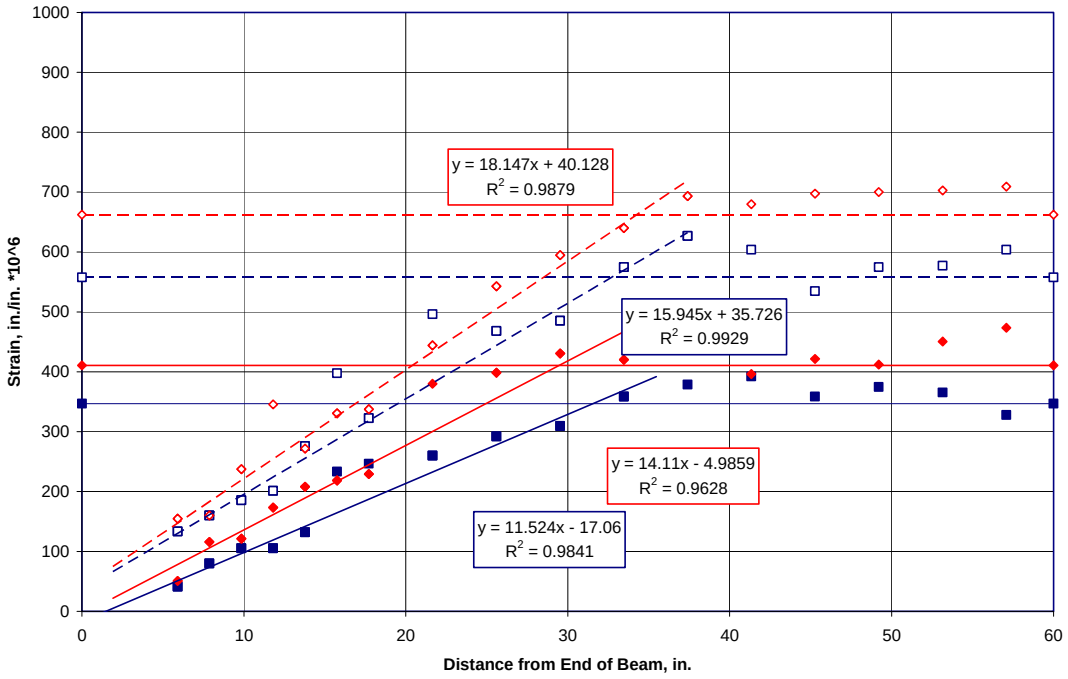

Figure B.115. Pour 4 Strand H Live End Surface Strains

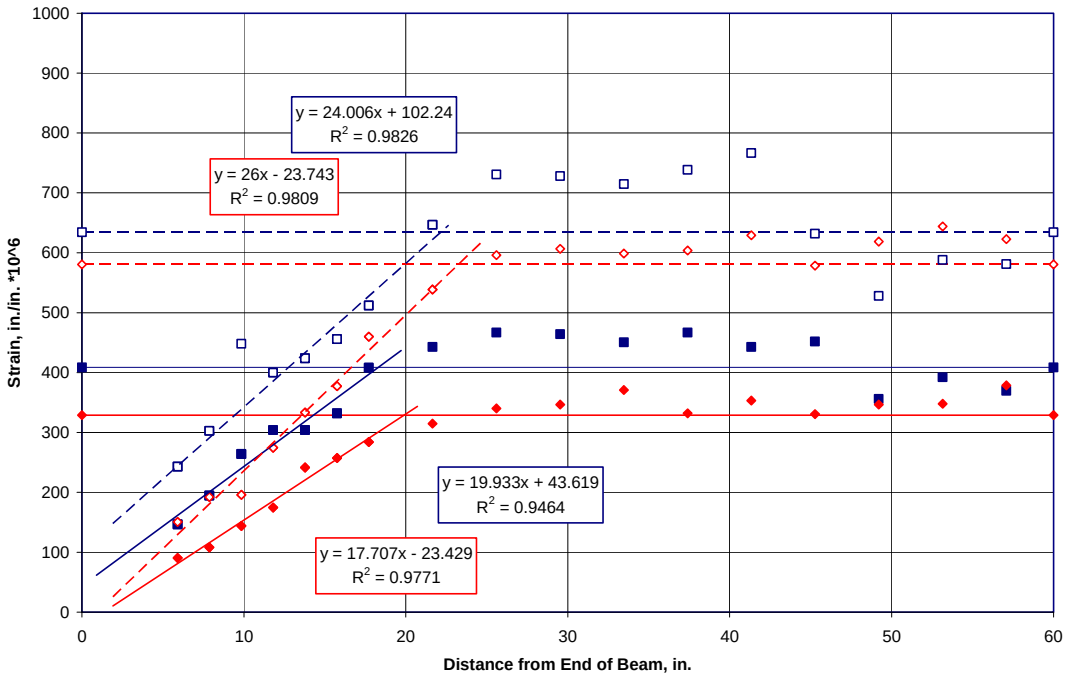

Figure B.116. Pour 4 Strand H Dead End Surface Strains

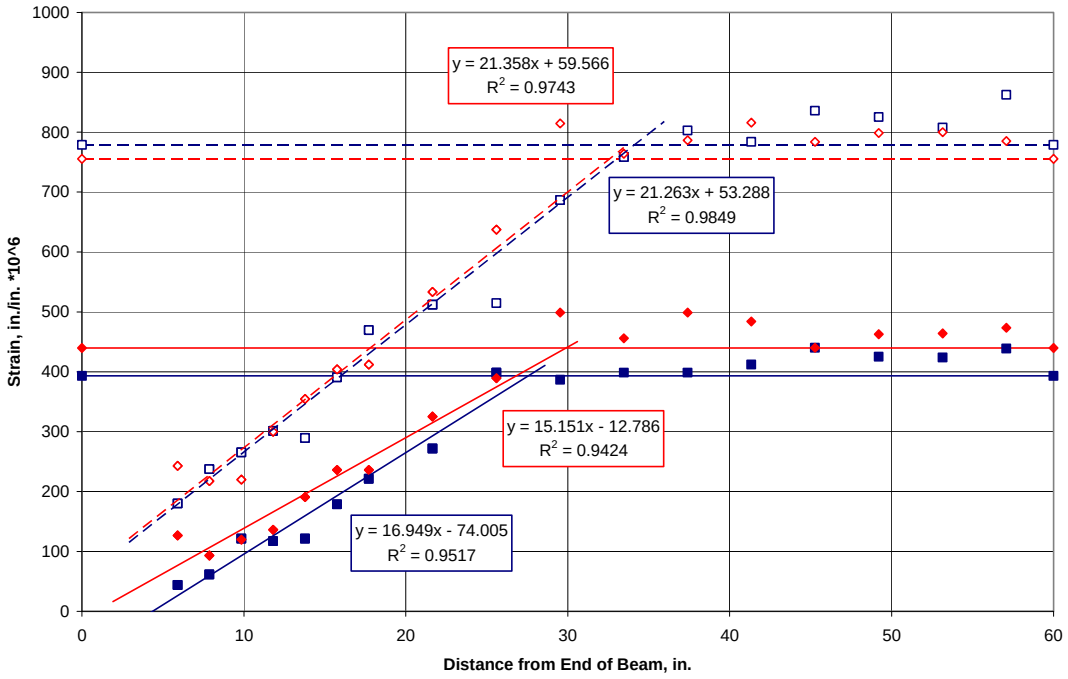

Figure B.117. Pour 4 Strand I Live End Surface Strains

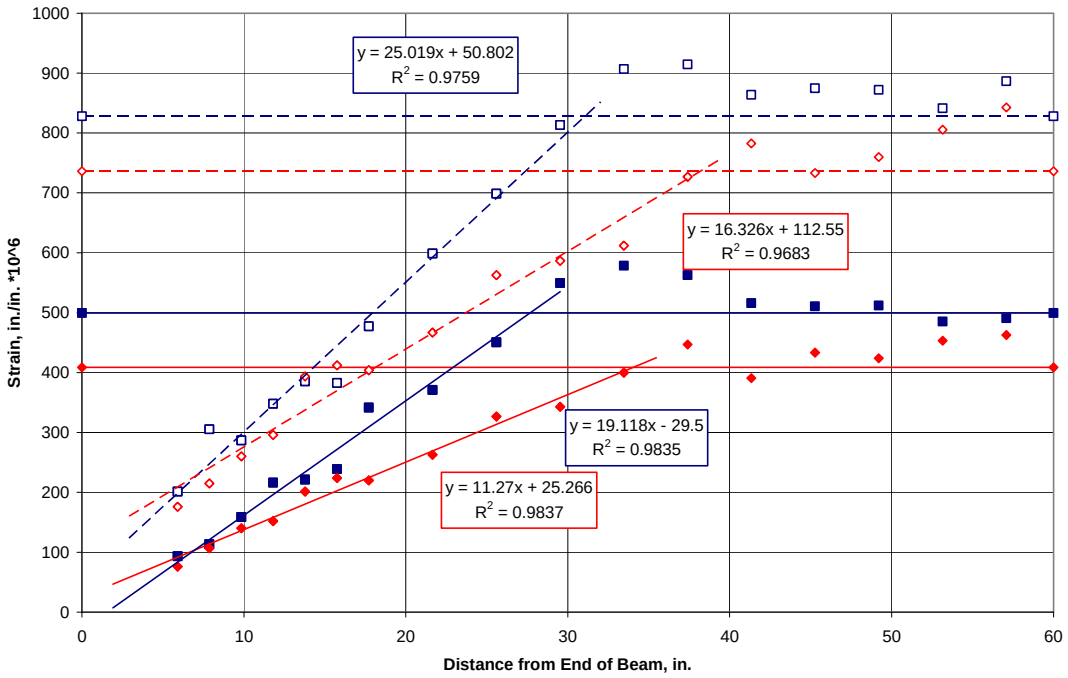

Figure B.118. Pour 4 Strand I Dead End Surface Strains

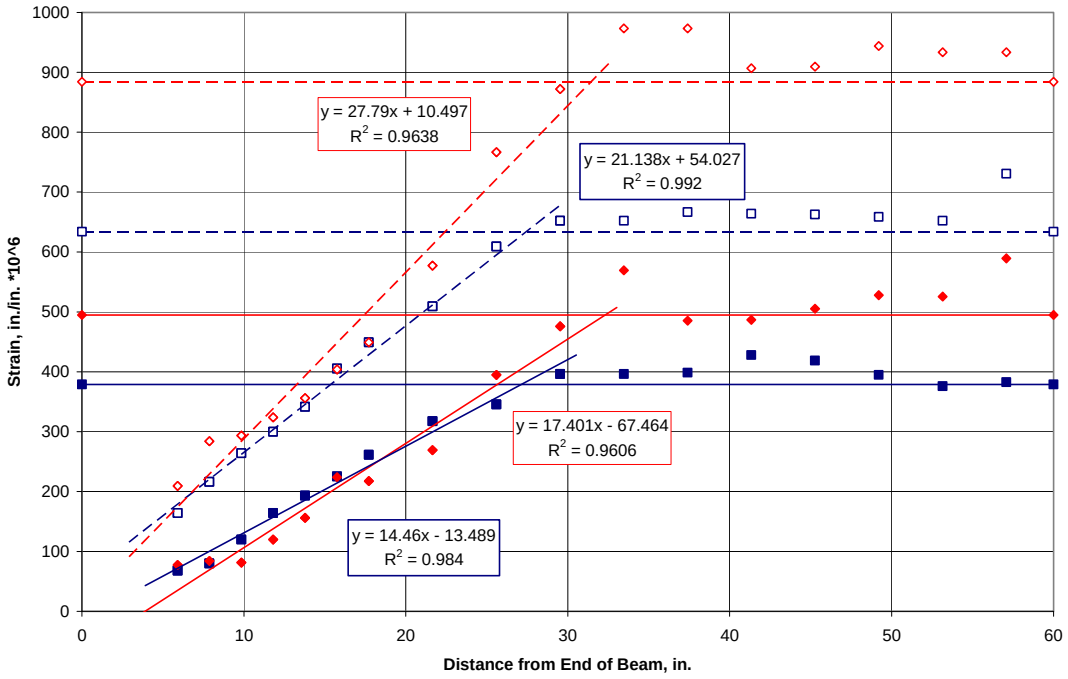

Figure B.119. Pour 4 Strand J Live End Surface Strains

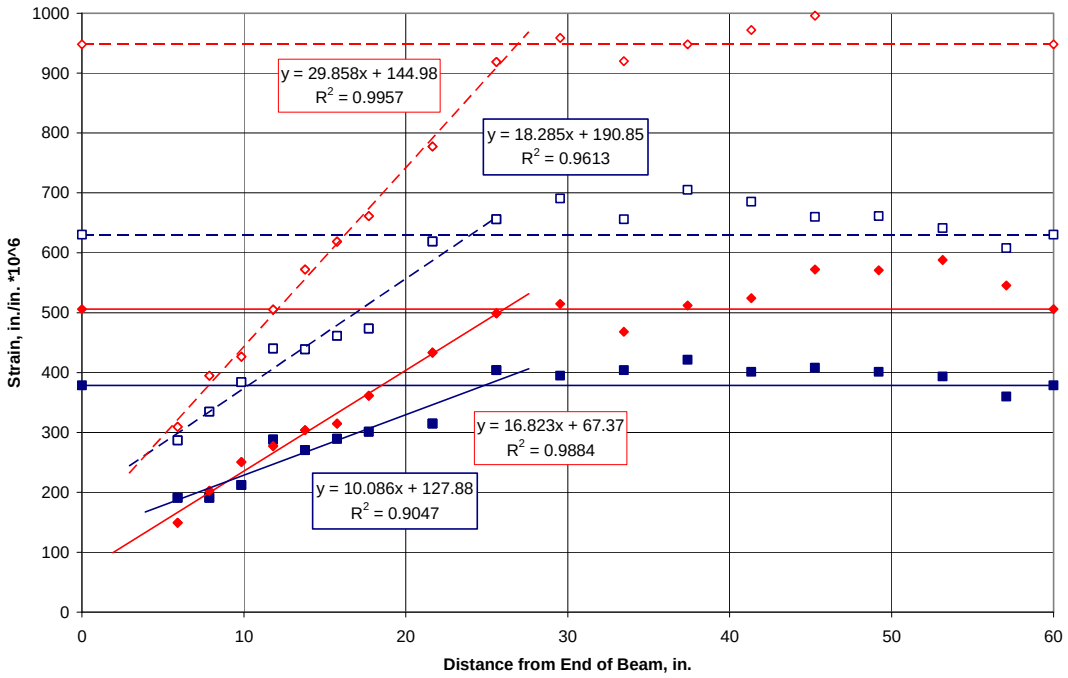

Figure B.120. Pour 4 Strand J Dead End Surface Strains

APPENDIX C

Moment versus Deflection and End-slip Plots

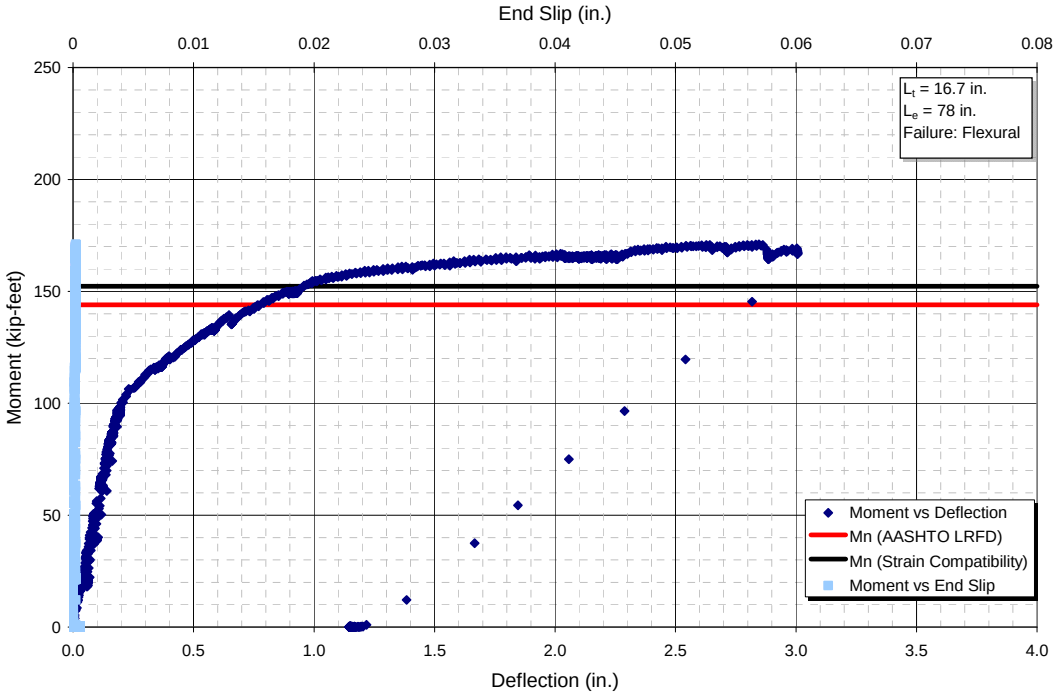

Figure C.1. 1.270.5N.RA

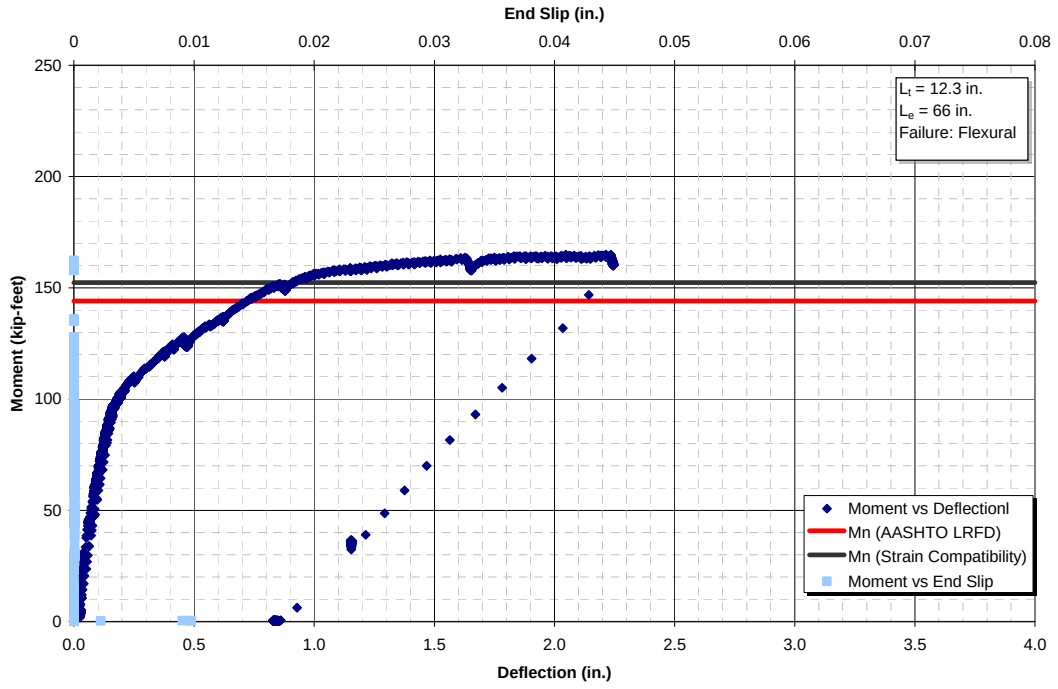

Figure C.1. 1.270.5N.RB

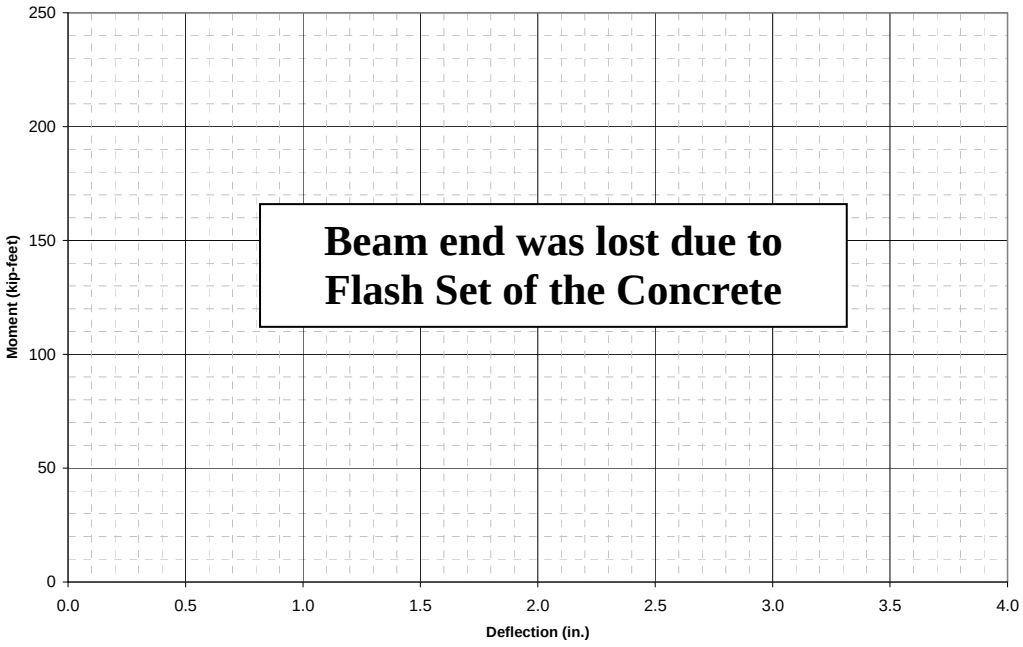

Figure C.3. 1.300.5N.RA

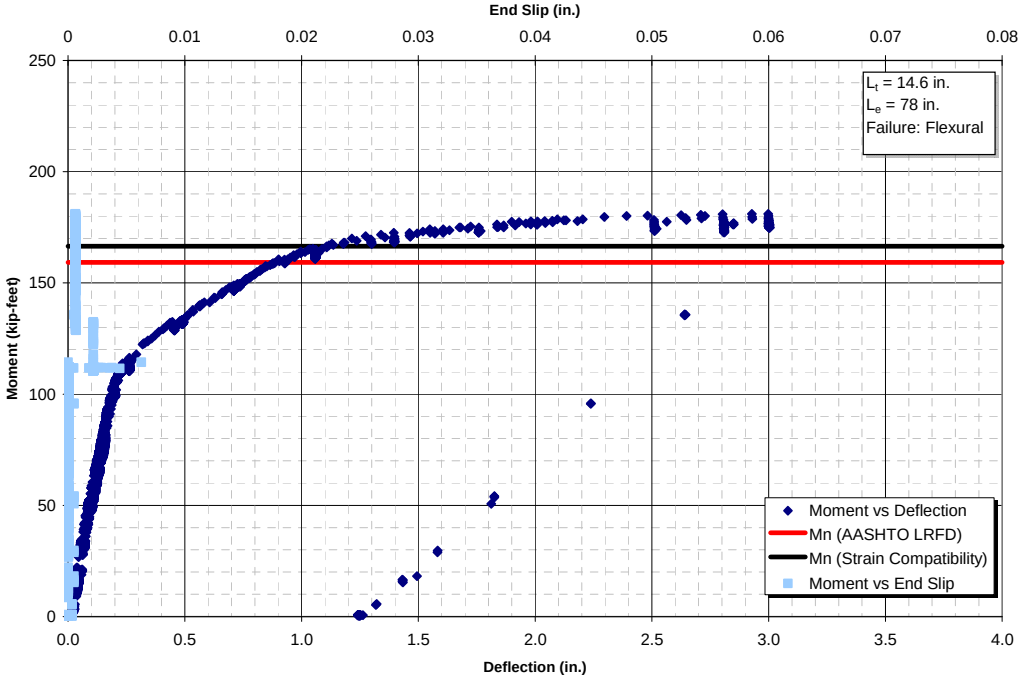

Figure C.4. 1.300.5N.RB

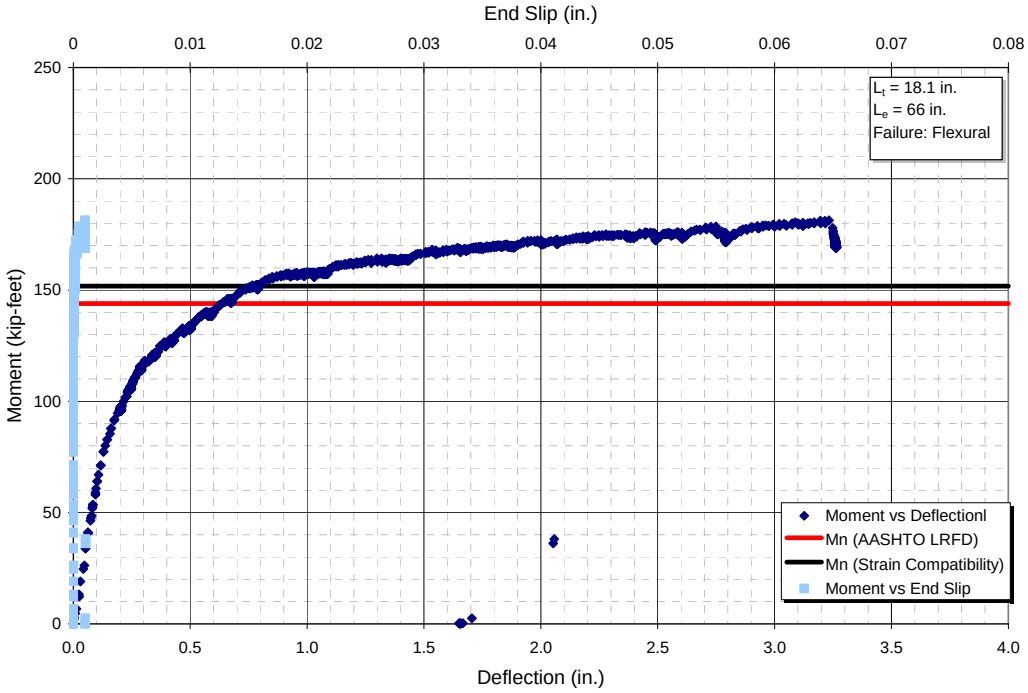

Figure C.5. 2.270.5N.RA

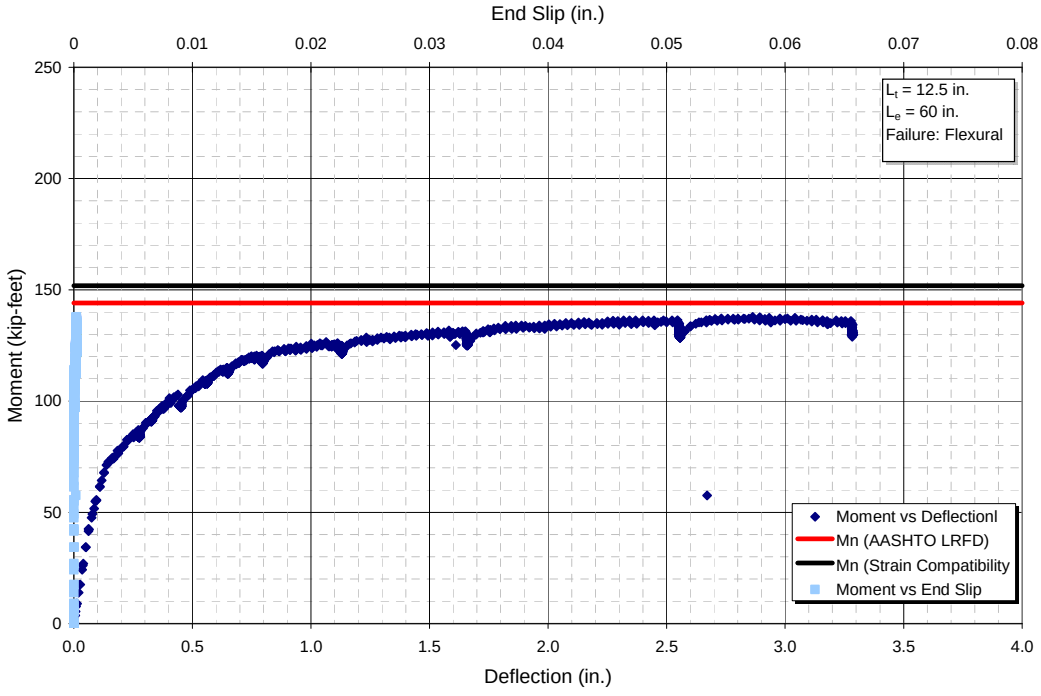

Figure C.6. 2.270.5N.RB

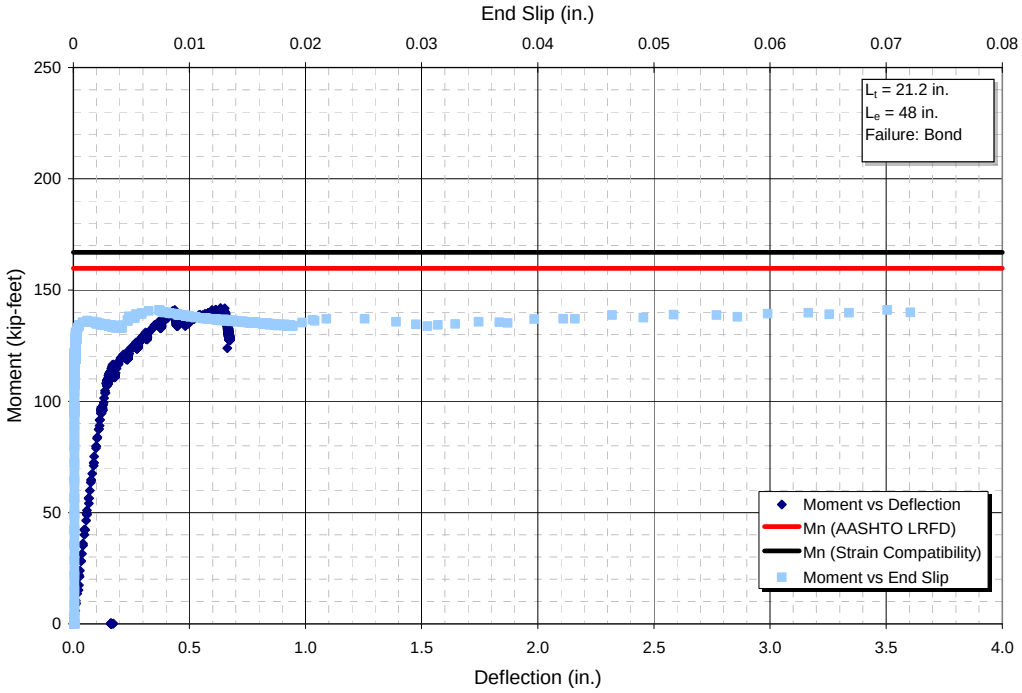

Figure C.7. 2.300.5N.RA

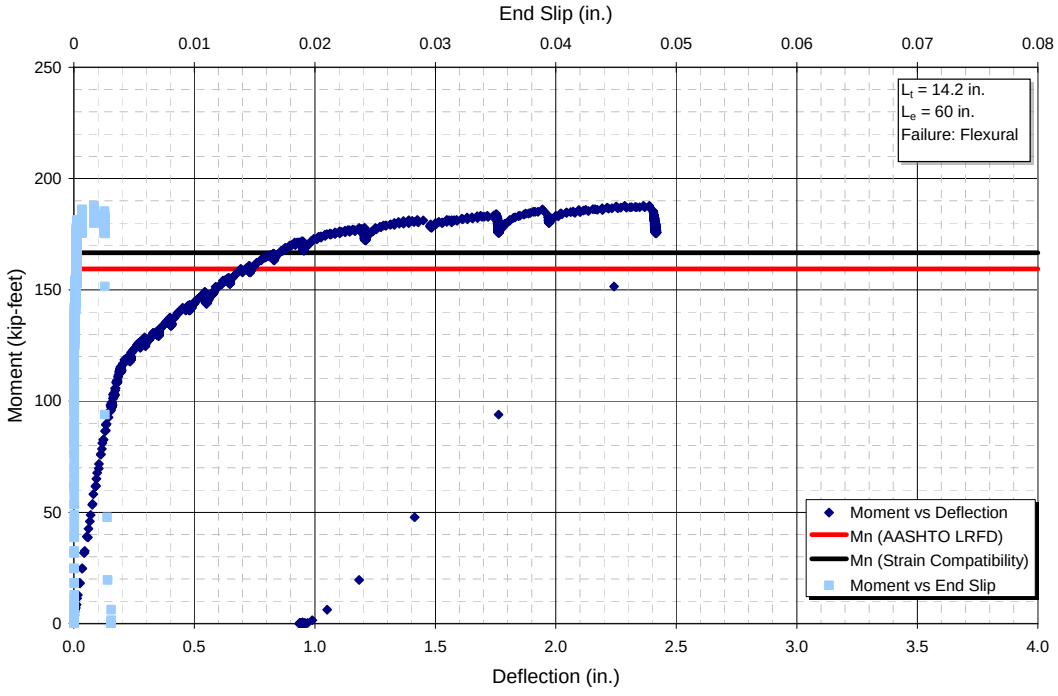

Figure C.8. 2.300.5N.RB

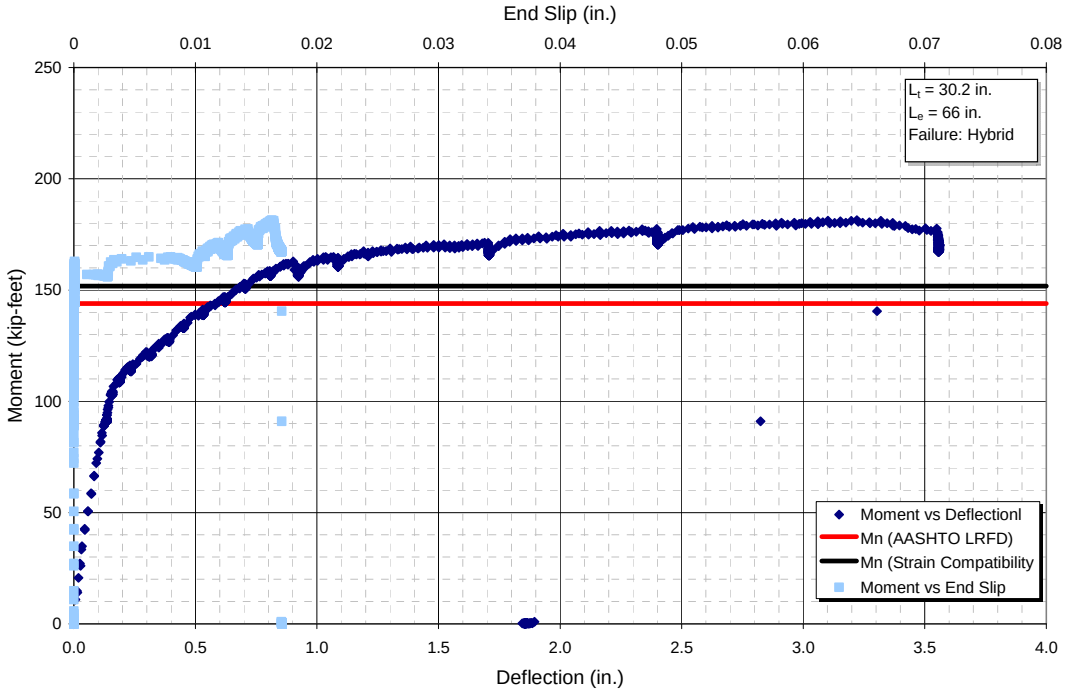

Figure C.9. 2.270.5N.UA

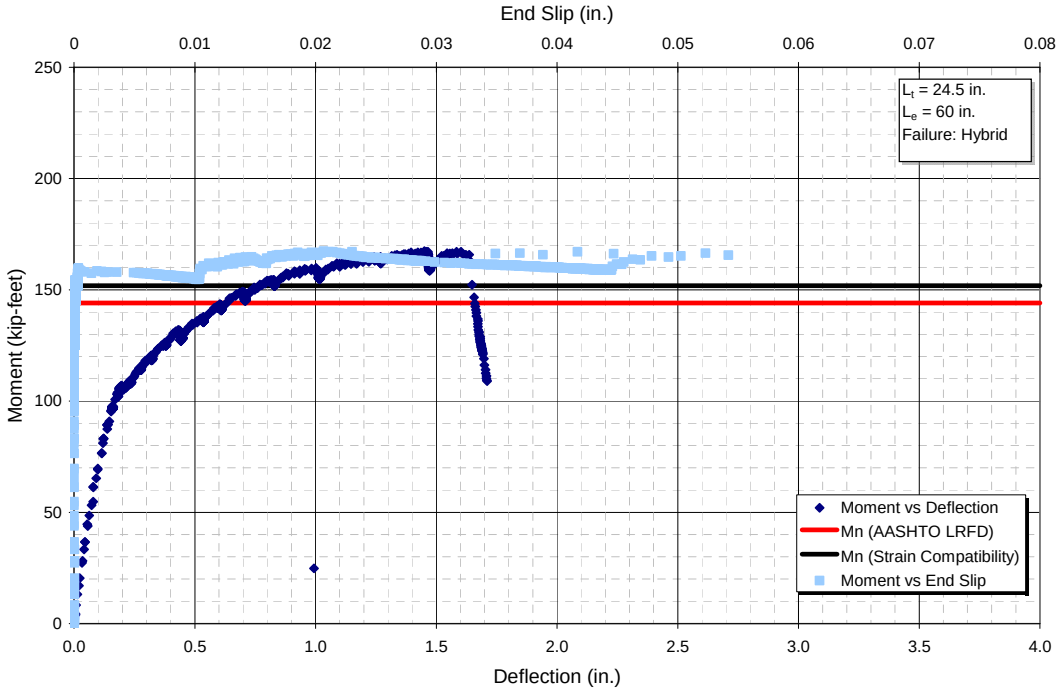

Figure C.10. 2.270.5N.UB

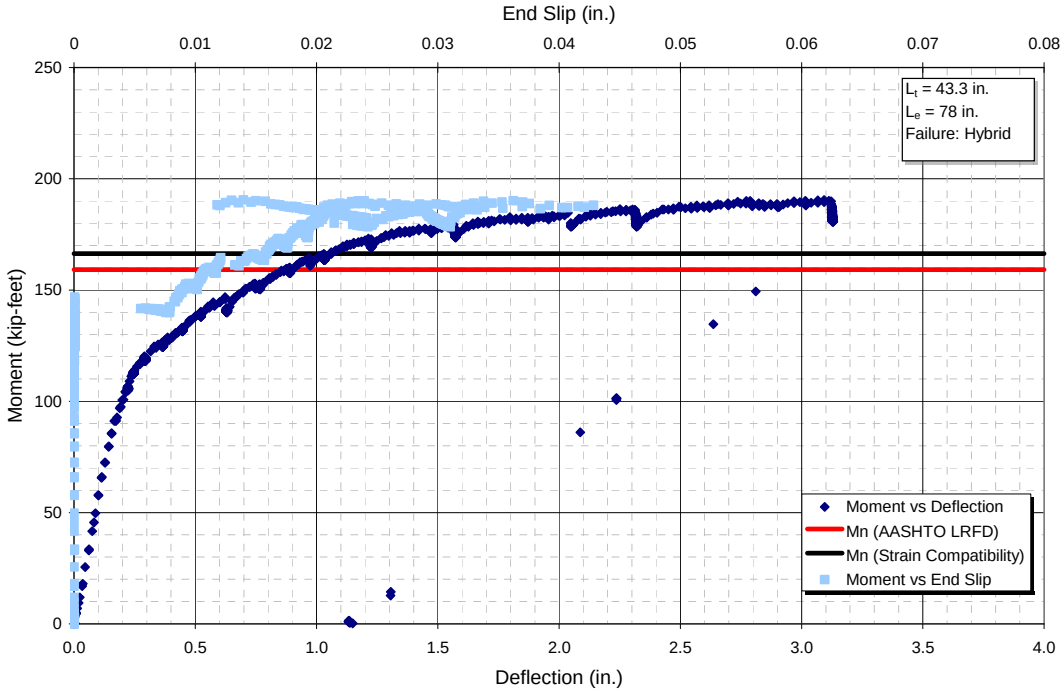

Figure C.11. 2.300.5N.UA

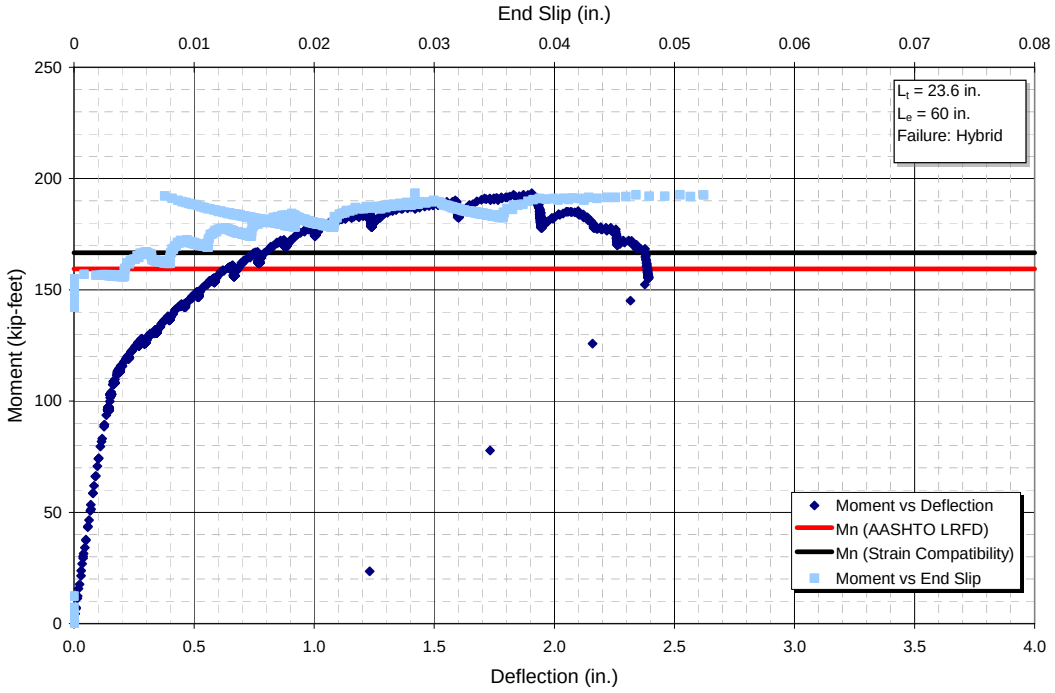

Figure C.12. 2.300.5N.UB

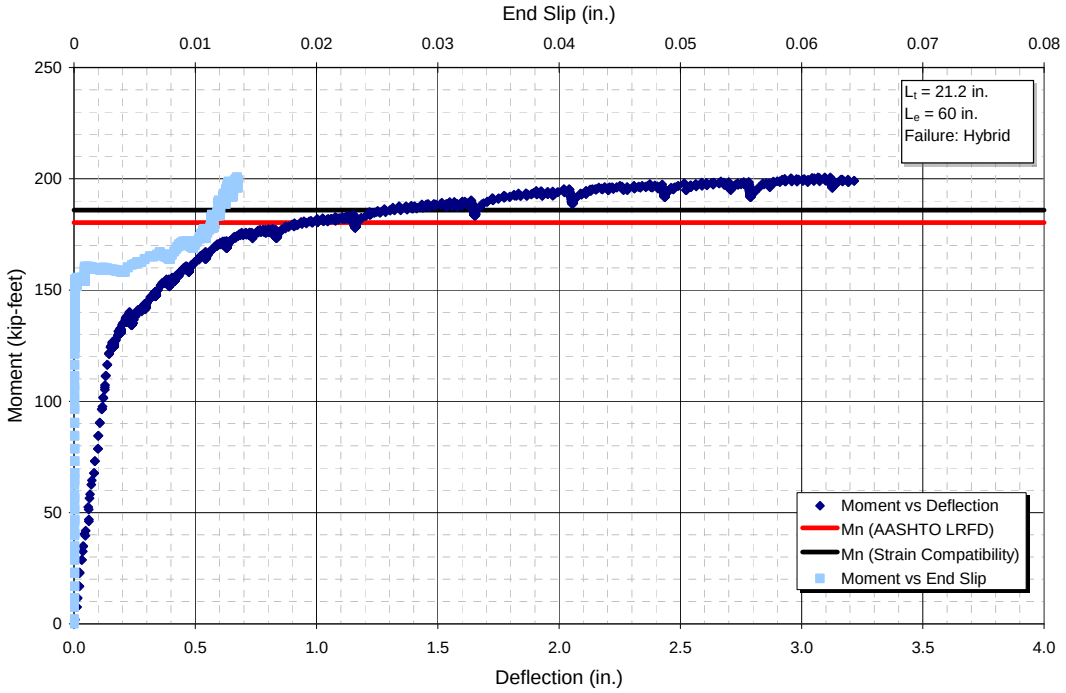

Figure C.13. 3.270.5S.RA

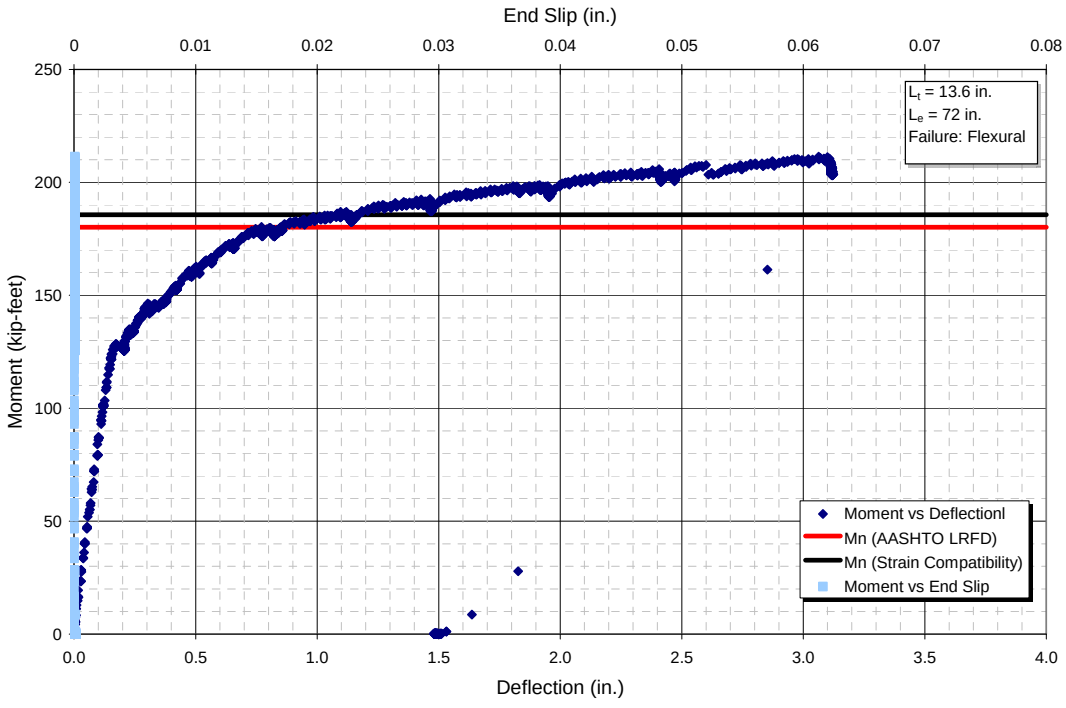

Figure C.14. 3.270.5S.RB

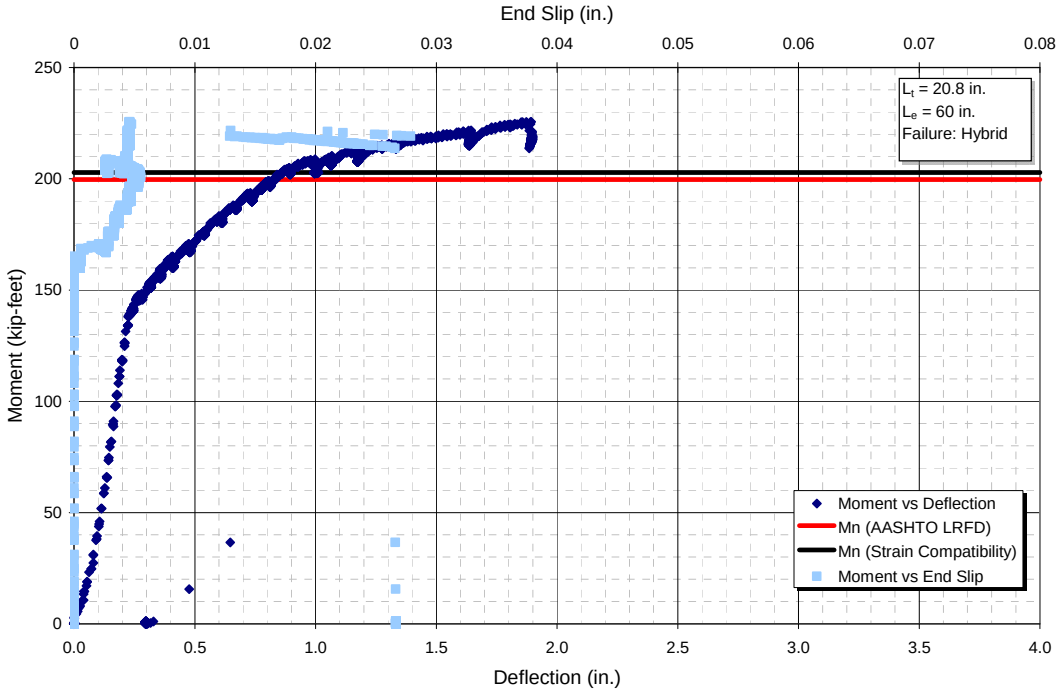

Figure C.15. 3.300.5S.RA

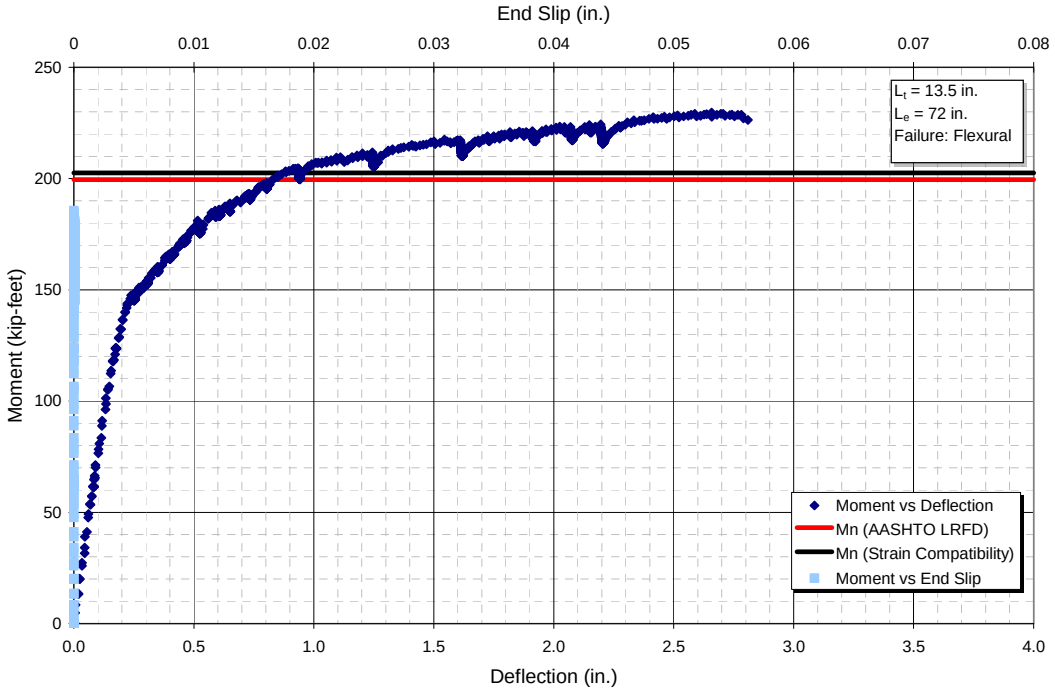

Figure C.16. 3.300.5S.RB

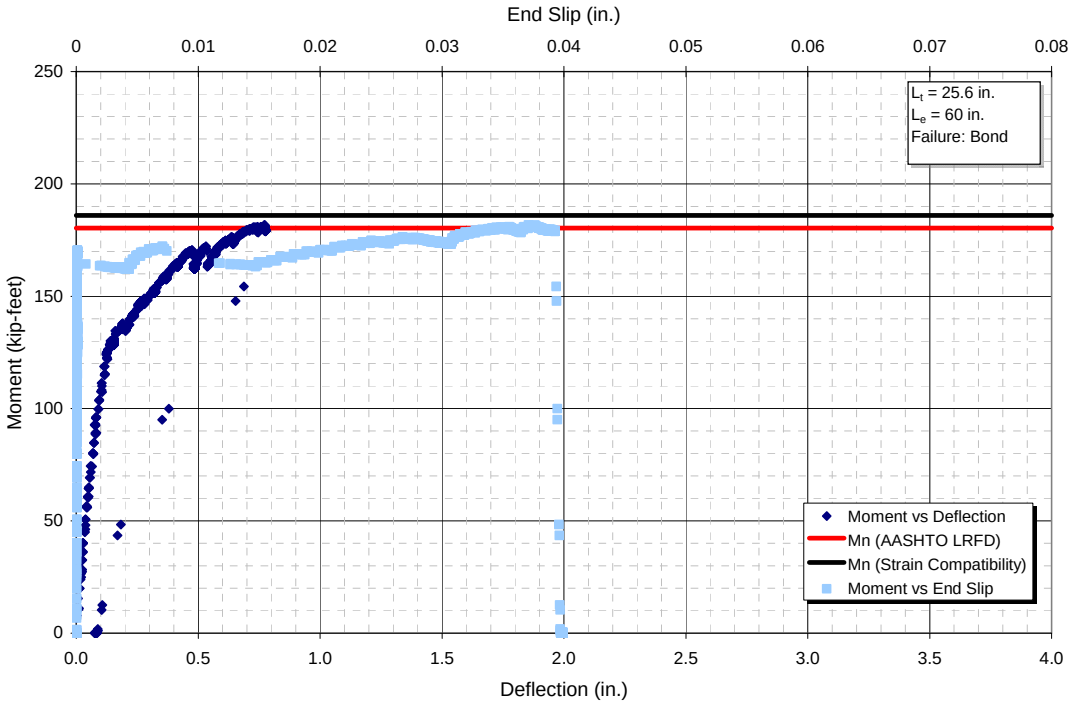

Figure C.17. 3.270.5S.UA

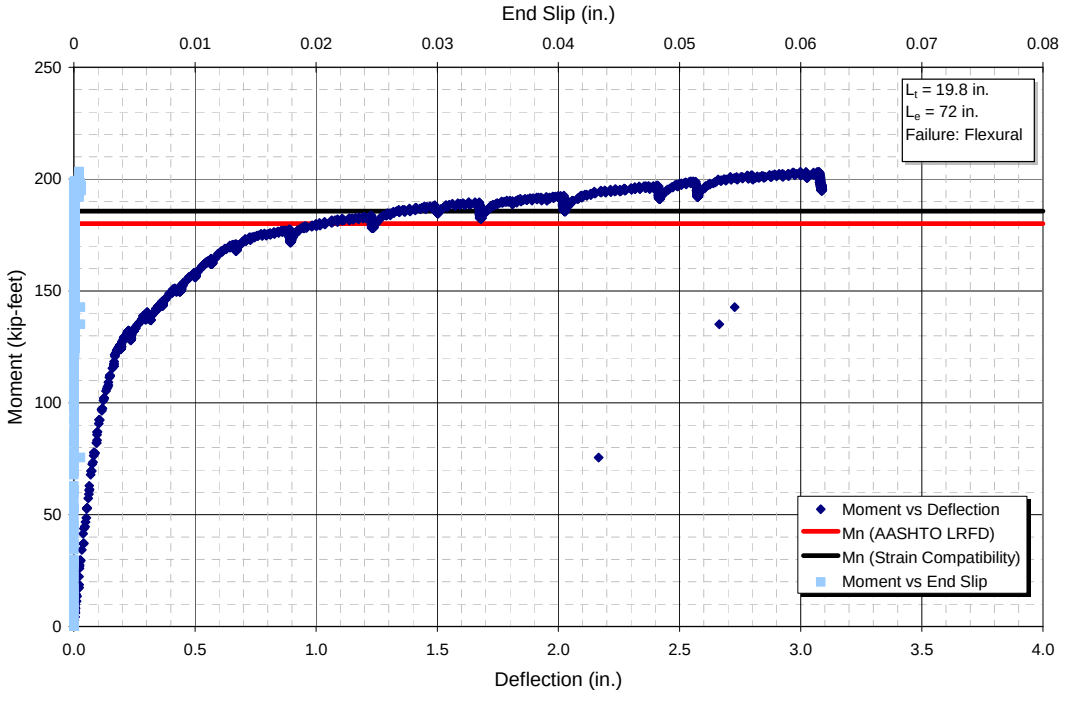

Figure C.18. 3.270.5S.UB

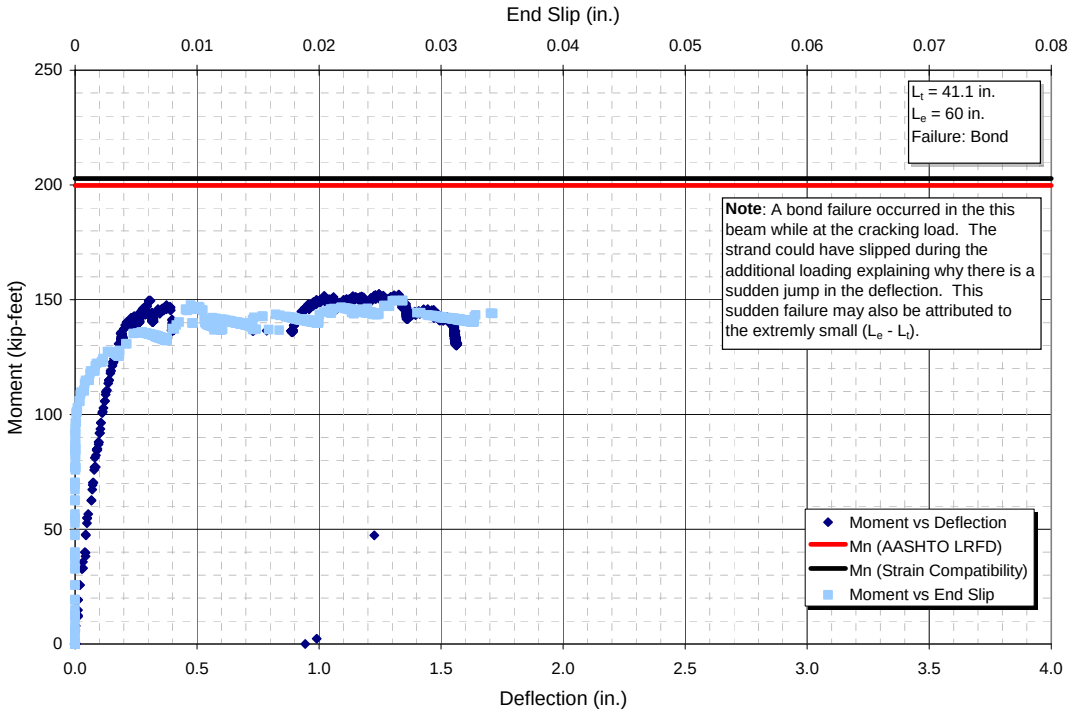

Figure C.19. 3.300.5S.UA

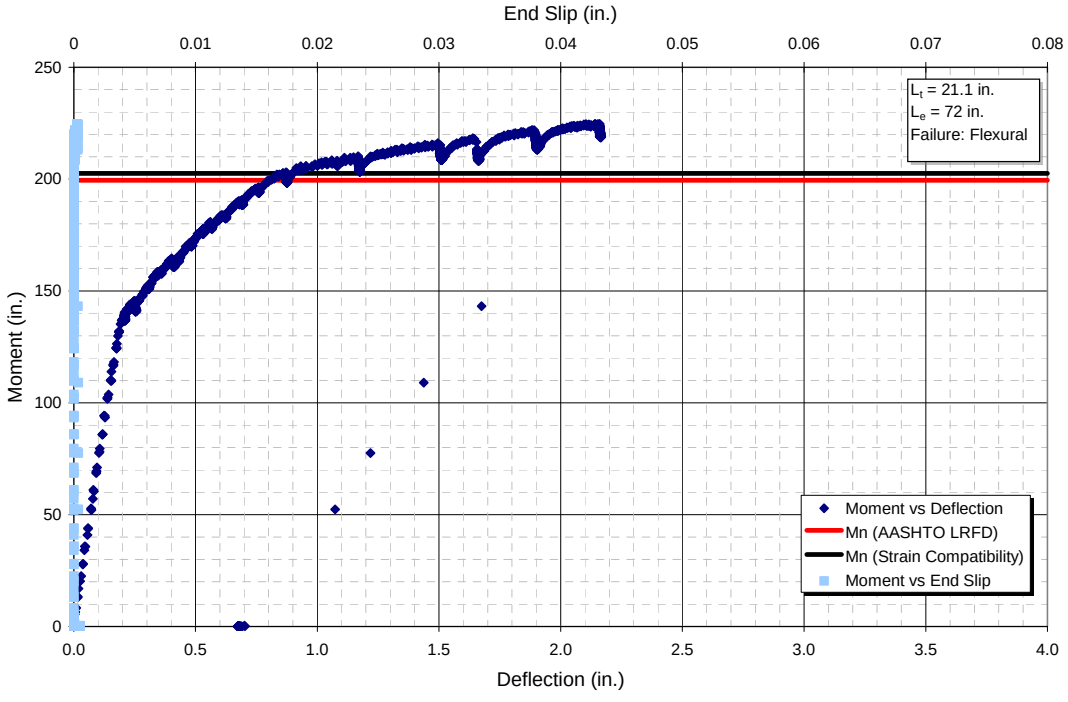

Figure C.20. 3.300.5S.UB

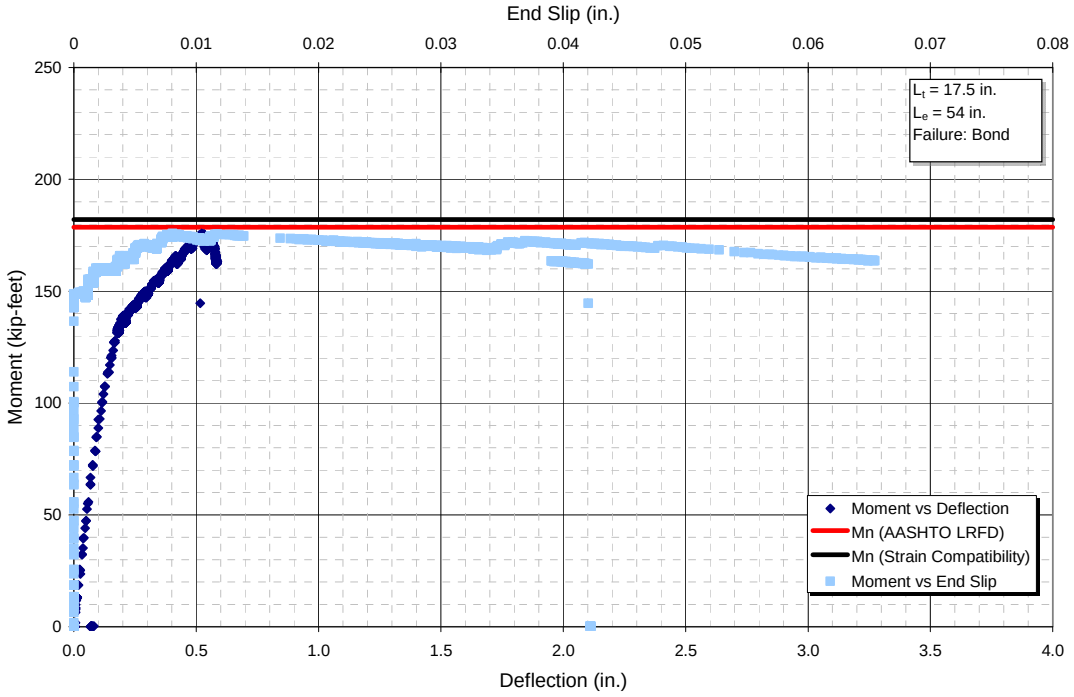

Figure C.21. 4.270.5S.RA

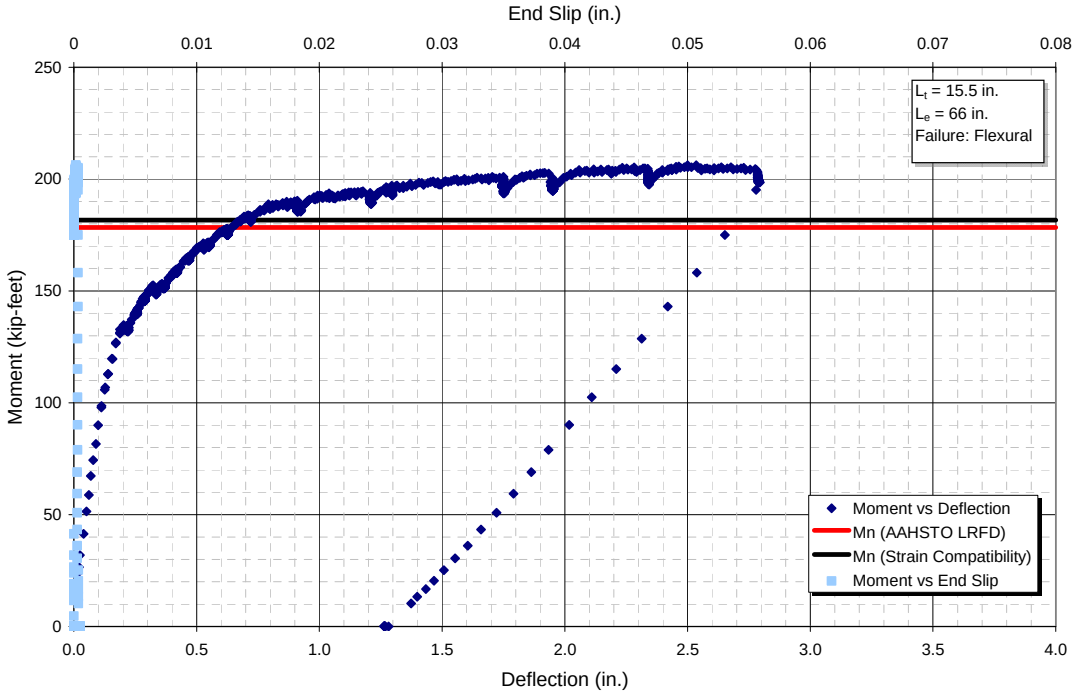

Figure C.22. 4.270.5S.RB

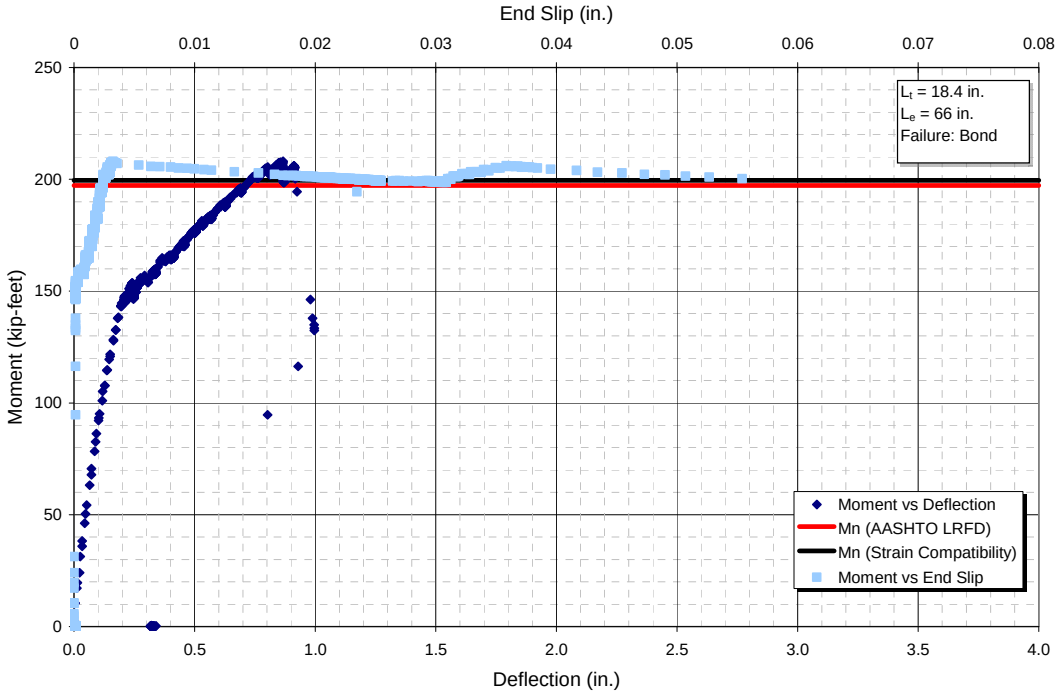

Figure C.23. 4.300.5S.RA

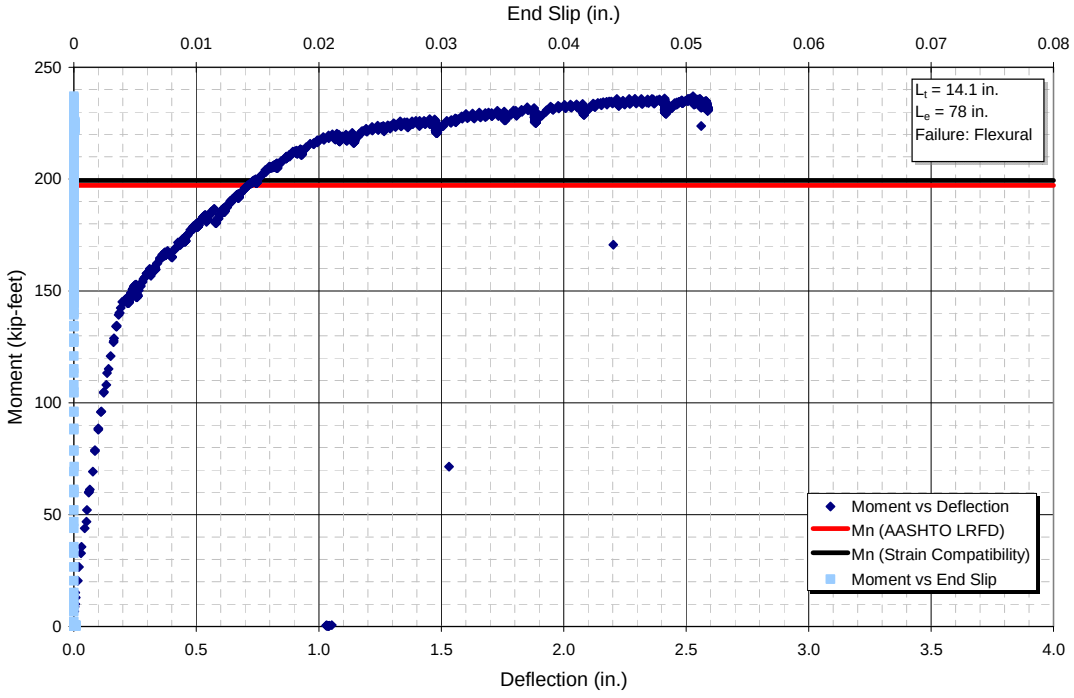

Figure C.24. 4.300.5S.RB

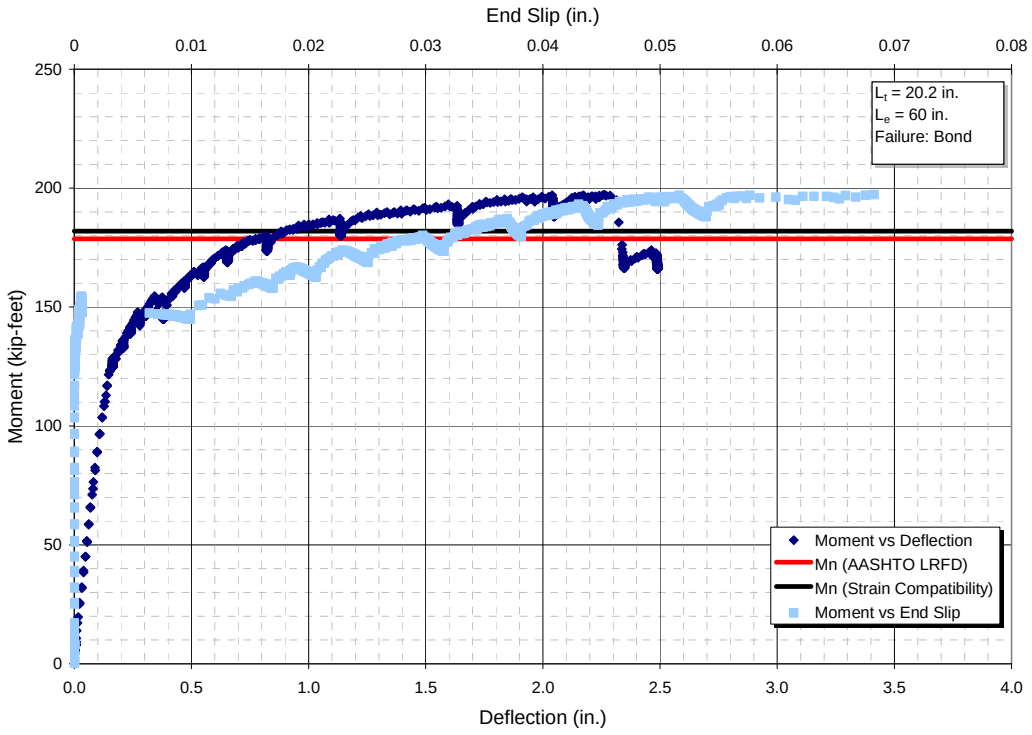

Figure C.25. 5.270.5S.RA

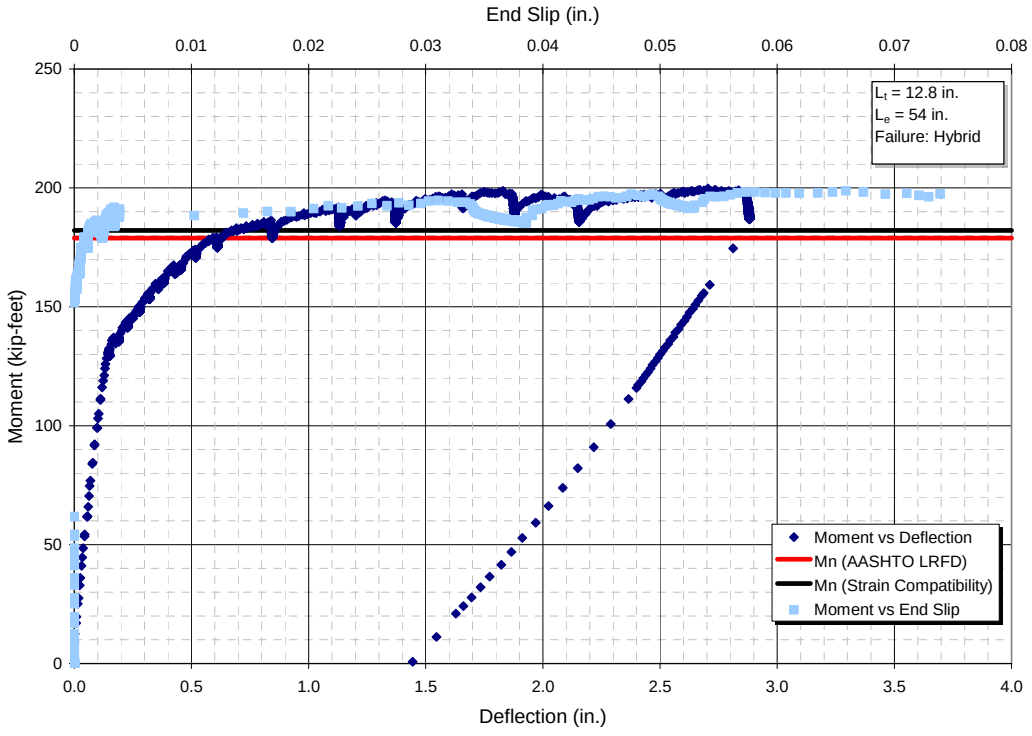

Figure C.26. 5.270.5S.RB

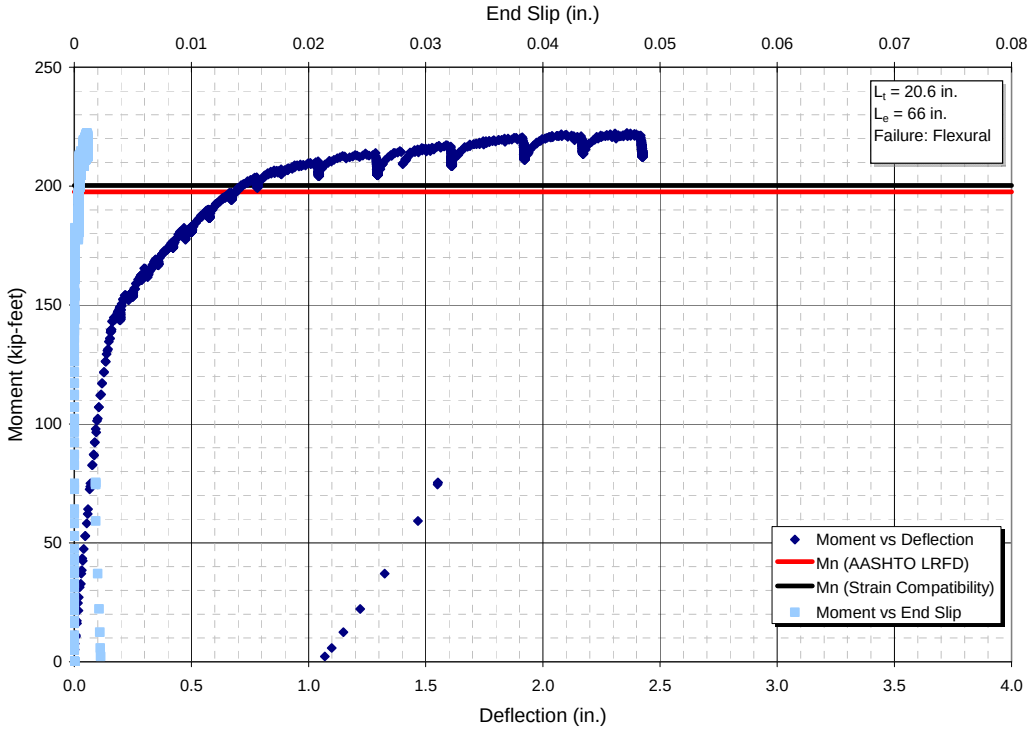

Figure C.27. 5.300.5S.RA

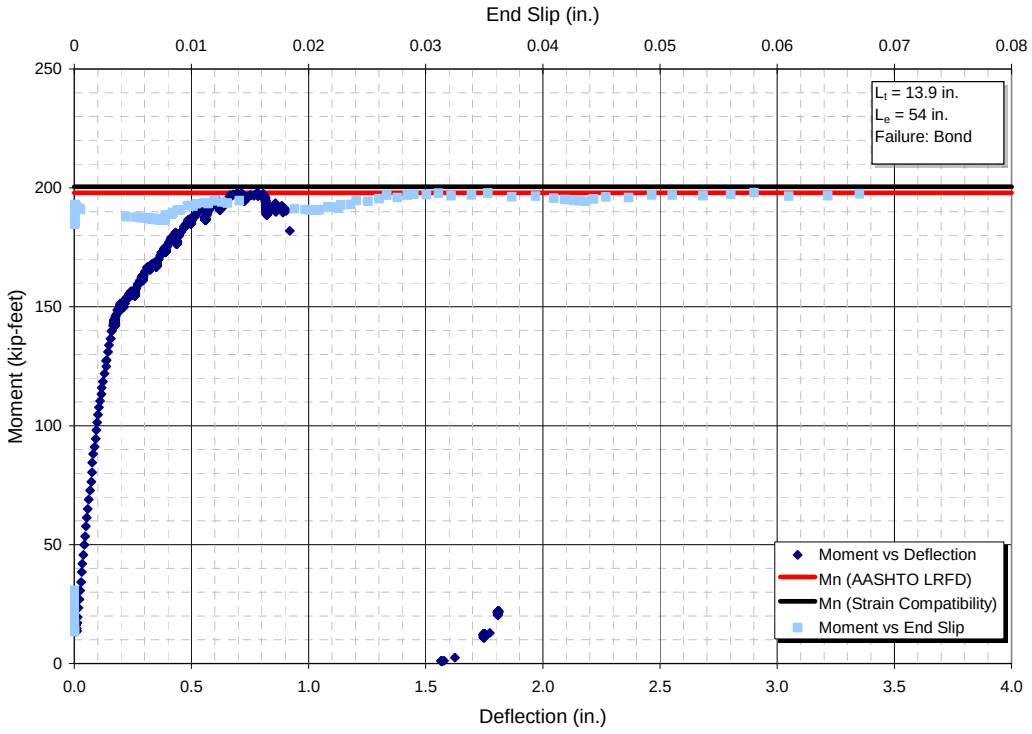

Figure C.28. 5.300.5S.RB

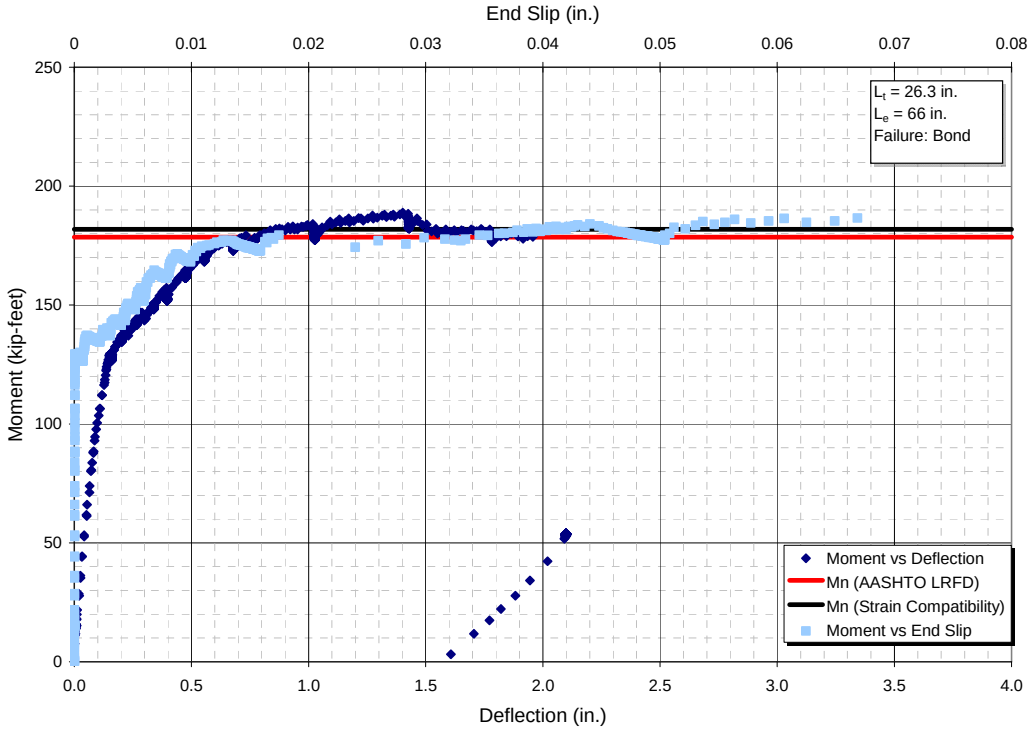

Figure C.29. 5.270.5S.UA

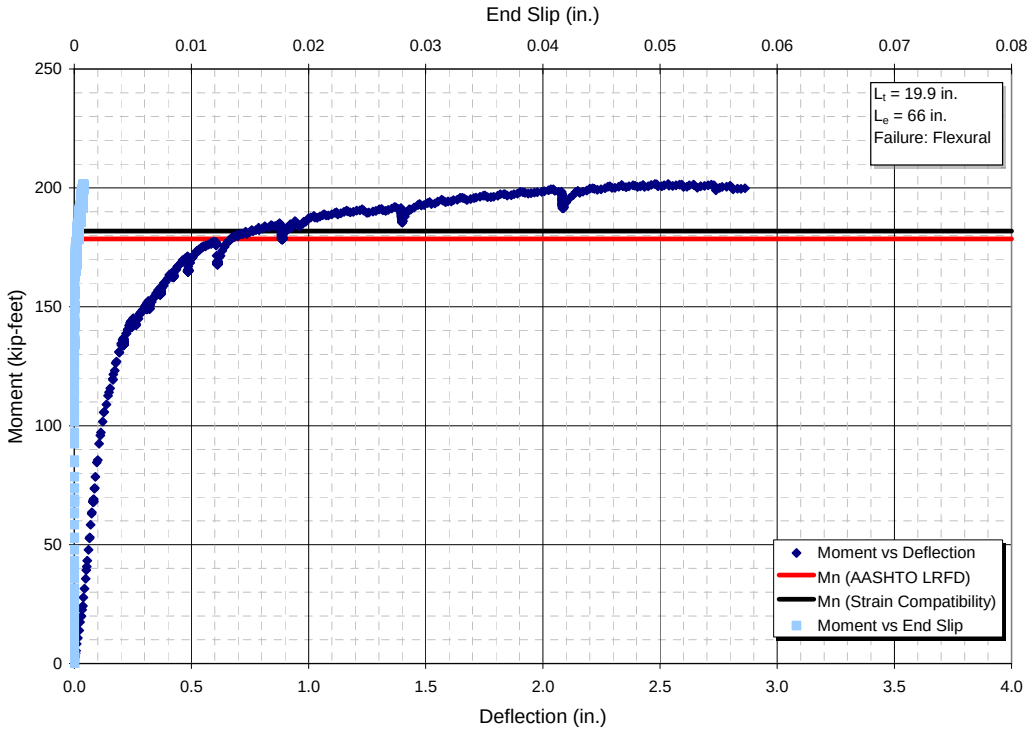

Figure C.30. 5.270.5S.UB

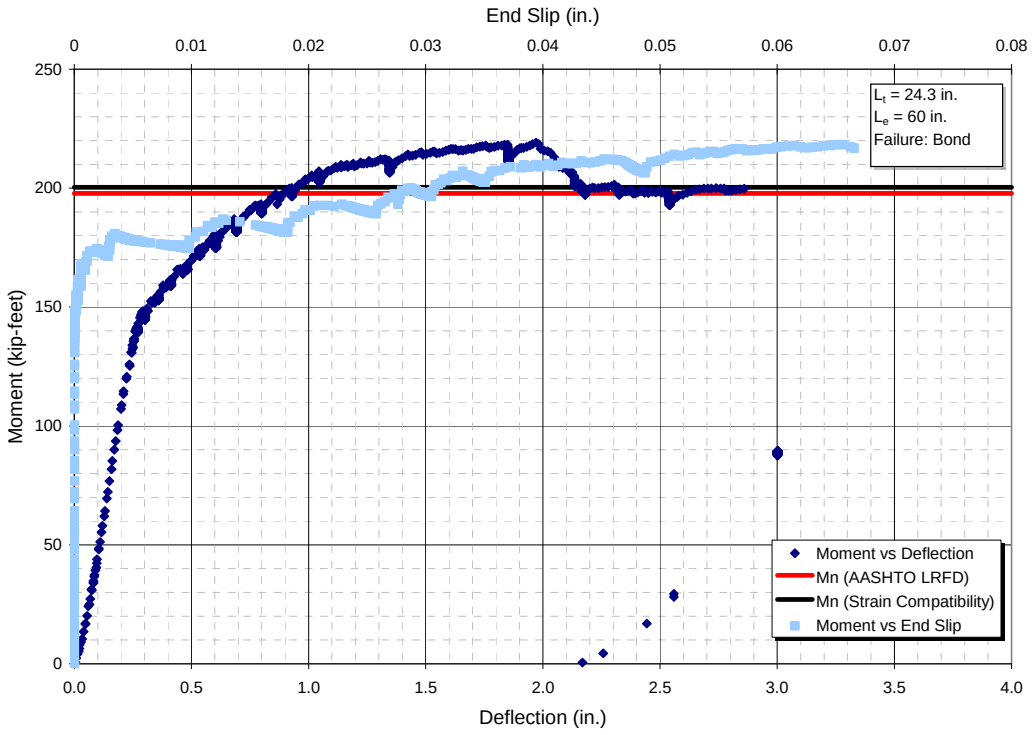

Figure C.31. 5.300.5S.UA

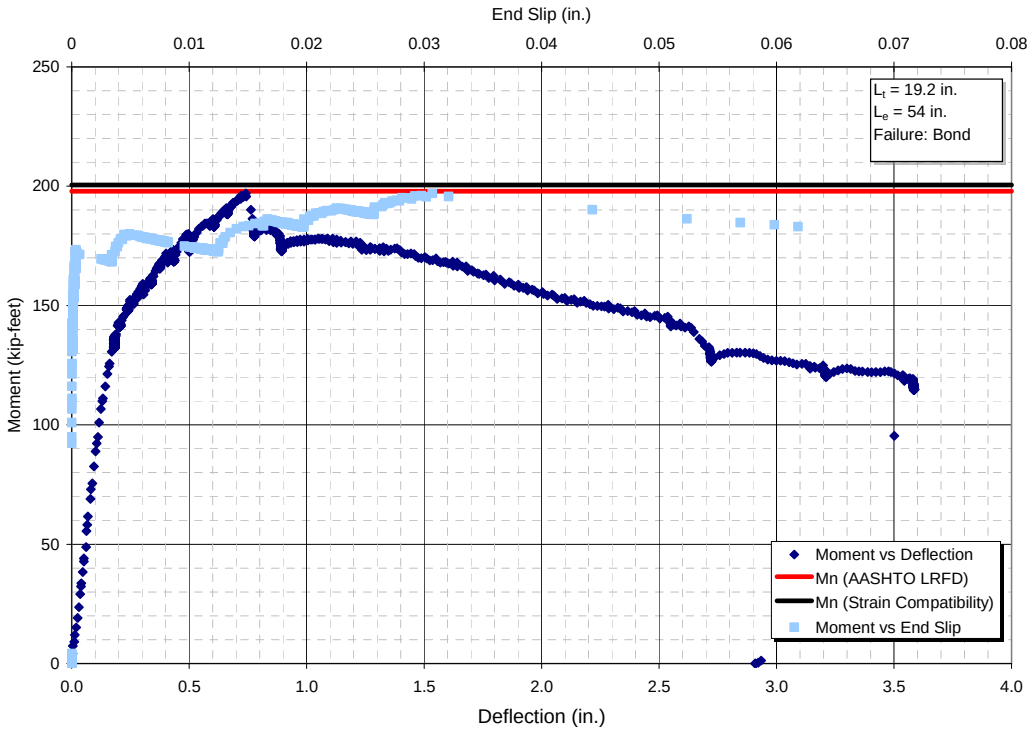

Figure C.32. 5.300.5S.UB

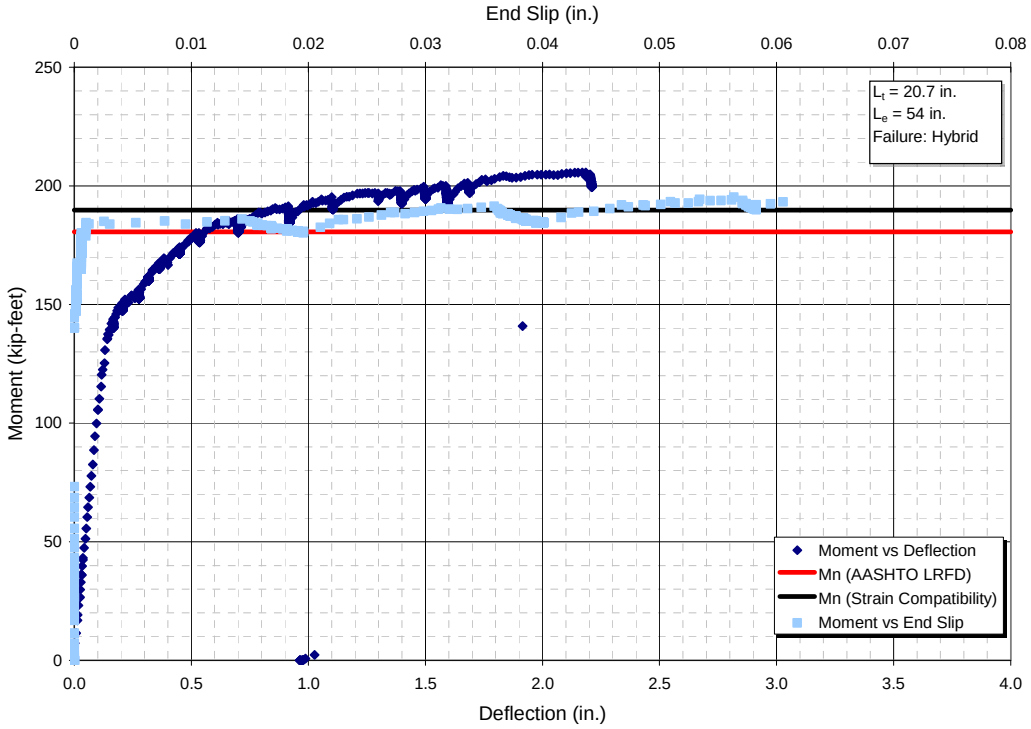

Figure C.33. 6.270.5S.RA

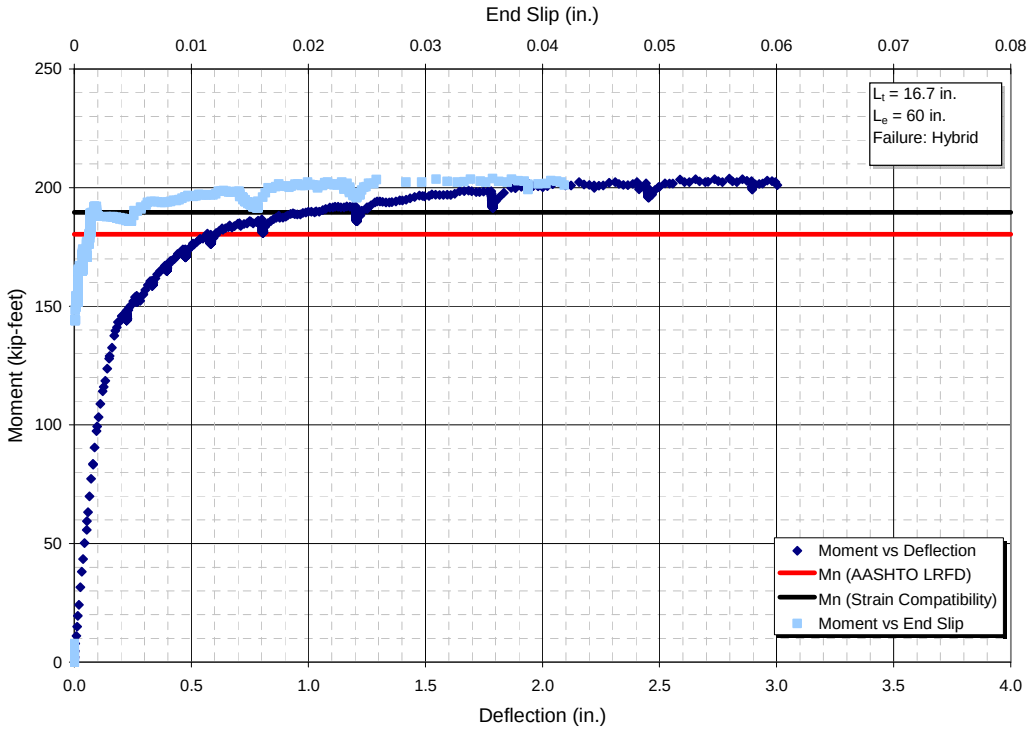

Figure C.34. 6.270.5S.RB

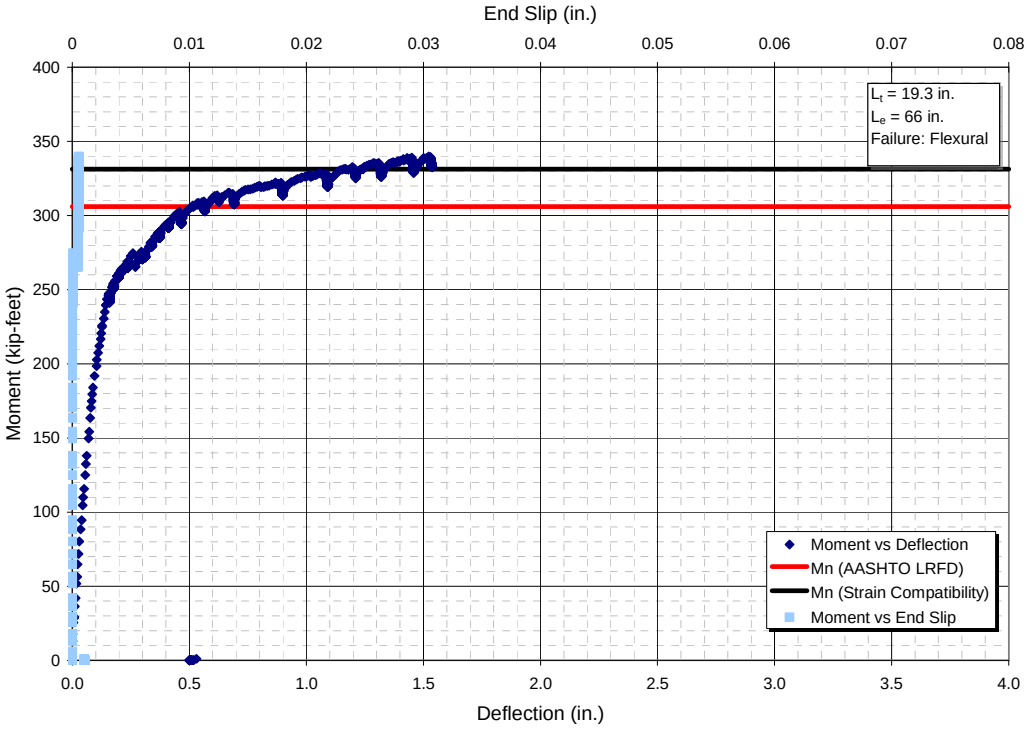

Figure C.35. 6.270.6N.RA

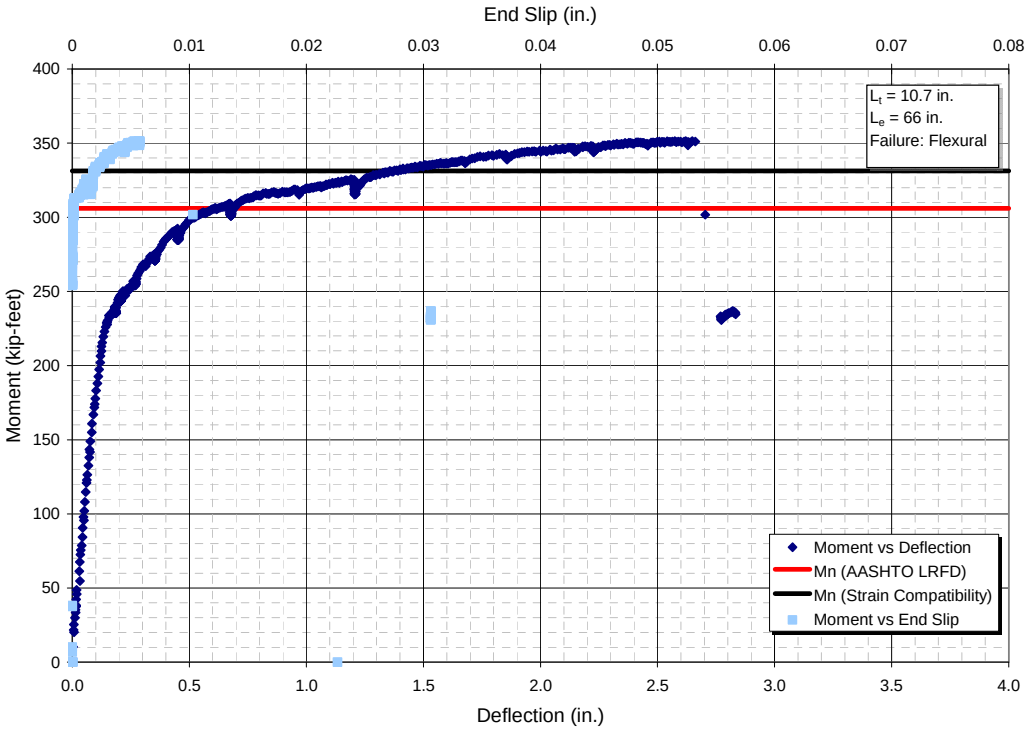

Figure C.36. 6.270.6N.RB

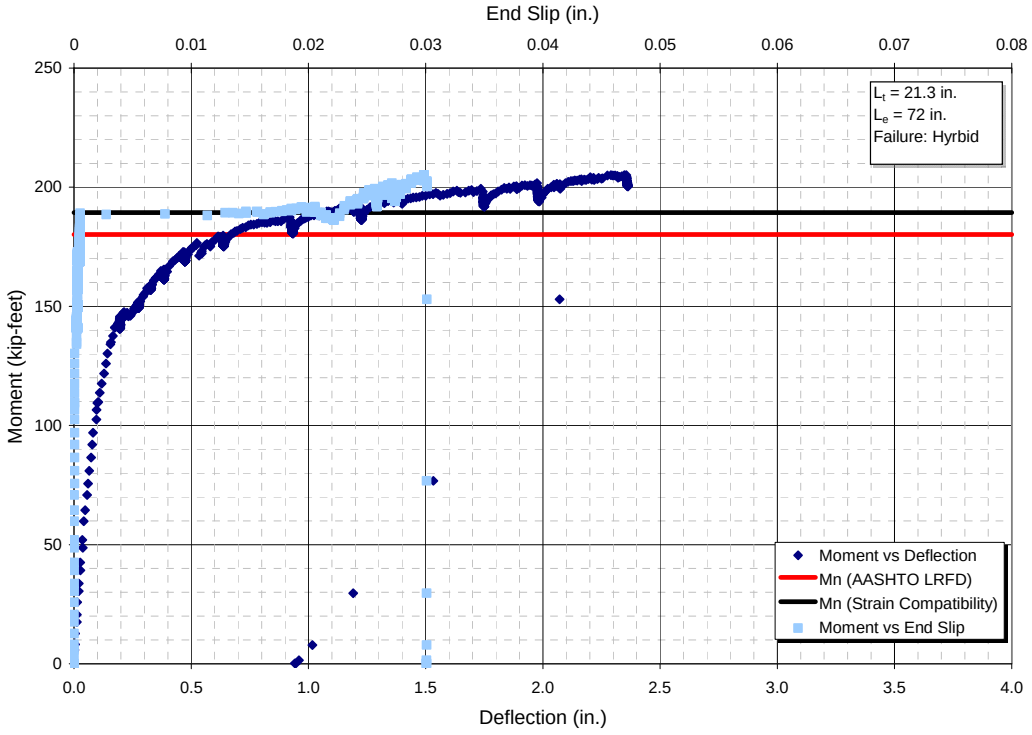

Figure C.37. 6.270.5S.UA

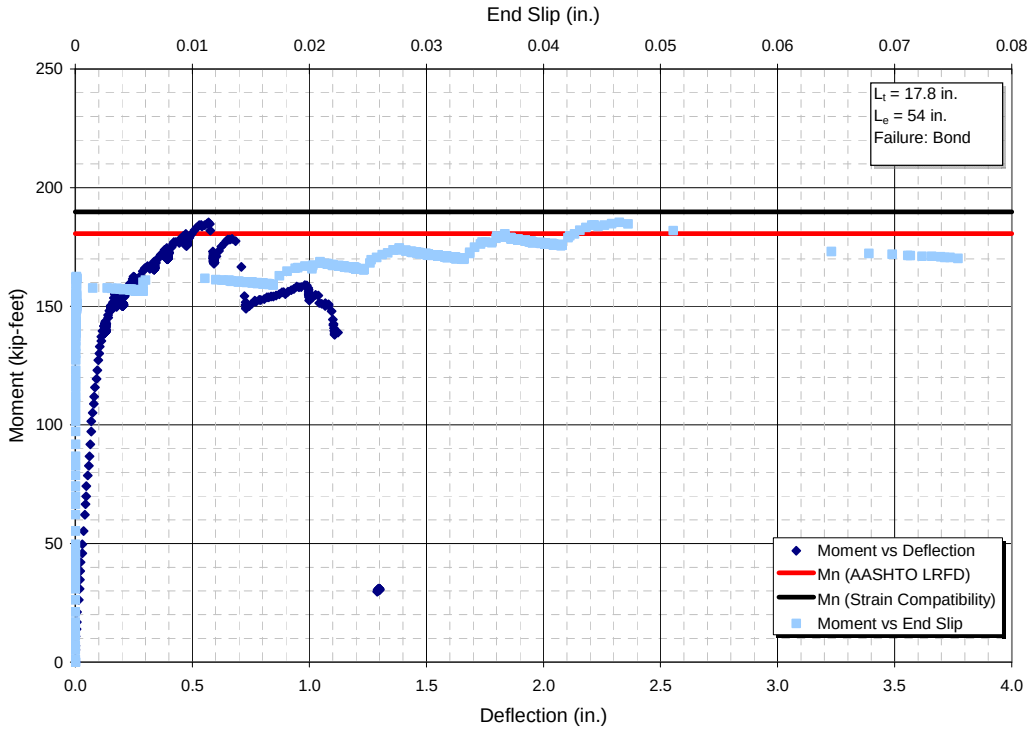

Figure C.38. 6.270.5S.UB

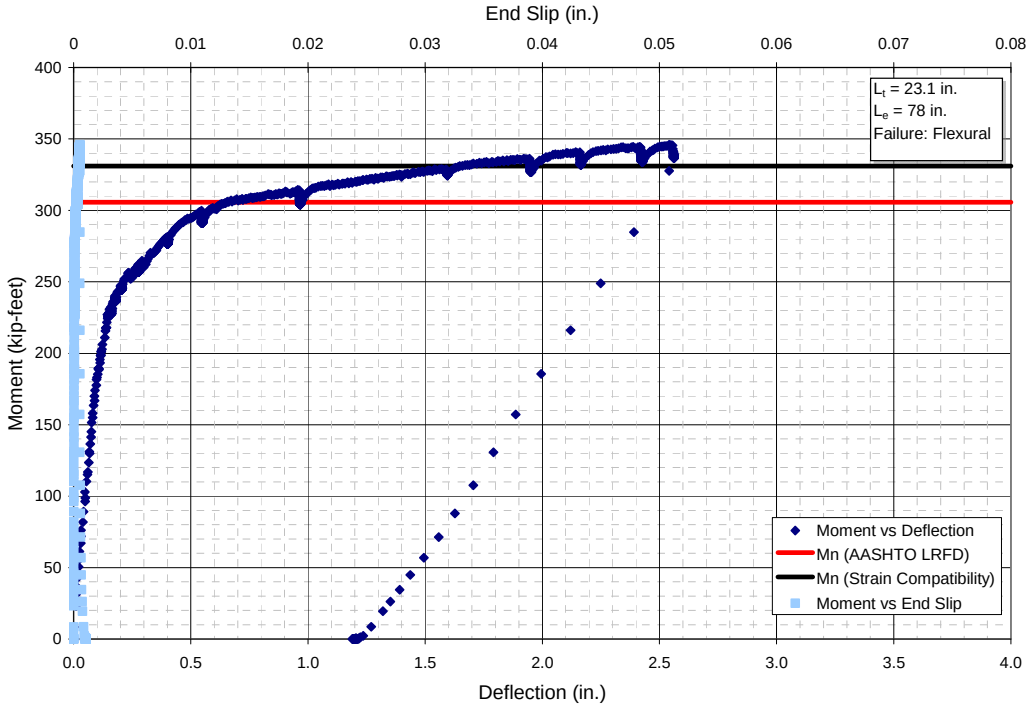

Figure C.39. 6.270.6N.UA

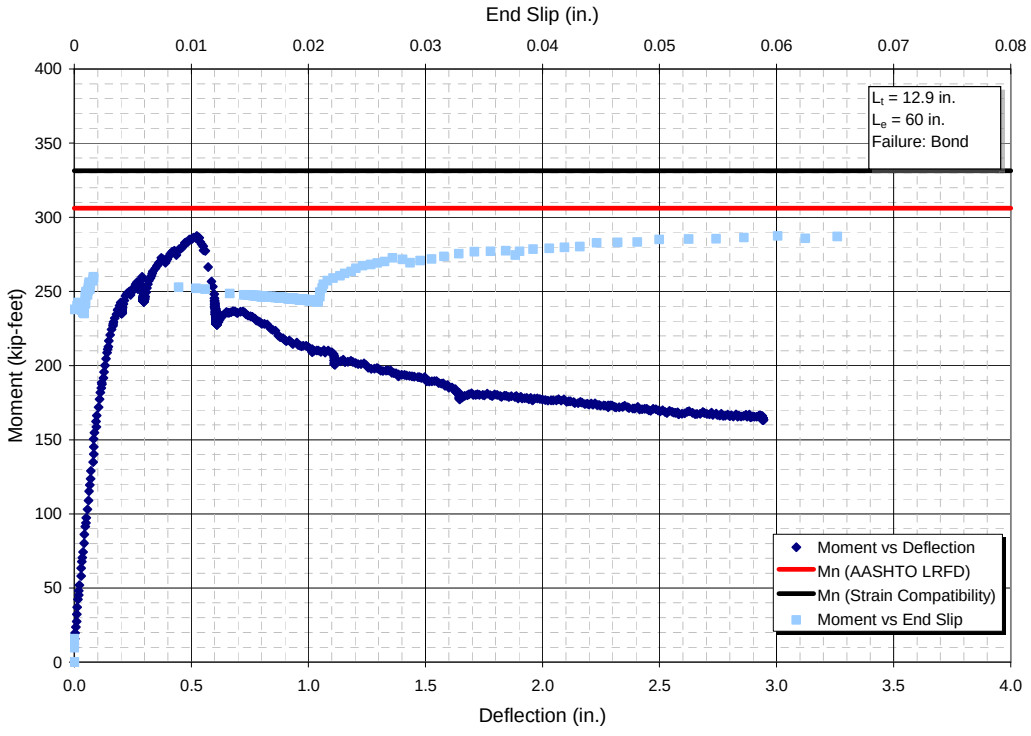

Figure C.40. 6.270.6N.UB

APPENDIX D

Additional Tables

Table D.1. Influence of Time (TSB-Pour 11)

	Strand	f_{sj} ksi	f_{si} ksi	f_{se} ksi	f'_{ci} psi	f'_c psi	Transfer Length (in.) Initial	Last	L/I
Live	A	202.50	188.72	178.00	4800	5900	21.15	22.81	1.08
	B	202.50	188.72	178.00	4800	5900	19.63	20.22	1.03
	C	202.50	188.72	178.00	4800	5900	18.30	19.71	1.08
	D	202.50	188.72	178.00	4800	5900	18.97	19.63	1.03
	E	202.50	188.72	178.00	4800	5900	18.77	20.38	1.09
	F	202.50	188.42	177.50	4800	5900	28.89	32.10	1.11
	G	202.50	188.42	177.50	4800	5900	25.73	30.24	1.18
	H	202.50	188.42	177.50	4800	5900	25.43	27.09	1.07
	I	202.50	186.65	174.64	4800	5900	23.74	24.05	1.01
	J	202.50	186.65	174.64	4800	5900	25.36	28.13	1.11
Dead	A	202.50	188.72	178.00	4800	5900	17.81	21.69	1.22
	B	202.50	188.72	178.00	4800	5900	16.32	17.57	1.08
	C	202.50	188.72	178.00	4800	5900	17.66	17.92	1.01
	D	202.50	188.72	178.00	4800	5900	16.37	16.91	1.03
	E	202.50	188.72	178.00	4800	5900	15.84	17.47	1.10
	F	202.50	188.42	177.50	4800	5900	46.76	47.87	1.02
	G	202.50	188.42	177.50	4800	5900	30.24	32.45	1.07
	H	202.50	188.42	177.50	4800	5900	24.70	25.39	1.03
	I	202.50	186.65	174.64	4800	5900	30.83	32.55	1.06
	J	202.50	186.65	174.64	4800	5900	24.19	24.29	1.00

Table D.2. Influence of Time (TSB-Pour 2)

	Strand	f_{sj} ksi	f_{si} ksi	f_{se} ksi	f'_{ci} psi	f'_c psi	Transfer Length (in.) Initial	Last	L/I
Live	A	202.50	189.57	179.91	5700	6600	19.35	21.15	1.09
	B	202.50	189.57	179.91	5700	6600	19.63	21.01	1.07
	C	202.50	189.57	179.91	5700	6600	18.27	18.71	1.02
	D	202.50	189.57	179.91	5700	6600	15.02	16.17	1.08
	E	202.50	189.57	179.91	5700	6600	16.06	16.06	1.00
	F	202.50	189.30	179.45	5700	6600	23.41	26.51	1.13
	G	202.50	189.30	179.45	5700	6600	21.69	25.93	1.20
	H	202.50	189.30	179.45	5700	6600	22.39	24.82	1.11
	I	202.50	187.66	176.81	5700	6600	21.45	22.01	1.03
	J	202.50	187.66	176.81	5700	6600	19.19	20.77	1.08
Dead	A	202.50	189.57	179.91	5700	6600	15.89	15.70	0.99
	B	202.50	189.57	179.91	5700	6600	15.53	16.10	1.04
	C	202.50	189.57	179.91	5700	6600	16.13	15.71	0.97
	D	202.50	189.57	179.91	5700	6600	14.50	14.92	1.03
	E	202.50	189.57	179.91	5700	6600	14.51	15.74	1.08
	F	202.50	189.30	179.45	5700	6600	20.35	23.82	1.17
	G	202.50	189.30	179.45	5700	6600	18.92	22.49	1.19
	H	202.50	189.30	179.45	5700	6600	14.26	15.07	1.06
	I	202.50	187.66	176.81	5700	6600	19.59	21.02	1.07
	J	202.50	187.66	176.81	5700	6600	16.31	20.53	1.26

Table D.3. Influence of Time (TSB-Pour 3)

	Strand	f_{sj} ksi	f_{si} ksi	f_{se} ksi	f'_{ci} psi	f'_c psi	Transfer Length (in.) Initial	Last	L/I
Live	A	202.50	189.04	179.43	6100	7000	22.55	23.71	1.05
	B	202.50	189.04	179.43	6100	7000	23.50	23.48	1.00
	C	202.50	189.04	179.43	6100	7000	19.04	18.96	1.00
	D	202.50	189.04	179.43	6100	7000	18.51	18.97	1.02
	E	202.50	189.04	179.43	6100	7000	17.55	17.68	1.01
	F	202.50	188.75	178.95	6100	7000	21.26	25.97	1.22
	G	202.50	188.75	178.95	6100	7000	23.98	26.00	1.08
	H	202.50	188.75	178.95	6100	7000	22.62	23.93	1.06
	I	202.50	187.03	176.23	6100	7000	25.15	26.82	1.07
	J	202.50	187.03	176.23	6100	7000	25.41	27.00	1.06
Dead	A	202.50	189.04	179.43	6100	7000	21.12	23.20	1.10
	B	202.50	189.04	179.43	6100	7000	17.30	18.63	1.08
	C	202.50	189.04	179.43	6100	7000	16.72	17.37	1.04
	D	202.50	189.04	179.43	6100	7000	16.38	16.74	1.02
	E	202.50	189.04	179.43	6100	7000	16.18	17.04	1.05
	F	202.50	188.75	178.95	6100	7000	34.22	36.72	1.07
	G	202.50	188.75	178.95	6100	7000	23.95	26.51	1.11
	H	202.50	188.75	178.95	6100	7000	17.39	20.67	1.19
	I	202.50	187.03	176.23	6100	7000	21.80	24.61	1.13
	J	202.50	187.03	176.23	6100	7000	24.41	26.53	1.09

Table D.4. Influence of Time (TSB-Pour 4)

	Strand	f_{sj} ksi	f_{si} ksi	f_{se} ksi	f'_{ci} psi	f'_c psi	Transfer Length (in.) Initial	Last	L/I
Live	A	202.50	188.00	177.20	5000	6100	29.34	32.14	1.10
	B	202.50	188.00	177.20	5000	6100	23.17	27.07	1.17
	C	202.50	188.00	177.20	5000	6100	20.71	22.69	1.10
	D	202.50	188.00	177.20	5000	6100	20.01	21.90	1.09
	E	202.50	188.00	177.20	5000	6100	18.84	19.79	1.05
	F	202.50	187.68	176.67	5000	6100	25.03	27.64	1.10
	G	202.50	187.68	176.67	5000	6100	25.52	30.32	1.19
	H	202.50	187.68	176.67	5000	6100	30.52	33.25	1.09
	I	202.50	185.80	173.69	5000	6100	28.71	33.35	1.16
	J	202.50	185.80	173.69	5000	6100	29.72	29.44	0.99
Dead	A	202.50	188.00	177.20	5000	6100	30.93	31.83	1.03
	B	202.50	188.00	177.20	5000	6100	21.38	25.78	1.21
	C	202.50	188.00	177.20	5000	6100	19.03	20.79	1.09
	D	202.50	188.00	177.20	5000	6100	17.25	18.60	1.08
	E	202.50	188.00	177.20	5000	6100	16.51	16.47	1.00
	F	202.50	187.68	176.67	5000	6100	25.70	31.10	1.21
	G	202.50	187.68	176.67	5000	6100	21.32	24.98	1.17
	H	202.50	187.68	176.67	5000	6100	19.11	22.70	1.19
	I	202.50	185.80	173.69	5000	6100	30.84	34.64	1.12
	J	202.50	185.80	173.69	5000	6100	25.47	25.46	1.00

Table D.5. Development Length/Flexural Test Results

		Specimen	f_{se}	f_{ps}	$f_{ps} - f_{se}$	f'_c	Failure Type	Curvature	M_{AASHTO}	M_{ACTUAL}	M_{ACTUAL}/M_{AASHTO}
Normal	Live	1.270.5N.RA	156	264	107	6500	Flexural	0.00376	144	171	1.19
		2.270.5N.RA	162	264	101	6400	Flexural	0.00373	144	181	1.26
		3.270.5S.RA	159	265	106	8200	Hybrid	0.00410	180	201	1.11
		4.270.5S.RA	159	264	105	6300	Bond	0.00357	179	176	0.98
		5.270.5S.RA	162	264	101	6500	Bond	0.00364	179	197	1.10
		6.270.5S.RA	174	265	90	8300	Hybrid	0.00408	181	206	1.14
		1.300.5N.RA	176	292	116	6500	NA	0.00000	NA	NA	NA
		2.300.5N.RA	180	292	112	6400	Bond	0.00351	160	142	0.89
		3.300.5S.RA	176	293	117	8200	Hybrid	0.00388	200	226	1.13
		4.300.5S.RA	176	292	116	6300	Bond*	0.00335	197	208	1.05
		5.300.5S.RA	181	292	111	6500	Flexural	0.00340	198	222	1.13
		6.270.6N.RA	173	266	93	8300	Flexural	0.00386	306	340	1.11
	Dead	1.270.5N.RB	158	264	106	6500	Flexural	0.00376	144	165	1.15
		2.270.5N.RB	162	264	101	6400	Flexural	0.00373	144	138	0.96
		3.270.5S.RB	159	265	106	8200	Flexural	0.00410	180	211	1.17
		4.270.5S.RB	157	264	107	6300	Flexural	0.00357	178	206	1.16
		5.270.5S.RB	162	264	101	6500	Hybrid	0.00364	179	200	1.12
		6.270.5S.RB	174	265	90	8300	Hybrid	0.00408	180	204	1.13
		1.300.5N.RB	176	292	116	6500	Flexural	0.00354	159	181	1.14
		2.300.5N.RB	180	292	112	6400	Flexural	0.00351	159	188	1.18
		3.300.5S.RB	176	293	117	8200	Flexural	0.00388	200	230	1.15
		4.300.5S.RB	175	292	117	6300	Flexural	0.00335	197	237	1.20
		5.300.5S.RB	181	292	111	6500	Bond	0.00340	198	198	1.00
		6.270.6N.RB	173	266	93	8300	Flexural	0.00386	306	351	1.15
Inverted	Live	2.270.5N.UA	162	264	102	6400	Hybrid	0.00373	144	181	1.26
		3.270.5S.UA	158	265	107	8200	Bond	0.00410	180	182	1.01
		5.270.5S.UA	162	264	101	6500	Bond	0.00364	179	189	1.06
		6.270.5S.UA	174	265	91	8300	Hybrid	0.00408	180	205	1.14
		2.300.5N.UA	180	292	113	6400	Bond	0.00351	159	190	1.20
		3.300.5S.UA	175	293	118	8200	Bond	0.00388	200	153	0.76
		5.300.5S.UA	181	292	111	6500	Bond	0.00340	198	219	1.11
		6.270.6N.UA	173	266	93	8300	Flexural	0.00386	306	346	1.13
	Dead	2.270.5N.UB	162	264	102	6400	Hybrid	0.00373	144	167	1.16
		3.270.5S.UB	158	265	107	8200	Flexural	0.00410	180	203	1.13
		5.270.5S.UB	162	264	102	6500	Flexural	0.00364	179	202	1.13
		6.270.5S.UB	174	265	91	8300	Bond	0.00408	181	185	1.03
		2.300.5N.UB	179	292	113	6400	Hybrid	0.00351	159	193	1.21
		3.300.5S.UB	175	293	118	8200	Flexural	0.00388	200	225	1.13
		5.300.5S.UB	181	292	112	6500	Bond	0.00340	198	197	1.00
		6.270.6N.UB	172	266	93	8300	Bond	0.00386	306	287	0.94

APPENDIX E

Additional Figures

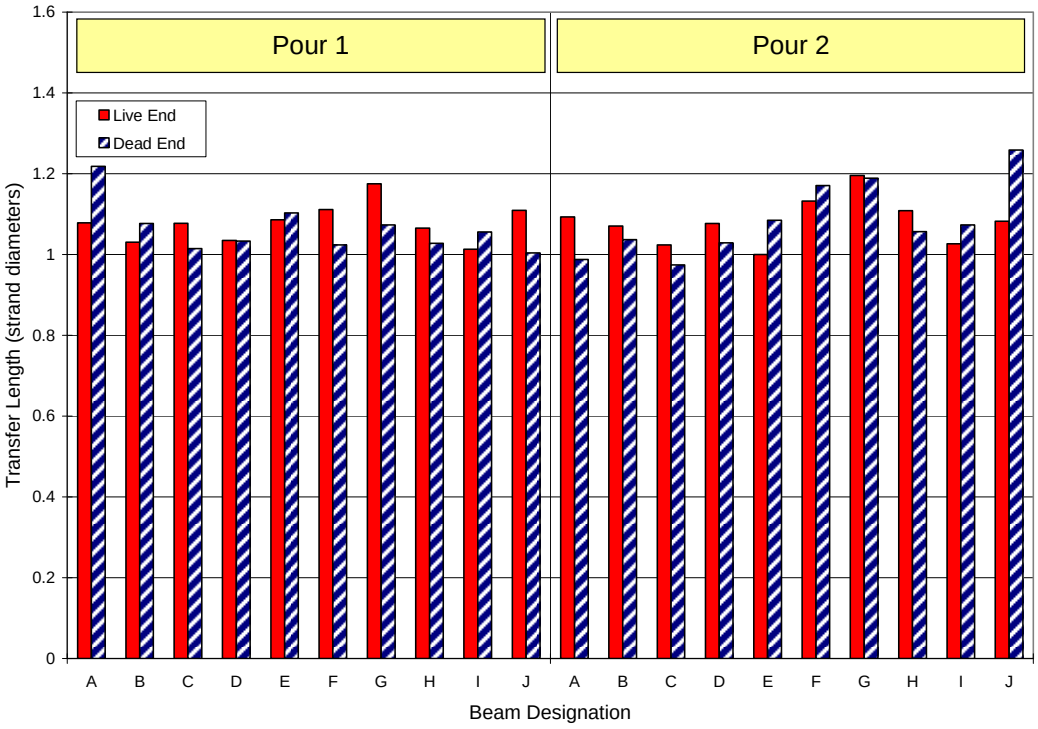

Figure E.1. Influence of Time (TSB-Pours 1 and 2)

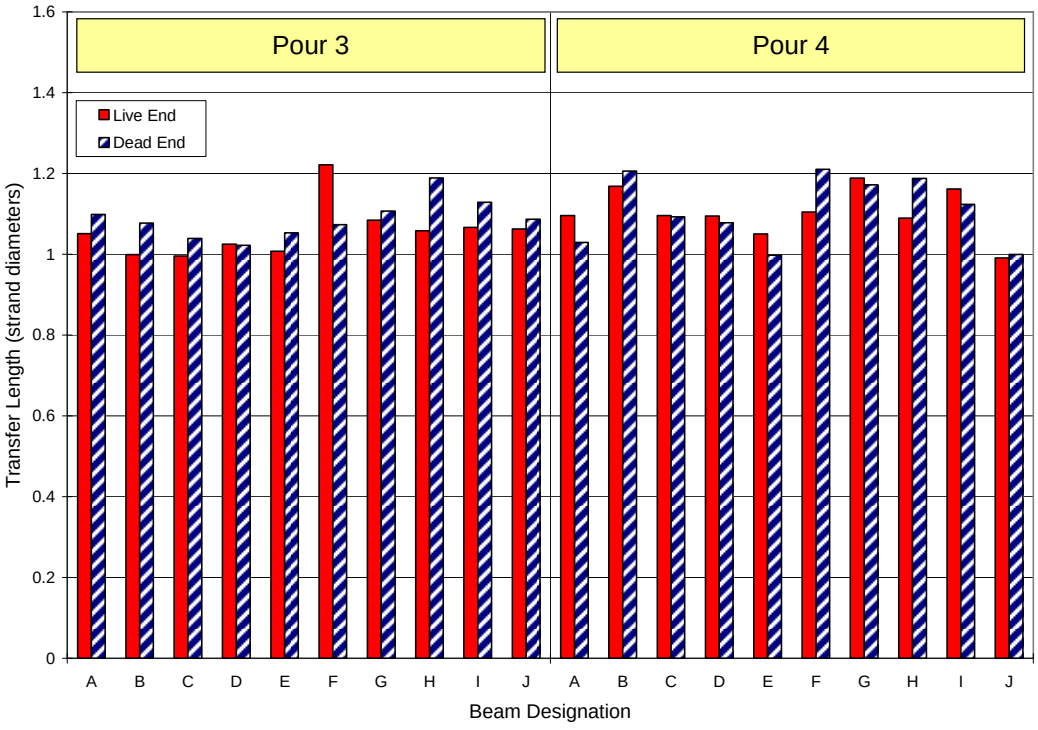

Figure E.2. Influence of Time (TSB-Pours 3 and 4)

APPENDIX F

Bond Model Input Files

```
$$=========================================================================
$$     4x4 Control Block with a jacking stress of 0.75fpu
$$=========================================================================

STRUDL ' '

UNITS INCH KIPS DEG FAH

$$=========================================================================
$$ SPECIFY JOINT COORDINATES
$$=========================================================================

JOINT COORDINATES GLOBAL

GENERATE 73 JOINTS ID 'A1',1 X 0. -
DIFF 0 72 AT 1. Y 0. Z 0.

GENERATE 73 JOINTS ID 'B1',1 X 0. -
DIFF 0 72 AT 1. Y 1. Z 0.

GENERATE 73 JOINTS ID 'C1',1 X 0. -
DIFF 0 72 AT 1. Y 2. Z 0.

GENERATE 73 JOINTS ID 'D1',1 X 0. -
DIFF 0 72 AT 1. Y 3. Z 0.

GENERATE 73 JOINTS ID 'E1',1 X 0. -
DIFF 0 72 AT 1. Y 4. Z 0.

GENERATE 74 JOINTS ID 'Cd0',1 X 0. -
DIFF -1 73 AT 1. Y 2. Z 0.

$$=========================================================================
$$ SPECIFY SUPPORT CONDITIONS
$$=========================================================================

STATUS SUPPORT -
'A73' 'B73' 'C73' 'D73' 'E73' -
'Cd0' TO 'Cd73'

JOINT RELEASES
'A73' 'B73' 'D73' 'E73' FOR Y Z MOM X Y Z
'Cd0' TO 'Cd72' FOR X Z MOM X Y Z

$$=========================================================================
$$ SPECIFY STRAND PROPERTIES
$$=========================================================================

TYPE PLANE TRUSS
GENERATE 73 MEMBERS ID 'STRND-0',1 FROM 'Cd0', 1 TO 'Cd1'

MEMBER PROPERTIES PRISMATIC AX 0.153
'STRND-0' TO 'STRND-72'

$$=========================================================================
$$ SPECIFY BOND ELEMENT PROPERTIES
$$=========================================================================
```

```
ELEMENT INC
'BOND-1'     'Cd1'     'C1'
'BOND-2'     'Cd2'     'C2'
'BOND-3'     'Cd3'     'C3'
'BOND-4'     'Cd4'     'C4'
'BOND-5'     'Cd5'     'C5'
'BOND-6'     'Cd6'     'C6'
'BOND-7'     'Cd7'     'C7'
'BOND-8'     'Cd8'     'C8'
'BOND-9'     'Cd9'     'C9'
'BOND-10'    'Cd10'    'C10'
'BOND-11'    'Cd11'    'C11'
'BOND-12'    'Cd12'    'C12'
'BOND-13'    'Cd13'    'C13'
'BOND-14'    'Cd14'    'C14'
'BOND-15'    'Cd15'    'C15'
'BOND-16'    'Cd16'    'C16'
'BOND-17'    'Cd17'    'C17'
'BOND-18'    'Cd18'    'C18'
'BOND-19'    'Cd19'    'C19'
'BOND-20'    'Cd20'    'C20'
'BOND-21'    'Cd21'    'C21'
'BOND-22'    'Cd22'    'C22'
'BOND-23'    'Cd23'    'C23'
'BOND-24'    'Cd24'    'C24'
'BOND-25'    'Cd25'    'C25'
'BOND-26'    'Cd26'    'C26'
'BOND-27'    'Cd27'    'C27'
'BOND-28'    'Cd28'    'C28'
'BOND-29'    'Cd29'    'C29'
'BOND-30'    'Cd30'    'C30'
'BOND-31'    'Cd31'    'C31'
'BOND-32'    'Cd32'    'C32'
'BOND-33'    'Cd33'    'C33'
'BOND-34'    'Cd34'    'C34'
'BOND-35'    'Cd35'    'C35'
'BOND-36'    'Cd36'    'C36'
'BOND-37'    'Cd37'    'C37'
'BOND-38'    'Cd38'    'C38'
'BOND-39'    'Cd39'    'C39'
'BOND-40'    'Cd40'    'C40'
'BOND-41'    'Cd41'    'C41'
'BOND-42'    'Cd42'    'C42'
'BOND-43'    'Cd43'    'C43'
'BOND-44'    'Cd44'    'C44'
'BOND-45'    'Cd45'    'C45'
'BOND-46'    'Cd46'    'C46'
'BOND-47'    'Cd47'    'C47'
'BOND-48'    'Cd48'    'C48'
'BOND-49'    'Cd49'    'C49'
'BOND-50'    'Cd50'    'C50'
'BOND-51'    'Cd51'    'C51'
'BOND-52'    'Cd52'    'C52'
'BOND-53'    'Cd53'    'C53'
'BOND-54'    'Cd54'    'C54'
'BOND-55'    'Cd55'    'C55'
```

```
'BOND-56'    'Cd56'    'C56'
'BOND-57'    'Cd57'    'C57'
'BOND-58'    'Cd58'    'C58'
'BOND-59'    'Cd59'    'C59'
'BOND-60'    'Cd60'    'C60'
'BOND-61'    'Cd61'    'C61'
'BOND-62'    'Cd62'    'C62'
'BOND-63'    'Cd63'    'C63'
'BOND-64'    'Cd64'    'C64'
'BOND-65'    'Cd65'    'C65'
'BOND-66'    'Cd66'    'C66'
'BOND-67'    'Cd67'    'C67'
'BOND-68'    'Cd68'    'C68'
'BOND-69'    'Cd69'    'C69'
'BOND-70'    'Cd70'    'C70'
'BOND-71'    'Cd71'    'C71'
'BOND-72'    'Cd72'    'C72'

NONLINEAR SPRING PROPERTIES
CURVE 'BOND' FORCE VS DISPL
0.0 0.0 -150.0 -1.0
END

ELEMENT PROPS
'BOND-1' TO 'BOND-72' TYPE 'NLS'

NONLINEAR SPRING ELEMENT DATA
STIFFNESS
'BOND-1' TO 'BOND-72' X CURVE 'BOND'
END

$$=====================================================================
$$ CONCRETE ELEMENT DATA
$$=====================================================================

TYPE PLANE STRESS
GENERATE 72 ELEMENTS ID 'AB-1', 1 FROM 'A1',1 TO 'A2',1 TO 'B2',1 TO
'B1',1
GENERATE 72 ELEMENTS ID 'BC-1', 1 FROM 'B1',1 TO 'B2',1 TO 'C2',1 TO
'C1',1
GENERATE 72 ELEMENTS ID 'CD-1', 1 FROM 'C1',1 TO 'C2',1 TO 'D2',1 TO
'D1',1
GENERATE 72 ELEMENTS ID 'DE-1', 1 FROM 'D1',1 TO 'D2',1 TO 'E2',1 TO
'E1',1

ELEMENT PROPERTIES TYPE 'IPLQ' THICK 4
'AB-1' TO 'AB-72'
'BC-1' TO 'BC-72'
'CD-1' TO 'CD-72'
'DE-1' TO 'DE-72'

$$=====================================================================
$$ SPECIFY MATERIAL PROPERTIES
$$=====================================================================
```

```
$$---------------------
$$ STEEL
$$---------------------
CONSTANTS
     E    28500 -
'STRND-0' TO 'STRND-72'

     G    10962 -
'STRND-0' TO 'STRND-72'

     POI  0.3 -
'STRND-0' TO 'STRND-72'

     DEN  2.83E-04 -
'STRND-0' TO 'STRND-72'

     CTE  6.50E-06 -
'STRND-0' TO 'STRND-72'

$$---------------------
$$ CONCRETE
$$---------------------
CONSTANTS
     E    3949 -
'AB-1' TO 'AB-72' -
'BC-1' TO 'BC-72' -
'CD-1' TO 'CD-72' -
'DE-1' TO 'DE-72'

     G    1688 -
'AB-1' TO 'AB-72' -
'BC-1' TO 'BC-72' -
'CD-1' TO 'CD-72' -
'DE-1' TO 'DE-72'

     POI  0.17 -
'AB-1' TO 'AB-72' -
'BC-1' TO 'BC-72' -
'CD-1' TO 'CD-72' -
'DE-1' TO 'DE-72'

     DEN  8.40E-05 -
'AB-1' TO 'AB-72' -
'BC-1' TO 'BC-72' -
'CD-1' TO 'CD-72' -
'DE-1' TO 'DE-72'

     CTE  5.50E-06 -
'AB-1' TO 'AB-72' -
'BC-1' TO 'BC-72' -
'CD-1' TO 'CD-72' -
'DE-1' TO 'DE-72'

$$=====================================================================
$$ SPECIFY TEMPERATURE LOADINGS
$$=====================================================================
```

```
LOADING 'TRANSFER' '-1100 TEMPERATURE CHANGE'
MEMBER TEMPERATURE LOADS
'STRND-0' TO 'STRND-72' AXIAL -1100

$$=====================================================================
$$ EXECUTE NONLINEAR ANALYSIS
$$=====================================================================

MAXIMUM NUMBER OF CYCLES 10
CONVERGENCE TOL 0.001
NONLINEAR ANALYSIS

LIST FORCES EXISTING -
'STRND-0' TO 'STRND-72'

LIST DISPLACEMENTS -
'C1' 'Cd1'
```

```
$$=========================================================================
$$    Top-strand Large Block with a jacking stress of 0.75fpu
$$=========================================================================

STRUDL ' '

UNITS INCH KIPS DEG FAH

$$=========================================================================
$$ SPECIFY JOINT COORDINATES
$$=========================================================================

JOINT COORDINATES GLOBAL

GENERATE 73 JOINTS ID 'A1',1 X 0. -
DIFF 0 72 AT 1 Y 24. Z 0.

GENERATE 73 JOINTS ID 'B1',1 X 0. -
DIFF 0 72 AT 1 Y 23. Z 0.

GENERATE 73 JOINTS ID 'C1',1 X 0. -
DIFF 0 72 AT 1 Y 22. Z 0.

GENERATE 73 JOINTS ID 'D1',1 X 0. -
DIFF 0 72 AT 1 Y 21. Z 0.

GENERATE 73 JOINTS ID 'E1',1 X 0. -
DIFF 0 72 AT 1 Y 20. Z 0.

GENERATE 73 JOINTS ID 'F1',1 X 0. -
DIFF 0 72 AT 1 Y 19. Z 0.

GENERATE 73 JOINTS ID 'G1',1 X 0. -
DIFF 0 72 AT 1 Y 18. Z 0.

GENERATE 73 JOINTS ID 'H1',1 X 0. -
DIFF 0 72 AT 1 Y 17. Z 0.

GENERATE 73 JOINTS ID 'I1',1 X 0. -
DIFF 0 72 AT 1 Y 16. Z 0.

GENERATE 73 JOINTS ID 'J1',1 X 0. -
DIFF 0 72 AT 1 Y 15. Z 0.

GENERATE 73 JOINTS ID 'K1',1 X 0. -
DIFF 0 72 AT 1 Y 14. Z 0.

GENERATE 73 JOINTS ID 'L1',1 X 0. -
DIFF 0 72 AT 1 Y 13. Z 0.

GENERATE 73 JOINTS ID 'M1',1 X 0. -
DIFF 0 72 AT 1 Y 12. Z 0.

GENERATE 73 JOINTS ID 'N1',1 X 0. -
DIFF 0 72 AT 1 Y 11. Z 0.

GENERATE 73 JOINTS ID 'O1',1 X 0. -
```

```
DIFF 0 72 AT 1 Y 10. Z 0.

GENERATE 73 JOINTS ID 'P1',1 X 0. -
DIFF 0 72 AT 1 Y 9. Z 0.

GENERATE 73 JOINTS ID 'Q1',1 X 0. -
DIFF 0 72 AT 1 Y 8. Z 0.

GENERATE 73 JOINTS ID 'R1',1 X 0. -
DIFF 0 72 AT 1 Y 7. Z 0.

GENERATE 73 JOINTS ID 'S1',1 X 0. -
DIFF 0 72 AT 1 Y 6. Z 0.

GENERATE 73 JOINTS ID 'T1',1 X 0. -
DIFF 0 72 AT 1 Y 5. Z 0.

GENERATE 73 JOINTS ID 'U1',1 X 0. -
DIFF 0 72 AT 1 Y 4. Z 0.

GENERATE 73 JOINTS ID 'V1',1 X 0. -
DIFF 0 72 AT 1 Y 3. Z 0.

GENERATE 73 JOINTS ID 'W1',1 X 0. -
DIFF 0 72 AT 1 Y 2. Z 0.

GENERATE 73 JOINTS ID 'X1',1 X 0. -
DIFF 0 72 AT 1 Y 1. Z 0.

GENERATE 73 JOINTS ID 'Y1',1 X 0. -
DIFF 0 72 AT 1 Y 0. Z 0.

$$================================

GENERATE 74 JOINTS ID 'Cd0',1 X 0. -
DIFF -1 73 AT 1 Y 22. Z 0.

GENERATE 74 JOINTS ID 'Hd0',1 X 0. -
DIFF -1 73 AT 1 Y 17. Z 0.

GENERATE 74 JOINTS ID 'Md0',1 X 0. -
DIFF -1 73 AT 1 Y 12. Z 0.

GENERATE 74 JOINTS ID 'Rd0',1 X 0. -
DIFF -1 73 AT 1 Y 7. Z 0.

GENERATE 74 JOINTS ID 'Wd0',1 X 0. -
DIFF -1 73 AT 1 Y 2. Z 0.

$$=====================================================================
$$ SPECIFY SUPPORT CONDITIONS
$$=====================================================================

STATUS SUPPORT -
'A73' 'B73' 'C73' 'D73' 'E73' 'F73' 'G73' 'H73' 'I73' 'J73' 'K73' 'L73'
'M73' 'N73' 'O73' 'P73' -
'Q73' 'R73' 'S73' 'T73' 'U73' 'V73' 'W73' 'X73' 'Y73'
```

```
JOINT RELEASES
'A73' 'B73' 'C73' 'D73' 'E73' 'F73' 'G73' 'H73' 'I73' 'J73' 'K73' 'L73'
'M73' 'N73' 'O73' 'P73' -
'Q73' 'R73' 'S73' 'T73' 'U73' 'V73' 'W73' 'X73' -
FOR Y Z MOM X Y Z

$$=====================================================================
$$ SPECIFY MASTER AND SLAVE JOINTS
$$=====================================================================

JOINT TIES
'Cd1' TO 'Cd73' EQUAL 'C1' TO 'C73'
'Cd0' EQUAL 'C1'

'Hd1' TO 'Hd73' EQUAL 'H1' TO 'H73'
'Hd0' EQUAL 'H1'

'Md1' TO 'Md73' EQUAL 'M1' TO 'M73'
'Md0' EQUAL 'M1'

'Rd1' TO 'Rd73' EQUAL 'R1' TO 'R73'
'Rd0' EQUAL 'R1'

'Wd1' TO 'Wd73' EQUAL 'W1' TO 'W73'
'Wd0' EQUAL 'W1'

SLAVE RELEASES
'Cd0' TO 'Cd72' 'Hd0' TO 'Hd72' 'Md0' TO 'Md72' 'Rd0' TO 'Rd72' 'Wd0'
TO 'Wd72' FOR X Z MOM X Y Z
'Cd73' 'Hd73' 'Md73' 'Rd73' 'Wd73' FOR Z MOM X Y Z

$$=====================================================================
$$ SPECIFY STRAND PROPERTIES
$$=====================================================================

TYPE PLANE TRUSS
GENERATE 73 MEMBERS ID 'STRNDA0',1 FROM 'Cd0', 1 TO 'Cd1'
GENERATE 73 MEMBERS ID 'STRNDB0',1 FROM 'Hd0', 1 TO 'Hd1'
GENERATE 73 MEMBERS ID 'STRNDC0',1 FROM 'Md0', 1 TO 'Md1'
GENERATE 73 MEMBERS ID 'STRNDD0',1 FROM 'Rd0', 1 TO 'Rd1'
GENERATE 73 MEMBERS ID 'STRNDE0',1 FROM 'Wd0', 1 TO 'Wd1'

MEMBER PROPERTIES PRISMATIC AX 0.153
'STRNDA0' TO 'STRNDA72'
'STRNDB0' TO 'STRNDB72'
'STRNDC0' TO 'STRNDC72'
'STRNDD0' TO 'STRNDD72'
'STRNDE0' TO 'STRNDE72'

$$=====================================================================
$$ SPECIFY BOND ELEMENT PROPERTIES
$$=====================================================================

ELEMENT INC
'BOND-C1'     'Cd1'     'C1'
'BOND-C2'     'Cd2'     'C2'
```

```
'BOND-C3'     'Cd3'     'C3'
'BOND-C4'     'Cd4'     'C4'
'BOND-C5'     'Cd5'     'C5'
'BOND-C6'     'Cd6'     'C6'
'BOND-C7'     'Cd7'     'C7'
'BOND-C8'     'Cd8'     'C8'
'BOND-C9'     'Cd9'     'C9'
'BOND-C10'    'Cd10'    'C10'
'BOND-C11'    'Cd11'    'C11'
'BOND-C12'    'Cd12'    'C12'
'BOND-C13'    'Cd13'    'C13'
'BOND-C14'    'Cd14'    'C14'
'BOND-C15'    'Cd15'    'C15'
'BOND-C16'    'Cd16'    'C16'
'BOND-C17'    'Cd17'    'C17'
'BOND-C18'    'Cd18'    'C18'
'BOND-C19'    'Cd19'    'C19'
'BOND-C20'    'Cd20'    'C20'
'BOND-C21'    'Cd21'    'C21'
'BOND-C22'    'Cd22'    'C22'
'BOND-C23'    'Cd23'    'C23'
'BOND-C24'    'Cd24'    'C24'
'BOND-C25'    'Cd25'    'C25'
'BOND-C26'    'Cd26'    'C26'
'BOND-C27'    'Cd27'    'C27'
'BOND-C28'    'Cd28'    'C28'
'BOND-C29'    'Cd29'    'C29'
'BOND-C30'    'Cd30'    'C30'
'BOND-C31'    'Cd31'    'C31'
'BOND-C32'    'Cd32'    'C32'
'BOND-C33'    'Cd33'    'C33'
'BOND-C34'    'Cd34'    'C34'
'BOND-C35'    'Cd35'    'C35'
'BOND-C36'    'Cd36'    'C36'
'BOND-C37'    'Cd37'    'C37'
'BOND-C38'    'Cd38'    'C38'
'BOND-C39'    'Cd39'    'C39'
'BOND-C40'    'Cd40'    'C40'
'BOND-C41'    'Cd41'    'C41'
'BOND-C42'    'Cd42'    'C42'
'BOND-C43'    'Cd43'    'C43'
'BOND-C44'    'Cd44'    'C44'
'BOND-C45'    'Cd45'    'C45'
'BOND-C46'    'Cd46'    'C46'
'BOND-C47'    'Cd47'    'C47'
'BOND-C48'    'Cd48'    'C48'
'BOND-C49'    'Cd49'    'C49'
'BOND-C50'    'Cd50'    'C50'
'BOND-C51'    'Cd51'    'C51'
'BOND-C52'    'Cd52'    'C52'
'BOND-C53'    'Cd53'    'C53'
'BOND-C54'    'Cd54'    'C54'
'BOND-C55'    'Cd55'    'C55'
'BOND-C56'    'Cd56'    'C56'
'BOND-C57'    'Cd57'    'C57'
'BOND-C58'    'Cd58'    'C58'
'BOND-C59'    'Cd59'    'C59'
```

```
'BOND-C60'    'Cd60'    'C60'
'BOND-C61'    'Cd61'    'C61'
'BOND-C62'    'Cd62'    'C62'
'BOND-C63'    'Cd63'    'C63'
'BOND-C64'    'Cd64'    'C64'
'BOND-C65'    'Cd65'    'C65'
'BOND-C66'    'Cd66'    'C66'
'BOND-C67'    'Cd67'    'C67'
'BOND-C68'    'Cd68'    'C68'
'BOND-C69'    'Cd69'    'C69'
'BOND-C70'    'Cd70'    'C70'
'BOND-C71'    'Cd71'    'C71'
'BOND-C72'    'Cd72'    'C72'

'BOND-H1'     'Hd1'     'H1'
'BOND-H2'     'Hd2'     'H2'
'BOND-H3'     'Hd3'     'H3'
'BOND-H4'     'Hd4'     'H4'
'BOND-H5'     'Hd5'     'H5'
'BOND-H6'     'Hd6'     'H6'
'BOND-H7'     'Hd7'     'H7'
'BOND-H8'     'Hd8'     'H8'
'BOND-H9'     'Hd9'     'H9'
'BOND-H10'    'Hd10'    'H10'
'BOND-H11'    'Hd11'    'H11'
'BOND-H12'    'Hd12'    'H12'
'BOND-H13'    'Hd13'    'H13'
'BOND-H14'    'Hd14'    'H14'
'BOND-H15'    'Hd15'    'H15'
'BOND-H16'    'Hd16'    'H16'
'BOND-H17'    'Hd17'    'H17'
'BOND-H18'    'Hd18'    'H18'
'BOND-H19'    'Hd19'    'H19'
'BOND-H20'    'Hd20'    'H20'
'BOND-H21'    'Hd21'    'H21'
'BOND-H22'    'Hd22'    'H22'
'BOND-H23'    'Hd23'    'H23'
'BOND-H24'    'Hd24'    'H24'
'BOND-H25'    'Hd25'    'H25'
'BOND-H26'    'Hd26'    'H26'
'BOND-H27'    'Hd27'    'H27'
'BOND-H28'    'Hd28'    'H28'
'BOND-H29'    'Hd29'    'H29'
'BOND-H30'    'Hd30'    'H30'
'BOND-H31'    'Hd31'    'H31'
'BOND-H32'    'Hd32'    'H32'
'BOND-H33'    'Hd33'    'H33'
'BOND-H34'    'Hd34'    'H34'
'BOND-H35'    'Hd35'    'H35'
'BOND-H36'    'Hd36'    'H36'
'BOND-H37'    'Hd37'    'H37'
'BOND-H38'    'Hd38'    'H38'
'BOND-H39'    'Hd39'    'H39'
'BOND-H40'    'Hd40'    'H40'
'BOND-H41'    'Hd41'    'H41'
'BOND-H42'    'Hd42'    'H42'
'BOND-H43'    'Hd43'    'H43'
```

```
'BOND-H44'    'Hd44'    'H44'
'BOND-H45'    'Hd45'    'H45'
'BOND-H46'    'Hd46'    'H46'
'BOND-H47'    'Hd47'    'H47'
'BOND-H48'    'Hd48'    'H48'
'BOND-H49'    'Hd49'    'H49'
'BOND-H50'    'Hd50'    'H50'
'BOND-H51'    'Hd51'    'H51'
'BOND-H52'    'Hd52'    'H52'
'BOND-H53'    'Hd53'    'H53'
'BOND-H54'    'Hd54'    'H54'
'BOND-H55'    'Hd55'    'H55'
'BOND-H56'    'Hd56'    'H56'
'BOND-H57'    'Hd57'    'H57'
'BOND-H58'    'Hd58'    'H58'
'BOND-H59'    'Hd59'    'H59'
'BOND-H60'    'Hd60'    'H60'
'BOND-H61'    'Hd61'    'H61'
'BOND-H62'    'Hd62'    'H62'
'BOND-H63'    'Hd63'    'H63'
'BOND-H64'    'Hd64'    'H64'
'BOND-H65'    'Hd65'    'H65'
'BOND-H66'    'Hd66'    'H66'
'BOND-H67'    'Hd67'    'H67'
'BOND-H68'    'Hd68'    'H68'
'BOND-H69'    'Hd69'    'H69'
'BOND-H70'    'Hd70'    'H70'
'BOND-H71'    'Hd71'    'H71'
'BOND-H72'    'Hd72'    'H72'

'BOND-M1'     'Md1'     'M1'
'BOND-M2'     'Md2'     'M2'
'BOND-M3'     'Md3'     'M3'
'BOND-M4'     'Md4'     'M4'
'BOND-M5'     'Md5'     'M5'
'BOND-M6'     'Md6'     'M6'
'BOND-M7'     'Md7'     'M7'
'BOND-M8'     'Md8'     'M8'
'BOND-M9'     'Md9'     'M9'
'BOND-M10'    'Md10'    'M10'
'BOND-M11'    'Md11'    'M11'
'BOND-M12'    'Md12'    'M12'
'BOND-M13'    'Md13'    'M13'
'BOND-M14'    'Md14'    'M14'
'BOND-M15'    'Md15'    'M15'
'BOND-M16'    'Md16'    'M16'
'BOND-M17'    'Md17'    'M17'
'BOND-M18'    'Md18'    'M18'
'BOND-M19'    'Md19'    'M19'
'BOND-M20'    'Md20'    'M20'
'BOND-M21'    'Md21'    'M21'
'BOND-M22'    'Md22'    'M22'
'BOND-M23'    'Md23'    'M23'
'BOND-M24'    'Md24'    'M24'
'BOND-M25'    'Md25'    'M25'
'BOND-M26'    'Md26'    'M26'
'BOND-M27'    'Md27'    'M27'
```

```
'BOND-M28'    'Md28'    'M28'
'BOND-M29'    'Md29'    'M29'
'BOND-M30'    'Md30'    'M30'
'BOND-M31'    'Md31'    'M31'
'BOND-M32'    'Md32'    'M32'
'BOND-M33'    'Md33'    'M33'
'BOND-M34'    'Md34'    'M34'
'BOND-M35'    'Md35'    'M35'
'BOND-M36'    'Md36'    'M36'
'BOND-M37'    'Md37'    'M37'
'BOND-M38'    'Md38'    'M38'
'BOND-M39'    'Md39'    'M39'
'BOND-M40'    'Md40'    'M40'
'BOND-M41'    'Md41'    'M41'
'BOND-M42'    'Md42'    'M42'
'BOND-M43'    'Md43'    'M43'
'BOND-M44'    'Md44'    'M44'
'BOND-M45'    'Md45'    'M45'
'BOND-M46'    'Md46'    'M46'
'BOND-M47'    'Md47'    'M47'
'BOND-M48'    'Md48'    'M48'
'BOND-M49'    'Md49'    'M49'
'BOND-M50'    'Md50'    'M50'
'BOND-M51'    'Md51'    'M51'
'BOND-M52'    'Md52'    'M52'
'BOND-M53'    'Md53'    'M53'
'BOND-M54'    'Md54'    'M54'
'BOND-M55'    'Md55'    'M55'
'BOND-M56'    'Md56'    'M56'
'BOND-M57'    'Md57'    'M57'
'BOND-M58'    'Md58'    'M58'
'BOND-M59'    'Md59'    'M59'
'BOND-M60'    'Md60'    'M60'
'BOND-M61'    'Md61'    'M61'
'BOND-M62'    'Md62'    'M62'
'BOND-M63'    'Md63'    'M63'
'BOND-M64'    'Md64'    'M64'
'BOND-M65'    'Md65'    'M65'
'BOND-M66'    'Md66'    'M66'
'BOND-M67'    'Md67'    'M67'
'BOND-M68'    'Md68'    'M68'
'BOND-M69'    'Md69'    'M69'
'BOND-M70'    'Md70'    'M70'
'BOND-M71'    'Md71'    'M71'
'BOND-M72'    'Md72'    'M72'

'BOND-R1'     'Rd1'     'R1'
'BOND-R2'     'Rd2'     'R2'
'BOND-R3'     'Rd3'     'R3'
'BOND-R4'     'Rd4'     'R4'
'BOND-R5'     'Rd5'     'R5'
'BOND-R6'     'Rd6'     'R6'
'BOND-R7'     'Rd7'     'R7'
'BOND-R8'     'Rd8'     'R8'
'BOND-R9'     'Rd9'     'R9'
'BOND-R10'    'Rd10'    'R10'
'BOND-R11'    'Rd11'    'R11'
```

```
'BOND-R12'    'Rd12'    'R12'
'BOND-R13'    'Rd13'    'R13'
'BOND-R14'    'Rd14'    'R14'
'BOND-R15'    'Rd15'    'R15'
'BOND-R16'    'Rd16'    'R16'
'BOND-R17'    'Rd17'    'R17'
'BOND-R18'    'Rd18'    'R18'
'BOND-R19'    'Rd19'    'R19'
'BOND-R20'    'Rd20'    'R20'
'BOND-R21'    'Rd21'    'R21'
'BOND-R22'    'Rd22'    'R22'
'BOND-R23'    'Rd23'    'R23'
'BOND-R24'    'Rd24'    'R24'
'BOND-R25'    'Rd25'    'R25'
'BOND-R26'    'Rd26'    'R26'
'BOND-R27'    'Rd27'    'R27'
'BOND-R28'    'Rd28'    'R28'
'BOND-R29'    'Rd29'    'R29'
'BOND-R30'    'Rd30'    'R30'
'BOND-R31'    'Rd31'    'R31'
'BOND-R32'    'Rd32'    'R32'
'BOND-R33'    'Rd33'    'R33'
'BOND-R34'    'Rd34'    'R34'
'BOND-R35'    'Rd35'    'R35'
'BOND-R36'    'Rd36'    'R36'
'BOND-R37'    'Rd37'    'R37'
'BOND-R38'    'Rd38'    'R38'
'BOND-R39'    'Rd39'    'R39'
'BOND-R40'    'Rd40'    'R40'
'BOND-R41'    'Rd41'    'R41'
'BOND-R42'    'Rd42'    'R42'
'BOND-R43'    'Rd43'    'R43'
'BOND-R44'    'Rd44'    'R44'
'BOND-R45'    'Rd45'    'R45'
'BOND-R46'    'Rd46'    'R46'
'BOND-R47'    'Rd47'    'R47'
'BOND-R48'    'Rd48'    'R48'
'BOND-R49'    'Rd49'    'R49'
'BOND-R50'    'Rd50'    'R50'
'BOND-R51'    'Rd51'    'R51'
'BOND-R52'    'Rd52'    'R52'
'BOND-R53'    'Rd53'    'R53'
'BOND-R54'    'Rd54'    'R54'
'BOND-R55'    'Rd55'    'R55'
'BOND-R56'    'Rd56'    'R56'
'BOND-R57'    'Rd57'    'R57'
'BOND-R58'    'Rd58'    'R58'
'BOND-R59'    'Rd59'    'R59'
'BOND-R60'    'Rd60'    'R60'
'BOND-R61'    'Rd61'    'R61'
'BOND-R62'    'Rd62'    'R62'
'BOND-R63'    'Rd63'    'R63'
'BOND-R64'    'Rd64'    'R64'
'BOND-R65'    'Rd65'    'R65'
'BOND-R66'    'Rd66'    'R66'
'BOND-R67'    'Rd67'    'R67'
'BOND-R68'    'Rd68'    'R68'
```

```
'BOND-R69'    'Rd69'    'R69'
'BOND-R70'    'Rd70'    'R70'
'BOND-R71'    'Rd71'    'R71'
'BOND-R72'    'Rd72'    'R72'

'BOND-W1'     'Wd1'     'W1'
'BOND-W2'     'Wd2'     'W2'
'BOND-W3'     'Wd3'     'W3'
'BOND-W4'     'Wd4'     'W4'
'BOND-W5'     'Wd5'     'W5'
'BOND-W6'     'Wd6'     'W6'
'BOND-W7'     'Wd7'     'W7'
'BOND-W8'     'Wd8'     'W8'
'BOND-W9'     'Wd9'     'W9'
'BOND-W10'    'Wd10'    'W10'
'BOND-W11'    'Wd11'    'W11'
'BOND-W12'    'Wd12'    'W12'
'BOND-W13'    'Wd13'    'W13'
'BOND-W14'    'Wd14'    'W14'
'BOND-W15'    'Wd15'    'W15'
'BOND-W16'    'Wd16'    'W16'
'BOND-W17'    'Wd17'    'W17'
'BOND-W18'    'Wd18'    'W18'
'BOND-W19'    'Wd19'    'W19'
'BOND-W20'    'Wd20'    'W20'
'BOND-W21'    'Wd21'    'W21'
'BOND-W22'    'Wd22'    'W22'
'BOND-W23'    'Wd23'    'W23'
'BOND-W24'    'Wd24'    'W24'
'BOND-W25'    'Wd25'    'W25'
'BOND-W26'    'Wd26'    'W26'
'BOND-W27'    'Wd27'    'W27'
'BOND-W28'    'Wd28'    'W28'
'BOND-W29'    'Wd29'    'W29'
'BOND-W30'    'Wd30'    'W30'
'BOND-W31'    'Wd31'    'W31'
'BOND-W32'    'Wd32'    'W32'
'BOND-W33'    'Wd33'    'W33'
'BOND-W34'    'Wd34'    'W34'
'BOND-W35'    'Wd35'    'W35'
'BOND-W36'    'Wd36'    'W36'
'BOND-W37'    'Wd37'    'W37'
'BOND-W38'    'Wd38'    'W38'
'BOND-W39'    'Wd39'    'W39'
'BOND-W40'    'Wd40'    'W40'
'BOND-W41'    'Wd41'    'W41'
'BOND-W42'    'Wd42'    'W42'
'BOND-W43'    'Wd43'    'W43'
'BOND-W44'    'Wd44'    'W44'
'BOND-W45'    'Wd45'    'W45'
'BOND-W46'    'Wd46'    'W46'
'BOND-W47'    'Wd47'    'W47'
'BOND-W48'    'Wd48'    'W48'
'BOND-W49'    'Wd49'    'W49'
'BOND-W50'    'Wd50'    'W50'
'BOND-W51'    'Wd51'    'W51'
'BOND-W52'    'Wd52'    'W52'
```

```
'BOND-W53'    'Wd53'    'W53'
'BOND-W54'    'Wd54'    'W54'
'BOND-W55'    'Wd55'    'W55'
'BOND-W56'    'Wd56'    'W56'
'BOND-W57'    'Wd57'    'W57'
'BOND-W58'    'Wd58'    'W58'
'BOND-W59'    'Wd59'    'W59'
'BOND-W60'    'Wd60'    'W60'
'BOND-W61'    'Wd61'    'W61'
'BOND-W62'    'Wd62'    'W62'
'BOND-W63'    'Wd63'    'W63'
'BOND-W64'    'Wd64'    'W64'
'BOND-W65'    'Wd65'    'W65'
'BOND-W66'    'Wd66'    'W66'
'BOND-W67'    'Wd67'    'W67'
'BOND-W68'    'Wd68'    'W68'
'BOND-W69'    'Wd69'    'W69'
'BOND-W70'    'Wd70'    'W70'
'BOND-W71'    'Wd71'    'W71'
'BOND-W72'    'Wd72'    'W72'

NONLINEAR SPRING PROPERTIES
CURVE 'BOND-C' FORCE VS DISPL
0.0 0.0 -150.0 -1.0
CURVE 'BOND-H' FORCE VS DISPL
0.0 0.0 -150.0 -1.0
CURVE 'BOND-M' FORCE VS DISPL
0.0 0.0 -150.0 -1.0
CURVE 'BOND-R' FORCE VS DISPL
0.0 0.0 -150.0 -1.0
CURVE 'BOND-W' FORCE VS DISPL
0.0 0.0 -150.0 -1.0
END

ELEMENT PROPS
'BOND-C1' TO 'BOND-C72' -
'BOND-H1' TO 'BOND-H72' -
'BOND-M1' TO 'BOND-M72' -
'BOND-R1' TO 'BOND-R72' -
'BOND-W1' TO 'BOND-W72' -
TYPE 'NLS'

NONLINEAR SPRING ELEMENT DATA
STIFFNESS
'BOND-C1' TO 'BOND-C72' X CURVE 'BOND-C'
'BOND-H1' TO 'BOND-H72' X CURVE 'BOND-H'
'BOND-M1' TO 'BOND-M72' X CURVE 'BOND-M'
'BOND-R1' TO 'BOND-R72' X CURVE 'BOND-R'
'BOND-W1' TO 'BOND-W72' X CURVE 'BOND-W'
END

$$=========================================================================
$$ CONCRETE ELEMENT DATA
$$=========================================================================
```

```
TYPE PLANE STRESS
GENERATE 72 ELEMENTS ID 'AB-1', 1 FROM 'B1',1 TO 'B2',1 TO 'A2',1 TO
'A1',1
GENERATE 72 ELEMENTS ID 'BC-1', 1 FROM 'C1',1 TO 'C2',1 TO 'B2',1 TO
'B1',1

GENERATE 72 ELEMENTS ID 'CD-1', 1 FROM 'D1',1 TO 'D2',1 TO 'C2',1 TO
'C1',1
GENERATE 72 ELEMENTS ID 'DE-1', 1 FROM 'E1',1 TO 'E2',1 TO 'D2',1 TO
'D1',1
GENERATE 72 ELEMENTS ID 'EF-1', 1 FROM 'F1',1 TO 'F2',1 TO 'E2',1 TO
'E1',1
GENERATE 72 ELEMENTS ID 'FG-1', 1 FROM 'G1',1 TO 'G2',1 TO 'F2',1 TO
'F1',1
GENERATE 72 ELEMENTS ID 'GH-1', 1 FROM 'H1',1 TO 'H2',1 TO 'G2',1 TO
'G1',1

GENERATE 72 ELEMENTS ID 'HI-1', 1 FROM 'I1',1 TO 'I2',1 TO 'H2',1 TO
'H1',1
GENERATE 72 ELEMENTS ID 'IJ-1', 1 FROM 'J1',1 TO 'J2',1 TO 'I2',1 TO
'I1',1
GENERATE 72 ELEMENTS ID 'JK-1', 1 FROM 'K1',1 TO 'K2',1 TO 'J2',1 TO
'J1',1
GENERATE 72 ELEMENTS ID 'KL-1', 1 FROM 'L1',1 TO 'L2',1 TO 'K2',1 TO
'K1',1
GENERATE 72 ELEMENTS ID 'LM-1', 1 FROM 'M1',1 TO 'M2',1 TO 'L2',1 TO
'L1',1

GENERATE 72 ELEMENTS ID 'MN-1', 1 FROM 'N1',1 TO 'N2',1 TO 'M2',1 TO
'M1',1
GENERATE 72 ELEMENTS ID 'NO-1', 1 FROM 'O1',1 TO 'O2',1 TO 'N2',1 TO
'N1',1
GENERATE 72 ELEMENTS ID 'OP-1', 1 FROM 'P1',1 TO 'P2',1 TO 'O2',1 TO
'O1',1
GENERATE 72 ELEMENTS ID 'PQ-1', 1 FROM 'Q1',1 TO 'Q2',1 TO 'P2',1 TO
'P1',1
GENERATE 72 ELEMENTS ID 'QR-1', 1 FROM 'R1',1 TO 'R2',1 TO 'Q2',1 TO
'Q1',1

GENERATE 72 ELEMENTS ID 'RS-1', 1 FROM 'S1',1 TO 'S2',1 TO 'R2',1 TO
'R1',1
GENERATE 72 ELEMENTS ID 'ST-1', 1 FROM 'T1',1 TO 'T2',1 TO 'S2',1 TO
'S1',1
GENERATE 72 ELEMENTS ID 'TU-1', 1 FROM 'U1',1 TO 'U2',1 TO 'T2',1 TO
'T1',1
GENERATE 72 ELEMENTS ID 'UV-1', 1 FROM 'V1',1 TO 'V2',1 TO 'U2',1 TO
'U1',1
GENERATE 72 ELEMENTS ID 'VW-1', 1 FROM 'W1',1 TO 'W2',1 TO 'V2',1 TO
'V1',1

GENERATE 72 ELEMENTS ID 'WX-1', 1 FROM 'X1',1 TO 'X2',1 TO 'W2',1 TO
'W1',1
GENERATE 72 ELEMENTS ID 'XY-1', 1 FROM 'Y1',1 TO 'Y2',1 TO 'X2',1 TO
'X1',1

ELEMENT PROPERTIES TYPE 'IPLQ' THICK 4
'AB-1' TO 'AB-72'
```

```
'BC-1' TO 'BC-72'

'CD-1' TO 'CD-72'
'DE-1' TO 'DE-72'
'EF-1' TO 'EF-72'
'FG-1' TO 'FG-72'
'GH-1' TO 'GH-72'

'HI-1' TO 'HI-72'
'IJ-1' TO 'IJ-72'
'JK-1' TO 'JK-72'
'KL-1' TO 'KL-72'
'LM-1' TO 'LM-72'

'MN-1' TO 'MN-72'
'NO-1' TO 'NO-72'
'OP-1' TO 'OP-72'
'PQ-1' TO 'PQ-72'
'QR-1' TO 'QR-72'

'RS-1' TO 'RS-72'
'ST-1' TO 'ST-72'
'TU-1' TO 'TU-72'
'UV-1' TO 'UV-72'
'VW-1' TO 'VW-72'

'WX-1' TO 'WX-72'
'XY-1' TO 'XY-72'

$$=========================================================================
$$ SPECIFY MATERIAL PROPERTIES
$$=========================================================================

$$---------------------
$$ STEEL
$$---------------------
CONSTANTS
     E    28500 -
'STRNDA0' TO 'STRNDA72' -
'STRNDB0' TO 'STRNDB72' -
'STRNDC0' TO 'STRNDC72' -
'STRNDD0' TO 'STRNDD72' -
'STRNDE0' TO 'STRNDE72'

     G    10962 -
'STRNDA0' TO 'STRNDA72' -
'STRNDB0' TO 'STRNDB72' -
'STRNDC0' TO 'STRNDC72' -
'STRNDD0' TO 'STRNDD72' -
'STRNDE0' TO 'STRNDE72'

     POI  0.3 -
'STRNDA0' TO 'STRNDA72' -
'STRNDB0' TO 'STRNDB72' -
'STRNDC0' TO 'STRNDC72' -
'STRNDD0' TO 'STRNDD72' -
'STRNDE0' TO 'STRNDE72'
```

```
     DEN  2.83E-04 -
'STRNDA0' TO 'STRNDA72' -
'STRNDB0' TO 'STRNDB72' -
'STRNDC0' TO 'STRNDC72' -
'STRNDD0' TO 'STRNDD72' -
'STRNDE0' TO 'STRNDE72'

     CTE  6.50E-06 -
'STRNDA0' TO 'STRNDA72' -
'STRNDB0' TO 'STRNDB72' -
'STRNDC0' TO 'STRNDC72' -
'STRNDD0' TO 'STRNDD72' -
'STRNDE0' TO 'STRNDE72'

$$--------------------
$$ CONCRETE
$$--------------------
CONSTANTS
     E    3949 -
'AB-1' TO 'AB-72' -
'BC-1' TO 'BC-72' -

'CD-1' TO 'CD-72' -
'DE-1' TO 'DE-72' -
'EF-1' TO 'EF-72' -
'FG-1' TO 'FG-72' -
'GH-1' TO 'GH-72' -

'HI-1' TO 'HI-72' -
'IJ-1' TO 'IJ-72' -
'JK-1' TO 'JK-72' -
'KL-1' TO 'KL-72' -
'LM-1' TO 'LM-72' -

'MN-1' TO 'MN-72' -
'NO-1' TO 'NO-72' -
'OP-1' TO 'OP-72' -
'PQ-1' TO 'PQ-72' -
'QR-1' TO 'QR-72' -

'RS-1' TO 'RS-72' -
'ST-1' TO 'ST-72' -
'TU-1' TO 'TU-72' -
'UV-1' TO 'UV-72' -
'VW-1' TO 'VW-72' -

'WX-1' TO 'WX-72' -
'XY-1' TO 'XY-72'

     G    1688 -
'AB-1' TO 'AB-72' -
'BC-1' TO 'BC-72' -

'CD-1' TO 'CD-72' -
'DE-1' TO 'DE-72' -
'EF-1' TO 'EF-72' -
```

```
'FG-1' TO 'FG-72' -
'GH-1' TO 'GH-72' -

'HI-1' TO 'HI-72' -
'IJ-1' TO 'IJ-72' -
'JK-1' TO 'JK-72' -
'KL-1' TO 'KL-72' -
'LM-1' TO 'LM-72' -

'MN-1' TO 'MN-72' -
'NO-1' TO 'NO-72' -
'OP-1' TO 'OP-72' -
'PQ-1' TO 'PQ-72' -
'QR-1' TO 'QR-72' -

'RS-1' TO 'RS-72' -
'ST-1' TO 'ST-72' -
'TU-1' TO 'TU-72' -
'UV-1' TO 'UV-72' -
'VW-1' TO 'VW-72' -

'WX-1' TO 'WX-72' -
'XY-1' TO 'XY-72'

     POI  0.17 -
'AB-1' TO 'AB-72' -
'BC-1' TO 'BC-72' -

'CD-1' TO 'CD-72' -
'DE-1' TO 'DE-72' -
'EF-1' TO 'EF-72' -
'FG-1' TO 'FG-72' -
'GH-1' TO 'GH-72' -

'HI-1' TO 'HI-72' -
'IJ-1' TO 'IJ-72' -
'JK-1' TO 'JK-72' -
'KL-1' TO 'KL-72' -
'LM-1' TO 'LM-72' -

'MN-1' TO 'MN-72' -
'NO-1' TO 'NO-72' -
'OP-1' TO 'OP-72' -
'PQ-1' TO 'PQ-72' -
'QR-1' TO 'QR-72' -

'RS-1' TO 'RS-72' -
'ST-1' TO 'ST-72' -
'TU-1' TO 'TU-72' -
'UV-1' TO 'UV-72' -
'VW-1' TO 'VW-72' -

'WX-1' TO 'WX-72' -
'XY-1' TO 'XY-72'

     DEN  8.40E-05 -
'AB-1' TO 'AB-72' -
```

```
'BC-1' TO 'BC-72' -

'CD-1' TO 'CD-72' -
'DE-1' TO 'DE-72' -
'EF-1' TO 'EF-72' -
'FG-1' TO 'FG-72' -
'GH-1' TO 'GH-72' -

'HI-1' TO 'HI-72' -
'IJ-1' TO 'IJ-72' -
'JK-1' TO 'JK-72' -
'KL-1' TO 'KL-72' -
'LM-1' TO 'LM-72' -

'MN-1' TO 'MN-72' -
'NO-1' TO 'NO-72' -
'OP-1' TO 'OP-72' -
'PQ-1' TO 'PQ-72' -
'QR-1' TO 'QR-72' -

'RS-1' TO 'RS-72' -
'ST-1' TO 'ST-72' -
'TU-1' TO 'TU-72' -
'UV-1' TO 'UV-72' -
'VW-1' TO 'VW-72' -

'WX-1' TO 'WX-72' -
'XY-1' TO 'XY-72'

     CTE  5.50E-06 -
'AB-1' TO 'AB-72' -
'BC-1' TO 'BC-72' -

'CD-1' TO 'CD-72' -
'DE-1' TO 'DE-72' -
'EF-1' TO 'EF-72' -
'FG-1' TO 'FG-72' -
'GH-1' TO 'GH-72' -

'HI-1' TO 'HI-72' -
'IJ-1' TO 'IJ-72' -
'JK-1' TO 'JK-72' -
'KL-1' TO 'KL-72' -
'LM-1' TO 'LM-72' -

'MN-1' TO 'MN-72' -
'NO-1' TO 'NO-72' -
'OP-1' TO 'OP-72' -
'PQ-1' TO 'PQ-72' -
'QR-1' TO 'QR-72' -

'RS-1' TO 'RS-72' -
'ST-1' TO 'ST-72' -
'TU-1' TO 'TU-72' -
'UV-1' TO 'UV-72' -
'VW-1' TO 'VW-72' -
```

```
'WX-1' TO 'WX-72' -
'XY-1' TO 'XY-72'

$$======================================================================
$$ SPECIFY TEMPERATURE LOADINGS
$$======================================================================

LOADING 'TRANSFER' '-1100 TEMPERATURE CHANGE'
MEMBER TEMPERATURE LOADS
'STRNDA0' TO 'STRNDA72' -
'STRNDB0' TO 'STRNDB72' -
'STRNDC0' TO 'STRNDC72' -
'STRNDD0' TO 'STRNDD72' -
'STRNDE0' TO 'STRNDE72' AXIAL -1100

$$======================================================================
$$ EXECUTE NONLINEAR ANALYSIS
$$======================================================================

MAXIMUM NUMBER OF CYCLES 10
CONVERGENCE TOL 0.001
NONLINEAR ANALYSIS

LIST FORCES EXISTING -
'STRNDA0' TO 'STRNDA72' -
'STRNDB0' TO 'STRNDB72' -
'STRNDC0' TO 'STRNDC72' -
'STRNDD0' TO 'STRNDD72' -
'STRNDE0' TO 'STRNDE72'

LIST DISPLACEMENTS -
'C1' 'Cd1' 'H1' 'Hd1' 'M1' 'Md1' 'R1' 'Rd1' 'W1' 'Wd1'
```

```
$$=========================================================================
$$    Small T-beam with a jacking stress of 0.67fpu
$$=========================================================================

STRUDL ' '

UNITS INCH KIPS DEG FAH

$$=========================================================================
$$ SPECIFY JOINT COORDINATES
$$=========================================================================

JOINT COORDINATES GLOBAL

GENERATE 193 JOINTS ID 'A1',1 X 0. -
DIFF 0 192 AT 0.5 Y 17. Z 0.

GENERATE 97 JOINTS ID 'B1',2 X 0. -
DIFF 0 96 AT 1 Y 16.5 Z 0.

GENERATE 193 JOINTS ID 'C1',1 X 0. -
DIFF 0 192 AT 0.5 Y 16. Z 0.

GENERATE 97 JOINTS ID 'D1',2 X 0. -
DIFF 0 96 AT 1 Y 15.5 Z 0.

GENERATE 193 JOINTS ID 'E1',1 X 0. -
DIFF 0 192 AT 0.5 Y 15. Z 0.

GENERATE 97 JOINTS ID 'F1',2 X 0. -
DIFF 0 96 AT 1 Y 14.5 Z 0.

GENERATE 193 JOINTS ID 'G1',1 X 0. -
DIFF 0 192 AT 0.5 Y 14. Z 0.

GENERATE 97 JOINTS ID 'H1',2 X 0. -
DIFF 0 96 AT 1 Y 13.5 Z 0.

GENERATE 193 JOINTS ID 'I1',1 X 0. -
DIFF 0 192 AT 0.5 Y 13. Z 0.

GENERATE 97 JOINTS ID 'J1',2 X 0. -
DIFF 0 96 AT 1 Y 12.5 Z 0.

GENERATE 193 JOINTS ID 'K1',1 X 0. -
DIFF 0 192 AT 0.5 Y 12. Z 0.

GENERATE 97 JOINTS ID 'L1',2 X 0. -
DIFF 0 96 AT 1 Y 11.5 Z 0.

GENERATE 193 JOINTS ID 'M1',1 X 0. -
DIFF 0 192 AT 0.5 Y 11. Z 0.

GENERATE 97 JOINTS ID 'N1',2 X 0. -
DIFF 0 96 AT 1 Y 10.5 Z 0.

GENERATE 193 JOINTS ID 'O1',1 X 0. -
```

```
DIFF 0 192 AT 0.5 Y 10. Z 0.

GENERATE 97 JOINTS ID 'P1',2 X 0. -
DIFF 0 96 AT 1 Y 9.5 Z 0.

GENERATE 193 JOINTS ID 'Q1',1 X 0. -
DIFF 0 192 AT 0.5 Y 9. Z 0.

GENERATE 97 JOINTS ID 'R1',2 X 0. -
DIFF 0 96 AT 1 Y 8.5 Z 0.

GENERATE 193 JOINTS ID 'S1',1 X 0. -
DIFF 0 192 AT 0.5 Y 8. Z 0.

GENERATE 97 JOINTS ID 'T1',2 X 0. -
DIFF 0 96 AT 1 Y 7.5 Z 0.

GENERATE 193 JOINTS ID 'U1',1 X 0. -
DIFF 0 192 AT 0.5 Y 7. Z 0.

GENERATE 97 JOINTS ID 'V1',2 X 0. -
DIFF 0 96 AT 1 Y 6.5 Z 0.

GENERATE 193 JOINTS ID 'W1',1 X 0. -
DIFF 0 192 AT 0.5 Y 6. Z 0.

GENERATE 97 JOINTS ID 'X1',2 X 0. -
DIFF 0 96 AT 1 Y 5.5 Z 0.

GENERATE 193 JOINTS ID 'Y1',1 X 0. -
DIFF 0 192 AT 0.5 Y 5. Z 0.

GENERATE 97 JOINTS ID 'Z1',2 X 0. -
DIFF 0 96 AT 1 Y 4.5 Z 0.

GENERATE 193 JOINTS ID 'AA1',1 X 0. -
DIFF 0 192 AT 0.5 Y 4. Z 0.

GENERATE 97 JOINTS ID 'BB1',2 X 0. -
DIFF 0 96 AT 1 Y 3.5 Z 0.

GENERATE 193 JOINTS ID 'CC1',1 X 0. -
DIFF 0 192 AT 0.5 Y 3. Z 0.

GENERATE 97 JOINTS ID 'DD1',2 X 0. -
DIFF 0 96 AT 1 Y 2.5 Z 0.

GENERATE 193 JOINTS ID 'EE1',1 X 0. -
DIFF 0 192 AT 0.5 Y 2. Z 0.

GENERATE 97 JOINTS ID 'FF1',2 X 0. -
DIFF 0 96 AT 1 Y 1.5 Z 0.

GENERATE 193 JOINTS ID 'GG1',1 X 0. -
DIFF 0 192 AT 0.5 Y 1. Z 0.

GENERATE 97 JOINTS ID 'HH1',2 X 0. -
```

```
DIFF 0 96 AT 1 Y 0.5 Z 0.

GENERATE 193 JOINTS ID 'II1',1 X 0. -
DIFF 0 192 AT 0.5 Y 0. Z 0.

$$================================

GENERATE 194 JOINTS ID 'EEd0',1 X 0. -
DIFF -1 1 AT 1 192 AT 0.5 Y 2. Z 0.

$$=============================================================================
$$ SPECIFY SUPPORT CONDITIONS
$$=============================================================================
STATUS SUPPORT -
'A193'  'B193'  'C193'  'D193'  'E193'  'F193'  'G193'  'H193'  'I193'
'J193'  -
'K193'  'L193'  'M193'  'N193'  'O193'  'P193'  'Q193'  'R193'  'S193'
'T193'  -
'U193'  'V193'  'W193'  'X193'  'Y193'  'Z193'  'AA193' 'BB193' 'CC193'
'DD193' -
'EE193' 'FF193' 'GG193' 'HH193' 'II1'   'II193'

JOINT RELEASES
'A193'  'B193'  'C193'  'D193'  'E193'  'F193'  'G193'  'H193'  'I193'
'J193'  -
'K193'  'L193'  'M193'  'N193'  'O193'  'P193'  'Q193'  'R193'  'S193'
'T193'  -
'U193'  'V193'  'W193'  'X193'  'Y193'  'Z193'  'AA193' 'BB193' 'CC193'
'DD193' -
'EE193' 'FF193' 'GG193' 'HH193' 'II193' -
FOR Y Z MOM X Y Z

JOINT RELEASES
'II1' -
FOR X Z MOM X Y Z

$$=============================================================================
$$ SPECIFY MASTER AND SLAVE JOINTS
$$=============================================================================

JOINT TIES
'EEd1' TO 'EEd193' EQUAL 'EE1' TO 'EE193'
'EEd0' EQUAL 'EE1'

SLAVE RELEASES
'EEd0' TO 'EEd192' FOR X Z MOM X Y Z
'EEd193' FOR Z MOM X Y Z

$$=============================================================================
$$ SPECIFY STRAND PROPERTIES
$$=============================================================================

TYPE PLANE TRUSS
GENERATE 193 MEMBERS ID 'STRND0',1 FROM 'EEd0', 1 TO 'EEd1'
GENERATE 192 MEMBERS ID 'REBAR1',1 FROM 'C1', 1 TO 'C2'

MEMBER PROPERTIES PRISMATIC AX 0.459
```

```
'STRND0' TO 'STRND192'

MEMBER PROPERTIES PRISMATIC AX 0.6
'REBAR1' TO 'REBAR192'

$$=====================================================================
$$ SPECIFY BOND ELEMENT PROPERTIES
$$=====================================================================

ELEMENT INC
'BOND-1'      'EEd1'      'EE1'
'BOND-2'      'EEd2'      'EE2'
'BOND-3'      'EEd3'      'EE3'
'BOND-4'      'EEd4'      'EE4'
'BOND-5'      'EEd5'      'EE5'
'BOND-6'      'EEd6'      'EE6'
'BOND-7'      'EEd7'      'EE7'
'BOND-8'      'EEd8'      'EE8'
'BOND-9'      'EEd9'      'EE9'
'BOND-10'     'EEd10'     'EE10'
'BOND-11'     'EEd11'     'EE11'
'BOND-12'     'EEd12'     'EE12'
'BOND-13'     'EEd13'     'EE13'
'BOND-14'     'EEd14'     'EE14'
'BOND-15'     'EEd15'     'EE15'
'BOND-16'     'EEd16'     'EE16'
'BOND-17'     'EEd17'     'EE17'
'BOND-18'     'EEd18'     'EE18'
'BOND-19'     'EEd19'     'EE19'
'BOND-20'     'EEd20'     'EE20'
'BOND-21'     'EEd21'     'EE21'
'BOND-22'     'EEd22'     'EE22'
'BOND-23'     'EEd23'     'EE23'
'BOND-24'     'EEd24'     'EE24'
'BOND-25'     'EEd25'     'EE25'
'BOND-26'     'EEd26'     'EE26'
'BOND-27'     'EEd27'     'EE27'
'BOND-28'     'EEd28'     'EE28'
'BOND-29'     'EEd29'     'EE29'
'BOND-30'     'EEd30'     'EE30'
'BOND-31'     'EEd31'     'EE31'
'BOND-32'     'EEd32'     'EE32'
'BOND-33'     'EEd33'     'EE33'
'BOND-34'     'EEd34'     'EE34'
'BOND-35'     'EEd35'     'EE35'
'BOND-36'     'EEd36'     'EE36'
'BOND-37'     'EEd37'     'EE37'
'BOND-38'     'EEd38'     'EE38'
'BOND-39'     'EEd39'     'EE39'
'BOND-40'     'EEd40'     'EE40'
'BOND-41'     'EEd41'     'EE41'
'BOND-42'     'EEd42'     'EE42'
'BOND-43'     'EEd43'     'EE43'
'BOND-44'     'EEd44'     'EE44'
'BOND-45'     'EEd45'     'EE45'
'BOND-46'     'EEd46'     'EE46'
'BOND-47'     'EEd47'     'EE47'
```

```
'BOND-48'     'EEd48'     'EE48'
'BOND-49'     'EEd49'     'EE49'
'BOND-50'     'EEd50'     'EE50'
'BOND-51'     'EEd51'     'EE51'
'BOND-52'     'EEd52'     'EE52'
'BOND-53'     'EEd53'     'EE53'
'BOND-54'     'EEd54'     'EE54'
'BOND-55'     'EEd55'     'EE55'
'BOND-56'     'EEd56'     'EE56'
'BOND-57'     'EEd57'     'EE57'
'BOND-58'     'EEd58'     'EE58'
'BOND-59'     'EEd59'     'EE59'
'BOND-60'     'EEd60'     'EE60'
'BOND-61'     'EEd61'     'EE61'
'BOND-62'     'EEd62'     'EE62'
'BOND-63'     'EEd63'     'EE63'
'BOND-64'     'EEd64'     'EE64'
'BOND-65'     'EEd65'     'EE65'
'BOND-66'     'EEd66'     'EE66'
'BOND-67'     'EEd67'     'EE67'
'BOND-68'     'EEd68'     'EE68'
'BOND-69'     'EEd69'     'EE69'
'BOND-70'     'EEd70'     'EE70'
'BOND-71'     'EEd71'     'EE71'
'BOND-72'     'EEd72'     'EE72'
'BOND-73'     'EEd73'     'EE73'
'BOND-74'     'EEd74'     'EE74'
'BOND-75'     'EEd75'     'EE75'
'BOND-76'     'EEd76'     'EE76'
'BOND-77'     'EEd77'     'EE77'
'BOND-78'     'EEd78'     'EE78'
'BOND-79'     'EEd79'     'EE79'
'BOND-80'     'EEd80'     'EE80'
'BOND-81'     'EEd81'     'EE81'
'BOND-82'     'EEd82'     'EE82'
'BOND-83'     'EEd83'     'EE83'
'BOND-84'     'EEd84'     'EE84'
'BOND-85'     'EEd85'     'EE85'
'BOND-86'     'EEd86'     'EE86'
'BOND-87'     'EEd87'     'EE87'
'BOND-88'     'EEd88'     'EE88'
'BOND-89'     'EEd89'     'EE89'
'BOND-90'     'EEd90'     'EE90'
'BOND-91'     'EEd91'     'EE91'
'BOND-92'     'EEd92'     'EE92'
'BOND-93'     'EEd93'     'EE93'
'BOND-94'     'EEd94'     'EE94'
'BOND-95'     'EEd95'     'EE95'
'BOND-96'     'EEd96'     'EE96'
'BOND-97'     'EEd97'     'EE97'
'BOND-98'     'EEd98'     'EE98'
'BOND-99'     'EEd99'     'EE99'
'BOND-100'    'EEd100'    'EE100'
'BOND-101'    'EEd101'    'EE101'
'BOND-102'    'EEd102'    'EE102'
'BOND-103'    'EEd103'    'EE103'
'BOND-104'    'EEd104'    'EE104'
```

```
'BOND-105'    'EEd105'    'EE105'
'BOND-106'    'EEd106'    'EE106'
'BOND-107'    'EEd107'    'EE107'
'BOND-108'    'EEd108'    'EE108'
'BOND-109'    'EEd109'    'EE109'
'BOND-110'    'EEd110'    'EE110'
'BOND-111'    'EEd111'    'EE111'
'BOND-112'    'EEd112'    'EE112'
'BOND-113'    'EEd113'    'EE113'
'BOND-114'    'EEd114'    'EE114'
'BOND-115'    'EEd115'    'EE115'
'BOND-116'    'EEd116'    'EE116'
'BOND-117'    'EEd117'    'EE117'
'BOND-118'    'EEd118'    'EE118'
'BOND-119'    'EEd119'    'EE119'
'BOND-120'    'EEd120'    'EE120'
'BOND-121'    'EEd121'    'EE121'
'BOND-122'    'EEd122'    'EE122'
'BOND-123'    'EEd123'    'EE123'
'BOND-124'    'EEd124'    'EE124'
'BOND-125'    'EEd125'    'EE125'
'BOND-126'    'EEd126'    'EE126'
'BOND-127'    'EEd127'    'EE127'
'BOND-128'    'EEd128'    'EE128'
'BOND-129'    'EEd129'    'EE129'
'BOND-130'    'EEd130'    'EE130'
'BOND-131'    'EEd131'    'EE131'
'BOND-132'    'EEd132'    'EE132'
'BOND-133'    'EEd133'    'EE133'
'BOND-134'    'EEd134'    'EE134'
'BOND-135'    'EEd135'    'EE135'
'BOND-136'    'EEd136'    'EE136'
'BOND-137'    'EEd137'    'EE137'
'BOND-138'    'EEd138'    'EE138'
'BOND-139'    'EEd139'    'EE139'
'BOND-140'    'EEd140'    'EE140'
'BOND-141'    'EEd141'    'EE141'
'BOND-142'    'EEd142'    'EE142'
'BOND-143'    'EEd143'    'EE143'
'BOND-144'    'EEd144'    'EE144'
'BOND-145'    'EEd145'    'EE145'
'BOND-146'    'EEd146'    'EE146'
'BOND-147'    'EEd147'    'EE147'
'BOND-148'    'EEd148'    'EE148'
'BOND-149'    'EEd149'    'EE149'
'BOND-150'    'EEd150'    'EE150'
'BOND-151'    'EEd151'    'EE151'
'BOND-152'    'EEd152'    'EE152'
'BOND-153'    'EEd153'    'EE153'
'BOND-154'    'EEd154'    'EE154'
'BOND-155'    'EEd155'    'EE155'
'BOND-156'    'EEd156'    'EE156'
'BOND-157'    'EEd157'    'EE157'
'BOND-158'    'EEd158'    'EE158'
'BOND-159'    'EEd159'    'EE159'
'BOND-160'    'EEd160'    'EE160'
'BOND-161'    'EEd161'    'EE161'
```

```
'BOND-162'    'EEd162'    'EE162'
'BOND-163'    'EEd163'    'EE163'
'BOND-164'    'EEd164'    'EE164'
'BOND-165'    'EEd165'    'EE165'
'BOND-166'    'EEd166'    'EE166'
'BOND-167'    'EEd167'    'EE167'
'BOND-168'    'EEd168'    'EE168'
'BOND-169'    'EEd169'    'EE169'
'BOND-170'    'EEd170'    'EE170'
'BOND-171'    'EEd171'    'EE171'
'BOND-172'    'EEd172'    'EE172'
'BOND-173'    'EEd173'    'EE173'
'BOND-174'    'EEd174'    'EE174'
'BOND-175'    'EEd175'    'EE175'
'BOND-176'    'EEd176'    'EE176'
'BOND-177'    'EEd177'    'EE177'
'BOND-178'    'EEd178'    'EE178'
'BOND-179'    'EEd179'    'EE179'
'BOND-180'    'EEd180'    'EE180'
'BOND-181'    'EEd181'    'EE181'
'BOND-182'    'EEd182'    'EE182'
'BOND-183'    'EEd183'    'EE183'
'BOND-184'    'EEd184'    'EE184'
'BOND-185'    'EEd185'    'EE185'
'BOND-186'    'EEd186'    'EE186'
'BOND-187'    'EEd187'    'EE187'
'BOND-188'    'EEd188'    'EE188'
'BOND-189'    'EEd189'    'EE189'
'BOND-190'    'EEd190'    'EE190'
'BOND-191'    'EEd191'    'EE191'
'BOND-192'    'EEd192'    'EE192'

$$=========================================================================
$$ NOTE: SPRING STIFFNESS MUST ACCOUNT FOR NUMBER OF STRANDS IN THIS
CASE, k(3 STRANDS) = 3*k(1 STRAND)
$$=========================================================================

NONLINEAR SPRING PROPERTIES
CURVE 'BOND' FORCE VS DISPL
0.0 0.0 -450.0 -1.0
END

ELEMENT PROPS
'BOND-1' TO 'BOND-192' -
TYPE 'NLS'

NONLINEAR SPRING ELEMENT DATA
STIFFNESS
'BOND-1' TO 'BOND-192' X CURVE 'BOND'
END

$$=========================================================================
$$ CONCRETE ELEMENT DATA
$$=========================================================================
```

```
TYPE PLANE STRESS
GENERATE 96 ELEMENTS ID 'AC-1',   1 FROM 'C1',2 TO 'C3',2 TO 'A3',2 TO
'A1',2 TO 'C2',2 TO 'B3',2 TO 'A2',2 TO 'B1',2
GENERATE 96 ELEMENTS ID 'CE-1',   1 FROM 'E1',2 TO 'E3',2 TO 'C3',2 TO
'C1',2 TO 'E2',2 TO 'D3',2 TO 'C2',2 TO 'D1',2

GENERATE 96 ELEMENTS ID 'EG-1',   1 FROM 'G1',2 TO 'G3',2 TO 'E3',2 TO
'E1',2 TO 'G2',2 TO 'F3',2 TO 'E2',2 TO 'F1',2
GENERATE 96 ELEMENTS ID 'GI-1',   1 FROM 'I1',2 TO 'I3',2 TO 'G3',2 TO
'G1',2 TO 'I2',2 TO 'H3',2 TO 'G2',2 TO 'H1',2
GENERATE 96 ELEMENTS ID 'IK-1',   1 FROM 'K1',2 TO 'K3',2 TO 'I3',2 TO
'I1',2 TO 'K2',2 TO 'J3',2 TO 'I2',2 TO 'J1',2
GENERATE 96 ELEMENTS ID 'KM-1',   1 FROM 'M1',2 TO 'M3',2 TO 'K3',2 TO
'K1',2 TO 'M2',2 TO 'L3',2 TO 'K2',2 TO 'L1',2
GENERATE 96 ELEMENTS ID 'MO-1',   1 FROM 'O1',2 TO 'O3',2 TO 'M3',2 TO
'M1',2 TO 'O2',2 TO 'N3',2 TO 'M2',2 TO 'N1',2

GENERATE 96 ELEMENTS ID 'OQ-1',   1 FROM 'Q1',2 TO 'Q3',2 TO 'O3',2 TO
'O1',2 TO 'Q2',2 TO 'P3',2 TO 'O2',2 TO 'P1',2
GENERATE 96 ELEMENTS ID 'QS-1',   1 FROM 'S1',2 TO 'S3',2 TO 'Q3',2 TO
'Q1',2 TO 'S2',2 TO 'R3',2 TO 'Q2',2 TO 'R1',2
GENERATE 96 ELEMENTS ID 'SU-1',   1 FROM 'U1',2 TO 'U3',2 TO 'S3',2 TO
'S1',2 TO 'U2',2 TO 'T3',2 TO 'S2',2 TO 'T1',2
GENERATE 96 ELEMENTS ID 'UW-1',   1 FROM 'W1',2 TO 'W3',2 TO 'U3',2 TO
'U1',2 TO 'W2',2 TO 'V3',2 TO 'U2',2 TO 'V1',2
GENERATE 96 ELEMENTS ID 'WY-1',   1 FROM 'Y1',2 TO 'Y3',2 TO 'W3',2 TO
'W1',2 TO 'Y2',2 TO 'X3',2 TO 'W2',2 TO 'X1',2

GENERATE 96 ELEMENTS ID 'YAA-1',  1 FROM 'AA1',2 TO 'AA3',2 TO 'Y3',2
TO 'Y1',2 TO 'AA2',2 TO 'Z3',2 TO 'Y2',2 TO 'Z1',2
GENERATE 96 ELEMENTS ID 'AACC-1', 1 FROM 'CC1',2 TO 'CC3',2 TO 'AA3',2
TO 'AA1',2 TO 'CC2',2 TO 'BB3',2 TO 'AA2',2 TO 'BB1',2
GENERATE 96 ELEMENTS ID 'CCEE-1', 1 FROM 'EE1',2 TO 'EE3',2 TO 'CC3',2
TO 'CC1',2 TO 'EE2',2 TO 'DD3',2 TO 'CC2',2 TO 'DD1',2
GENERATE 96 ELEMENTS ID 'EEGG-1', 1 FROM 'GG1',2 TO 'GG3',2 TO 'EE3',2
TO 'EE1',2 TO 'GG2',2 TO 'FF3',2 TO 'EE2',2 TO 'FF1',2
GENERATE 96 ELEMENTS ID 'GGII-1', 1 FROM 'II1',2 TO 'II3',2 TO 'GG3',2
TO 'GG1',2 TO 'II2',2 TO 'HH3',2 TO 'GG2',2 TO 'HH1',2

ELEMENT PROPERTIES TYPE 'IPQQ' THICK 24
'AC-1' TO 'AC-96'
'CE-1' TO 'CE-96'

ELEMENT PROPERTIES TYPE 'IPQQ' THICK 6
'EG-1' TO 'EG-96'
'GI-1' TO 'GI-96'

ELEMENT PROPERTIES TYPE 'IPQQ' THICK 4
'IK-1' TO 'IK-96'
'KM-1' TO 'KM-96'
'MO-1' TO 'MO-96'
'OQ-1' TO 'OQ-96'
'QS-1' TO 'QS-96'
'SU-1' TO 'SU-96'
'UW-1' TO 'UW-96'

ELEMENT PROPERTIES TYPE 'IPQQ' THICK 6
```

```
'WY-1' TO 'WY-96'
'YAA-1' TO 'YAA-96'

ELEMENT PROPERTIES TYPE 'IPQQ' THICK 8
'AACC-1' TO 'AACC-96'
'CCEE-1' TO 'CCEE-96'
'EEGG-1' TO 'EEGG-96'
'GGII-1' TO 'GGII-96'

$$=========================================================================
$$ SPECIFY MATERIAL PROPERTIES
$$=========================================================================

MATERIAL STEEL -
'REBAR1' TO 'REBAR192'

$$---------------------
$$ STEEL
$$---------------------
CONSTANTS
     E    28500 -
'STRND0' TO 'STRND192'

     G    10962 -
'STRND0' TO 'STRND192'

     POI  0.3 -
'STRND0' TO 'STRND192'

     DEN  2.83E-04 -
'STRND0' TO 'STRND192'

     CTE  6.50E-06 -
'STRND0' TO 'STRND192'

$$---------------------
$$ CONCRETE
$$---------------------
CONSTANTS
     E    4150 -
'AC-1' TO 'AC-96' -
'CE-1' TO 'CE-96' -

'EG-1' TO 'EG-96' -
'GI-1' TO 'GI-96' -

'IK-1' TO 'IK-96' -
'KM-1' TO 'KM-96' -
'MO-1' TO 'MO-96' -
'OQ-1' TO 'OQ-96' -
'QS-1' TO 'QS-96' -
'SU-1' TO 'SU-96' -
'UW-1' TO 'UW-96' -

'WY-1' TO 'WY-96' -
'YAA-1' TO 'YAA-96' -
```

```
'AACC-1' TO 'AACC-96' -
'CCEE-1' TO 'CCEE-96' -
'EEGG-1' TO 'EEGG-96' -
'GGII-1' TO 'GGII-96'

     G    1773 -
'AC-1' TO 'AC-96' -
'CE-1' TO 'CE-96' -

'EG-1' TO 'EG-96' -
'GI-1' TO 'GI-96' -

'IK-1' TO 'IK-96' -
'KM-1' TO 'KM-96' -
'MO-1' TO 'MO-96' -
'OQ-1' TO 'OQ-96' -
'QS-1' TO 'QS-96' -
'SU-1' TO 'SU-96' -
'UW-1' TO 'UW-96' -

'WY-1' TO 'WY-96' -
'YAA-1' TO 'YAA-96' -

'AACC-1' TO 'AACC-96' -
'CCEE-1' TO 'CCEE-96' -
'EEGG-1' TO 'EEGG-96' -
'GGII-1' TO 'GGII-96'

     POI  0.17 -
'AC-1' TO 'AC-96' -
'CE-1' TO 'CE-96' -

'EG-1' TO 'EG-96' -
'GI-1' TO 'GI-96' -

'IK-1' TO 'IK-96' -
'KM-1' TO 'KM-96' -
'MO-1' TO 'MO-96' -
'OQ-1' TO 'OQ-96' -
'QS-1' TO 'QS-96' -
'SU-1' TO 'SU-96' -
'UW-1' TO 'UW-96' -

'WY-1' TO 'WY-96' -
'YAA-1' TO 'YAA-96' -

'AACC-1' TO 'AACC-96' -
'CCEE-1' TO 'CCEE-96' -
'EEGG-1' TO 'EEGG-96' -
'GGII-1' TO 'GGII-96'

     DEN  8.40E-05 -
'AC-1' TO 'AC-96' -
'CE-1' TO 'CE-96' -

'EG-1' TO 'EG-96' -
'GI-1' TO 'GI-96' -
```

```
'IK-1' TO 'IK-96' -
'KM-1' TO 'KM-96' -
'MO-1' TO 'MO-96' -
'OQ-1' TO 'OQ-96' -
'QS-1' TO 'QS-96' -
'SU-1' TO 'SU-96' -
'UW-1' TO 'UW-96' -

'WY-1' TO 'WY-96' -
'YAA-1' TO 'YAA-96' -

'AACC-1' TO 'AACC-96' -
'CCEE-1' TO 'CCEE-96' -
'EEGG-1' TO 'EEGG-96' -
'GGII-1' TO 'GGII-96'

     CTE  5.50E-06 -
'AC-1' TO 'AC-96' -
'CE-1' TO 'CE-96' -

'EG-1' TO 'EG-96' -
'GI-1' TO 'GI-96' -

'IK-1' TO 'IK-96' -
'KM-1' TO 'KM-96' -
'MO-1' TO 'MO-96' -
'OQ-1' TO 'OQ-96' -
'QS-1' TO 'QS-96' -
'SU-1' TO 'SU-96' -
'UW-1' TO 'UW-96' -

'WY-1' TO 'WY-96' -
'YAA-1' TO 'YAA-96' -

'AACC-1' TO 'AACC-96' -
'CCEE-1' TO 'CCEE-96' -
'EEGG-1' TO 'EEGG-96' -
'GGII-1' TO 'GGII-96'

$$=========================================================================
$$ SPECIFY TEMPERATURE LOADINGS NOTE: -980 F IS EQUIVALENT TO 0.67*fpu
$$=========================================================================

LOADING 'TRANSFER' '-980 TEMPERATURE CHANGE'
MEMBER TEMPERATURE LOADS
'STRND0' TO 'STRND192' AXIAL -980

$$=========================================================================
$$ EXECUTE NONLINEAR ANALYSIS
$$=========================================================================

MAXIMUM NUMBER OF CYCLES 10
CONVERGENCE TOL 0.001
NONLINEAR ANALYSIS

LIST FORCES EXISTING -
```

```
'STRND0' TO 'STRND192'

LIST DISPLACEMENTS -
'EE1' 'EEd1'
```